

AD-A245 237



2

WL-TR-91-4111

**DURABILITY AND  
DAMAGE TOLERANCE OF  
ALUMINUM CASTINGS**



M. W. OZELTON  
S. J. MOCARSKI  
P. G. PORTER

NORTHROP CORPORATION  
AIRCRAFT DIVISION  
ONE NORTHROP AVENUE  
HAWTHORNE, CALIFORNIA 90250



October 1991

Final Technical Report  
For Period September 1985 - June 1991

Approved for Public Release: Distribution Unlimited

MATERIALS DIRECTORATE  
WRIGHT LABORATORY  
AIR FORCE SYSTEMS COMMAND  
WRIGHT-PATTERSON AFB, OHIO 45433-6533

92-02019



92 1 21 21

NOTICE

When Government drawings, specifications, or other data are used for any purpose other than in connection with a definitely Government-related procurement, the United States Government thereby incurs no responsibility nor any obligation whatsoever. The fact that the government may have formulated, or in any way supplied the said drawings, specifications, or other data, is not to be regarded by implication or otherwise as in any manner construed, as licensing the holder or any other person or corporation, or as conveying any rights or permission to manufacture use, or sell any patented invention that may in any way be related thereto.

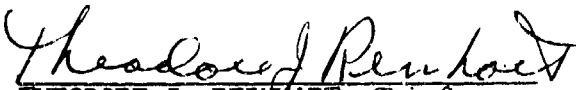
This report is releasable to the National Technical Information Service (NTIS). At NTIS, it will be available to the general public, including foreign nations.

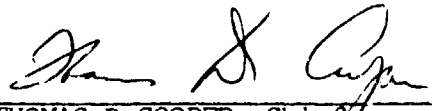
This technical report has been reviewed and is approved for publication.

  
MARY ANN PHILLIPS, Project Engineer  
Engineering & Design Data  
Materials Engineering Branch

  
CLAYTON L. HARMSWORTH, Tech.Mgr.  
Engineering & Design Data  
Materials Engineering Branch

FOR THE COMMANDER

  
THEODORE J. REINHART, Chief  
Materials Engineering Branch  
Systems Support Division  
Materials Directorate

  
THOMAS D. COOPER, Chief  
Systems Support Division  
Materials Directorate  
Wright Laboratory

If your address has changed, if you wish to be removed from our mailing list, or if the addressee is no longer employed by your organization please notify WL/MLSE, WPAFB, OH 45433-6533 to help us maintain a current mailing list.

Copies of this report should not be returned unless return is required by security considerations, contractual obligations, or notice on a specific document.

| REPORT DOCUMENTATION PAGE   |  |   | Form Approved<br>OMB No 0704 0188  |  |
|---|--|---|--|--|
| Public reporting burden for this collection of information is estimated to average 1 hour per response, including the time for reviewing instructions, searching existing data sources, gathering and maintaining the data needed, and completing and reviewing the collection of information. Send comments regarding this burden estimate or any other aspect of this collection of information, including suggestions for reducing this burden, to Washington Headquarters Service, Directorate for Information Operations and Reports, 1215 Jefferson Davis Highway, Suite 1204, Arlington, VA 22202-4302, and to the Office of Management and Budget, Paperwork Reduction Project (0704-0188), Washington, DC 20503.   |  |   |  |  |
| 1. AGENCY USE ONLY (Leave blank)  | 2. REPORT DATE<br>October 1991                           | 3. REPORT TYPE AND DATES COVERED<br>Final, 1 Sept 1985 - 30 June 1991 |  |  |
| 4. TITLE AND SUBTITLE<br>Durability and Damage Tolerance of Aluminum Castings   |  |   | 5. FUNDING NUMBERS<br>F33615-85-C-5015<br>PE 62102F<br>Project 2418<br>Task 01<br>Work Unit 42 |  |
| 6. AUTHOR(S)<br>M. W. Ozelton, S. J. Mocarski, and P. G. Porter   |  |   |  |  |
| 7. PERFORMING ORGANIZATION NAME(S) AND ADDRESS(ES)<br>Northrop Corporation<br>Aircraft Division<br>One Northrop Avenue<br>Hawthorne, CA 90250   |  |   | 8. PERFORMING ORGANIZATION<br>REPORT NUMBER<br>NOR 91-25                                       |  |
| 9. SPONSORING/MONITORING AGENCY NAME(S) AND ADDRESS(ES)<br>Materials Laboratory (WL/MLSE)<br>Wright Laboratory<br>Wright-Patterson AFB<br>Dayton, OH 45433-6533   |  |   | (Mary Ann Phillips)<br>(513-255-5128)<br>WL-TR-91-4111   |  |
| 11. SUPPLEMENTARY NOTES   |  |   |  |  |
| 12a. DISTRIBUTION/AVAILABILITY STATEMENT<br>Approved for public release; distribution is unlimited  |  |   | 12b. DISTRIBUTION CODE   |  |
| 13. ABSTRACT (Maximum 200 words)<br>A durability and damage tolerance (DADT) data base for aluminum casting alloys D357-T6 and B201-T7 was developed and the applicability of ultrasonic and low frequency eddy-current NDI methods to castings was assessed. Relationships among composition, heat treatment, solidification rate, microstructure, and mechanical properties were investigated using multiple regression analyses. Sr (silicon modifier) and Ag had the most significant impact on the properties of D357-T6 and B201-T7 respectively. Constant amplitude fatigue data were used to calculate an equivalent initial flaw size for both alloys. Spectrum fatigue results for D357-T6 were used to assess the applicability of current military DADT specifications to aluminum castings. The effect of intentionally-added defects (D357-T6) and nonoptimum microstructure (D357-T6 and B201-T7) on mechanical properties was determined. Four large, complex aerospace castings were produced and tested to confirm that the property data base, which was obtained for cast plates, is applicable to aircraft applications. A D357 specification for durability and damage tolerance applications was submitted to the Society of Automotive Engineers. |  |   |  |  |
| 14. SUBJECT TERMS<br>Aluminum castings, D357, B201, mechanical properties, durability, damage tolerance, fatigue, fracture toughness, specifications, equivalent initial flaw size, nondestructive inspection.  |  |   | 15. NUMBER OF PAGES<br>502   |  |
|   |  |   | 16. PRICE CODE   |  |
| 17. SECURITY CLASSIFICATION OF REPORT<br>Unclassified   | 18. SECURITY CLASSIFICATION OF THIS PAGE<br>Unclassified | 19. SECURITY CLASSIFICATION OF ABSTRACT<br>Unclassified               | 20. LIMITATION OF ABSTRACT<br>UL   |  |

## SUMMARY

A durability and damage tolerance data base for aluminum casting alloys A357-T6 and A201-T7 was developed. AMS material specifications for premium quality aluminum castings issued in 1986 were selected for use during the program. The specifications included new alloy designations, which were used throughout this final report. The designations are D357 (AMS 4241) and B201 (AMS 4242).

A new ultrasonic NDI method called Frequency Attenuation Inflection (FAI) was evaluated to determine the type and amount of defects in D357 and B201 aluminum castings. Results were compared with standard X-ray radiography and microstructural data. The effects of surface roughness, material thickness, and nonparallel surfaces on the FAI results were determined.

An in-service low frequency eddy-current method was evaluated for detecting the presence of cracks under fasteners in D357 and B201 substructures through aluminum face sheets of varying thickness. Both titanium and steel fasteners were used.

Relationships among chemical composition, heat treatment, solidification rate, microstructure, and mechanical properties of the premium quality casting alloys D357-T6 and B201-T7 were investigated. Tensile, notched tensile, and fatigue life properties, as well as microstructural features, were determined as a function of solidification rate, aging treatment, and alloy composition. Multiple regression analyses were conducted to determine correlations among the process variables and mechanical properties. Sr (silicon modifier) and Ag had the most significant effect on the properties of D357-T6 and B201-T7, respectively.

Specifications for both alloys were developed and a durability and damage tolerance (DADT) property data base for D357-T6 and B201-T7 cast plates produced by three commercial foundries was obtained. Tensile, fatigue, and fracture toughness properties were determined and microstructural and

fractographic evaluations were performed. The fatigue data (stress-life and crack growth rate) were used to calculate an equivalent initial flaw size for both alloys to assess the applicability of current military DADT specifications to castings. The DADT property data base was used as a baseline to assess the effect of defects (D357-T6) and nonoptimum microstructure (D357-T6 and B201-T7) on mechanical properties.

Four large, complex aerospace castings (wing pylons) were produced and tested to confirm that the data base developed for cast plates can be applied to large aircraft castings.

Where required, modifications to existing specifications (material and DADT) were recommended based on the program results.

A revised version of AMS 4241 specification (D357) for use in the manufacture of durability and damage tolerance aircraft components was submitted to the Society of Automotive Engineers. If approved, this will be a new specification for DADT applications.

PREFACE

This final report report covers the work performed under Contract F33615-85-C-5015 from September 1985 to June 1991 by Northrop Corporation, Aircraft Division, Hawthorne, California, under Project Number 2418. The program was administered under the technical direction of Mary Ann Phillips, WL/MLSE, Wright-Patterson AFB, Ohio 45433-6533.

The work was performed by Northrop's Metallic and Ceramic Materials and Processes Research and Technology Department. Dr. M. W. Ozelton was the Program Manager; Mr. S. J. Mocarski (1988-1991) and Mr. G. R. Turk (1985-1988) were the Principal Investigators. The contributions of the following Northrop personnel are acknowledged: P. G. Porter, durability, damage tolerance, and equivalent initial flaw size analyses; W. R. Sheppard, NDI analyses; K. J. Oswalt for many invaluable castings technology discussions; S. Hsu, mechanical testing; D. R. Drott, H. E. Langman, J. T. Findley, and M. A. Arrieta for coordinating and carrying out the many and varied activities to obtain the test data; H. S. Richardson for preparing the manuscript; and G. L. Young for data tabulation and plotting.

The major subcontractors for the program were Alcoa, Premium Castings Division, Corona, California; Hitchcock Industries Inc., Minneapolis, Minnesota; Fansteel Wellman Dynamics, Creston, Iowa; and Dr. L. Adler of Ohio State University (NDI consultant).



|                      |                                     |
|----------------------|-------------------------------------|
| <b>Accession For</b> |                                     |
| NTIS GRA&I           | <input checked="" type="checkbox"/> |
| DTIC TAB             | <input type="checkbox"/>            |
| Unannounced          | <input type="checkbox"/>            |
| Justification        |                                     |
| By                   |                                     |
| Distribution/        |                                     |
| Availability Codes   |                                     |
| Dist                 | Avail and/or<br>Special             |
| A-1                  |                                     |

## CONTENTS

| <u>Section</u> |  | <u>Page</u> |
|----------------|--|-------------|
| 1              | INTRODUCTION .....   | 1           |
| 2              | OBJECTIVE .....  | 3           |
| 3              | PROGRAM APPROACH .....   | 5           |
|                | 3.1 Phase I - DADT of Aluminum Castings Quality Assessment .....               | 5           |
|                | 3.1.1 Task 1 - NDI Assessment .....  | 5           |
|                | 3.1.2 Task 2 - Alloy Characterization .....                                    | 5           |
|                | 3.1.3 Task 3 - Effects of Defects on DADT Properties .....                     | 5           |
|                | 3.1.4 Task 4 - Applicability of DADT Specifications to Aluminum Castings ..... | 7           |
|                | 3.2 Phase II - DADT of Aluminum Castings Quality Verification .....            | 7           |
|                | 3.3 Phase III - DADTAC Program Consolidation .....                             | 7           |
| 4              | PHASE I, TASK 1 - NDI ASSESSMENT .....   | 9           |
|                | 4.1 Introduction .....   | 9           |
|                | 4.2 NDI Methods .....  | 11          |
|                | 4.2.1 FAI Technique .....  | 11          |
|                | 4.2.2 Ultrasonic C-Scan .....  | 15          |
|                | 4.2.3 Radiography .....  | 15          |
|                | 4.2.4 Eddy Current Technique .....   | 17          |
|                | 4.3 Defect-Containing Plates for FAI Method Evaluations .....                  | 23          |
|                | 4.4 Results and Discussion .....   | 23          |
|                | 4.4.1 FAI Evaluation of the Full-Thickness Plates .....                        | 26          |
|                | 4.4.2 Correlation Between FAI Results for Plates and Slices .....              | 30          |
|                | 4.4.3 Correlation Between FAI and X-ray Assessments .....                      | 36          |
|                | 4.4.4 Correlation Between FAI and Microstructural Measurements .....           | 38          |
|                | 4.4.5 Effect of Nonparallel Surfaces on FAI Results .....                      | 43          |

CONTENTS (Continued)

| <u>Section</u>                                      | <u>Page</u> |
|---|-------------|
| 4.4.6 Weld Defect Evaluation .....                  | 43          |
| 4.4.7 Eddy Current Crack Detection Results .....    | 46          |
| 4.5 Conclusions .....                               | 49          |
| 5 PHASE I, TASK 2 - D357-T6 SCREENING TESTS .....   | 51          |
| 5.1 Introduction .....                              | 51          |
| 5.2 Experimental Procedures .....                   | 52          |
| 5.2.1 Process Variables .....                       | 52          |
| 5.2.2 Test Procedures .....                         | 58          |
| 5.2.3 Microstructural Characterization .....        | 58          |
| 5.2.4 Data Analysis .....                           | 58          |
| 5.3 Results and Discussion .....                    | 61          |
| 5.3.1 Composition .....                             | 62          |
| 5.3.2 Microstructure .....                          | 64          |
| 5.3.3 Tensile Properties .....                      | 74          |
| 5.3.4 Notched Tensile Strength and NTS/YS Ratio ... | 79          |
| 5.3.5 Fatigue Life .....                            | 83          |
| 5.3.6 Regression Analysis .....                     | 85          |
| 5.4 Conclusions .....                               | 88          |
| 5.5 Recommendations .....                           | 89          |
| 6 PHASE I, TASK 2 - B201-T7 SCREENING TESTS .....   | 91          |
| 6.1 Introduction .....                              | 91          |
| 6.2 Experimental Procedures .....                   | 91          |
| 6.2.1 Process Variables .....                       | 91          |
| 6.2.2 Test Procedures .....                         | 96          |
| 6.2.3 Microstructural Characterization .....        | 96          |
| 6.2.4 Data Analysis .....                           | 96          |
| 6.3 Results and Discussion .....                    | 96          |
| 6.3.1 Composition .....                             | 96          |
| 6.3.2 Microstructure .....                          | 97          |
| 6.3.3 Tensile Properties .....                      | 100         |
| 6.3.4 Notched Tensile Strength and NTS/YS Ratio ... | 105         |
| 6.3.5 Fatigue Life .....                            | 108         |
| 6.3.6 Regression Analysis .....                     | 109         |
| 6.4 Conclusions .....                               | 112         |
| 6.5 Recommendations .....                           | 113         |

CONTENTS (Continued)

| <u>Section</u> |  | <u>Page</u> |
|----------------|--|-------------|
| 7              | PHASE I, TASK 2 - PROPERTY VERIFICATION .....  | 115         |
|                | 7.1 Introduction .....   | 115         |
|                | 7.2 Experimental Procedures .....  | 115         |
|                | 7.2.1 Production of Castings .....   | 115         |
|                | 7.2.2 Test Procedures .....  | 125         |
|                | 7.2.3 Equivalent Initial Flaw Size Analysis .....  | 127         |
|                | 7.3 D357-T6 Results .....  | 131         |
|                | 7.3.1 Composition .....  | 132         |
|                | 7.3.2 Microstructure .....   | 132         |
|                | 7.3.3 Tensile Properties .....   | 138         |
|                | 7.3.4 Fatigue Properties .....   | 141         |
|                | 7.3.5 Fracture Toughness .....   | 147         |
|                | 7.3.6 Equivalent Initial Flaw Size Analysis .....  | 150         |
|                | 7.4 B201-T7 Results .....  | 154         |
|                | 7.4.1 Composition .....  | 154         |
|                | 7.4.2 Microstructure .....   | 154         |
|                | 7.4.3 Tensile Properties .....   | 160         |
|                | 7.4.4 Fatigue Properties .....   | 160         |
|                | 7.4.5 Fracture Toughness .....   | 166         |
|                | 7.4.6 Stress Corrosion .....   | 169         |
|                | 7.4.7 Equivalent Initial Flaw Size Analysis .....  | 169         |
|                | 7.4.8 Effect of HIPing on Porosity .....   | 172         |
|                | 7.5 Conclusions .....  | 175         |
| 8              | PHASE I, TASK 3 - EFFECT OF METALLURGICAL FEATURES AND<br>DISCONTINUITIES ON MECHANICAL PROPERTIES ..... | 177         |
|                | 8.1 Introduction .....   | 177         |
|                | 8.2 Experimental Procedures .....  | 178         |
|                | 8.2.1 Production of Castings .....   | 178         |
|                | 8.2.2 Test Procedures .....  | 181         |
|                | 8.3 Effect of Defects on the Properties of D357-T6 .....   | 185         |
|                | 8.3.1 Composition .....  | 185         |
|                | 8.3.2 Microstructure .....   | 185         |
|                | 8.3.3 Ultrasonic NDI Evaluation of the Defect-<br>Containing Plates .....                                | 187         |
|                | 8.3.4 Tensile Properties .....   | 192         |

CONTENTS (Continued)

| <u>Section</u>   | <u>Page</u> |
|--|-------------|
| 8.3.5 Fatigue Properties .....   | 197         |
| 8.3.6 Fracture Toughness .....   | 208         |
| 8.4 Effect of Nonoptimum Microstructure on the Properties<br>of D357-T6 .....          | 208         |
| 8.4.1 Composition .....  | 208         |
| 8.4.2 Microstructure .....   | 212         |
| 8.4.3 Tensile Properties .....   | 216         |
| 8.4.4 Fatigue Properties .....   | 216         |
| 8.4.5 Fracture Toughness .....   | 220         |
| 8.5 Effect of Nonoptimum Microstructure on the Properties<br>of B201-T7 .....          | 220         |
| 8.5.1 Composition .....  | 220         |
| 8.5.2 Microstructure .....   | 220         |
| 8.5.3 Tensile Properties .....   | 226         |
| 8.5.4 Fatigue Properties .....   | 226         |
| 8.5.5 Fracture Toughness .....   | 230         |
| 8.5.6 Stress Corrosion Cracking .....  | 230         |
| 8.6 Conclusions .....  | 231         |
| 8.6.1 Effect of Defects on D357-T6 Mechanical<br>Properties .....                      | 231         |
| 8.6.2 Nonoptimum D357-T6 .....   | 231         |
| 8.6.3 Nonoptimum B201-T7 .....   | 233         |
| 9 PHASE I, TASK 4 - APPLICABILITY OF DADT SPECIFICATIONS TO<br>ALUMINUM CASTINGS ..... | 235         |
| 9.1 Introduction .....   | 235         |
| 9.2 Durability and Damage Tolerance Assessment .....                                   | 235         |
| 9.2.1 FAI Assessment .....   | 236         |
| 9.2.2 Damage Tolerance Analysis .....  | 236         |
| 10 PHASE II - DADT OF ALUMINUM CASTINGS QUALITY VERIFICATION                           | 237         |
| 10.1 Introduction .....  | 237         |
| 10.2 Casting Selection .....   | 237         |
| 10.3 Production of Castings .....  | 238         |
| 10.4 Castings Properties .....   | 240         |

CONTENTS (Continued)

| <u>Section</u>   | <u>Page</u> |
|--|-------------|
| 10.4.1 Composition .....   | 240         |
| 10.4.2 Microstructure .....  | 240         |
| 10.4.3 Tensile Properties .....  | 242         |
| 10.4.4 Fatigue Properties .....  | 247         |
| 10.4.5 Fracture Toughness .....  | 249         |
| 10.4.6 FAI Assessment of the Pylons .....  | 253         |
| 10.4.7 Equivalent Initial Flaw Size Analysis of the<br>Pylons .....                    | 253         |
| 10.4.8 Summary .....   | 255         |
| 10.5 Durability and Damage Tolerance Analysis .....                                    | 255         |
| 10.5.1 Element Testing .....   | 256         |
| 10.5.2 DADT Analysis Method .....  | 262         |
| 10.5.3 Data Requirements .....   | 265         |
| 10.5.4 Analysis .....  | 266         |
| 10.5.5 Test Results .....  | 269         |
| 10.5.6 Analytical Correlation .....  | 276         |
| 10.5.7 Fractographic Analysis .....  | 278         |
| 10.6 Conclusions .....   | 281         |
| 11 PHASE III - DATA CONSOLIDATION .....  | 285         |
| 11.1 Material Specifications .....   | 285         |
| 11.1.1 D357-T6 .....   | 285         |
| 11.1.2 B201-T7 .....   | 308         |
| 11.2 Process Specifications .....  | 308         |
| 11.2.1 D357-T6 .....   | 309         |
| 11.2.2 B201-T7 .....   | 311         |
| 11.3 Applicability of MIL-A-87221 and MIL-A-83444 to<br>Premium Quality Castings ..... | 312         |
| 12 SUMMARY OF DADTAC PROGRAM CONCLUSIONS .....   | 315         |
| 12.1 Phase I, Task 1 - NDI Assessment .....  | 315         |
| 12.2 Phase I, Task 2 - Screening Tests .....   | 315         |
| 12.3 Phase I, Task 2 - Property Verification .....                                     | 315         |
| 12.4 Phase I, Task 3 - Effect of Defects .....   | 316         |
| 12.5 Phase II - Castings Qualify Verification .....                                    | 316         |
| 12.6 Phase III - Data Consolidation .....  | 316         |
| 13 SPECIAL CONSIDERATIONS .....  | 319         |

CONTENTS (Continued)

|  | <u>Page</u> |
|--|-------------|
| REFERENCES .....   | 321         |
| APPENDIX A Phase I, Task 2 - D357-T6 Screening<br>Test Data .....  | 325         |
| APPENDIX B Phase I, Task 2 - B201-T7 Screening<br>Test Data .....  | 339         |
| APPENDIX C Phase I, Task 2 - D357-T6 Verification<br>Test Data .....   | 353         |
| APPENDIX D Phase I, Task 2 - B201-T7 Verification<br>Test Data .....   | 371         |
| APPENDIX E Phase I, Task 3 - D357-T6 Discontinuity<br>Assessment .....   | 385         |
| APPENDIX F Phase I, Task 3 - D357-T6 Nonoptimum<br>Microstructure Assessment .....   | 413         |
| APPENDIX G Phase I, Task 3 - B201-T7 Nonoptimum<br>Microstructure Assessment .....   | 419         |
| APPENDIX H Phase II, Task 4 - Aircraft Castings<br>Evaluation .....  | 425         |
| APPENDIX I Phase II, Task 4 - Element Test Data .....  | 435         |
| APPENDIX J Phase III - Recommended Changes to AMS 4241<br>(D357) for Durability and Damage Tolerance<br>Applications .....   | 463         |
| APPENDIX K Phase III - Recommended Changes to AMS 4242<br>(B201) .....   | 487         |
| APPENDIX L Phase I, Task 3 - Hydrogen Content and<br>Equivalent Initial Flaw Size of Gas<br>Porosity Fatigue Specimens ..... | 501         |

## LIST OF FIGURES

| <u>Figure</u> |   | <u>Page</u> |
|---------------|---|-------------|
| 1             | Program Outline .....   | 6           |
| 2             | FAI Equipment .....   | 12          |
| 3             | Schematic Illustration of the FAI Method .....  | 14          |
| 4             | C-Scan Ultrasonic Imaging System .....  | 16          |
| 5             | Combinations of Fac Sheet, Fasteners, and Substructure<br>Used for In-Service Eddy Current Inspection .....   | 18          |
| 6             | In-Service Eddy Current Inspection Test Equipment .....   | 19          |
| 7             | Schematic Illustration of the Probes Used With Steel<br>and Titanium Fasteners .....                          | 20          |
| 8             | Multisegment Eddy Current Probe .....   | 21          |
| 9             | Typical Eddy Current Probe Output .....   | 22          |
| 10            | Typical Gas Porosity in Grade C D357 .....  | 40          |
| 11            | Typical Shrinkage Porosity in Grade D B201 .....  | 40          |
| 12            | Typical Less-Dense Foreign Material in Grade C D357 .....   | 41          |
| 13            | C-Scan of Weld Defects in D357 .....  | 45          |
| 14            | Gating, Riserling, and Chill Placement Used for the<br>D357 Process Variable Plates .....                     | 57          |
| 15            | Fatigue Test Specimen .....   | 60          |
| 16            | D357 Dendrite Arm Spacing vs. Distance From the<br>Center of the Chill .....                                  | 66          |
| 17            | Effect of Strontium on the D357-T6 Microstructure .....   | 72          |
| 18            | D357-T6 NTS/YS Ratio vs. Percent Strontium for Plates<br>That Were Within the Composition Specification ..... | 82          |
| 19            | Gating, Riserling, and Chill Placement Used for the<br>B201 Process Variable Plates .....                     | 92          |

LIST OF FIGURES (Continued)

| <u>Figure</u> |   | <u>Page</u> |
|---------------|---|-------------|
| 20            | Rigging System Used by Alcoa to Produce D357 Plates .....   | 119         |
| 21            | Rigging System Used by Hitchcock Industries to Produce<br>D357 Plates .....   | 120         |
| 22            | Rigging System Used by Fansteel Wellman Dynamics to<br>Produce D357 Plates .....  | 122         |
| 23            | Typical D357-T6 Microstructure .....  | 134         |
| 24            | Backscatter SEM Micrograph of D357-T6 .....   | 137         |
| 25            | TEM Micrograph of D357-T6 Showing Si Particles .....  | 137         |
| 26            | TEM Micrograph of D357-T6 Showing a Needle-Shaped Phase<br>Containing Ti .....  | 137         |
| 27            | a. TEM Micrograph of D357-T6 Showing a Needle-Shaped<br>Particle Containing Ti and Smaller Mg <sub>2</sub> Si Particles.. | 139         |
|               | b. Selected Area Diffraction Pattern of the Needle<br>Phase of Figure 27a .....   | 139         |
| 28            | D357-T6 Stress-Life Fatigue Data .....  | 142         |
| 29            | D357-T6 Strain-Life Fatigue Data .....  | 144         |
| 30            | D357-T6 Fatigue Crack Growth Rate Data .....  | 145         |
| 31            | Typical Crack Initiation Sites in D357-T6 Fatigue<br>Specimens .....  | 146         |
| 32            | Relationship Between Fracture Toughness and Yield<br>Strength for D357-T6 .....   | 149         |
| 33            | Weibull Distribution of D357-T6 EIFS Data .....   | 152         |
| 34            | Measurement of Defect Size in D357-T6 .....   | 155         |
| 35            | Typical B201-T7 Microstructure .....  | 156         |
| 36            | TEM Micrograph of B201-T7 Showing the Theta Phase .....   | 158         |
| 37            | Backscatter SEM Image of B201-T7 .....  | 159         |
| 38            | STEM Micrograph of B201-T7 Showing a Phase Rich in<br>Al, Cu, Fe, and Mn .....  | 159         |

LIST OF FIGURES (Continued)

| <u>Figure</u> |  | <u>Page</u> |
|---------------|--|-------------|
| 39            | TEM Micrograph of B201-T7 Showing a Phase Rich in Al, Cu, and Mn .....                   | 159         |
| 40            | TEM Micrograph of B201-T7 Showing a Phase Rich in Al and Ti .....                        | 159         |
| 41            | B201-T7 Stress-Life Fatigue Data .....   | 162         |
| 42            | B201-T7 Strain-Life Fatigue Data .....   | 164         |
| 43            | B201-T7 Fatigue Crack Growth Rate Data .....   | 165         |
| 44            | Foreign Material on a B201-T7 Fatigue Fracture Surface...                                | 167         |
| 45            | Relationship Between Fracture Toughness and Yield Strength of B201-T7 .....              | 170         |
| 46            | Weibull Distribution of B201-T7 EIFS Data .....  | 173         |
| 47            | Microstructure of D357-T6 Weld .....   | 189         |
| 48            | Stress-Life Fatigue Data for D357-T6 Containing Gas Porosity .....                       | 198         |
| 49            | Stress-Life Fatigue Data for D357-T6 Containing Shrinkage Porosity .....                 | 198         |
| 50            | Stress-Life Fatigue Data for D357-T6 Containing Less-Dense Foreign Material .....        | 199         |
| 51            | Stress-Life Fatigue Data for Grade A/B and Weld-Repaired D357-T6 .....                   | 199         |
| 52            | Grade A/B and Grade B D357-T6 Stress-Life Fatigue Data for Small Test Specimens .....    | 201         |
| 53            | Constant Amplitude Fatigue Crack Growth Rate of Grade B (Gas Porosity) D357-T6 .....     | 202         |
| 54            | Constant Amplitude Fatigue Crack Growth Rate of Grade C (Gas Porosity) D357-T6 .....     | 203         |
| 55            | Constant Amplitude Fatigue Crack Growth Rate of Grade D (Gas Porosity) D357-T6 .....     | 204         |
| 56            | Constant Amplitude Fatigue Crack Growth Rate of Grade B (Foreign Material) D357-T6 ..... | 205         |

LIST OF FIGURES (Continued)

| <u>Figure</u> |  | <u>Page</u> |
|---------------|--|-------------|
| 57            | Constant Amplitude Fatigue Crack Growth Rate of Grade A/B D357-T6 .....                | 206         |
| 58            | Constant Amplitude Fatigue Crack Growth Rate of Weld-Repaired D357-T6 .....            | 207         |
| 59            | Typical Microstructure of D357-T6 With Nonoptimum Microstructure .....                 | 213         |
| 60            | Backscatter SEM Micrograph of Nonoptimum D357-T6 .....                                 | 214         |
| 61            | TEM Micrograph of Nonoptimum D357-T6 Showing a Small Precipitate .....                 | 214         |
| 62            | Selected Area Diffraction Pattern of the Precipitate in Figure 61 .....                | 215         |
| 63            | TEM Micrograph of Nonoptimum D357-T6 Showing a Needle-Shaped Phase Containing Ti ..... | 215         |
| 64            | Stress-Life Fatigue Data for D357-T6 With Nonoptimum Microstructure .....              | 218         |
| 65            | Fatigue Crack Growth Rate of D357-T6 With Nonoptimum Microstructure .....              | 219         |
| 66            | Typical Optical Microstructure of Nonoptimum B201-T7 ....                              | 222         |
| 67            | SEM Image of Nonoptimum B201-T7 Showing Typical Constituent Phases .....               | 224         |
| 68            | Main Strengthening Phase in Nonoptimum B201-T7 .....                                   | 224         |
| 69            | Typical Grain Boundary Precipitates in Nonoptimum B201-T7 .....                        | 225         |
| 70            | Blocky Precipitate Commonly Observed in Nonoptimum B201-T7 .....                       | 225         |
| 71            | Stress-Life Fatigue Data for B201-T7 With Nonoptimum Microstructure .....              | 228         |
| 72            | Fatigue Crack Growth Rate of B201-T7 With Nonoptimum Microstructure .....              | 229         |
| 73            | F-5 Inboard Wing Pylon .....   | 239         |
| 74            | Typical Microstructure in a Na-Modified D357-T6 Pylon ...                              | 243         |

LIST OF FIGURES (Continued)

| <u>Figure</u> |   | <u>Page</u> |
|---------------|---|-------------|
| 75            | Typical Microstructure in a Sr-Modified D357-T6 Pylon ...   | 243         |
| 76            | Typical Microstructure of a D357-T6 Cast Plate .....  | 243         |
| 77            | Stress-Life Fatigue Data for D357-T6 Pylons .....   | 248         |
| 78            | Fatigue Crack Initiating From a Pore in a Pylon<br>Fatigue Specimen .....                               | 250         |
| 79            | Two Large Inclusions Observed in a Pylon Fatigue<br>Specimen .....                                      | 250         |
| 80            | Constant Amplitude Fatigue Crack Growth Rate of D357-T6<br>Pylons .....                                 | 251         |
| 81            | Weibull Distribution for D357-T6 Pylons and Verification<br>Plates.....                                 | 254         |
| 82            | Modified F-18 Wing Root Spectrum .....  | 258         |
| 83            | Multihole Durability Specimen .....   | 258         |
| 84            | Damage Tolerance Specimen With a Precracked Hole .....  | 260         |
| 85            | Damage Tolerance Specimen With a Surface Flaw .....   | 260         |
| 86            | Location of Multihole Durability Specimens in the Cast<br>Plates .....                                  | 261         |
| 87            | Flow Chart of Unified Crack Growth Analysis<br>Requirements .....                                       | 263         |
| 88            | Strain-Life Data for D357-T6 and B201-T7 .....  | 267         |
| 89            | Cyclic Stress-Strain Curves for D357-T6 and B201-T7 .....   | 267         |
| 90            | Determination of $m_1$ Under Spectrum Loading for<br>D357-T6 and 7050-T7451 Plate .....                 | 271         |
| 91            | Correlation Between Test and Analysis for D357-T6<br>Under Spectrum Loading .....                       | 272         |
| 92            | Spectrum Crack Growth Correlation for Surface Flawed<br>Specimens Tested at 35 ksi Maximum Stress ..... | 273         |
| 93            | Spectrum Crack Growth Correlation for Surface Flawed<br>Specimens Tested at 40 ksi Maximum Stress ..... | 273         |

LIST OF FIGURES (Continued)

| <u>Figure</u> |   | <u>Page</u> |
|---------------|---|-------------|
| 94            | Spectrum Crack Growth Correlation for Surface Flawed Specimens Tested at 42 ksi Maximum Stress .....  | 274         |
| 95            | Spectrum Crack Growth Correlation for Precracked Hole Specimens Tested at 23 ksi Maximum Stress ..... | 274         |
| 96            | Spectrum Crack Growth Correlation for Precracked Hole Specimens Tested at 27 ksi Maximum Stress ..... | 275         |
| 97            | Correlation Between Analysis and Test Results for Multihole Specimens (Total Life) .....              | 277         |
| 98            | Hole Number Assignment for Multihole Durability Specimens .....                                       | 280         |
| 99            | Single Silicon Particle Initiating a Fatigue Crack .....  | 282         |
| 100           | Cluster of Silicon Particles Initiating a Fatigue Crack .   | 282         |
| 101           | Cavity Observed in Specimen Q6A2 .....  | 282         |
| 102           | Shrinkage Pore Observed in Specimen Q5C1 .....  | 283         |
| 103           | Microcrack in Specimen Q3D3 .....   | 283         |
| 104           | Combined Plate and Pylon Stress-Life Fatigue Data for D357-T6 .....                                   | 289         |
| 105           | EIFS Weibull Analysis of 7050-T7451 Plate .....   | 291         |
| 106           | Variation of Inferred Sudden Death EIFS of 7050-T7451 Plate Based on Fatigue Life .....               | 293         |
| 107           | Weibull Distribution of D357-T6 Pylon and Foundry A Verification Plate Data .....                     | 296         |
| 108           | Variation of Inferred Sudden Death EIFS of D357-T6 Based on Fatigue Life .....                        | 299         |
| 109           | Variation of D357-T6 Specification Fatigue Requirements vs. Specimen Diameter .....                   | 301         |
| 110           | Relationship Between Fatigue Life and Bulk Hydrogen Content of D357-T6 .....                          | 305         |
| 111           | Bulk Hydrogen Content of D357-T6 vs. Equivalent Initial Flaw Size .....                               | 307         |
| 112           | Weibull Distribution of 7050-T7451 EIFS Data .....  | 313         |

## LIST OF TABLES

| <u>Table</u> |  | <u>Page</u> |
|--------------|--|-------------|
| 1            | Defect Types and Plate Thickness of D357 and E201 Defect-Containing Plates .....           | 24          |
| 2            | Defect Plates Selected for FAI Evaluation .....  | 25          |
| 3            | FAI Pore Radius Data for Defect-Containing Plates .....                                    | 27          |
| 4            | FAI Percent Porosity Data for Defect-Containing Plates ..                                  | 28          |
| 5            | Correlations Between FAI Data for Plates and Slices .....                                  | 31          |
| 6            | Effect of Dynamic Range on FAI Measurements .....  | 34          |
| 7            | Correlation Between FAI Results and X-Ray Radiographic Grade for the Plate Slices .....    | 37          |
| 8            | Comparison of FAI and Microstructural Analysis Data .....                                  | 39          |
| 9            | Effect of Nonparallel Surfaces on Defect Detection Capabilities of the FAI Technique ..... | 44          |
| 10           | FAI Evaluation of Results for Plates Containing Weld Defects .....                         | 47          |
| 11           | Eddy Current Inspection Results .....  | 48          |
| 12           | Composition Specification for the D357-T6 Screening Plates .....                           | 53          |
| 13           | Composition Variations for the D357-T6 Screening Plates..                                  | 54          |
| 14           | D357-T6 Screening Plate Process Variables .....  | 56          |
| 15           | Screening Test Specifications .....  | 59          |
| 16           | Composition of the D357 Screening Plates .....   | 63          |
| 17           | Effect of Process Variables on the Dendrite Arm Spacing of D357-T6 .....                   | 65          |
| 18           | Effect of Process Variables on the Silicon Particle Aspect Ratio of D357-T6 .....          | 67          |

LIST OF TABLES (Continued)

| <u>Table</u> | <u>Page</u>   |
|--------------|---|
| 19           | Effect of Process Variables on the Silicon Particle Area of D357-T6 ..... 68      |
| 20           | Effect of Process Variables on the Silicon Particle Spacing of D357-T6 ..... 69   |
| 21           | Effect of Process Variables on the Percent Porosity of D357-T6 ..... 73           |
| 22           | Effect of Process Variables on the Ultimate Tensile Strength of D357-T6 ..... 75  |
| 23           | Effect of Process Variables on the Yield Strength of D357-T6 ..... 76             |
| 24           | Effect of Process Variables on the Elongation of D357-T6 ..... 77                 |
| 25           | Effect of Process Variables on the Notched Tensile Strength of D357-T6 ..... 80   |
| 26           | Effect of Process Variables on the NTS/YS Ratio of D357-T6 ..... 81               |
| 27           | Effect of Process Variables on the Fatigue Life of D357-T6 ..... 84               |
| 28           | Linear and Nonlinear Regression Analysis Results for D357-T6 ..... 86             |
| 29           | Composition Specification for the B201-T7 Screening Plates ..... 93               |
| 30           | Composition Variations for the B201-T7 Screening Plates ..... 93                  |
| 31           | Process Variables for the B201-T7 Screening Plates ..... 95                       |
| 32           | Composition of the B201 Screening Plates ..... 98                                 |
| 33           | Effect of Process Variables on the Grain Size of B201-T7 ..... 99                 |
| 34           | Effect of Process Variables on the Ultimate Tensile Strength of B201-T7 ..... 101 |
| 35           | Effect of Process Variables on the Yield Strength of B201-T7 ..... 102            |

LIST OF TABLES (Continued)

| <u>Table</u> |   | <u>Page</u> |
|--------------|---|-------------|
| 36           | Effect of Process Variables on the Elongation of B201-T7 .....                        | 103         |
| 37           | Effect of Process Variables on the Notched Tensile Strength of B201-T7 .....          | 106         |
| 38           | Effect of Process Variables on the NTS/YS Ratio of B201-T7 .....                      | 107         |
| 39           | Effect of Process Variables on the Fatigue Life of B201-T7 .....                      | 110         |
| 40           | Linear and Nonlinear Regression Analysis Results for B201-T7 .....                    | 111         |
| 41           | Composition Specification for the D357-T6 Verification Plates .....                   | 117         |
| 42           | Composition Specification for the B201-T7 Verification Plates .....                   | 123         |
| 43           | Verification Tests for D357-T6 and B201-T7 .....                                      | 126         |
| 44           | D357 Verification Material Melt Compositions .....                                    | 133         |
| 45           | DAS and Si Particle Morphology Data for 1.25-inch-thick D357-T6 Plates.....           | 136         |
| 46           | Tensile Properties of 1.25-inch-thick Water- and Glycol-Quenched D357-T6 Plates ..... | 140         |
| 47           | Fatigue Crack Initiation Sites for D357-T6 Fatigue Specimens .....                    | 145         |
| 48           | Average D357-T6 Fracture Toughness and Notched Tensile Strength Data .....            | 148         |
| 49           | D357-T6 Equivalent Initial Flaw Size Data .....                                       | 151         |
| 50           | Comparison of Predicted and Measured EIFS for D357-T6 .....                           | 153         |
| 51           | B201 Verification Material Melt Compositions .....                                    | 156         |
| 52           | Tensile Properties of 1.25-inch-thick B201-T7 Plates ....                             | 161         |
| 53           | B201-T7 Fracture Toughness and Notched Tensile Strength Data .....                    | 168         |

LIST OF TABLES (Continued)

| <u>Table</u> |  | <u>Page</u> |
|--------------|--|-------------|
| 54           | B201-T7 Equivalent Initial Flaw Size Data .....  | 171         |
| 55           | Comparison of Predicted and Measured EIFS for B201-T7 ...  | 174         |
| 56           | Number of Plates Produced for Each Defect/Grade<br>Combination .....   | 179         |
| 57           | Number of Tests Performed to Determine the Effect of<br>Defects on the Mechanical Properties of D357-T6 .....                                  | 183         |
| 58           | Number of Tests Performed to Determine the Effect of<br>Nonoptimum Microstructure on the Mechanical Properties<br>of D357-T6 and B201-T7 ..... | 184         |
| 59           | Composition of D357 With Intentionally-Added Defects ....  | 186         |
| 60           | DAS and Si Particle Morphology Data for the Phase I,<br>Task 3 Defect-Containing D357 Plates .....   | 188         |
| 61           | FAI Data for the Phase I, Task 3 Defect-Containing<br>D357-T6 Plates .....   | 191         |
| 62           | D357-T6 Tensile Properties Versus Defect Type and Grade .  | 193         |
| 63           | D357-T6 Tensile Test Results Out of Specification .....  | 194         |
| 64           | D357-T6 Tensile Property Data Within the AMS 4241<br>Specification .....   | 196         |
| 65           | Spectrum Fatigue Data for Defect-Containing D357-T6 .....  | 209         |
| 66           | Average Fracture Toughness of Defect-Containing D357-T6 .  | 210         |
| 67           | Composition of D357-T6 With Nonoptimum Microstructure ...  | 211         |
| 68           | DAS and Si Particle Morphology for D357-T6 With Nonoptimum<br>Microstructure .....   | 213         |
| 69           | Tensile Properties of D357-T6 With Nonoptimum<br>Microstructure .....  | 217         |
| 70           | Composition of B201-T7 With Nonoptimum Microstructure ...  | 221         |
| 71           | Tensile Properties of B201-T7 With Nonoptimum<br>Microstructure .....  | 227         |
| 72           | Ratio of Mechanical Properties of Defect-Containing<br>D357 and Average Values for Verification Material .....                                 | 232         |

LIST OF TABLES (Continued)

| <u>Table</u> |  | <u>Page</u> |
|--------------|--|-------------|
| 73           | D357-T6 Plate and Pylon Melt Compositions .....  | 241         |
| 74           | Average DAS and Si Particle Morphology Data for D357-T6<br>Plates and Pylons .....       | 244         |
| 75           | Average Tensile Properties of D357-T6 Plates and Pylons .                                | 245         |
| 76           | D357-T6 Pylon Fracture Toughness and Notched Tensile<br>Strength Data .....              | 252         |
| 77           | DADT Test Matrix .....   | 257         |
| 78           | Stress Intensity Correction Factor for Each DADT<br>Specimen Geometry .....              | 270         |
| 79           | Data for Cracks Observed at Fracture Surfaces of Multihole<br>Durability Specimens ..... | 279         |
| 80           | Maximum EIFS and Minimum Fatigue Life vs. Specimen Size<br>and Number of Tests .....     | 300         |
| 81           | Maximum Average EIFS and Minimum Fatigue Life vs.<br>Specimen Size .....                 | 300         |
| 82           | Silicon Particle Morphology and Porosity for All D357-T6<br>Verification Plates .....    | 310         |

SECTION 1  
INTRODUCTION

The use of castings for aircraft applications offers the potential for significant cost and weight savings compared with built-up structures. Recurring cost reductions greater than 30 percent are possible through reduced machining and assembly costs. Weight savings can be achieved, for example, by eliminating lap joints and fasteners. A reduction in fastener holes decreases the number of potential flaw initiation sites. Castings also allow greater shape flexibility compared with built-up structures.

Castings are not currently used in fatigue-critical aircraft structure because of the inability to accurately inspect thick sections, and a lack of durability and damage tolerance (DADT) data and design allowables that take into account the effects of inherent casting discontinuities and microstructural features on DADT properties. The absence of the required DADT data for castings precludes compliance with the current military DADT specifications, MIL-A-83444 and MIL-A-87221. As a result, it is not possible to take advantage of the inherent cost and weight savings of castings for fatigue-critical aircraft applications.

The goals of the "Durability and Damage Tolerance of Aluminum Castings" (DADTAC) program were to (1) investigate a nondestructive inspection (NDI) technique that has the potential for providing a quantitative assessment of the discontinuities present in aluminum castings, (2) identify the process variables and discontinuities that influence the DADT properties, (3) characterize the DADT properties of the aluminum casting alloys A357 and A201, and (4) recommend revisions to material, process, and DADT specifications.

The alloys evaluated in the DADTAC program were required to meet the tensile properties and composition of AMS specifications 4241 [1] (D357) and 4242 [2] (B201), respectively, though a requirement for a silicon modifier was added to AMS 4241. Therefore, A357 and A201 are referred to as D357 and B201, respectively, throughout this final report, per the AMS specifications.

The program results and conclusions are described in Sections 4 through 12. Data are summarized as averages where possible to simplify their presentation. The individual test results are included in Appendices A-I for those readers who wish to analyze the results in more detail. The recommended specification revisions for D357 and B201 are described in detail in Appendices J and K, respectively. Appendix L includes the hydrogen gas content of failed fatigue specimens. The hydrogen gas measurements were obtained by Wright Laboratory for specimens tested in Phase I, Task 3.

## SECTION 2

### OBJECTIVE

The overall objective of the DADTAC program was to generate durability and damage tolerance data for premium quality aluminum castings and advance foundry technology to expedite the use of these castings in primary aircraft structures.

SECTION 3  
PROGRAM APPROACH

The DADTAC program, which consists of three phases, is summarized in Figure 1. A brief description of the technical activities associated with each phase is provided below.

3.1 PHASE I - DADT OF ALUMINUM CASTINGS QUALITY ASSESSMENT

3.1.1 Task 1 - NDI Assessment

A state-of-the-art NDI method for determining the soundness of the cast plates and components tested during the program was evaluated in conjunction with the program NDI consultant, Dr. L. Adler of Ohio State University. The objective was to establish more accurate information of the size, location, and types of discontinuities in the test castings than is currently available using conventional radiographic methods.

3.1.2 Task 2 - Alloy Characterization

Concurrent with Task 1, the effects of process variables on the durability and damage tolerance (DADT) properties of D357-T6 and B201-T7 were assessed. Screening tests were conducted to identify the process variables that provided the optimum balance of tensile and DADT properties for each of the two alloys. Additional castings were then made using the process variables that provided the optimum properties, and their DADT properties were comprehensively characterized. This material became the baseline for the technical effort during the remainder of the program.

3.1.3 Task 3 - Effects of Defects on DADT Properties

The effects of discontinuities and metallurgical features (microstructure) on the DADT properties of D357-T6 were determined. Because emphasis during the program was on D357-T6, only the effect of microstructure on properties was determined for B201-T7.

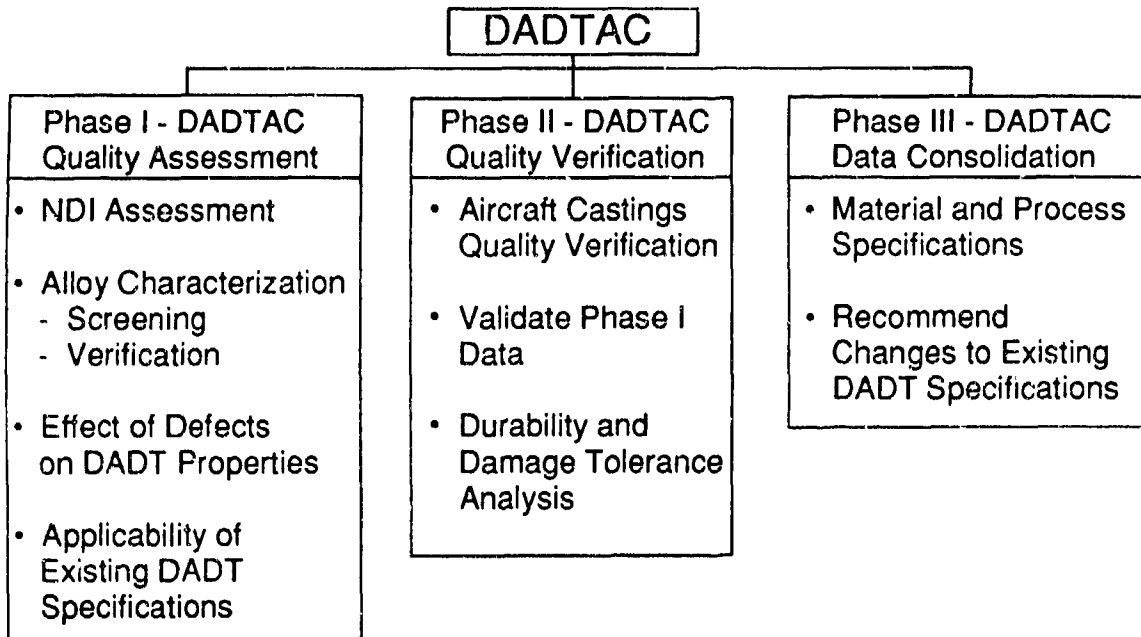


Figure 1. Program Outline

#### 3.1.4 Task 4 - Applicability of DADT Specifications to Aluminum Castings

The applicability of the MIL-A-83444 and MIL-A-87221 specifications to D357-T6 and B201-T7 aluminum castings was assessed, based on the data generated in Tasks 1-3.

#### 3.2 PHASE II - DADT OF ALUMINUM CASTINGS QUALITY VERIFICATION

During Phase II, the DADT properties obtained during Phase I, Task 2 were confirmed by testing specimens excised from D357 aircraft castings. After considering several existing castings, an inboard F-5 wing pylon was chosen. Four castings of the selected design were produced based on the processing and material specification guidelines from Phase I, and were then subjected to NDI and DADT property evaluations. The results were compared with those obtained during Phase I to ensure that the process requirements can be scaled-up from small cast plates to a large aircraft casting.

In addition, cast plates were produced from which specially-designed element test specimens were excised to assess the durability and damage tolerance characteristics of D357. Test results were compared with analytically-derived life predictions using Phase I test data.

#### 3.3 PHASE III - DADTAC PROGRAM DATA CONSOLIDATION

In Phase III, the results of Phases I and II were consolidated. Revisions to material and process specifications were recommended for premium quality aluminum castings for primary aircraft structure. A D357-T6 specification for durability and damage tolerance applications was submitted to the Society of Automotive Engineers for review and approval as an AMS specification. Modifications to existing damage tolerance specifications, such as MIL-A-83444 and MIL-A-87221, were also investigated. MIL-A-87221 replaced MIL-A-83444.

SECTION 4  
PHASE I, TASK 1 - NDI ASSESSMENT

4.1 INTRODUCTION

The objectives of this task were (1) to select and evaluate the most promising nondestructive inspection (NDI) method for detecting and quantifying casting defects, and (2) to evaluate an eddy current technique for detecting the presence of cracks similar to those sometimes found in aircraft substructure.

To implement castings in fatigue critical applications, defects in cast components must be detected and quantified to assure acceptable durability. Inspection of castings for internal defects has conventionally been accomplished by X-ray radiography. However, conventional radiography sensitivity is limited to detecting defects that are greater than about one percent of the part thickness. As part thickness increases, the minimum detectable flaw size increases and small flaws may not be detected. With these limitations, defects that may be detrimental to mechanical properties may remain undetected in thicker sections. Current Air Force-sponsored research in computer tomography and backscatter imaging tomography (BIT) has significantly advanced the ability to radiographically evaluate thick castings. Defect detection and sizing capabilities are greatly improved. BIT is especially important for the NDI of thick structures, in which resolution of near-surface defects are critical. However, these methods will be neither cost-effective nor applicable for a foundry environment.

NDI methods were considered with a view to selecting an alternate or complementary method to radiography that would allow both qualitative and quantitative assessment of defects in castings that are thicker than about 0.75 inch. An ultrasonic technique named Frequency Attenuation Inflection (FAI) was chosen because of the promising results shown during initial evaluations by Northrop before commencing the contract activities. The FAI technique was developed by Dr. L. Adler [3] at Ohio State University (OSU) and

tailored for this program through a cooperative effort between Dr. Adler and Northrop NDI personnel.

The DADTAC contract evaluations included testing D357 and B201 cast plates that contained a range of typical casting defects. A total of 34 D357 and B201 plates in two thicknesses were cast (1.25 inch and 3.0 inch). Each plate was inspected using both standard X-ray radiography with a one percent sensitivity and ultrasonic C-scan methods. Six of the 34 plates that contained representative amounts and types of casting defects were then selected, based on the radiographic and C-scan results, for a detailed NDI analysis. The detailed analysis consisted of inspecting the six plates using the FAI technique, followed by slicing the as-cast plates into thinner plates and reinspecting the slices using radiography, C-scans, and the FAI method. Microstructural analyses of the defects using image analysis were also conducted to determine the type and amount of defects present. The results of the microstructural and NDI analyses were then compared to assess the accuracy of the FAI technique compared with the conventional methods for detecting defects in castings. The effects of surface roughness and nonparallel surfaces on the defect detection sensitivity of the FAI technique were also determined. Cast surfaces are often not flat or parallel, and the effect of these conditions on defect detection capabilities must be evaluated. In addition, welding defects were intentionally produced in two otherwise defect-free plates and were evaluated by X-ray, C-scan, and FAI methods.

In the second portion of Task 1, an eddy current technique for detecting cracks emanating from fastener holes was evaluated. Cracks originating from fastener holes are the most common in-service flaws and can be difficult to detect without removing the fasteners. The eddy current method was developed for wrought material structures by Northrop under an Air Force contract (F33615-81-C-5100) entitled "Manufacturing Technology for Advanced Second Layer NDE System." The approach in the current program was to prepare simulated component substructures from D357 and B201 with fatigue-induced cracks of different lengths emanating from holes. Face sheets of 7075-T6 of three different thicknesses were fastened to the pre-cracked subcomponents using steel or titanium fasteners, and the eddy current technique was used to detect the presence of the cracks. The two types of fasteners were used

because steel (magnetic) and titanium (nonmagnetic) require the use of different probes and different crack detection evaluation methods. Both the location and the magnitude of the cracks were determined. The results were compared with the known location and dimensions of the fatigue-induced cracks.

## 4.2 NDI METHODS

### 4.2.1 FAI Technique

The equipment used for the FAI evaluations consisted of an ultrasonic transducer mounted on a traveling bridge assembly. Ultrasonic pulse signals were transmitted through water to the casting and were reflected back to the transducer and monitored by a computer. The time delays in signal transmission/reception and the changes in the signal characteristics were then analyzed using the computer to give the pore size and overall average percent porosity in the area under the transducer.

Figure 2 is a block diagram that illustrates the FAI system. The computer digitized and stored the ultrasonic waveforms and performed the defect parameter calculations. A transducer and pulser/receiver with usable bandwidths between 2 and 20 megahertz were used to generate ultrasonic pulses. Both the front and back surface echoes were digitized and stored using a Tektronix transient digitizer. Waveforms were digitized with a temporal resolution of less than 2 nanoseconds between points. Control over gating and gain was exercised by the computer. The distance from the transducer to the front surface of the plates and the specimen thickness were determined by the computer from the time delays required in gating. Waveforms were time-averaged to reduce noise. A correlation routine was used to remove the effects of electrical and mechanical jitter during waveform averaging. Using this routine, the shift in time between waveforms due to jitter was determined before the waveforms were averaged. Waveforms were then shifted by the appropriate time delay and averaged.

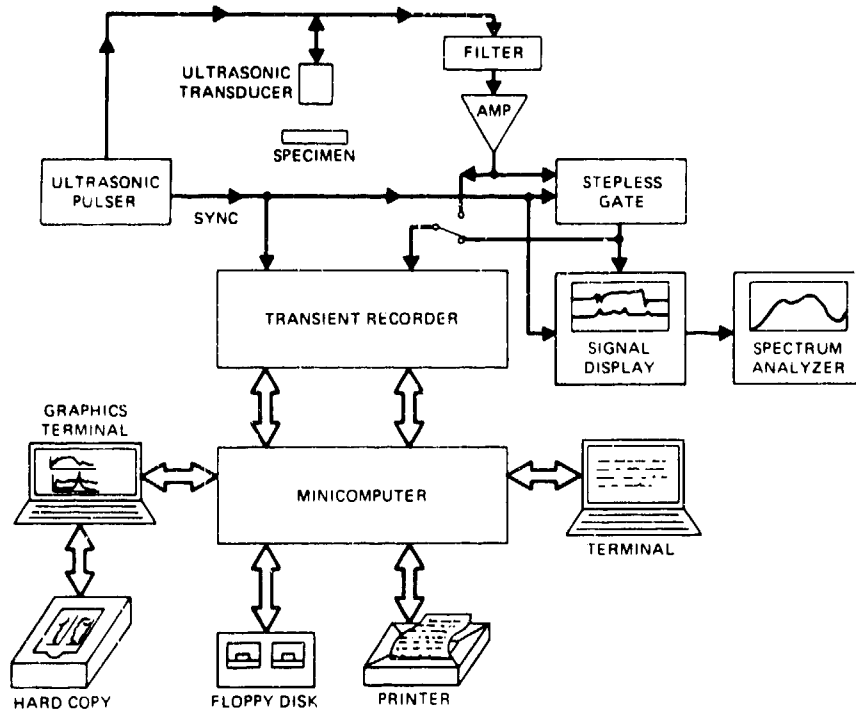


Figure 2. FAI Equipment

The frequency spectrums of the front and back surface waveforms were calculated using a fast Fourier transform algorithm. Figure 3 shows typical front and back surface echoes and their resulting frequency spectra. The spectrum of the back surface signal is deconvolved by the spectrum of the front surface signal. Attenuation coefficients, with appropriate corrections for all geometric losses, are obtained for the selected frequency range. The inflection or turning point in the attenuation versus frequency plot is used to determine the average pore size and volume fraction in the cylindrical volume sampled by the transducer. Inflection occurs at the intersection of the low frequency and high frequency scattering parameters and is dependent on pore size.

For isotropic materials, a fairly sharp peak in the derivative of the attenuation versus frequency curve is predicted by theory and observed in experiment [4]. This peak occurs for aluminum at an average pore radius  $R$  (in cm) of

$$R = 0.108/f_p \quad \text{Eq. 4-1}$$

where  $f_p$  is the frequency in megahertz at which the peak occurs, and 0.108 is a factor accounting for the effective size of a pore and Poisson's ratio.

The average percent porosity,  $C$ , was determined by measuring the attenuation at  $f_p$ , and calculated using the following equation [4]:

$$C = 122 \cdot \alpha_p \cdot R \quad \text{Eq. 4-2}$$

where  $\alpha_p$  is the attenuation in nepers/cm at  $f_p$ ,  $R$  is the average pore radius in cm, and 122 is a factor which is related to the average cross section of a pore and to Poisson's ratio. The mathematical assumptions made in developing the FAI technique were based on the assumption that the defects are spherical voids.

The equations for  $R$  and  $C$  (Eqs. 4-1 and 4-2, respectively) do not account for multiple scattering of the ultrasonic waves by the pores, which makes the equations accurate only for relatively low levels of porosity (<6 percent). This is a common assumption in calculations of this type [5]. The

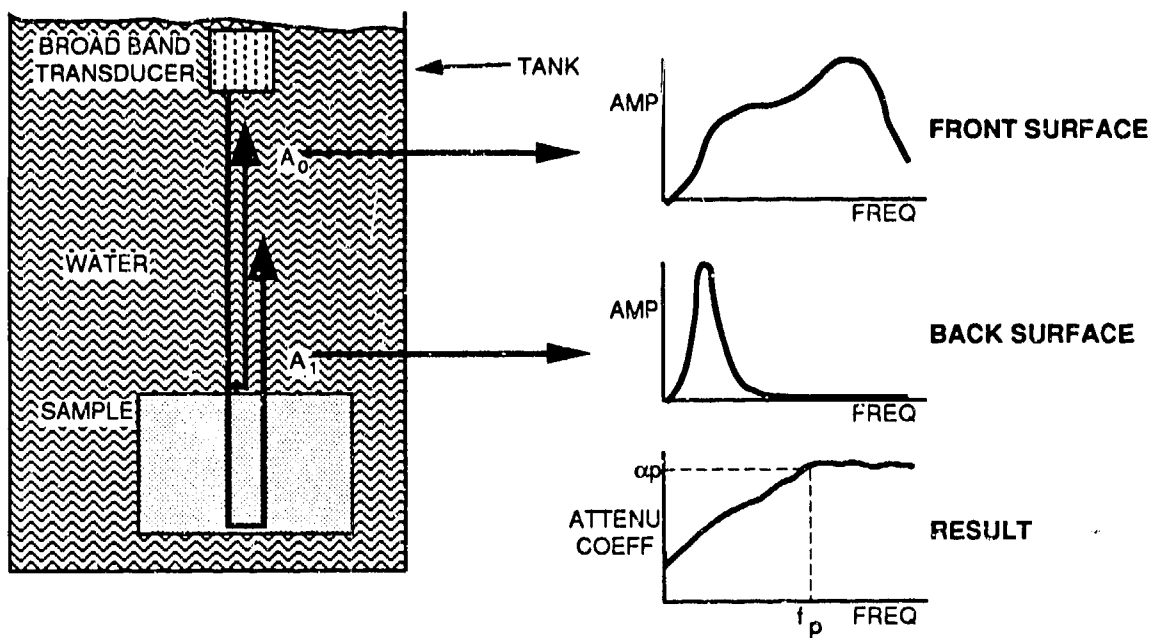


Figure 3. Schematic Illustration of the FAI Method

amount of porosity found in cast materials is usually less than 6 percent (see Table 21), indicating that this assumption is unlikely to introduce a large error in calculating the percent porosity and pore radius.

An attenuation correction factor due to scattering of the ultrasonic waves from grain boundaries was not included in the preceding calculations due to its relatively minor effect on ultrasonic scattering compared to that caused by porosity. However, during the course of the program a lower limit for percent porosity of 0.2 percent was determined experimentally for the FAI technique due to grain boundary effects. Below 0.2 percent porosity, the attenuation of ultrasound due to grain boundary scattering approaches that due to the porosity.

#### 4.2.2 Ultrasonic C-Scan

A block diagram of the ultrasonic C-scan system used for casting evaluations is shown in Figure 4. A DEC PDP 11/23 computer was used for data acquisition and storage, and for control of the transducer mounted on the bridge assembly. A Gould image processor was used to manipulate the data and then present them on a monitor.

A pulse/echo arrangement with a 0.5-inch-diameter, 10-MHz, center frequency ultrasonic transducer and 5.9-inch focal distance was used for the C-scans. Specimens were scanned using a point-to-point resolution of 0.04 inch. The peak magnitude of the back surface echo was digitized to 12 bits resolution. Attenuation levels of the resulting C-scans were displayed on a monitor in eight bit gray scale for analysis.

#### 4.2.3 Radiography

Radiographs achieving a one percent sensitivity were taken of the defect-containing plates both by the foundries and a Northrop-approved X-ray laboratory and were evaluated according to ASTM specification E155.

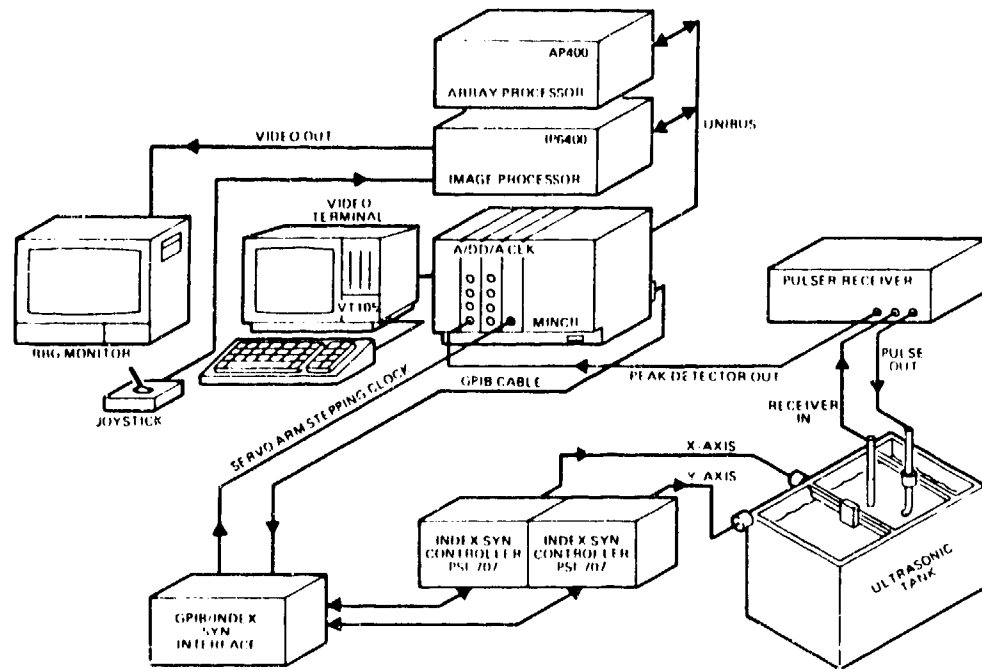


Figure 4. C-Scan Ultrasonic Imaging System

#### 4.2.4 Eddy Current Technique

The material combinations used for the in-service inspection investigation are shown in Figure 5, and a schematic of the eddy current probe test equipment is shown in Figure 6. Three thicknesses of 7075-T6 face sheets were used in conjunction with both D357-T6 and B201-T7 substructure. A total of five different crack lengths were produced in 0.25-inch- and 0.75-inch-thick D357 and B201 fatigue specimens by constant amplitude fatigue loading. Both steel and titanium fasteners were used in the evaluations to determine their effect on crack detection capability.

Two multisegment eddy current probes capable of detecting flaws in both the first and second layers of bolted aluminum structures were used in these investigations. A sketch depicting the differences between the two probes is shown in Figure 7, and a photograph of the simulated face sheet, substructure (fatigue specimen), and the probe used with the steel fastener is shown in Figure 8. The probes consist of a central drive coil and an outer ring segmented into 16 separate sensing coils. The drive coil generates an eddy current which encircles the fastener and penetrates the face sheet and underlying substructure. Cracks initiating at substructure fastener holes cause a perturbation of the eddy current and are detected as a change in the open circuit voltage of the sensing coils. The crack length and location can be determined simultaneously without moving the probe or removing the fastener.

A graphical representation of a low frequency eddy current probe response to substructure fastener hole cracks is shown in Figure 9. The two peaks on the graph indicate that the substructure contained two cracks located at positions number 6 and 14. The predicted crack lengths were 0.24 inch and 0.26 inch long, and are similar to the optical measurements of 0.227 inch and 0.257 inch. The derived crack lengths were determined from the output of the eddy current probe (in millivolts), using an empirically determined conversion factor, which depends upon the thickness of the face sheet and substructure, as well as the face sheet, substructure, and fastener materials. Determination of the conversion factor for different applications was conducted through an evaluation of a standard which incorporates a known crack length and the same material types and thickness as those to be inspected.

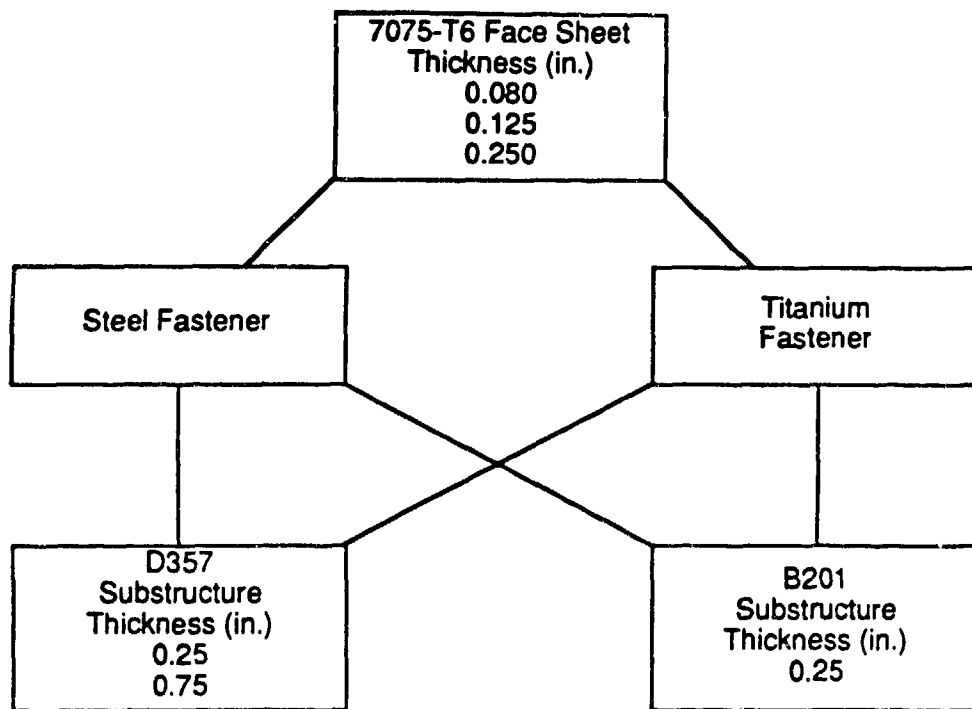


Figure 5. Combinations of Face Sheet, Fasteners, and Substructure Used for In-Service Eddy Current Inspection

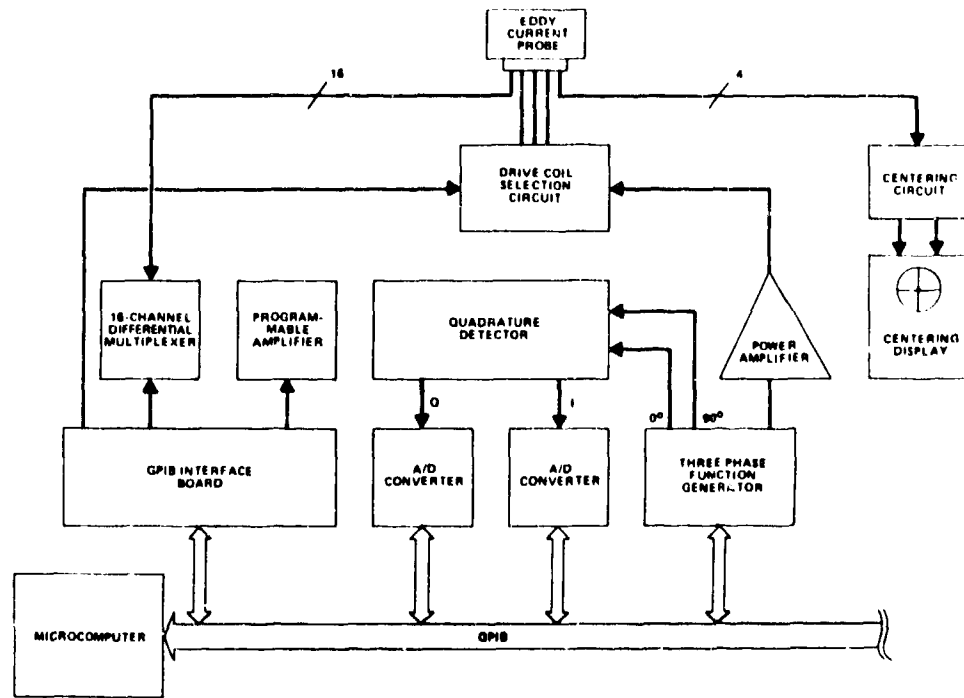
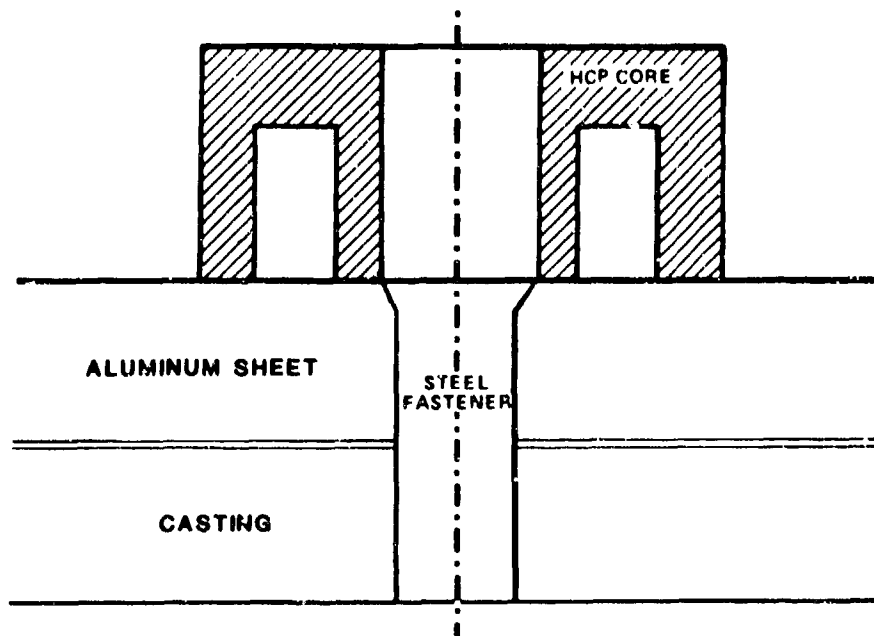
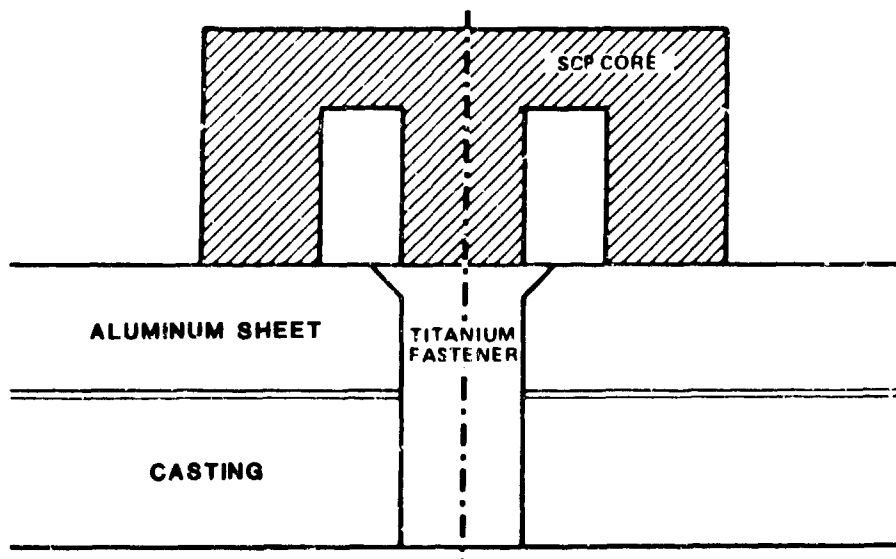


Figure 6. In-Service Eddy Current Inspection Test Equipment



a. Steel Fastener (Magnetic) - Hollow Center Probe (HCP)



b. Titanium Fastener (Nonmagnetic) - Solid Center Probe (SCP)

Figure 7. Schematic Illustration of the Probes Used With Steel and Titanium Fasteners

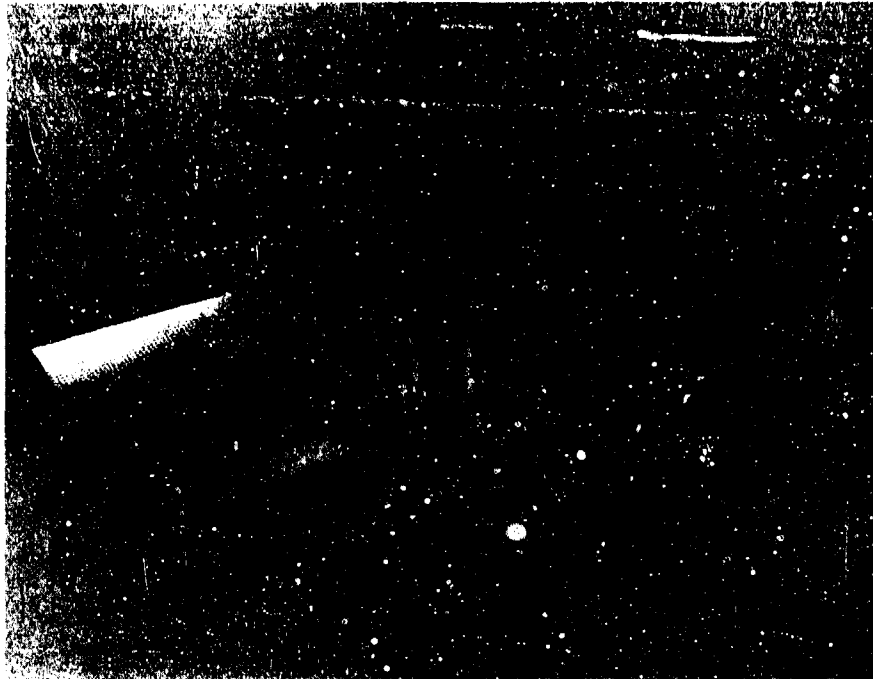


Figure 8. Multisegment Eddy Current Probe

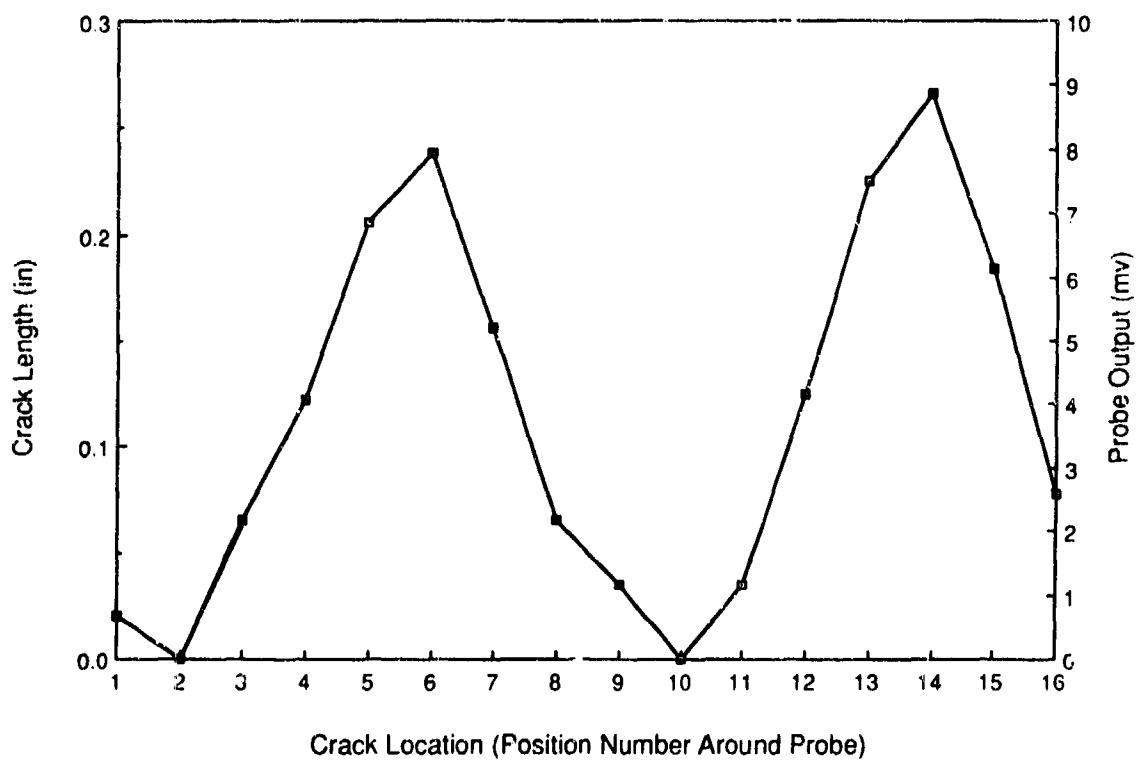


Figure 9. Typical Eddy Current Probe Output

#### 4.3 DEFECT-CONTAINING PLATES FOR FAI METHOD EVALUATIONS

Thirty-four cast plates that contained gas porosity, gas holes, shrinkage porosity, shrinkage sponge, cold shuts, and less-dense and more-dense foreign material were cast specifically for this task by Alcoa (D357) and Hitchcock Industries (B201). The alloys, defect types, and plate thicknesses are listed in Table 1. All plates were 6 x 6 x 1.25 inch or 3 inch thick. Two defect-free plates were also cast for evaluation of welding defects (lack of penetration, lack of fusion, porosity, and cracks).

The gas defects were produced by intentionally not degassing the melt, pouring at a higher than normal melt temperature, adding ammonium chloride wrapped in aluminum foil to the melt, or blowing argon gas into the mold during pouring. Shrinkage defects were produced by nonoptimum chill and riser placement. The cold shut was produced by interrupting the pour. Less-dense foreign material was introduced into the casting by overagitating the melt to capture aluminum oxide in the molten aluminum, by pouring the melt into the risers instead of the pouring cup, or by removing all filters and screens from the runner system. The more-dense foreign material defects were obtained by introducing tungsten and iron filings into the melt during pouring.

The weld defects, lack of penetration and fusion, porosity, and cracks, were produced by using non-standard GTA welding procedures. Dirty electrodes were used, the surfaces of the castings were not cleaned, plates were improperly heated, and the weld grooves were intentionally not filled.

#### 4.4 RESULTS AND DISCUSSION

The defect-containing plates used for the FAI evaluations were initially screened using X-ray radiography and C-scans. The objective of the screening process was to identify six plates that provided a selection of alloy/defect/plate thickness combinations for detailed FAI evaluation. The six plates that were selected are described in Table 2 and were selected because (1) the defects were well-dispersed, (2) they offered a comparison of the defect detection capability for different plate thicknesses, and (3) in some cases more than one grade (B, C) was available for a given defect.

TABLE 1. DEFECT TYPES AND PLATE THICKNESS OF D357 AND B201 DEFECT-CONTAINING PLATES

| DEFECT                      | GRADE <sup>(1)</sup> | PLATE THICKNESS <sup>(2)</sup> (IN) |     |      |
|-----------------------------|----------------------|-------------------------------------|-----|------|
|                             |                      | D357                                |     | B201 |
|                             |                      | 1.25                                | 3.0 | 1.25 |
| Gas Holes                   | B                    | X <sup>(3)</sup>                    | X   | X    |
| Gas Porosity                | B                    | X                                   | X   | X    |
|                             | C                    |                                     |     | X    |
| Shrinkage Cavity            | B                    | X                                   | X   | X    |
|                             | C                    | X                                   | X   | X    |
| Shrinkage Sponge            | B                    | X                                   | X   | X    |
|                             | C                    | X                                   | X   | X    |
| Less Dense Foreign Material | B                    | X                                   | X   | X    |
|                             | C                    | X                                   | X   | X    |
| More Dense Foreign Material | B                    | X                                   | X   | X    |
| Cold Shut                   | B                    | X                                   | X   | X    |
| Segregation                 | B                    | -                                   | -   | X    |
| Weld Repair Defect          | B                    | X                                   | -   | X    |

(1) According to MIL-A-2175

(2) All plates were 6 x 6 x the indicated thickness

(3) 'X' indicates the plates that were produced

TABLE 2. DEFECT PLATES SELECTED FOR FAI EVALUATION

| ALLOY | THICKNESS<br>(INCH) | DEFECT             | TARGET<br>GRADE |
|-------|---------------------|--------------------|-----------------|
| B201  | 1.25                | Shrinkage Sponge   | B               |
|       | 1.25                | Less Dense Foreign | C               |
| D357  | 3.0                 | Gas Porosity       | B               |
|       | 1.25                | Gas Porosity       | B               |
|       | 3.0                 | Less Dense Foreign | B               |
|       | 3.0                 | Shrinkage Sponge   | B               |

The six plates were initially evaluated by Dr. Adler at Ohio State University (OSU) and then by Northrop to determine if similar results could be obtained.

All six plates were initially evaluated with sandblasted surfaces, which represented an as-cast or finished casting surface. Both surfaces of each plate were then machined smooth and the evaluation was repeated to determine the effect of surface roughness on the FAI results. The plates were cut into slices, which were then evaluated. A comparison was made between the results for the thinner slices and those for the full-thickness plates. The slices had machined surfaces.

After completing the FAI evaluation on the slices, areas of several plates were selected for microstructural characterization to provide a comparison between the results obtained microstructurally and those predicted from the FAI analysis. In addition, FAI results for plates with nonparallel sides were obtained because many castings have complex shapes.

For the in-service eddy current inspection effort, fatigue cracks were initiated at fastener holes in D357 and B201 specimens. Face sheets of three thicknesses of 7075-T6 were installed over the precracked substructure using steel or titanium fasteners. The effectiveness of the eddy current method for qualitatively and quantitatively detecting the presence of the cracks was evaluated.

The results from the evaluations outlined above are discussed in the following subsections.

#### 4.4.1 FAI Evaluation of the Full-Thickness Plates

Prior to conducting the FAI tests, a grid consisting of nine 2 x 2-inch squares was marked on one surface of each plate and each square was identified with a number from 1 to 9. Both Ohio State University (Dr. Adler) and Northrop obtained measurements at the center of each of the nine squares using a 0.5-inch-diameter probe, so that the data from the two sources could be compared. The results are shown in Tables 3 and 4, which include the pore radius and average percent porosity data for sandblasted and machined (smooth) surfaces, respectively.

TABLE 3. FAI PORE RADIUS DATA FOR DEFECT-CONTAINING PLATES

| DEFECT/<br>ALLOY                           | GRADE/<br>THICKNESS   | AVERAGE PORE RADIUS* ( $\mu\text{m}$ ) |          |                          |          |
|--|-----------------------|--|----------|--------------------------|----------|
|  |                       | NORTHROP                               |          | OHIO STATE<br>UNIVERSITY |          |
|  |                       | SAND-<br>BLASTED                       | MACHINED | SAND-<br>BLASTED         | MACHINED |
| Shrinkage<br>Sponge/<br>D357               | Grade B/<br>3 inches  | 79                                     | 79       | 77                       | 65       |
| Shrinkage<br>Sponge/<br>B201               | Grade B/<br>1.25 inch | 151                                    | 139      | 140                      | 119      |
| Gas<br>Porosity/<br>D357                   | Grade B/<br>3 inches  | 163                                    | 151      | 147                      | 133      |
| Gas<br>Porosity/<br>D357                   | Grade B/<br>1.25 inch | 134                                    | 130      | 116                      | 101      |
| Less-Dense<br>Foreign<br>Material/<br>B201 | Grade C/<br>1.25 inch | 67                                     | 67       | 61                       | 52       |
| Less-Dense<br>Foreign<br>Material/<br>D357 | Grade B/<br>3 inches  | 60                                     | 70       | **                       | **       |

\* Average of nine areas per plate

\*\* None detected

TABLE 4. FAI PERCENT POROSITY DATA FOR DEFECT-CONTAINING PLATES

| DEFECT/<br>ALLOY                           | GRADE/<br>THICKNESS   | AVERAGE POROSITY* (%) |          |                          |          |
|--|-----------------------|-----------------------|----------|--------------------------|----------|
|  |                       | NORTHROP              |          | OHIO STATE<br>UNIVERSITY |          |
|  |                       | SAND-<br>BLASTED      | MACHINED | SAND-<br>BLASTED         | MACHINED |
| Shrinkage<br>Sponge/<br>D357               | Grade B/<br>3 inches  | 0.3                   | 0.3      | 0.3                      | 0.3      |
| Shrinkage<br>Sponge/<br>B201               | Grade B/<br>1.25 inch | 1.4                   | 1.5      | 1.6                      | 1.3      |
| Gas<br>Porosity/<br>D357                   | Grade B/<br>3 inches  | 0.7                   | 0.6      | 0.7                      | 0.6      |
| Gas<br>Porosity/<br>D357                   | Grade B/<br>1.25 inch | 1.3                   | 1.3      | 1.1                      | 1.1      |
| Less-Dense<br>Foreign<br>Material/<br>B201 | Grade C/<br>1.25 inch | 0.4                   | 0.2      | 0.4                      | 0.4      |
| Less-Dense<br>Foreign<br>Material/<br>D357 | Grade B/<br>3 inches  | 0.2                   | 0.1      | **                       | **       |

\* Average of nine areas per plate

\*\* None detected

Because the plates were relatively thick, an accurate radiographic assessment of defect content and grade could not be made, particularly for the 3-inch-thick plates. The grades shown in Tables 3 and 4 were those that were targeted for each plate.

The results of the joint evaluations by Northrop and Ohio State University (OSU) show that the pore radius and percent porosity data were within experimental scatter for both sandblasted and machined surfaces. Therefore, it was concluded that the FAI technology developed at OSU by Dr. Adler had been duplicated in Northrop's NDI Research Laboratory.

The differences in the average pore radius and percent porosity results for the sandblasted and machined surfaces were small. The overall trend indicated a slightly lower value for the machined surfaces than for those that were sandblasted, which is in good agreement with analytical predictions derived at OSU [4].

The average RMS roughness values for the sandblasted and machined plate surfaces were 210 and 62 microinches, respectively. The increased roughness of the sandblasted surfaces provided a higher value for pore radius and percent porosity because of increased ultrasonic wave scattering compared with the machined surface. However, a compensation factor could be developed to minimize the discrepancy. This can be accomplished by assuming a Gaussian distribution of the RMS surface roughness, which can be determined by mechanical or ultrasonic means. By fitting the spectral attenuation of the front surface echo to an analytical equation, the attenuation of the back surface echo can be calculated. A complete derivation and explanation of the effects of surface roughness on ultrasonic attenuation can be found in Reference 4.

The FAI evaluations of the plates that contained less-dense foreign material did not indicate increased ultrasonic scattering due to the presence of foreign material. The data represent low background levels of other discontinuities, such as porosity. There was no difference between these measurements and those obtained for squares in the same plate that did not contain foreign material. This result was not unexpected since the FAI method

was derived from a model which assumed the defects to be unfilled spherical pores. All defect size predictions are based on this assumption. Unfortunately, the interaction of ultrasound with less-dense foreign material is significantly different from its interaction with a void or gas-filled pore. Thus, a different defect model is required to size foreign material. Foreign material can be detected using ultrasound but an extended feasibility study (such as that in Reference 3) is necessary to establish the detectability of different foreign materials depending on size and concentration.

#### 4.4.2 Correlation Between FAI Results for Plates and Slices

After evaluating the six 1.25 inch and the 3.0 inch thick plates, they were cut into slices, each of which was about 0.6 inch thick. Two slices were obtained from the 1.25 inch thick plates and four or five were obtained from the 3.0 inch thick plates. All slices were 6 x 6 inches in area. The surfaces of the slices were machined parallel and were marked with the same 2 x 2-inch-square grid pattern that was used for the plates so that the NDI evaluations of the slices coincided exactly with those for the whole plates. Therefore, it was possible to provide a defect map of the thick plates from the data for the slices, which allowed a determination of the effect of thickness on the FAI results to be made. Some material was lost due to saw cuts and machining, which represented about 15 percent of the original plate thickness.

Each slice was individually X-rayed by an independent laboratory that serves the casting community to determine if the soundness and the defect content were as expected and in agreement with the data obtained for the thicker plates. X-ray radiography is subject to defect detection limitations for 1.25-inch-thick material, even using a one percent sensitivity, and would detect only the very largest defects in 3-inch-thick material.

The FAI data (Northrop) for the plates and slices, summarized in Table 5, are the average percent porosity and pore radius values for the nine squares in each plate and corresponding slices. The results for the three types of defects shown in Table 5 are discussed separately below.

TABLE 5. CORRELATION BETWEEN FAI DATA FOR PLATES AND SLICES

| DEFECT<br>GRADE/ALLOY       | PLATE<br>THICKNESS<br>(INCH) | PERCENT POROSITY |           | PORE RADIUS ( $\mu\text{m}$ ) |           |
|-----------------------------|------------------------------|------------------|-----------|-------------------------------|-----------|
|                             |                              | PLATE(1)         | SLICES(2) | PLATE(1)                      | SLICES(2) |
| <u>Gas Porosity</u>         |                              |                  |           |                               |           |
| Grade B/D357                | 3                            | 0.6              | 1.4       | 151                           | 93        |
| Grade B/D357                | 1.25                         | 1.3              | 1.6       | 130                           | 105       |
| <u>Shrinkage Sponge</u>     |                              |                  |           |                               |           |
| Grade B/D357 <sup>(3)</sup> | 3                            | 0.3              | 0.3       | 79                            | 73        |
| Grade B/B201                | 1.25                         | 1.5              | 2.3       | 139                           | 94        |
| <u>Foreign Material</u>     |                              |                  |           |                               |           |
| Grade B/D357                | 3                            | 0.1              | 0.1       | 70                            | 10        |
| Grade C/B201                | 1.25                         | 0.2              | 0.2       | 67                            | 38        |

(1) Machined surfaces - Northrop data

(2) All the slices were approximately 0.6 inch thick

(3) Plate was supposed to contain shrinkage sponge, but actually contained gas porosity

Gas Porosity Plates. X-ray radiography of the slices cut from each of the two gas porosity plates (3 inches and 1.25 inches thick) showed that the overall plate soundness grades were similar to those of the slices. Fifty-four individual 2 x 2-inch squares were graded. Of these, 36 squares were Grade B gas porosity; the remaining 18 squares were Grade C gas porosity. Twelve of the Grade C squares were in the 3-inch-thick plate.

There was a significant difference between the FAI results for the 3-inch-thick plate and corresponding slices. The average percent porosity and pore radius for the plate and slices was 0.6 percent and 1.4 percent, and 150  $\mu\text{m}$  and 93  $\mu\text{m}$ , respectively. For the 1.25-inch-thick plate, the differential between the plate and slice data was much less, i.e. 1.3 percent versus 1.6 percent, respectively, for the percent porosity and 129  $\mu\text{m}$  versus 105  $\mu\text{m}$  for pore radius, respectively. These differences probably result from the nonuniform distribution of defects and/or the dynamic range of the system, as discussed below.

Porosity assessment by FAI is based on assuming an even porosity distribution, i.e., the pore radius and the percent porosity should be the same at different depths. Since this is often not the case, the overall parameters represent an average, which is calculated from the overall ultrasonic attenuation. Therefore, the mutual effect of the percent porosity and pore radius on each other should be taken into consideration. For example, for a given pore radius, a higher percent porosity should be weighted more in the overall average pore radius than a lower percent porosity because the contribution to the total attenuation is higher. Similarly, for a given percent porosity, the contribution of smaller pores should be weighted more in the overall average percent porosity. For the data shown in Table 5 this mutual interaction was neglected and both volume fractions and pore radii were averaged independently of the other parameter. The averages of the thin slices were compared to the overall values for the original thick plates to determine the effect of thickness on the FAI results.

The dynamic range of the system influences the ability to accurately determine the percent porosity and pore radius. Whenever the attenuation exceeds the dynamic range of the system, the resulting measured attenuation

value is saturated, and the actual attenuation is underestimated. This occurs mainly in thick samples, and can be recognized from the detected signal. Attenuation saturation plays an important role in the FAI method by setting the limit for accurate measurement and indicating the need to increase the dynamic range of the system by spatial averaging, increasing the resolution of the system, or refinement of data reduction methods.

The dynamic range of the equipment used in the current work was 60 dB. The data for all the plates and slices were reanalyzed, taking the dynamic range into consideration (Table 6). For the total data base (54 squares) only 57 percent and 52 percent of the pore radius and the percent porosity values, respectively, of the plates were essentially the same as those for the slices. For those areas for which the attenuation was below the dynamic range of the equipment (<60 dB), the agreement between plate and slice data improved significantly, i.e., to 91 percent and 85 percent for the pore radius and the percent porosity, respectively. By increasing the dynamic range of the system, the discrepancies between the data for the thick plates and the slices can be significantly reduced. A dynamic range increase to 120 dB, which is reasonably achievable using a different instrumentation approach, will allow accurate measurements for a 3-inch-thick casting with porosity concentrations above about one percent.

Shrinkage Sponge Plates. The shrinkage sponge defect intended to be included in the 3-inch-thick D357 plate was not substantiated by an evaluation of the slices, which indicated that the plate contained mainly gas porosity. Radiography of the 3-inch-thick plate was inconclusive regarding identification of defect type and level. Five slices were obtained from this plate, providing 45 squares for FAI evaluation. The top 4 slices were graded by X-ray radiography as Grade B gas porosity. Some Grade B, C, and D foreign material was found in the bottom slice.

The 1.25-inch-thick B201 plate showed a much stronger correlation between X-ray data for the plate and the two slices. The presence of shrinkage sponge was confirmed in both slices; one slice was entirely Grade B and the other was entirely Grade D. These radiographic assessments demonstrate that certain size defects in very thick plates (3 inches) may not be detected using conventional X-ray radiography.

TABLE 6. EFFECT OF DYNAMIC RANGE ON FAI MEASUREMENTS

| POROSITY | DIFFERENTIAL<br>BETWEEN PLATES <sup>(1)</sup><br>AND SLICES <sup>(2)</sup> | AGREEMENT BETWEEN<br>PLATE AND SLICE RESULTS(%) |  |
|----------|--|---|--|
|          |  | TOTAL<br>DATA<br>BASE <sup>(1)</sup>            | DATA WITHIN<br>60 dB DYNAMIC<br>RANGE <sup>(3)</sup> |
| Radius   | <10 $\mu\text{m}$  | 57  | 91   |
|          | 10-20 $\mu\text{m}$  | 13  | 9  |
|          | >20 $\mu\text{m}$  | 30  | 0  |
| Percent  | <0.1%  | 52  | 85   |
|          | 0.1-0.2%   | 9   | 15   |
|          | >0.2%  | 39  | 0  |

- (1) Nine squares from each of the six plates (54 squares total)  
(2) Average for the squares from the slices that comprised each of the 54 squares in the plate  
(3) Only those squares for which saturation was not indicated (31 squares)

The average percent porosity determined by FAI for the 3-inch-thick plate that was supposed to contain shrinkage sponge and the individual slices was the same (0.3 percent, Table 5). The average pore radius values were also very similar, 79  $\mu\text{m}$  and 73  $\mu\text{m}$  for the plate and slices, respectively. These data represent gas porosity and not shrinkage sponge, which was not present in the plate or slices. The results for the four slices that contained the Grade B gas porosity were significantly different from those described in the previous section, indicating a wide range of possible porosity contents for radiographic Grade B. These slices were a very good Grade B (low porosity) as opposed to the previously described Grade B gas porosity specimens, which were almost Grade C.

For the 1.25-inch-thick B201 plate that was verified as containing shrinkage sponge, the percent porosity was 1.3 percent and 2.3 percent in the plate and slices, respectively. The corresponding average pore radii were 138  $\mu\text{m}$  and 94  $\mu\text{m}$ . The differences between the plate and slice results are consistent with those for the gas porosity data described in the previous section, and are probably also due to the defect size distribution and the limited dynamic range of the FAI system.

Foreign Material Plates. The 3-inch-thick D357 plate was Grade B according to X-ray radiography. Two of the nine squares contained less-dense foreign material (LDFM); the remaining squares contained some Grade B gas porosity. The four slices cut from the plate showed that most of the squares were Grade A/B (no observed defects). All the LDFM was in the slice cut from the bottom of the plate. Six squares were rated as Grade C for LDFM; the remaining three were Grade B gas porosity.

The 1.25-inch-thick B201 plate was rated as Grade C because of the level of LDFM in two of the nine squares. The remaining areas were Grade B gas porosity. However, of the 18 squares in the two slices cut from this plate, 17 were rated as Grade A, and one was found to contain Grade C LDFM.

The square that contained LDFM showed average pore radius and percent porosity values that were similar to the slices that were defect-free, indicating that FAI was unable to determine the size of the LDFM. This is

discussed in more detail in the next section where the overall correlation of FAI and X-ray radiography is described.

#### 4.4.3 Correlation Between FAI and X-Ray Assessments

All of the individual squares from the slices cut from the six defect-containing plates were individually inspected using X-ray radiography and the FAI method. All the results are shown in Table 7. They are listed according to the various defect types and the corresponding FAI average values and ranges for percent porosity. As determined by radiography of the slices, forty-four defect-free (Grade A/B) squares were found among the total of 171 that were characterized.

The Grade A/B material had average percent porosity and pore radius values of 0.2 percent and 16  $\mu\text{m}$ , respectively. The material that contained gas porosity and shrinkage sponge had percent porosity and average pore radius values that were significantly higher than that rated as Grade A/B. Statistical analysis showed that the uncertainties in the FAI values due to experimental error are about 20  $\mu\text{m}$  and 0.2 percent for pore radius and percent porosity, respectively. Considering this experimental error margin, the specimens graded as defect-free by radiography were also found to be defect-free by FAI.

For gas porosity, the average percent porosity and pore radius values were qualitatively consistent with the X-ray radiography grades, with Grade C having higher values than Grade B. Also, within each radiographic grade, the different severities of porosity observed in the X-ray radiography correlates well with the FAI-predicted levels. The apparent severity of porosity observed by radiography was a function of both the FAI-predicted concentration and average pore radius, as would be expected. Similar trends were observed in the data for the Grade B and D shrinkage sponge (SS) material. The average measured percent porosity for Grade D SS material was slightly higher than Grade B SS material, 2.6 percent versus 2.1 percent.

The previously mentioned dynamic range limitation caused some underestimation in Grade B material, and even more in Grade C material, thereby resulting in additional overlap of FAI data for these categories.

TABLE 7. CORRELATION BETWEEN FAI RESULTS AND X-RAY  
RADIOGRAPHIC GRADE FOR THE PLATE SLICES

| GRADE                              | FAI DATA         |         |                               |         | NO. OF<br>SQUARES<br>EXAMINED |
|------------------------------------|------------------|---------|-------------------------------|---------|-------------------------------|
|                                    | PERCENT POROSITY |         | PORE RADIUS ( $\mu\text{m}$ ) |         |                               |
|                                    | AVERAGE          | RANGE   | AVERAGE                       | RANGE   |                               |
| A/B                                | 0.2              | 0-0.5   | 16                            | 0-60    | 44                            |
| <u>Gas Porosity</u>                |                  |         |                               |         |                               |
| B                                  | 0.6              | 0-2.0   | 50                            | 0-120   | 69                            |
| C                                  | 1.7              | 1.5-1.9 | 117                           | 90-140  | 24                            |
| <u>Shrinkage Sponge</u>            |                  |         |                               |         |                               |
| B                                  | 2.1              | 1.8-2.4 | 93                            | 80-110  | 9                             |
| D                                  | 2.6              | 1.4-2.9 | 97                            | 80-110  | 9                             |
| <u>Less-Dense Foreign Material</u> |                  |         |                               |         |                               |
| B                                  | 0.2              | 0-0.4   | 78                            | 0-110   | 5                             |
| C                                  | 0.2              | 0-0.5   | 54                            | 0-110   | 9                             |
| D                                  | 0.2              | 0.1-0.3 | 105                           | 100-110 | 2                             |

No correlations between radiographic grade and FAI data for the LDFM defects were obtained. The percent porosity values of 0.2 percent were equal to those obtained for the defect-free Grade A/B material. The average pore radius data also did not seem to indicate the presence of LDFM; values were similar to those obtained for gas and shrinkage porosity.

In summary, there is a qualitative correlation between FAI and X-ray radiography results for gas porosity and shrinkage sponge. Further development of the FAI method is required before this approach can be applied to foreign material.

#### 4.4.4 Correlation Between FAI and Microstructural Measurements

After completing the FAI investigation of the plate slices, portions of several plates were selected for microstructural examination. The objective was to correlate the FAI-predicted data with actual microstructural measurements.

The ultrasonic probe was circular in cross-section and characterized a cylinder of about 0.5 inch diameter. The microstructural specimens were taken from the center of this circular area on the plane that was parallel with the axis of the cylinder. Image analysis was used to determine the average size of a given defect.

The selected defects and grade levels are shown in Table 8. Typical micrographs of three types of defect (gas porosity, shrinkage sponge, and foreign material) are shown in Figures 10, 11, and 12. The average percent porosity measured using the FAI and microstructural methods for Grade B gas porosity material was 0.7 percent and 0.5 percent, respectively. For Grade C gas porosity material, the equivalent results were 1.7 percent and 1.3 percent. The agreement between FAI and microstructural data for Grades B and C was excellent. In each case, the FAI method predicted a slightly higher value than that determined from the microstructure. The overestimation of percent porosity by the FAI method is probably due to the difference in measurement methods between FAI and image analysis. The FAI values for percent porosity and pore radius are determined on a volumetric basis while

TABLE 8. COMPARISON OF FAI AND MICROSTRUCTURAL ANALYSIS DATA

| DEFECT<br>TYPE <sup>(1)</sup> /<br>GRADE <sup>(2)</sup> | PERCENT POROSITY   |                               | PORE RADIUS ( $\mu\text{m}$ ) |                               |
|---|--------------------|-------------------------------|-------------------------------|-------------------------------|
|   | FAI <sup>(3)</sup> | MICROSTRUCTURE <sup>(4)</sup> | FAI <sup>(3)</sup>            | MICROSTRUCTURE <sup>(4)</sup> |
| GP/B  | 1.6                | 1.4                           | 110                           | 98                            |
|   | 0.1                | 0.05                          | 100                           | 12                            |
|   | <u>0.4</u>         | <u>0.1</u>                    | <u>100</u>                    | <u>11</u>                     |
| AVG   | 0.7                | 0.5                           | 103                           | 40                            |
| GP/C  | 1.6                | 1.0                           | 110                           | 89                            |
|   | 1.8                | 1.6                           | 120                           | 97                            |
|   | <u>1.6</u>         | <u>1.4</u>                    | <u>130</u>                    | <u>86</u>                     |
| AVG   | 1.7                | 1.3                           | 120                           | 91                            |
| SS/B  | 1.9                | 1.3                           | 80                            | 15                            |
| SS/D  | 2.3                | 1.2                           | 80                            | 19                            |
| LDFM/D  | 1.0                | (5)                           | 180                           | (5)                           |

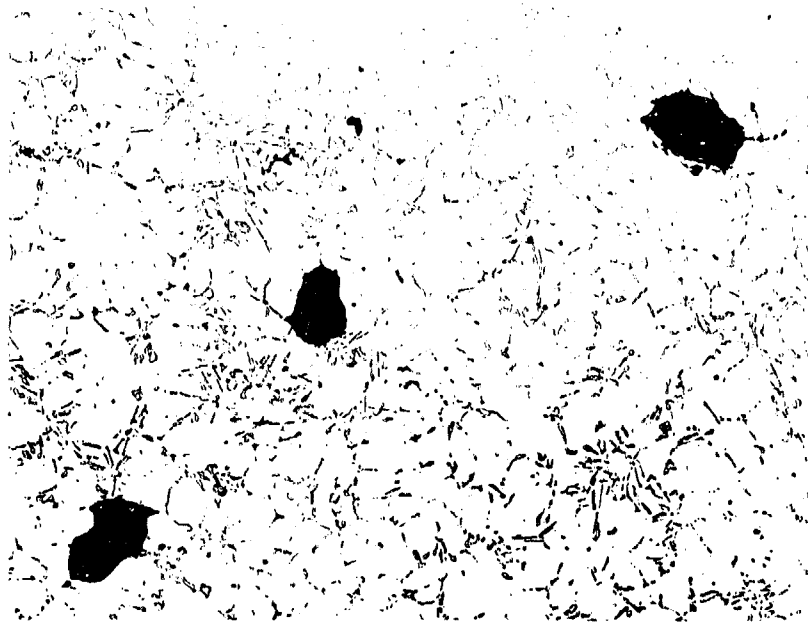
(1) GP - gas porosity; SS - shrinkage sponge; LDFM - less-dense foreign material

(2) According to MIL-A-2157

(3) Volumetric data

(4) Surface cross-section data

(5) Complex shape--specific numbers could not be assigned



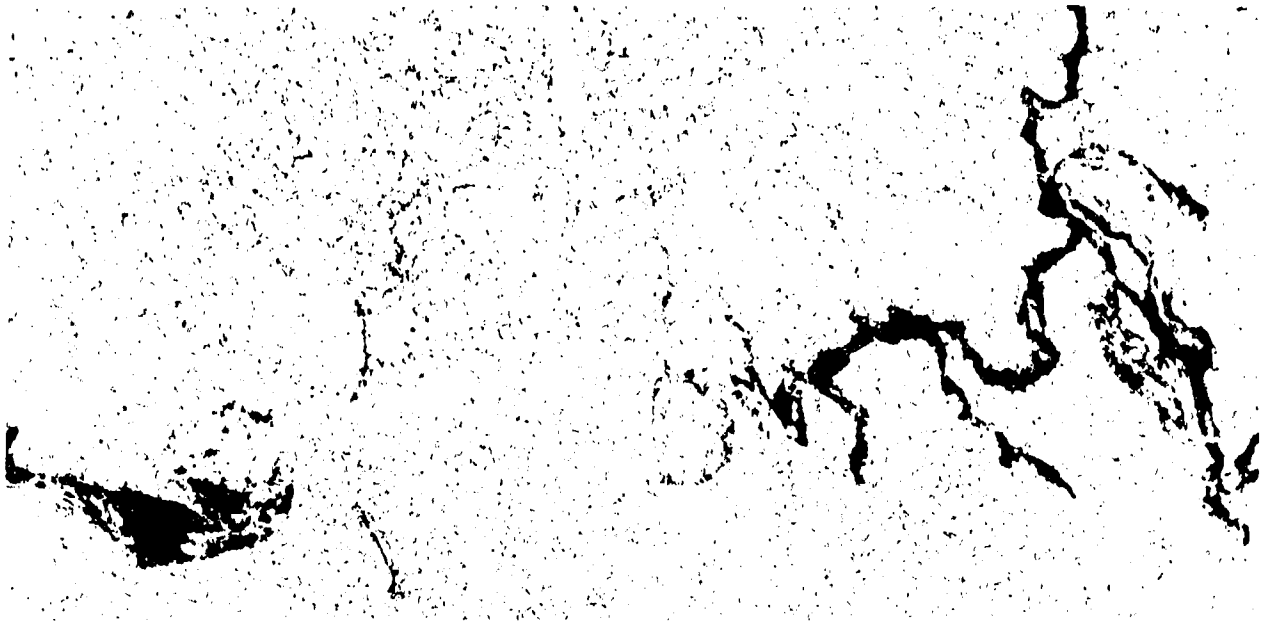
50X

Figure 10. Typical Gas Porosity in Grade C D357



50X

Figure 11. Typical Shrinkage Sponge in Grade D B201



50X

Figure 12. Typical Less-Dense Foreign Material in Grade C D357

the same values obtained from microstructural analysis were determined on a cross-sectional basis. The microstructural data, therefore, do not allow a full defect evaluation because the entire defect is not sampled. In addition, the FAI values are not completely accurate due to the nonspherical shapes of the pores. The theory upon which FAI is based assumes that the pores are spherical, which is not the case in practice (Figure 10); most of the pores tend to be elliptical.

Similar to the percent porosity, the FAI average pore radius values for gas porosity were higher than those obtained by microstructural analysis. The average FAI and microstructural pore radii for Grade B porosity were 103  $\mu\text{m}$  and 40  $\mu\text{m}$ , respectively. For Grade C, the equivalent results were 120  $\mu\text{m}$  and 91  $\mu\text{m}$ . Similar to the percent porosity assessment, the measured average pore radii for Grade C material were higher than that of Grade B material. The average pore radius measurements from the FAI method were observed to be approximately equal to the longer axis of the elliptically shaped pores, which supports the conclusion that the discrepancy is related to the nonspherical nature of the gas pores.

The correlation between data from the FAI and the microstructural methods for the shrinkage sponge was not as good as that for gas porosity. Two grade levels (B and D) were evaluated. The percent porosity obtained using the FAI and microstructural methods was 1.9 percent and 1.3 percent, respectively, for Grade B, and 2.3 percent and 1.2 percent for Grade D. The equivalent data for the average pore radius were 80  $\mu\text{m}$  and 15  $\mu\text{m}$  (Grade B) and 80  $\mu\text{m}$  and 19  $\mu\text{m}$  (Grade D). The FAI percent porosity data correlated better with the X-ray grades than did the microstructural results. It is difficult to attempt a correlation of this type, particularly for pore radius measurements, because of (1) the difficulty of accurately assigning a dimension to a defect that has a relatively complex shape (Figure 11), and (2) because the FAI model assumes that the defects are spherical.

The situation for foreign material was complicated. A typical LDFM inclusion has a very complex shape (Figure 12) and cannot be readily assigned specific dimensions. The deviation from a spheroidal shape is even greater than that for gas porosity and shrinkage sponge. For LDFM shown in Figure 12,

the percent porosity and pore radius measurements obtained using the FAI method were 1.0 percent and 180  $\mu\text{m}$ , respectively. The percent porosity value falls in the range typical of those for gas porosity and shrinkage sponge (Table 8). The average pore radius (180  $\mu\text{m}$ ) was larger than those typical of gas porosity and shrinkage sponge. However, the LDFM (Figure 12) was much bigger than the other two defects shown in Figures 10 and 11. The data indicate that the FAI method, as currently designed, cannot be used to identify foreign materials in castings.

#### 4.4.5 Effect of Nonparallel Surfaces on FAI Results

Because the surfaces of castings are often not parallel, the effect of nonparallel surfaces on the FAI results was determined. The measurements were performed on one of the slices discussed in Section 4.4.2. The slice was D357 and was determined by X-ray radiography and FAI measurements to have a very uniform distribution of Grade B gas porosity. Surfaces of the nine squares were machined so that they were at angles in the range of 2 degrees to 10 degrees compared with the opposing surface. The FAI results as a function of angle are shown in Table 9. For a given location, the FAI measurements were taken both before (parallel sides) and after machining (nonparallel sides). The average pore radius for parallel and nonparallel sides was, within experimental scatter, the same for a given angle. However, the measured average percent porosity showed an increase from about 1.4 percent for parallel sides to 2.1 percent for the 10 degree angle.

The above results suggest that the effectiveness of the FAI method, without compensating for nonparallel sides, may be reduced if the angle between opposing sides of the casting is greater than about 7 degrees (Table 9).

#### 4.4.6 Weld Defect Evaluation

The welding defects, i.e., lack of fusion and penetration, cracks, and porosity, were produced in one plate of both D357 and B201 using GTA welding. The defects were initially detected by both radiography and C-scan and then by the FAI method. Figure 13 shows a C-scan of the weld defects in the D357

TABLE 9. EFFECT OF NONPARALLEL SURFACES ON DEFECT DETECTION CAPABILITIES OF THE FAI TECHNIQUE

| ANGLE <sup>(2)</sup><br>(DEG.) | AVERAGE PORE RADIUS <sup>(1)</sup> ( $\mu\text{m}$ ) |                         | AVERAGE PERCENT POROSITY <sup>(1)</sup> |                         |
|--------------------------------|--|-------------------------|---|-------------------------|
|                                | NONPARALLEL  | PARALLEL <sup>(3)</sup> | NONPARALLEL                             | PARALLEL <sup>(3)</sup> |
| 0                              | --   | 100                     | --                                      | 1.4                     |
| 2                              | 90   | 100                     | 1.6                                     | 1.5                     |
| 5                              | 100  | 80                      | 1.7                                     | 1.5                     |
| 7                              | 130  | 110                     | 1.9                                     | 1.6                     |
| 10                             | 110  | 100                     | 2.1                                     | 1.5                     |

(1) Data obtained for a 0.75-inch-thick slice of an D357-T6 plate that contained Grade B gas porosity

(2) Between opposing surfaces

(3) Value before machining the angle

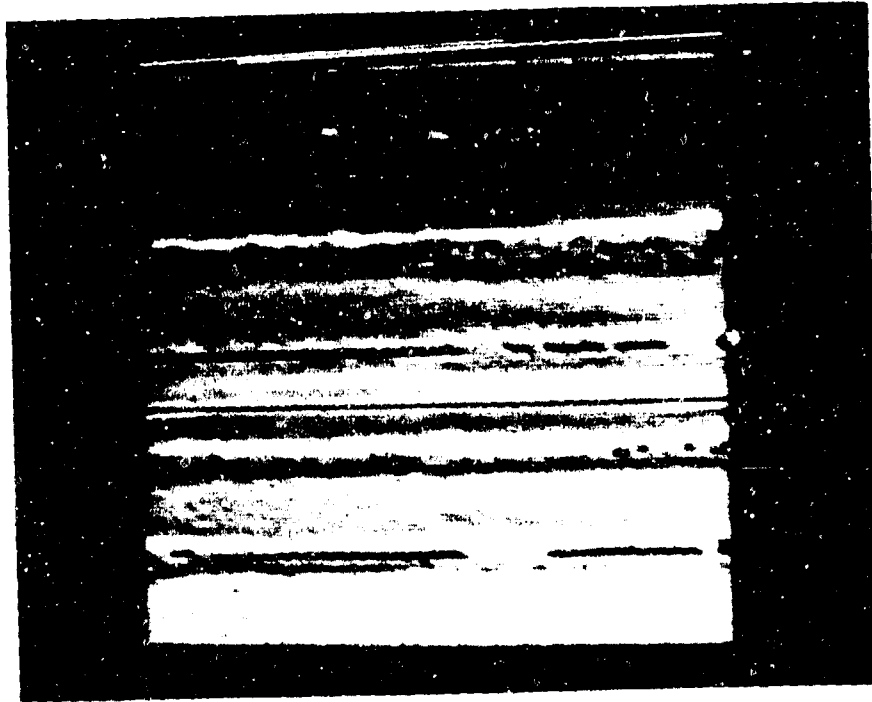


Figure 13. C-Scan of Weld Defects in D357  
(Defects: Cracking, lack of penetration and fusion, porosity)

plate. Six locations evenly spaced along each of the welds were chosen for evaluation by FAI, yielding a total of 29 test locations. The defects at each of these locations were then characterized by radiography for comparison with the FAI results. None of the welds were defect-free (Grade 1). All welds contained defects of Grade 2, indicating that the welds were not acceptable. Welding specifications do not assign defect Grades B, C, and D to defective welds. Instead, the welds are graded as passed (Grade 1) or failed (Grade 2).

The results of the FAI evaluations and the defect type are listed in Table 10. Percent porosity and pore radius values were obtained at all 29 locations examined. The severity level of the defects is not determined by radiography standards, and the accuracy of the FAI results could not be exactly assessed. However, because weld defects are radiographically graded in a pass/fail manner, it was assumed that any reading greater than that obtained from essentially defect-free material indicates a defective weld. Further development of the FAI technique is required, though, to fully define the FAI values corresponding to defect-free material. Once this has been accomplished, assessment of weld quality by FAI on a pass/fail basis should be feasible.

#### 4.4.7 Eddy Current Crack Detection Results

The results of the eddy current inspections are summarized in Table 11. The actual crack lengths, determined from optical measurements, are listed along with the corresponding probe outputs and predicted crack lengths determined for each face sheet thickness/cast material/fastener combination. With the steel fastener installed, all of the cracks in both D357 and B201 were detected through three face sheets of three thicknesses. With the titanium fastener installed, all cracks could be detected and quantified except for the shortest crack/thickest face sheet combination of 0.049 inch/0.25 inch. Difficulty in detecting this crack was due to interference between the low probe output (0.2 mv) and the system noise. The 0.049-inch-long crack could be detected and quantified through the other two face sheets, which were 0.08 inch and 0.125 inch thick. Based on these results, a lower threshold of about 1.0 mv should be used to account for system noise.

TABLE 10. FAI EVALUATION RESULTS FOR PLATES CONTAINING WELD DEFECTS

| DEFECT<br>TYPE      | ALLOY | PERCENT<br>POROSITY | PORE<br>RADIUS<br>( $\mu\text{m}$ ) |
|---------------------|-------|---------------------|-------------------------------------|
| None                | D357  | 0.4                 | 152                                 |
|                     | B201  | 0.3                 | 65                                  |
| Foreign<br>Material | D357  | 0.5                 | 91                                  |
|                     | B201  | 1.2                 | 133                                 |
| Gas Hole            | D357  | 0.3                 | 180                                 |
| Crack               | D357  | 0.4                 | 50                                  |
|                     | B201  | 0.4                 | 176                                 |
| No Fusion           | D357  | 0.4                 | 150                                 |
|                     | B201  | 0.4                 | 176                                 |

TABLE 11. IN-SERVICE EDDY CURRENT INSPECTION RESULTS

| FASTENER MATERIAL | SUBSTRUCTURE MATERIAL-THICKNESS (IN) | ACTUAL CRACK LENGTH | 7075-T6 FACE SHEET THICKNESS (IN) |               |               |                             |                   |                             |                   |
|-------------------|--------------------------------------|---------------------|-----------------------------------|---------------|---------------|-----------------------------|-------------------|-----------------------------|-------------------|
|                   |                                      |                     | 0.250                             | 0.125         | 0.080         | PREDICTED CRACK LENGTH (IN) | PROBE OUTPUT (mV) | PREDICTED CRACK LENGTH (IN) | PROBE OUTPUT (mV) |
| Steel             | D357-0.25                            | 0.049               | 0.05                              | 0.04          | 0.04          | 1.0                         | 1.6               | 0.04                        | 2.1               |
|                   | D357-0.25                            | 0.141               | 0.15                              | 0.14          | 0.14          | 5.0                         | 11.0              | 0.14                        | 18.7              |
|                   | D357-0.75                            | 0.257 and 0.227     | 0.26 and 0.24                     | 0.26 and 0.23 | 0.26 and 0.23 | 8.3 and 7.5                 | 23.9 and 20.8     | 0.26 and 0.25               | 38.8 and 37.9     |
|                   | B201-0.25                            | 0.049               | 0.05                              | 0.05          | 0.05          | 1.0                         | 2.3               | 0.05                        | 3.5               |
|                   | B201-0.25                            | 0.077               | 0.07                              | 0.07          | 0.07          | 1.7                         | 3.0               | 0.07                        | 6.1               |
|                   |                                      |                     |                                   |               |               |                             |                   |                             |                   |
| Titanium          | D357-0.25                            | 0.049               | 0                                 | 0.05          | 0.05          | 0.2                         | 0.9               | 0.06                        | 2.9               |
|                   | D357-0.25                            | 0.141               | 0.14                              | 0.14          | 0.14          | 1.8                         | 10.3              | 0.13                        | 27.3              |
|                   | D357-0.75                            | 0.257 and 0.227     | 0.24 and 0.24                     | 0.24 and 0.23 | 0.24 and 0.23 | 3.7 and 3.2                 | 22.0 and 19.5     | 0.24 and 0.24               | 59.8 and 59.5     |
|                   | B201-0.25                            | 0.049               | 0                                 | 0.05          | 0.05          | 0.4                         | 1.3               | 0.06                        | 3.7               |
|                   | B201-0.25                            | 0.077               | 0.07                              | 0.08          | 0.08          | 0.9                         | 3.0               | 0.07                        | 6.8               |
|                   |                                      |                     |                                   |               |               |                             |                   |                             |                   |

These results clearly indicate that this eddy current technique may be used for in-service inspections to accurately detect and measure cracks originating from fastener holes underneath face sheet materials.

#### 4.5 CONCLUSIONS

1. The FAI results for pore radius and percent porosity showed a qualitative correlation with X-ray grades for castings that contained gas or shrinkage porosity. By strengthening the data base, it may be possible to use the FAI method to provide quantitative correlations.
2. The FAI technique requires further development before data for foreign materials can be correlated with X-ray results.
3. The FAI percent porosity measurements decrease as the angle between the opposing sides of the specimen increases above about 7 degrees. This may limit the use of the FAI method unless it can be further developed for use with castings that have non-parallel sides.
4. The FAI technique can be used as a pass/fail method for evaluating weld repairs in castings.
5. Because the dynamic range was found to be a limiting factor for the FAI method, it should be maximized to reduce the discrepancies between the data obtained for material of different thicknesses.
6. The in-service eddy current technique can be used to detect the presence of cracks in component substructure and for determining their length.
7. Though a good correlation between FAI results and X-ray and microstructural data for gas porosity exists, without significant additional evaluation and development, the FAI method cannot be used as a foundry tool for grading aluminum castings.

SECTION 5  
PHASE I, TASK 2 - D357-T6 SCREENING TESTS

5.1 INTRODUCTION

The overall Task 2 objective was to define the process variables (solidification rate, aging condition, composition) that provide the optimum balance of tensile and DADT properties of B201-T7 and D357-T6 using screening tests, and to characterize the DADT properties of material produced according to the best process conditions. The screening test data for D357-T6 are discussed in this section. Average properties are presented in Section 5; the individual test results are included in Appendix A.

Cast plates of D357 (radiographic quality of Grade B, or better) were produced to determine (1) the effect of composition, solidification rate, and aging conditions on DADT properties and (2) if optimization of DADT properties conflicts with the requirements for obtaining the best static (tensile) properties. The range of compositions was based on the AMS specification 4241 [1]. The target tensile properties were 50 ksi UTS, 40 ksi YS, and 3 percent elongation. Solidification rates and aging parameters were selected to be typical of those used by foundries. The solution heat treatment conditions were the same for all the cast plates.

The screening tests were tension, notched tension, fatigue life, and microstructural analyses. The ratio of the notched tensile strength (NTS) to tensile yield strength (YS) was used as an indicator of fracture toughness. The microstructural analyses included determination of the dendrite arm spacing (DAS), and the area, aspect ratio, and spacing of the silicon particles. The amount of porosity present in each cast plate was also estimated using image analysis.

Multiple regression analyses were conducted to determine the relationships between the process variables, and the mechanical properties and microstructural features.

## 5.2 EXPERIMENTAL PROCEDURES

### 5.2.1 Process Variables

Forty-eight D357 plates with variations of composition, solidification rate, and aging parameters were cast by Alcoa. Each plate was 0.75 x 6 x 12 inches. The same pattern, and gating and risering system shown in Figure 14 were used to produce each plate.

The plates were produced based on the composition specification shown in Table 12. With the exception of the addition of Sr as a Si particle modifier, the specification is the same as AMS 4241 [1] (Draft 40GC). This initial draft was subsequently modified and approved for general release. The modifications were (1) an increase in the lower limit for Ti from 0.04 percent to 0.10 percent and (2) a decrease in the maximum limit for Fe from 0.20 percent to 0.12 percent.

The composition of 36 of the 48 plates was varied within the limits allowed by the specification. Due to the number of tests that would be required to evaluate the effect of all the key elements individually, some were grouped together, for example Ti, Mn, and Be. Cast plates were made with close to the minimum or maximum percentages of each element or group of elements. The target for those elements not being specifically varied was the middle of the allowed composition range. The Sr addition was 0.008 percent to 0.016 percent, except for those plates where it was specifically omitted. Strontium was included to promote the formation of low aspect ratio silicon particles in all parts of each plate to improve fatigue properties by reducing the stress concentration associated with irregularly shaped particles.

In addition to the 36 plates that were within the AMS 4241 composition guidelines, 12 plates were made with compositions outside the specification. The composition ranges stipulated in the specification are relatively narrow and, therefore, correlations between properties and alloying element content could be difficult to detect. These additional plates were made to increase the possibility of detecting correlations using regression analyses. A summary of the D357 composition variations evaluated, both within and outside the specification, is shown in Table 13. Forty-eight combinations of the

TABLE 12. COMPOSITION SPECIFICATION FOR THE D357-F6 SCREFFING PLATES

| ELEMENT(1)    | RANGE (WT %) |       |
|---------------|--------------|-------|
|               | MIN.         | MAX.  |
| Silicon       | 6.5          | 7.5   |
| Magnesium     | 0.55         | 0.6   |
| Titanium      | 0.04         | 0.20  |
| Beryllium     | 0.04         | 0.07  |
| Strontium     | 0.008        | 0.016 |
| Iron          | --           | 0.20  |
| Manganese     | --           | 0.10  |
| Others, each  | --           | 0.05  |
| Others, total | --           | 0.15  |
| Aluminum      | Balance      |       |

(1) AMS 4241 (Draft 40GC) plus Sr addition

TABLE 13. COMPOSITION VARIATIONS FOR THE D357-T6 SCREENING PLATES

| COMPOSITION VARIABLES | COMPOSITION DEVIATION FROM SPECIFICATION MID-RANGE |      |      |
|-----------------------|--|------|------|
|                       | Below Min.   | Min. | Max. |
| Si                    | (1)  | X    | X    |
| Mg                    | X  | X    | X    |
| Ti, Mn, Be            | (1)  | X    | X    |
| Fe                    | N/A  | (1)  | X    |
| Ti                    | X  | (1)  | (1)  |
| Fe, Be                | X  | (1)  | (1)  |
| Nominal               | Without Sr   |      |      |
| Nominal               | With Sr  |      |      |

(1) Not evaluated

three process variables (composition, solidification rate, aging parameters) were produced, as shown in Table 14.

Two solidification rates were achieved by varying the pour temperature and the chill material. Copper or iron chills were placed along the center of the plates (Figure 14) to vary the solidification rate. Pour temperatures of 1380°F and 1440°F were used with the copper and iron chills, respectively. The solidification rate was not measured directly, but subsequent DAS and mechanical property data indicated that the plates with the Cu chills had been solidified more rapidly than those with the Fe chills. These plates are referred to as the fast and slow solidification plates in the remainder of this report.

The solution heat treatment parameters were the same for all 48 plates. The plates were heated for 16 hours at  $1010 \pm 10^\circ\text{F}$ , which is within the requirements of AMS 4241. The plates were quenched in room temperature water with a delay time of less than 8 seconds.

The two aging temperature/time combinations were (1)  $315 \pm 5^\circ\text{F}$  for 12 hours, and (2)  $335 \pm 5^\circ\text{F}$  for 6 hours. These combinations were selected following consultations with several foundries as being representative of the temperature and time ranges typically used for aging D357 castings to the T6 condition. Heat treatment of all the screening plates was conducted by Northrop.

All the D357-T6 castings for screening were Grade B or better, according to MIL-A-2175. The plates were radiographically inspected to a one percent sensitivity both by the foundry and subsequently by an independent laboratory. The melt composition of each plate was provided by the foundry and was subsequently verified for each plate by Northrop using inductively coupled plasma (ICP) analysis. The foundry melt analysis is used throughout this report for quoting plate compositions.

TABLE 14. D357-T6 SCREENING PLATE PROCESS VARIABLES

| COMPOSITION <sup>(1)</sup> | SLOW SOLIDIFICATION |              | FAST SOLIDIFICATION |              |
|----------------------------|---------------------|--------------|---------------------|--------------|
|                            | AGING PARAMETERS    |              | AGING PARAMETERS    |              |
|                            | 315°F/12 hrs.       | 335°F/6 hrs. | 315°F/12 hrs.       | 335°F/6 hrs. |
| Si                         |                     |              |                     |              |
| Max.                       | X                   | X            | X                   | X            |
| Min.                       | X                   | X            | X                   | X            |
| Mg                         |                     |              |                     |              |
| Max.                       | X                   | X            | X                   | X            |
| Min.                       | X                   | X            | X                   | X            |
| Below Min.                 | X                   | X            | X                   | X            |
| Ti, Mn, Be                 |                     |              |                     |              |
| Max.                       | X                   | X            | X                   | X            |
| Min.                       | X                   | X            | X                   | X            |
| Fe                         |                     |              |                     |              |
| Max.                       | X                   | X            | X                   | X            |
| Ti                         |                     |              |                     |              |
| Below Min.                 | X                   | X            | X                   | X            |
| Fe, Be                     |                     |              |                     |              |
| Below Min.                 | X                   | X            | X                   | X            |
| Nominal                    |                     |              |                     |              |
| No Sr                      | X                   | X            | X                   | X            |
| With Sr                    | X                   | X            | X                   | X            |

(1) Other elements were mid-range of the specification

(2) Each "X" represents one cast plate (total of 48 plates)

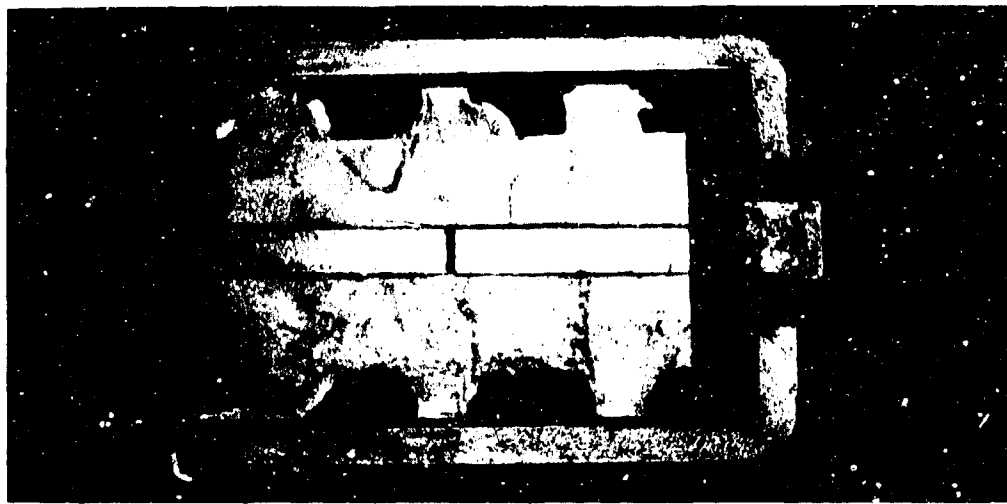
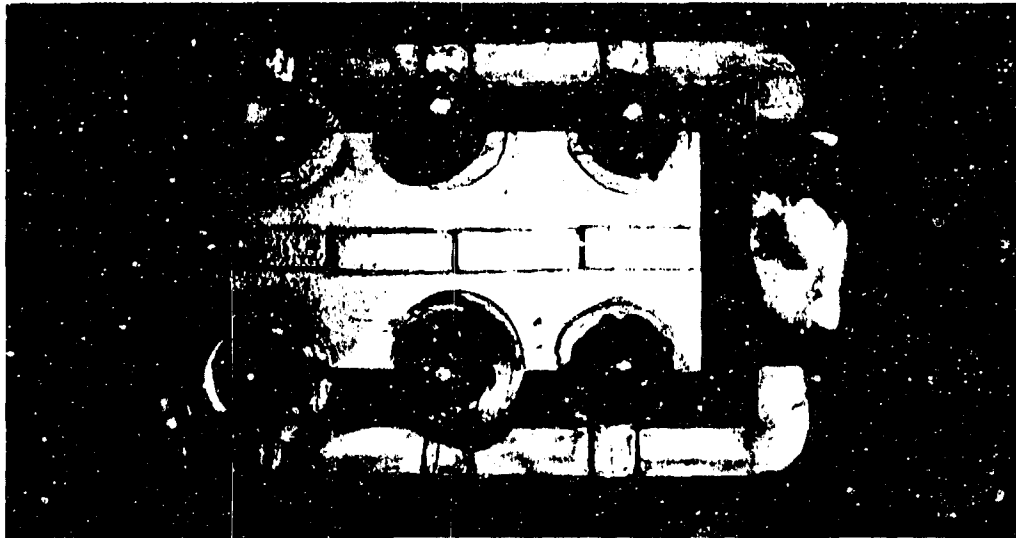


Figure 14. Gating, Risering, and Chill Placement Used for the D357 Process Variable Plates

### 5.2.2 Test Procedures

Tension, notched tension, and fatigue life tests were performed in accordance with the ASTM specifications shown in Table 15. Two specimens per plate were tested for each of these three mechanical properties. The specimens were excised from the same location in each of the 48 plates for consistency. The fatigue specimen, which is shown in Figure 15, is a simple simulation of aircraft components that contain holes for inserting fasteners during aircraft assembly. Holes act as stress concentrators and are a common cause of fatigue problems. All the D357-T6 fatigue specimens were tested to failure using constant amplitude loading, a net maximum tensile stress of 20 ksi, and a stress ratio (R) of 0.1.

### 5.2.3 Microstructural Characterization

The specific measurements for characterizing the microstructure of each of the 48 plates were (1) dendrite arm spacing (DAS), (2) silicon particle aspect ratio, area, and spacing, and (3) percent porosity.

The DAS was measured using a line intercept method [6] at the edge and center (under the chill) of each of the 48 plates, and for four of the plates as a function of distance from the center of the plates. The percent porosity was determined at the center of each plate. The silicon particle morphology was measured at the edge of all 48 plates. The percent porosity and the Si particle morphology were investigated using an Omnicon 3500 Image Analyzer.

### 5.2.4 Data Analysis

The test matrix (Table 14) was completed for each mechanical property and microstructural parameter. For mechanical properties, results from two tests were averaged for each "X" shown in Table 14 (a total of 96 tests for each property).

The average properties for the process variables were obtained by averaging the test results for the rows and columns in Table 14. The general effect of composition was obtained by averaging the data in each row (eight

TABLE 15. SCREENING TEST SPECIFICATIONS

| TEST            | SPECIFICATION |
|-----------------|---------------|
| Tension         | ASTM B557     |
| Notched Tension | ASTM E602     |
| Fatigue Life    | ASTM E466     |

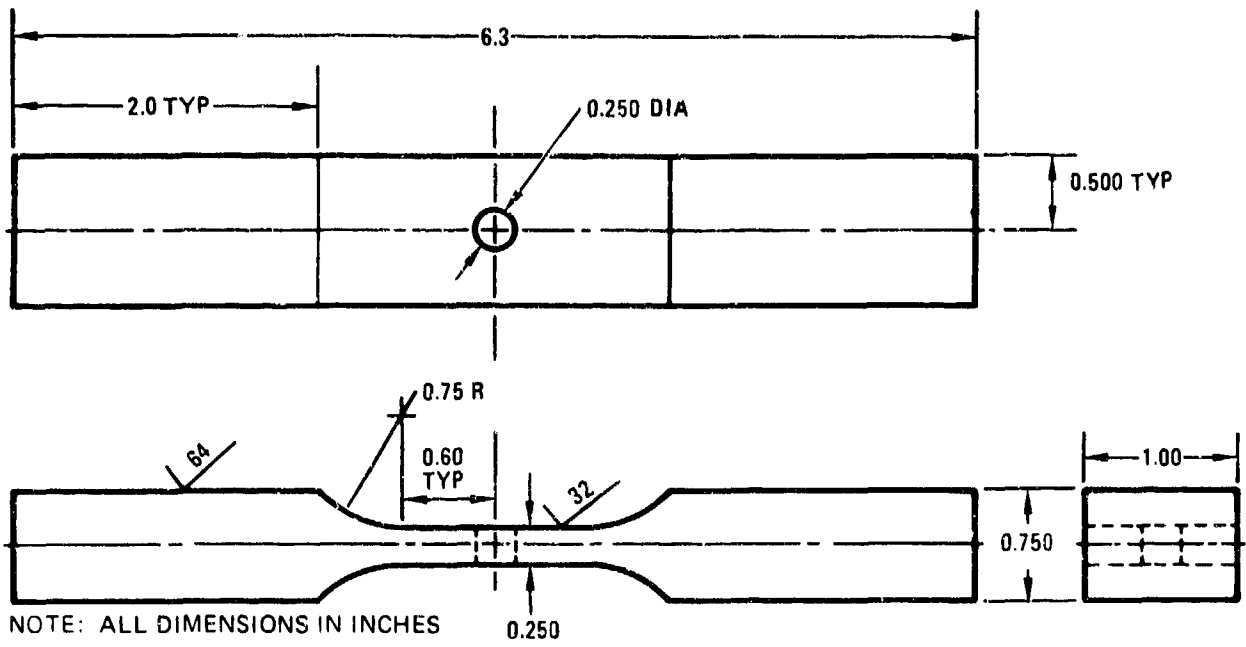


Figure 15. Fatigue Test Specimen

tests per row). The general effects of solidification rate and aging condition were determined by averaging the data in the four columns. For the plates that were within the composition specification, 18 individual test results per column were averaged. An average of six results was obtained per column for the plates that were outside the composition specification.

The plates that were outside the AMS composition specification were made specifically to enhance the regression analyses. All the individual test results for each composition variant shown in Table 14 were included in the regression analyses. Both linear and nonlinear multiple analyses were conducted. The linear analysis assumed a 5 percent probability of error for accepting or rejecting a variable in the final relationship, providing a broad indication of the relevant variables before progressing to the nonlinear analysis. The nonlinear analysis is considered to give a more accurate definition of the correlation equation due to its inclusion of cross-product and second order terms. However, the acceptance/rejection criterion was tightened from five percent to one percent probability of error to reduce the number of unrepresentative cross-product items which might otherwise appear in the final equation.

The results of the regression analyses are presented as the percent variation in the dependent variables (mechanical properties and microstructural features) explained by the independent variables (composition, solidification rate, and aging temperature/time).

### 5.3 RESULTS AND DISCUSSION

The average hardness (Rockwell B) for the plates that were within the composition specification (WCS) was 46 after solution heat treatment and quench (SHT) and 69 after aging. The conductivity values (percent of IACS) for these conditions were 34 percent and 36 percent, respectively. For the plates that were outside the composition specification (OCS), the hardness of the SHT and the aged plates was 45 and 71, respectively. The corresponding conductivity values were 36 percent and 39 percent.

The properties for each plate are presented in the following subsections as a function of the process variables for plates that are (1) within the composition specification, and (2) outside the composition specification. The data are averages of two or more tests.

The average property values cited and discussed in Section 5.3 as a function of the process variables were obtained from the data tabulated in Tables 17 through 27 as follows:

1. Solidification Rate. Average of the data points in the two adjacent columns under fast or slow solidification.
2. Composition. Average of the four data points in each row representing a particular composition variation.
3. Aging. Average of the data points in the columns (not adjacent) for the two sets of aging parameters.
4. Strontium. Data for unmodified plates (no Sr) are shown in the row designated 0.00 Sr; the average is shown at the end of the row. For modified plates, all the remaining data were averaged according to items 1 through 3 above.

#### 5.3.1 Composition

The chemical composition of the 12 composition variants was based on the AMS specification shown in Table 12. Nine of the variants were held within the composition specification; the composition of the other three variants was outside the specification. The average contents of the alloying elements that were specifically controlled are summarized in Table 16. The target for the elements that were not specifically controlled was the mid-range of the specification.

TABLE 16. COMPOSITION OF THE D357 SCREENING PLATES

| ELEMENT<br>CONTENT (1) | ELEMENT (WT %) |      |      |       |                 |      |              |
|------------------------|----------------|------|------|-------|-----------------|------|--------------|
|                        | Si             | Mg   | Fe   | Sr    | Ti-Mn-Be        | Ti   | Fe-Be        |
| Max.                   | 7.41           | 0.60 | 0.18 | 0.016 | 0.19-0.10-0.053 | (2)  | (2)          |
| Min.                   | 6.53           | 0.56 | (2)  | 0.008 | 0.07-0.00-0.04  | (2)  | (2)          |
| Below Min.             | (2)            | 0.45 | (2)  | (2)   | (2)             | 0.00 | 0.027-0.0005 |

(1) All other elements were mid-range of the specification  
 (2) Not evaluated

Note: Plates of nominal composition were also evaluated

### 5.3.2 Microstructure

#### Dendrite Arm Spacing (DAS)

The DAS results are summarized in Table 17. For the WCS material, the average DAS at the plate edge and under the chill was 0.0028 inch and 0.0014 inch, respectively. Variations in alloy composition had no effect on the DAS. The overall average DAS measured at the edge of each of the 18 plates that were solidified at the faster rate (Cu chill) was slightly smaller than that for the 18 plates solidified at the slower rate (Fe chill), i.e., 0.0027 inch versus 0.0029 inch. The overall average DAS under both the Cu and Fe chills was the same, i.e. 0.0014 inch. However, detailed determination of the dependence of DAS on distance from the center of four WCS plates (Figure 16) showed that DAS increased approximately linearly with distance from the center of the plate, and that the faster solidification rate (Cu chill) resulted in a smaller DAS, which typically improves mechanical properties [7].

The DAS for the OCS plates was similar to those that were within the composition specification. The overall average values for the OCS plates under the chill and at the plate edge were 0.0014 inch and 0.0024 inch, respectively.

#### Silicon Particle Morphology

The aspect ratio, area, and spacing of the Si particles in each plate were determined using image analysis. The data for all the 48 plates are summarized in Tables 18, 19, and 20, respectively.

##### a. Aspect Ratio

For the WCS plates, the overall average aspect ratio was 1.86; for the Sr-containing plates (Table 18) it was 1.82. A noticeably higher average aspect ratio of 2.19 was obtained for the plates that did not contain Sr. The average silicon particle aspect ratio of the plates solidified at the faster rate was lower than that of the slow solidification rate material (1.82 versus 1.90).

TABLE 17. EFFECT OF PROCESS VARIABLES ON THE DENDRITE ARM SPACING OF D357-T6

| COMPOSITION (1)<br>(WT. %)            | SPECIMEN<br>LOCATION | AVERAGE DAS ( $10^{-4}$ IN.) |           |                           |           | AVERAGE |
|---------------------------------------|----------------------|------------------------------|-----------|---------------------------|-----------|---------|
|                                       |                      | AGE                          |           | AGE                       |           |         |
|                                       |                      | (SLOW SOLIDIFICATION) (2)    |           | (FAST SOLIDIFICATION) (3) |           |         |
|                                       |                      | 315°F/12HR                   | 335°F/6HR | 315°F/12HR                | 335°F/6HR |         |
| (a) Within Composition Specification  |                      |                              |           |                           |           |         |
| 0.19Ti-0.10Mn-0.053Be                 | Chill                | 14                           | 17        | 14                        | 13        | 15      |
|                                       | Edge                 | 30                           | 33        | 29                        | 26        | 30      |
| 0.27Ti-0.00Mn-0.04Be                  | Chill                | 15                           | 13        | 12                        | 12        | 13      |
|                                       | Edge                 | 27                           | 31        | 28                        | 25        | 28      |
| 0.60Mg                                | Chill                | 14                           | 14        | 14                        | 14        | 14      |
|                                       | Edge                 | 29                           | 28        | 27                        | 26        | 28      |
| 0.56Mg                                | Chill                | 16                           | 14        | 12                        | 13        | 14      |
|                                       | Edge                 | 28                           | 26        | 25                        | 25        | 26      |
| 7.41Si                                | Chill                | 13                           | 14        | 15                        | 14        | 14      |
|                                       | Edge                 | 25                           | 24        | 24                        | 26        | 25      |
| 6.13Si                                | Chill                | 14                           | 13        | 14                        | 14        | 14      |
|                                       | Edge                 | 28                           | 32        | 30                        | 27        | 29      |
| 0.19Fe                                | Chill                | 13                           | 14        | 15                        | 16        | 15      |
|                                       | Edge                 | 30                           | 31        | 22                        | 28        | 28      |
| 0.10Sr                                | Chill                | 14                           | 16        | 13                        | 12        | 14      |
|                                       | Edge                 | 30                           | 31        | 27                        | 27        | 29      |
| Average                               | Chill                | 14                           | 14        | 14                        | 14        | 14      |
|                                       | Edge                 | 28                           | 30        | 27                        | 26        | 28      |
| (b) Outside Composition Specification |                      |                              |           |                           |           |         |
| 0.45Mg                                | Chill                | 15                           | 14        | 13                        | 14        | 14      |
|                                       | Edge                 | 20                           | 23        | 28                        | 25        | 24      |
| 0.77Ti                                | Chill                | 14                           | 21        | 13                        | 12        | 15      |
|                                       | Edge                 | 23                           | 27        | 23                        | 20        | 27      |
| 0.17Be-0.1005Be                       | Chill                | 14                           | 17        | 14                        | 13        | 14      |
|                                       | Edge                 | 22                           | 26        | 28                        | 25        | 25      |
| Average                               | Chill                | 14                           | 17        | 13                        | 13        | 14      |
|                                       | Edge                 | 22                           | 25        | 26                        | 23        | 24      |

(1) Other elements; mid-range of the specification

(2) Fe chill; 1440°F pour temperature

(3) Ti chill; 1380°F pour temperature

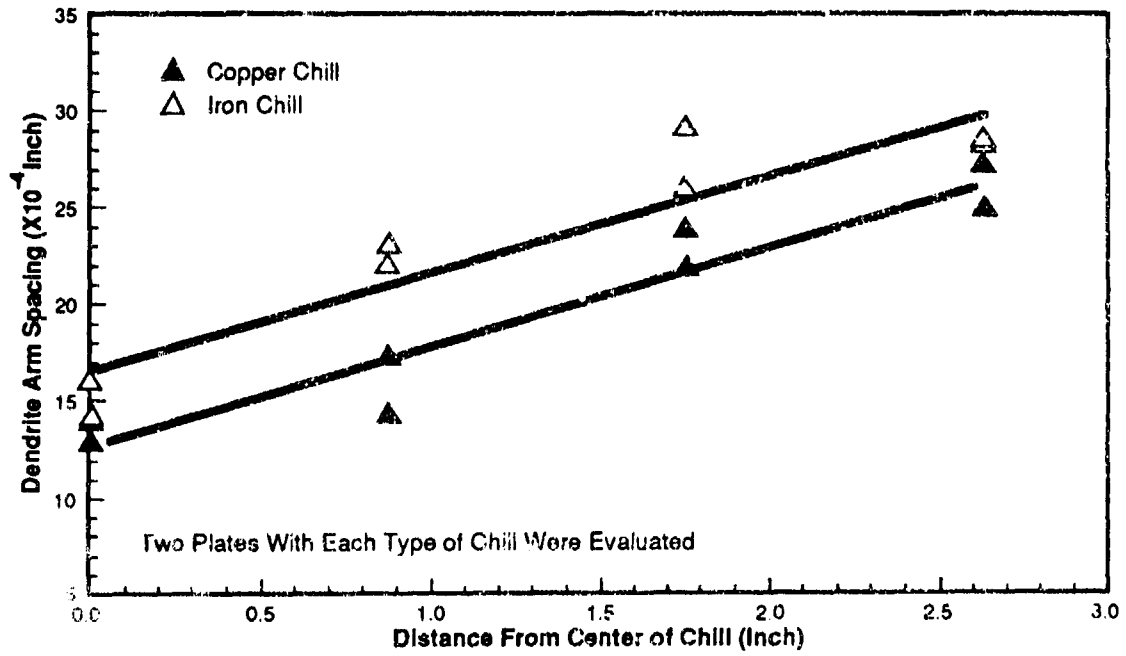


Figure 16. D357 Dendrite Arm Spacing Versus Distance from the Center of the Chill

TABLE 13. EFFECT OF PROCESS VARIABLES ON THE SILICON PARTICLE ASPECT RATIO OF D357-T6

| COMPOSITION <sup>(1)</sup><br>(WT %)         | SILICON PARTICLE ASPECT RATIO        |           |                                      |           | AVG. |
|--|--------------------------------------|-----------|--------------------------------------|-----------|------|
|  | AGE                                  |           | AGE                                  |           |      |
|  | (SLOW SOLIDIFICATION) <sup>(2)</sup> |           | (FAST SOLIDIFICATION) <sup>(3)</sup> |           |      |
|  | 315°F/12HR                           | 335°F/6HR | 315°F/12HR                           | 335°F/6HR |      |
| <u>(a) Within Composition Specification</u>  |                                      |           |                                      |           |      |
| 0.19Ti-0.11Mn-0.053Be                        | 1.78                                 | 1.96      | 1.74                                 | 1.75      | 1.81 |
| 0.07Ti-0.00Mn-0.04Be                         | 1.80                                 | 1.70      | 1.80                                 | 1.70      | 1.75 |
| 0.50Mg                                       | 1.83                                 | 2.00      | 1.71                                 | 1.73      | 1.82 |
| 0.56Mg                                       | 1.81                                 | 1.80      | 1.90                                 | 1.76      | 1.82 |
| 7.41Si                                       | 2.00                                 | 1.99      | 1.80                                 | 1.80      | 1.90 |
| 6.53Si                                       | 1.92                                 | 1.89      | 1.78                                 | 1.73      | 1.83 |
| 0.18Fe                                       | 1.73                                 | 1.92      | 1.76                                 | 1.89      | 1.83 |
| 0.00Sr                                       | 2.06                                 | 2.29      | 2.20                                 | 2.19      | 2.19 |
| Nominal                                      | 1.77                                 | 1.80      | 1.75                                 | 1.75      | 1.77 |
| Average                                      | 1.86                                 | 1.93      | 1.83                                 | 1.81      | 1.86 |
| <u>(b) Outside Composition Specification</u> |                                      |           |                                      |           |      |
| 0.45Mg                                       | 1.72                                 | 1.75      | 1.76                                 | 1.76      | 1.75 |
| 0.00Ti                                       | 1.77                                 | 1.87      | 1.74                                 | 1.74      | 1.78 |
| 0.027Fe-0.0005Be                             | 1.78                                 | 1.72      | 1.81                                 | 1.74      | 1.76 |
| Average                                      | 1.76                                 | 1.78      | 1.77                                 | 1.75      | 1.76 |

(1) Other elements were mid-range of the specification

(2) Fe chill; 1440°F pour temperature

(3) Cu chill; 1380°F pour temperature

TABLE 19. EFFECT OF PROCESS VARIABLES ON THE SILICON PARTICLE AREA OF D357-T6

| COMPOSITION <sup>(1)</sup><br>(WT %)         | SILICON PARTICLE AREA ( $\mu\text{m}^2$ ) |           |                                      |           | AVG. |
|--|---|-----------|--------------------------------------|-----------|------|
|  | AGE                                       |           | AGE                                  |           |      |
|  | (SLOW SOLIDIFICATION) <sup>(2)</sup>      |           | (FAST SOLIDIFICATION) <sup>(3)</sup> |           |      |
|  | 315°F/12HR                                | 335°F/6HR | 315°F/12HR                           | 335°F/6HR |      |
| <u>(a) Within Composition Specification</u>  |   |           |                                      |           |      |
| 0.19Ti-0.11Mn-0.053Be                        | 16  | 21        | 19                                   | 16        | 18   |
| 0.07Ti-0.00Mn-0.04Be                         | 21  | 20        | 18                                   | 15        | 18   |
| 0.60Mg                                       | 25  | 19        | 18                                   | 19        | 20   |
| 0.56Mg                                       | 17  | 24        | 14                                   | 15        | 18   |
| 7.41Si                                       | 18  | 21        | 20                                   | 19        | 19   |
| 6.53Si                                       | 23  | 22        | 23                                   | 19        | 22   |
| 0.18Fe                                       | 18  | 32        | 18                                   | 24        | 23   |
| 0.00Sr                                       | 83  | 108       | 66                                   | 70        | 82   |
| Nominal                                      | 20  | 27        | 19                                   | 22        | 22   |
| Average                                      | 27  | 33        | 24                                   | 24        | 27   |
| <u>(b) Outside Composition Specification</u> |   |           |                                      |           |      |
| 0.45Mg                                       | 16  | 18        | 19                                   | 17        | 17   |
| 0.00Ti                                       | 19  | 23        | 19                                   | 18        | 20   |
| 0.027Fe-0.0005Be                             | 16  | 18        | 22                                   | 19        | 19   |
| Average                                      | 17  | 19        | 20                                   | 18        | 19   |

(1) Other elements were mid-range of the specification

(2) Fe chill; 1440°F pour temperature

(3) Cu chill; 1380°F pour temperature

TABLE 20. EFFECT OF PROCESS VARIABLES ON THE SILICON PARTICLE SPACING OF D357-T6

| COMPOSITION(1)<br>(WT %)                     | SILICON PARTICLE SPACING ( $\mu\text{m}$ ) |           |                                      |           | AVG. |
|--|--|-----------|--------------------------------------|-----------|------|
|  | AGE  |           | AGE                                  |           |      |
|  | (SLOW SOLIDIFICATION) <sup>(2)</sup>       |           | (FAST SOLIDIFICATION) <sup>(3)</sup> |           |      |
|  | 315°F/12HR                                 | 335°F/6HR | 315°F/12HR                           | 335°F/6HR |      |
| <u>(a) Within Composition Specification</u>  |  |           |                                      |           |      |
| 0.19Ti-0.11Mn-0.053Be                        | 38   | 34        | 29                                   | 33        | 34   |
| 0.07Ti-0.00Mn-0.04Be                         | 42   | 34        | 36                                   | 32        | 36   |
| 0.60Mg                                       | 44   | 37        | 44                                   | 40        | 41   |
| 0.56Mg                                       | 41   | 34        | 30                                   | 32        | 34   |
| 7.41Si                                       | 40   | 41        | 41                                   | 43        | 41   |
| 6.53Si                                       | 30   | 28        | 39                                   | 34        | 33   |
| 0.18Fe                                       | 29   | 35        | 34                                   | 38        | 34   |
| 0.00Sr                                       | 76   | 64        | 59                                   | 63        | 66   |
| Nominal                                      | 53   | 51        | 39                                   | 53        | 49   |
| Average                                      | 44   | 40        | 39                                   | 41        | 41   |
| <u>(b) Outside Composition Specification</u> |  |           |                                      |           |      |
| 0.45Mg                                       | 35   | 45        | 35                                   | 47        | 41   |
| 0.00Ti                                       | 47   | 57        | 42                                   | 42        | 47   |
| 0.027Fe-0.0005Be                             | 37   | 44        | 41                                   | 49        | 43   |
| Average                                      | 40   | 49        | 39                                   | 46        | 44   |

(1) Other elements were mid-range of the specification

(2) Fe chill; 1440°F pour temperature

(3) Cu chill; 1380°F pour temperature

For the OCS plates, the overall average aspect ratio was 1.76, which is slightly lower than the value for the WCS plates. No significant effect of solidification rate was observed.

b. Area

The overall average Si particle area (Table 19) was  $27 \mu\text{m}^2$ . The average for the WCS Sr-containing variants was  $20 \mu\text{m}^2$  and showed only minor variations due to composition changes. The average Si particle area in the Sr-free plates, however, was over four times greater than that of the plates that contained Sr ( $82 \mu\text{m}^2$  versus  $20 \mu\text{m}^2$ ).

The effect of solidification rate on aspect ratio was much greater for the Sr-free than for the Sr-containing plates. The average Si particle area for plates without Sr that were solidified at the faster and slower rates was 68 and  $95 \mu\text{m}^2$ , respectively. For plates containing Sr, the values were 19 and  $21 \mu\text{m}^2$ , respectively.

The average Si particle area determined for the OCS plates was  $19 \mu\text{m}^2$ . There was no significant effect of solidification rate or composition. The results were essentially the same as those for the WCS Sr-containing plates.

c. Spacing

The overall average Si particle spacing for the WCS plates was  $41 \mu\text{m}$  (Table 20). The average Si particle spacing for the Sr-containing variants and those that did not contain Sr was  $36 \mu\text{m}$  and  $66 \mu\text{m}$ , respectively. For the Sr-free plates, the faster solidification rate (Cu chill) produced a slightly smaller average spacing than that for the material solidified slowly (Fe chill),  $61 \mu\text{m}$  versus  $70 \mu\text{m}$ . No effect of solidification rate was observed for the Sr-containing plates.

The average spacing for the OCS plates was  $44 \mu\text{m}$ , i.e. slightly higher than the WCS material ( $41 \mu\text{m}$ ). The average values for the slow and fast solidification rates were  $44.5 \mu\text{m}$  and  $42.5 \mu\text{m}$ , respectively.

The effect of Sr content on the Si particle aspect ratio, area, and spacing is illustrated in Figure 17. The photomicrographs are typical of material taken from the edge of the plate. The Si particles of the Sr-free material are larger, more irregularly shaped, and are spaced further apart compared with those observed in the Sr-containing material. Large, irregularly shaped particles of the type seen in the material without Sr can be detrimental to DADT properties, particularly fatigue crack initiation [8,9].

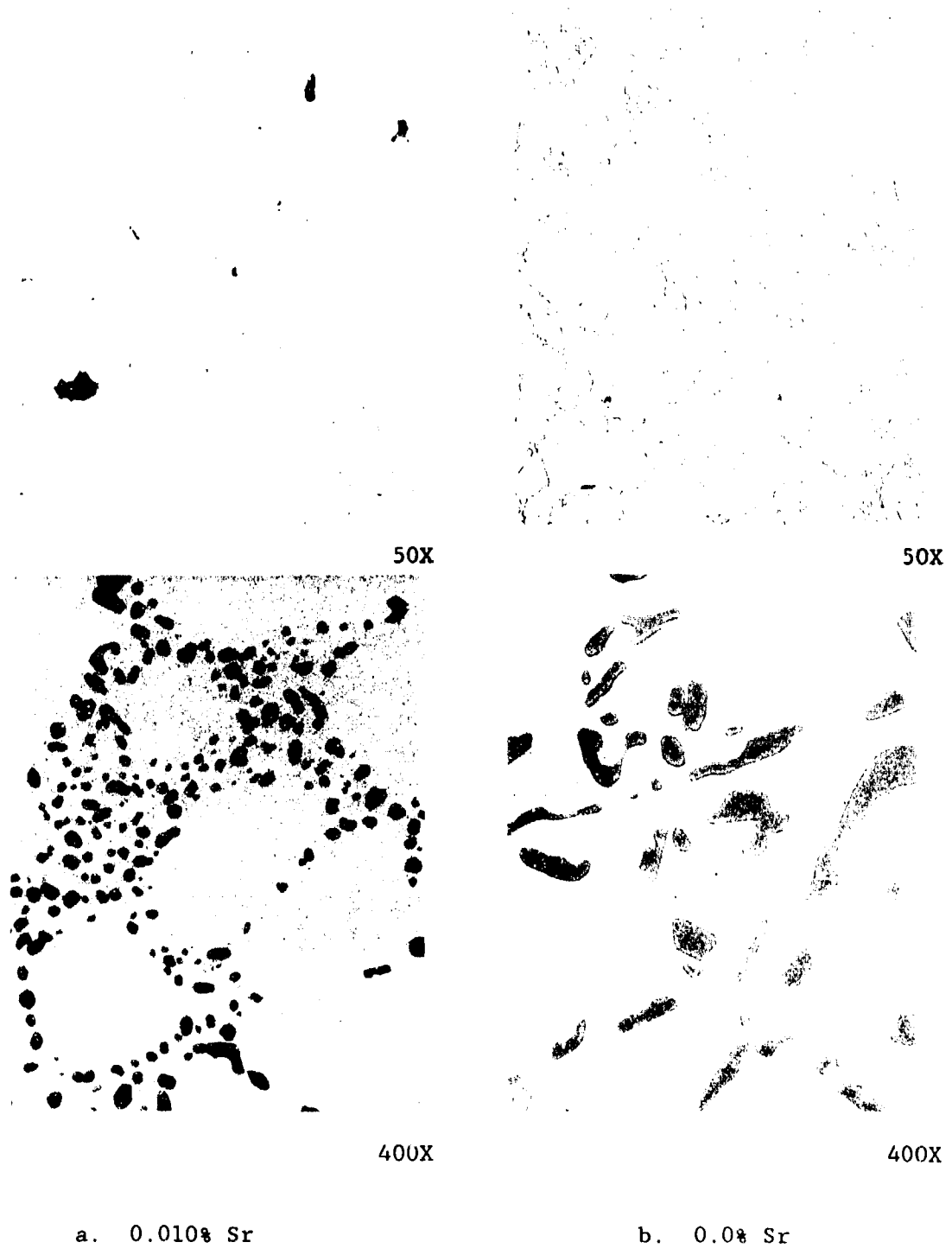
Though the Sr modified the Si particles, there was no effect on DAS (Table 17). For material under the chill, the Si particle morphology was equivalent for both the solidification rates. However, the addition of a modifier such as Sr will promote the formation of an optimum Si particle morphology in parts of a casting that are not under or near a chill. This may be particularly important for DADT properties, which may be more sensitive to Si particle morphology than static properties.

The mechanism by which Sr modifies the Si particle morphology is not fully understood, although several possible explanations have been described [10]. Sr may change the equilibrium at the solid-liquid interface due to solute build-up, producing a hard-to-detect ternary phase. Sr may also change the nucleation kinetics and inhibit growth of the Si particles on the preferred [111] plane.

#### Percent Porosity

The percent porosity for each plate was determined using image analysis. The data were obtained from specimens taken from the center of the plate under the chill. Each result presented is the average of about 50 fields of view within the microstructure specimen. The data are summarized in Table 21.

For the WCS plates, the average porosity of the material solidified at the slower rate (Fe chill) was about three times that of the fast solidification material (Cu chill). This is probably due to the increased time available for dissolution of hydrogen from the melt at the slower solidification rate [10] and/or a greater hydrogen content in the higher



a. 0.010% Sr

b. 0.0% Sr

Figure 17. Effect of Strontium on the D357-T6 Microstructure

TABLE 21. EFFECT OF PROCESS VARIABLES ON THE PERCENT POROSITY OF D357-T6

| COMPOSITION <sup>(1)</sup><br>(WT %)         | PERCENT POROSITY                     |           |                                      |           | AVG.  |
|--|--------------------------------------|-----------|--------------------------------------|-----------|-------|
|  | AGE                                  |           | AGE                                  |           |       |
|  | (SLOW SOLIDIFICATION) <sup>(2)</sup> |           | (FAST SOLIDIFICATION) <sup>(3)</sup> |           |       |
|  | 315°F/12HR                           | 335°F/6HR | 315°F/12HR                           | 335°F/6HR |       |
| <u>(a) Within Composition Specification</u>  |                                      |           |                                      |           |       |
| 0.19Ti-0.11Mn-0.053Be                        | 0.030                                | 0.040     | 0.001 <sup>(4)</sup>                 | 0.001     | 0.018 |
| 0.07Ti-0.00Mn-0.04Be                         | 0.050                                | 0.001     | 0.030                                | 0.010     | 0.023 |
| 0.60Mg                                       | 0.040                                | 0.020     | 0.001                                | 0.040     | 0.025 |
| 0.56Mg                                       | 0.010                                | 0.001     | 0.001                                | 0.001     | 0.003 |
| 7.41Si                                       | 0.001                                | 0.070     | 0.030                                | 0.060     | 0.040 |
| 6.53Si                                       | 0.060                                | 0.010     | 0.001                                | 0.020     | 0.023 |
| 0.18Fe                                       | 0.050                                | 0.010     | 0.001                                | 0.001     | 0.016 |
| 0.00Sr                                       | 0.050                                | 0.030     | 0.001                                | 0.001     | 0.021 |
| Nominal                                      | 0.001                                | 0.030     | 0.001                                | 0.001     | 0.010 |
| Average                                      | 0.047                                | 0.024     | 0.007                                | 0.015     | 0.023 |
| <u>(b) Outside Composition Specification</u> |                                      |           |                                      |           |       |
| 0.45Mg                                       | 0.001                                | 0.001     | 0.001                                | 0.110     | 0.028 |
| 0.00Ti                                       | 0.001                                | 0.030     | 0.001                                | 0.001     | 0.008 |
| 0.027Fe-0.0005Be                             | 0.001                                | 0.001     | 0.001                                | 0.001     | 0.001 |
| Average                                      | 0.001                                | 0.011     | 0.001                                | 0.037     | 0.012 |

(1) Other elements were mid-range of the specification

(2) Fe chill; 1440°F pour temperature

(3) Cu chill; 1380°F pour temperature

(4) No porosity detected--below the detection limit of the equipment

temperature melt. However, even with the same melt gas content, a slower solidification rate would tend to promote the formation of more gas porosity than that for material solidified more rapidly. The actual hydrogen content of the melt was not determined, but bubbles were not detected in the vacuum test samples from any of the melts. The other process variables had no effect on the percent porosity. X-ray inspection showed all plates to be Grade B or better.

All the OCS plates were also Grade B, or better, according to X-ray radiography. Unlike the WCS plates, no significant effect of solidification rate on the percent porosity was observed. Only two of the 12 plates contained a detectable amount of porosity (one each for slow and fast solidification rate material).

### 5.3.3 Tensile Properties

The tensile property data are summarized in Tables 22, 23, and 24 for the plates that were within and outside the composition specification. The overall average tensile properties are 51 ksi/43 ksi/5 percent and 51 ksi/42 ksi/8 percent for the WCS and OCS plates, respectively.

The average ultimate and yield strengths for the two groups of materials were very similar, though the elongation of the OCS material was higher than that of the WCS material. The results are discussed in more detail below.

#### Ultimate Tensile Strength

The UTS (Table 22) was not significantly affected by any of the composition variants. A slightly higher value was obtained for the WCS plates solidified at the faster rate compared with those solidified more slowly, i.e., 52.2 ksi versus 50.7 ksi. A slightly higher UTS (52.1 ksi) was obtained for the WCS variants that were aged at 335°F for 6 hours compared with those that were aged at 315°F for 12 hours (50.7 ksi).

The UTS of the OCS plates was not significantly affected by aging conditions, solidification rate, or composition.

TABLE 22. EFFECT OF PROCESS VARIABLES ON THE ULTIMATE TENSILE STRENGTH OF D357-T6

| COMPOSITION(1)<br>(WT %)                     | AVERAGE ULTIMATE TENSILE STRENGTH (ksi) |           |                           |           | AVG. |
|--|---|-----------|---------------------------|-----------|------|
|  | AGE                                     |           | AGE                       |           |      |
|  | (SLOW SOLIDIFICATION) (2)               |           | (FAST SOLIDIFICATION) (3) |           |      |
|  | 315°F/12HR                              | 335°F/6HR | 315°F/12HR                | 335°F/6HR |      |
| <u>(a) Within Composition Specification</u>  |   |           |                           |           |      |
| 0.19Ti-0.10Mn-0.053Be                        | 50.4                                    | 50.3      | 51.2                      | 53.4      | 51.3 |
| 0.07Ti-0.00Mn-0.04Be                         | 49.0                                    | 51.8      | 49.1                      | 54.2      | 51.0 |
| 0.60Mg                                       | 49.7                                    | 51.8      | 52.0                      | 54.6      | 52.0 |
| 0.56Mg                                       | 50.1                                    | 52.1      | 53.5                      | 54.1      | 52.5 |
| 7.41Si                                       | 49.5                                    | 51.4      | 51.0                      | 51.8      | 50.9 |
| 6.53Si                                       | 49.8                                    | 53.2      | 51.6                      | 51.4      | 51.5 |
| 0.18Fe                                       | 50.0                                    | 51.2      | 52.2                      | 52.0      | 51.4 |
| 0.00Sr                                       | 49.6                                    | 51.2      | 52.5                      | 52.7      | 51.5 |
| Nominal                                      | 51.5                                    | 49.5      | 50.7                      | 51.4      | 50.8 |
| Average                                      | 50.0                                    | 51.4      | 51.5                      | 52.8      | 51.4 |
| <u>(b) Outside Composition Specification</u> |   |           |                           |           |      |
| 0.45Mg                                       | 50.6                                    | 51.8      | 50.5                      | 49.0      | 50.5 |
| 0.00Ti                                       | 51.0                                    | 48.9      | 52.0                      | 51.5      | 50.9 |
| 0.027Fe-0.0005Be                             | 52.5                                    | 51.8      | 49.0                      | 52.3      | 51.4 |
| Average                                      | 51.4                                    | 50.8      | 50.5                      | 51.0      | 50.9 |

(1) Other elements were mid-range of the specification

(2) Fe chill; 1440°F pour temperature

(3) Cu chill; 1380°F pour temperature

TABLE 23. EFFECT OF PROCESS VARIABLES ON THE YIELD STRENGTH OF D357-T6

| COMPOSITION(1)<br>(WT %)                     | AVERAGE YIELD STRENGTH (ksi) |           |                          |           | AVG. |
|--|------------------------------|-----------|--------------------------|-----------|------|
|  | AGE                          |           | AGE                      |           |      |
|  | (SLOW SOLIDIFICATION)(2)     |           | (FAST SOLIDIFICATION)(3) |           |      |
|  | 315°F/12HR                   | 335°F/6HR | 315°F/12HR               | 335°F/6HR |      |
| <u>(a) Within Composition Specification</u>  |                              |           |                          |           |      |
| 0.19Ti-0.10Mn-0.053Be                        | 42.1                         | 43.6      | 41.8                     | 44.5      | 43.0 |
| 0.07Ti-0.00Mn-0.04Be                         | 41.9                         | 43.8      | 41.6                     | 44.6      | 43.0 |
| 0.60Mg                                       | 41.2                         | 44.7      | 43.1                     | 45.7      | 43.7 |
| 0.56Mg                                       | 42.0                         | 43.9      | 42.8                     | 45.8      | 43.6 |
| 7.41Si                                       | 41.9                         | 44.5      | 41.8                     | 44.0      | 43.0 |
| 6.53Si                                       | 41.6                         | 44.7      | 42.0                     | 43.8      | 43.0 |
| 0.18Fe                                       | 42.8                         | 45.2      | 43.3                     | 45.0      | 44.1 |
| 0.00Sr                                       | 42.5                         | 45.5      | 43.0                     | 44.3      | 43.8 |
| Nominal                                      | 42.8                         | 42.4      | 41.6                     | 45.1      | 43.0 |
| Average                                      | 42.1                         | 44.2      | 42.3                     | 44.8      | 43.4 |
| <u>(b) Outside Composition Specification</u> |                              |           |                          |           |      |
| 0.45Mg                                       | 40.1                         | 42.8      | 38.9                     | 41.0      | 40.7 |
| 0.00Ti                                       | 41.8                         | 41.8      | 42.0                     | 43.2      | 42.2 |
| 0.027Fe-0.0005Be                             | 42.8                         | 44.9      | 42.8                     | 44.4      | 43.7 |
| Average                                      | 41.6                         | 43.2      | 41.2                     | 42.9      | 42.2 |

(1) Other elements were mid-range of the specification

(2) Fe chill; 1440°F pour temperature

(3) Cu chill; 1380°F pour temperature

TABLE 24. EFFECT OF PROCESS VARIABLES ON THE ELONGATION OF D357-T6

| COMPOSITION <sup>(1)</sup><br>(WT %)         | AVERAGE ELONGATION (%)               |           |                                      |           | AVG. |
|--|--------------------------------------|-----------|--------------------------------------|-----------|------|
|  | AGE                                  |           | AGE                                  |           |      |
|  | (SLOW SOLIDIFICATION) <sup>(2)</sup> |           | (FAST SOLIDIFICATION) <sup>(3)</sup> |           |      |
|  | 315°F/12HR                           | 335°F/6HR | 315°F/12HR                           | 335°F/6HR |      |
| <u>(a) Within Composition Specification</u>  |                                      |           |                                      |           |      |
| 0.19Ti-0.10Mn-0.053Be                        | 5.2                                  | 1.5       | 6.5                                  | 6.8       | 5.0  |
| 0.07Ti-0.00Mn-0.04Be                         | 4.0                                  | 5.0       | 3.5                                  | 9.2       | 5.4  |
| 0.60Mg                                       | 4.5                                  | 4.2       | 6.0                                  | 7.0       | 5.4  |
| 0.56Mg                                       | 4.6                                  | 5.5       | 9.5                                  | 7.0       | 6.7  |
| 7.41Si                                       | 4.0                                  | 3.2       | 6.8                                  | 5.2       | 4.8  |
| 6.53Si                                       | 5.1                                  | 6.0       | 9.0                                  | 5.7       | 6.5  |
| 0.18Fe                                       | 3.2                                  | 3.0       | 5.2                                  | 5.2       | 4.2  |
| 0.00Sr                                       | 2.5                                  | 1.8       | 5.5                                  | 4.2       | 3.5  |
| Nominal                                      | 5.8                                  | 4.1       | 5.3                                  | 3.6       | 4.7  |
| Average                                      | 4.3                                  | 3.8       | 6.4                                  | 6.0       | 5.1  |
| <u>(b) Outside Composition Specification</u> |                                      |           |                                      |           |      |
| 0.45Mg                                       | 11.2                                 | 7.6       | 13.6                                 | 6.3       | 9.7  |
| 0.00Ti                                       | 6.0                                  | 3.2       | 7.2                                  | 6.7       | 5.8  |
| 0.027Fe-0.0005Be                             | 10.9                                 | 6.8       | 10.1                                 | 5.6       | 8.3  |
| Average                                      | 9.3                                  | 5.9       | 10.3                                 | 6.2       | 7.9  |

(1) Other elements were mid-range of the specification

(2) Fe chill; 1440°F pour temperature

(3) Cu chill; 1380°F pour temperature

In summary, the UTS (WCS plates) was influenced only by solidification rate and aging procedures.

#### Tensile Yield Strength

Similar to the UTS, the yield strength (Table 23) was not significantly affected by composition. On average, the WCS plates had a slightly higher yield strength than the OCS plates (43.4 ksi versus 42.2 ksi, respectively). The variant that differed most from the overall average value was the low Mg (0.45 percent) variant (OCS), with a yield strength of 40.7 ksi. The solidification rate did not affect the yield strength of either the WCS or the OCS plates.

The aging conditions had the most significant effect on yield strength. The material aged at 335°F for 6 hours had a higher yield strength than that aged at 315°F for 12 hours. For the WCS plates the averages were 44.5 ksi and 42.2 ksi, respectively. For the OCS plates, the yield strength values were 43.0 ksi and 41.4 ksi, respectively.

In summary, the yield strength was influenced mainly by the aging conditions. The OCS plates had a slightly lower yield strength than those that were within the composition specification.

#### Elongation

The composition had a greater effect on elongation to failure (Table 24) than it had on either the ultimate or the yield strengths. The WCS variants that did not contain Sr had the lowest average value (3.5 percent). The OCS plates had the highest elongation, particularly the low Mg (9.7 percent) and the low Fe/Be (8.3 percent) variants.

The plates that were solidified at the faster rate had an average elongation of 6.2 percent (WCS) and 8.2 percent (OCS). For the WCS plates, the elongation for the rapidly solidified material was higher (6.2 percent) than those that were solidified more slowly (4.0 percent). For the OCS plates, the difference in elongation due to solidification rate was not

significant (7.8 percent and 8.2 percent for the slow and fast solidification rate plates, respectively).

For the WCS plates, the aging conditions had no effect on the average elongation. The values were 5.3 percent and 4.9 percent for the 315°F/12 hour and 335°F/6 hour combinations, respectively. For the OCS plates, the average elongation for the 335°F/6 hour aging combination plates was 6 percent, compared with 9.8 percent for those that were aged at 315°F for 12 hours.

In summary, composition, solidification rate, and aging condition (OCS plates only) all influenced the elongation to failure.

#### 5.3.4 Notched Tensile Strength and NTS/YS Ratio

The average NTS and NTS/YS ratio data for each plate are shown in Tables 25 and 26, respectively. The overall average NTS values for WCS and OCS material are 52.5 ksi and 54.9 ksi, respectively. The corresponding NTS/YS ratios are 1.21 and 1.30.

The Sr-free plates had a significantly lower NTS (44.1 ksi) than any other composition variant. The Sr-free material also had by far the lowest NTS/YS ratio (1.01). The modified Si particle morphology, which is due to the presence of Sr, clearly has a beneficial affect on the NTS and the NTS/YS ratio, indicating that Sr should significantly improve fracture toughness in those areas of a casting that do not benefit from being near a chill. The effect of Sr on Si particle morphology was shown in Figure 17. The effect of Sr on the NTS/YS ratio is plotted in Figure 18 for the WCS plates and shows that the highest NTS/YS ratio was obtained for material that contained about 0.013 percent Sr.

The low Fe/Be OCS variant had the highest NTS (58.5 ksi) and a NTS/YS ratio (1.34) that was significantly higher than the average value for the WCS material (1.21). The highest NTS/YS ratio (1.37) was obtained for the OCS low Mg material. These results indicate that the low OCS Fe/Be and Mg variants should each have excellent fracture toughness, which is consistent with the excellent ductility obtained for both variants.

TABLE 25. EFFECT OF PROCESS VARIABLES ON THE NOTCHED TENSILE STRENGTH OF D357-T6

| COMPOSITION(1)<br>(WT %)                     | AVERAGE NOTCHED TENSILE STRENGTH (ksi) |           |                          |           | AVG. |
|--|--|-----------|--------------------------|-----------|------|
|  | AGE                                    |           | AGE                      |           |      |
|  | (SLOW SOLIDIFICATION)(2)               |           | (FAST SOLIDIFICATION)(3) |           |      |
|  | 315°F/12HR                             | 335°F/6HR | 315°F/12HR               | 335°F/6HR |      |
| <u>(a) Within Composition Specification</u>  |  |           |                          |           |      |
| 0.19Ti-0.10Mn-0.053Be                        | 51.9                                   | 48.4      | 56.0                     | 56.9      | 53.3 |
| 0.07Ti-0.00Mn-0.04Be                         | 55.7                                   | 53.6      | 55.2                     | 58.9      | 55.9 |
| 0.60Mg                                       | 51.6                                   | 53.9      | 56.0                     | 56.9      | 54.6 |
| 0.56Mg                                       | 48.8                                   | 54.4      | 57.7                     | 58.1      | 54.7 |
| 7.41Si                                       | 51.1                                   | 52.2      | 53.0                     | 50.0      | 51.6 |
| 6.53Si                                       | 48.8                                   | 50.8      | 55.2                     | 56.0      | 52.7 |
| 0.18Fe                                       | 52.8                                   | 48.6      | 53.8                     | 52.3      | 51.9 |
| 0.00Sr                                       | 43.2                                   | 42.7      | 46.0                     | 44.4      | 44.1 |
| Nominal                                      | 55.9                                   | 52.4      | 55.8                     | 49.8      | 53.5 |
| Average                                      | 51.1                                   | 50.8      | 54.3                     | 53.7      | 52.5 |
| <u>(b) Outside Composition Specification</u> |  |           |                          |           |      |
| 0.45Mg                                       | 58.0                                   | 55.1      | 56.0                     | 52.9      | 55.5 |
| 0.00Ti                                       | 52.9                                   | 44.9      | 51.2                     | 54.1      | 50.8 |
| 0.027Fe-0.0005Be                             | 61.2                                   | 57.0      | 57.5                     | 58.0      | 58.5 |
| Average                                      | 57.4                                   | 52.4      | 54.9                     | 55.0      | 54.9 |

(1) Other elements were mid-range of the specification

(2) Fe chill; 1440°F pour temperature

(3) Cu chill; 1380°F pour temperature

TABLE 26. EFFECT OF PROCESS VARIABLES ON THE NTS/YS RATIO OF D357-T6

| COMPOSITION(1)<br>(WT %)                     | AVERAGE NTS/YS RATIO     |           |                          |           | AVG. |
|--|--------------------------|-----------|--------------------------|-----------|------|
|  | AGE                      |           | AGE                      |           |      |
|  | (SLOW SOLIDIFICATION)(2) |           | (FAST SOLIDIFICATION)(3) |           |      |
|  | 315°F/12HR               | 335°F/6HR | 315°F/12HR               | 335°F/6HR |      |
| <u>(a) Within Composition Specification</u>  |                          |           |                          |           |      |
| 0.19Ti-0.10Mn-0.053Be                        | 1.23                     | 1.11      | 1.34                     | 1.28      | 1.24 |
| 0.07Ti-0.00Mn-0.04Be                         | 1.33                     | 1.22      | 1.33                     | 1.32      | 1.30 |
| 0.60Mg                                       | 1.26                     | 1.21      | 1.30                     | 1.25      | 1.25 |
| 0.56Mg                                       | 1.16                     | 1.24      | 1.35                     | 1.26      | 1.25 |
| 7.41Si                                       | 1.22                     | 1.17      | 1.27                     | 1.14      | 1.20 |
| 6.53Si                                       | 1.17                     | 1.14      | 1.32                     | 1.27      | 1.22 |
| 0.18Fe                                       | 1.24                     | 1.08      | 1.24                     | 1.16      | 1.18 |
| 0.00Sr                                       | 1.02                     | 0.94      | 1.07                     | 1.00      | 1.01 |
| Nominal                                      | 1.31                     | 1.24      | 1.34                     | 1.11      | 1.25 |
| Average                                      | 1.21                     | 1.15      | 1.28                     | 1.20      | 1.21 |
| <u>(b) Outside Composition Specification</u> |                          |           |                          |           |      |
| 0.45Mg                                       | 1.45                     | 1.29      | 1.44                     | 1.29      | 1.37 |
| 0.00Ti                                       | 1.26                     | 1.07      | 1.22                     | 1.25      | 1.20 |
| 0.027Fe-0.0005Be                             | 1.43                     | 1.27      | 1.35                     | 1.31      | 1.34 |
| Average                                      | 1.38                     | 1.21      | 1.33                     | 1.28      | 1.30 |

(1) Other elements were mid-range of the specification

(2) Fe chill; 1440°F pour temperature

(3) Cu chill; 1380°F pour temperature

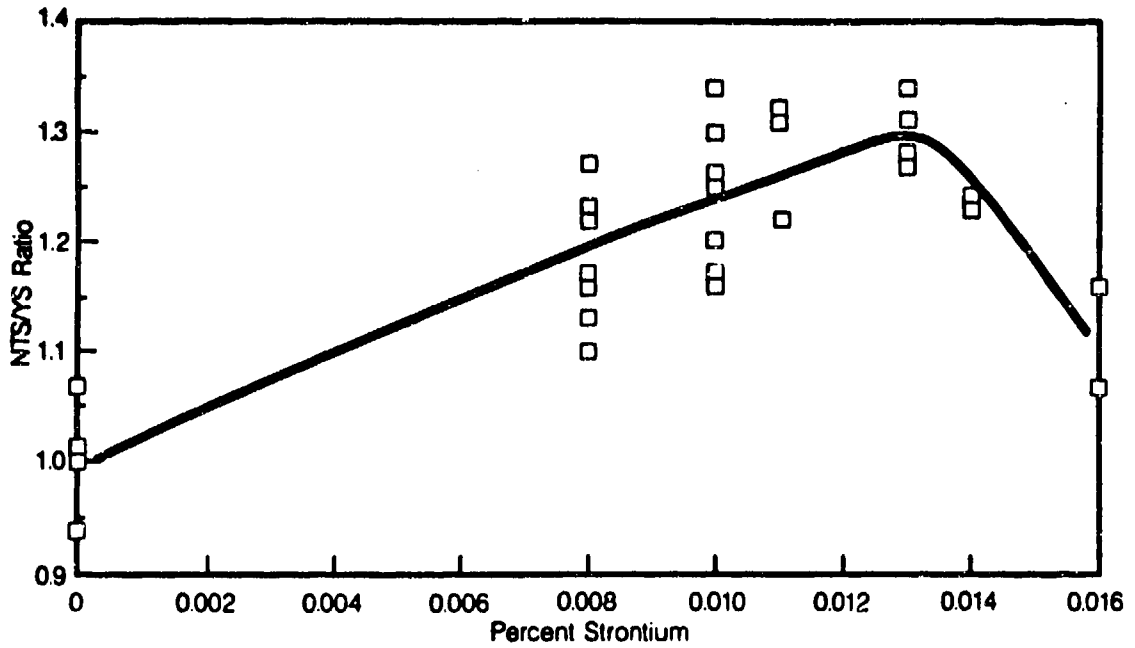


Figure 18. D357-T6 NTS/YS Ratio Versus Percent Strontium for Plates That Were Within the Composition Specification

The solidification rate also influenced both the NTS and the NTS/YS ratio. For the WCS plates, the NTS averaged 54 ksi and 51 ksi for the fast and slow solidification rates, respectively. For the OCS variants, the average NTS was the same for both solidification rates, about 55 ksi. The NTS/YS ratio was 1.24 for the fast solidification rate WCS material, compared with 1.18 for the slow solidification rate material. For the OCS variants, the NTS/YS ratio was the same (1.30) for the two solidification rates.

The aging conditions did not influence the NTS of the WCS material. The NTS for the 315°F/12 hour combination was, however, higher than the 335°F/6 hour material for the OCS variants, 56.1 ksi versus 53.7 ksi. The NTS/YS ratio was slightly higher for the 315°F/12 hour aging condition than for the 335°F/6 hour age for both the WCS (1.24 and 1.17) and the OCS (1.35 and 1.24) variants. The variations in the NTS/YS ratio were due to the change in yield strength with aging condition.

In summary, NTS and NTS/YS ratio improvements were obtained by including Sr to modify the Si particle morphology. The fast solidification rate was also beneficial, compared with the slower rate. Low levels of Mg and Fe/Be in specific OCS plate variants resulted in high NTS and NTS/YS ratio values.

#### 5.3.5 Fatigue Life

The fatigue life data are summarized in Table 27 for plates that were both within and outside the composition specification. All the data in Table 27 are log averages of the fatigue life results for each plate. A minimum of two specimens were tested for each plate. Additional tests were conducted where a considerable discrepancy between the two test results was obtained. All fatigue tests were conducted under constant amplitude loading using a net maximum stress of 20 ksi, and an R ratio of 0.1.

Significant scatter of the fatigue life data for individual specimens was obtained, which is typical for most materials. The precise location of casting defects in the specimen influences fatigue life, which would be shorter if the defects were located near the area of peak stress (near the hole). The overall averages were  $117 \times 10^3$  and  $66 \times 10^3$  cycles to failure for

TABLE 27. EFFECT OF PROCESS VARIABLES ON THE FATIGUE LIFE OF D357-T6

| COMPOSITION <sup>(1)</sup>                   | LOG AVERAGE FATIGUE LIFE ( $10^3$ CYCLES TO FAILURE)* |           |                                      |           | AVERAGE |
|--|---|-----------|--------------------------------------|-----------|---------|
|  | AGE   |           | AGE                                  |           |         |
|  | (SLOW SOLIDIFICATION) <sup>(2)</sup>                  |           | (FAST SOLIDIFICATION) <sup>(3)</sup> |           |         |
|  | 315°F/12HR  | 335°F/6HR | 315°F/12HR                           | 335°F/6HR |         |
| <u>(a) Within Composition Specification</u>  |   |           |                                      |           |         |
| 0.19Ti-0.10Mn-0.053Be                        | 98  | 104       | 193                                  | 222       | 149     |
| 0.07Ti-0.00Mn-0.04Be                         | 168   | 136       | 163                                  | 199       | 165     |
| 0.60Mg                                       | 78  | 102       | 373                                  | 165       | 150     |
| 0.56Mg                                       | 145   | 86        | 620                                  | 523       | 252     |
| 7.41Si                                       | 66  | 59        | 117                                  | 58        | 76      |
| 6.53Si                                       | 94  | 131       | 103                                  | 92        | 104     |
| 0.18Fe                                       | 70  | 84        | 102                                  | 350       | 118     |
| 0.00Sr                                       | 53  | 75        | 175                                  | 79        | 99      |
| Nominal                                      | 57  | 66        | 40                                   | 44        | 51      |
| Log Average                                  | 85  | 90        | 156                                  | 144       | 117     |
| <u>(b) Outside Composition Specification</u> |   |           |                                      |           |         |
| 0.45Mg                                       | 78  | 59        | 88                                   | 56        | 69      |
| 0.00Ti                                       | 78  | 54        | 56                                   | 71        | 64      |
| 0.027Fe-0.0005Be                             | 82  | 73        | 53                                   | 54        | 64      |
| Log Average                                  | 79  | 62        | 64                                   | 60        | 66      |

\* Specimen with a hole;  $K_t = 2.42$ ; net maximum stress = 20 ksi

(1) Other elements were mid-range of the specification

(2) Fe chill; 1440°F pour temperature

(3) Cu chill; 1380°F pour temperature

the WCS and OCS materials, respectively. There were differences in fatigue life between the composition variants that were at the maximum and minimum composition limits for a given alloying element or group of elements. However, because of the scatter in the results, differences in the average fatigue life values for the compositional variants shown in Table 27 were considered to be insignificant.

The WCS material that was solidified at the faster rate had a longer average fatigue life ( $150 \times 10^3$  cycles) compared with that for the slow solidification rate material ( $88 \times 10^3$  cycles). This higher average fatigue life is attributed to a lower percentage porosity in these plates (0.011 percent) compared with the material solidified more slowly (0.035 percent) as shown in Table 21. Fatigue cracks typically initiate at pores in casting alloys [11].

No significant effect of aging conditions on the fatigue life of the WCS variants was apparent.

Even considering the large amount of scatter in the data, the average fatigue life for the OCS plates ( $66 \times 10^3$  cycles to failure) was significantly shorter than that of the WCS plates. No significant effects of composition, solidification rate, or aging conditions were observed.

In summary, the fatigue life of the WCS D357-T6 appears to be related to the percent porosity, even though all the plates were Grade B, or better.

#### 5.3.6 Regression Analysis

Linear and nonlinear regression analyses were conducted as described in Section 5.2.4. The results are summarized in Table 28. The percent variation in each dependent variable (e.g., mechanical property) explained by the independent variables in the linear analysis (e.g., composition) are listed. The individual contributions of the independent variables in the nonlinear analysis are not shown because they cannot be defined due to the cross-correlation terms generated. However, the total contribution of the relevant variables is listed. In general, the results of the regression analyses

TABLE 28. LINEAR AND NONLINEAR REGRESSION ANALYSIS RESULTS FOR D357-T6

| PROPERTY                 | LINEAR (1)                                       |                     |    |    |    |    |    |    |                               |                               |    | NONLINEAR (2) |
|--------------------------|--|---------------------|----|----|----|----|----|----|-------------------------------|-------------------------------|----|---------------|
|                          | PERCENT VARIATION EXPLAINED BY PROCESS VARIABLES |                     |    |    |    |    |    |    |                               |                               |    |               |
|                          | AGING PARAMETERS                                 | SOLIDIFICATION RATE | Mg | Sr | Fe | Be | Si | Mn | TOTAL VARIATION EXPLAINED (%) | TOTAL VARIATION EXPLAINED (%) |    |               |
| UTS                      | 12   | 13                  | -  | -  | -  | -  | -  | -  | -                             | 25                            | 0  |               |
| YS                       | 50   | -                   | 15 | -  | 14 | 5  | -  | -  | -                             | 84                            | 77 |               |
| EL                       | -  | 13                  | 25 | -  | -  | -  | -  | -  | -                             | 38                            | 60 |               |
| NTS                      | -  | -                   | -  | 37 | -  | 7  | -  | -  | -                             | 44                            | 81 |               |
| NTS/YS                   | 16   | -                   | 8  | 31 | 13 | -  | -  | -  | -                             | 68                            | 78 |               |
| FATIGUE LIFE             | -  | 11                  | -  | -  | 9  | -  | -  | -  | -                             | 20                            | 57 |               |
| DAS (3)                  | -  | -                   | -  | -  | -  | -  | 11 | 22 | -                             | 33                            | 47 |               |
| PERCENT POROSITY         | -  | -                   | -  | -  | -  | -  | -  | -  | -                             | 0                             | 14 |               |
| Si PARTICLE AREA         | -  | -                   | -  | 55 | 4  | -  | 6  | -  | -                             | 65                            | 92 |               |
| Si PARTICLE ASPECT RATIO | -  | -                   | -  | 52 | 8  | -  | 4  | -  | -                             | 64                            | 76 |               |
| Si PARTICLE SPACING      | -  | -                   | -  | 32 | -  | -  | -  | 14 | -                             | 46                            | 68 |               |

(1) 5% error level  
 (2) 1% error level  
 (3) At the edge of the plate

support the overall trends observed from the data discussed in previous subsections.

The effect of aging condition consisted of concurrently varying temperature and time and is represented in the regression analyses only by the aging temperature for the two temperature/time combinations evaluated (335°F/6 hours and 315°F/12 hours). The solidification rate was represented by the average DAS for the fast (0.0021 inch) and slow (0.0024 inch) rates at a point midway between the center and edge of the plate (Figure 16).

All the WCS and OCS data were included in the data set. The results for the linear and nonlinear analyses are discussed separately below.

#### Linear Analysis

The criterion used to accept or reject the contribution of an independent variable to the variation of the dependent variable was a 5 percent probability of error. This large percentage was chosen so that the best indication of the contributing variables could be determined.

The dependent variables with the largest explained variations were yield strength, NTS, NTS/YS ratio, and Si particle size area, spacing, and aspect ratio. With the exception of yield strength, the Sr content had the most significant effect on these parameters. The yield strength was primarily influenced by the aging parameters (50 percent) with smaller contributions from Mg (15 percent) and Fe (14 percent).

Other significant contributions to the variation in the dependent variables were elongation (25 percent - Mg), and DAS at the edge of the plate (22 percent - Mn). The relationship observed earlier (Section 5.3.2) between solidification rate and percent porosity was not confirmed by the regression analysis.

## Nonlinear Analysis

A tighter acceptance/rejection criterion of one percent was used in this analysis. Despite this fact, the total percentage variation explained by the nonlinear analysis was usually greater than that determined by the linear analysis. If the nonlinear percentage is lower but similar to the linear value, a linear relationship is indicated. If the nonlinear percentage is greater than the linear percentage, the increase is due to the inclusion of second-order and/or cross-product terms. For example, the total percent variation in the NTS/YS ratio increased from 68 percent (linear analysis) to 78 percent (nonlinear analysis). By plotting the data (Figure 18), it was shown that a nonlinear relationship existed between the NTS/YS ratio and the Sr content.

Other increases in the total percent variation explained were noted for elongation, NTS, fatigue life, DAS, and Si particle area, aspect ratio, and spacing, indicating nonlinear relationships.

The UTS showed a reduction in the percent variation explained from 25 percent (linear) to zero percent (nonlinear). This reduction is probably due to the tighter (1 percent) error level for the nonlinear analysis and the fact that the linear correlation was relatively weak. For the percent porosity, the percent variation explained increased from zero percent (linear) to 14 percent (nonlinear). Even the latter is too small to indicate a significant correlation between percent porosity and any of the independent variables.

### 5.4 CONCLUSIONS

The combined conclusions from both the tabulated data and the regression analyses regarding the effect of process variables on the mechanical properties and microstructural features of D357-T6 are as follows:

#### 1. Composition

- The addition of Sr improved:

- Si particle morphology of material that was not under the chill
- NTS and NTS/YS ratio (up to 0.013 percent Sr) and ductility
- Low Fe/Be and Mg material (OCS) had the highest ductility and NTS/YS ratio
- Low Fe/Be material (OCS) had the highest NTS
- Low Mg material (OCS) had the lowest yield strength and highest ductility

2. Solidification Rate

- The faster solidification rate (Cu chill) improved ultimate strength, ductility, NTS, NTS/YS ratio, and the fatigue life of the WCS plates
- There was no significant effect of solidification rate on the properties of OCS plates

3. Aging Temperature/Time

- The yield strength was higher for the 335°F/6 hours aging condition than for 315°F/12 hours (WCS and OCS plates)
- Ductility, NTS, and the NTS/YS ratio were higher for the OCS plates that were aged at 315°F for 12 hours than those aged at 335°F for 6 hours

4. Property Optimization

The requirements for optimizing the DADT and tensile properties of D357-T6 do not conflict.

5.5 RECOMMENDATIONS

1. To obtain the best balance of mechanical properties, the approved AMS 4241 specification, with the addition of a Si modifier, such as Sr, should be used for producing the Task 2, Phase I, D357-T6 verification plates and for the remainder of the DADTAC program.

2. The plates for subsequent characterization of DADT properties should have a DAS below 0.0024 inch in designated areas.
  
3. D357-T6 should be solution treated according to AMS 4241 [1] ( $1010 \pm 10^\circ\text{F}$ ). The quenching and precipitation heat treatment procedure should be established by the foundry to achieve the required casting properties.

SECTION 6  
PHASE I, TASK 2 - B201-T7 SCREENING TESTS

6.1 INTRODUCTION

The overall objective, procedures, and test methods for the B201-T7 screening test subtask were the same as those described in Section 5.1 for D357-T6. The composition for the cast plates was based on the AMS 4242 (Draft 40GD) specification [2]. The target tensile properties were 60 ksi UTS, 50 ksi YS, and 3 percent elongation. Average properties are presented in Section 6; individual test results are included in Appendix B.

6.2 EXPERIMENTAL PROCEDURES

6.2.1 Process Variables

Thirty-two plates with variations of composition, solidification rate, and aging parameters were produced by Hitchcock Industries. Twenty-four plates were within the AMS 4242 composition specification; the remaining eight plates were intentionally outside the specification to strengthen the regression analysis. Each plate was 0.75 inch thick x 6 inches wide x 12 inches long. The same pattern, and gating and risering systems were used to produce each plate. Figure 19 shows the orientation of the gates, risers, and chills (drag only) used to produce these plates.

The plates were produced using the composition specification AMS 4242 (Draft 40GD), which is shown in Table 29. This initial draft was subsequently modified and approved for general release. The modifications were (1) a change in the range for Ag from 0.5-1.0 percent to 0.4-0.8 percent, and (2) the Mg range was changed from 0.25-0.35 percent to 0.20-0.30 percent.

A summary of the B201 composition variations evaluated is shown in Table 30.

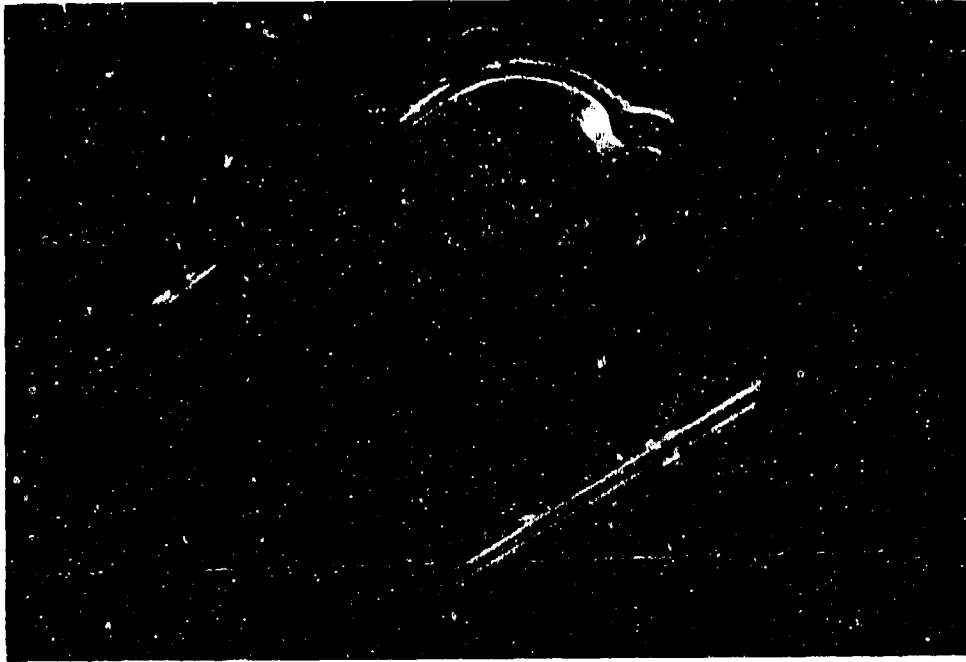


Figure 19. Gating, Riser, and Chill Placement Used for the B201 Process Variable Plates

TABLE 29. COMPOSITION SPECIFICATION FOR THE B201-T7 SCREENING PLATES

| ELEMENT <sup>(1)</sup> | RANGE (WT %) |      |
|------------------------|--------------|------|
|                        | MIN.         | MAX. |
| Copper                 | 4.5          | 5.0  |
| Silver                 | 0.5          | 1.0  |
| Maganese               | 0.20         | 0.50 |
| Magnesium              | 0.25         | 0.35 |
| Titanium               | 0.15         | 0.35 |
| Iron                   | --           | 0.05 |
| Silicon                | --           | 0.05 |
| Others, each           | --           | 0.05 |
| Others, total          | --           | 0.15 |
| Aluminum               | Balance      |      |

(1) AMS 4242 (Draft 40GD)

TABLE 30. COMPOSITION VARIATIONS FOR THE B201-T7 SCREENING PLATES

| COMPOSITION VARIABLES | DEVIATION FROM MID-RANGE OF<br>COMPOSITION SPECIFICATION <sup>(1)</sup> |      |      |       |
|-----------------------|---|------|------|-------|
|                       | BELOW   |      |      | ABOVE |
|                       | MIN.  | MIN. | MAX. | MAX.  |
| Ti, Mn                | (2)   | X    | (2)  | X     |
| Cu, Ag, Mg            | (2)   | X    | X    | X     |
| Fe, Si                | (2)   | (2)  | (2)  | X     |
| Ti                    | X   | (2)  | (2)  | (2)   |
| Nominal               |   |      |      |       |

(1) AMS 4242

(2) Not evaluated

It was not possible to vary all the key elements individually; Ti-Mn, Cu-Ag-Mg, and Fe-Si were combined to form three groups of elements. The target for those elements not being specifically varied was the middle of the allowed composition range.

Two different solidification rates were achieved by varying the pour temperature and chill material. Copper or iron chills were placed along the center of the plates and pour temperatures of 1350°F and 1450°F, respectively, were used to obtain two solidification rates. Similar to D357, the Cu- and Fe-chilled B201 plates are referred to in this report as fast and slow solidification rate plates, respectively.

All plates were hot isostatically pressed (HIPed) to reduce the amount of microshrinkage that can sometimes be present in B201. This step was taken to reduce the number of potential sites for fatigue crack initiation. HIPing was undertaken by step heating the plates up to 950°F and holding for 3 hours in an inert gas atmosphere at 15,000 psi. Improvements in mechanical properties, particularly fatigue life, were previously demonstrated [12].

All 32 plates were solution treated identically. They were held at 940°F for 2 hours, 960°F for 2 hours, and 980°F for 16 hours and then quenched in room temperature water with a maximum quench delay time of 8 seconds.

The effect of two different aging temperature/time combinations was evaluated. These were (1) 360 ± 5°F for 8 hours, and (2) 380 ± 5°F for 5 hours. These combinations were selected following consultations with foundries as being within the range of temperatures and times typically used for aging B201 castings to the T7 condition.

The variations in the three process variables (composition, solidification rate, and aging parameters) provided a total of 32 combinations, as shown in Table 31.

All plates were Grade B, or better, according to MIL-A-2175. The inspection and composition verification procedures were the same as those for D357, described in Section 5.2.1.

TABLE 31. PROCESS VARIABLES FOR THE B201-T7 SCREENING PLATES

| COMPOSITION(1) | SLOW SOLIDIFICATION |           | FAST SOLIDIFICATION |           |
|----------------|---------------------|-----------|---------------------|-----------|
|                | AGING PARAMETERS    |           | AGING PARAMETERS    |           |
|                | 360°F/8Hr           | 380°F/5Hr | 360°F/8Hr           | 380°F/5Hr |
| Ti, Mn         |                     |           |                     |           |
| Max.           | X                   | X         | X                   | X         |
| Min.           | X                   | X         | X                   | X         |
| Cu, Ag, Mg     |                     |           |                     |           |
| Max.           | X                   | X         | X                   | X         |
| Min.           | X                   | X         | X                   | X         |
| Above Max.     | X                   | X         | X                   | X         |
| Fe, Si         |                     |           |                     |           |
| Max.           | X                   | X         | X                   | X         |
| Ti             |                     |           |                     |           |
| Below Min.     | X                   | X         | X                   | X         |
| Nominal        | X                   | X         | X                   | X         |

(1) Other elements were mid-range of the specification (AMS 4242)

Note: Each "X" represents one cast plate (total of 32 plates)

### 6.2.2 Test Procedures

The B201 screening tests were identical to those described in Section 5.2.2 for D357 except that the net maximum stress for the constant amplitude fatigue life testing was raised to 25 ksi.

### 6.2.3 Microstructural Characterization

The grain size was measured at both the edge and the center (under the chill) of each plate. The percent porosity in each plate was also determined, using image analysis. The effectiveness of the HIPing in reducing the amount of microshrinkage was confirmed by determining the ultrasonic attenuation in each plate both before and after HIPing.

### 6.2.4 Data Analysis

Data were analyzed as described in Section 5.2.4 for D357.

## 6.3 RESULTS AND DISCUSSION

The hardness and conductivity values for each plate were taken after solution heat treatment (SHT) and again after aging. The average hardness (Rockwell B) of the 24 WCS plates was 60 after SHT and 82 after aging. For the OCS plates, the values were 67 and 91, respectively. The conductivity (percent of IACS) for the WCS materials was 28 percent (SHT) and 33 percent (aged). For the OCS plates, the corresponding values were 32 percent and 33 percent. The properties are summarized and discussed in the following subsections. Data averaging was the same as described for D357 in Section 5.3.

### 6.3.1 Composition

Melt analyses were supplied by Hitchcock Industries and confirmed by Northrop. Four plates were made for each composition variant (Table 31). The average contents of the alloying elements that were specifically controlled

are summarized in Table 32. The target for the elements that were not specifically controlled was the mid-range of the specification.

### 6.3.2 Microstructure

The grain size and percent porosity were determined at two locations in each plate, under the chill and at the edge of the plate. The results are discussed below.

#### Grain Size

The grain size results are presented in Table 33. The overall WCS average grain size was 0.0042 inch under the chill and 0.0046 inch at the edge of the plate. Composition had a noticeable effect on these values. The variants with high levels of Ti/Mn or Fe/Si had the smallest average grain sizes. The low Ti/Mn and Cu/Ag/Mg variants had larger-than-average grain sizes. The observed effect of varying the Ti/Mn content is to be expected because Ti is added as a grain refiner. The Ti was added to each melt with the same delay time before pouring. Thus, the observed effect of Ti is not due to variations in the residence time in the melt before pouring.

The solidification rate had the anticipated effect; the faster rate produced a smaller average grain size at the chill (0.0038 inch) than the slower rate (0.0047 inch). The effect of solidification rate was much more pronounced for the low Ti/Mn than for the high Ti/Mn variant, as might be expected. The high levels produced a small grain size even when the solidification rate was slow, indicating that the grain size was relatively independent of solidification rate. The grain size of the high Fe/Si variant was also relatively independent of solidification rate.

For the OCS plates, the overall average grain size was 0.0064 inch, both under the chill and at the edge of the plate. The average values for the high Ag-Cu-Mg variants were especially high. The values for the very low Ti variant were similar to those for the WCS plates that had a Ti level near the specification minimum.

TABLE 32. COMPOSITION OF THE B201 SCREENING PLATES

| ELEMENT<br>CONTENT(1) | ELEMENT (WT %) |                |             |       |
|-----------------------|----------------|----------------|-------------|-------|
|                       | Ti-Mn          | Cu-Ag-Mg       | Fe-Si       | Ti    |
| Above Max.            | (2)            | 5.25-1.45-0.43 | (2)         | (2)   |
| Max.                  | 0.35-0.43      | 4.95-0.98-0.32 | 0.041-0.043 | (2)   |
| Min.                  | 0.19-0.24      | 4.65-0.57-0.26 | (2)         | (2)   |
| Below Min.            | (2)            | (2)            | (2)         | 0.052 |

(1) All other elements were mid-range of the specification

(2) Not evaluated

Note: Plates of nominal composition were also evaluated

TABLE 33. EFFECT OF PROCESS VARIABLES ON THE GRAIN SIZE OF B201-T7

| COMPOSITION(1)                               | SPECIMEN<br>LOCATION | GRAIN SIZE (10 <sup>-4</sup> IN.) |           |                          |           | AVG. |
|--|----------------------|-----------------------------------|-----------|--------------------------|-----------|------|
|  |                      | AGE                               |           | AGE                      |           |      |
|  |                      | (SLOW SOLIDIFICATION)(2)          |           | (FAST SOLIDIFICATION)(3) |           |      |
|  |                      | 360°F/8HR                         | 380°F/5HR | 360°F/8HR                | 380°F/5HR |      |
| <u>(a) Within Composition Specification</u>  |                      |                                   |           |                          |           |      |
| 0.35Ti-0.43Mn                                | Chill                | 24                                | 33        | 28                       | 24        | 27   |
|  | Edge                 | 33                                | 33        | 28                       | 24        | 30   |
| 0.19Ti-0.24Mn                                | Chill                | 67                                | 79        | 33                       | 33        | 53   |
|  | Edge                 | 67                                | 79        | 47                       | 33        | 57   |
| 4.95Cu-0.98Ag<br>-0.32Mg                     | Chill                | 40                                | 47        | 40                       | 47        | 44   |
|  | Edge                 | 56                                | 56        | 33                       | 47        | 48   |
| 4.65Cu-0.57Ag<br>-0.26Mg                     | Chill                | 47                                | 57        | 40                       | 47        | 48   |
|  | Edge                 | 67                                | 67        | 33                       | 47        | 54   |
| 0.041Fe-0.043Si                              | Chill                | 20                                | 24        | 33                       | 28        | 26   |
|  | Edge                 | 28                                | 28        | 40                       | 28        | 31   |
| Nominal                                      | Chill                | 55                                | 70        | 50                       | 55        | 58   |
|  | Edge                 | 60                                | 60        | 55                       | 60        | 58   |
| Average                                      | Chill                | 42                                | 52        | 38                       | 38        | 42   |
|  | Edge                 | 52                                | 54        | 39                       | 39        | 46   |
| <u>(b) Outside Composition Specification</u> |                      |                                   |           |                          |           |      |
| 0.052Ti                                      | Chill                | 47                                | 56        | 47                       | 56        | 52   |
|  | Edge                 | 56                                | 67        | 47                       | 56        | 57   |
| 5.25Cu-1.45Ag-<br>0.43Mg                     | Chill                | 90                                | 70        | 70                       | 75        | 76   |
|  | Edge                 | 75                                | 70        | 65                       | 70        | 70   |
| Average                                      | Chill                | 69                                | 63        | 59                       | 66        | 64   |
|  | Edge                 | 66                                | 69        | 56                       | 63        | 64   |

(1) Other elements were mid-range of the specification

(2) Fe chill; 1450°F pour temperature

(3) Cu chill; 1350°F pour temperature

### Percent Porosity

Similar to the D357 screening plates, an assessment of the percent porosity present in each B201 plate was obtained using the microstructure specimen excised from underneath the chill. Unlike D357, almost no gas or shrinkage porosity was detected in any of the 20 B201 plates. Microshrinkage porosity was sealed by HIPing. Ultrasonic attenuation measurements taken both before and after HIPing confirmed the reduction of microshrinkage. The average ultrasonic attenuation was reduced from 3.21 to 0.59 dB/cm by HIPing.

### 6.3.3 Tensile Properties

Tensile properties are summarized in Tables 34, 35, and 36. The overall average WCS tensile properties were 65 ksi (UTS), 59 ksi (YS), and seven percent elongation, which were significantly higher than the target values (60/50/3). The equivalent values for the OCS plates were 72 ksi (UTS), 67 ksi (YS) and three percent elongation. Stress corrosion tests were conducted on B201 from both aging conditions to confirm that the material was in the overaged (T7) condition. Specimens were exposed for 30 days to alternate immersion in salt water at a stress of 37.5 ksi. No failures were experienced. The results for each of the three tensile properties are discussed separately below.

#### Ultimate Strength

The UTS (Table 34) was highest for those variants that had the highest levels of Cu/Ag/Mg (69.6 ksi average). This is as expected because these are the main strengthening elements added to B201. The lowest UTS (62.3 ksi) was obtained for the plates that contained the maximum levels of Fe and Si impurities. The UTS of the low Ti/Mn variant was slightly greater than that of the high Ti/Mn variant, 65.8 ksi versus 63.3 ksi.

The UTS was slightly higher for material solidified at the faster rate than for slower solidification rate material (66 ksi versus 64 ksi). The UTS was slightly higher (66 ksi) for the plates that were aged at 360°F for 8 hours than those aged at 380°F for 5 hours (64 ksi).

TABLE 34. EFFECT OF PROCESS VARIABLES ON THE ULTIMATE TENSILE STRENGTH OF B201-T7

| COMPOSITION <sup>(1)</sup><br>(WT %)         | AVERAGE ULTIMATE TENSILE STRENGTH (ksi) |           |                                      |           | AVG. |
|--|---|-----------|--------------------------------------|-----------|------|
|  | AGE                                     |           | AGE                                  |           |      |
|  | (SLOW SOLIDIFICATION) <sup>(2)</sup>    |           | (FAST SOLIDIFICATION) <sup>(3)</sup> |           |      |
|  | 360°F/8HR                               | 380°F/5HR | 360°F/8HR                            | 380°F/5HR |      |
| <u>(a) Within Composition Specification</u>  |   |           |                                      |           |      |
| 0.35Ti-0.43Mn                                | 64.3                                    | 61.4      | 65.0                                 | 62.4      | 63.3 |
| 0.19Ti-0.24Mn                                | 66.5                                    | 65.6      | 66.1                                 | 65.2      | 65.8 |
| 4.95Cu-0.98Ag-0.32Mg                         | 70.1                                    | 69.3      | 69.8                                 | 69.2      | 69.6 |
| 4.65Cu-0.57Ag-0.26Mg                         | 65.2                                    | 64.7      | 65.1                                 | 63.8      | 64.7 |
| 0.041Fe-0.043Si                              | 64.5                                    | 60.0      | 64.3                                 | 60.3      | 62.3 |
| Nominal                                      | 60.4                                    | 59.6      | 71.3                                 | 69.6      | 65.2 |
| Average                                      | 65.2                                    | 63.4      | 66.9                                 | 65.1      | 65.1 |
| <u>(b) Outside Composition Specification</u> |   |           |                                      |           |      |
| 0.052Ti                                      | 68.6                                    | 67.2      | 69.0                                 | 67.6      | 68.1 |
| 5.25Cu-1.45Ag-0.43Mg                         | 74.4                                    | 74.0      | 77.5                                 | 75.9      | 75.5 |
| Average                                      | 71.5                                    | 70.6      | 73.2                                 | 71.8      | 71.8 |

(1) Other elements were mid-range of the specification

(2) Fe chill; 1450°F pour temperature

(3) Cu chill; 1350°F pour temperature

TABLE 35. EFFECT OF PROCESS VARIABLES ON THE YIELD STRENGTH OF B201-T7

| COMPOSITION <sup>(1)</sup><br>(WT %)         | AVERAGE YIELD STRENGTH (ksi)         |           |                                      |           | AVG. |
|--|--------------------------------------|-----------|--------------------------------------|-----------|------|
|  | AGE                                  |           | AGE                                  |           |      |
|  | (SLOW SOLIDIFICATION) <sup>(2)</sup> |           | (FAST SOLIDIFICATION) <sup>(3)</sup> |           |      |
|  | 360°F/8HR                            | 380°F/5HR | 360°F/8HR                            | 380°F/5HR |      |
| <u>(a) Within Composition Specification</u>  |                                      |           |                                      |           |      |
| 0.35Ti-0.43Mn                                | 59.2                                 | 56.1      | 58.5                                 | 56.0      | 57.5 |
| 0.19Ti-0.24Mn                                | 61.0                                 | 59.8      | 60.3                                 | 59.0      | 60.0 |
| 4.95Cu-0.98Ag-0.32Mg                         | 64.8                                 | 63.5      | 63.8                                 | 63.2      | 63.8 |
| 4.65Cu-0.57Ag-0.26Mg                         | 58.5                                 | 57.4      | 58.1                                 | 56.4      | 57.6 |
| 0.041Fe-0.043Si                              | 59.0                                 | 55.5      | 58.7                                 | 55.5      | 57.2 |
| Nominal                                      | 59.7                                 | 58.3      | 62.7                                 | 62.0      | 60.7 |
| Average                                      | 60.4                                 | 58.4      | 60.4                                 | 58.7      | 59.5 |
| <u>(b) Outside Composition Specification</u> |                                      |           |                                      |           |      |
| 0.052Ti                                      | 64.0                                 | 62.4      | 64.1                                 | 62.5      | 63.2 |
| 5.25Cu-1.45Ag-0.43Mg                         | 72.5                                 | 70.1      | 72.4                                 | 69.8      | 71.2 |
| Average                                      | 68.2                                 | 66.2      | 68.2                                 | 66.2      | 67.2 |

(1) Other elements were mid-range of the specification

(2) Fe chill; 1450°F pour temperature

(3) Cu chill; 1350°F pour temperature

TABLE 36. EFFECT OF PROCESS VARIABLES ON THE ELONGATION OF B201-T7

| COMPOSITION <sup>(1)</sup><br>(WT %)         | AVERAGE ELONGATION (%)               |                    |                                      |           | AVG. |
|--|--------------------------------------|--------------------|--------------------------------------|-----------|------|
|  | AGE                                  |                    | AGE                                  |           |      |
|  | (SLOW SOLIDIFICATION) <sup>(2)</sup> |                    | (FAST SOLIDIFICATION) <sup>(3)</sup> |           |      |
|  | 360°F/8HR                            | 380°F/5HR          | 360°F/8HR                            | 380°F/5HR |      |
| <u>(a) Within Composition Specification</u>  |                                      |                    |                                      |           |      |
| 0.35Ti-0.43Mn                                | 7.2                                  | 5.2                | 10.7                                 | 2.3       | 6.3  |
| 0.19Ti-0.24Mn                                | 6.2                                  | 6.1                | 9.6                                  | 9.5       | 7.9  |
| 4.95Cu-0.98Ag-0.32Mg                         | 4.4                                  | 6.0                | 8.7                                  | 7.3       | 6.6  |
| 4.65Cu-0.57Ag-0.26Mg                         | 7.2                                  | 8.8                | 9.5                                  | 9.7       | 8.8  |
| 0.041Fe-0.043Si                              | 7.0                                  | 5.7                | 8.6                                  | 7.2       | 7.1  |
| Nominal                                      | 0.3                                  | 0.5                | 9.3                                  | 8.3       | 4.6  |
| Average                                      | 6.4 <sup>(4)</sup>                   | 6.3 <sup>(4)</sup> | 9.4                                  | 7.4       | 6.9  |
| <u>(b) Outside Composition Specification</u> |                                      |                    |                                      |           |      |
| 0.052Ti                                      | 3.0                                  | 2.9                | 3.2                                  | 3.1       | 3.1  |
| 5.25Cu-1.45Ag-0.43Mg                         | 1.4                                  | 2.4                | 5.7                                  | 5.3       | 3.7  |
| Average                                      | 2.2                                  | 2.6                | 4.5                                  | 4.2       | 3.4  |

(1) Other elements were mid-range of the specification

(2) Fe chill; 1450°F pour temperature

(3) Cu chill; 1350°F pour temperature

(4) Data for the nominal composition variant were not used to compute the average value because they were below the minimum specification requirement

In summary, the UTS of the WCS variants was slightly influenced by composition, aging conditions, and solidification rate.

The UTS of both the OCS variants was higher than the average for the WCS plates, particularly the above-maximum levels of Ag-Cu-Mg, the main strengthening elements. The effects of solidification rate and aging conditions were similar to those for the WCS plates. Increased solidification rate (72.6 ksi versus 71.0) and the 360°F/8 hour age (72.4 versus 71.2) gave a higher UTS.

### Yield Strength

The WCS yield strength (Table 35) was dependent upon the levels of Cu/Ag/Mg and Ti/Mn. The average yield strength was 58 ksi for the low Cu/Ag/Mg levels and 64 ksi for the maximum levels. The high Ti/Mn variant had an average yield strength of 58 ksi, while the low Ti/Mn variant had an average yield strength of 60 ksi. The lowest average yield strength (57 ksi) was obtained for the high Fe/Si material.

There was no significant effect of solidification rate on yield strength.

A slight difference in yield strength was observed for the two aging conditions; the 360°F/8hr age gave a higher value (60 ksi) than that for material aged at 380°F for 5 hours (58 ksi). This was similar to the trend observed by the UTS.

In summary, the yield strength of the WCS B201-T7 variants was influenced by composition and the aging conditions.

The yield strength for the OCS material was much higher than the WCS variant, particularly for the above-maximum Ag-Cu-Mg plates. Similar to the WCS material, the yield strength was influenced by the aging conditions.

### Elongation.

The elongation to failure of the WCS variants showed (Table 36) a dependence upon composition. At the higher Cu/Ag/Mg content, the elongation was less than that at the lower Cu/Ag/Mg level, 6.6 percent versus 8.8 percent, respectively. The low Ti/Mn variant had an elongation slightly greater than that of the high Ti/Mn variant, 7.9 percent versus 6.3 percent. The nominal composition material that was solidified at the lower rate had a very low ductility (0.5 percent), which is clearly anomalous. One of the low ductility specimens was metallographically examined; extensive porosity with oxidized pore surfaces was observed, which probably resulted in the low ductility.

Higher elongation values were obtained at the faster solidification rate (eight percent versus six percent). The elongation to failure was essentially independent of the aging combinations.

In summary, the elongation to failure of the WCS material was mainly influenced by composition and by the solidification rate.

The average ductility of both of the OCS variants was low. Solidification rate had a significant effect on the results for the above-maximum Ag-Cu-Mg material. No effect of aging conditions was observed.

#### 6.3.4 Notched Tensile Strength and NTS/YS Ratio

The notched tensile strength and NTS/YS ratio data are summarized in Tables 37 and 38, respectively. The overall average NTS value for the WCS plates was 86.2 ksi. As a function of composition, the NTS ranged from 82.0 ksi (high Fe/Si) to 89.2 ksi (low Ti/Mn). The high Ti/Mn variant had a NTS of 87.2 ksi. Both the high and low Cu/Ag/Mg variants had the same NTS (85.5 ksi).

TABLE 37. EFFECT OF PROCESS VARIABLES ON THE NOTCHED TENSILE STRENGTH OF B201-T7

| COMPOSITION(1)<br>(WT %)                     | AVERAGE NOTCHED TENSILE STRENGTH (ksi) |           |                          |           | AVG. |
|--|--|-----------|--------------------------|-----------|------|
|  | AGE                                    |           | AGE                      |           |      |
|  | (SLOW SOLIDIFICATION)(2)               |           | (FAST SOLIDIFICATION)(3) |           |      |
|  | 360°F/8HR                              | 380°F/5HR | 360°F/8HR                | 380°F/5HR |      |
| <u>(a) Within Composition Specification</u>  |  |           |                          |           |      |
| 0.35Ti-0.43Mn                                | 85.5                                   | 84.2      | 91.2                     | 87.8      | 87.2 |
| 0.19Ti-0.24Mn                                | 87.3                                   | 87.2      | 91.9                     | 90.5      | 89.2 |
| 4.95Cu-0.98Ag-0.32Mg                         | 81.2                                   | 83.9      | 86.0                     | 91.3      | 85.6 |
| 4.65Cu-0.57Ag-0.26Mg                         | 83.2                                   | 80.9      | 89.0                     | 88.7      | 85.5 |
| 0.041Fe-0.043Si                              | 89.0                                   | 74.0      | 90.0                     | 75.2      | 82.0 |
| Nominal                                      | 83.3                                   | 78.3      | 97.3                     | 90.9      | 87.5 |
| Average                                      | 84.9                                   | 81.4      | 90.9                     | 87.4      | 86.2 |
| <u>(b) Outside Composition Specification</u> |  |           |                          |           |      |
| 0.052Ti                                      | 74.6                                   | 71.8      | 70.7                     | 74.2      | 72.8 |
| 5.25Cu-1.45Ag-0.43Mg                         | 79.4                                   | 77.9      | 89.7                     | 85.6      | 83.2 |
| Average                                      | 77.0                                   | 74.8      | 80.2                     | 79.9      | 78.0 |

(1) Other elements were mid-range of the specification

(2) Fe chill; 1450°F pour temperature

(3) Cu chill; 1350°F pour temperature

TABLE 38. EFFECT OF PROCESS VARIABLES ON THE NTS/YS RATIO OF B201-T7

| COMPOSITION(1)<br>(WT%)                      | AVERAGE NTS/YS RATIO     |           |                          |           | AVG. |
|--|--------------------------|-----------|--------------------------|-----------|------|
|  | AGE                      |           | AGE                      |           |      |
|  | (SLOW SOLIDIFICATION)(2) |           | (FAST SOLIDIFICATION)(3) |           |      |
|  | 360°F/8HR                | 380°F/5HR | 360°F/8HR                | 380°F/5HR |      |
| <u>(a) Within Composition Specification</u>  |                          |           |                          |           |      |
| 0.35Ti-0.43Mn                                | 1.45                     | 1.50      | 1.56                     | 1.57      | 1.52 |
| 0.19Ti-0.24Mn                                | 1.43                     | 1.46      | 1.52                     | 1.53      | 1.49 |
| 4.95Cu-0.98Ag-0.32Mg                         | 1.25                     | 1.32      | 1.35                     | 1.45      | 1.34 |
| 4.65Cu-0.57Ag-0.26Mg                         | 1.42                     | 1.41      | 1.53                     | 1.57      | 1.48 |
| 0.041Fe-0.043Si                              | 1.51                     | 1.33      | 1.53                     | 1.36      | 1.43 |
| Nominal                                      | 1.39                     | 1.34      | 1.55                     | 1.46      | 1.44 |
| Average                                      | 1.41                     | 1.39      | 1.51                     | 1.49      | 1.45 |
| <u>(b) Outside Composition Specification</u> |                          |           |                          |           |      |
| 0.052Ti                                      | 1.17                     | 1.15      | 1.10                     | 1.19      | 1.15 |
| 5.25Cu-1.45Ag-0.43Mg                         | 1.09                     | 1.12      | 1.24                     | 1.23      | 1.17 |
| Average                                      | 1.13                     | 1.13      | 1.17                     | 1.21      | 1.16 |

(1) Other elements were mid-range of the specification

(2) Fe chill; 1450°F pour temperature

(3) Cu chill; 1350°F pour temperature

The average NTS was higher for material solidified at the faster rate (88 ksi versus 84 ksi) than that for the slow solidification rate material. The 360°F/8 hour aging condition resulted in a slightly higher NTS than the 380°F/6 hour age (87 ksi versus 84 ksi).

For the OCS plates, a very low NTS was obtained for the low Ti variant (72.8 ksi). Material solidified at the faster rate had a higher NTS value than for the slow solidification rate material (80 ksi versus 76 ksi), which is the same trend as that for the WCS material.

As a function of composition, the average NTS/YS ratio for the WCS material ranged from 1.34 to 1.52, the average value being 1.45. The high and low values were obtained for the high Ti/Mn and high Cu/Ag/Mg variants, respectively. The ratio was higher (1.50) for the fast solidification rate than that for material solidified more slowly (1.41). No effect of aging conditions on the NTS/YS ratio was observed.

In summary, the NTS of the WCS material was influenced by composition, solidification rate, and aging condition. The NTS/YS ratio was affected by composition and solidification rate.

The average value (1.16) and the range of NTS/YS values for the OCS plates were much lower than the WCS material, indicating that their toughness is probably low. No effect of solidification rate or aging conditions was observed.

#### 6.3.5 Fatigue Life

At least two fatigue specimens from each plate were tested at a net maximum stress of 25 ksi. This is a higher stress than that used for D357-T6 because B201-T7 has an inherently longer fatigue life at a given stress. The same stress could not be used for the two alloys because there would have been a significant number of runouts (B201-T7) or a very short fatigue life (D357-T6). The choice of two stress levels was acceptable because the objective was to determine the effect of process variables on the fatigue life of each alloy, rather than to compare the results for the two alloys. Where

considerable discrepancy between the two results occurred, additional tests were run. The data are summarized in Table 39. Log average values are quoted. The data scatter was significant, which is not unusual for this type of test. The overall log average fatigue life for the WCS plates was  $151 \times 10^3$  cycles. The average fatigue life range for the WCS variants was  $70 \times 10^3$  to  $373 \times 10^3$  cycles. Because of the amount of data scatter, there were no apparent correlations between fatigue life and any of the three process variables.

The average fatigue life of the OCS plates ( $78 \times 10^3$  cycles) was lower than for the WCS material. No correlation with the process variables was observed.

#### 6.3.6 Regression Analysis

Linear and nonlinear regression analyses were conducted as described in Section 5.2.4. The results are summarized in Table 40. The overall approach was the same as that for D357-T6, described in Section 5.3.6. The regression analysis results reported in the First Interim Report were slightly different from those described below because the data for the OCS material were not available when the report was published in 1988.

The Ag content accounted for significant portions of the total percent variation explained in the ultimate and yield strengths and had a smaller effect on the NTS/YS ratio. The data presented in Tables 34 and 35 showed that the combined Cu/Ag/Mg level significantly influenced the tensile strength. Clearly, from the regression analysis, Ag was the main contributor of these three elements.

In the Interim Report, Ti content showed a strong correlation with grain size and, to a lesser extent, yield strength. Since Ti is added as a grain refiner, the correlation was to be expected and was noted from the data presented in Table 33. However, inclusion of the OCS data showed a much lower correlation with grain size (reduced from 45 percent to 9 percent) and an increased correlation with NTS and the NTS/YS ratio (from 0 percent to 24 percent and 42 percent, respectively).

TABLE 39. EFFECT OF PROCESS VARIABLES ON THE FATIGUE LIFE OF B201-T7

| COMPOSITION(1)                               | LOG AVERAGE FATIGUE LIFE (10 <sup>3</sup> CYCLES TO FAILURE)* |           |                          |           | AVG. |
|--|---|-----------|--------------------------|-----------|------|
|  | AGE   |           | AGE                      |           |      |
|  | (SLOW SOLIDIFICATION)(2)                                      |           | (FAST SOLIDIFICATION)(3) |           |      |
|  | 360°F/8HR   | 380°F/5HR | 360°F/8HR                | 380°F/5HR |      |
| <u>(a) Within Composition Specification</u>  |   |           |                          |           |      |
| 0.35Ti-0.43Mn                                | 145   | 169       | 135                      | 278       | 174  |
| 0.19Ti-0.24Mn                                | 179   | 373       | 190                      | 150       | 222  |
| 4.95Cu-0.98Ag-0.32Mg                         | 157   | 150       | 125                      | 131       | 141  |
| 4.65Cu-0.57Ag-0.26Mg                         | 118   | 137       | 147                      | 113       | 128  |
| 0.041Fe-0.043Si                              | 147   | 119       | 158                      | 122       | 137  |
| Nominal                                      | 116   | 70        | 72                       | 365       | 121  |
| Log Average                                  | 142   | 159       | 132                      | 173       | 151  |
| <u>(b) Outside Composition Specification</u> |   |           |                          |           |      |
| 0.052Ti                                      | 134   | 48        | 63                       | 93        | 79   |
| 5.25Ag-1.45Cu-0.43Mg                         | 82  | 53        | 105                      | 79        | 78   |
| Average                                      | 105   | 51        | 82                       | 85        | 78   |

\*Specimen with a hole; Kt = 2.42; net maximum stress = 25 ksi

(1) Other elements were mid-range of the specification

(2) Fe chill; 1450°F pour temperature

(3) Cu chill; 1350°F pour temperature

TABLE 40. LINEAR AND NONLINEAR REGRESSION ANALYSIS RESULTS FOR B201-J7

| PROPERTY      | LINEAR ANALYSIS (1)                              |                     |    |    |    |    |    |    |   |   | NONLINEAR ANALYSIS (2)            |                                   |
|---------------|--|---------------------|----|----|----|----|----|----|---|---|-----------------------------------|-----------------------------------|
|               | PERCENT VARIATION EXPLAINED BY PROCESS VARIABLES |                     |    |    |    |    |    |    |   |   | TOTAL PERCENT VARIATION EXPLAINED | TOTAL PERCENT VARIATION EXPLAINED |
|               | AGING PARAMETERS                                 | SOLIDIFICATION RATE | Ag | Si | Fe | Ti | Mn | Mg |   |   |                                   |                                   |
| UTS           | -  | -                   | 62 | -  | -  | 11 | -  | -  | - | - | 73                                | 73                                |
| YS            | -  | -                   | 74 | -  | -  | 17 | -  | -  | - | - | 96                                | 97                                |
| EL            | -  | 45                  | -  | -  | -  | -  | -  | -  | - | - | 45                                | 44                                |
| NTS           | -  | 16                  | -  | 10 | -  | 24 | 11 | -  | - | - | 61                                | 55                                |
| NTS/YS        | -  | 6                   | -  | -  | 8  | 42 | -  | 30 | - | - | 86                                | 88                                |
| Fatigue Life  | -  | -                   | -  | -  | 14 | -  | -  | -  | - | - | 14                                | 27                                |
| Grain Size(3) | -  | 22                  | -  | 44 | -  | 9  | 3  | -  | - | - | 81                                | 85                                |

(1) 5% error level  
 (2) 1% error level  
 (3) At the edge of the plate

Inclusion of the OCS data showed an increase in the correlations between Si and grain size (from 0 percent to 44 percent), and solidification rate and elongation (from 23 percent to 45 percent).

The percent variations explained in all the dependent variables except fatigue life were similar for the linear and nonlinear analyses, indicating that linear relationships probably exist. The correlation between fatigue life and the process variables was low for both linear and nonlinear analyses.

#### 6.4 CONCLUSIONS

The combined conclusions from both the tabulated data and the regression analyses regarding the effect of process variables on the mechanical properties and microstructural features of B201-T7 are as follows:

##### 1. Composition

- Higher Cu/Ag/Mg levels increased UTS and YS, and reduced EL and the NTS/YS ratio
- The high Fe/Si levels provided the lowest UTS value
- Higher Ti/Mn levels slightly decreased the UTS, YS, and EL, but gave the highest NTS/YS ratio
- The lowest ductility (3.1 percent) was obtained for low Ti (OCS) material.

##### 2. Solidification Rate

The faster solidification rate (Cu chill) increased ductility, NTS, and the NTS/YS ratio.

##### 3. Aging Temperature/Time

The 360°F/8 hour aging condition gave higher average UTS, YS, and NTS values than those for material aged at 380°F for 5 hours.

#### 4. Property Optimization

The requirements for optimizing the DADT and tensile properties of B201-T7 do not conflict. The benefits of HIPing were demonstrated by the reduction in ultrasonic attenuation in HIPed plates compared with plates that had not been HIPed.

#### 6.5 RECOMMENDATIONS

1. The approved AMS 4242 specification should be used for producing the B201-T7 verification plates for the remaining portion of Task 2, Phase I, and for the plates required for Task 3, Phase I. All the plates should be HIPed.
2. The plates for subsequent DADT characterization on the DADTAC program should have a maximum grain size of 0.0035 inch. This may be obtained through Ti additions and/or chilling, which will also minimize the formation of shrinkage sponge.

SECTION 7  
PHASE I, TASK 2 - PROPERTY VERIFICATION

7.1 INTRODUCTION

The objective of the property verification subtask was to perform a detailed DADT characterization for D357-T6 and B201-T7 made according to the optimum material and processing conditions determined during the Screening Subtask described in Sections 5 and 6. D357-T6 and B201-T7 plates were cast by Hitchcock Industries, Fansteel Wellman Dynamics, and Alcoa according to specifications derived from the screening evaluations. The specifications were based on the process variables that provided the best overall balance of tensile and DADT properties. The use of three foundries to produce material to the same specification enabled property variations that might be typical of the casting industry to be determined. The test results for the three foundries are described for Foundries A, B, or C; this designation does not correspond to the order listed above.

Because a large amount of data was obtained during the verification subtask, average property values are typically presented in Section 7. The individual test results are included in Appendices C (D357-T6) and D (B201-T7).

7.2 EXPERIMENTAL PROCEDURES

7.2.1 Production of Castings

Plates with dimensions 16 x 6 x 1.25 inches were used for the verification evaluations. The 1.25 inch plate thickness enabled valid fracture toughness specimens to be obtained. However, a limited number of plates of the thickness (0.75 inch) used in the screening evaluations of Phase I, Task 2 (Sections 5 and 6) were also evaluated to assure that the verification material properties were similar to those obtained from the best screening task plates.

The requirements given to the foundries are outlined in the following sections. Key mechanical and microstructural properties were specified, but the foundries were given the freedom to select the production methods that would best enable them to produce plates with the required properties. All areas of the plates were designated.

#### 7.2.1.1 D357-T6

Screening evaluation data (Section 5) indicated that there was no conflict in the requirements for optimizing tensile and DADT properties. Therefore, the AMS 4241 composition specification [1] was used, Table 41, with the addition of a silicon modifier, which was shown in the screening evaluations (Section 5) to improve mechanical properties, particularly the NTS/YS ratio (an indicator of toughness) and ductility. Although Sr was used during the screening evaluation, two foundries (Alcoa and Fansteel Wellman Dynamics) preferred to use sodium for the verification plates based on prior experience with modifiers. Hitchcock Industries used Sr.

Each foundry produced two plates of the same size as the screening plates (12 x 6 x 0.75 inch) and eight larger plates (16 x 6 x 1.25 inch). The smaller plates, which were the same size as those used in the screening evaluation portion of Phase I, Task 2, were tested to assure that the properties of the optimally-produced screening material could be reproduced using the verification material specifications. Because castings are often quenched in a glycol/water solution to reduce distortion (by reducing the cooling rate) of complex-shaped parts and/or those that have significant thickness variations, three of the eight large plates were quenched in a room temperature glycol (25 percent)/water solution; the remaining plates were quenched in room temperature water. The rigging system and aging treatments were the same for the glycol-quenched and water-quenched plates.

The minimum tensile properties specified were based on the results obtained during the screening evaluations and were identical to the AMS 4241 specification for designated areas, as follows:

TABLE 41. COMPOSITION SPECIFICATION<sup>(1)</sup> FOR THE D357 VERIFICATION PLATES

| ELEMENT       | RANGE (WT %) |       |
|---------------|--------------|-------|
|               | MIN.         | MAX.  |
| Silicon       | 6.5          | 7.5   |
| Magnesium     | 0.55         | 0.6   |
| Titanium      | 0.10         | 0.20  |
| Beryllium     | 0.04         | 0.07  |
| Strontium     | } (2)        | 0.008 |
| Sodium        |              | 0.001 |
| Iron          | -            | 0.12  |
| Manganese     | -            | 0.10  |
| Others, each  | -            | 0.05  |
| Others, total | -            | 0.15  |
| Aluminum      | Balance      |       |

(1) AMS 4241 plus Si modifier

(2) Sr or Na was used, not both

Ultimate tensile strength - 50 ksi  
Yield strength at 0.2% offset - 40 ksi  
Elongation - 3%

The foundries selected their preferred aging procedures to meet the mechanical property requirements.

No weld repair was allowed, and each plate was required to be Grade B or better by one percent sensitivity radiography according to MIL-STD-2175.

The rigging systems and the heat treatment procedures used by the three foundries are described below.

#### Alcoa

The rigging, shown in Figure 20, consisted of a tapered down sprue leading into a pouring well and runner system which fed the vertical mold cavity. Three 1.25-inch-thick copper chills were used, and a fiberglass screen was placed between the pouring well and runner to trap foreign material.

The plates were solution heat treated for 15 hours at 1015°F in a drop bottom furnace. The temperature was controlled to within +5°F and -10°F. The plates were quenched in room temperature water or a 25 percent glycol-water solution, and were artificially aged at 335±5°F for 6 hours.

#### Hitchcock Industries

The rigging for the plates is shown in Figure 21. Eight 2 x 2 x 1.5-inch-thick iron chills placed end on end were used in the center of the horizontal cope, and one 3 x 3 x 16-inch-long copper chill was used in the drag to obtain directional and rapid solidification. Eight insulated risers spaced at approximately 4-inch intervals were used to feed the casting during solidification. The mold cavity was gravity fed through an insulated gating system which contained ceramic filters to trap foreign material.

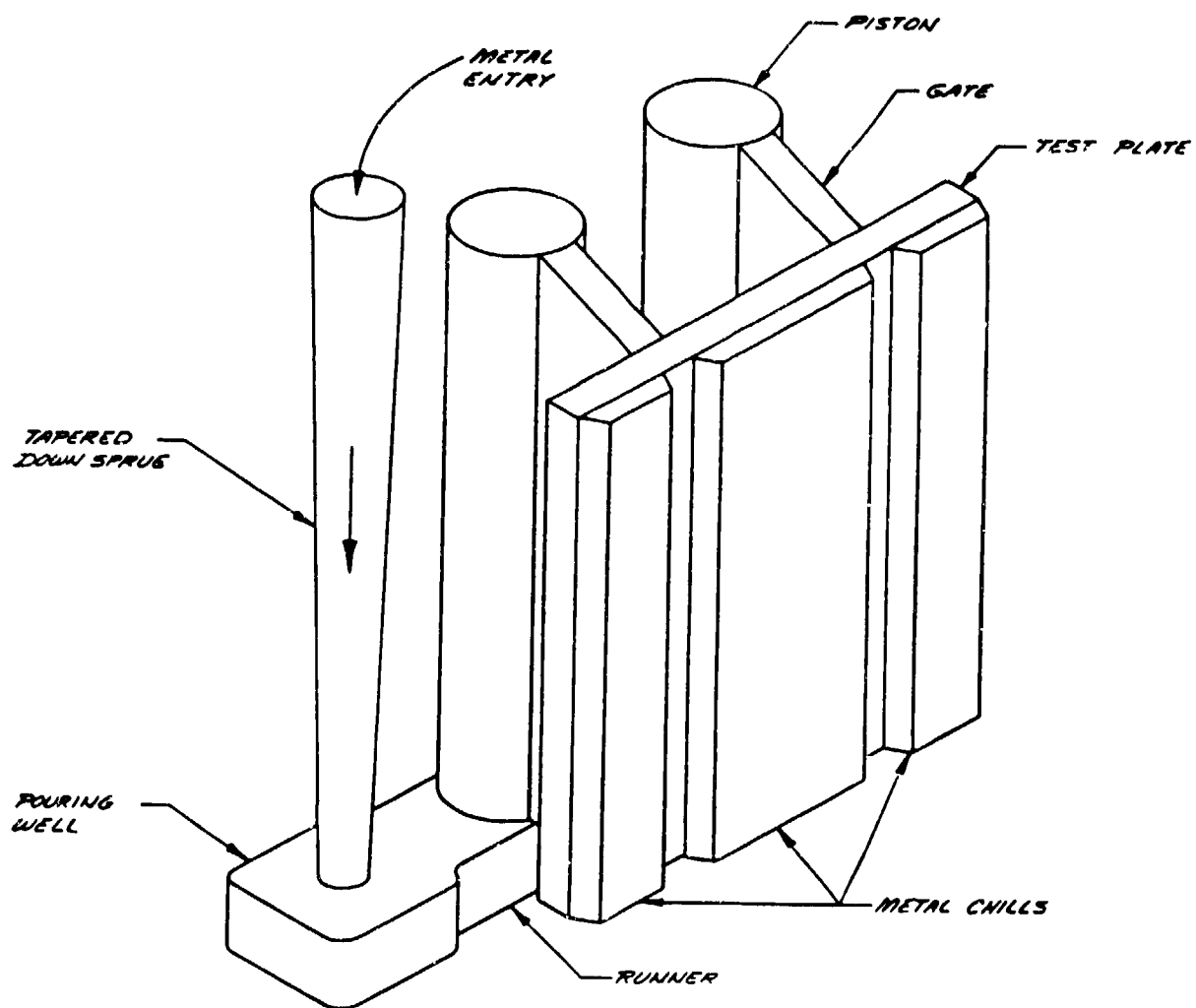
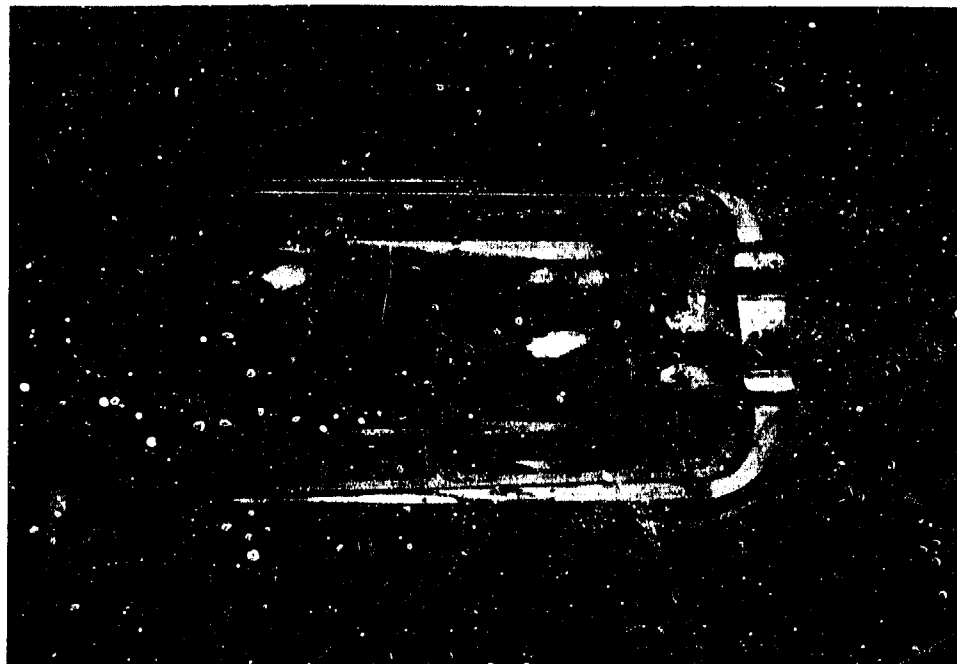


Figure 20. Rigging System Used by Alcoa to Produce D357 Plates



a. Cope Side of Casting



b. Runner and Filter System

Figure 21. Rigging System Used by Hitchcock Industries to Produce D357 Plates

The plates were solution heat treated at  $1010 \pm 5^\circ\text{F}$  for 24 hours and quenched in room temperature water or a 25 percent glycol-water solution. The plates were then artificially aged at  $315 \pm 5^\circ\text{F}$  for 13.5 hours.

#### Fansteel Wellman Dynamics

The rigging for the D357 plates produced by Fansteel Wellman Dynamics is shown in Figure 22. A 2 x 4 x 16-inch-long copper chill was used in both the cope and the drag. Ten 1.5-inch-diameter insulated risers spaced at approximately 4-inch intervals were used to feed the casting during solidification. The mold cavity was gravity fed through the gating system, which contained ceramic foam filters to trap foreign material.

Attached bars, shown in Figure 22, were co-cast with the plates to verify heat treatment. The water- and glycol-quenched plates were solution heat treated at  $1010^\circ\text{F}$  for 19 hours and 16 hours, respectively, prior to quenching at room temperature. Following a 24-hour hold at room temperature, all the plates were aged for 6 hours at  $335^\circ\text{F}$ .

#### 7.2.1.2 B201-T7

Similar to D357-T6, the screening evaluation data showed that there was no conflict in the requirements for optimizing tensile and DADT properties. Consequently, the composition specified in AMS 4242 (Table 42) [2] was used for the verification plates. Each foundry produced two 0.75-inch-thick plates and five 1.25-inch-thick plates and selected their preferred aging treatment to meet the mechanical property requirements. All areas of the plates required designated properties and all of the plates were quenched in room temperature water. To minimize microshrinkage, which may have a deleterious effect on fatigue life, all B201 plates were HIPed. HIPing consisted of step-heating the as-cast plates to  $950^\circ\text{F}$  and holding for three hours in an inert gas atmosphere at 15,000 psi.

The specified minimum tensile properties were based on the results obtained during the screening evaluations and were identical to the AMS 4242 specification requirements for designated areas, as follows:

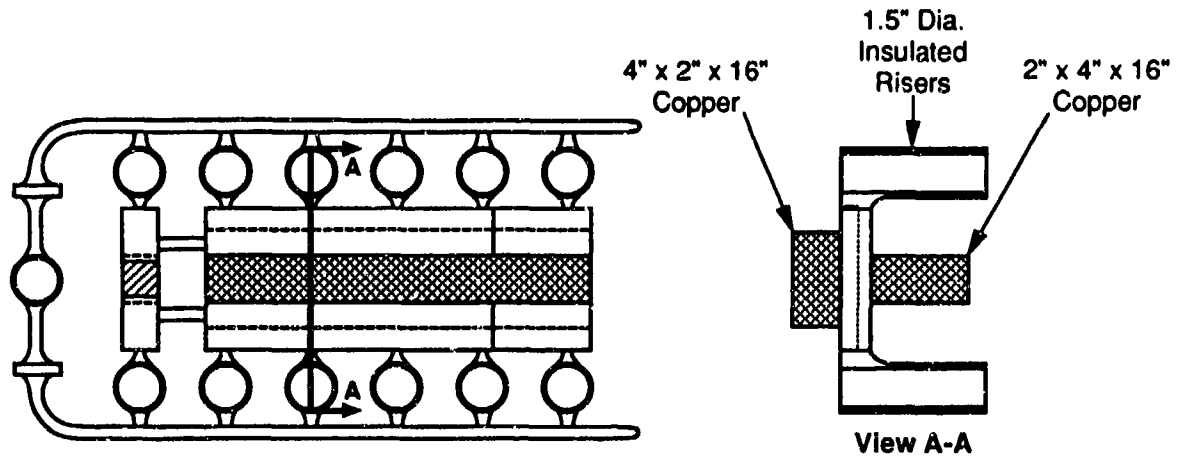


Figure 22. Rigging System Used by Fansteel Wellman Dynamics to Produce D357 Plates

TABLE 42. COMPOSITION SPECIFICATION<sup>(1)</sup> FOR THE B201 VERIFICATION PLATES

| ELEMENT       | RANGE (WT %) |      |
|---------------|--------------|------|
|               | MIN.         | MAX. |
| Copper        | 4.50         | 5.0  |
| Silver        | 0.40         | 0.8  |
| Maganese      | 0.20         | 0.50 |
| Magnesium     | 0.20         | 0.30 |
| Titanium      | 0.15         | 0.35 |
| Iron          | -            | 0.05 |
| Silicon       | -            | 0.05 |
| Others, each  | -            | 0.05 |
| Others, total | -            | 0.15 |
| Aluminum      | Balance      |      |

(1) AMS 4242

Ultimate tensile strength - 60 ksi  
Yield strength at 0.2% offset - 50 ksi  
Elongation - 3%

Similar to D357-T6, weld repairs were not allowed, and each plate was required to be of a Grade B or better radiographic quality (1 percent sensitivity).

Similar to the D357 plates, each foundry designed its own rigging system and selected the solution heat treat and aging parameters for achieving the T7 temper and the required mechanical properties. The rigging systems and heat treatment procedures used by the three foundries are described below.

#### Alcoa

The rigging for plates was the same as that used for the D357 plates (Figure 20).

The plates were loaded into a furnace below 500°F and solution heat treated as follows:

2 hours at 940±10°F  
2 hours at 960±10°F  
16 hours at 980±10°F

The plates were then quenched in room temperature water and artificially aged for 5 hours at 380±5°F.

#### Hitchcock Industries

The rigging for the plates was similar to that shown in Figure 21 except that no chills were used in the cope. One 2 x 3 x 16-inch-long copper chill was used in the drag to obtain directional solidification. Eight insulated risers spaced at approximately 4-inch intervals were used to feed the casting during solidification. The mold cavity was gravity fed through an insulated gating system which contained ceramic filters to trap foreign material.

The plates were loaded into a furnace below 500°F and solution heat treated as follows:

2 hours at 940±10°F  
2 hours at 950±10°F  
16 hours at 980±10°F

The plates were then quenched in room temperature water and aged for 8 hours at 360±5°F.

#### Fansteel Wellman Dynamics

The rigging system was similar to that used for D357, shown in Figure 22, except that two steel chills (2.5 x 2.5 x 8 inch) instead of copper were used in the cope to promote directional solidification. The plates were loaded into a furnace below 500°F and solution heat treated as follows:

2 hours at 920±10°F  
2 hours at 950±10°F  
2 hours at 970±10°F  
16 hours at 980±10°F

The plates were quenched into room temperature water and then naturally aged at room temperature for 24 hours, followed by artificial aging at 360±5°F for 8 hours.

#### 7.2.2 Test Procedures

The 1.25-inch-thick plates used for the verification evaluations were radiographically inspected to assure that all material was Grade B or better. They were then comprehensively evaluated using the tests shown in Table 43. The test specimens were excised randomly from the 1.25-inch-thick plates to determine the between-plate and foundry-to-foundry mechanical property variability.

TABLE 43. VERIFICATION TESTS FOR D357-T6 AND B201-T7

| TEST                                       | SPECIFICATION                        | NUMBER OF TESTS |                  |                 |
|--|--------------------------------------|-----------------|------------------|-----------------|
|  |                                      | D357-T6         |                  | B201-T7         |
|  |                                      | WATER<br>QUENCH | GLYCOL<br>QUENCH | WATER<br>QUENCH |
| Tensile                                    | ASTM B557                            | 28              | 15               | 26              |
| Notched Tensile                            | ASTM E602                            | 34              | 15               | 26              |
| Fracture Toughness                         | ASTM B646 <sup>(1)</sup>             | 7               | 4                | 7               |
| Constant Amplitude<br>Fatigue Crack Growth | ASTM E647                            | 6               | 3                | 6               |
| Stress-Life Fatigue<br>Smooth              | ASTM E466                            | 14              | 12               | 15              |
| Notched                                    |                                      | 10              | 0                | 8               |
| Stress Corrosion                           | ASTM G47                             | 0               | 0                | 3               |
| Strain-Life Fatigue                        | ASTM E606 <sup>(2)</sup><br>and E466 | 12              | 0                | 12              |
| Metallography                              | ASTM E112                            | 13              | 8                | 15              |
| Chemical Analysis                          | NA                                   | 15              | 6                | 15              |

- (1) In addition to the ASTM 646 standard test, short bar testing was performed using the method currently under review by ASTM
- (2) A new specification is under review by ASTM

For the 0.75-inch-thick verification plates, only tensile and notched tensile tests were conducted. The results were compared with the screening test data to assure that the properties obtained from the optimized screening evaluation plates (Sections 5 and 6) had been reproduced in the verification plates.

The composition of each plate was determined using Inductively Coupled Plasma (ICP) analysis to confirm the foundry melt results. The DAS of the D357 plates was measured using a line intercept method [6] and the silicon particle morphology was characterized using an Omnicon 3500 image analyzer. Specimens were excised from random locations throughout the plates.

### 7.2.3 Equivalent Initial Flaw Size Analysis

Durability and damage tolerance analysis requirements for aircraft structure are defined in MIL-A-83444 and MIL-A-87221. For damage tolerance analysis of wrought alloys, the presence of a flaw is assumed so that defects that may occur in critical areas of a part during manufacturing are accounted for. Castings contain inherent flaws such as microporosity, microshrinkage, or foreign material that may not be detectable by normal NDI methods. A limited amount of these defects is acceptable in premium quality aluminum castings for aerospace applications. An equivalent initial flaw size (EIFS) must be determined for castings to account for these inherent flaws. The EIFS of D357 and B201 was determined from the Phase I, Task 2 (verification) fatigue data using a method developed previously under a Northrop IR&D Program [13]. The methodology for determining the EIFS and how it may be applied to both durability and damage tolerance analyses are summarized below.

#### 7.2.3.1 Determination of Equivalent Initial Flaw Size

Stress-life fatigue results for smooth round bar specimens ( $K_t = 1.0$ ) were used to obtain an estimate of the inherent material EIFS. The value of EIFS ( $a_0$ ), which initiates a crack in a smooth round bar fatigue specimen, is based on the following relationship [13].

$$a_0 = \left\{ a_i^{(1-m/2)} - (1-m/2)C(\beta\Delta S\sqrt{\pi}/Q)^m N_i \right\}^{1/(1-m/2)} \quad \text{Eq. 7-1}$$

where

$a_i$  - a selected flaw size defining initiation which is close to, but in excess of  $a_0$  by at least 0.01 inch.

$m$  &  $C$  - the slope and intercept, respectively, of the Paris equation representing the  $da/dn$  vs  $\Delta K$  plot. The  $da/dn$  test must be run at the same stress ratio as the stress-life fatigue tests for the EIFS analysis.

$\beta$  - the stress intensity correction factor for a semicircular surface flaw of a depth equal to the average of  $a_0$  and  $a_i$ .

$\Delta S$  - the elastic stress range of the fatigue specimen.

$N_i$  - the number of cycles for the fatigue crack to grow to  $a_i$  from  $a_0$ .

$Q$  - a crack shape factor, equal to  $2.464 - 0.212 (S_{\max}/\sigma_y)^2$ .

where  $S_{\max}$  - the maximum fatigue stress.

$\sigma_y$  - yield strength.

The value of  $N_i$  is determined from the number of cycles to failure, using the following relationship:

$$(N_f/N_i) = 1 + \frac{(a_i + a_0)^{m/2}}{(a_i - a_0)^{m/2}} \sum_{a=a_i}^{a_c} \left\{ \frac{\Delta a}{\left(\frac{\beta_a}{\beta_i}\right)^m \times (2\bar{a})^{m/2}} \right\} \quad \text{Eq. 7-2}$$

where  $\bar{a}$  - the crack length at the midpoint of the assumed interval,  $\Delta a$ .

$\beta_{\bar{a}}$  - the stress intensity correction factor at crack length  $\bar{a}$ .

The EIFS solution involves an interpolation between Equations 7-1 and 7-2 because each one contains  $a_0$ . An adequate convergence occurs within seven or eight iterations, depending on the initial value of  $a_i$  assumed.

#### 7.2.3.2 Application to Durability Analysis

The durability analysis was performed using the Northrop sequence crack initiation program, LOOPIN8 [14], using data generated from round bar strain-life fatigue test specimens. These specimens have the same general geometry as those used to obtain the EIFS (Section 7.2.3.1).

Using the average EIFS, obtained as described in Section 7.2.3.1, the ratio between  $N_i$  and  $N_f$  for each alloy can be derived from Equation 7-2 for a selected value of initiation flaw size ( $a_i$ ). Hence, the failure lives obtained during the strain-life tests can be converted to the cycles required to initiate a crack of the selected size. Using these converted data, the LOOPIN8 program is then used to predict the life to initiate a crack from the material EIFS ( $a_0$ ) to the predefined initiation flaw size ( $a_i$ ).

#### 7.2.3.3 Application to Damage Tolerance Analysis

Damage tolerance analysis is based on the assumption that crack growth starts from a "rogue" flaw. For wrought alloys, the size of this flaw is generally defined [15] as a 0.050-inch corner flaw at the edge of a hole. Reductions in the assumed value of this flaw are negotiable between the

supplier and the customer based on a demonstration of manufacturing quality. However, if the basic quality of the material is such that similar or greater rogue flaws can exist regardless of the care taken to produce the finished article, then the upper bound of the inherent material equivalent initial flaw size becomes the limiting design factor.

The upper bound values for D357 and B201 castings were derived from the EIFS distributions obtained from smooth round bar fatigue test results using a "sudden death" analysis, as described below.

#### Sudden Death Analysis

Sudden death testing [16] is a method that can be used for determining the upper bound defect size for the general population based on the fatigue life results for specimens that contain random distributions of casting defects. Crack initiation will usually occur at the largest defect located at or near the surface of the gauge section of the specimen. The failure of the specimen can be assumed to be the "sudden death" failure of the set of defects contained within the surface volume of the specimen. The largest defect is represented by the shortest fatigue life.

The smooth round bar fatigue specimens used in the DADTAC program had a 1.6-inch-long by 0.50-inch-diameter gauge section. The volume of material in the critical initiation zone of these specimens is equivalent to that obtained in a similar depth of material at the edge of approximately seventy 0.25-inch-diameter x 0.25-inch-deep holes. This estimate is based on an assumption that the critical high stress concentration region for a hole extends twenty degrees either side of the hole axis aligned normal to the primary load direction. This is considered to be a conservative assumption as a more localized stress concentration would tend to increase the number of holes represented by the smooth bar specimen.

According to the theory of ranking [16], the lowest value in a set of 70 specimens clusters about the one percent probability level of the general population. If the lowest life represents the highest equivalent initial flaw size in each set of 70, then the EIFS values obtained from an analysis of the

round bar tests will be clustered about the 99 percent probability level of the EIFS values obtained for a typical defect population.

The ranked results are analyzed assuming a Weibull distribution to obtain the median and upper 95 percent confidence limit statistics of the "sudden death" population. The median and upper 95 percent confidence limit of the general population are obtained by translating the "sudden death" median line and confidence limit upward until the Weibull median value of the "sudden death" line coincides with the 99 percent probability value.

EIFS values for castings obtained from different vendors were grouped using variance analysis [17]. An estimate of the maximum inherent material rogue flaw size was obtained from the 99.9 percent probability and 95 percent confidence value read from the above derived general population distribution. If this value exceeds the current requirements of MIL-A-83444 it indicates that the basic material quality is more critical for the castings evaluated under the DADTAC program than the upper flaw sizes currently assumed for wrought alloys based on manufacturing quality. A value less than the current MIL-A-83444 specification requirement would indicate that castings can be considered for use in a damage tolerant design by applying the same criteria used for wrought alloys.

### 7.3 D357-T6 RESULTS

The main emphasis for D357 was to evaluate cast plates that were quenched in room temperature water. However, a few D357 plates were quenched in glycol to determine if the quench medium significantly influenced the mechanical properties. All other process parameters for the glycol-quenched plates were the same as for the water-quenched plates.

For the water-quenched plates, only those that fully met the specified microstructural and tensile properties, as well as radiographic quality and chemical composition, were used for evaluating DADT properties. To fully evaluate the effect of the quench, all of the glycol-quenched plate test results were compared with data from the water-quenched plates. However, only data from those glycol-quenched plates which fully met all the specification requirements were included in the subsequent DADT analyses (e.g., EIFS).

All the water-quenched and glycol-quenched D357-T6 plates from Foundries A and C met the tensile property specification requirements. The DADT test specimens, therefore, were excised from these plates at random locations. For Foundry B, three water-quenched plates did not meet the tensile property requirements; both had one low elongation value (<3 percent) out of the two tensile specimens tested from each plate. Therefore, with one exception, only the remaining three Foundry B plates were used for the DADT characterization described in this section. The exception is the use of plate V208, which had to be used for notched fatigue tests because of material shortage.

Full details of the plates used and their properties are included in Appendix C.

#### 7.3.1 Composition

A combined total of 31 plates (1.25-inch- and 0.75-inch-thick) cast from 13 different melts by three foundries were used for the verification evaluations. The composition of each of these melts and the specification ranges for each element are listed in Table 44. The compositions were within the range specified from the screening subtask of this program (Table 41). The melt analyses were confirmed by ICP chemical analyses on samples taken from the plates.

#### 7.3.2 Microstructure

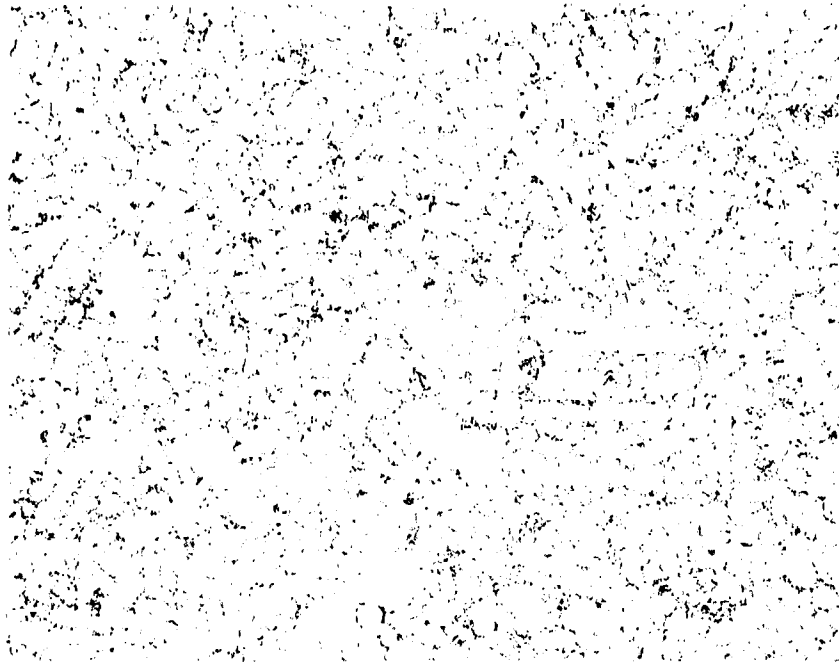
The microstructure of the D357-T6 plates was characterized using optical, transmission and scanning transmission electron microscopy (TEM and STEM), and scanning electron microscopy (SEM). The DAS and silicon particle morphology of each plate were determined. A typical optical micrograph of D357-T6 is shown in Figure 23.

The DAS of specimens taken from various locations throughout the plates ranged from 0.0008 inch to 0.0020 inch, which is within the requirement ( $\leq 0.0024$  inch) specified for the verification plates.

TABLE 44. D357 VERIFICATION MATERIAL MELT COMPOSITIONS

| COMPOSITION (WT %)                  |             |              |               |      |               |       |       |      |
|-------------------------------------|-------------|--------------|---------------|------|---------------|-------|-------|------|
| Fe                                  | Si          | Mg           | Ti            | Mn   | Be            | Na    | Sr    | Al   |
| 0.03                                | 7.03        | 0.6          | 0.12          | 0.00 | 0.050         | 0.002 | -     | Bal. |
| 0.03                                | 6.99        | 0.6          | 0.11          | 0.00 | 0.070         | 0.003 | -     | Bal. |
| 0.03                                | 7.27        | 0.6          | 0.10          | 0.00 | 0.060         | 0.009 | -     | Bal. |
| 0.04                                | 7.37        | 0.6          | 0.11          | 0.00 | 0.050         | 0.012 | -     | Bal. |
| 0.11                                | 6.67        | 0.6          | 0.16          | 0.01 | 0.061         | -     | 0.008 | Bal. |
| 0.10                                | 7.35        | 0.6          | 0.15          | 0.01 | 0.070         | -     | 0.014 | Bal. |
| 0.11                                | 6.80        | 0.6          | 0.17          | 0.01 | 0.059         | -     | 0.011 | Bal. |
| 0.10                                | 7.07        | 0.6          | 0.15          | 0.01 | 0.069         | -     | 0.014 | Bal. |
| 0.11                                | 7.20        | 0.6          | 0.16          | 0.01 | 0.070         | -     | 0.007 | Bal. |
| 0.10                                | 7.07        | 0.6          | 0.15          | 0.01 | 0.069         | -     | 0.014 | Bal. |
| 0.06                                | 7.11        | 0.6          | 0.12          | 0.01 | 0.55          | 0.002 | -     | Bal. |
| 0.06                                | 7.13        | 0.6          | 0.12          | 0.01 | 0.56          | 0.003 | -     | Bal. |
| 0.06                                | 7.10        | 0.6          | 0.13          | 0.01 | 0.51          | 0.003 | -     | Bal. |
| <u>AMS 4241 Specification Range</u> |             |              |               |      |               |       |       |      |
| <0.12                               | 6.5-<br>7.5 | 0.55-<br>0.6 | 0.10-<br>0.20 | <0.1 | 0.04-<br>0.07 | *     | *     | Bal. |

\* Not specified in AMS 4241; however, those amounts used are within the 0.05 wt. % limit set for "other" elements



50X

As polished

Figure 23. Typical D357-T6 Microstructure

The average DAS values, as well as the Si particle area, spacing, and aspect ratio for water-quenched and glycol-quenched material from both foundries are listed in Table 45, along with a comparison to the corresponding data obtained previously for the screening material. The DAS for material from the three foundries was similar, with all values being below the specification maximum of 0.0024 inch. The average DAS of the verification material was slightly less than that of the screening material. The average DAS for the glycol-quenched plates from two of the three foundries (A and B) was less than that for the water-quenched material. The glycol-quenched and water-quenched plates were made to the same specification using identical processing conditions except for the quench medium. There was no variation in chill or mold materials which would affect the DAS. Therefore, the consistent difference in the DAS for the glycol-quenched and water-quenched plates is considered to be coincidental and not a result of processing differences. The DAS for glycol-quenched Foundry C plates was slightly higher than for the water-quenched material.

The silicon particle data for the verification material from the three foundries were also similar, and were similar to those obtained previously for the screening material. The percent porosity, which was determined using the optical metallography specimens, was low for all of the verification plates, as it was in the screening plates.

The microstructure of randomly selected samples was evaluated using SEM, TEM, STEM, SAD patterns, and EDX analyses. Four different phases were observed, although the exact stoichiometry of three could not be determined.

A typical SEM micrograph of D357-T6, Figure 24, shows three phase morphologies in addition to the aluminum matrix. Using EDX analyses, the shapes identified by Numbers 1 and 2 were determined to be Al-Fe, but the stoichiometry could not be determined. The phase identified by Number 3 was determined by EDXA to be Si. Smaller Si particles were also observed in the TEM micrograph, Figure 25. An X-ray map of the microstructure confirmed that these particles were Si. Long needle-shaped particles were also observed in the microstructure of Figure 26, and were shown by X-ray mapping to contain Ti. Mg and Fe X-ray maps of this microstructure were also generated, but

TABLE 45. DAS AND SI PARTICLE MORPHOLOGY DATA FOR  
1.25-INCH-THICK D357-T6 PLATES

| Si PARTICLE MORPHOLOGY              |        |               |                             |                              |                 |                 |
|-------------------------------------|--------|---------------|-----------------------------|------------------------------|-----------------|-----------------|
| FOUNDRY                             | QUENCH | DAS<br>(inch) | AREA<br>( $\mu\text{m}^2$ ) | SPACING<br>( $\mu\text{m}$ ) | ASPECT<br>RATIO | POROSITY<br>(%) |
| A                                   | Water  | 0.0012        | 16                          | 38                           | 1.6             | 0               |
|                                     | Glycol | 0.0010        | 12                          | 36                           | 1.6             | 0               |
| B                                   | Water  | 0.0018        | 18                          | 44                           | 1.6             | 0.083           |
|                                     | Glycol | 0.0013        | 23                          | 40                           | 1.6             | 0               |
| C                                   | Water  | 0.0011        | 14                          | 50                           | 1.7             | 0               |
|                                     | Glycol | 0.0012        | 13                          | 62                           | 1.7             | 0               |
| Average                             | Water  | 0.0014        | 16                          | 44                           | 1.6             | 0.028           |
|                                     | Glycol | 0.0012        | 16                          | 46                           | 1.6             | 0               |
| Average of<br>Screening<br>Data [3] |        | 0.0016        | 20                          | 36                           | 1.8             | 0.023           |



Figure 24. Backscatter SEM Micrograph of D357-T6



Figure 25. TEM Micrograph of D357-T6 Showing Si Particles



Figure 26. TEM Micrograph of D357-T6 Showing a Needle-Shaped Phase Containing Ti

neither element was detected. A closer examination of the Ti-containing needles was conducted to determine their stoichiometry. Figures 27a and b show a typical needle and its SAD pattern, respectively. Examination of the pattern, as well as two others obtained at different orientations, did not reveal the composition or stoichiometry of the phase. Another phase is also seen in Figure 27a, which was identified by EDXA to be  $Mg_2Si$ , the main strengthening phase.

Sodium was used to modify the as-cast microstructure of the specimen that was examined in the TEM. However, X-ray mapping and diffraction patterns of various areas of the microstructure failed to locate Na. Some controversy exists about the exact modification mechanism caused by Na. However, one theory [18] is that modification is accomplished through an interaction between Na and P, an impurity element. In the absence of Na, P forms AlP, which promotes the formation of large Si particles. When Na is added, the compound NaP is formed, which suppresses this tendency, resulting in a finer microstructure.

### 7.3.3 Tensile Properties

The average tensile properties of D357-T6 plates are shown in Table 46. Tests were conducted on both water- and glycol-quenched material from the 1.25-inch-thick plates. A limited number of tensile tests were also conducted on the 0.75-inch-thick plates (water-quenched only). These smaller plates were evaluated to assure that those properties obtained for the screening material could be reproduced in plates of the same size produced to the AMS 4241 specification composition limits. The combined average tensile properties for the 0.75-inch-thick verification plates from all three foundries were 53.6 ksi ultimate strength, 45.3 ksi yield strength, and 5.9 percent elongation. These values were similar to the results from the screening tests, i.e., 51.4 ksi, 43.4 ksi, and 5.1, respectively.

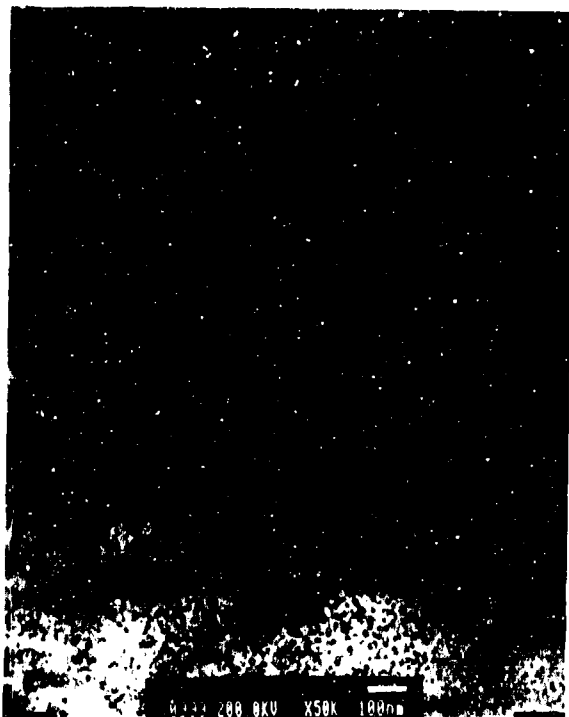


Figure 27a. TEM Micrograph of D357-T6 Showing a Needle-Shaped Particle Containing Ti and Smaller  $Mg_2Si$  Particles



Figure 27b. Selected Area Diffraction Pattern of the Needle Phase of Figure 27a

TABLE 46. TENSILE PROPERTIES OF THE 1.25-INCH-THICK, WATER-  
AND GLYCOL-QUENCHED\* D357-T6 PLATES

| FOUNDRY     | QUENCH**<br>MEDIUM | UTS (ksi) |       | YS (ksi) |       | El (%) |         |
|-------------|--------------------|-----------|-------|----------|-------|--------|---------|
|             |                    | AVG.      | RANGE | AVG.     | RANGE | AVG.   | RANGE   |
| A           | Water              | 54        | 51-55 | 45       | 44-47 | 5.9    | 3.5-8.5 |
|             | Glycol             | 53        | 51-55 | 43       | 42-44 | 6.6    | 5.5-9.0 |
| B           | Water              | 52        | 50-53 | 45       | 44-46 | 4.5    | 3.0-5.6 |
|             | Glycol             | 49        | 48-50 | 42       | 41-43 | 3.4    | 2.5-4.3 |
| C           | Water              | 54        | 53-55 | 47       | 46-48 | 5.4    | 3.9-8.2 |
|             | Glycol             | 51        | 50-52 | 44       | 43-44 | 4.9    | 4.6-5.2 |
| Average     | Water              | 53        |       | 46       |       | 5.2    |         |
|             | Glycol             | 51        |       | 43       |       | 5.0    |         |
| Target Min. |                    | 50        |       | 40       |       | 3.0    |         |

\* 25% glycol solution

\*\* Room temperature

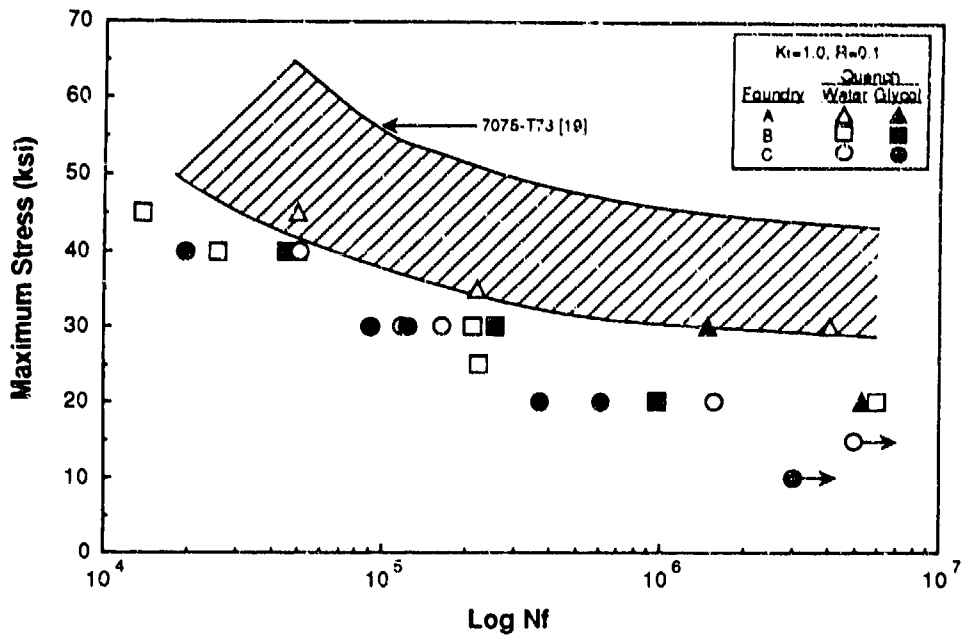
The average and minimum tensile properties for the 1.25-inch-thick water-quenched material from foundries A and C were slightly higher than those from Foundry B. All of the individual test specimens from the Foundry A plates met the 50/40/3 tensile property requirements. Three Foundry B plates each had one tensile test result that had a percent elongation less than the 3.0 percent minimum requirement. Subsequent DADT evaluations of material from Foundry B were conducted only on those plates that fully met the tensile property specification requirements. The average tensile property data for Foundry B material shown in Table 46 include only those water-quenched plates that were within the specification.

The average and minimum tensile property data for glycol-quenched plates are also shown in Table 46. Strength levels are in general slightly lower than those for the water-quenched material. The reduction in strength is probably associated with a lower level of Mg remaining in solution following the quench, resulting in less  $Mg_2Si$ , the strengthening phase, following artificial aging. Two of 15 elongation values (Foundry B) for the glycol-quenched plates were below the 3.0 percent minimum. Also, all the UTS values for glycol-quenched Foundry B material were below the 50 ksi minimum.

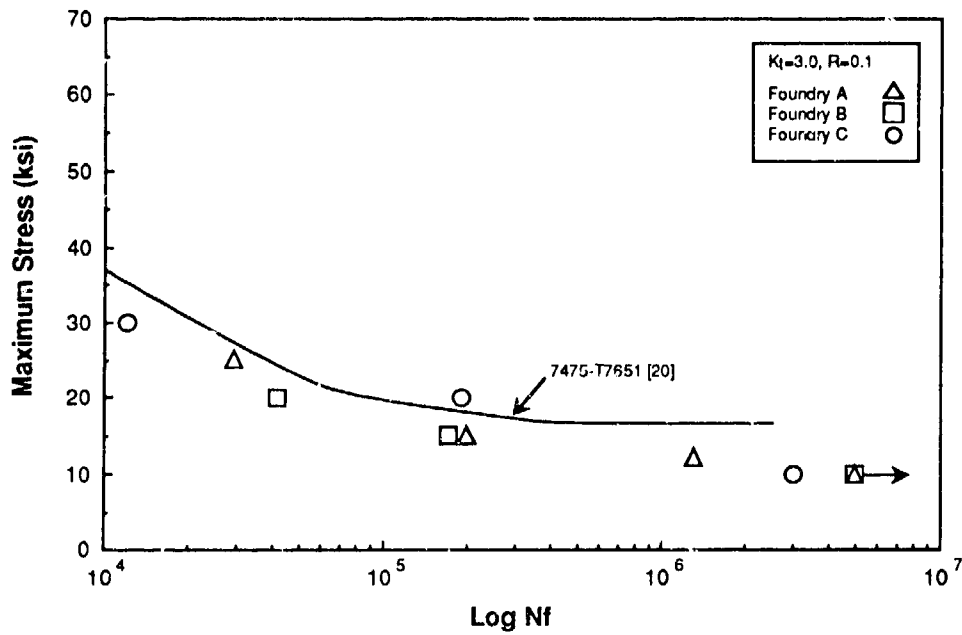
#### 7.3.4 Fatigue Properties

##### 7.3.4.1 Stress-Life

The smooth and notched stress-life data for D357-T6 ( $K_t = 1.0$  and 3.0) are shown in Figure 28a and b, respectively. The smooth fatigue data are compared to 7075-T73 [19], a wrought alloy commonly used in fatigue critical aircraft applications. The fatigue lives of material from Foundry A are longer than those for Foundries B and C for a given stress level. The fatigue lives of the glycol- and water-quenched material are indistinguishable. The average fatigue life of D357-T6 is less than that of 7075-T73, and is presumably due to lower D357-T6 strength and the larger size of the inherent defects found in castings, which will tend to reduce the initiation life, as discussed in Section 7.3.4.3.



a. Smooth Fatigue ( $K_t = 1.0$ )



b. Notched Fatigue ( $K_t = 3.0$ )

Figure 28. D357-T6 Stress-Life Fatigue Data

The notched fatigue data are compared with 7475-T76 [20], which has a longer life than D357-T6 at a given stress, though the difference is not as pronounced as that for the smooth fatigue results.

#### 7.3.4.2 Strain-Life

The strain-life data are shown in Figure 29 as log strain amplitude versus log of the number of cycles to failure ( $N_f$ ). The specimens were tested using an R ratio of -1.0 and a  $K_t$  of 1.0, with strain amplitudes ranging from 0.010 to 0.002, which resulted in fatigue lives ranging from approximately 50 to 1,000,000 cycles. These data were generated for use in the durability analysis (Sections 7.2.3.2 and 10.5). Data from the three foundries were indistinguishable.

#### 7.3.4.3 Fatigue Crack Growth Rate

The range of constant amplitude fatigue crack growth rate (FCGR) data for water- and glycol-quenched material are shown in Figure 30. Also included are data obtained under a previous Northrop program for A357-T6 [21], and 7075-T7351 plate [22]. The DADTAC D357-T6 data are similar to the previous A357-T6 data and are slightly better than that of 7075-T7351. Based on these data, the difference in the total fatigue life between the cast and wrought materials (Figure 28) can be attributed to the ease of crack initiation. Fatigue cracks probably initiate more readily in castings than in wrought material, due to the presence of inherent defects such as dross and/or porosity. Several fatigue life specimens were fractographically examined to determine the crack initiation site. Out of 12 specimens examined, 11 initiated a fatigue crack from a defect located at or near the surface. No clearly defined defect was associated with the fatigue crack initiation of the twelfth specimen. The results are shown in Table 47. All of the defects were porosity and/or dross. Typical sites are shown in Figures 31a and b.

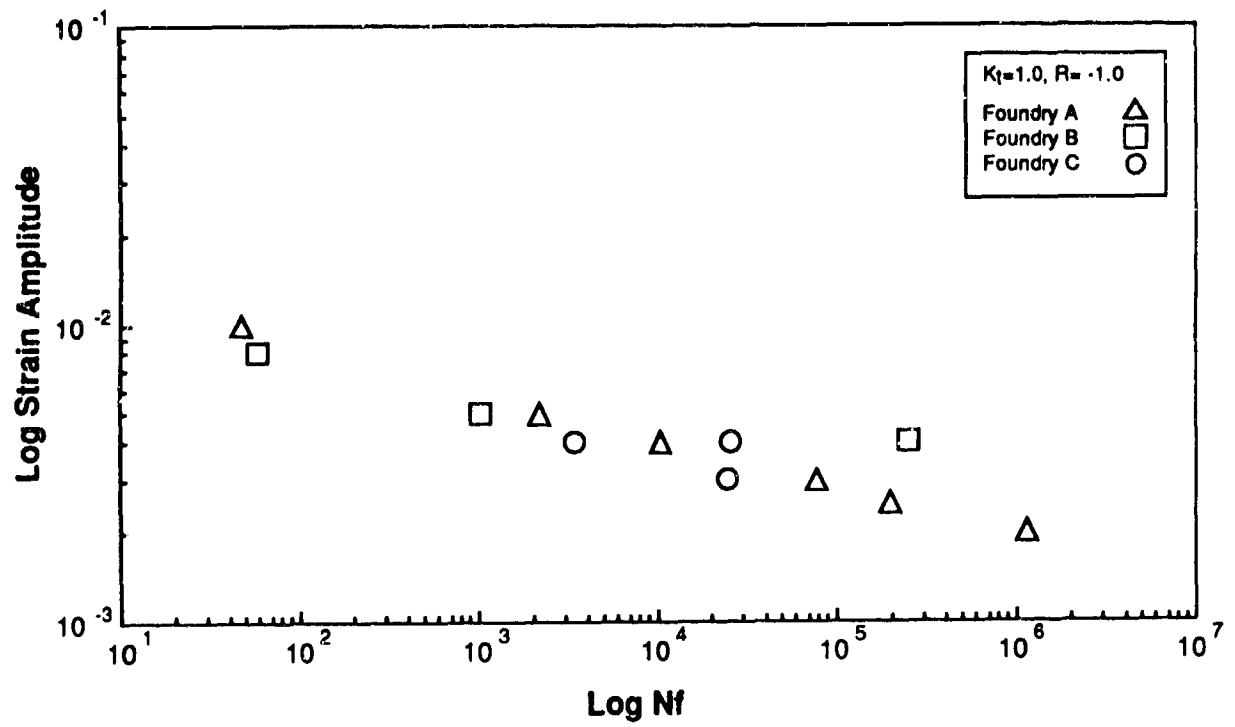


Figure 29. D357-T6 Strain-Life Fatigue Data

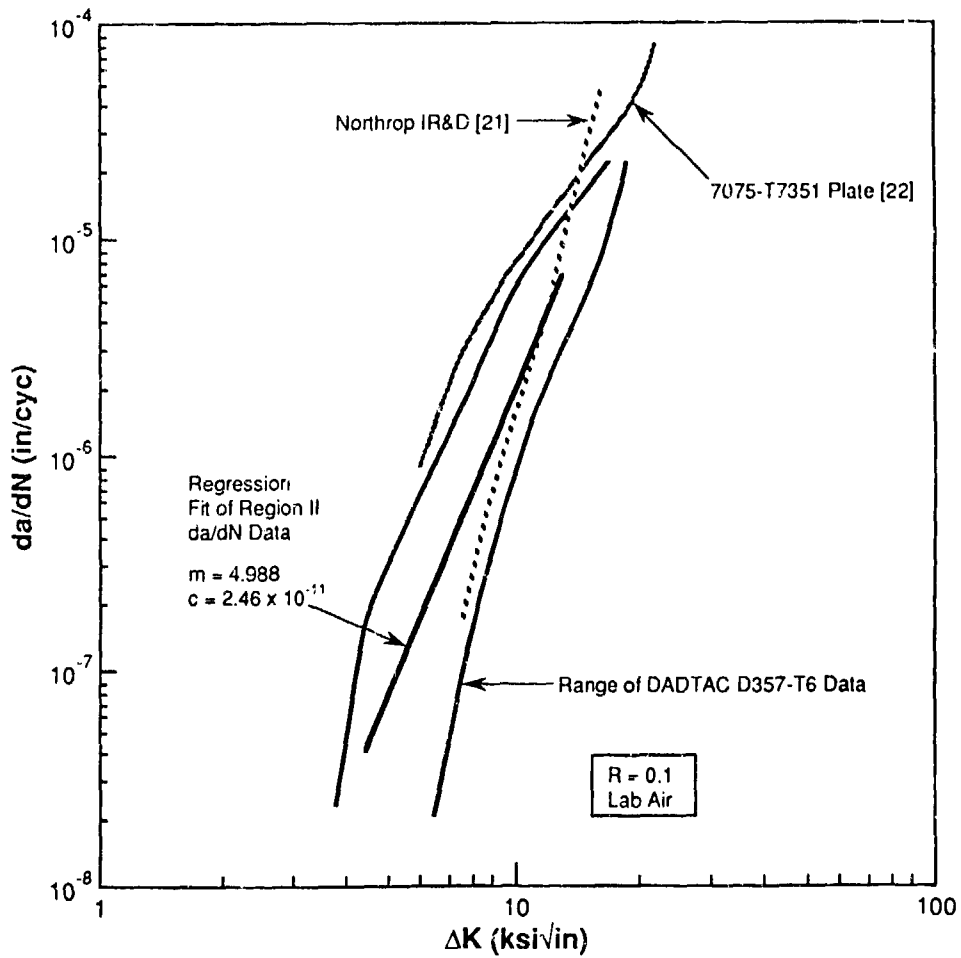
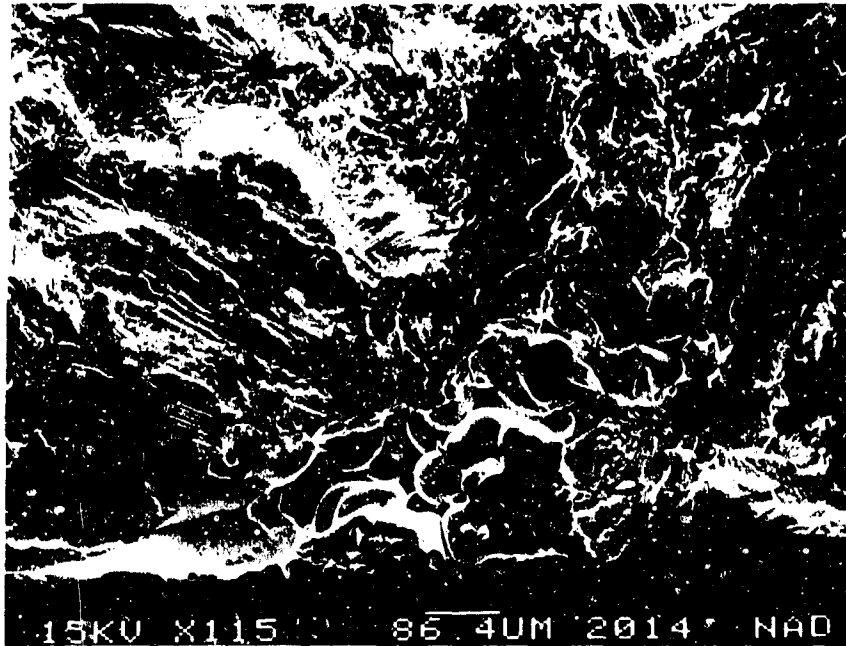


Figure 30. D357-T6 Fatigue Crack Growth Rate Data

TABLE 47. FATIGUE CRACK INITIATION SITES FOR D357-T6 FATIGUE SPECIMENS

| NUMBER OF FATIGUE SPECIMENS WITH CRACK INITIATION SITE |      |                     |        |
|--|------|---------------------|--------|
| Dross  | Pore | Both Dross and Pore | Other* |
| 4  | 4    | 3                   | 1      |

\* No observable defect



a. SEM Micrograph of a Pore



b. Backscatter SEM Micrograph of Foreign Material

Figure 31. Typical Crack Initiation Sites in D357-T6 Fatigue Specimens

#### 7.3.4.4. Spectrum Fatigue Life

Two specimens (Figure 15) were tested under spectrum fatigue loading using an F-18 spectrum (F18C2) at 32 ksi gross maximum stress. The total time to failure for the two specimens was 14,131 and 17,731 flight hours (average - 15,931 flight hours). These data were obtained to provide a baseline for assessing the effect of defects and nonoptimum microstructure on spectrum fatigue life (Section 8).

#### 7.3.5 Fracture Toughness

The average fracture toughness results for water-quenched and glycol-quenched D357-T6 are shown in Table 48. Compact tension and short bar fracture toughness, as well as NTS/YS ratio data were obtained. A short bar test specimen was removed from five of the tested compact tension specimens to provide a direct comparison of the results for the two test methods. Invalid  $K_Q$  results were obtained from the compact tension tests for all the water-quenched material due to excessive crack front curvature, which is often observed in castings due to residual stresses incurred during quenching. Valid  $K_{IC}$  results were obtained for glycol-quenched plates, presumably because of the slower cooling rate associated with the glycol.

An average of 24 ksi/in was obtained for water-quenched material by both compact tension ( $K_Q$ ) and short bar ( $K_{IV}$ ) test methods. The fracture toughness of the glycol-quenched material was slightly less than that of the water-quenched material, 22 ksi/in for both compact tension ( $K_{IC}$ ) and short bar ( $K_{IV}$ ) test methods. The average fracture toughness values for the glycol-quenched and water-quenched plates from each of the foundries was similar.

The compact tension and short bar fracture toughness values are shown as a function of yield strength in Figure 32. The fracture toughness ranged from approximately 21 to 25 ksi/in, with most of the lowest values (21 to 22 ksi/in,  $K_{IC}$ ) being obtained for the glycol-quenched material. There was no clear correlation between the fracture toughness and yield strength, probably because the yield strength range was relatively narrow. Other work [23] has shown that there is an inverse relationship between fracture toughness and yield strength.

TABLE 48. AVERAGE D357-T6 FRACTURE TOUGHNESS AND NOTCHED TENSILE STRENGTH DATA

| FOUNDRY | QUENCH MEDIUM | FRACTURE TOUGHNESS (ksi $\sqrt{\text{in.}}$ ) |                |                  | NTS (ksi) | YS (ksi) | NTS/YS |
|---------|---------------|---|----------------|------------------|-----------|----------|--------|
|         |               | K <sub>IC</sub>                               | K <sub>Q</sub> | K <sub>IV*</sub> |           |          |        |
| A       | Water         | --  | 25             | 25               | 63        | 45       | 1.4    |
|         | Glycol        | 21  | --             | 22               | 58        | 43       | 1.3    |
| B       | Water         | --  | 24             | 24               | 62        | 45       | 1.4    |
|         | Glycol        | 22  | --             | 22               | 58        | 42       | 1.4    |
| C       | Water         | --  | 23             | --               | 53        | 47       | 1.1    |
|         | Glycol        | 22  | --             | --               | 44        | 44       | 1.0    |
| AVERAGE | Water         | --  | 24             | 24               | 59        | 46       | 1.3    |
|         | Glycol**      | 22  | --             | 22               | 53        | 43       | 1.2    |

\* Short bar test  
 \*\* 25% glycol solution

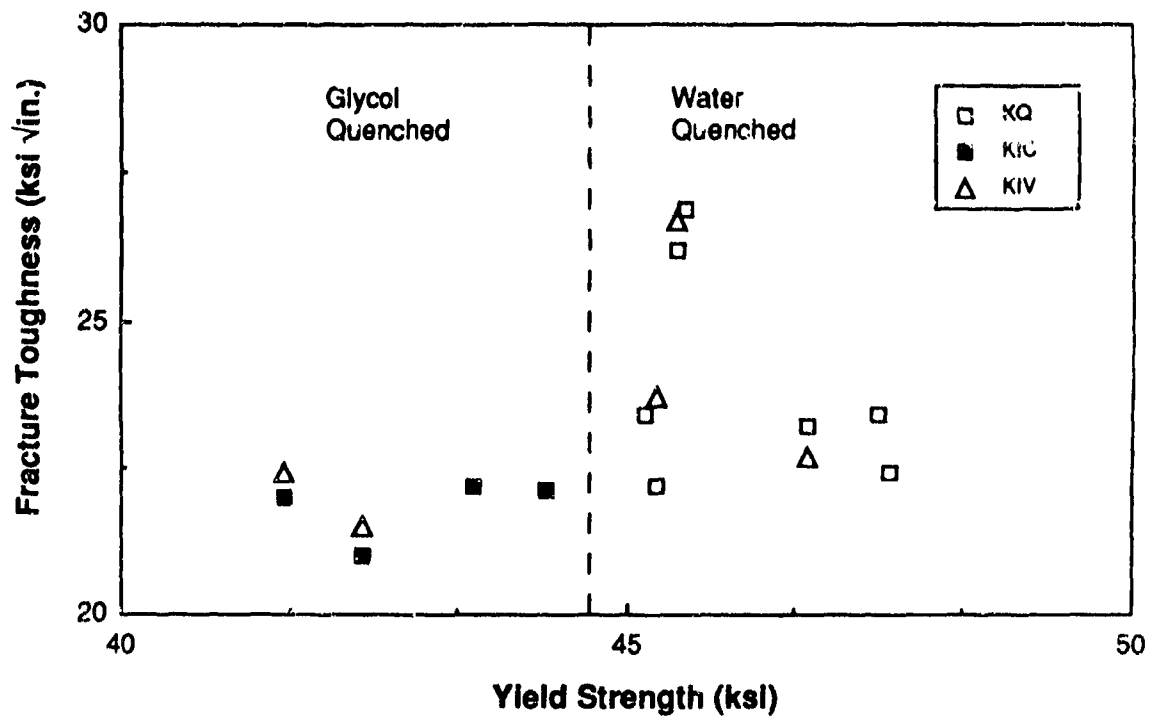


Figure 32. Relationship Between Fracture Toughness and Yield Strength for D357-T6

### 7.3.6 Equivalent Initial Flaw Size Analysis

The method for determining the equivalent initial flaw size was described in Section 7.2.3.1. The calculated values for individual specimens excised from material from all three foundries are shown in Table 49, along with the corresponding fatigue life and maximum applied stress. Testing of specimens that did not fail after  $5 \times 10^6$  cycles was terminated and an EIFS was not calculated.

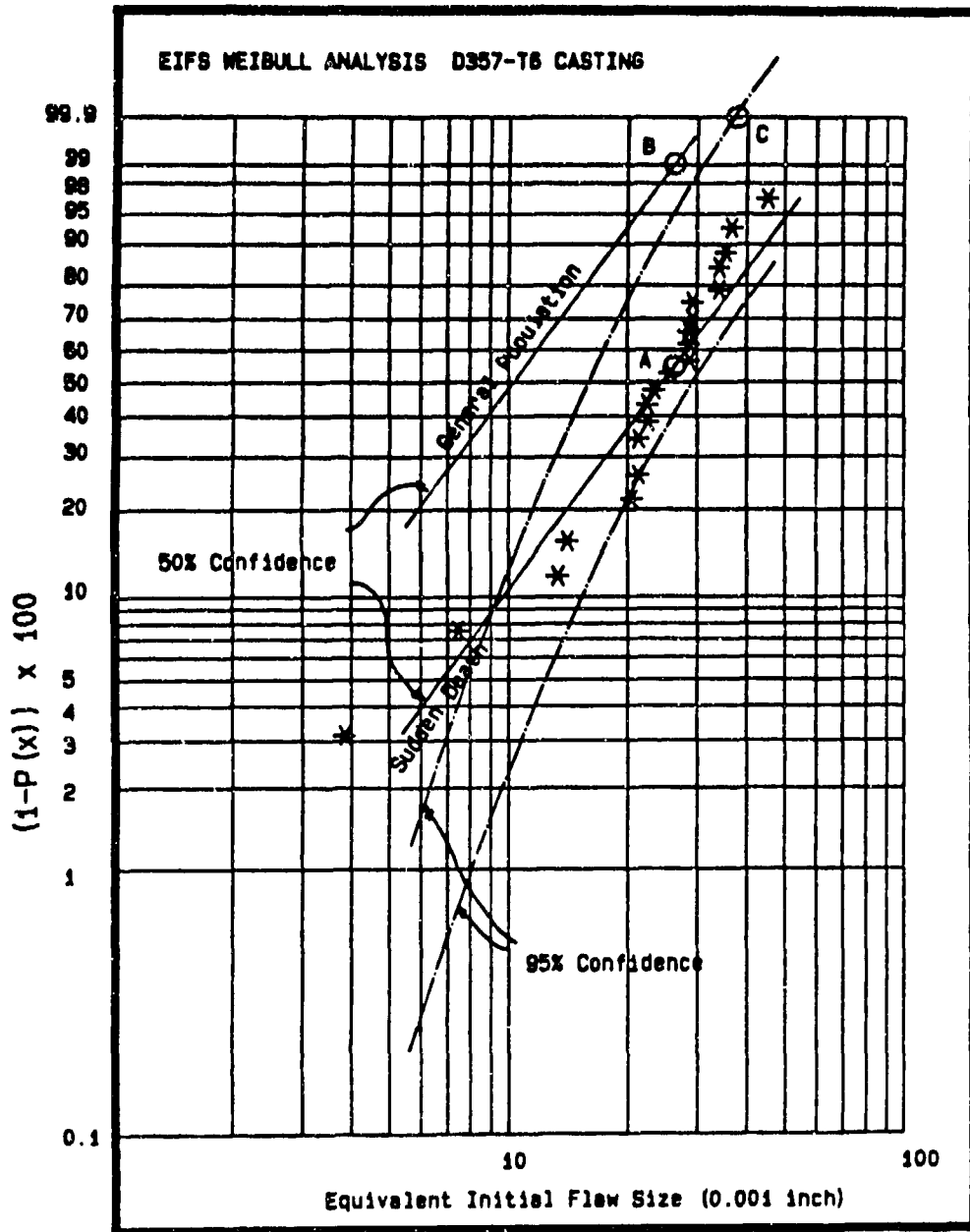
The data indicate that the EIFS for Foundry A is significantly lower than that for Foundries B and C. This is consistent with the S/N fatigue data shown in Figure 28; the results for test specimens from Foundry A material are at the higher end of the overall band of data. The combined EIFS data for all three foundries were then analyzed as described in Section 7.2.3.3 to determine the value of the maximum inherent material rogue flaw size (99.9 percent probability and 95 percent confidence) that should be used to design a cast DADT critical component to a specific life. The data are presented as a Weibull distribution in Figure 33. For D357-T6, the maximum flaw size was determined to be 0.036 inch, which is less than the 0.050-inch flaw that is typically assumed for damage tolerance analysis of wrought materials [15]. A defect of this size may be detected in material up to about 3 inches thick using X-ray radiography at a one percent sensitivity. Based on this information, Grade B, or better, D357-T6 castings up to the maximum thickness evaluated under the DADTAC program (1.25 inch) can be considered for use in a damage tolerance design.

The fracture surfaces of selected fatigue specimens were examined to determine the size of the crack initiation sites and were compared to those derived from the EIFS analysis, Table 50. The measured values were obtained by determining the semicircular area within which the flaw would fit. The center of the semicircle was on the surface of the specimen. Measured values were not obtained for all the fatigue specimens because exact identification of the complete crack initiation site was not possible due to the presence of multiple defects. The derived values are within an order of magnitude of the measured values. Discrepancies between the measured and derived values are probably due to the inability to accurately account for the effects of the

TABLE 49. D357-T6 EQUIVALENT INITIAL FLAW SIZE DATA

| FOUNDRY | MAXIMUM STRESS (ksi) | CYCLES TO FAILURE ( $\times 10^3$ ) | EIFS (inch)   |
|---------|----------------------|-------------------------------------|---------------|
| A       | 30                   | 4069                                | 0.0039        |
|         | 30*                  | 1474                                | 0.0073        |
|         | 35                   | 220                                 | 0.0139        |
|         | 45                   | 50                                  | 0.0149        |
|         | 40*                  | 50                                  | 0.0211        |
|         | 40                   | 50                                  | <u>0.0211</u> |
|         | Avg.                 |                                     | <u>0.0137</u> |
| B       | 30*                  | 254                                 | 0.0201        |
|         | 30                   | 213                                 | 0.0220        |
|         | 40*                  | 45                                  | 0.0223        |
|         | 45                   | 14                                  | 0.0292        |
|         | 20*                  | 982                                 | 0.0293        |
|         | 40                   | 26                                  | 0.0295        |
|         | 25                   | 223                                 | <u>0.0341</u> |
| Avg.    |                      | <u>0.0266</u>                       |               |
| C       | 40                   | 50                                  | 0.0210        |
|         | 20                   | 1569                                | 0.0232        |
|         | 30                   | 118                                 | 0.0251        |
|         | 30*                  | 123                                 | 0.0289        |
|         | 30                   | 165                                 | 0.0294        |
|         | 30*                  | 91                                  | 0.0334        |
|         | 40*                  | 20                                  | 0.0334        |
|         | 20*                  | 618                                 | 0.0362        |
|         | 20*                  | 373                                 | <u>0.0450</u> |
|         | Avg.                 |                                     | <u>0.0306</u> |

\* Glycol-quenched



Note: Weibull Mean (A) of the Sudden Death Data Clusters About the 99% Probability Level of the General Population (B). The Maximum Expected Flow (99.9% Probability With 95% Confidence) is Indicated by Point (C)

Figure 33. Weibull Distribution of D357-T6 EIFS Data

TABLE 50. COMPARISON OF PREDICTED AND MEASURED EQUIVALENT INITIAL FLAW SIZE FOR D357-T6

| SPECIMEN | EIFS (in) |          |
|----------|-----------|----------|
|          | PREDICTED | MEASURED |
| V111     | 0.0039    | 0.0175   |
| V115     | 0.0073    | 0.0375   |
| V116     | 0.0211    | 0.0343   |
| V209     | 0.0292    | 0.0096   |
| V210     | 0.0341    | 0.0162   |
| V211     | 0.0201    | 0.0062   |
| V213     | 0.0293    | 0.0137   |

shape (sometimes very complex) and orientation of the crack initiation sites relative to the specimen surface. The difficulty of accurately measuring defects is illustrated in Figures 34a and b. The measured defect size is indicated by the semicircle enclosing each defect with the center of the semicircle placed on the edge of the specimen. (A semicircle was used because DADT analyses assumes the presence of a semicircular flaw in the material.) It can be clearly seen that the semicircle encloses much more material than the defect, and that the size of the semicircle is highly dependent upon the aspect ratio of the defect. In contrast, the EIFS analysis determines the semicircular area which has the same effect on fatigue properties as a highly aspected defect. Highly aspected defects can cause the measured defect size to be either greater than or less than the predicted defect size (the EIFS). From this comparison, it was concluded that the approach being used to predict the EIFS from smooth fatigue data is viable.

#### 7.4 B201-T7 RESULTS

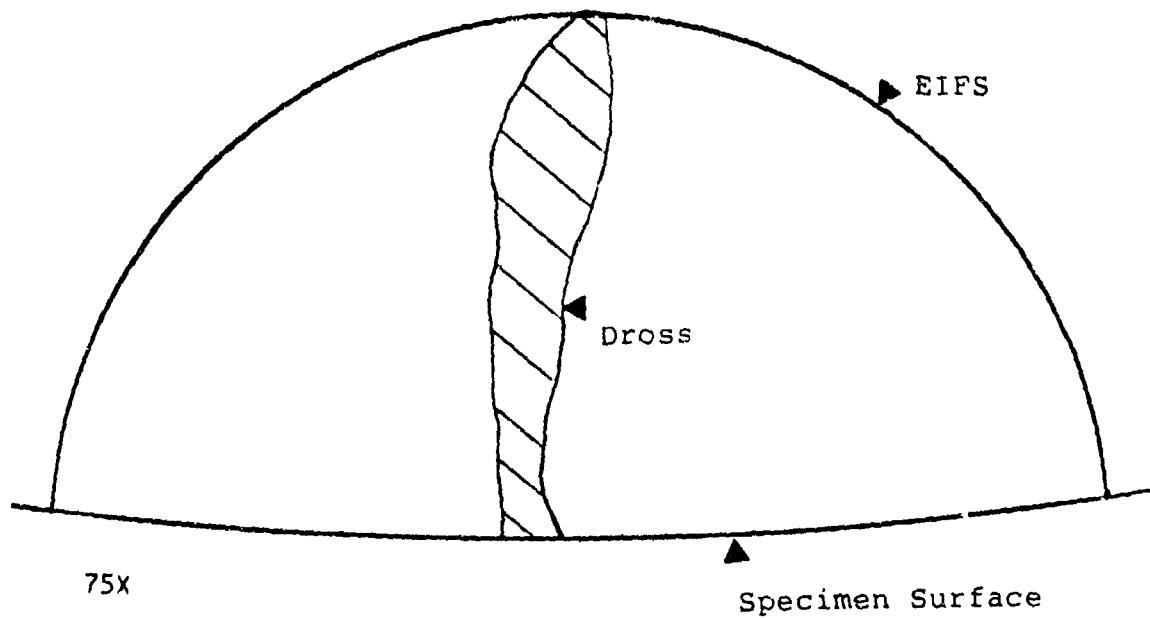
##### 7.4.1 Composition

Twenty plates cast (both 1.25 inch thick and 0.75 inch thick) from eight different melts by three foundries were used for the B201 verification evaluations. The composition of each of these melts and the ranges for each element are listed in Table 51. All of the compositions were within the specified range (AMS 4242) [2]. Reported compositions of the plates were confirmed by ICP tests at Northrop.

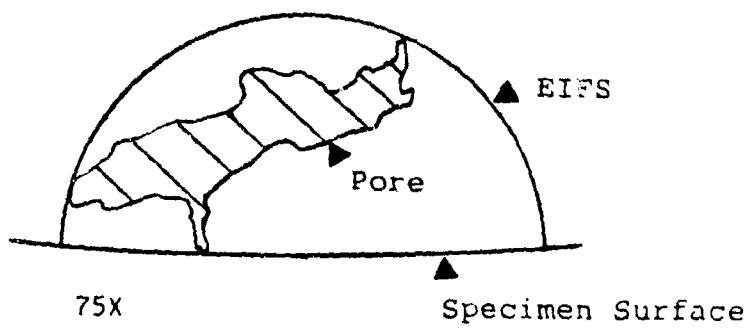
##### 7.4.2 Microstructure

The microstructure of the B201-T7 plates was characterized using optical, TEN, STEM, and SEM methods, and the grain size and percent porosity of each plate were determined.

The grain size at random locations in plates from all three foundries ranged from 0.0024 inch to 0.0039 inch. A typical micrograph of the B201-T7 microstructure is shown in Figure 35.



a. Dross

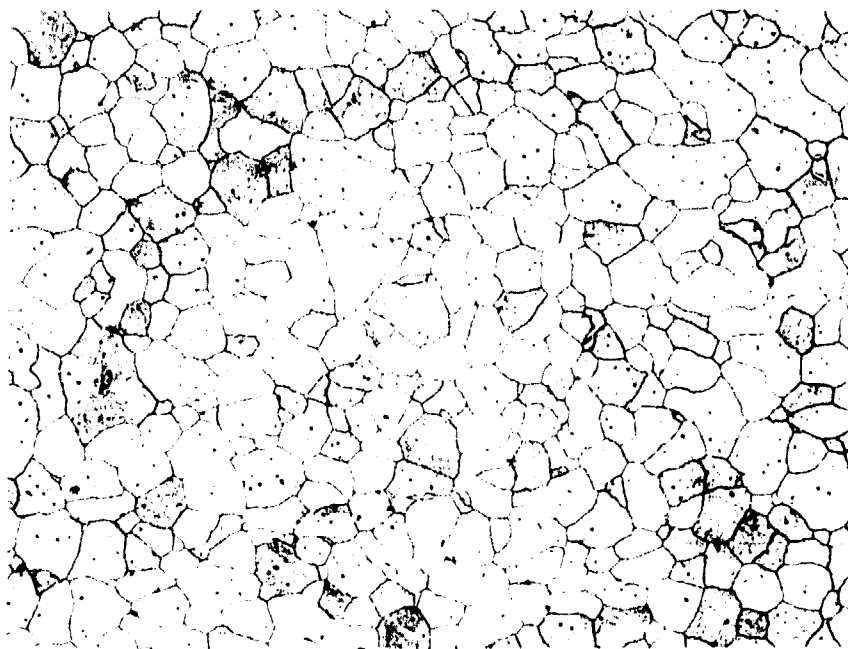


b. Pore

Figure 34. Measurement of Defect Size in D357-T6

TABLE 51. B201 VERIFICATION MATERIAL MELT COMPOSITIONS

| COMPOSITION (WT %)            |       |       |       |       |       |       |      |
|-------------------------------|-------|-------|-------|-------|-------|-------|------|
| Cu                            | Ag    | Mg    | Mn    | Ti    | Fe    | Si    | Al   |
| 4.59                          | 0.56  | 0.27  | 0.28  | 0.19  | 0.02  | 0.04  | Bal. |
| 4.55                          | 0.55  | 0.30  | 0.28  | 0.18  | 0.01  | 0.02  | Bal. |
| 4.54                          | 0.40  | 0.27  | 0.22  | 0.17  | 0.01  | 0.05  | Bal. |
| 4.75                          | 0.44  | 0.24  | 0.33  | 0.16  | 0.02  | 0.05  | Bal. |
| 4.69                          | 0.64  | 0.28  | 0.28  | 0.28  | 0.04  | 0.04  | Bal. |
| 4.93                          | 0.69  | 0.28  | 0.28  | 0.28  | 0.04  | 0.04  | Bal. |
| 4.59                          | 0.65  | 0.26  | 0.27  | 0.24  | 0.04  | 0.02  | Bal. |
| 4.63                          | 0.57  | 0.25  | 0.31  | 0.18  | 0.02  | 0.01  | Bal. |
| <u>AMS 4242 Specification</u> |       |       |       |       |       |       |      |
| 4.5-                          | 0.40- | 0.20- | 0.20- | 0.15- | ≤0.05 | ≤0.05 | Bal. |
| 5.0                           | 0.80  | 0.30  | 0.50  | 0.35  |       |       |      |



50X

Kellers Etch

Figure 35. Typical B201-T7 Microstructure

The microstructure was examined further by SEM, STEM, and TEM. SAD diffraction patterns and EDXA of various phases were taken, and five different phases were identified. The most prominent of these five was the strengthening phase  $\text{CuAl}_2$ , ( $\theta$ ), Figure 36, found as small platelets on the (100) plane of the aluminum matrix. A grain boundary phase and associated precipitate-free zone were also observed in Figure 36. EDX analysis of the grain boundary area identified the presence of Al and Cu, suggesting the phase was equilibrium  $\text{CuAl}_2$ .  $\text{CuAl}_2$  was also seen as a large blocky constituent phase, Number 2 in Figure 37. Other large constituents were also observed in Figure 37. The constituent labeled Number 1 contained Cu and Fe. The constituents indicated by Numbers 3 and 4 were rich in Ti, and those indicated by Numbers 5 and 6 contained Cu, Fe, and Mn.

Two grain boundary phases were also observed in addition to the equilibrium  $\text{CuAl}_2$  phase. One was the Al, Cu, Fe, and Mn rich phase mentioned previously, Number 1 in Figure 38; the other was rich in Al, Cu, and Mn, Number 2. A large blocky Al, Cu, and Mn phase was also observed in the matrix, Figure 39. Figure 40 shows an Al-Ti phase, which was  $\text{Al}_3\text{Ti}$ ,  $\text{Al}_{24}\text{Ti}_6$ , or  $\text{Al}_{23}\text{Ti}_9$ .

The  $\text{CuAl}_2$  phase identified above has been reported [24] for alloys containing Ag to be omega, an altered form of theta, the main strengthening precipitate in Al-Cu alloys. The addition of Ag to Al-Cu alloys promotes the formation of the omega strengthening precipitate during aging above about 210°F and causes a marked increase in age hardening. Silver was also shown by regression analyses (Section 6.3.6) to increase the strength of B201-T7. Omega essentially replaces theta and is thought to be a monoclinic or hexagonal form of the theta phase, which itself is body-centered tetragonal. Omega forms on the (111) plane of the matrix as a uniform dispersion of large very thin, hexagonally shaped plates, and is thought to be coherent with the matrix along the (111) plane and at the ends of the precipitate. Omega may be more stable than theta, as evidenced by creep testing [24]. In addition, the precipitation mechanism associated with the omega phase seems to be different from that of the theta phase.

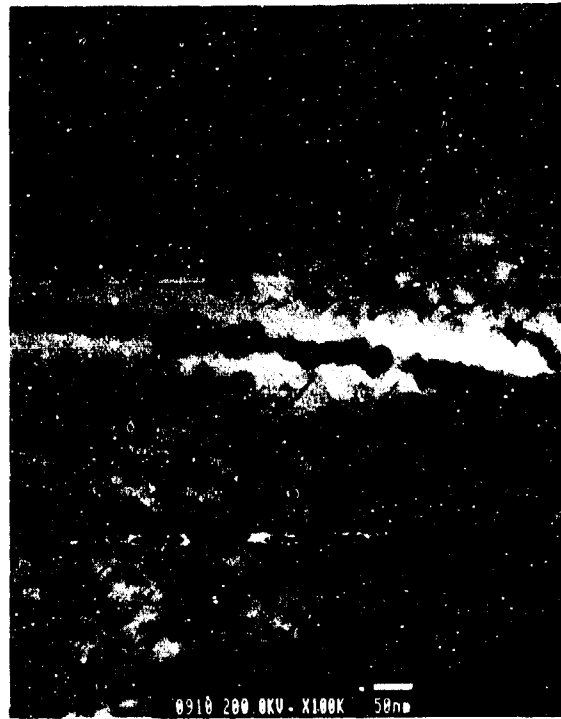


Figure 36. TEM Micrograph of B201-T7 Showing the Theta Phase



Figure 37. Backscatter SEM Image of B201-T7



Figure 38. STEM Micrograph of B201-T7 Showing a Phase Rich in Al, Cu, Fe, and Mn



Figure 39. TEM Micrograph of B201-T7 Showing a Phase Rich in Al, Cu, and Mn



Figure 40. TEM Micrograph of B201-T7 Showing a Phase Rich in Al and Ti

Scanning diffractometry of B201 was also conducted to identify phases. Analysis of the diffraction pattern led to the identification of only two phases,  $Al_2O_3$  and delta ( $Al_4Cu_9$ ). Phases containing other alloying elements were not detected due to the relatively small amount (<1 weight percent) of all alloying elements in B201 except for Cu.

#### 7.4.3 Tensile Properties

The average and minimum (indicated by the ranges) tensile property values of the 1.25-inch-thick B201-T7 plates from all three foundries are shown in Table 52. Test results were also obtained for the 0.75-inch-thick plates to provide a direct comparison with those obtained in the screening portion of Phase I, Task 2. Average tensile properties of 66.5 ksi ultimate strength, 59.1 ksi yield strength, and 8.3 percent elongation to failure were obtained for the 0.75-inch-thick verification plates with minimum values of 64/55/6.5. These properties are similar to those obtained for the screening material (65/57/7).

All the individual tensile properties for the 1.25-inch-thick verification plates from all three foundries exceeded the specified minimum of 60 ksi ultimate strength, 50 ksi yield strength, and 3 percent elongation. Material from Foundry B had the highest strength; material from Foundries A and C had similar properties. Stress corrosion tests were conducted (Section 7.4.6) and confirmed that the alloys were in the T7 condition.

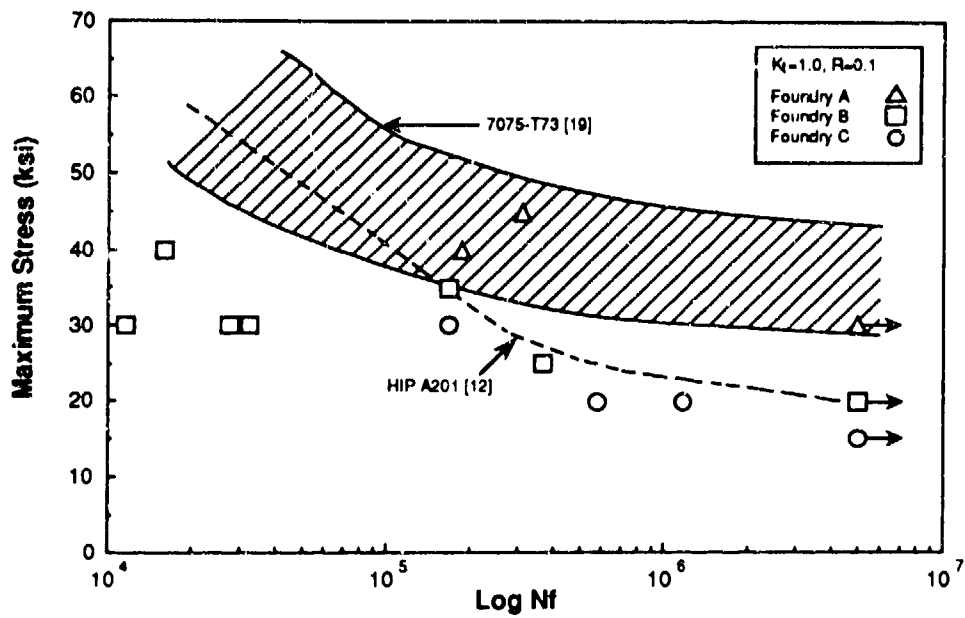
#### 7.4.4 Fatigue Properties

##### 7.4.4.1 Stress-Life

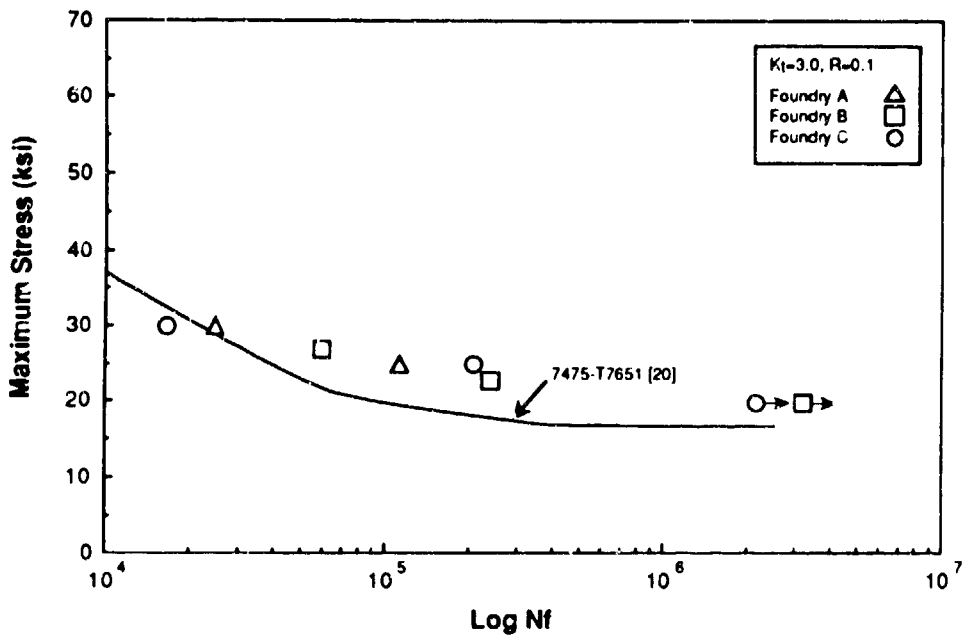
The smooth and notched stress-life ( $K_t = 1.0$  and  $3.0$ ) data for B201-T7 from the three foundries are shown in Figure 41. The smooth fatigue data are compared to results for A201-T7 material obtained under a previous Northrop/Navy contract [12], and 7075-T73 [19], an alloy commonly used in fatigue-critical aircraft applications. The fatigue lives for B201-T7 from Foundries B and C are similar and are shorter than those for Foundry A material.

TABLE 52. TENSILE PROPERTIES OF 1.25-INCH-THICK B201-T7 PLATES

| FOUNDRY     | UTS (ksi) |       | YS (ksi) |       | El (%) |          |
|-------------|-----------|-------|----------|-------|--------|----------|
|             | AVG.      | RANGE | AVG.     | RANGE | AVG.   | RANGE    |
| A           | 66        | 65-67 | 57       | 54-58 | 8.7    | 8.3-11.0 |
| B           | 70        | 68-73 | 63       | 60-66 | 8.2    | 7.5-8.8  |
| C           | 67        | 64-70 | 60       | 58-62 | 8.3    | 6.5-9.5  |
| Average     | 68        |       | 60       |       | 8.4    |          |
| Target Min. | 60        |       | 50       |       | 3.0    |          |



a. Smooth Fatigue ( $K_t = 1.0$ )



b. Notched Fatigue ( $K_t = 3.0$ )

Figure 41. B201-T7 Stress-Life Fatigue Data

Eight fatigue specimens ( $K_t = 1.0$ ) were fractographically evaluated to determine the nature of the crack initiation site. For five specimens, foreign material (dross) was observed at the initiation site. In two specimens, porosity was found; in the remaining specimen there was no indication of a microstructural discontinuity.

Two specimens of Foundry A material were evaluated, which showed the best fatigue life results. One contained dross, which was an internal flaw; the other specimen was the one that did not contain any noticeable discontinuities. Two Foundry B specimens contained dross; a third contained porosity. For all three Foundry C specimens, dross was present at the initiation site.

The notched ( $K_t = 3.0$ ) fatigue data are compared with 7475-T76 [20]. The fatigue data for the two alloys are very similar, with those for B201-T7 being slightly better than 7475-T76.

#### 7.4.4.2 Strain-Life

The strain-life data, plotted as log strain amplitude vs. log of the number of cycles to failure ( $N_f$ ), are shown in Figure 42. The specimens were tested using an R ratio of -1.0 and a  $K_t$  of 1.0, with strain amplitudes ranging from 0.008 to 0.002. These strain amplitudes resulted in fatigue lives ranging from approximately 500 to 200,000 cycles. These data were generated for use in the durability analysis (Sections 7.2.3.2 and 10.5).

#### 7.4.4.3 Fatigue Crack Growth Rate

The range of fatigue crack growth rate (constant amplitude) data for B201-T7 from the three foundries is shown in Figure 43. Also included are data for A201-T7 tested under a Northrop/Navy contract [12], and 7075-T7351 plate [22], an alloy used in fatigue critical aircraft applications. The DADTAC program data are similar to the Northrop/Navy contract A201-T7 data. However, B201-T7 had a slightly slower fatigue crack growth rate than 7075-T7351. Because the FCGR for B201 castings and 7075-T7351 is similar, the

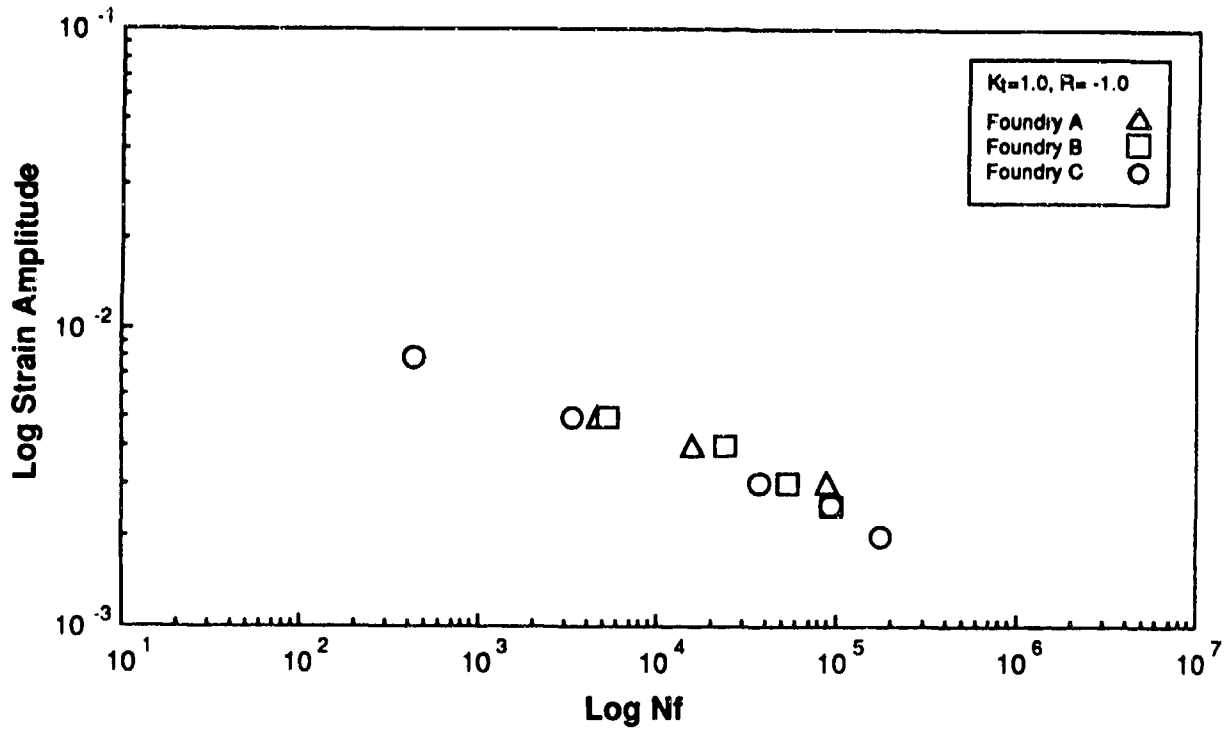


Figure 42. B201-T7 Strain-Life Fatigue Data

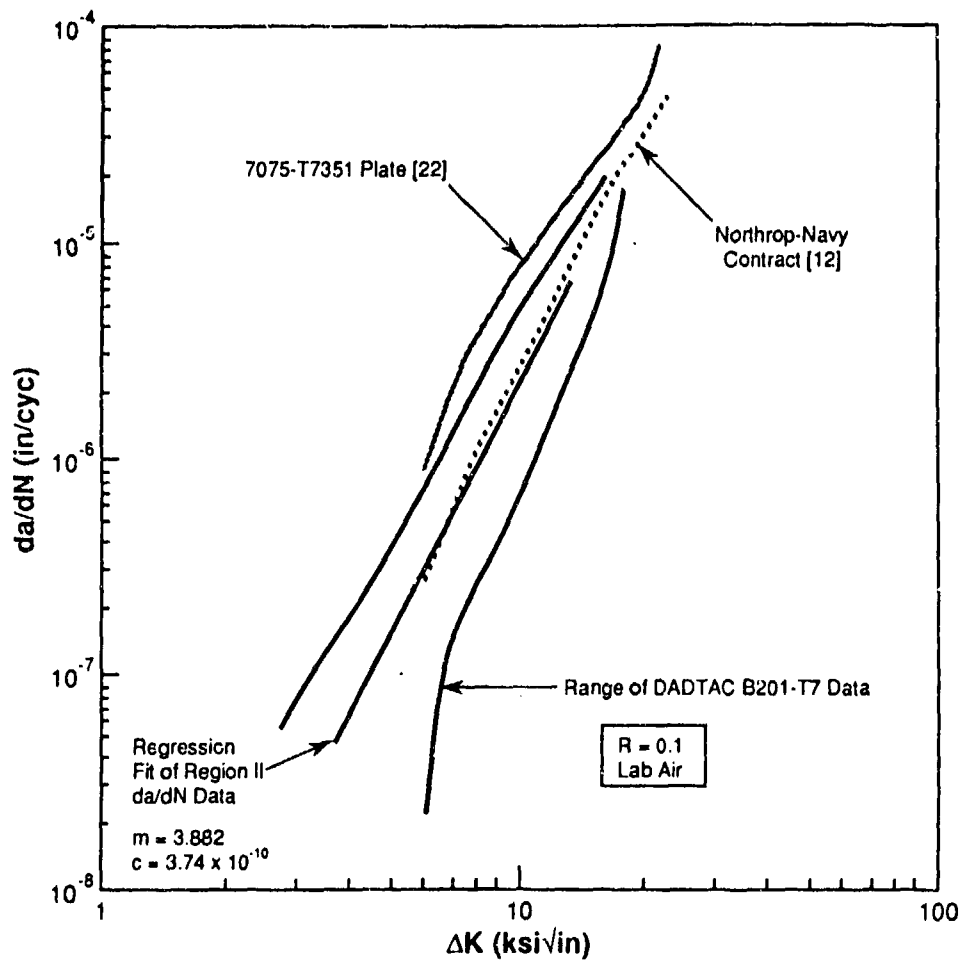


Figure 43. B201-T7 Fatigue Crack Growth Rate Data

difference in total fatigue life (Figure 41) can be attributed to the reduced crack initiation resistance of the cast material, which is presumably due to the presence of inherent defects such as dross and/or porosity.

Each fatigue life specimen was fractographically examined to determine the crack initiation site(s). Out of eight specimens examined, fatigue cracks in seven of them initiated at defects. It was not possible to detect a defect associated with the crack initiation in the remaining specimen. The defects were either gas porosity, shrinkage porosity, or foreign material. A typical foreign material defect is shown in Figure 44.

#### 7.4.4.4 Spectrum Fatigue Life

Similar to D357-T6, two specimens were tested under spectrum loading to provide a baseline for assessing the effect of nonoptimum microstructure on fatigue life (Section 8). The fatigue lives were 26,762 and 14,731 flight hours for maximum stresses of 32 ksi and 40 ksi, respectively. The spectrum was an F-18 wing root spectrum (F18C2); the specimen configuration is shown in Figure 15.

#### 7.4.5 Fracture Toughness

The individual and average compact tension and short bar fracture toughness values, as well as average NTS/YS ratios, of B201-T7 are shown in Table 53. The short bar test specimens were excised from the broken compact tension specimens to provide a direct comparison of the two test methods. An average  $K_Q$  value of 39.4 ksi/in was obtained from compact tension testing, which is similar to the average  $K_{IV}$  value of 40.4 ksi/in obtained from the short bar test. The average  $K_Q$  values for Foundries A, B, and C were 43, 29, and 47 ksi/in, respectively. The Foundry B toughness value was significantly lower than for the other two foundries. From Table 53, it can be seen that the yield strength of the Foundry B material is higher than that from Foundries A and C, indicating that it may have been overaged. The lower NTS/YS ratio is in agreement with the fracture toughness data. One of Foundry B's fracture toughness specimens was fractographically examined but no clear explanation for the low values was obtained.

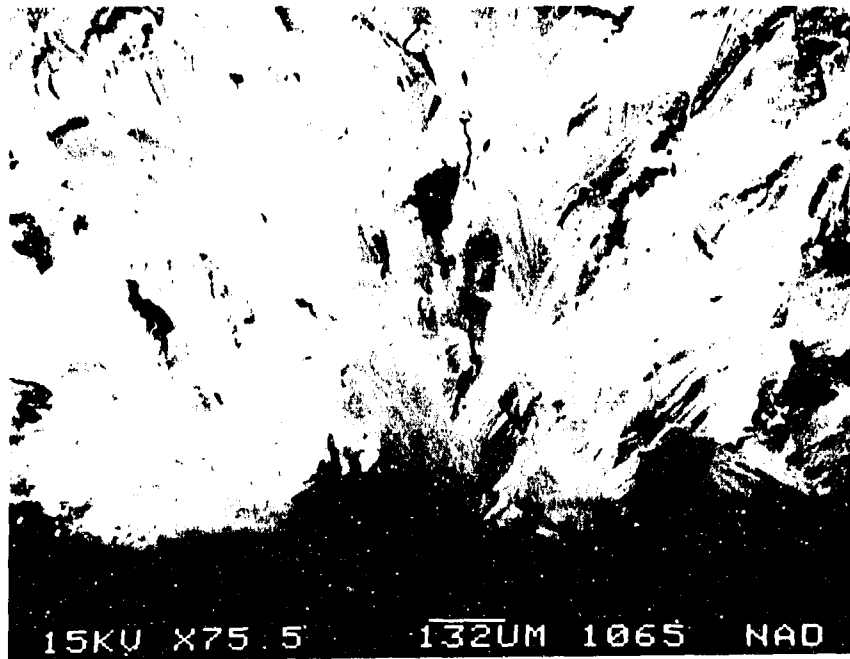


Figure 44. Foreign Material on a B201-T7  
Fatigue Specimen Fracture Surface

TABLE 53. B201-T7 FRACTURE TOUGHNESS AND NOTCHED TENSILE STRENGTH DATA

| FOUNDRY | FRACTURE TOUGHNESS (ksi/in) |                   | NTS<br>(ksi) | YS<br>(ksi) | NTS/YS |
|---------|-----------------------------|-------------------|--------------|-------------|--------|
|         | K <sub>Q</sub>              | K <sub>IV</sub> * |              |             |        |
| A       | 46                          | 56                | 92.7         | 57.7        | 1.62   |
|         | 39                          | 41                | 88.6         | 57.2        | 1.55   |
| B       | 27                          | 27                | 81.5         | 62.5        | 1.37   |
|         | 32                          | 31                | 84.8         | 65.8        | 1.29   |
| C       | 49                          | 43                | 90.7         | 60.3        | 1.50   |
|         | 46                          | 44                | 86.0         | 60.1        | 1.44   |
| AVERAGE | 40                          | 40                | 87.3         | 60.6        | 1.46   |

\* Short bar test

Invalid  $K_Q$  results were obtained for all the compact tension tests due to excessive crack front curvature, similar to the water-quenched D357-T6 specimens (Section 7.3.5).

Individual specimen data and the relationship between fracture toughness and yield strength is shown in Figure 45. The fracture toughness decreased with increasing yield strength and ranged from 27 to 46 ksi/in. The corresponding short bar results ranged from 27 to 58 ksi/in.

#### 7.4.6 Stress Corrosion

Stress corrosion tests were conducted on B201 from all three foundries. Direct tension, alternate immersion tests were conducted; specimens were exposed to a 3.5 percent NaCl solution for 30 days at 75 percent of the material yield strength. No failures were experienced after the 30 day exposure, indicating that each plate had been heat treated to the T7 (overaged) condition.

#### 7.4.7 Equivalent Initial Flaw Size Analysis

The method for determining the equivalent initial flaw size was described in Section 7.2.3.1. The calculated values for individual specimens excised from material from each of the three foundries are shown in Table 54, along with the fatigue life and maximum applied stress. Testing of specimens that did not fail after  $5 \times 10^6$  cycles was terminated and an EIFS was not calculated.

The data indicate that the EIFS for material from Foundry A is less than that for Foundries B and C. This is consistent with the stress-life fatigue data shown in Figure 41; the results for Foundry A material are at the higher end of the overall data band. Data for Foundries B and C are similar.

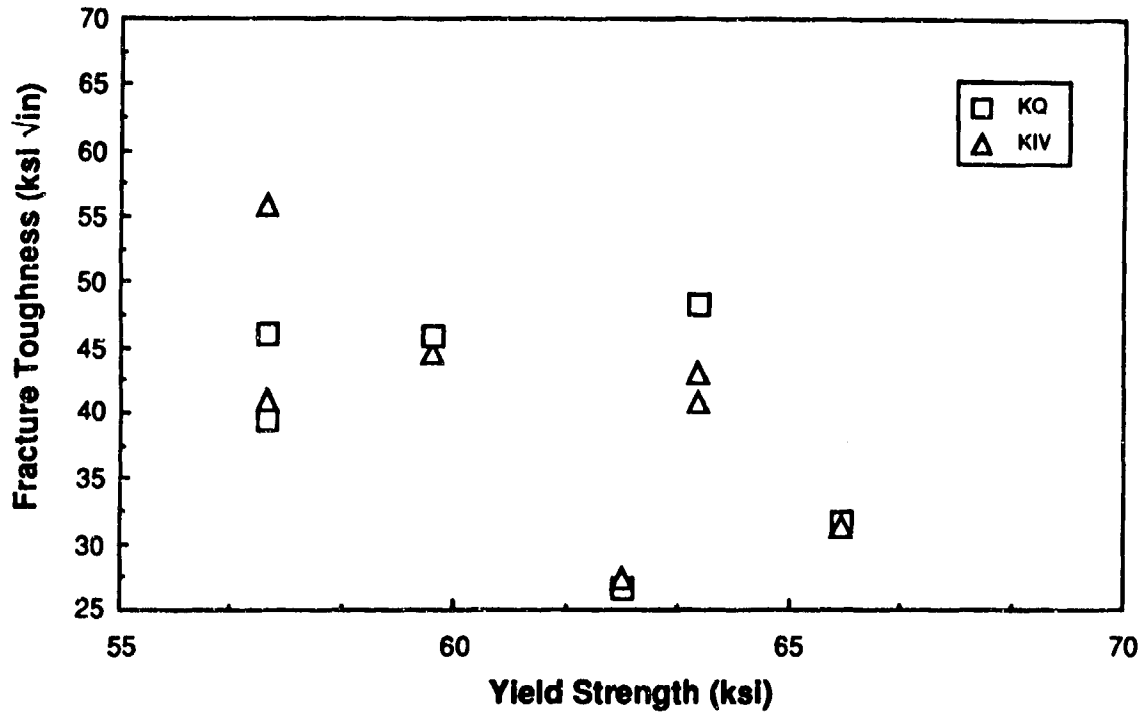


Figure 45. Relationship Between Fracture Toughness and Yield Strength of B201-T7

TABLE 54. B201-T7 EQUIVALENT INITIAL FLAW SIZE DATA

| FOUNDRY | MAXIMUM STRESS (ksi) | CYCLES TO FAILURE ( $\times 10^3$ ) | EIFS (INCH)   |
|---------|----------------------|-------------------------------------|---------------|
| A       | 40                   | 187                                 | 0.0037        |
|         | 45                   | 309                                 | 0.0014        |
|         | 30                   | 5,000*                              | --            |
|         | 20                   | 5,000*                              | --            |
|         | Avg.                 |                                     | <u>0.0025</u> |
| B       | 25                   | 39                                  | 0.0111        |
|         | 30                   | 28                                  | 0.0404        |
|         | 35                   | 188                                 | 0.0067        |
|         | 20                   | 5,000*                              | -             |
|         | Avg.                 |                                     | <u>0.0194</u> |
| C       | 40                   | 16                                  | 0.0289        |
|         | 20                   | 118                                 | 0.0086        |
|         | 20                   | 573                                 | 0.0160        |
|         | 30                   | 168                                 | 0.0118        |
|         | 15                   | 5,000*                              | -             |
|         | Avg.                 |                                     | <u>0.0163</u> |

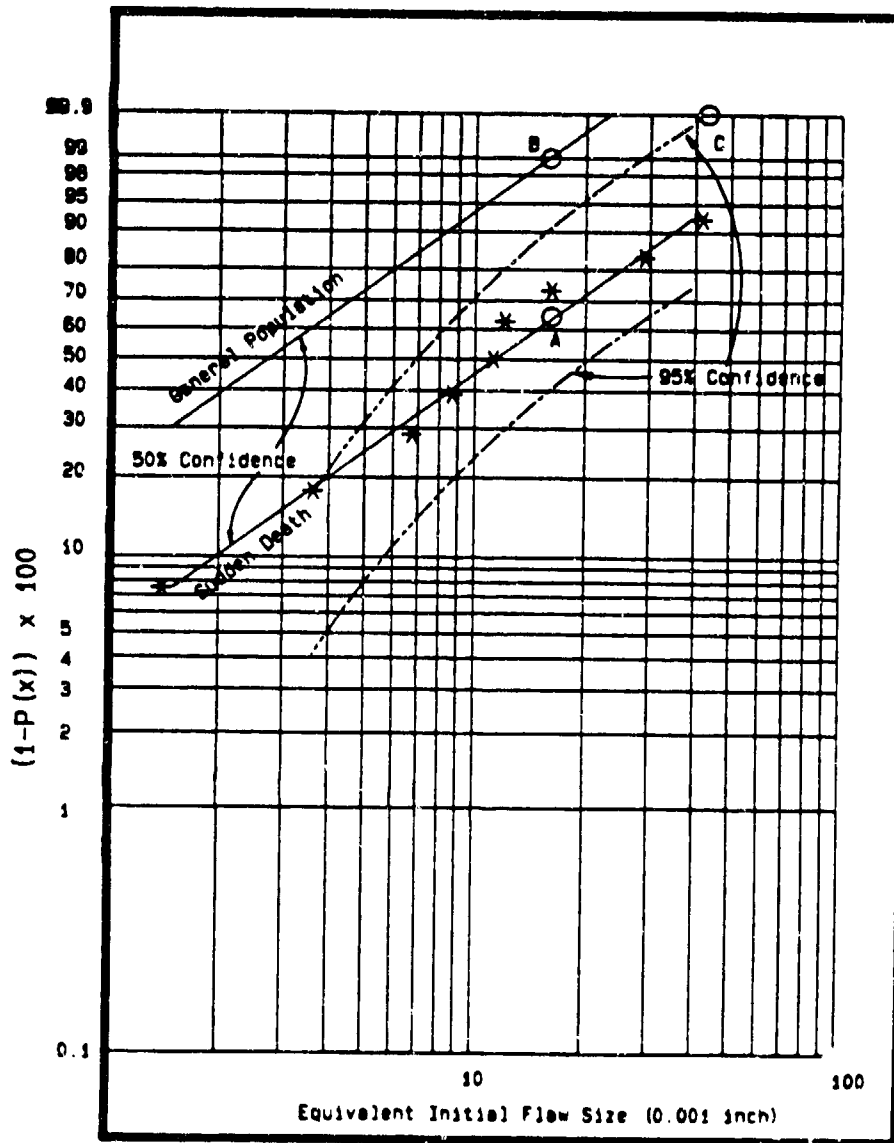
\* No failure

The EIFS data were then analyzed as described in Section 7.2.3.3 to determine the maximum inherent rogue flaw size (99.9 percent probability and 95 percent confidence) that should be used to design a cast DADT critical component to a specific life. The data are presented as a Weibull distribution in Figure 46. For B201-T7, the maximum flaw size was determined to be 0.042 inch, which is less than the 0.050-inch flaw that is typically assumed for damage tolerance analysis [15]. A flaw of this size can be detected in material up to about 4 inches thick by X-ray radiography using 1 percent sensitivity. Based on this information, Grade B or better B201-T7 castings up to the maximum thickness evaluated under the DADTAC program (1.25 inch) can be considered for use in a damage tolerance design.

The fracture surfaces of the fatigue specimens were examined to determine the size of the crack initiation sites. A comparison of these measured values and those derived from the EIFS analysis is shown in Table 55. The measured values were obtained by determining the semicircular area within which the flaw would fit, with the center of the semicircle on the surface of the specimen. The derived values are within an order of magnitude of the measured values. Discrepancies between the measured and derived values are probably due to the inability to accurately account for the effects of the shape and orientation of the crack initiation sites as discussed in Section 7.3.6.

#### 7.4.8 Effect of HIPing on Porosity

HIPing was shown [12] to improve the mechanical properties of A201-T7, particularly fatigue life and, consequently, all cast B201 plates evaluated during the DADTAC program were similarly HIPed. To ensure that the cast B201 verification plates had been HIPed, the amount of porosity present in 10 B201 plates was determined using the FAI method (Section 4) both before and after HIPing. The average porosity before HIPing was 0.34 percent (range 0.2 to 0.8 percent); after HIPing, porosity was reduced to 0.08 percent (range 0 to 0.2 percent) i.e., a reduction of about 75 percent.



Note: Weibull Mean (A) of the Sudden Death Data Clusters About the 99% Probability Level of the General Population (B). The Maximum Expected Flaw (99.9% Probability With 95% Confidence) is Indicated by Point (C)

Figure 46. Weibull Distribution of B201-T7 EIFS Data

TABLE 55. COMPARISON OF PREDICTED AND MEASURED EQUIVALENT INITIAL FLAW SIZE FOR B201-T7

| SPECIMEN | EIFS (in) |          |
|----------|-----------|----------|
|          | PREDICTED | MEASURED |
| V156     | 0.0037    | 0.0025   |
| V256     | 0.0111    | 0.0037   |
| V355     | 0.0118    | 0.0366   |
| V356     | 0.0086    | 0.0316   |
| V357     | 0.0160    | 0.0075   |

## 7.5 CONCLUSIONS

- Tensile properties of the verification material were similar to those of the screening plates.
- The fatigue crack growth rates of D357-T6 and B201-T7 castings are similar, but are slightly slower than those of 7075-T7351.
- Based on an evaluation of the smooth fatigue ( $K_t = 1.0$ ) specimen fracture surfaces, the overall fatigue life, and the FCGR, crack initiation occurs sooner in castings than in 7075-T7351 due to the presence of inherent defects.
- The equivalent initial flaw size for D357-T6 (0.036 inch) and B201-T7 (0.042 inch) is less than the value assumed for wrought alloys (0.050 inch). Therefore, for castings up to 1.25 inch thick, these alloys can be considered for damage tolerance applications based on the existing damage tolerance specifications (MIL-A-83444 and MIL-A-87221).
- The average fracture toughness ( $K_Q$ ) of D357-T6 was adequate (24 ksi/in). Though the overall average value for B201-T7 was excellent (40 ksi/in), there was significant variability in the average value for each foundry, ranging from 29 to 47 ksi/in.
- The agreement between the compact tension and short bar fracture toughness test results was excellent.

## SECTION 8

### PHASE I, TASK 3 - EFFECT OF MICROSTRUCTURE AND DISCONTINUITIES ON MECHANICAL PROPERTIES

#### 8.1 INTRODUCTION

Prior to Task 3 of Phase I, emphasis was on defining the product and process parameters that provide the best balance of mechanical properties for both D357-T6 and B201-T7 (Grade B or better). The objective of Task 3 was to determine the effect of intentionally introduced defects (D357-T6 only), nonoptimum microstructure (D357-T6 and B201-T7), and weld repair (D357-T6) on mechanical properties. Cast plates, 16 x 6 x 1.25 inch, were made by Alcoa (D357-T6) and Hitchcock Industries (B201-T7).

To determine the effect of defects on properties, the initial goal was to cast D357-T6 plates that contained gas porosity, shrinkage porosity, and foreign material at grades ranging from A/B (essentially defect-free) to C. However, the material produced ranged from Grade A/B to Grade D (Section 8.2.2). For the effect of microstructure on properties, D357-T6 and B201-T7 plates with an excessively coarse microstructure were produced. The alloys were held within the AMS 4241 and 4242 composition specifications, respectively, and heat treated the same as the verification plates, with which the test data were compared.

The process parameters for producing the defect-containing and poor microstructure plates were maintained as close as possible to those used for making the Phase I, Task 2 verification material. However, some deviations were necessary to intentionally introduce additional defects or produce a coarse microstructure (Section 8.2.1).

To determine the effect of weld repair on the mechanical properties of Grade B D357-T6 plates, grooves were machined in the Alcoa-produced plates coincident with the gage sections of the various specimens to be excised from the plates. The grooves were then repaired by Alcoa using D357 filler wire (without silicon modifier) and standard commercial welding procedures.

Further details regarding the defect-containing, coarse microstructure, and weld-repaired plates are contained in Section 8.2.

Because of the large volume of data obtained during this Task, in most instances average property values are presented in this section. The individual test results are included in Appendices E, F, and G.

## 8.2 EXPERIMENTAL PROCEDURES

### 8.2.1 Production of Castings

#### 8.2.1.1 Effect of Defects

The goal was to produce D357-T6 plates containing gas porosity, shrinkage porosity, and less-dense foreign material at Grades B and C, as well as essentially defect-free material (Grade A/E), while maintaining the composition and DAS to be the same as the verification material. The rigging for producing the castings was the same as that used by Alcoa for the Task 2 verification plates (Figure 20). Grade B or better material was produced using standard foundry procedures for aerospace grade castings. To produce lower quality material (Grade C or worse), the following methods were employed.

Gas Porosity. The melt was not degassed.

Shrinkage Porosity. The chills were coated with excessive amounts of Silocel mold wash (0.030 to 0.040 inch), which is an insulator and therefore reduces heat transfer, leading to non-directional solidification and the formation of shrinkage porosity.

Less-Dense Foreign Material. Molten metal, including the  $Al_2O_3$  dross on the surface, was poured down the tops of the risers.

Six plates of each of the defects and grades shown in Table 56 were produced. Each plate was evaluated by X-rays, both by Alcoa and independently by a commercial radiographic facility, according to MIL-A-2175.

TABLE 56. NUMBER OF PLATES PRODUCED FOR EACH DEFECT/GRADE COMBINATION

| GRADE | DEFECT |              |                    |                  |             |
|-------|--------|--------------|--------------------|------------------|-------------|
|       | NONE   | GAS POROSITY | SHRINKAGE POROSITY | FOREIGN MATERIAL | WELD REPAIR |
| A/B   | 6      | --           | --                 | --               | 6           |
| B     | --     | 6            | 6                  | 6                | --          |
| C     | --     | 6            | 6                  | 6                | --          |

All plates were solution treated at 1015°F for 15 hours and quenched in room temperature water. They were then artificially aged for 6 hours at 335±5°F, the same heat treatment conditions used for the Task 2 verification plates to achieve the AMS 4241 tensile property requirements.

#### 8.2.1.2 Nonoptimum Microstructure

The average D357-T6 DAS and B201-T7 grain size for the water-quenched Task 2 verification plates was 0.0014 inch and 0.0030 inch, respectively. To determine the effect of nonoptimum microstructure on mechanical properties, D357-T6 and B201-T7 plates with coarse microstructures were produced.

For D357-T6, Alcoa initially produced plates using Fe chills instead of the Cu chills that were used for the verification material. However, these plates had a DAS of 0.0015 inch which was the same as the verification material. Additional plates were then made employing mold walls coated with about 0.04 inch of Silocel mold wash to reduce the solidification rate. Also, the silicon modifier was omitted. These plates had a DAS of 0.0029 inch, which was almost twice that of the verification material, and were used to evaluate the effect of nonoptimum microstructure on mechanical properties.

No minimum mechanical property specifications were provided to the foundry. The D357-T6 plates were heat treated as described above for the defect-containing plates.

For B201-T7, a coarse microstructure was achieved by the nonoptimum (early) addition of the titanium grain refiner prior to pouring, and by the use of Fe chills and a low pouring temperature to provide a slow solidification rate. An average grain size of 0.011 inch (Section 8.5.2) was obtained for these plates.

No minimum mechanical property specifications were given to the foundries. The B201-T7 plates were heat treated and HIPed as described in Section 7.2.1.2.

### 8.2.1.3 Weld Repair of D357

Six D357 plates identical to the Phase 1, Task 2 verification material were produced (Section 7) by Alcoa. The layout of specimens to be excised from the plates was determined and the plates were sectioned and welded so that approximately a 1-inch-long portion of the gage section of each tensile and fatigue specimen comprised a significant amount of weld repaired material. For the compact tension (C(T)) fracture toughness and fatigue crack growth specimens, the plates were welded so that there was a 1-inch-wide strip of weld-repaired material behind the notch after final machining. The strip was the full thickness of the specimen and ran from the notch to the specimen edge so that failure occurred in 100 percent weld-repaired material.

The welding was carried out by Alcoa using D357 filler wire (without Si-modifier) and the standard procedures for production castings. After welding, the plates were heat treated according to the procedures described in Section 7.2.1.1. The soundness of the welds was confirmed by radiography according to MIL-A-2175 to be Grade A/B, i.e., essentially defect-free.

### 8.2.2 Test Procedures

Upon receipt of the D357-T6 plates that contained the intentionally-added defects, the soundness was determined by radiography. In addition, several areas of each plate were evaluated using the FAI technique described in Section 4 to aid in specimen layout and to provide data for comparison to previous FAI results. Based on the X-ray and FAI data, specimens were machined from the plates with the intention of obtaining equal numbers of specimens for each required grade/defect combination. Each specimen was then individually radiographed to determine if, after machining, the grade and defect(s) present were the same as those intended. In many cases, the grade/defect combination of the machined specimens changed, sometimes significantly. This was particularly true for specimens machined from plates containing shrinkage porosity and foreign material, because these types of defect preferentially formed at the plate surfaces. As a result of changes in the grade and defect following machining, there was an imbalance between the numbers of specimens of each grade/defect combination available for testing.

At all grade levels, specimens that contained gas porosity were most prevalent. A smaller number of specimens that contained shrinkage porosity were obtained. Because a majority of the foreign material was located at the surface of the plates and was unavoidably machined away during specimen preparation, only a few less-dense foreign material specimens were available. This distribution of the number of specimens resulted in a large data base for gas porosity, with fewer data for shrinkage porosity and even fewer for foreign material. However, the distribution is representative of normal D357-T6 production; that is, gas porosity is the most commonly observed defect.

After machining, only a limited number of Grade A/B specimens were obtained. Because all of the specimens were thinner than the plates (1.25 inch), some of the defects that were not detected in the plates by radiography were revealed in the specimen X-rays. Consequently, the specimens could not be rated as Grade A/B.

The composition of the plates was determined by Inductively Coupled Plasma (ICP) analysis to confirm the foundry melt analyses. The DAS of the D357 plates was measured using a line intercept method [6], and the silicon particle morphology was evaluated using an Omnicom 3500 image analyzer. Specimens were excised from random locations throughout the plates.

The final test matrix for determining the effect of defects on the mechanical properties of D357-T6 is shown in Table 57. The X-ray ratings are based on results for the individual specimens, not the plates from which they were excised. The test matrix for determining the effect of a coarse microstructure on the mechanical properties of D357-T6 and B201-T7 is shown in Table 58. The tests were conducted according to the specifications shown in Table 43.

TABLE 57. NUMBER OF TESTS PERFORMED TO DETERMINE THE EFFECT OF DEFECTS ON THE MECHANICAL PROPERTIES OF D357-T6

| DEFECT/<br>GRADE LEVEL   | TYPE AND NUMBER OF TESTS |                                 |                          |                             |                       |
|--------------------------|--------------------------|---------------------------------|--------------------------|-----------------------------|-----------------------|
|                          | TENSILE                  | S/N<br>FATIGUE<br>( $K_t = 1$ ) | CONST.<br>AMPL.<br>FCGR* | SPECTRUM<br>FATIGUE<br>LIFE | FRACTURE<br>TOUGHNESS |
| Grade A/B                | 15                       | 6                               | 2                        | --                          | 3                     |
| Grade B                  |                          |                                 |                          |                             |                       |
| Gas Porosity             | 8                        | 16                              | 4                        | 2                           | 3                     |
| Shrinkage Porosity       | 10                       | 11                              | --                       | 1                           | 3                     |
| Foreign Material         | 3                        | 5                               | 1                        | --                          | --                    |
| Grade C                  |                          |                                 |                          |                             |                       |
| Gas Porosity             | 12                       | 15                              | 2                        | 4                           | 2                     |
| Shrinkage Porosity       | 3                        | 5                               | --                       | --                          | 1                     |
| Foreign Material         | 3                        | 2                               | --                       | --                          | --                    |
| Grade D                  |                          |                                 |                          |                             |                       |
| Gas Porosity             | 3                        | 11                              | 4                        | 3                           | --                    |
| Weld Repair              | 6                        | 8                               | 3                        | 3                           | 3                     |
| Total Number<br>of Tests | 63                       | 79                              | 16                       | 13                          | 15                    |

\* Constant amplitude fatigue crack growth rate

TABLE 58. NUMBER OF TESTS PERFORMED TO DETERMINE THE EFFECT OF  
NONOPTIMUM MICROSTRUCTURE ON THE MECHANICAL PROPERTIES  
OF D357-T6 AND A201-T7

| TYPE AND NUMBER OF TESTS |         |                                 |                                 |                         |                             |                       |       |
|--------------------------|---------|---------------------------------|---------------------------------|-------------------------|-----------------------------|-----------------------|-------|
| ALLOY                    | TENSILE | S/N<br>FATIGUE<br>( $K_t = 1$ ) | S/N<br>FATIGUE<br>( $K_t = 3$ ) | CONST.<br>AMP.<br>FCGR* | SPECTRUM<br>FATIGUE<br>LIFE | FRACTURE<br>TOUGHNESS | SCC** |
| D357-T6                  | 9       | 8                               | 8                               | 2                       | 2                           | 2                     | --    |
| B201-T7                  | 10      | 7                               | 9                               | 2                       | 2                           | 2                     | 3     |
| Total                    | 19      | 15                              | 17                              | 4                       | 4                           | 4                     | 3     |

\* Constant amplitude fatigue crack growth rate

\*\* Stress corrosion cracking

### 8.3 EFFECTS OF DEFECTS ON THE PROPERTIES OF D357-T6

#### 8.3.1 Composition

A total of 48 plates were cast by Alcoa from ten different melts. Material that contained a range of specific defects, including essentially defect-free material, and plates for weld repair were produced. The composition of each of the melts and the specification range for each element are listed in Table 59. With the exception of one melt (571374 - low Ti), from which some of the tensile and other specimens were excised, all elements were within specification. The silicon particle morphology was modified using Na.

The specimens from plates made from melt 571374 (identified as D41-D45) were tested and included in the data base because a) all the microstructural characteristics of these plates were similar to those of the verification material, and the same as the other defect-containing plates, and b) there would have been a shortage of material for testing had these plates been rejected. Ti is added to D357 to assure grain refinement. A fine microstructure was observed in plates D41-D45, indicating that the lower Ti level did not have an adverse effect. All the results for specimens excised from plates D41-D45 are shown in Appendix E, along with data for all the other plates. Some of the tensile results for plates D41-D45 were below specification (Appendix Tables E2, E3, and E4). However, this was also observed for specimens containing the same defect type/grade excised from other plates.

#### 8.3.2 Microstructure

The microstructure of the D357-T6 defect-containing plates was characterized using optical microscopy and image analysis. Typical examples of gas porosity, shrinkage porosity and less-dense foreign material observed in D357-T6 are shown in Figures 10, 11, and 12.

TABLE 59. COMPOSITION OF D357 WITH INTENTIONALLY ADDED DEFECTS

| LOT NUMBER                          | MELT COMPOSITION (WT %) |      |      |       |       |       |       |      |
|-------------------------------------|-------------------------|------|------|-------|-------|-------|-------|------|
|                                     | Fe                      | Si   | Mg   | Ti    | Mn    | Be    | Na    | Al   |
| 571252                              | 0.08                    | 6.9  | 0.6  | 0.14  | 0     | 0.05  | 0.005 | Bal. |
| 571253                              | 0.09                    | 6.9  | 0.6  | 0.13  | 0     | 0.05  | 0.002 | Bal. |
| 571254                              | 0.08                    | 6.8  | 0.6  | 0.14  | 0     | 0.06  | 0.007 | Bal. |
| 571256                              | 0.08                    | 7.0  | 0.6  | 0.14  | 0     | 0.06  | 0.005 | Bal. |
| 571257                              | 0.08                    | 6.8  | 0.6  | 0.14  | 0     | 0.05  | 0.005 | Bal. |
| 571258                              | 0.08                    | 6.9  | 0.6  | 0.11  | 0     | 0.07  | 0.004 | Bal. |
| 571259                              | 0.08                    | 6.9  | 0.6  | 0.11  | 0     | 0.07  | 0.004 | Bal. |
| 571260                              | 0.09                    | 7.0  | 0.6  | 0.15  | 0     | 0.05  | 0.004 | Bal. |
| 571261                              | 0.09                    | 7.0  | 0.6  | 0.15  | 0     | 0.05  | 0.004 | Bal. |
| 571374                              | 0.08                    | 7.3  | 0.6  | 0.07* | 0     | 0.06  | 0.001 | Bal. |
| <u>AMS 4241 Specification Range</u> |                         |      |      |       |       |       |       |      |
|                                     | <0.12                   | 6.5  | 0.55 | 0.10  | <0.10 | 0.04  | **    | Bal. |
|                                     |                         | -7.5 | -0.6 | -0.20 |       | -0.07 |       |      |

\* Out of specification

\*\* Not specified in AMS 4241; however, amounts used are within the 0.05 wt % limit set for "other" elements. Alcoa was requested to maintain the Na between 0.001 and 0.01%

DAS determinations were made from the grips of tensile specimens excised from the six plates produced for each of the intended defect/grade combinations. The range of DAS values was 0.008 to 0.0020 inch, all of which were within the Phase 1, Task 2 Verification specification requirement (0.0024 inch). This range of DAS values indicated that the microstructure was acceptable.

The average DAS values, as well as the Si particle area, spacing, and aspect ratio, and the percent porosity of the Task 3 plates and the Task 2 verification material are listed in Table 60. The DAS, Si particle area and aspect ratio for the defect-containing plates were very similar to the verification material. The average Si particle spacing was higher (60  $\mu\text{m}$  vs. 44  $\mu\text{m}$ ). Only the aspect ratio was similar for the weld material; the particle size area and spacing were significantly higher and lower, respectively, than the verification material.

A typical microstructure of the weld material is shown in Figure 47.

### 4.3.3 Ultrasonic NDI Evaluation of the Defect-Containing Plates

In Phase 1, Task 1, NDI Assessment, the frequency attenuation inflection (FAI) method was evaluated to assess its effectiveness in providing a quantitative determination of defects present in aluminum castings. It was shown (Section 4) that there was a reasonably good correlation between FAI measurements and X-ray grades and microstructural characterization for gas porosity, less so for shrinkage porosity, with no correlation for foreign material. To add to the data base obtained in Task 1, and to try to aid in characterizing the material to be tested in Task 3, an FAI evaluation of the plates that contained intentionally-added defects was conducted. The approach was to select the location of the specimens that would be machined from a plate using X-ray radiography and obtain an FAI reading from the material at the center of the intended gage section after machining. In this way, the FAI reading would be representative of material that was later mechanically

TABLE 60. DAS AND Si PARTICLE MORPHOLOGY DATA FOR THE PHASE I,  
TASK 3 DEFECT-CONTAINING D357 PLATES

| DEFECT<br>(GRADE)        | DAS<br>(inch) | SILICON PARTICLE MORPHOLOGY |                              |                 |      | POROSITY<br>(%) |
|--------------------------|---------------|-----------------------------|------------------------------|-----------------|------|-----------------|
|                          |               | AREA<br>( $\mu\text{m}^2$ ) | SPACING<br>( $\mu\text{m}$ ) | ASPECT<br>RATIO |      |                 |
| None                     |               |                             |                              |                 |      |                 |
| Grade A/B                | 0.0013        | 16                          | 60                           | 1.8             | 0    |                 |
| Gas Porosity             |               |                             |                              |                 |      |                 |
| Grade B                  | 0.0019        | 17                          | 56                           | 1.9             | 1.1  |                 |
| Grade C                  | 0.0017        | 16                          | 63                           | 2.0             | 1.7  |                 |
| Shrinkage Porosity       |               |                             |                              |                 |      |                 |
| Grade B                  | 0.0015        | 19                          | 60                           | 1.7             | 0.8  |                 |
| Grade C                  | 0.0015        | 19                          | 64                           | 1.9             | 1.7  |                 |
| Foreign Material         |               |                             |                              |                 |      |                 |
| Grade B                  | 0.0012        | 16                          | 56                           | 2.0             | 1.6  |                 |
| Grade C                  | 0.0012        | 15                          | 64                           | 1.8             | 0.6  |                 |
| Weld Repair              | *             | 35                          | 20                           | 1.8             | 0    |                 |
| Verification<br>Material | 0.0014        | 16                          | 44                           | 1.6             | 0.03 |                 |

\* Very fine microstructure; DAS could not be measured

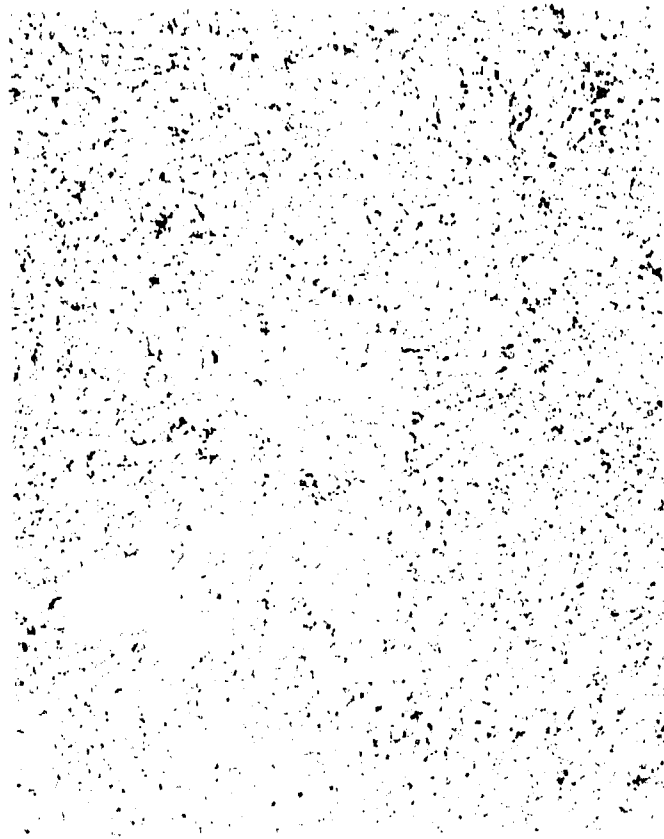


Figure 47. Microstructure of D357-T6 Weld

tested. The evaluation was conducted prior to machining the specimens because the circular cross-section of many of the specimens would influence the accuracy of the result (Section 4.4.5).

The results of the FAI investigation are shown in Table 61. Three to five plates were evaluated for each grade. Approximately 10 readings per plate were taken. The values shown in Table 60 are the average of 30 to 50 individual measurements. For both gas porosity and shrinkage porosity the average pore radius and percent porosity for Grade B material are both lower than those for Grade C, indicating a good qualitative correlation. The trend was not observed for the foreign material. These trends are typical of those seen during the Phase I, Task 1 FAI evaluation (Section 4.4.3), though the average pore radius and percent porosity values were not the same as those in Task 1 (Table 7). With the exception of results obtained for Grade D shrinkage porosity material, the average values for both parameters were higher for the Task 3 measurements than for those made in Task 1. Also, for shrinkage porosity, the differences between the Grade B and C radius and between Grade B and C percent porosity values were much greater in Task 3 than in Task 1.

The percent porosity values (Table 61) for gas porosity and foreign material are very similar to those obtained by image analysis (Table 60) for the same grades (1.2 percent versus 1.1 percent and 1.8 percent versus 1.7 percent for Grades B and C gas porosity, respectively; 1.8 percent versus 1.6 percent and 0.7 percent versus 0.6 percent for Grades B and C foreign material, respectively). The comparison for shrinkage porosity was qualitatively good, i.e., the values for Grade B were higher than those for Grade C. However, the quantitative agreement was poor. As discussed in Section 4, this is probably due to the fact that, unlike gas porosity, shrinkage porosity is not spherical.

The good quantitative agreement between the FAI and image analysis results for plates that contained foreign material almost certainly reflects the background gas porosity present in that material rather than the isolated gross particles that were observed. As discussed in Section 4, the FAI approach needs to be modified to be able to adequately accommodate foreign material.

TABLE 61. FAI DATA FOR THE PHASE I, TASK 3 DEFECT-CONTAINING D357-T6 PLATES

| X-RAY GRADE        | FAI RESULTS       |                                    |
|--------------------|-------------------|------------------------------------|
|                    | AVG. POROSITY (%) | AVG. PORE RADIUS ( $\mu\text{m}$ ) |
| A/B                | <0.1*             | *                                  |
| Gas Porosity       |                   |                                    |
| Grade E            | 1.2               | 130                                |
| Grade C            | 1.8               | 161                                |
| Shrinkage Porosity |                   |                                    |
| Grade B            | 1.4               | 126                                |
| Grade C            | 2.4               | 190                                |
| Foreign Material   |                   |                                    |
| Grade B            | 1.8               | 138                                |
| Grade C            | 0.7               | 81                                 |

\* Below the level of detection

The excellent correlation for gas porosity is encouraging. However, because the absolute values obtained for Tasks 1 and 3 material were widely different, further work beyond the scope of the current program is required.

The average hydrogen content of Task 3 plates that contained Grades B, C and D gas porosity was 1.3, 1.4, and  $1.8 \pm 0.3$  ppm, respectively. The hydrogen content increased with decreasing soundness, as would be expected.

#### 8.3.4 Tensile Properties

The tensile property data for material that contained different types and amounts of intentionally-added defects are summarized in Table 62. As discussed in Section 8.2.2, the gage section of each tensile specimen was radiographically graded. Average values and ranges for ultimate and yield strengths and percent elongation are given for each defect/grade combination. In many cases, test results, particularly the elongation, were below the values specified in AMS 4241. The data for the verification material evaluated in Task 2, Phase I (Section 7.3.3) are shown for comparison. The number of specimens that failed to meet the AMS 4241 property requirements is shown in Table 63.

Though adjustments were made to the manufacturing process to obtain material that contained different defects, the microstructure of all the plates was similar to the verification material (Table 60) and therefore comparison of results exhibited by the various defect/grade combinations should be meaningful. Some general observations are summarized below.

- The average properties are highest for Grade A/B, weld repair (also rated Grade A/B by radiography), and Grade B foreign material
- Only 48 percent of the specimens attained the minimum elongation specification (3 percent)
- All specimens met the 40 ksi minimum yield strength requirement (40 ksi)

TABLE 62. D357-T6 TENSILE PROPERTIES VS. DEFECT TYPE AND GRADE

| DEFECT/GRADE          | UTS (ksi) |       | YS (ksi) |       | El (%) |         |
|-----------------------|-----------|-------|----------|-------|--------|---------|
|                       | AVG.      | RANGE | AVG.     | RANGE | AVG.   | RANGE   |
| Baseline              |           |       |          |       |        |         |
| Grade A/B (15)*       | 54        | 53-55 | 48       | 47-48 | 3.9    | 1.1-5.0 |
| Gas Porosity          |           |       |          |       |        |         |
| Grade B (8)           | 51        | 47-52 | 45       | 42-46 | 3.3    | 2.1-4.3 |
| Grade C (12)          | 50        | 49-53 | 45       | 43-47 | 2.1    | 0.9-4.1 |
| Grade D (3)           | 49        | 48-49 | 44       | 44-45 | 1.5    | 1.3-1.7 |
| Shrinkage Porosity    |           |       |          |       |        |         |
| Grade B (10)          | 51        | 50-53 | 46       | 44-48 | 2.7    | 1.5-7.9 |
| Grade C (3)           | 51        | 50-51 | 46       | 45-46 | 2.9    | 2.2-3.9 |
| Foreign Material      |           |       |          |       |        |         |
| Grade B (3)           | 54        | 51-55 | 46       | 45-48 | 4.6    | 3.1-7.5 |
| Grade C (3)           | 51        | 45-52 | 44       | 41-46 | 2.4    | 1.2-4.7 |
| Weld Repair           |           |       |          |       |        |         |
| Grade A/B (6)         | 55        | 54-56 | 47       | 46-48 | 5.1    | 3.5-8.0 |
| Verification Material | 53        | 50-55 | 45       | 44-48 | 5.0    | 3.0-8.5 |

\* The numbers in parentheses show the number of tests performed

TABLE 63. D357-T6 TENSILE TEST RESULTS OUT OF SPECIFICATION\*

| DEFECT/GRADE                    | TOTAL<br>NO.<br>OF<br>TESTS | RESULTS OUT OF SPECIFICATION |         |         |
|---------------------------------|-----------------------------|------------------------------|---------|---------|
|                                 |                             | UTS                          | YS      | E1      |
|                                 |                             | No. (%)**                    | No. (%) | No. (%) |
| <u>Phase I, Task 3</u>          |                             |                              |         |         |
| Baseline                        |                             |                              |         |         |
| Grade A/B                       | 15                          | 0 (0)                        | 0 (0)   | 4 (27)  |
| Gas Porosity                    |                             |                              |         |         |
| Grade B                         | 8                           | 2 (25)                       | 0 (0)   | 3 (38)  |
| Grade C                         | 12                          | 3 (25)                       | 0 (0)   | 10 (83) |
| Grade D                         | 3                           | 3 (100)                      | 0 (0)   | 3 (100) |
| Shrinkage Porosity              |                             |                              |         |         |
| Grade B                         | 10                          | 1 (10)                       | 0 (0)   | 9 (90)  |
| Grade C                         | 3                           | 3 (100)                      | 0 (0)   | 2 (67)  |
| Foreign Material                |                             |                              |         |         |
| Grade B                         | 3                           | 0 (0)                        | 0 (0)   | 0 (0)   |
| Grade C                         | 3                           | 1 (33)                       | 0 (0)   | 2 (67)  |
| Weld Repair                     |                             |                              |         |         |
| Grade A/B                       | 6                           | 0 (0)                        | 0 (0)   | 0 (0)   |
| Total                           | 63                          | 13 (21)                      | 0 (0)   | 33 (52) |
| <u>Verification Material***</u> | 48                          | 1 (2)                        | 0 (0)   | 17 (35) |

\* AMS 4241 (50/40/3)

\*\* Percent of total number of test results that were out of specification

\*\*\* Water quenched material only

- Seventy-nine percent of specimens met the minimum ultimate tensile strength requirement (50 ksi)
- For the defect type that was most rigorously evaluated (gas porosity), a correlation appears to exist between percent elongation and grade level. The average elongation value decreased (Table 62) and the percentage of specimens that did not meet the minimum requirement increased (Table 63) as the soundness deteriorated from Grade B to Grade D.

A breakdown of the tensile data as a function of grade is shown in Table 64. The percent of data that met the AMS 4241 specification is shown irrespective of the type of defect present. A clear correlation is evident; the reduction from 94 percent for Grade A/B to 33 percent for Grade D indicates that, in general, properties degrade with decreasing soundness. The data for the initial Grade B Task 2 verification plates are also included for comparison (87 percent of the test results met the AMS 4241 specification). If the verification plates that were remade by Foundry C are included, the number meeting AMS 4241 specification increases to about 95 percent. This still falls short of a 100 percent success rate, which was the goal for the verification material.

Two specimens were selected for fractographic analysis to try to determine if there were any microstructural characteristics that were responsible for the low ductility values. The specimens were from plates D30 (Grade B gas porosity) and D32 (Grade B shrinkage porosity). The specimen from plate D30, which had a 2.1 percent elongation, showed no unusual features compared with a similar specimen (from plate D70) that had a 4.3 percent elongation. However, a Grade B shrinkage porosity specimen from plate D32 exhibited extensive porosity and an oxide inclusion at the edge of the specimen, which probably contributed to the low ductility.

From Table 63 it is evident that most of the specimens that failed to meet the AMS specification exhibited low percent elongation. Coupled with the fact that all specimens significantly exceeded the minimum yield strength requirement (40 ksi) it is possible that the aging treatment, which was the

TABLE 64. D357-T6 TENSILE PROPERTY DATA WITHIN THE AMS 4241 SPECIFICATION<sup>(1)</sup>

| GRADE                 | NO. OF TEST RESULTS <sup>(1)</sup> | DATA MEETING MINIMUM REQUIREMENTS (%) |
|-----------------------|------------------------------------|---------------------------------------|
| A/B <sup>(2)</sup>    | 63                                 | 94                                    |
| B                     | 63                                 | 76                                    |
| C                     | 54                                 | 61                                    |
| D                     | 9                                  | 33                                    |
| Verification Material | 144                                | 87                                    |

(1) The ultimate and yield strengths, and percent elongation are counted as three separate data points

(2) Including weld repair data, which was Grade A/B

same as that used for the Task 2, Phase I, verification material, was not optimum for the defect-containing plates. The correlation shown in Table 64 should still be valid, but with optimized aging treatment the percentage of data points that meet the specification minimum, particularly the elongation, would probably be increased for each grade.

### 8.3.5 Fatigue Properties

#### 8.3.5.1 Stress-Life

The stress-life ( $K_t = 1.0$ ) data for D357-T6 containing gas porosity, shrinkage porosity, foreign material, or weld repair are shown in Figures 48 through 51. Typical data for 7075-T73, a commonly-used wrought aluminum alloy, are also shown for comparison. The data points for all four of the defect categories fall within the same broad band. However, as is shown most clearly for gas and shrinkage porosity, the fatigue life data for Grades C and D form a tighter band than for Grade B and also fall at, or slightly below, the lower edge of the Grade B values. The Grade A/B data fall along the upper edge of the scatter for Grade B gas and shrinkage porosity material.

The above data suggest that, for Grade C or worse, the defects are sufficiently large and/or occur at a frequency that shortens the fatigue life. For Grade B some of the defects are sufficiently small so that fatigue crack initiation occurs later for a given stress. However, the lowest fatigue life is very similar for all the defect/Grade B-D combinations.

The results for essentially defect-free material (Grade A/B) are shown in Figures 48-51. These specimens were smaller (0.25-inch-diameter gage section) than the standard specimen used throughout the program (0.5 inch diameter) because of the shortage of Grade A/B material. It was recognized that the smaller specimen might influence the results, possibly increasing the fatigue life because the chance of a defect occurring at the specimen surface would be decreased due to a reduction in the surface area of the gage length. Conversely, the fatigue life could possibly be decreased because a defect of given size would represent a larger percentage of the cross sectional area. To assess the possibility of the fatigue life being affected, some small Grade B gas porosity specimens were also tested. The results, which are plotted in

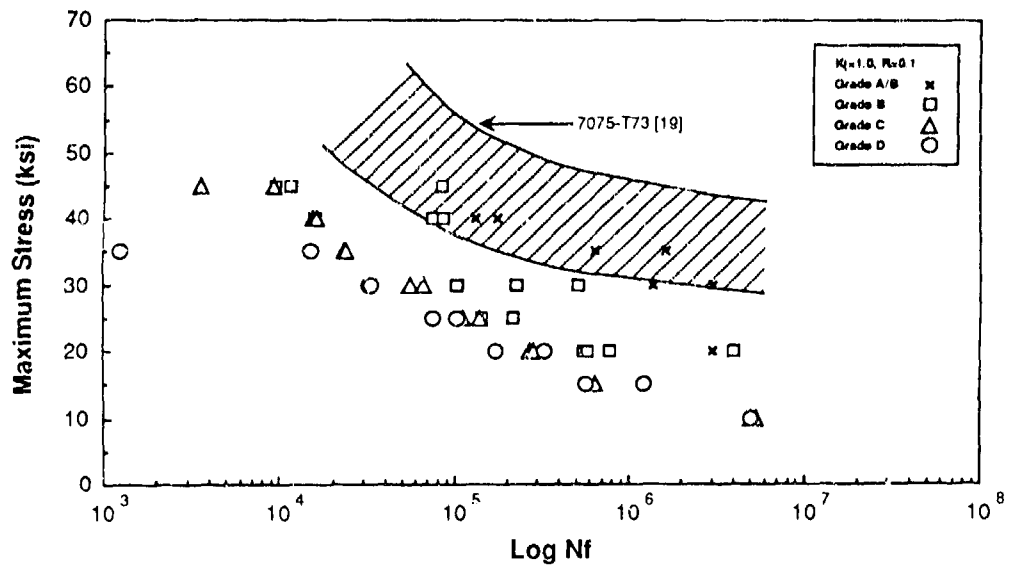


Figure 48. Stress-Life Fatigue Data for D357-T6 Containing Gas Porosity

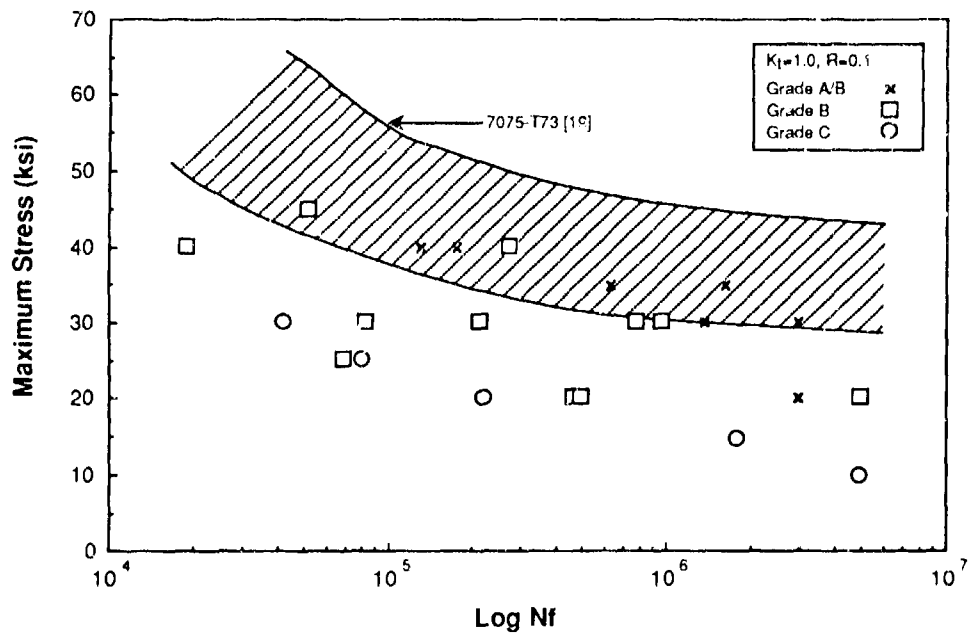


Figure 49. Stress-Life Fatigue Data for D357-T6 Containing Shrinkage Porosity

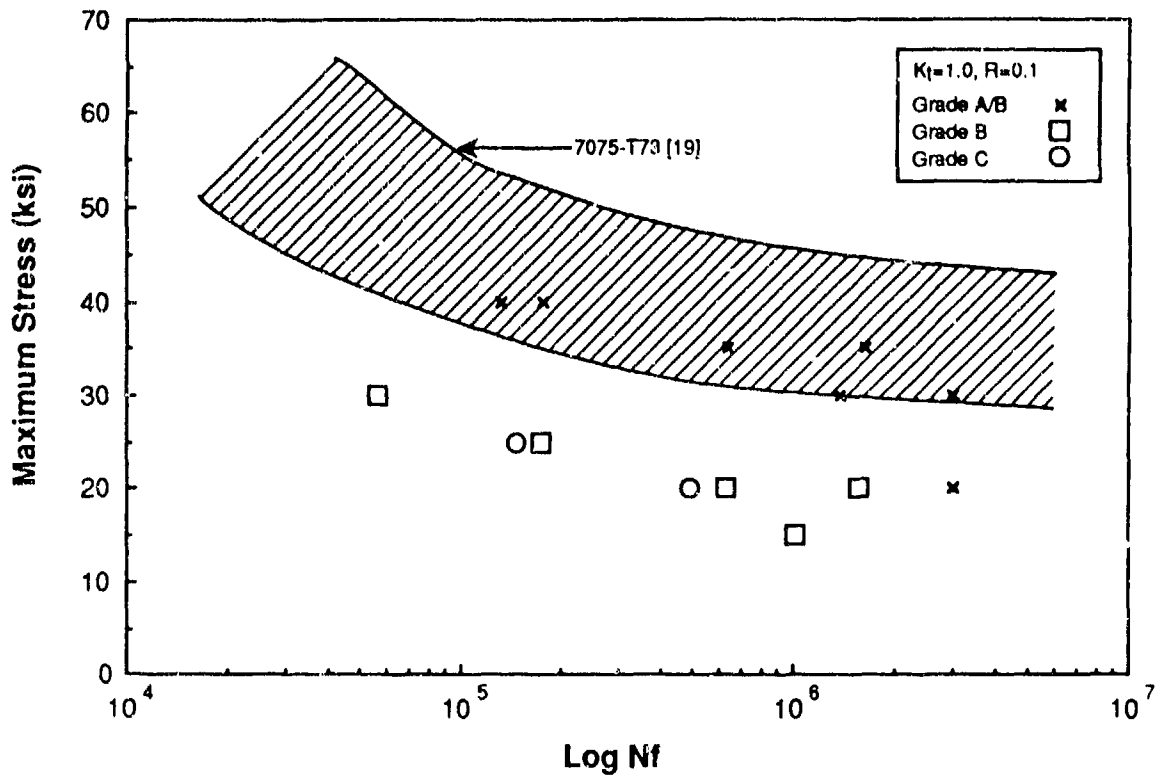


Figure 50. Stress-Life Fatigue Data for D357-T6 Containing Less-Dense Foreign Material.

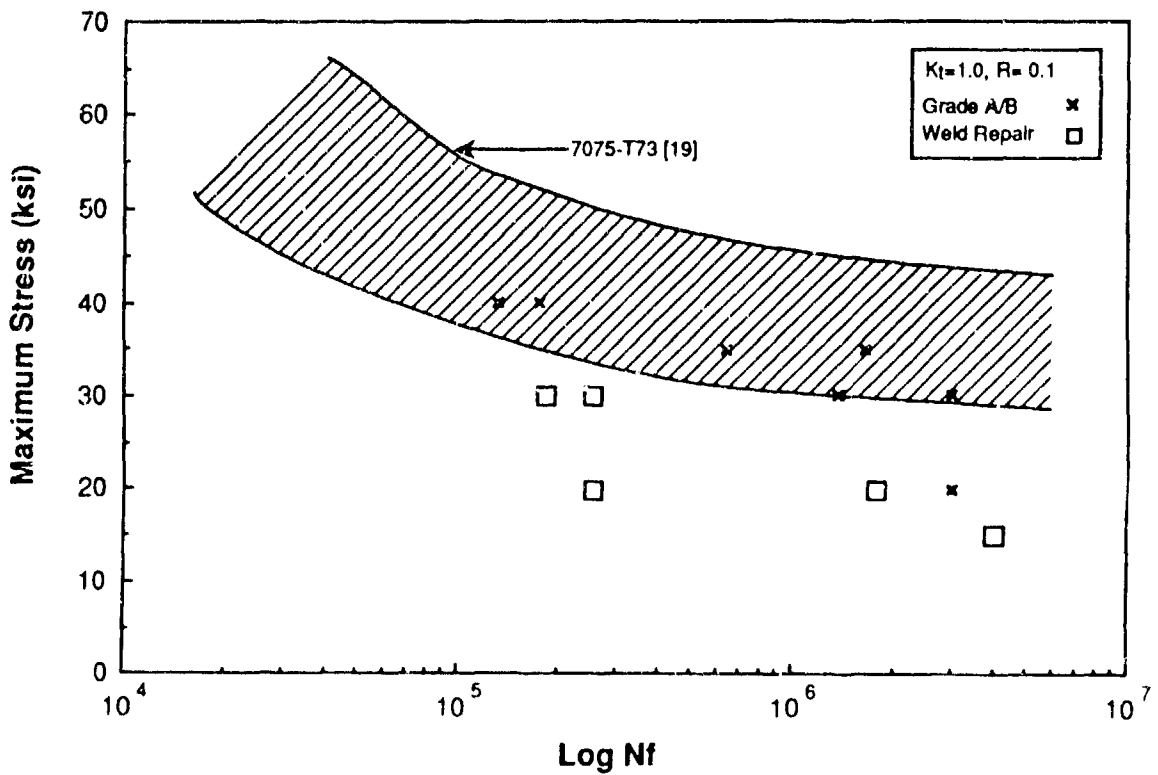


Figure 51. Stress-Life Fatigue Data for Grade A/B and Weld-Repaired D357-T6

Figure 52, indicate that the fatigue life for Grade A/B material is still better than that for Grade B gas porosity. Thus, the overall conclusion that the fatigue life deteriorates progressively as the soundness is reduced from Grade A/B to Grades C and D is valid.

Nine of the defect-containing fatigue specimens were fractographically analyzed to determine details of the crack initiation site. Seven of the specimens were determined by radiography to contain either gas porosity (3 specimens) or shrinkage porosity (4 specimens). The other two specimens were weld repaired or contained foreign material. Porosity was found at the initiation site of six of the gas porosity and shrinkage porosity specimens and at the initiation site of the weld repair specimen. Inclusions were observed at the initiation sites of the foreign material specimen and one of the shrinkage porosity specimens. All the defects at the initiation sites were located at the specimen surface.

#### 8.3.5.2 Fatigue Crack Growth Rate

Constant amplitude fatigue crack growth rate (FCGR) data were obtained for Grades B, C, and D gas porosity, Grade B foreign material, Grade A/B, and weld repair (also Grade A/B) material. Specimens were machined for other grade/defect combinations but X-ray radiography indicated that the defects were not located along the line that the crack would propagate during testing; consequently, these specimens were not tested. The FCGR data are shown in Figures 53-58, and are presented as a band covering all the specimens that were tested. The numbers of specimens tested are indicated in each figure.

There was no significant difference between the FCGR behavior for the various grade/defect combinations. For some materials, the band was wider than for others, but the data were generally scattered about the mean for the Phase I, Task 2 verification material. For Grade D gas porosity material, the band was significantly wider in the high  $\Delta K$  region than for any other material (Figure 55). Overall, the FCGR is slower than that for 7075-7351 [22], a wrought aluminum alloy used for aerospace applications, except in the high  $\Delta K$  region, which reflects the fact that the fracture toughness of 7075-T7351 is higher than that of D357-T6.

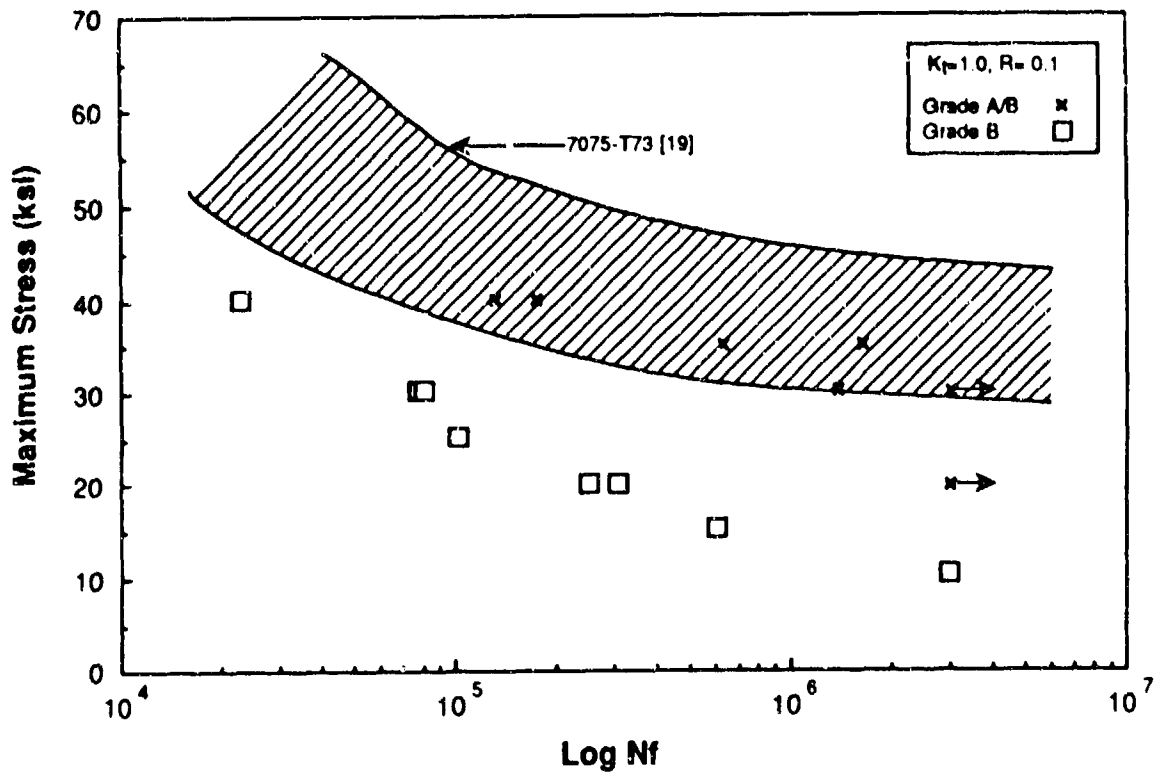


Figure 52. Grade A/B and Grade B Stress-Life Fatigue Data for Small Test Specimens

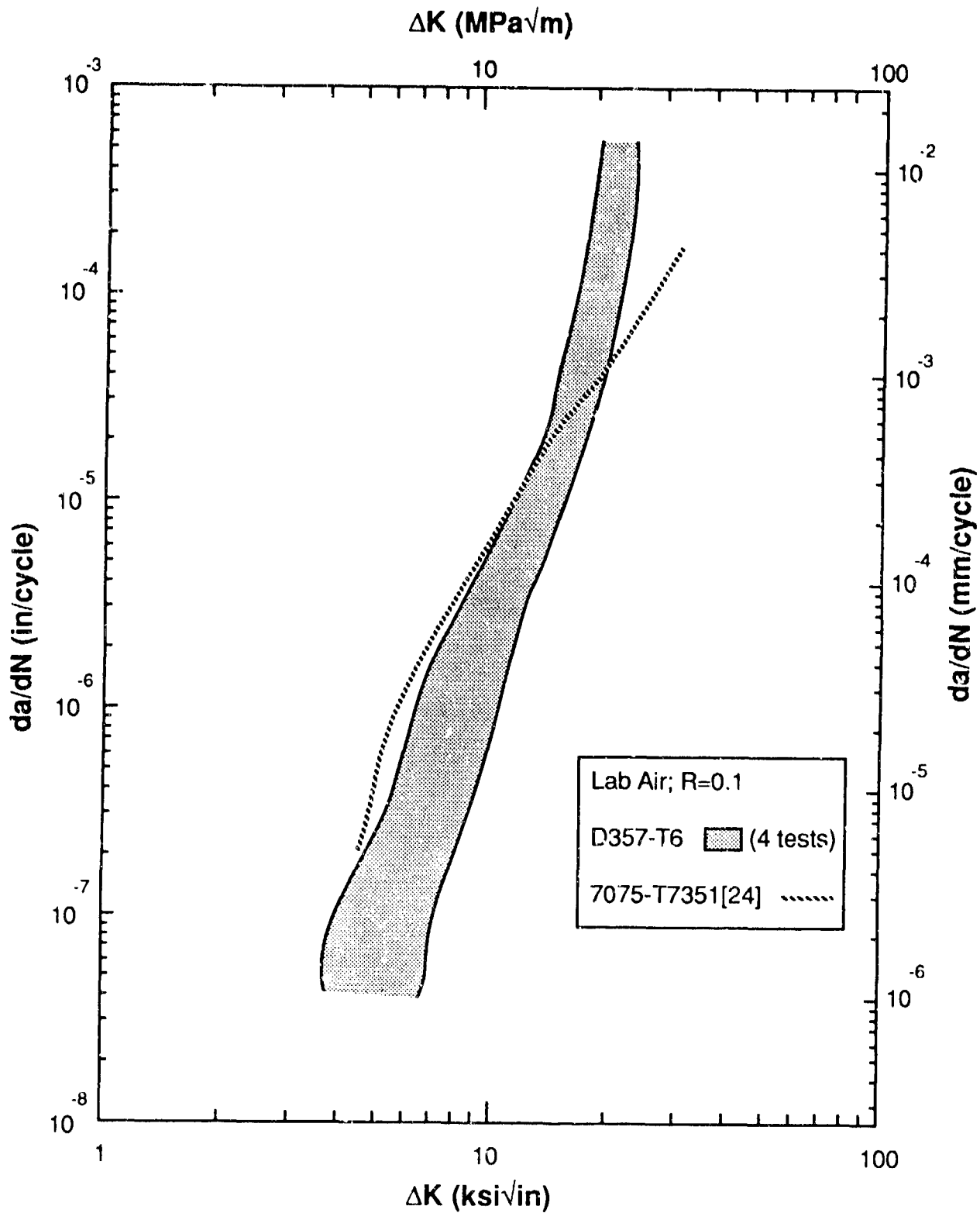


Figure 53. Constant Amplitude Fatigue Crack Growth Rate of Grade B (Gas Porosity) D357-T6



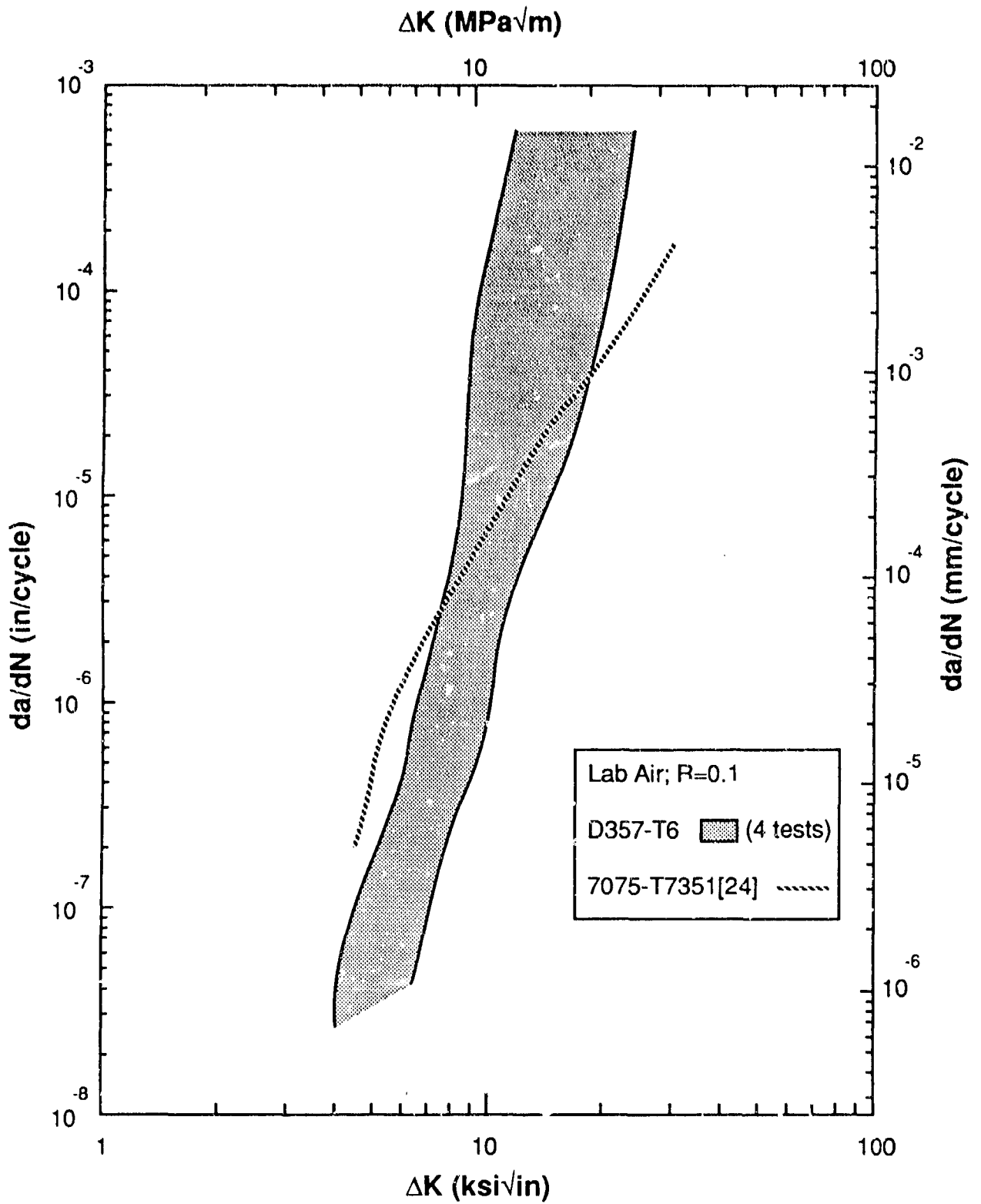


Figure 55. Constant Amplitude Fatigue Crack Growth Rate of Grade D (Gas Porosity) D357-T6

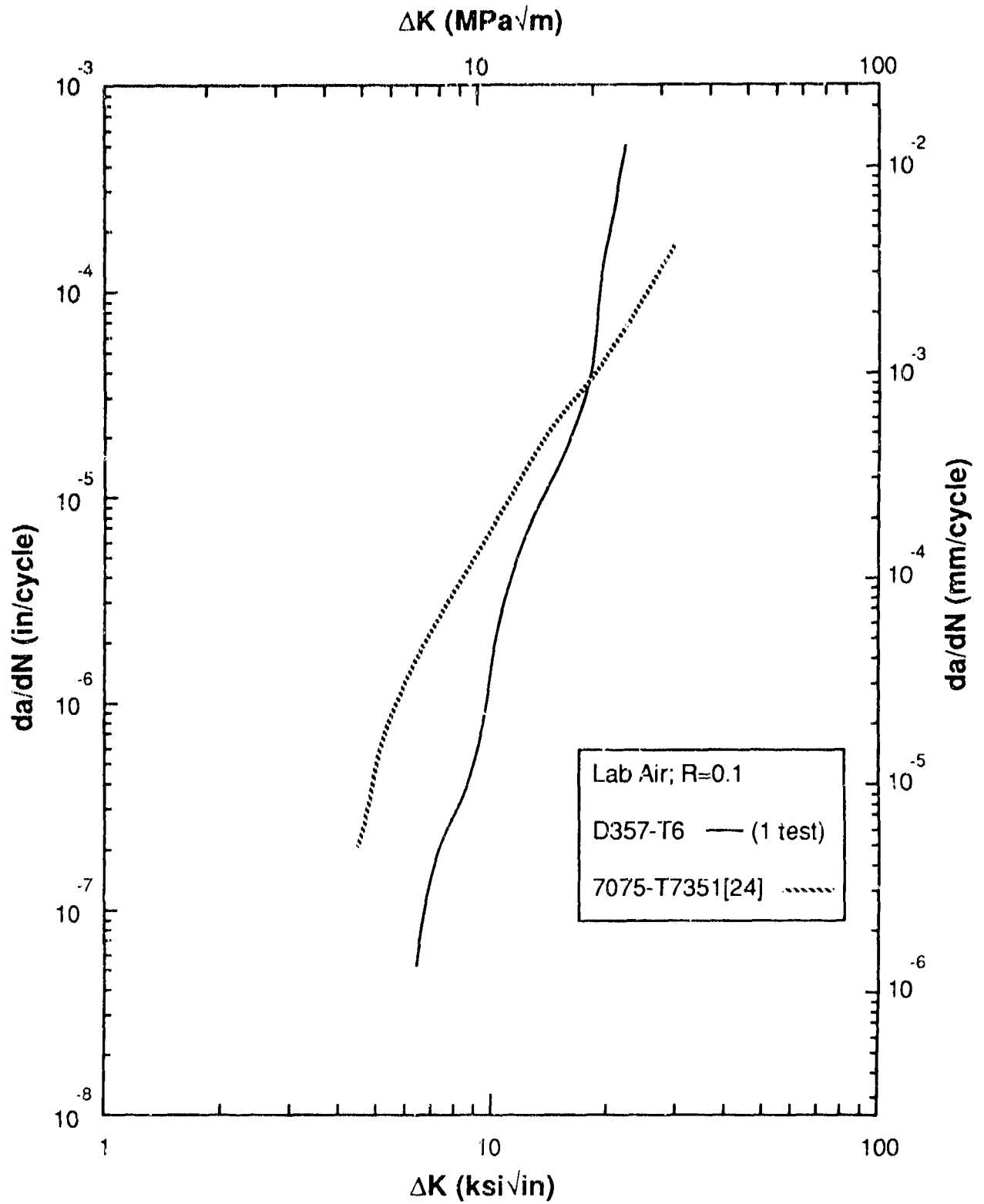


Figure 56. Constant Amplitude Fatigue Crack Growth Rate of Grade B (Foreign Material) D357-T6

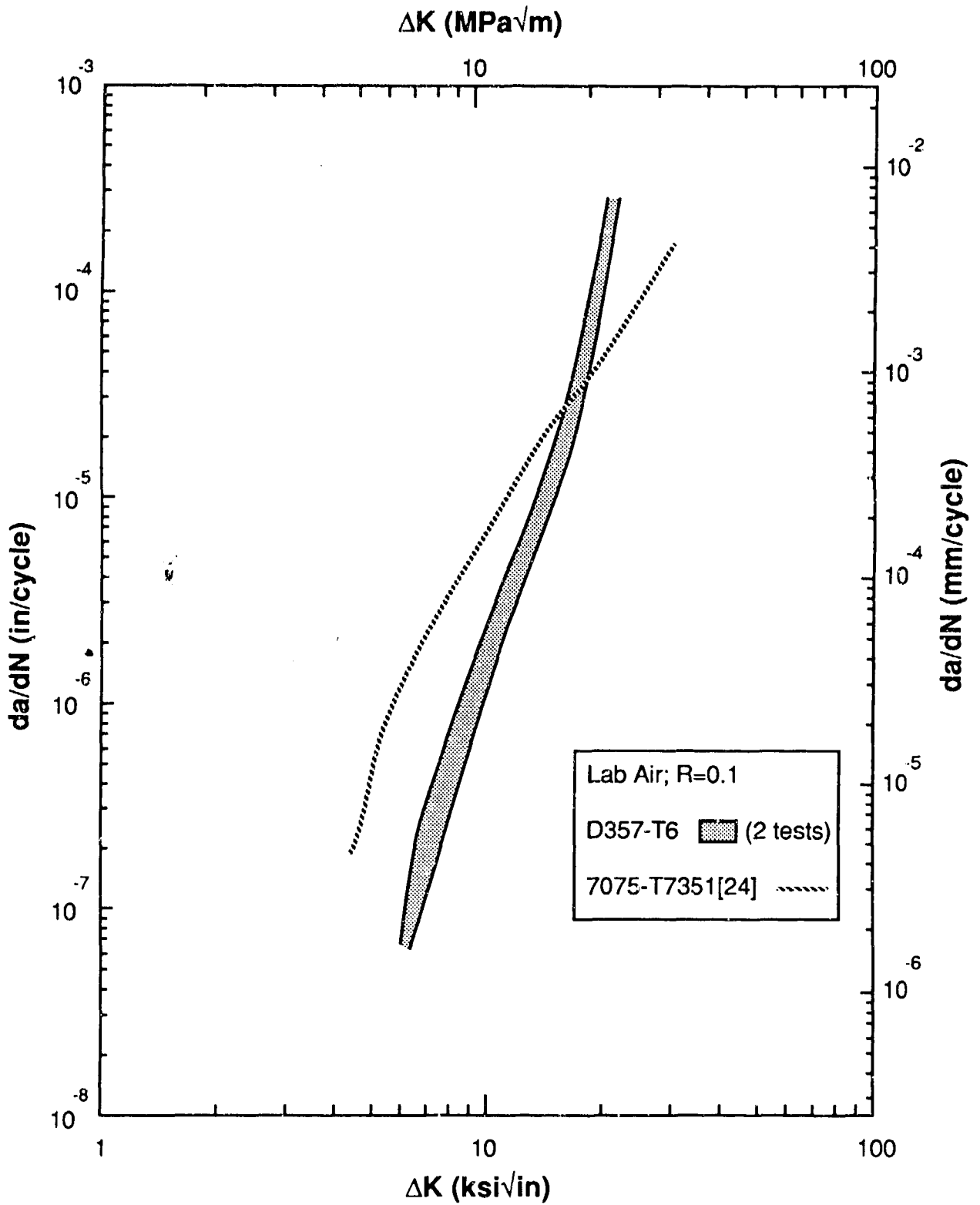


Figure 57. Constant Amplitude Fatigue Crack Growth Rate of Grade A/B D357-T6

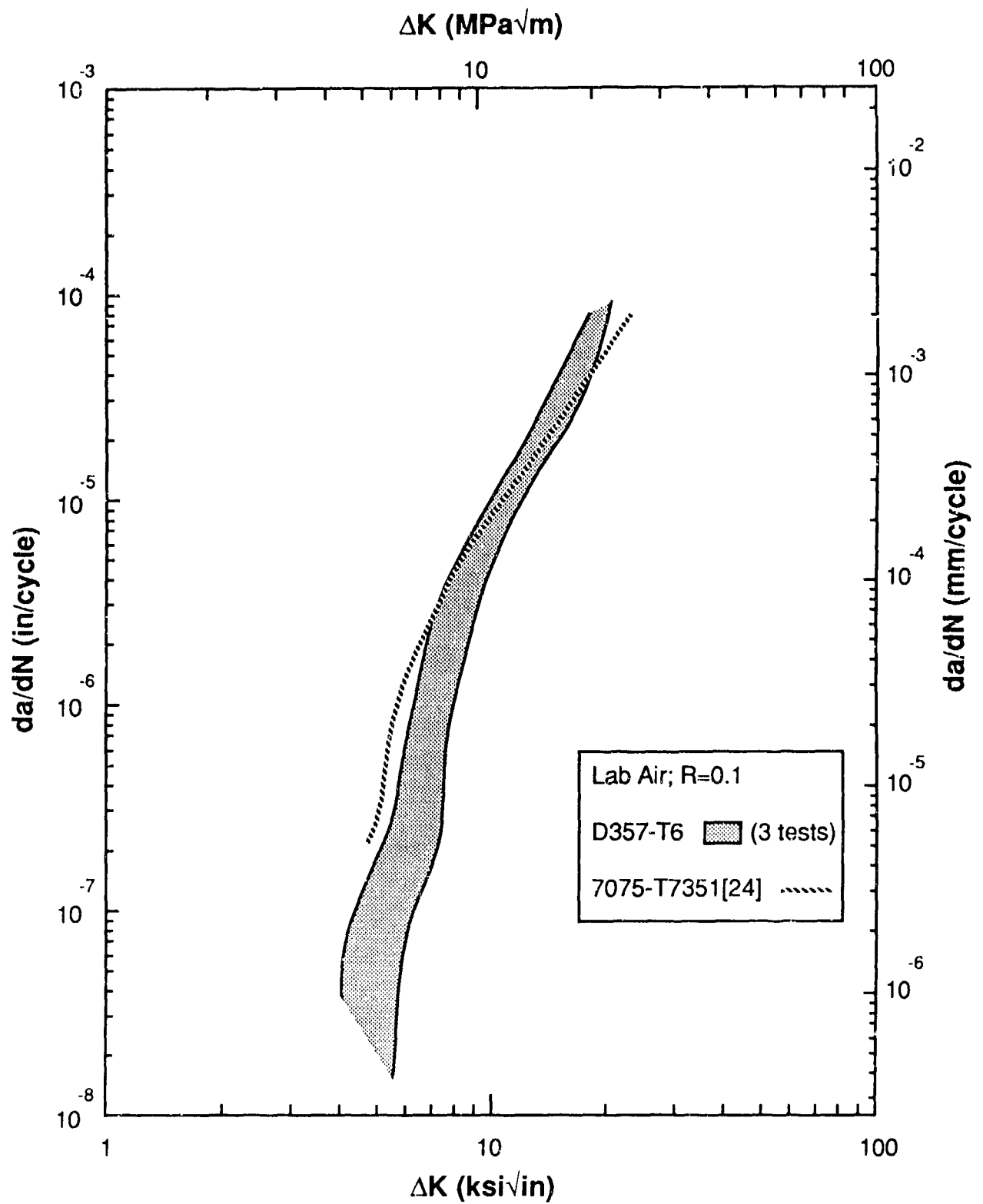


Figure 58. Constant Amplitude Fatigue Crack Growth Rate of Weld-Repaired D357-T6

### 8.3.5.3 Spectrum Fatigue Life

A small number of fatigue tests were conducted under spectrum loading to determine if there were any trends that were not observed during constant amplitude load testing. An F/A-18 aircraft wing root spectrum was selected, and a flat specimen with a hole in the center of the gage section (Figure 15) was used. The data are presented in Table 65 for gross maximum stress of 32 ksi. There was a significant amount of data scatter, but one clear trend that emerged is that the life for the Grades C and D specimens was much lower than for the Grade B or weld repair (Grade A/B) material.

### 8.3.6 Fracture Toughness

The fracture toughness data for D357-T6 that contained a range of different types and amounts of defect are shown in Table 66. Invalid  $K_Q$  values were all due to excessive crack front curvature, which is often observed in castings due to residual stresses incurred during quenching. The best fracture toughness values were obtained for Grade A/B and weld repair (also Grade A/B) materials, with weld repair being the highest (32 ksi/in). Values for Grades B and C gas and shrinkage porosity were very similar to the Grade B verification material evaluated during Phase I, Task 2.

## 8.4 EFFECT OF NONOPTIMUM MICROSTRUCTURE ON THE PROPERTIES OF D357-T6

### 8.4.1 Composition

A total of seven plates was cast by Alcoa to provide material that had a coarse, nonoptimum microstructure. Of these seven plates, only two had a microstructure and DAS that were significantly different from the verification material (Section 8.2.1.2). These two plates were used for the evaluation of nonoptimum microstructure. The composition of the melt from which the two plates were produced is shown in Table 67. A silicon modifier was not used. The plates were Grade B.

TABLE 65. SPECTRUM<sup>(1)</sup> FATIGUE DATA FOR DEFECT-CONTAINING D357-T6

| DEFECT/GRADE          | AVERAGE LIFE <sup>(2)</sup><br>(X1000 FLIGHT HOURS) | NO. OF<br>TESTS |
|-----------------------|---|-----------------|
| Grade B               |   |                 |
| Gas Porosity          | 38  | 2               |
| Shrinkage Porosity    | 45  | 1               |
| Grade C               |   |                 |
| Gas Porosity          | 7   | 4               |
| Grade D               |   |                 |
| Gas Porosity          | 8   | 3               |
| Weld Repair           | 31  | 3               |
| Verification Material | 16  | 2               |

(1) F/A-18 wing root spectrum (F18C2)

(2) 32 ksi gross maximum stress

TABLE 66. AVERAGE FRACTURE TOUGHNESS OF DEFECT-CONTAINING D357-T6

| GRADE/DEFECT               | $K_{IC}$<br>(ksi/in) | $K_Q$<br>(ksi/in) |
|----------------------------|----------------------|-------------------|
| Grade A/B                  | --                   | 27 (3)            |
| Grade B                    |                      |                   |
| Gas Porosity               | 21 (1)               | 22 (2)            |
| Shrinkage Porosity         | 20 (1)               | 24 (2)            |
| Grade C                    |                      |                   |
| Gas Porosity               | 22 (1)               | 23 (1)            |
| Shrinkage Porosity         | 23 (1)               | --                |
| Weld Repair<br>(Grade A/B) | --                   | 32 (3)            |
| Verification Material      |                      |                   |
| Water Quench               | --                   | 24 (7)            |
| Glycol Quench              | 22 (4)               | --                |

Note: The figures in parentheses denote the number of specimens tested

TABLE 67. COMPOSITION OF D357 WITH NONOPTIMUM MICROSTRUCTURE

| LOT<br>NUMBER                 | COMPOSITION (WT %) |      |       |       |      |       |     |
|-------------------------------|--------------------|------|-------|-------|------|-------|-----|
|                               | Si                 | Mg   | Ti    | Fe    | Mn   | Be    | Al  |
| 571531                        | 6.96               | 0.60 | 0.10  | 0.07  | 0    | 0.05  | Bal |
| <u>AMS 4241 Specification</u> |                    |      |       |       |      |       |     |
|                               | 6.5                | 0.55 | 0.10  | <0.12 | <0.1 | 0.04  | Bal |
|                               | -7.5               | -0.6 | -0.20 |       |      | -0.07 |     |

#### 8.4.2 Microstructure

The microstructure of the nonoptimum D357-T6 was characterized using optical, scanning and transmission electron microscopy (SEM and TEM), and image analysis. The DAS and silicon particle morphology were determined and are shown in Table 68, with those for the verification material produced in Phase I, Task 2 for comparison. The nonoptimum material clearly had a much coarser microstructure than the verification plates. An optical micrograph of a typical area is shown in Figure 59. A micrograph of the verification material taken at the same magnification is shown in Figure 23.

A typical SEM micrograph is given in Figure 60 and reveals the presence of two phases in the aluminum matrix. EDXA spectra of these two phases identified the elongated phase as Si and the coarser, lighter constituent as an Al-Fe phase. Both phases were observed in the verification material (Section 7.3.2). However, the silicon particles in the nonoptimum material are generally larger and more irregularly shaped (with a higher aspect ratio) compared to the primary silicon in the verification plates. In addition, the small ( $\leq 0.2$  micron) Si particles identified throughout the verification material are observed far less frequently in the nonoptimum plates. As shown in the TEM micrograph in Figure 61, a small, approximately 10-nanometer precipitate phase was observed homogeneously distributed throughout the primary silicon in the nonoptimum material. EDXA and selected area diffraction (SAD) analyses of this phase, however, failed to reveal its structure or composition. A SAD pattern generated from the precipitate phase, Figure 62, reveals a crystallographic orientation with the aluminum matrix.

As in the verification material, long needle-shaped particles were also observed in the nonoptimum plates (Figure 63). An X-ray map confirmed that these particles contain Ti. X-ray mapping further revealed the presence of Si along the surface of these particles, suggesting that silicon precipitates at the interface between the particles and the aluminum matrix. The stoichiometry of the needle-shaped phase could not be determined from SAD patterns. Attempts to locate an Mg-Si strengthening phase (e.g.,  $Mg_2Si$ ) using SAD analysis were also unsuccessful. However, analysis of SAD patterns obtained along the  $[011]_{Al}$  and  $[111]_{Al}$  orientations suggest that the strengthening mechanism in this nonoptimum material consists of GP zones.

TABLE 68. DAS AND Si PARTICLE MORPHOLOGY OF D357-T6 WITH NONOPTIMUM MICROSTRUCTURE

| MATERIAL     | AVERAGE<br>DAS<br>( $10^{-4}$ INCH) | SILICON PARTICLE MORPHOLOGY |                              |                 |
|--------------|-------------------------------------|-----------------------------|------------------------------|-----------------|
|              |                                     | AREA<br>( $\mu\text{m}^2$ ) | SPACING<br>( $\mu\text{m}$ ) | ASPECT<br>RATIO |
| Nonoptimum   | 29                                  | 95                          | 90                           | 2.2             |
| Verification | 14                                  | 16                          | 44                           | 1.6             |



X50

Figure 59. D357-T6 With Nonoptimum Microstructure

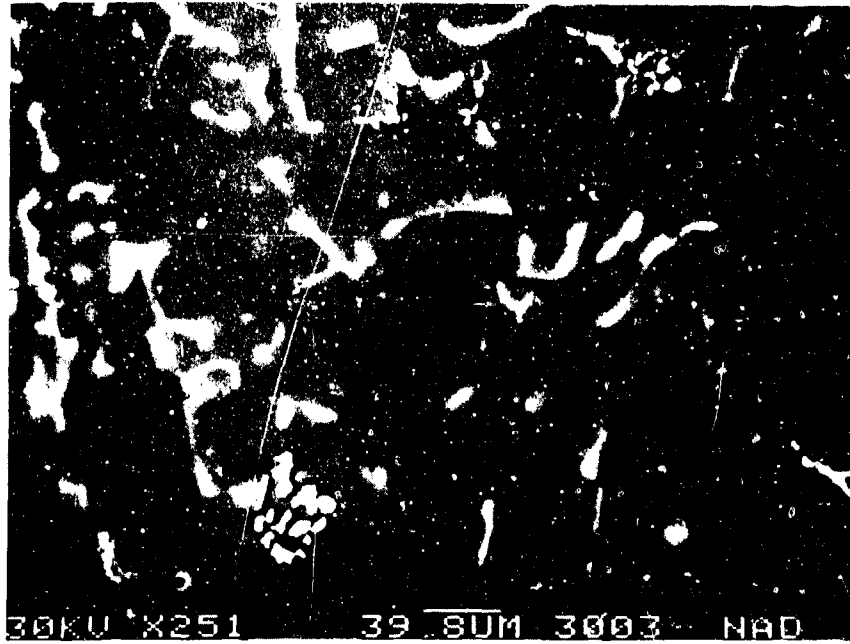


Figure 60. Backscatter SEM Micrograph of Nonoptimum D357-T6



Figure 61. TEM Micrograph of Nonoptimum D357-T6 Showing a Small Precipitate

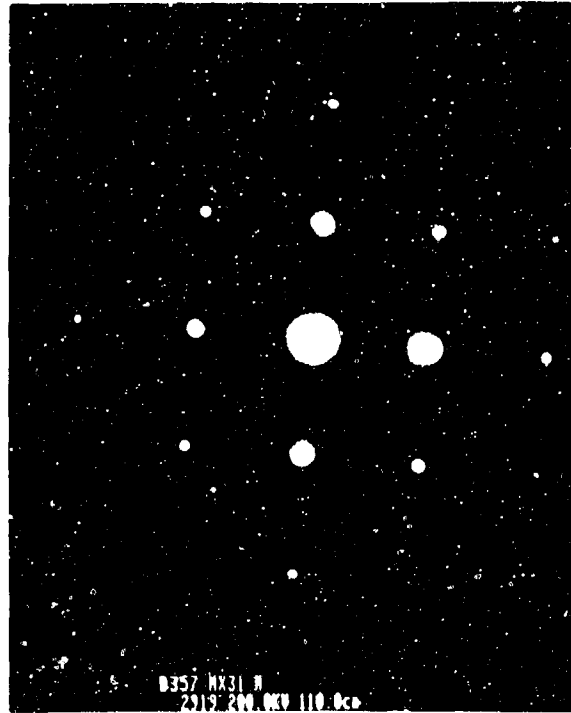


Figure 62. Selected Area Diffraction Pattern of the Precipitate in Figure 61



Figure 63. TEM Micrograph of Nonoptimum D357-T6 Showing a Needle-Shaped Phase Containing Ti

### 8.4.3 Tensile Properties

The tensile properties of D357-T6 with the nonoptimum microstructure are shown in Table 69. The average and all individual values for UTS and elongation failed to meet the AMS 4241 specification requirements. The average yield strength was within specification and was only 2 ksi lower than the value obtained for the verification material. The lower properties for the nonoptimum materials are presumed to be due to the presence of larger silicon particles with a higher aspect ratio.

### 8.4.4 Fatigue Properties

#### 8.4.4.1 Stress-Life

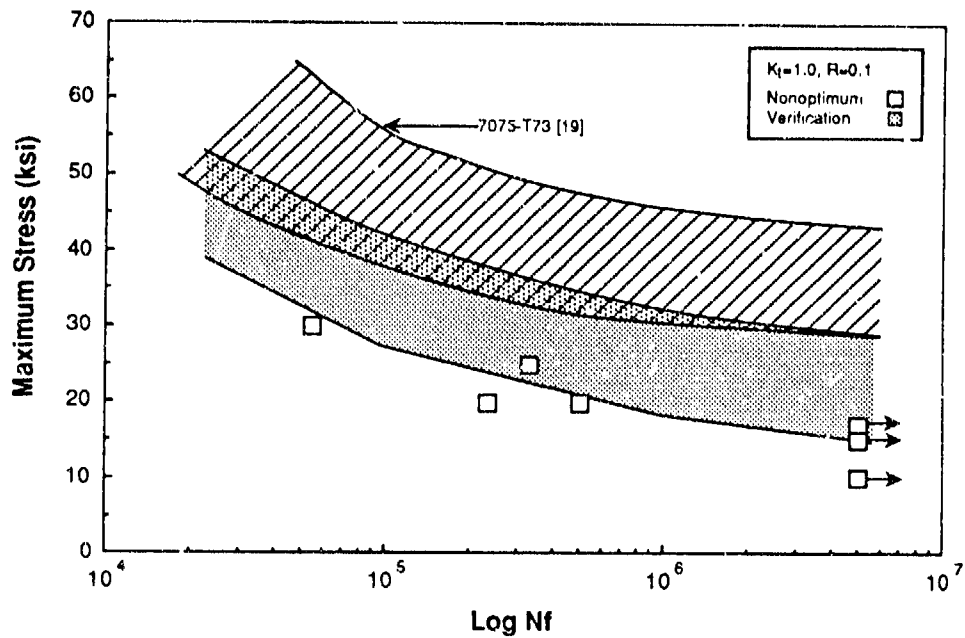
The stress life data ( $K_t = 1.0$  and  $3.0$ ) for D357-T6 with nonoptimum microstructure are shown in Figure 64. Data for 7075-T73 and the Phase I, Task 2 verification material are also shown for comparison. The smooth stress-life data (Figure 64a) for the D357-T6 with nonoptimum microstructure fall close to or slightly below the lower boundary of the scatter for the verification material. The notched stress-life data are indistinguishable from those of the verification data (Figure 64b). The overall conclusion is that the smooth fatigue life is slightly reduced by coarsening the D357-T6 microstructure. The notched fatigue life is relatively unaffected.

#### 8.4.4.2 Fatigue Crack Growth Rate

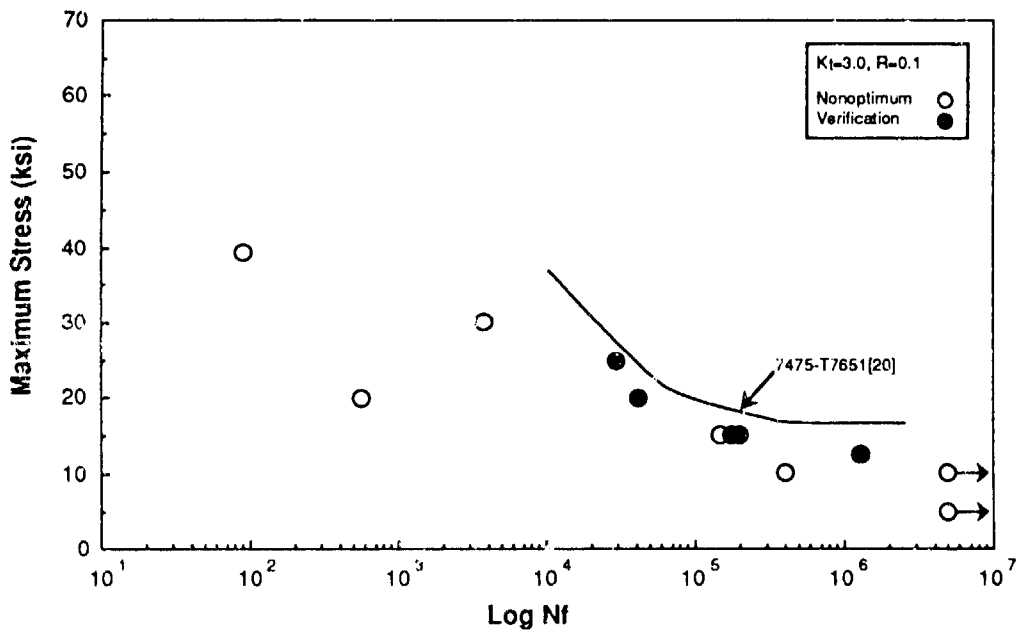
Fatigue crack growth rate (FCGR) data were obtained and are presented in Figure 65. The FCGR was the same as the verification material, i.e., slightly slower than 7075-T7351, and was therefore unaffected by the coarse microstructure.

TABLE 69. TENSILE PROPERTIES OF D357-T6 WITH NONOPTIMUM MICROSTRUCTURE

| MATERIAL     | UTS (ksi) |       | YS (ksi) |       | El (%) |         |
|--------------|-----------|-------|----------|-------|--------|---------|
|              | AVG.      | RANGE | AVG.     | RANGE | AVG.   | RANGE   |
| Nonoptimum   | 47        | 46-48 | 43       | 42-44 | 0.9    | 0.6-1.1 |
| Verification | 53        | 50-55 | 45       | 44-48 | 5.0    | 3.0-8.5 |



a. Smooth Fatigue ( $K_t = 1.0$ )



b. Notched Fatigue ( $K_t = 3.0$ )

Figure 64. Stress-Life Fatigue Data for D357-T6 With Nonoptimum Microstructure



#### 8.4.4.3 Spectrum Fatigue Life

The fatigue life using an F-18 spectrum (F18C2) was determined at both 32 ksi and 40 ksi gross maximum stress. The fatigue life for these two stress levels was 1456 and 144 flight hours, respectively. The value at 32 ksi was significantly lower than the 15,931 flight hours obtained for the verification material (Section 7.3.4.4), also tested at 32 ksi maximum stress. This result indicates that the spectrum fatigue life may be reduced by the coarse, nonoptimum microstructure.

#### 8.4.5 Fracture Toughness

The average fracture toughness (two tests) of the nonoptimum microstructure D357-T6 was 17.7 ksi/in. Valid  $K_{IC}$  values were obtained (17.1 and 18.3 ksi/in). In comparison, the average value for the verification material, 24 ksi/in ( $K_Q$ ), is considerably higher. A comparison with data for defect-containing material reveals that fracture toughness was affected far more by coarsening the microstructure (large, high aspect ratio silicon particles) than by introducing significant amounts of porosity (Grade C, Table 66).

### 8.5 EFFECT OF NONOPTIMUM MICROSTRUCTURE ON THE PROPERTIES OF B201-T7

#### 8.5.1 Composition

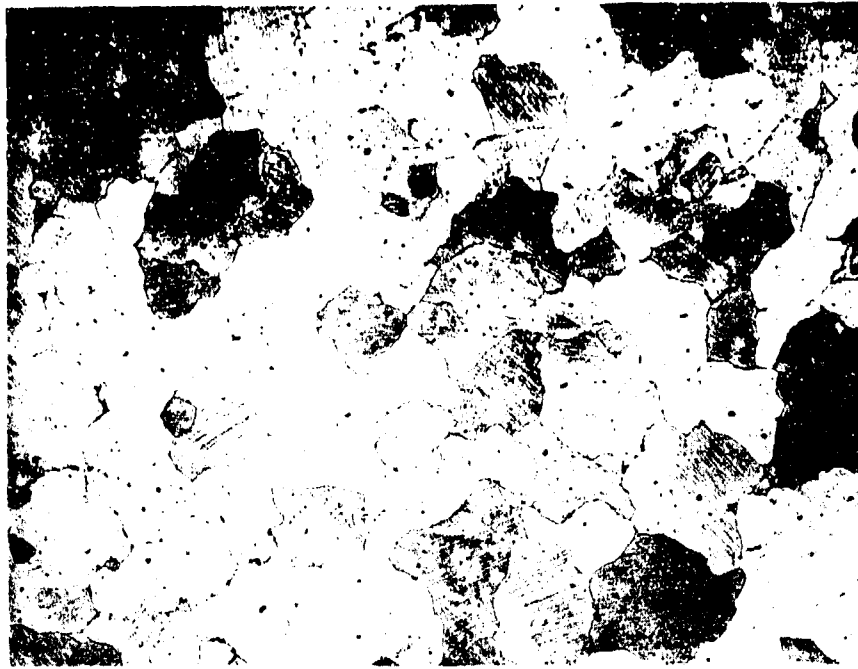
Four 16 x 6 x 1.25-inch B201-T7 plates were cast from the same melt by Hitchcock Industries to provide material that had a nonoptimum microstructure. Details are included in Section 8.2.1.2. The composition of the plates (foundry melt analysis), which is shown in Table 70, was confirmed by Northrop to be within specification. The plates were evaluated by radiography and determined to be Grade B or better.

#### 8.5.2 Microstructure

The microstructure of the nonoptimum B201-T7 was initially characterized using optical microscopy. A typical area is shown in Figure 66.

TABLE 70. COMPOSITION OF B201-T7 WITH NONOPTIMUM MICROSTRUCTURE

| COMPOSITION (WT %)            |       |       |       |       |      |      |      |
|-------------------------------|-------|-------|-------|-------|------|------|------|
| Cu                            | Ag    | Mg    | Mn    | Ti    | Fe   | Si   | Al   |
| 4.8                           | 0.68  | 0.30  | 0.23  | 0.21  | 0.02 | 0.03 | Bal. |
| <u>AMS 4242 Specification</u> |       |       |       |       |      |      |      |
| 4.5                           | 0.40  | 0.20  | 0.20  | 0.15  | 0.05 | 0.05 | Bal. |
| -5.0                          | -0.80 | -0.30 | -0.50 | -0.35 |      |      |      |



X50

Figure 66. Typical Optical Microstructure of Nonoptimum B201-T7

The average grain size of this material was 0.011 inch, which is more than three times greater than that for the verification material (0.0032 inch). The grain size range was 0.0085 to 0.013 inch. After determining that a coarse, nonoptimum microstructure had been obtained, additional detailed microstructural analysis was undertaken using SEM and TEM methods.

Using SEM in the backscattered electron imaging mode, several constituent phases were observed (Figure 67). Energy dispersive X-ray analysis (EDXA) was performed on several phases, numbered 1 through 5 in Figure 67. Phases 1 and 2 were rich in Cu and Al and are probably equilibrium theta ( $\text{Al}_2\text{Cu}$ ). Phases 3 through 5 contained Cu, Fe, and Mn. Both types of phase (1 and 2, 3 through 5) were detected in the verification material. EDXA of the matrix (denoted as "m" in Figure 67) showed the presence of Al and Cu, as would be expected.

Further examination of the nonoptimum B201-T7 was conducted using TEM and selected area diffraction (SAD). The main strengthening phase was identified (Figure 68) and was determined by EDXA to be rich in Al and Cu. Analysis of the diffraction data indicated that the strengthening phase is theta prime ( $\text{Al}_2\text{Cu}$ ).

Typical grain boundary precipitates identified by TEM are shown in Figure 69. The boundary contains a small precipitate surrounded by a precipitate-free zone. EDXA of the grain boundary phase revealed the presence of only Al and Cu, similar to the grain boundary phase observed in verification material. The grain boundary precipitate is believed to be theta or theta prime ( $\text{Al}_2\text{Cu}$ ).

Another phase observed throughout the microstructure of the nonoptimum material is shown in Figure 70. It contained Al, Cu and Mn and was also seen in the verification material. It's exact identity could not be determined. Other phases observed in the verification material included a grain boundary phase containing Al, Cu, Fe and Mn and a lath-shaped phase (composed of Al and Cu) with a distinct orientation to the matrix.

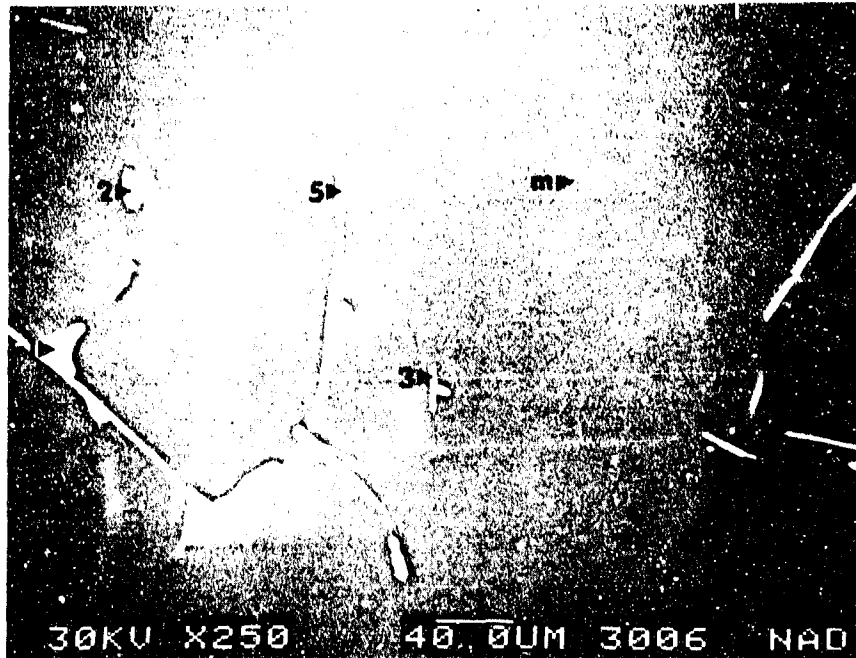


Figure 67. SEM Image of Nonoptimum B201-T7 Showing Typical Constituent Phases

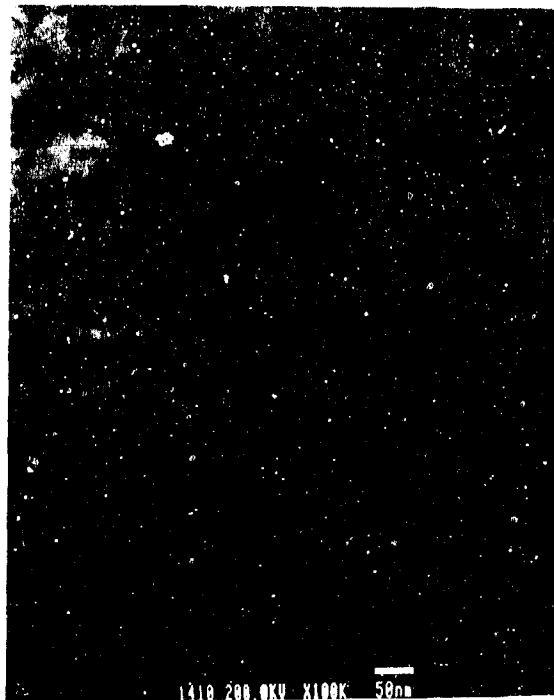


Figure 68. Main Strengthening Phase in Nonoptimum B201-T7



Figure 69. Typical Grain Boundary Precipitates in Nonoptimum B201-T7

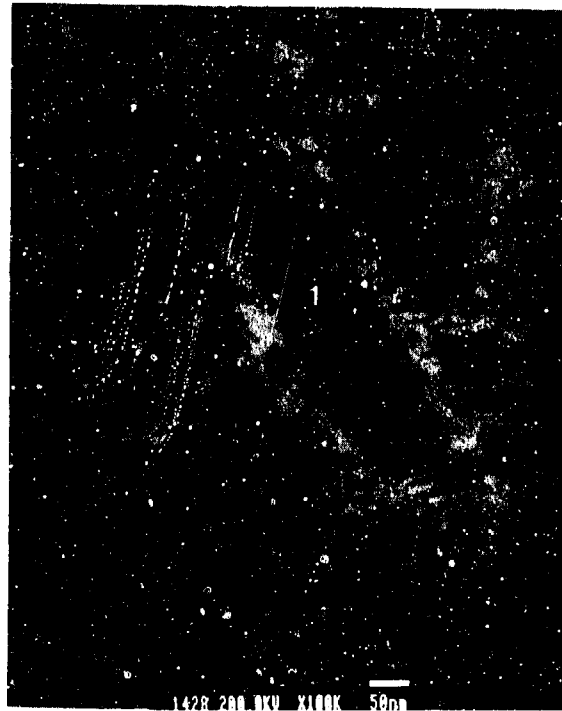


Figure 70. Blocky Precipitate Commonly Observed in Nonoptimum B201-T7

The above microstructural analysis suggests that, with the exception of the large grain size, the microstructure of the nonoptimum B201-T7 was essentially the same as that of the verification material evaluated under Task 2, Phase 1. Any mechanical property differences between the two materials can therefore be attributed to the grain size difference, which was significant (0.0032 inch versus 0.011 inch)

### 8.5.3 Tensile Properties

The tensile properties of B201-T7 with nonoptimum microstructure are shown in Table 71. The average values for all three properties were slightly lower than those for the verification material but were well above the AMS 4242 requirement of 60/50/3. Based on these data, it is therefore concluded that the tensile properties are relatively insensitive to grain size. The decrease in tensile properties observed for B201-T7 was much less than that observed for D357-T6 (Section 8.4.3).

### 8.5.4 Fatigue Properties

#### 8.5.4.1 Stress-Life

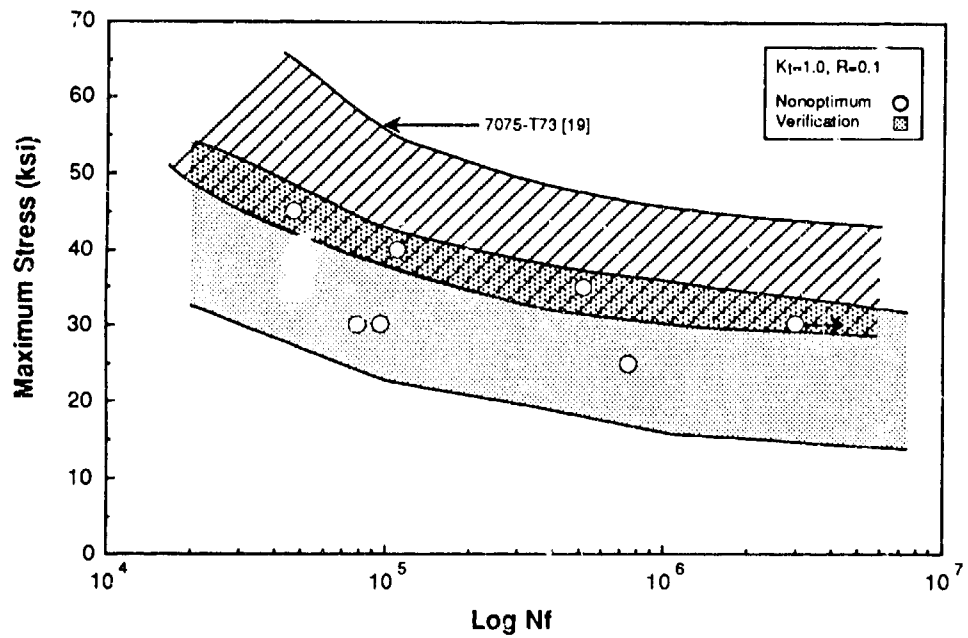
The stress-life ( $K_t = 1.0$  and  $3.0$ ) data are shown in Figure 71 and are compared with those for the verification material evaluated in Task 2 of Phase I. The smooth and notched fatigue data points (Figures 71a and b) fall within the scatter for the verification material. Thus, it is concluded that the coarse microstructure did not significantly influence fatigue life.

#### 8.5.4.2 Fatigue Crack Growth Rate

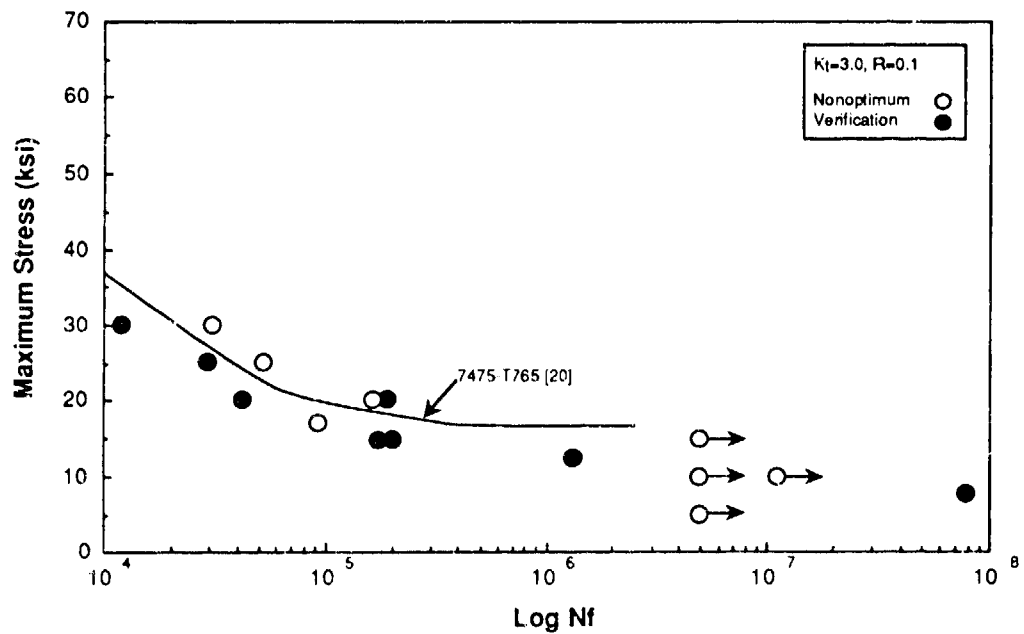
The constant amplitude fatigue crack growth rate (FCGR) data for the nonoptimum microstructure B201-T7 are shown in Figure 72. Two tests were conducted. The data coincide with the lower extreme of the scatter for the verification material, indicating that the FCGR may be lower for the coarse, nonoptimum microstructure material. This is consistent with observations for other alloys; a fine-grain material typically exhibits a more rapid FCGR than does a coarse material.

TABLE 71. TENSILE PROPERTIES OF B201-T7 WITH NONOPTIMUM MICROSTRUCTURE

| MATERIAL     | UTS (ksi) |       | YS (ksi) |       | El (%) |          | GRAIN SIZE ( $10^{-4}$ in) |        |
|--------------|-----------|-------|----------|-------|--------|----------|----------------------------|--------|
|              | AVG.      | RANGE | AVG.     | RANGE | AVG.   | RANGE    | AVG.                       | RANGE  |
| Nonoptimum   | 65        | 64-68 | 59       | 58-61 | 6.9    | 3.3-11.0 | 110                        | 85-130 |
| Verification | 68        | 65-73 | 60       | 54-66 | 8.4    | 6.5-11.0 | 32                         | 26- 40 |



a. Smooth Fatigue ( $K_t = 1.0$ )



b. Notched Fatigue ( $K_t \approx 3.0$ )

Figure 71. Stress-Life Fatigue Data for B201-T7 With Nonoptimum Microstructure



#### 8.5.4.3 Spectrum Fatigue Life

Similar to D357-T6, the effect of coarse microstructure on spectrum fatigue life was determined using an F-18 wing root spectrum (F18C2). At gross maximum stress levels of 32 and 40 ksi, fatigue lives of 17,763 and 14,581 flight hours, respectively, were obtained. For the verification material (Section 7.4.4.4), the fatigue lives were 26,762 and 14,731 flight hours, respectively, at the same stress levels. The data indicate a decrease in life at 32 ksi, but the decrease is much smaller than that observed for D357-T6. Although the amount of data available is limited, it is concluded that a coarse microstructure had little effect on the spectrum fatigue life of B201-T7 at a stress of 40 ksi; a more significant effect was observed at 32 ksi.

#### 8.5.5 Fracture Toughness

The average fracture toughness obtained for B201-T7 with the nonoptimum microstructure was 46 ksi/in. The average was based on two tests, both of which yielded invalid  $K_Q$  values because of excessive crack front curvature. The individual results were 46.7 and 45.4 ksi/in. The average fracture toughness for the verification material, which includes two values for material made by Foundry B that were significantly lower than those for material made by Foundries A and C, was 39.4 ksi/in. The fracture toughness of the coarse B201-T7 was within the scatter of the verification material. It is concluded, therefore, that the large grain size did not influence fracture toughness.

#### 8.5.6 Stress Corrosion Cracking

Direct tension, alternate immersion SCC tests were conducted on the nonoptimum B201-T7 to ensure that the material had been overaged to the T7 temper. One specimen from each of three plates was exposed to a 3.5 percent NaCl solution for 30 days at a constant load equal to 75 percent of the yield strength. No failures were experienced, indicating that each plate had been heat treated to the T7 condition.

## 8.6 CONCLUSIONS

### 8.6.1 Effect of Defects on D357-T6 Mechanical Properties

The overall trends for the effect of defects on the mechanical properties of D357-T6 are summarized in Table 72; the average properties for the various defect/grade combinations are shown as a ratio with the average verification material properties. The following conclusions are based on a combination of Table 72 data and results described in Section 8.3.

- There was a correlation between soundness and tensile properties that met the AMS 4241 specification minimum values (Table 64). Ductility decreased with decreasing soundness
- The best overall mechanical properties were exhibited by Grade A/B (essentially defect-free) and weld repair material
- The fatigue crack growth rate was insensitive to the amount and type of defect present in D357-T6
- There was a significant difference in the fatigue life of Grade A/B and Grades B, C and D D357-T6. The scatter band for Grade B was wider than the other grades, spanning the gap between Grades A/B and D
- Because the lower edge of the data scatter is the same for Grades B, C, and D, the fatigue life ( $K_t = 1.0$ ) can only be improved by achieving essentially defect-free material (Grade A/B)
- The weld material, which had the finest microstructure, had the highest fracture toughness (32 ksi/in), followed by Grade A/B (27 ksi/in). The fracture toughness of Grades B and C gas and shrinkage porosity material was the same (average 22 ksi/in)
- FAI ultrasonic inspection data showed the same qualitative trends observed in Task 1 (Section 4) for porosity. However, the absolute porosity and pore radius values were higher

### 8.6.2 Nonoptimum D357-T6

- The ultimate strength and ductility for the D357-T6 with the coarse microstructure and high DAS (0.0029 inch) were significantly lower than for optimized material

TABLE 72. RATIO OF MECHANICAL PROPERTIES OF DEFECT-CONTAINING D357 AND AVERAGE VALUES FOR VERIFICATION MATERIAL

| DEFECT/GRADE     | PROPERTY(1) |      |      |                    |                        |
|------------------|-------------|------|------|--------------------|------------------------|
|                  | TENSION(2)  |      |      | FRACTURE TOUGHNESS | STRESS-LIFE FATIGUE(3) |
|                  | UTS         | YS   | E1   |                    |                        |
| Grade A/B        | 1.02        | 1.07 | 0.75 | 1.13               | 14.0                   |
| Gas Porosity     |             |      |      |                    |                        |
| B                | 0.96        | 1.00 | 0.63 | 0.92               | 0.89                   |
| C                | 0.94        | 0.93 | 0.40 | 0.96               | 0.50                   |
| D                | 0.92        | 0.98 | 0.29 | --                 | 0.33                   |
| Shrinkage        |             |      |      |                    |                        |
| B                | 0.96        | 1.02 | 0.52 | 0.92               | 1.00                   |
| C                | 0.96        | 1.02 | 0.56 | 0.96               | 0.44                   |
| Foreign Material |             |      |      |                    |                        |
| B                | 1.02        | 1.02 | 0.88 | --                 | 0.61                   |
| C                | 0.96        | 1.02 | 0.46 | --                 | 0.61                   |
| Weld Repair      | 1.04        | 1.04 | 0.98 | 1.33               | 1.16                   |

(1) Ratio = Average value for defect/grade combination divided by verification data average

(2) Water-quenched verification material

(3) Lower bound fatigue life ( $K_t = 1.0$ ) at 30 ksi stress

- The constant amplitude fatigue life and crack growth rate of nonoptimum D375-T6 were the same as that observed for the verification material. However, limited spectrum fatigue life testing indicated that the life was shorter than for the verification material
- The fracture toughness (17.7 ksi/in) was about 25 percent lower than the toughness of the verification material
- Overall, the observed property trends support the commonly accepted view that the best balance of D357-T6 properties is obtained by achieving a fine microstructure.

#### 8.6.3 Nonoptimum B201-T7

There was no significant effect on any of the properties evaluated by increasing the grain size of B201-T7 from 0.0032 inch to 0.011 inch.

## SECTION 9

### PHASE I, TASK 4 - APPLICABILITY OF DADT SPECIFICATIONS TO ALUMINUM CASTINGS

#### 9.1 INTRODUCTION

Upon completion of Phase I, Tasks 1 to 3 (Sections 4 to 8), an assessment was made of the applicability of MIL-STD-1530A, MIL-A-83444, and MIL-A-87221 specifications to premium quality aluminum castings based on the data obtained in the program. MIL-STD-1530A defines the overall requirements necessary to achieve structural integrity of USAF airplanes. Acceptance methods of contractor compliance are specified and the appropriate detailed specifications are listed, including MIL-A-83444 for damage tolerance. Durability and damage tolerance requirements are described in MIL-A-87221, which is a relatively recent specification.

#### 9.2 DURABILITY AND DAMAGE TOLERANCE ASSESSMENT

Upon completion of Phase I, Task 3, two investigations that were intended to promote the use of aluminum castings for durability and damage tolerance applications had been completed. These were (1) an assessment of the FAI NDI method for characterizing casting defects (Section 4) and (2) the equivalent initial flaw size (EIFS) analysis (Section 7), which related specifically to damage tolerance. Life predictions based on fatigue data generated during the program were also initiated during Phase I, Task 4, forming part of the durability analysis for aluminum castings. The durability analysis was completed later in the program and is discussed in its entirety in Section 10.5; results from multihole specimens tested under spectrum fatigue loading were used to compare actual and predicted fatigue lives. A brief summary of the FAI method and the EIFS analysis results and their implications with regard to DADT specifications is included below. Details of these and the durability analyses are described in the above-noted sections of this report. An overall summary is included in Section 11.3.

### 9.2.1 FAI Assessment

The FAI method was selected for evaluation because it offered the potential for providing a quantitative assessment of the typical defects found in aluminum castings. Measurement of both average defect size and the volume percent present in the casting is possible using this method. Improvement in such measurements would facilitate the application of DADT specifications because it is known that fatigue life is particularly dependent upon the type, size, and distribution of defects present in a casting. The effects of defects on mechanical properties was demonstrated in Task 3, confirming the need for the best possible NDI methods so that advantage can be taken of the inherent advantages of castings (e.g., cost reduction) for DADT applications.

It was shown (Sections 4.4 and 8.3.3) that there is a good correlation between FAI results and X-ray and microstructure data for gas porosity but not for shrinkage sponge or foreign material. It was concluded that, without a significant amount of additional evaluation and development, the FAI method cannot be used as a foundry NDI tool for grading aluminum castings for DADT applications.

### 9.2.2 Damage Tolerance Analysis

A maximum initial equivalent flaw size was derived for both Grade B D357 and B201 during Phase I, Task 2 (property verification - Sections 7.3.6 and 7.4.7). The EIFS for the two alloys was determined to be 0.036 inch and 0.042 inch, respectively (99.9 percent probability, 95 percent confidence). These values are less than the 0.050 inch flaw that is typically assumed for damage tolerance analysis of wrought materials (MIL-A-83444) [15]. Defects in the range 0.036 to 0.042 inch may be detectable in material up to about 3 inches thick using X-ray radiography at a 1 percent sensitivity. Based on this information, Grade B or better D357 or B201 castings up to the maximum thickness evaluated under the DADTAC program (1.25 inch) can be considered for use in damage tolerance design.

## SECTION 10

### PHASE II - DADT OF ALUMINUM CASTINGS QUALITY VERIFICATION

#### 10.1 INTRODUCTION

During Phase I, a mechanical property data base was developed for D357-T6 and B201-T7 cast plates produced according to optimum material specifications. Also, the effect of casting defects (D357-T6) and nonoptimum microstructure (D357-T6 and B201-T7) on the baseline mechanical properties was determined. The overall goal in Phase II was to demonstrate that the optimum D357-T6 alloy can be used to manufacture a large complex aircraft casting while retaining the mechanical properties demonstrated in Phase I for the cast plates. In addition, specially-designed durability and damage tolerance fatigue specimens were tested to verify life predictions based on an analysis of Phase I data. These DADT specimens were excised from additional plates.

The selection and evaluation of the aircraft casting, as well as the fatigue data analysis and life prediction assessment conducted in Phase II are described in the following subsections. As in previous sections, average data are listed; the individual test results can be found in Appendices H (cast aircraft component) and I (cast plates).

#### 10.2 CASTING SELECTION

The criteria for selecting the aerospace casting for evaluation in Phase II were as follows:

- The casting should be a large production aircraft part
- The configuration of the casting should be relatively complex, with a wide range of wall thickness
- Tooling was readily available
- Production processes were established.

After reviewing potential castings with Alcoa, the subcontractor for this effort, the one that best met the above criteria was the F-5 inboard wing pylon (Figure 73a). The casting weighs approximately 65 pounds, is about 5 feet long, and has a complex configuration. Two of the other castings that were considered were the centerline and outboard wing pylons. Alcoa cast over 2,000 inboard wing pylons over the life of the F-5 program. The pylon is one of two (inboard and outboard) suspended under each wing for carrying armaments.

### 10.3 PRODUCTION OF CASTINGS

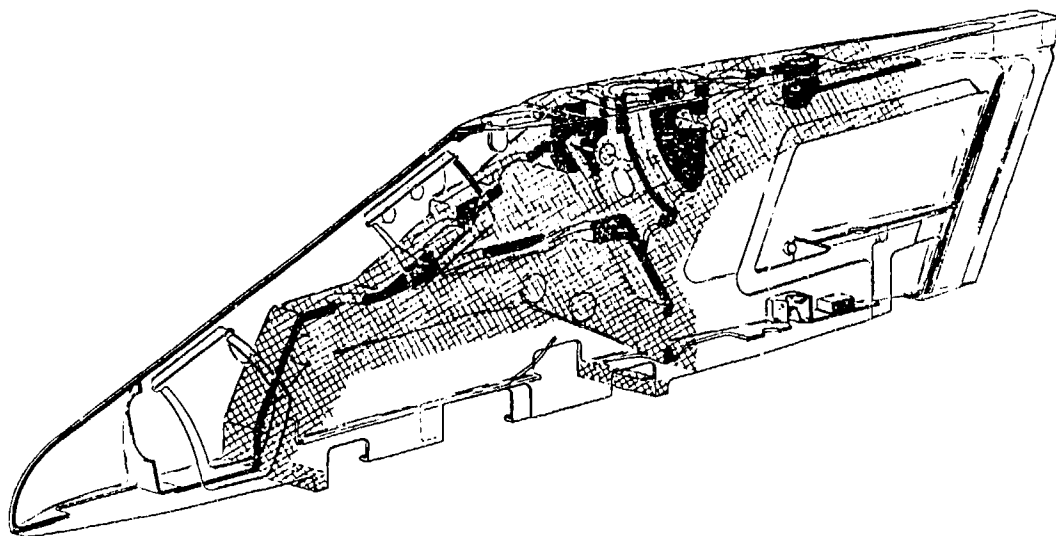
Four D357-T6 wing pylons and 14 D357-T6 plates were cast by Alcoa according to the composition requirements of AMS 4241 specification with the addition of a silicon modifier. The plates were produced using procedures that were the same as those used for the Task 2, Phase I verification plates. The pylons were produced using the same tooling and production methods as those employed for production aircraft pylons. The plates and pylons were solution treated for 15 hours at  $1010 \pm 10^\circ\text{F}$  and aged for 5.5 hours at  $325^\circ\text{F}$ . They were quenched in room temperature water.

The composition specification for both the plates and the pylons was the same. The use of sodium or strontium was included in the specification because of the benefits to silicon particle morphology seen during the Phase I testing. Alcoa preferred to use sodium because they had much more experience with sodium than with strontium and felt they could provide better castings as a result. However, because much of the Phase I data were obtained using Sr-modified material, Alcoa was requested to cast two of the four pylons using strontium to determine if the type of modifier influenced mechanical properties. The silicon modifier for the 14 plates and the other two pylons was sodium. In all parts of the cast plates and in designated areas of the pylons (Figure 73b), tensile properties were required (AMS 4241) to meet the following minimum values:

|                              |        |
|------------------------------|--------|
| Tensile Strength             | 50 ksi |
| Yield Strength (0.2% offset) | 40 ksi |
| Elongation                   | 3      |



a. F-5 Inboard Wing Pylon



b. Designated Areas of Pylon (Crosshatch)

Figure 73. F-5 Inboard Wing Pylon

Minimum tensile properties in nondesignated areas of the pylons were 45 ksi ultimate strength, 36 ksi yield strength, and 2 percent elongation.

In lieu of the DAS procedures defined in AMS 4241, a maximum DAS of 0.0024 inch throughout the plates and in the designated areas of the pylons was specified. This value was selected based on the results of Phase I testing (Section 5). All castings were required to be Grade B quality, or better, based on radiographic analysis (1 percent sensitivity). Because the castings were sectioned for mechanical property evaluation, the attached coupons were not tested.

#### 10.4 CASTINGS PROPERTIES

Chemical, microstructural, and mechanical property evaluations were conducted on the cast plates and pylons. Pylon test results were compared to those obtained during the Phase I verification subtask to ensure that the process requirements can be scaled up to a large aircraft casting. Tensile results for the cast plates were used to qualify material for the DADT element fatigue testing (Section 10.5.5). Based on radiographic analysis, all castings were determined to be Grade B quality.

##### 10.4.1 Composition

Fourteen plates, cast from two different melts, and four inboard wing pylons, cast from four different melts, were evaluated. The composition of each of these melts is listed in Table 73. The compositions were within the AMS 4241 (plus silicon modifier) specification; two of the pylons were cast from melts modified using strontium. The melt compositions were confirmed by ICP chemical analysis conducted by Northrop on samples taken from the plates and pylons.

##### 10.4.2 Microstructure

The microstructure of the cast plates and pylons was characterized using optical microscopy and image analysis. DAS, percent porosity, and silicon particle morphology for each of the pylons and for selected plates were

TABLE 73. D357-T6 PLATE AND PYLON MELT COMPOSITIONS

| COMPOSITION (WT %)    |      |       |       |       |       |        |         |      |
|-----------------------|------|-------|-------|-------|-------|--------|---------|------|
| Fe                    | Si   | Mg    | Ti    | Mn    | Be    | Na     | Sr      | Al   |
| <u>Plate Melts</u>    |      |       |       |       |       |        |         |      |
| 0.08                  | 6.91 | 0.60  | 0.12  | 0.00  | 0.06  | 0.002  | --      | Bal. |
| 0.08                  | 6.87 | 0.60  | 0.13  | 0.00  | 0.06  | 0.005  | --      | Bal. |
| <u>Pylon Melts</u>    |      |       |       |       |       |        |         |      |
| 0.07                  | 7.00 | 0.60  | 0.12  | 0.00  | 0.05  | 0.006  | --      | Bal. |
| 0.08                  | 6.88 | 0.59  | 0.12  | 0.00  | 0.05  | 0.009  | --      | Bal. |
| 0.08                  | 6.90 | 0.59  | 0.13  | 0.00  | 0.06  | --     | 0.011   | Bal. |
| 0.08                  | 7.15 | 0.60  | 0.12  | 0.00  | 0.05  | --     | 0.014   | Bal. |
| <u>Specification*</u> |      |       |       |       |       |        |         |      |
| <0.12                 | 6.5- | 0.55- | 0.10- | <0.10 | 0.04- | 0.001- | 0.008-  | Bal. |
|                       | 7.5  | 0.6   | 0.20  |       | 0.07  | 0.01** | 0.014** |      |

\* AMS 4241 plus silicon modifier

\*\* Na concentration = 0.00% when Sr is used as modifier;  
Sr concentration = 0.00% when Na is used

determined. A typical micrograph of the sodium-modified D357-T6 pylon microstructure is shown in Figure 74; the microstructure of strontium-modified D357-T6 is shown in Figure 75. A typical micrograph of the plate microstructure is given in Figure 76.

The average DAS values, Si particle area, aspect ratio, and particle spacing for plate and pylon castings are listed in Table 74. Corresponding data obtained during Phase I verification testing for water-quenched D357-T6 are listed for comparison. The DAS of specimens taken from selected plates (three plates from each of the two melts) ranged from 0.0009 inch to 0.0014 inch, which is less than the maximum specification requirement of 0.0024 inch. Similarly, the DAS of specimens excised from each of the four pylons was below the maximum specification value, ranging from 0.0009 inch to 0.0017 inch. The average DAS values for the sodium and strontium modified pylons were each similar to that of the verification material. The specimens that were used to determine DAS for the pylons were excised from thick, designated sections of the castings.

The silicon particle morphology of the plates and pylons is similar to that of the verification material. The silicon particle area, spacing, and aspect ratio obtained for sodium-modified pylons is nearly identical to those obtained for strontium-modified castings. The percent porosity was low in each of the cast plates and pylons, similar to that for the verification material.

#### 10.4.3 Tensile Properties

The tensile properties of the D357-T6 plates and pylons are summarized in Table 75. A total of 28 tensile tests were conducted to evaluate the tensile properties of the 14 plates (two specimens per plate). For the pylons, 16 specimens (four per pylon) were machined from both designated and nondesignated sections and tested (a total of 32 specimens). Average ultimate strength and elongation results for the cast plates and pylons (both Na- and Sr-modified) were similar to the values from the verification tests. Although easily meeting the minimum specification requirements, the average yield strengths were slightly lower in the Phase II castings than in the Phase I verification test plates, i.e., 42 ksi versus 45 ksi.

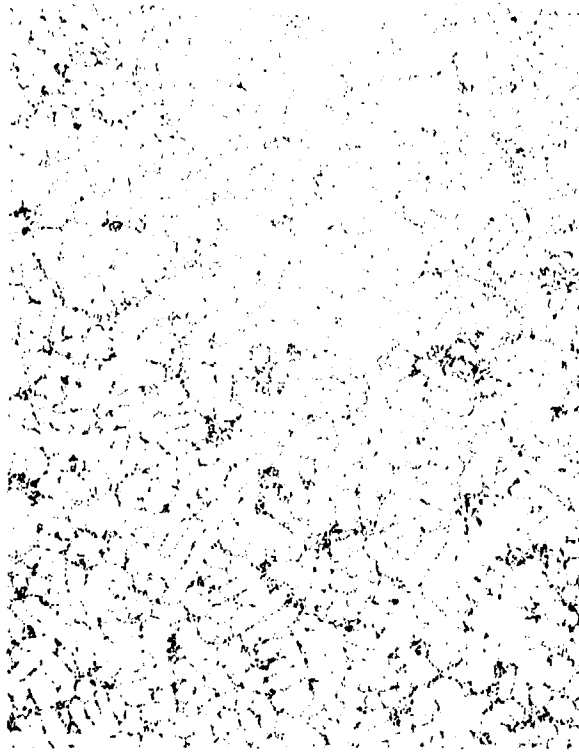


Figure 74. Typical Microstructure in Na-Modified D357-T6 Cast Pylon

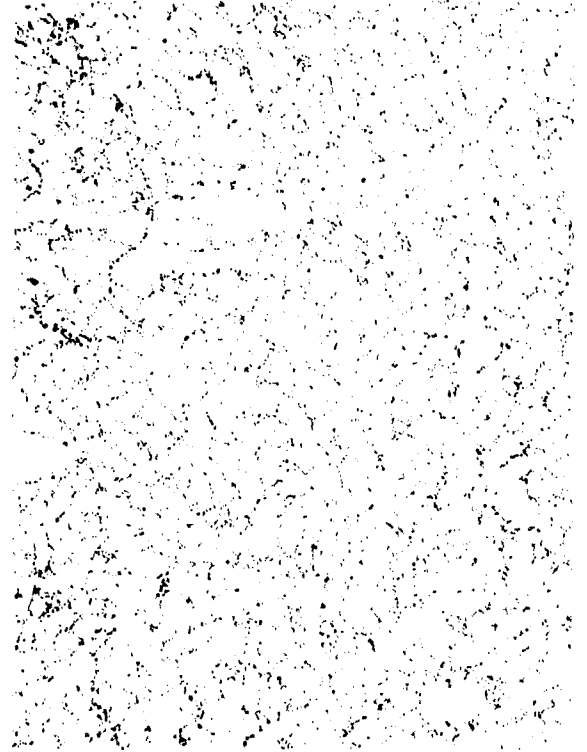


Figure 75. Typical Microstructure in a Sr-Modified D357-T6 Cast Pylon



Figure 76. Typical Microstructure of a D357-T6 Cast Plate (Na-Modified)

TABLE 74. AVERAGE DAS AND Si PARTICLE MORPHOLOGY DATA FOR  
D357-T6 PLATES AND PYLONS

| CASTING                  | SILICON<br>MODIFIER | DAS<br>(inch) | Si PARTICLE MORPHOLOGY      |                              |                 | POROSITY<br>(%) |
|--------------------------|---------------------|---------------|-----------------------------|------------------------------|-----------------|-----------------|
|                          |                     |               | AREA<br>( $\mu\text{m}^2$ ) | SPACING<br>( $\mu\text{m}$ ) | ASPECT<br>RATIO |                 |
| Plates                   | Na                  | 0.0011        | 14                          | 42                           | 1.9             | 0               |
| Pylons                   | Na                  | 0.0014        | 19                          | 47                           | 1.9             | 0.013           |
|                          | Sr                  | 0.0015        | 18                          | 50                           | 1.9             | 0               |
| Verification<br>Material | *                   | 0.0014        | 17                          | 43                           | 1.6             | 0.028           |

\* Two foundries used Na; one used Sr

TABLE 75. AVERAGE TENSILE PROPERTIES OF D357-T6 PLATES AND PYLONS

| CASTING                  | SILICON<br>MODIFIER | UTS (ksi) |       | YS (ksi) |       | El (%) |       |          |
|--------------------------|---------------------|-----------|-------|----------|-------|--------|-------|----------|
|                          |                     | AVG.      | RANGE | AVG.     | RANGE | AVG.   | RANGE |          |
| Plates                   | Designated          | Na        | 52    | 49-54    | 42    | 38-44  | 8.9   | 5.4-14.5 |
| Pylons                   | Designated          | Na        | 51    | 49-52    | 42    | 39-44  | 6.3   | 3.5- 8.6 |
|                          |                     | Sr        | 52    | 49-54    | 42    | 39-43  | 10.0  | 8.0-11.7 |
|                          | Non-designated      | Na        | 52    | 52-53    | 42    | 41-42  | 7.4   | 6.9- 8.0 |
|                          |                     | Sr        | 53    | 52-53    | 40    | 40-41  | 10.5  | 9.8-11.2 |
| Verification<br>Material | Designated          | *         | 53    |          | 46    |        | 5.2   |          |
| Specification<br>Min.    | Designated          | --        | 50    |          | 40    |        | 3.0   |          |
|                          | Non-designated      | --        | 45    |          | 36    |        | 2.0   |          |

\* Two foundries used Na; one used Sr

NOTE: Two plates were not used for DADT testing because of unacceptable tensile results (see text and Appendix Table H); results for these plates are not included in the above averages.

Some of the individual test results for the pylons and the plates were below the AMS specification tensile property requirements (Appendix H, Tables H1, H2, and H3). Of a total of 48 individual test results for designated material, three UTS and three YS results were slightly below the specification minimum. Thus, only 88 percent of the data points met or exceeded the specification minimum value. This is the same percentage pass rate that was observed for the verification plates. Unlike the verification material, for the pylons it was the ultimate and yield strengths and not the percent elongation that usually did not meet the minimum requirement. On average, the results were low by only 0.2 ksi. There was no difference in the number of specimens that failed to meet the specification for the Na- and Sr-modified pylons; in each case, there were three occurrences. There was no indication of inclusions on the fracture surfaces of these specimens. The DAS, soundness and composition were also within specification.

Because the average pylon elongation value exceeded the average verification value and the pylon failures were in ultimate and yield strength, it is probable that the pylons were underaged as a result of nonoptimized aging parameters. The aging conditions used by Alcoa were the same as those employed to make many of the same wing pylons over more than 20 years of F-5 production. However, since the composition of the four pylons that were made for the DADTAC program was different from those made previously, presumably they may require different aging conditions. Under the contract it was not possible to optimize the aging parameters for the pylons to obtain the best balance of mechanical properties.

The average elongation of the Sr-modified pylons was significantly higher than pylons that were modified using Na (10.0 percent versus 6.3 percent for the designated areas). The average ultimate and yield strengths for the Na- and Sr-modified material were similar (Appendix Table H1). The reason for the difference in elongation is not clear. The silicon particle morphology was essentially identical for both materials (Table 74). It is possible that the difference could be due to a need for different aging parameters, depending upon which modifier is being used.

Similar to the designated area material, nondesignated areas of the Sr-modified castings had a slightly different yield strength/elongation combination than the Na-modified pylons (40.4 ksi/10.5 percent and 41.8/7.5 percent, respectively). This further supports the conclusion that the aging parameters required to obtain targeted mechanical properties for Na- and Sr-modified D357 may not be identical.

The detailed tensile results for the 14 plates are shown in Appendix Table H3. As in the case of the pylons, some of the test results did not meet the minimum requirement. For two plates (Q13 and Q14), both of the two ultimate tensile strength results were below 50 ksi. One elongation value was also low. These two plates were rejected and were not used for the subsequent element tests conducted with the plate material. Two additional plates (Q6 and Q7) each exhibited one yield and one ultimate strength value below specification. However, because results from a second specimen from each plate were within specification and there was a material shortage, these two plates were used for the element testing.

#### 10.4.4 Fatigue Properties

##### 10.4.4.1 Smooth Stress-Life

Stress-life ( $K_t = 1.0$ ) constant amplitude fatigue data for the four D357-T6 pylons are shown in Figure 77 along with a comparison with data for verification material, and 7075-T73 [19], a wrought alloy commonly used in fatigue critical aircraft applications. Two specimens (0.375-inch-diameter gage section) per pylon were tested. No discernable difference in fatigue life data was observed between Na- and Sr-modified material. The fatigue lives exhibited by the pylons are similar to those exhibited by the verification material. Although demonstrating lower or similar crack growth rates (Section 10.4.4.2), the total fatigue life for the D357-T6 specimens is significantly less than that of 7075-T73. This is probably indicative of shorter crack initiation lives for cast material.

The presence of inherent defects such as dross and porosity enhances fatigue crack initiation in cast materials. Fractographic examination of six

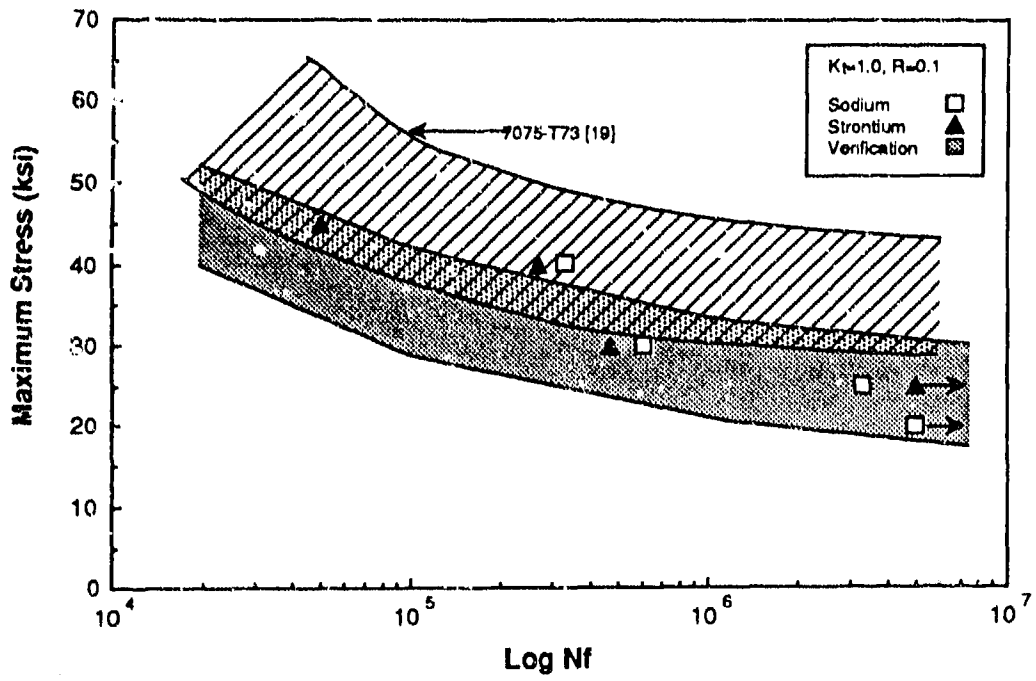


Figure 77. Stress-Life Fatigue Data for D357-T6 Pylons

pylon fatigue life specimens revealed that three fatigue cracks initiated at a defect located at or near the surface. In two of these specimens, a large (>200 micron) dross inclusion acted as the initiation site. In the third specimen, the fatigue crack initiated at a pore. A micrograph of the pore and resulting fatigue crack is given in Figure 78.

None of the remaining three specimens exhibited defects near the surface. However, in each of these specimens, dross inclusions were observed within the interior of the gage section. A micrograph of a specimen in which two large inclusions were observed is shown in Figure 79. This particular specimen (P96S2), tested at a gross stress level of 25 ksi, failed after  $3.3 \times 10^6$  cycles (Appendix I), which is shorter than the  $5 \times 10^6$  cycle lifetime exhibited by a second specimen tested at 25 ksi. Overall, the amount of dross observed in the pylon smooth fatigue specimens suggests that the quality of the pylons, particularly in the designated areas from which these specimens were machined, could be improved. Although the data shown in Figure 77 are similar to that exhibited by the verification material, micrographic analysis has shown that large defects can still exist and may reduce the time to initiate a fatigue crack.

#### 10.4.4.2 Fatigue Crack Growth Rate

The range of constant amplitude fatigue crack growth rate (FCGR) data obtained from the four pylons is shown in Figure 80. Also shown are the data for the Phase I verification material and 7075-T73 plate [22]. The pylon and verification plate FCGR data are similar. The fatigue crack growth rate of D357-T6 is slightly slower than that of 7075-T73. Therefore, the shorter fatigue lives (Figure 77) can be attributed to a shorter crack initiation phase in cast material, presumably because of higher distribution density of larger defects in Grade B castings.

#### 10.4.5 Fracture Toughness

Fracture toughness data for the D357-T6 pylons are shown in Table 76. One compact tension and four notched tensile specimens per pylon were tested. Fracture toughness specimens were excised from the thick attach pad at the top

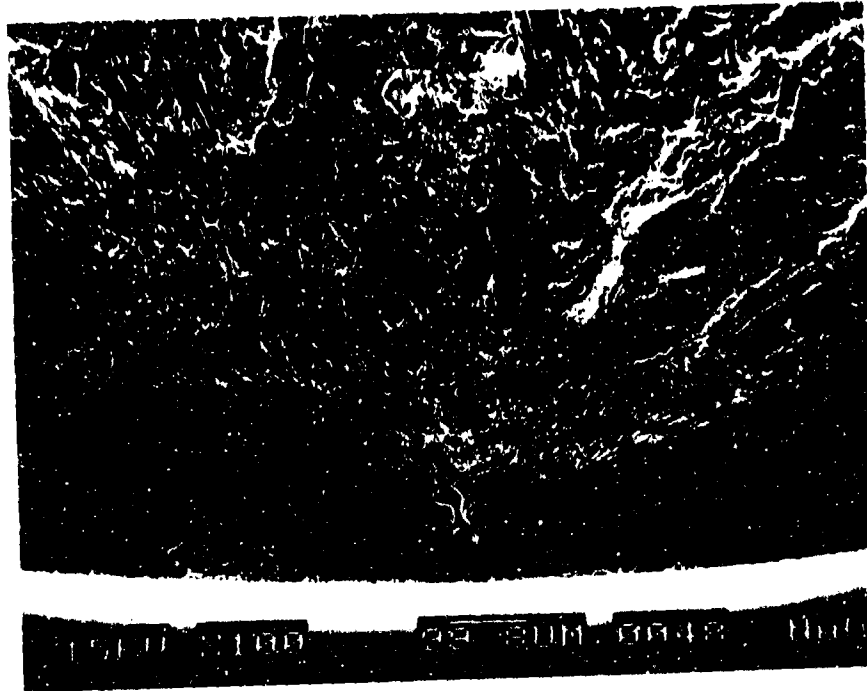


Figure 78. Fatigue Crack Initiating From a Pore in a Pylon Fatigue Specimen

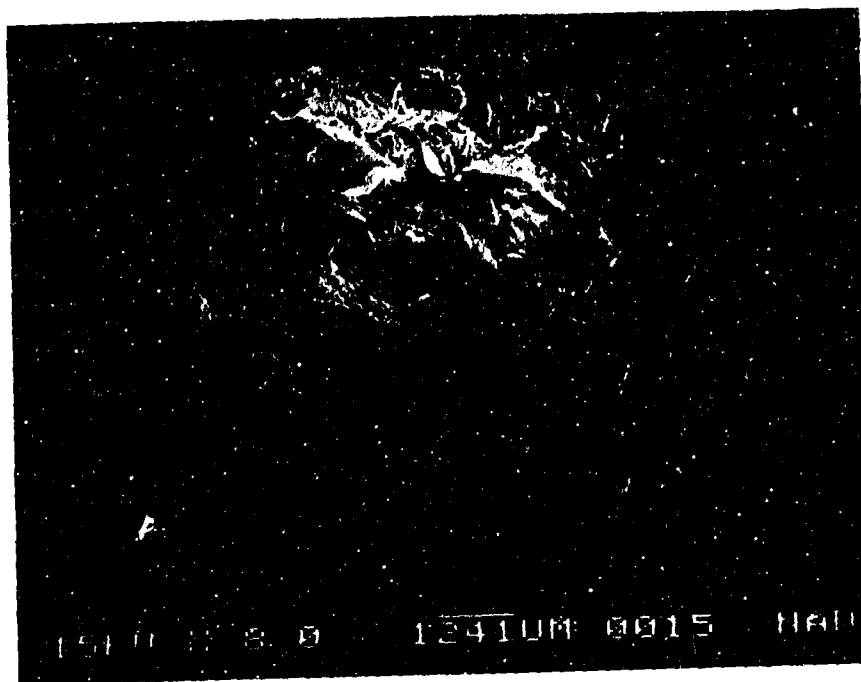


Figure 79. Two Large Inclusions Observed in a Pylon Fatigue Specimen



TABLE 76. D357-T6 PYLON FRACTURE TOUGHNESS AND NOTCHED TENSILE STRENGTH DATA\*

| SILICON<br>MODIFIER      | PYLON<br>NO. | KQ<br>(ksi./in) | NTS<br>(ksi) | YS<br>(ksi) | NTS/YS |
|--------------------------|--------------|-----------------|--------------|-------------|--------|
| Na                       | 95           | 25.5            | 61.0         | 42.4        | 1.44   |
|                          | 96           | 25.4            | 60.1         | 41.8        | 1.44   |
|                          | Average      | 25.5            | 60.6         | 42.1        | 1.44   |
| Sr                       | 97           | 28.1            | 61.6         | 41.3        | 1.49   |
|                          | 98           | 27.2            | 62.0         | 41.8        | 1.49   |
|                          | Average      | 27.7            | 61.8         | 41.6        | 1.49   |
| Verification<br>Material |              | 24.0            | 59.0         | 46.0        | 1.38   |

\* Specimens excised from designated area of the pylon

of the pylon (Figure 73) where it would mate with the aircraft structure. The pad is a designated area. Pylons that contained Na modifier, had an average  $K_Q$  value of 25.5 ksi/in. The average  $K_Q$  value of the Sr-modified material was slightly higher at 27.7 ksi/in, which is consistent with the higher elongation values observed for this material. The average NTS/YS ratio of the Sr-modified material was also slightly higher than that of the Na-modified material, 1.49 versus 1.44. None of the fracture toughness results met the criteria for valid  $K_{IC}$  values due to the presence of excessive crack front curvature.

The average fracture toughness and NTS values obtained for the pylons were higher than the average values determined for the Phase I verification material. Average NTS/YS ratios were also higher because of the contribution of these higher NTS values and lower average yield strengths.

#### 10.4.6 FAI Assessment of the Pylons

Frequency Attenuation Inflection (FAI, Section 4) measurements were made on specimens excised from selected areas of one of the pylons (P95) to further assess both the soundness of the casting and the FAI method. Fifteen specimens of varying thickness were machined from different areas in the casting and analyzed using FAI and X-ray radiography. Metallographic analysis was also conducted on the specimens to confirm the FAI results.

Results from FAI inspection showed that all specimens contained less than 0.1 percent porosity (the minimum detection capability of the equipment). X-ray inspection showed that each of the specimens was Grade B. Metallographic analysis indicated that there was <0.01 percent porosity in all the specimens, which also supported the FAI results.

#### 10.4.7 Equivalent Initial Flaw Size Analysis of the Pylons

An EIFS analysis was performed using the smooth fatigue data obtained for the four cast inboard pylons. The Weibull analysis is shown in Figure 81 and also includes data for cast verification plates for the three individual foundries. The average EIFS for the six specimens evaluated was 0.0109 inch.

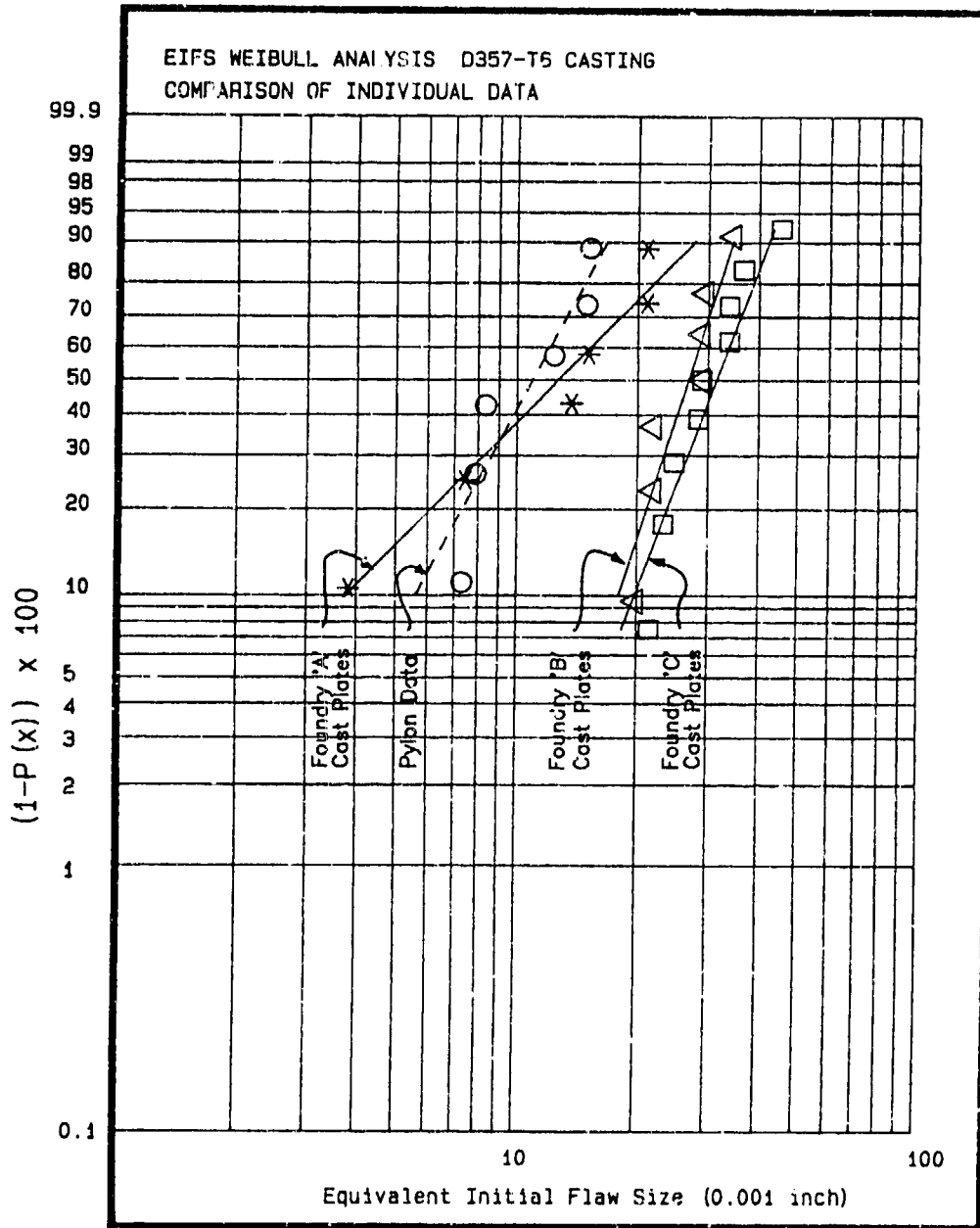


Figure 81. Weibull Distribution for D357-T6 Pylons and Verification Plates

This is better than the best verification material, made by Foundry A, which had an average EIFS of 0.0137 inch (Table 49). The Weibull analysis in Figure 81 also shows the similarity between the EIFS data for the pylons and the verification plates made by Foundry A.

#### 10.4.8 Summary

In general, the overall properties for the pylons were similar to those obtained for the verification material evaluated in Phase I, including the percentage of test results that did not meet the AMS 4241 specification tensile property requirements. The main difference between the pylon and verification data sets was the balance between yield strength and elongation. This suggests that the number of out-of-specification test results might have been reduced by additional aging of the pylons.

However, because pylons containing Sr modifier exhibited significantly higher elongation values than Na-modified pylons (10.0 percent versus 6.3 percent, respectively, for designated areas), further heat treatment optimization for each of the two types of material is perhaps required. The overall conclusion is that with heat treatment optimization, the Phase I material and process requirements can be successfully scaled up for producing large, complex aircraft castings.

#### 10.5 DURABILITY AND DAMAGE TOLERANCE ANALYSIS

A unified analytical method was developed [13] at Northrop under an IR&D program to predict both the crack initiation and crack growth portions of the total fatigue life under variable amplitude loading. This method was applied to the DADTAC program results to determine if accurate life predictions can be made for premium quality aluminum castings. The applicability of MIL-A-83444 and MIL-A-87221 to premium quality aluminum castings was also assessed.

Test specimens were excised from 14 D357-T6 plates cast by Alcoa. Tensile properties for each of these plates were determined to ensure that the material met the AMS 4241 requirements. Details of the tensile testing are discussed in Sections 10.3 and 10.4. Only 12 of the 14 available plates were

used for the durability and damage tolerance tests because two of them were judged to be unacceptable based on the tensile test results.

#### 10.5.1 Element Testing

Three types of specimen were used to characterize D357-T6 under spectrum loading. These specimens were specifically designed to evaluate the crack initiation and growth phases of damage, and included a multihole durability specimen without precracks and two damage tolerance (DT) specimen configurations. One of the DT specimen configurations had a single hole with a corner precrack; the other configuration had a surface precrack. The test matrix is shown in Table 77. All specimens were randomly excised from the 12 available D357-T6 cast plates. However, their location in each plate was noted to determine if it influenced the test results.

Two 7050-T7451 multihole durability specimens were also tested to provide baseline data for evaluating the D357-T6 results. 7050-T7451 is a wrought aluminum alloy commonly used in fatigue-critical aircraft applications.

##### 10.5.1.1 Test Spectrum

A modified version of a typical F-18 wing root spectrum was used for all fatigue tests. The negative load levels were removed so that observation of crack initiation and growth would not be restricted by the use of lateral buckling constraints that would have been required. The spectrum tape data consisted of event-sequenced wing root loads representing a block of 300 flight hours and normalized by the maximum spectrum load. This spectrum is illustrated by the exceedence curve shown in Figure 82.

##### 10.5.1.2 Specimen Geometry and Test Requirements

Durability Tests. The multihole durability specimen configuration is shown in Figure 83. Each specimen contained 14 holes, each having the same elastic stress concentration. Twelve D357-T6 and two 7050-T7451 specimens

TABLE 77. DADT TEST MATRIX

| SPECIMEN<br>TYPE     | NO. OF<br>SPECIMENS |
|----------------------|---------------------|
| Multihole Durability | 12                  |
| Damage Tolerance     |                     |
| - Surface Crack      | 4                   |
| - Precracked Hole    | 6*                  |

\* One specimen was weld-repaired after two lifetimes of growth and then tested to failure

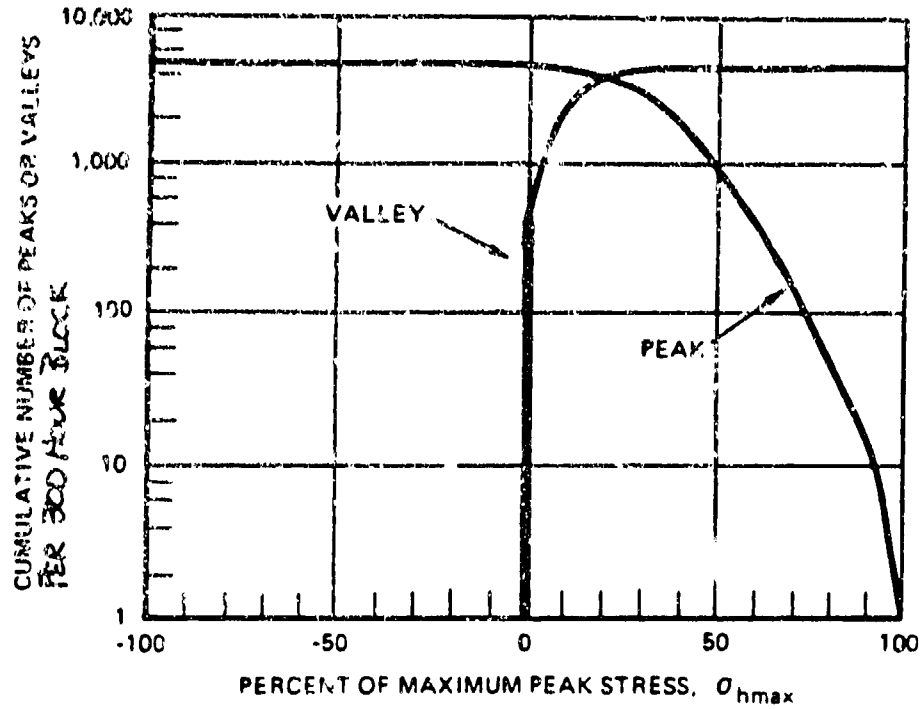


Figure 82. Modified F-18 Wing Root Spectrum

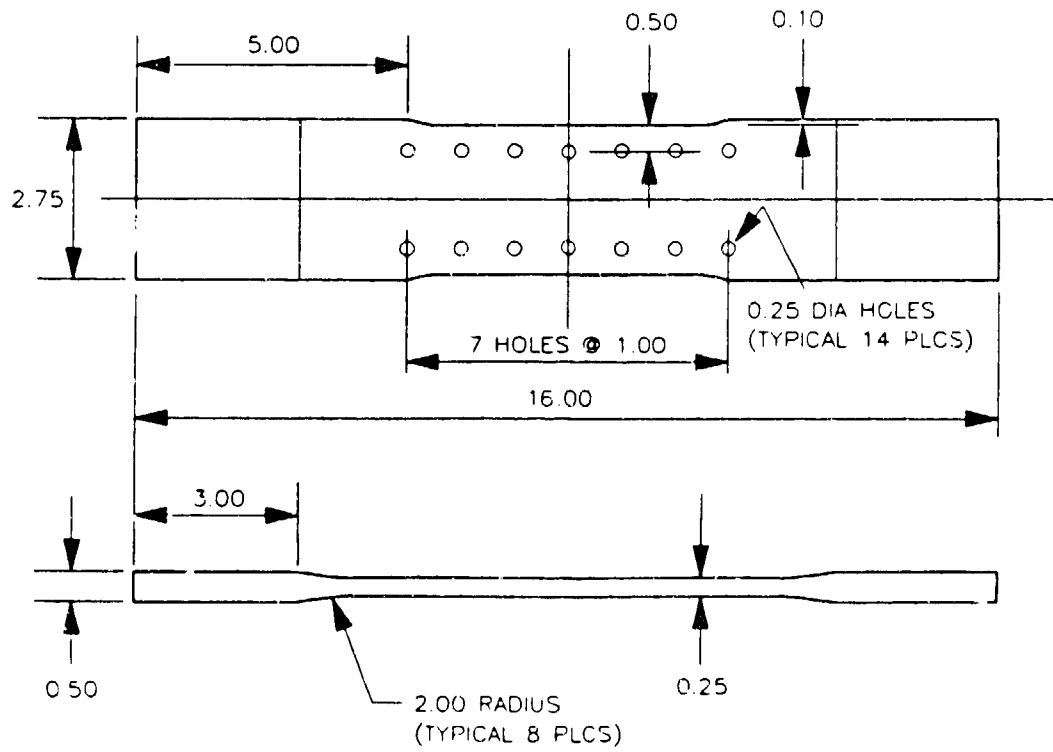


Figure 83. Multihole Durability Specimen

were tested to failure over a range of spectrum severity levels. All holes were visually monitored at regular intervals to detect the first sign of crack initiation. The time for each crack to initiate was noted. The extent of the visible surface crack length was monitored throughout the test. The test was stopped at the first occurrence of a crack breaking out to the edge of the specimen. At the end of the test a metallographic examination of each specimen was conducted at the four holes that contained the largest cracks to determine the size, location and nature of the initiating defect.

Crack Growth From a Precracked Hole. The configuration of the damage tolerance specimen with the precracked hole is shown in Figure 84. A 0.02-inch corner flaw was introduced using EDM and sharpened under constant amplitude fatigue loading to 0.05 inch. Six specimens were tested over a range of spectrum severity levels. Five of these specimens were tested to failure. One specimen which did not fail after two lifetimes of crack growth was weld repaired and the test was continued to failure. Crack growth was monitored at regular intervals on all specimens. The weld repair exercise was performed to determine if the crack growth characteristics of weld-repaired material were significantly different from those of the parent alloy. After repairing the cracked area, the hole was reamed to its original diameter and the specimen fatigue testing was continued.

Crack Growth From a Surface Flaw. The surface flaw damage tolerance specimen is shown in Figure 85. A 0.04 x 0.02-inch EDM flaw was introduced and sharpened under constant amplitude fatigue loading to a length of 0.01 inch. Four specimens were tested over a range of spectrum severity levels. Crack growth was monitored at regular intervals on all specimens.

#### 10.5.1.3 Specimen Fabrication

General Layout. The 12 plates were randomly numbered, keeping track of the individual heat lot identification. The blanks for the multihole durability specimens were located according to the scheme shown in Figure 86. The preflawed damage tolerance specimen blanks were machined from the remaining plate material such that approximately an equal number were obtained from each heat lot.

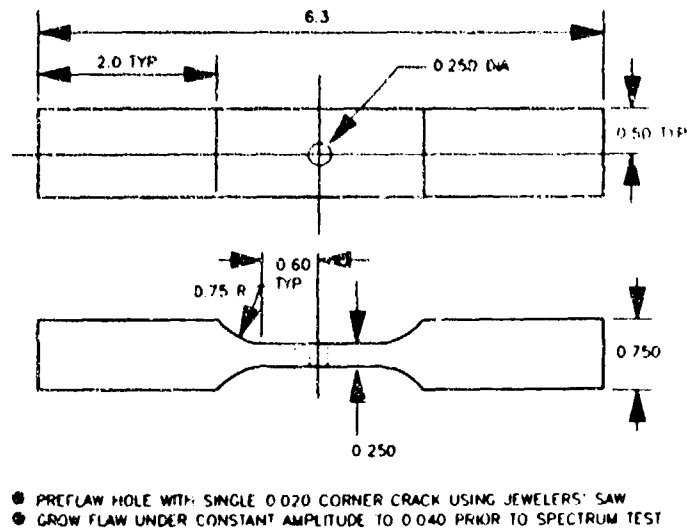


Figure 84. Damage Tolerance Specimen With a Precracked Hole

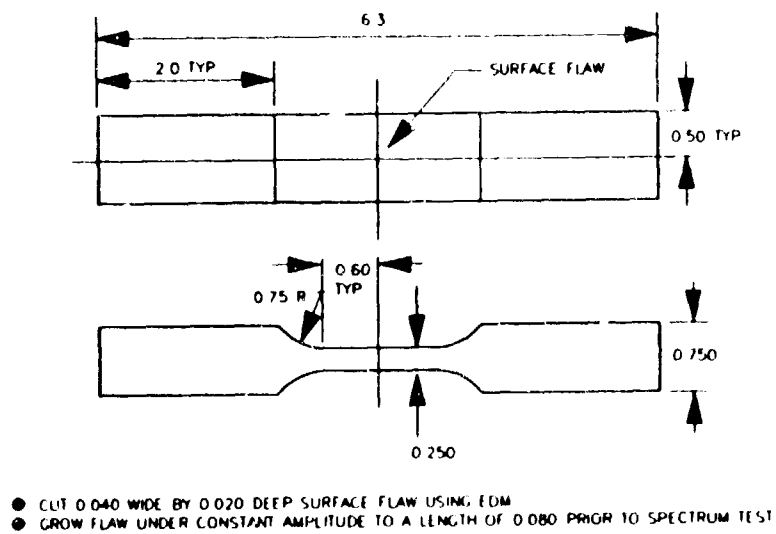


Figure 85. Damage Tolerance Specimen With a Surface Flaw

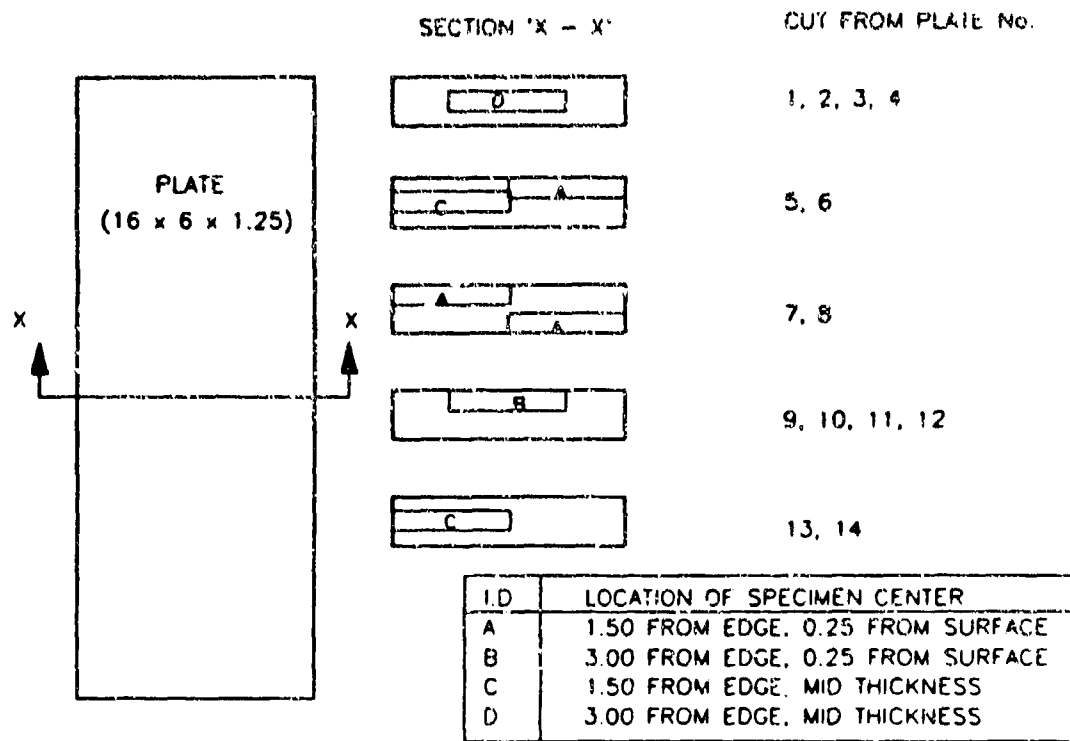


Figure 86. Location of Multihole Durability Specimens in the Cast Plates

Multihole Durability Specimens. The multihole durability specimens were fabricated as defined in Figures 83 and 86. Each specimen was identified using the code QX-Y-Z, where X identified the plate number (i.e., '1' through '12'), Y identified the location (i.e., 'A' through 'D'), and Z identified the specimen number for that location (i.e., '1' through '6' for location 'A', and '1' through '4' for locations 'B' through 'D'). Identification was also made of the specimen surfaces that were in proximity to the plate edge and planar surface so that the location of each crack initiation site could be established relative to its position in the original cast plate.

Precracked Damage Tolerance Specimens. The precracked specimens were fabricated as shown in Figures 84 and 85. Each specimen was identified using the code QX-Y-Z, where X identified the plate number, Y identified the specimen type as precracked hole or surface flaw (i.e., 'H' or 'S'), and Z identified the specimen number for that type (i.e., '1' through '6').

Tensile Specimens. Two tensile specimens were also excised from each plate. These results are discussed in Sections 10.3 and 10.4.

#### 10.5.2 DADT Analysis Method

The analysis method used to correlate the results of the durability and damage tolerance testing employed the Northrop 'LOOPINC' computer program [25]. This method is based on the unified crack initiation and crack growth approach outlined in Reference 15. The data requirements and basic approach are illustrated in Figure 87.

The basic premise of the method hinges on the numerical integration of the reciprocal of the changing analytical crack growth rate throughout the total length of the assumed crack. The local crack growth rate is obtained from:

$$\frac{(da/dn)_2}{(da/dn)_1} = \left( \frac{\beta_2}{\beta_1} \right)^{m_1} \left( \frac{a_2}{a_1} \right)^{\frac{m_1}{2}} \quad \text{Eq. 10-1}$$

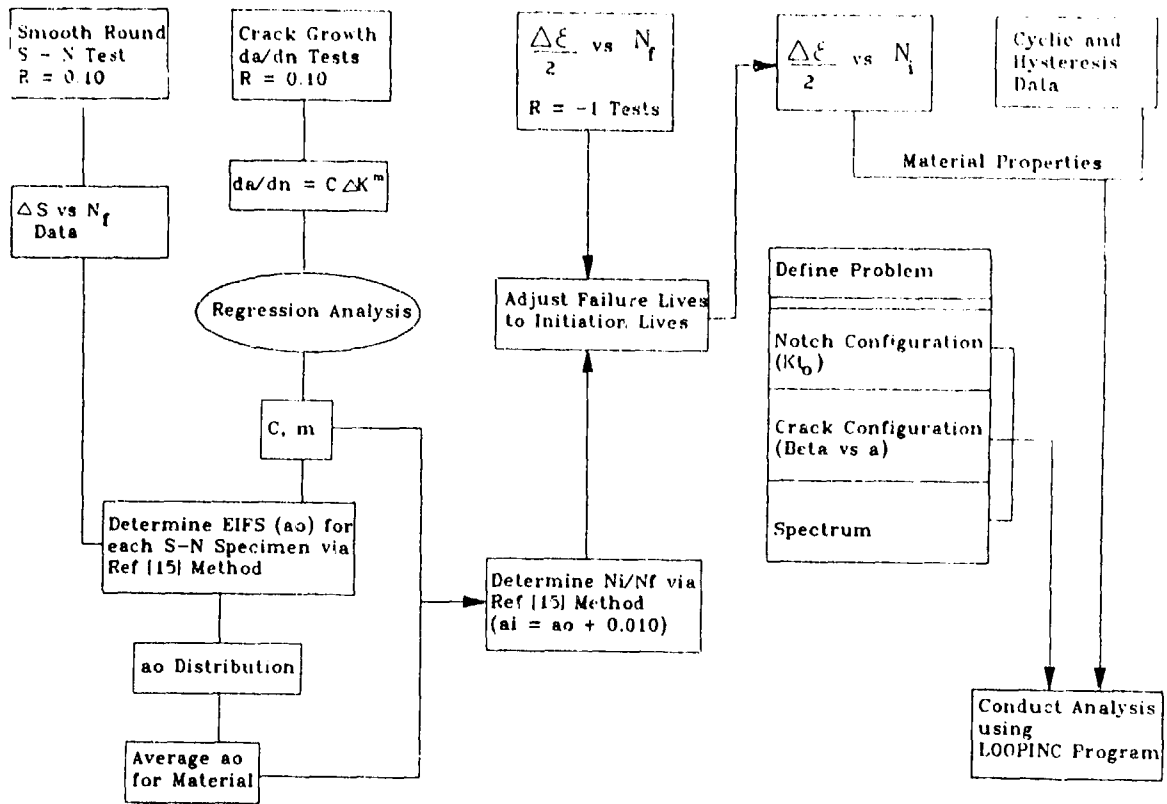


Figure 87. Flow Chart of Unified Crack Growth Analysis Requirements

where:

$(da/dn)_2$  - crack growth rate at crack length  $a_2$

$(da/dn)_1$  - crack growth rate at crack length  $a_1$

$\beta_1$  - stress intensity correction factor at crack length  $a_1$ , including all secondary effects such as crack shape, back surface correction, etc.

$\beta_2$  - stress intensity correction factor at crack length  $a_2$ , including all secondary effects

$m_1$  - exponent from the best fit regression on the analytical spectrum crack initiation life trend

$$N_i = C_N (K_t S_{max})^{-m_1}$$

$N_i$  - time to initiate a crack of length 0.010 inch from a notch subjected to a spectrum normalized by a design condition elastic notch stress of  $(K_t S_{max})$ .

At initiation:

$$a_1 = 0.010/2 = 0.005$$

$$K_{t_{a_1}} = K_{t_o} \left( \frac{\beta_1}{\beta_o} \right)$$

and  $(da/dn)_1 = N_i$  based on a spectrum notch severity of

$$(K_{t_{a_1}} S_{max})$$

Hence, Equation 10-1 becomes:

$$(da/dn)_2 = \left( \frac{\beta_2}{\beta_{0.005}} \right)^{m_1} \left( \frac{a_2}{0.005} \right)^{\frac{m_1}{2}} \left( \frac{0.010}{N_i} \right) \quad \text{Eq. 10-2}$$

and the time to grow the crack from length  $a_p$  to  $a_q$  can be obtained from:

$$N_{pq} = \int_{a_2 = a_p}^{a_2 = a_q} (dn/da)_2 \cdot \Delta a \quad \text{Eq. 10-3}$$

Note that a constant incremental value of  $\Delta a = 0.010$  is used in the analysis.

### 10.5.3 Data Requirements

Determination of the spectrum crack initiation life ( $N_i$ ) for the D357-T6 test specimens was based on the Northrop LOOPINC method [25]. This method utilizes smooth round bar cyclic and hysteresis stress-strain data to track the values at the elastically constrained, plastically deforming material immediately local to the notch. The resulting hysteresis loops are then correlated with the cyclic life observed during strain-controlled tests performed at various constant strain ratios on similar smooth round bar specimens. The total life to failure ( $N_f$ ) provided by these tests is adjusted to give the number of cycles for the generation of a 0.010-inch crack ( $N_i$ ) by the following relationship [15].

$$(N_f/N_i) = 1 + \frac{\left(\frac{a_i}{2}\right)^{m/2}}{0.010} \sum_{\bar{a}=a_i}^{a_c} \left[ \frac{\Delta a}{\left(\frac{\beta_a}{\beta_i}\right) \bar{a}^{m/2}} \right] \quad \text{Eq. 10-4}$$

Where:

$a_i$  = 0.010 (i.e., crack size after an initial growth of 0.010 inch)

$\Delta a$  = Size of the numerical integration interval (assumed to be 0.010)

$\bar{a}$  = Crack size at the mid point of the current interval

$\beta_{\bar{a}}$  = Stress intensity correction factor for a crack of length "a" growing in a round bar

$\beta_i$  = Stress intensity correction factor at the midpoint of the initiation interval, i.e., at a crack length of 0.0050 inch

$m$  = Paris equation slope of the  $(da/dn)$  vs  $\Delta K$  line derived from crack growth data

(A value of  $m = 4.988$  was obtained for D357-T6)

The use of Equation 10-4 provided a value of  $N_f/N_i = 1.095$  for the smooth round bar specimens used to determine the strain life data for D357-T6.

Fully-reversed ( $R = -1.0$ ) strain-life data were obtained for D357-T6 and B201-T7 and are shown in Figure 88. The associated cyclic stress-strain curves are shown in Figure 89. A regression fit of the fully-reversed ( $R = -1.0$ ) D357-T6 strain-life data (Figure 88) gave the following relationship:

$$\frac{\Delta\epsilon}{2} = 0.0162(N_f)^{-0.1552} \quad \text{Eq. 10-5}$$

(based on nine data points;  $r^2 = 0.975$ )

Modifying Equation 10-5 in terms of  $N_i$ :

$$\frac{\Delta\epsilon}{2} = 0.0162 (1.095N_f)^{-0.1552} = 0.016(N_i)^{-0.1552} \quad \text{Eq. 10-6}$$

The data trend represented by Equation 10-6 was used for the fully reversed strain life data utilized by the Northrop LOOPINC crack growth program in the analysis of the D357-T6 spectrum test life prediction.

#### 10.5.4 Analysis

##### 10.5.4.1 Specimen Notch Stress Concentration

The basic stress concentration factor was determined for each of the three specimen configurations as shown below:

Multihole Durability Specimen. For a row of holes located in a specimen of constant width, the stress concentration at the end holes is higher than that at intermediate holes. Therefore, the width of the multihole specimen was increased near the end holes so that the elastic notch stress was the same for all holes. The holes in each row had a diameter of 0.25 inch and were spaced 1.00 inch apart. Except for the end holes, each had an edge distance of 0.50 inch, measured from the center of the hole, providing a stress concentration factor of  $K_t = 2.84$  based on the gross section stress [14]

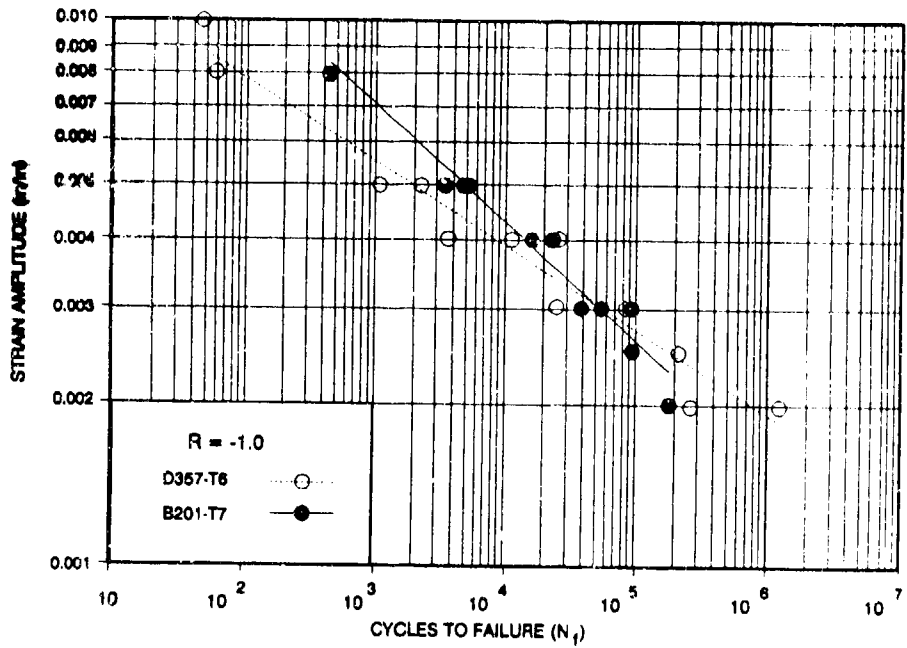


Figure 88. Strain-Life Data for D357-T6 and B201-T7

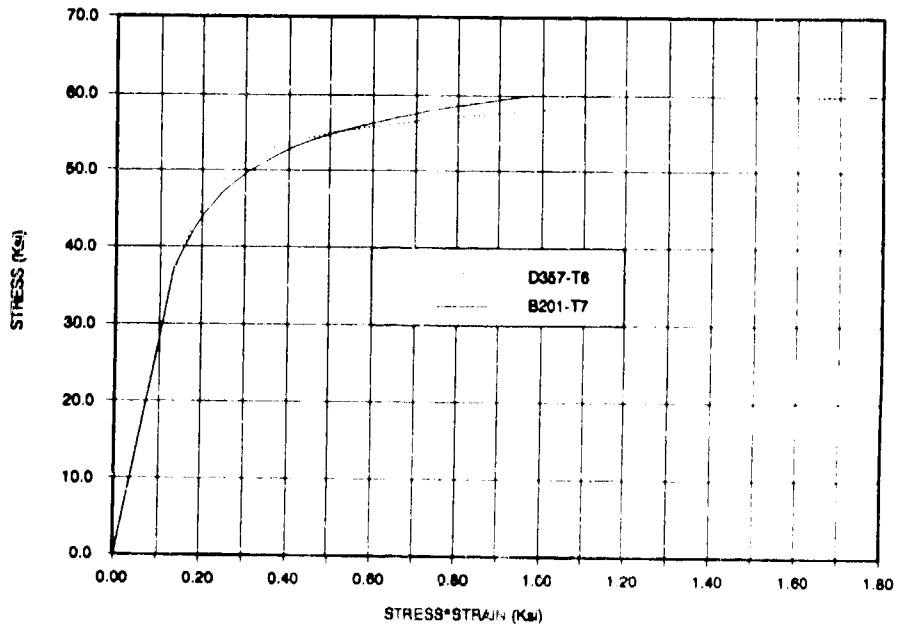


Figure 89. Cyclic Stress-Strain Curves for D357-T6 and B201-T7

Except where the end holes are located, the width of the specimen was 2.55 inches. The end holes are located in line with the other holes, but the width of the specimen at that point is 2.75 inches, providing an edge distance of 0.60 inch. The nominal stress concentration factor for the end holes is 3.03 [14]. Hence,  $(K_t S)_{\text{end}} / (K_t S)_{\text{int}} = (3.03/2.75) / (2.84/2.55) = 0.99$ , i.e., the stress concentrations at end and intermediate holes are equivalent. DADT analysis was conducted using the geometry of the intermediate holes.

Single Hole Crack Growth Specimen. A single 0.25-inch-diameter hole centrally located in a width of 1.00 inch has a gross section stress concentration factor of  $K_t = 3.24$  [14].

Surface Crack Specimen. Prior to crack initiation, the surface flaw specimen is assumed to have a stress concentration factor of unity.

#### 10.5.4.2 Net Section Yield

Although the analytical method is not valid above net section yield, the specimens were tested above this value to determine if the failure mode was significantly different. The average tensile yield strength for the D357-T6 plates used for the DADT analysis was 42 ksi (Table 75), which is close to the minimum value of 40 ksi given in MIL-HDBK-5 for a Class 2 designated area. The MIL-HDBK-5 value was used to determine the gross stress level at which each of the specimen configurations would experience net section yielding, as follows:

##### Multihole Specimen

$$\text{Gross area} = 2.55 \times 0.25 = 0.6375 \text{ sq. in.}$$

$$\text{Net area} = (2.55 - 0.50) \times 0.25 = 0.5125 \text{ sq. in.}$$

$$\text{At net yield: Gross stress} = 40 \times 0.5125 / 0.6375 = \underline{32.16 \text{ ksi}}$$

##### Single Hole Specimen

$$\text{Gross area} = 1.00 \times 0.25 = 0.25 \text{ sq. in.}$$

$$\text{Net area} = (1.00 - 0.25) \times 0.25 = 0.1875 \text{ sq. in.}$$

$$\text{At net yield: Gross stress} = 40 \times 0.1875 / 0.25 = \underline{30.0 \text{ ksi}}$$

### Surface Crack Specimen

Gross area =  $1.00 \times 0.25 = 0.25$  sq. in.

At net yield: Gross stress = 40 ksi

#### 10.5.4.3 Stress Intensity Correction Factors

The stress intensity correction factors used in the analysis are shown in Table 78. These values were determined for a single crack from the standard solutions for the geometries tested and include all secondary effects, such as back surface, edge proximity and crack shape. A uniform (radial arc) crack shape was assumed until the crack exceeded the thickness, at which time a through-crack geometry was assumed.

#### 10.5.4.4 Determination of Spectrum Crack Growth Exponent ' $m_1$ '

The strain-life data obtained for D357-T6 were established over a life range from 10 to 1,000,000 cycles. The maximum strains associated with these lives ranged from 0.0112 to 0.0020 inch/inch. The spectrum crack initiation life trend was determined over a range of elastic notch stresses equivalent to the above strains. Assuming a Young's modulus of 10.4 Msi gives a maximum spectrum elastic notch stress range of 116,480 - 20,800 psi. The spectrum crack growth exponent ( $m_1$ ) for the DADT analysis of D357-T6 was based on the analytical crack initiation life trend obtained over this range of elastic notch stress. The analytical crack initiation life trend versus the maximum spectrum elastic notch stress for D357-T6 is shown in Figure 90a, from which a value of  $m_1 = 4.706$  was obtained. A similar analysis was conducted for 7050-T7451 plate; the derivation of  $m_1$  under the spectrum loading used for D357-T6 is shown in Figure 90b. A value of  $m_1 = 3.535$  was obtained.

#### 10.5.5 Test Results

The results of the DADT tests are summarized in Figure 91. Crack growth trends are also presented in Figures 92 through 96 for the precracked surface flaw, and for precracked hole specimens tested at stress levels below the net section yield.

TABLE 78. STRESS INTENSITY CORRECTION FACTOR FOR EACH DADT SPECIMEN GEOMETRY

| CRACK LENGTH (in) | MULTI-HOLE SPECIMEN | SINGLE HOLE SPECIMEN | SURFACE CRACK SPECIMEN |
|-------------------|---------------------|----------------------|------------------------|
| 0.0000            | 2.304               | 2.328                | 0.686                  |
| 0.0050            |                     | 2.130                |                        |
| 0.0065            | 2.054               |                      |                        |
| 0.0100            |                     |                      | 0.686                  |
| 0.0150            | 1.814               | 1.842                |                        |
| 0.0250            | 1.613               | 1.643                | 0.689                  |
| 0.0350            | 1.468               | 1.498                |                        |
| 0.0450            | 1.357               | 1.388                |                        |
| 0.0500            |                     |                      | 0.693                  |
| 0.0550            | 1.270               | 1.302                |                        |
| 0.0650            | 1.202               | 1.233                |                        |
| 0.0750            | 1.146               | 1.178                |                        |
| 0.0850            | 1.102               | 1.135                |                        |
| 0.0950            | 1.065               | 1.100                |                        |
| 0.1000            |                     |                      | 0.712                  |
| 0.1050            | 1.035               | 1.072                |                        |
| 0.1150            | 1.011               | 1.049                |                        |
| 0.1250            | 0.991               | 1.030                |                        |
| 0.1350            | 0.977               | 1.019                |                        |
| 0.1450            | 0.967               | 1.011                |                        |
| 0.1500            |                     |                      | 0.755                  |
| 0.1550            | 0.960               | 1.006                |                        |
| 0.1650            | 0.955               | 1.005                |                        |
| 0.1750            | 0.953               | 1.007                |                        |
| 0.1850            | 0.959               | 1.020                |                        |
| 0.1950            | 0.970               | 1.039                |                        |
| 0.2000            |                     |                      | 0.847                  |
| 0.2050            | 0.988               | 1.063                |                        |
| 0.2150            | 1.017               | 1.095                |                        |
| 0.2250            | 1.055               | 1.138                |                        |
| 0.2350            | 1.110               | 1.212                |                        |
| 0.2450            | 1.182               | 1.305                |                        |
| 0.2500            |                     |                      | 1.184                  |
| 0.2550            | 1.349               | 1.499                |                        |
| 0.2650            | 1.369               | 1.526                |                        |
| 0.2750            | 1.390               | 1.553                |                        |
| 0.2850            | 1.424               | 1.654                |                        |
| 0.2950            | 1.458               | 1.754                |                        |
| 0.3000            |                     |                      | 1.302                  |
| 0.3050            | 1.507               | 1.853                |                        |
| 0.3150            | 1.570               | 1.951                |                        |
| 0.3250            | 1.633               | 2.047                |                        |
| 0.3350            | 1.784               | 20.964               |                        |
| 0.3450            | 1.971               | 39.587               |                        |
| 0.3500            |                     |                      | 1.490                  |
| 0.3550            | 20.643              | 57.937               |                        |
| 0.3650            | 57.517              | 76.350               |                        |
| 0.3750            | 93.891              | 93.899               |                        |
| 0.4000            |                     |                      | 1.820                  |
| 0.4500            |                     |                      | 2.586                  |
| 0.4750            |                     |                      | 3.673                  |
| 0.5000            |                     |                      | 100.000                |

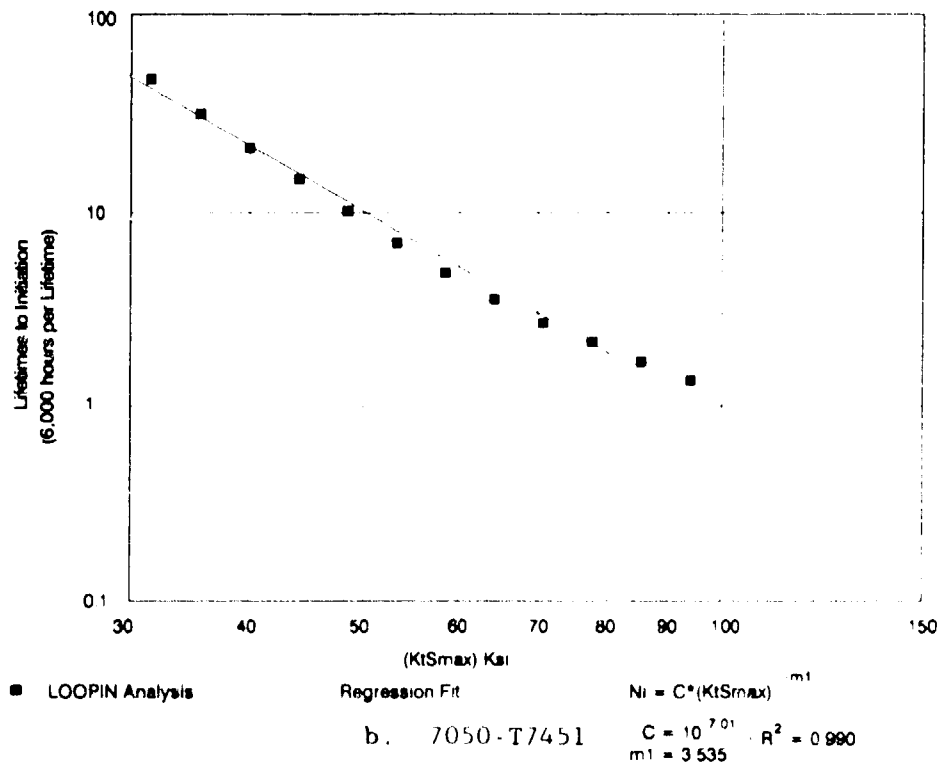
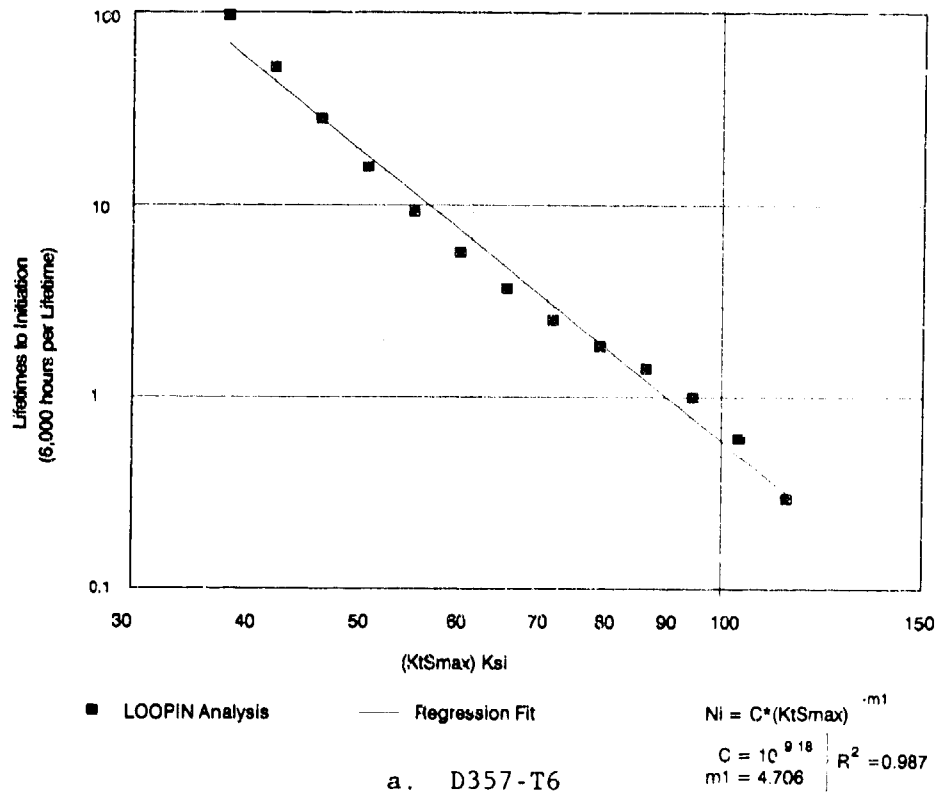
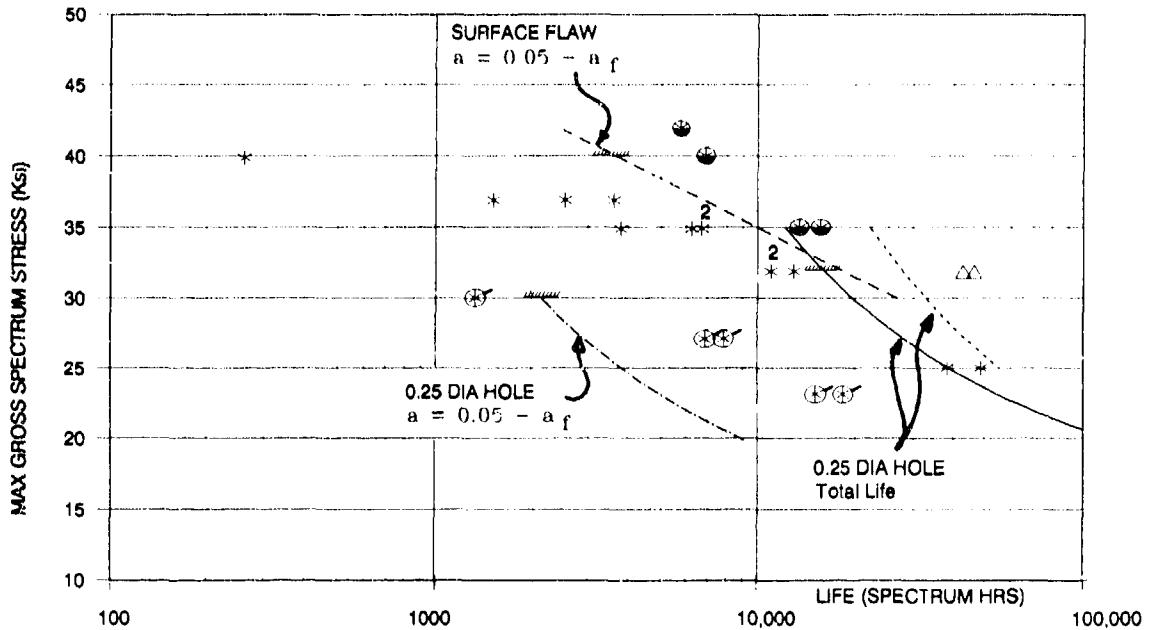


Figure 90. Determination of  $m_1$  Under Spectrum Loading for D357-T6 and 7050-T7451 Plate



|          |   | Test | Analysis (m1 = 4.706) |
|----------|---|------|-----------------------|
| D357-TG  | Hole with No Precrack (Total Life)        | *    | —————                 |
|          | Life from 0.050 Inch Surface Crack        | ●    | - - - - -             |
|          | Life for Hole with 0.05 Inch Corner Crack | ⊗    | - · - · -             |
| 7050-T74 | Hole with No Precrack (Total Life)        | △    | Analysis (m1 = 3.535) |

Note: Indicates Gross Stress at which the Specimen encounters Net Section Yield

Figure 91. Correlation Between Test and Analysis for D357-T6 Under Spectrum Loading

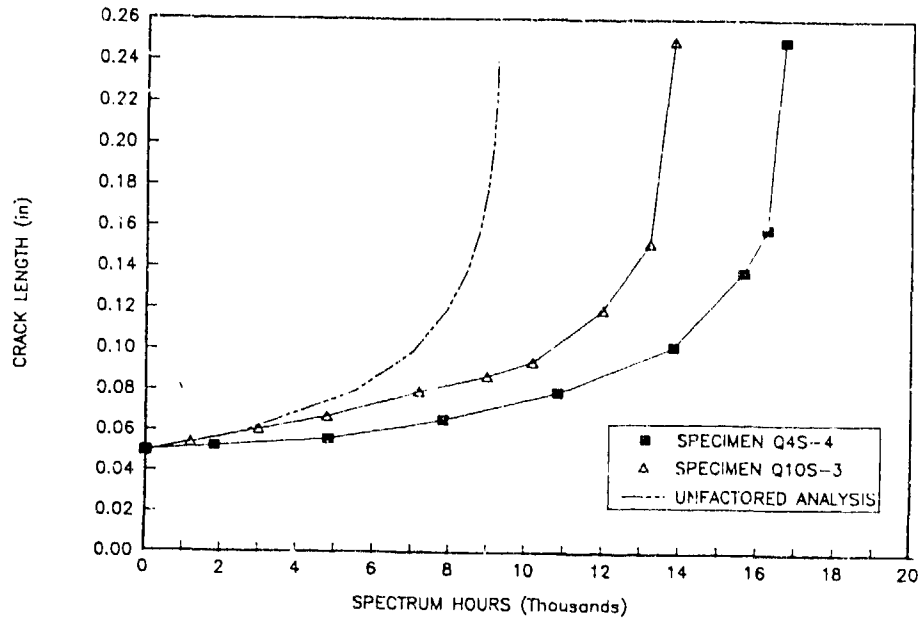


Figure 92. Spectrum Growth Correlation for Surface Flawed Specimens Tested at 35 ksi Maximum Stress ( $\beta_1 = 0.686$ )

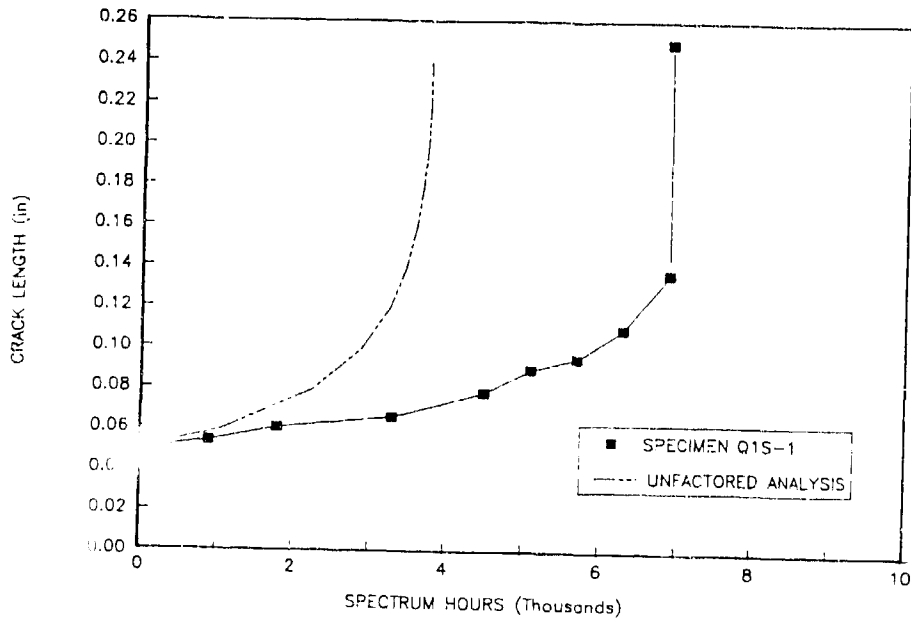


Figure 93. Spectrum Growth Correlation for Surface Flawed Specimens Tested at 40 ksi Maximum Stress ( $\beta_1 = 0.686$ )

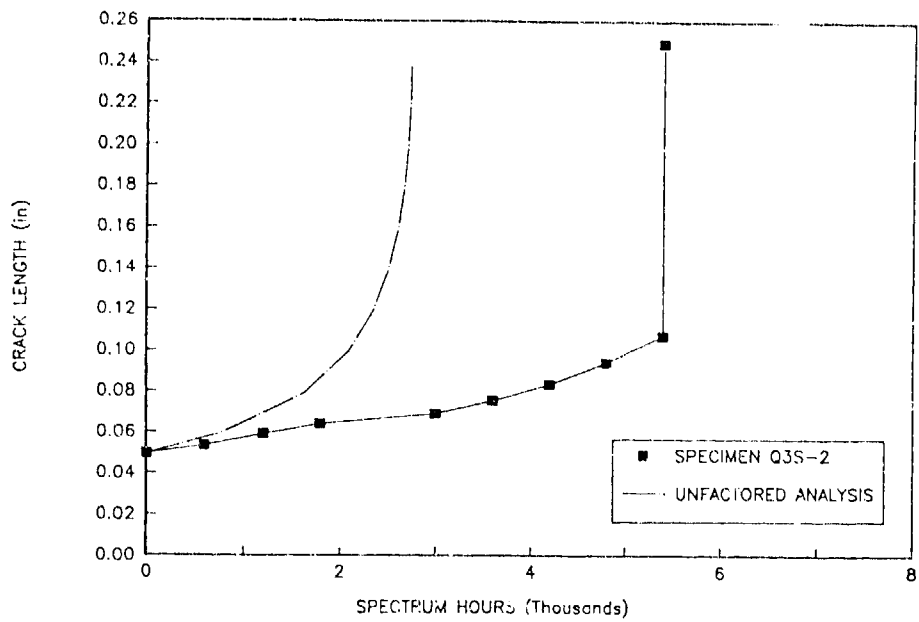


Figure 94. Spectrum Growth Correlation for Surface Flawed Specimens Tested at 42 ksi Maximum Stress ( $\beta_i = 0.686$ )

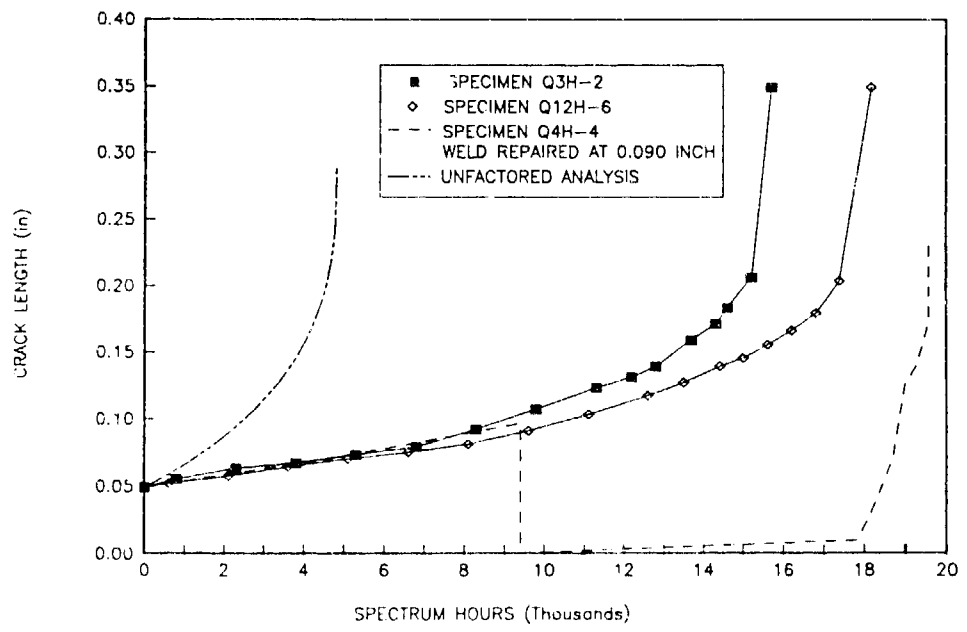


Figure 95. Spectrum Growth Correlation for Precracked Hole Specimens Tested at 23 ksi Gross Maximum Stress

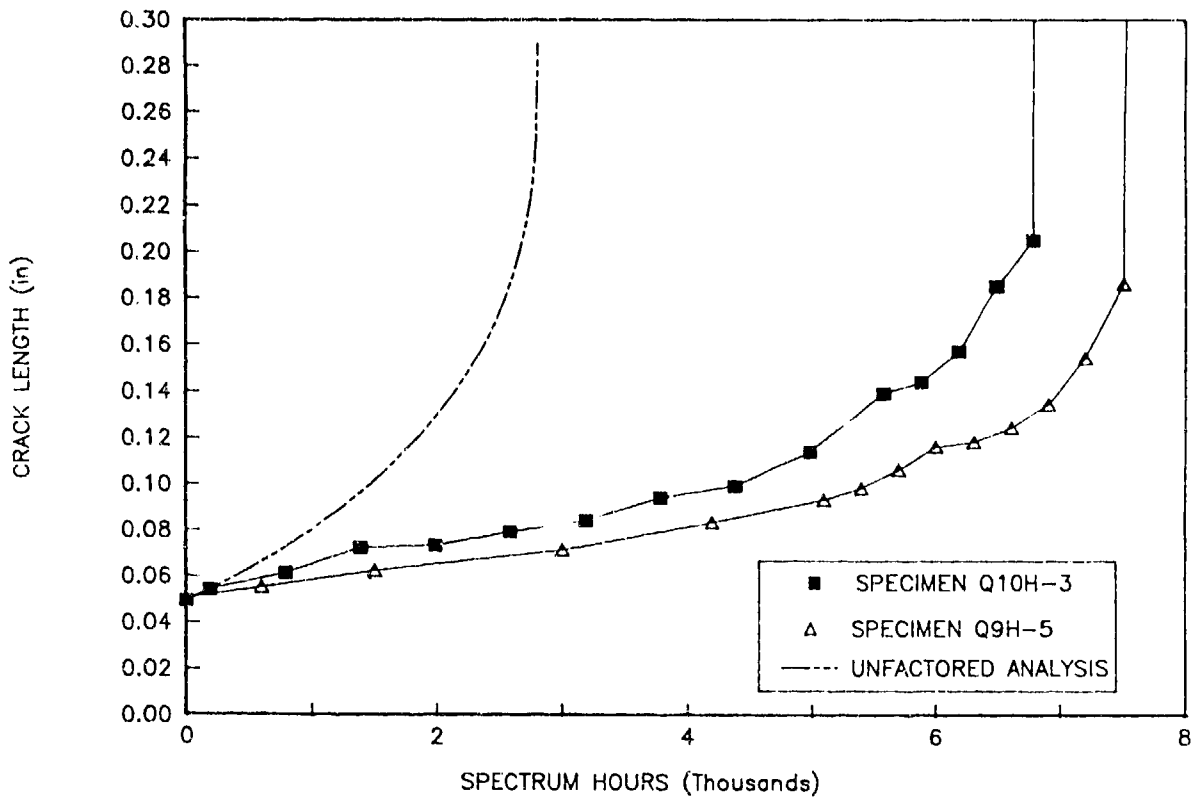


Figure 96. Spectrum Growth Correlation for Precracked Hole Specimens Tested at 27 ksi Gross Maximum Stress

The following observations were made:

- Crack growth of the precracked specimens was well-behaved; no significant interruptions or accelerations were noted
- Tests repeated at maximum spectrum stresses below the net section yield of the specimen gave similar results
- As expected, the life trends were significantly reduced for those specimens that were tested above the net section yield.

#### 10.5.6 Analytical Correlation

Figures 91 through 97 include the life trends predicted by the unified crack growth method. The following observations were made with respect to this correlation:

- Figures 91 and 97 show that the total life prediction for the multihole specimens was accurate when the maximum net section spectrum stress was below the yield strength. Although the method projected unconservative results at stress levels above the net section yield, these higher levels can be assumed to be outside normal durability analysis requirements.
- The analytical prediction for the total life for 7050-T7451 tested at a maximum stress of 32 ksi is also reasonably accurate (67 percent of demonstrated lives).
- Figure 97 also shows that specimens excised from the corner of the casting (location A, Figure 86) gave lower lives than those from the other locations.

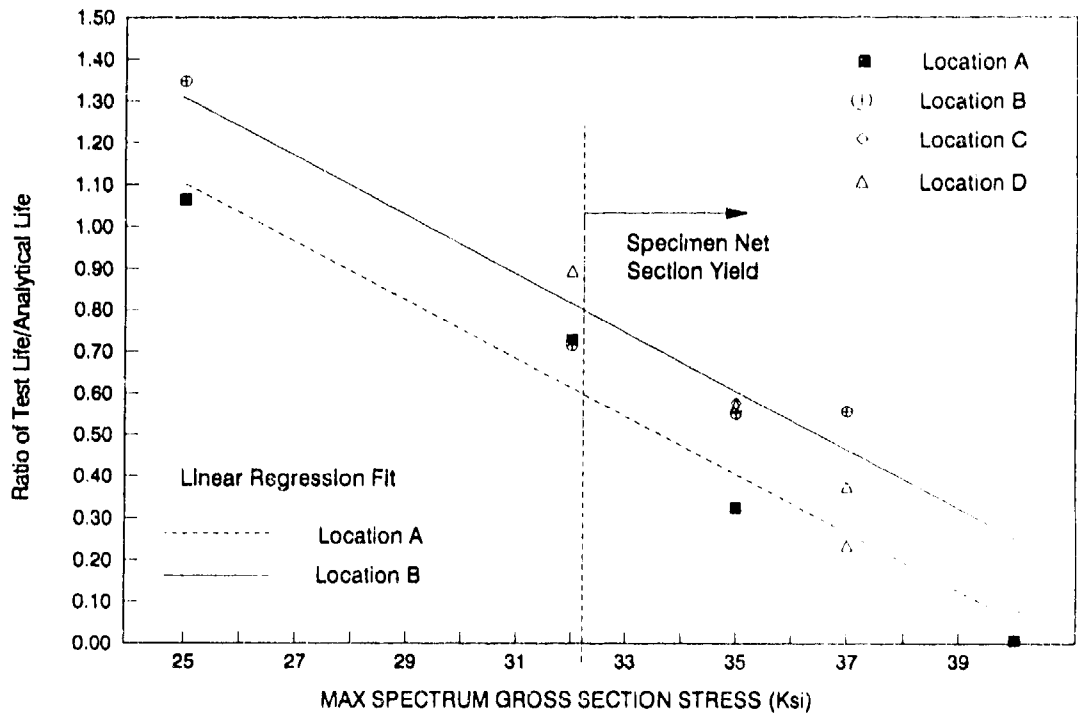


Figure 97. Correlation Between Analysis and Test Results for Multihole Specimens (Total Life)

- Although the shapes of the analytically predicted and observed curves are consistent, the unified method predicted shorter crack growth lives from an initial 0.05-inch precrack than those obtained by test. However, small changes in the assumed stress intensity correction factor solution can have a significant effect on the local crack growth rate, particularly for larger crack lengths. For example, a constant reduction in the stress intensity correction factors for crack lengths above 0.050 inch to 80 to 85 percent of the values used would be sufficient to match the analysis with the observed results.

#### 10.5.7 Fractographic Analysis

Each of the 12 multihole durability specimens was fractographically examined to identify the crack initiation sites. On average, four cracks per specimen were examined. The cracks which were chosen were those that had propagated the farthest or were located at the fracture surface. SEM analysis was used to identify the initiation site.

Table 79 provides data for the cracks that first appeared at the fracture surfaces of each specimen prior to failure. Further data on additional cracks observed in the specimens are included in Appendix I. The location and propagation direction of the cracks are identified by the hole number, the face on which the crack appeared, and the crack growth direction. Figure 98 illustrates the hole numbering scheme. The time at which the cracks were first observed and recorded and the crack length at initiation are also indicated in Table 79. Where possible, initiation sites are identified.

Because of obscure fractographic features, initiation sites for many of the cracks could not be identified. As shown in Table 79 and Appendix I, the initiation sites for approximately half of the cracks analyzed could not be determined. Inspection of the areas along the hole surfaces adjacent to these cracks suggest that they originated at a single silicon particle or a cluster of particles. As demonstrated by the data in Table 79, eutectic silicon particles are common initiation sites in D357. An example of a single silicon

TABLE 79. DATA FOR CRACKS OBSERVED AT FRACTURE SURFACES OF MULTIHOLE DURABILITY SPECIMENS

| SPECIMEN | GROSS STRESS (ksi) | HOLE NUMBER <sup>(1)</sup> | TIME AT CRACK INITIATION (FLIGHT HOURS) | CRACK LENGTH AT INITIATION (INCH) | TOTAL LIFE (FLIGHT HOURS) | INITIATION SITE |
|----------|--------------------|----------------------------|---|-----------------------------------|---------------------------|-----------------|
| Q8A6     | 25                 | 2-F-O                      | 31,200                                  | 0.020                             | 38,428                    | NI              |
| Q10B2    | 25                 | 11-F-O                     | 44,400                                  | 0.040                             | 48,928                    | NI              |
| Q3D3     | 32                 | 9-F-O                      | 11,400                                  | 0.022                             | 13,528                    | NI              |
| Q12B4    | 32                 | 10-R-I                     | 8,400                                   | 0.026                             | 10,828                    | NI              |
| Q7A3     | 32                 | 2-F-I                      | 9,000                                   | 0.010                             | 11,053                    | Si Particles    |
| Q4D4     | 35                 | 12-F-I                     | 6,600                                   | 0.020                             | 6,628                     | NI              |
| Q5C1     | 35                 | 2-F-O                      | 4,800                                   | 0.008                             | 6,755                     | Si Particles    |
| Q6A2     | 35                 | 13-R-O                     | 3,600                                   | 0.018                             | 3,755                     | Cavity          |
| Q11B3    | 35                 | 2-R-O                      | 6,300                                   | 0.028                             | 6,455                     | Si Particles    |
| Q1D1     | 37                 | 12-F-I                     | 900                                     | 0.010                             | 1,528                     | NI              |
| Q2D2     | 37                 | 5-R-O                      | 2,400                                   | 0.006                             | 2,419                     | NI              |
| Q9B1     | 37                 | 13-R-O                     | 3,600                                   | 0.022                             | 3,628                     | Si Particles    |
| Q5A1     | 40                 | (2)                        | (3)                                     | (3)                               | 28                        | NI              |
| Q6C2     | 40                 | (2)                        | (3)                                     | (3)                               | 253                       | NI              |

(1) F - Front; R - Rear; I - Inboard; O - Outboard

(2) No fatigue cracks were observed in the specimen

(3) Due to high stress, specimen failed quickly and data were not obtained

NI - Not identified

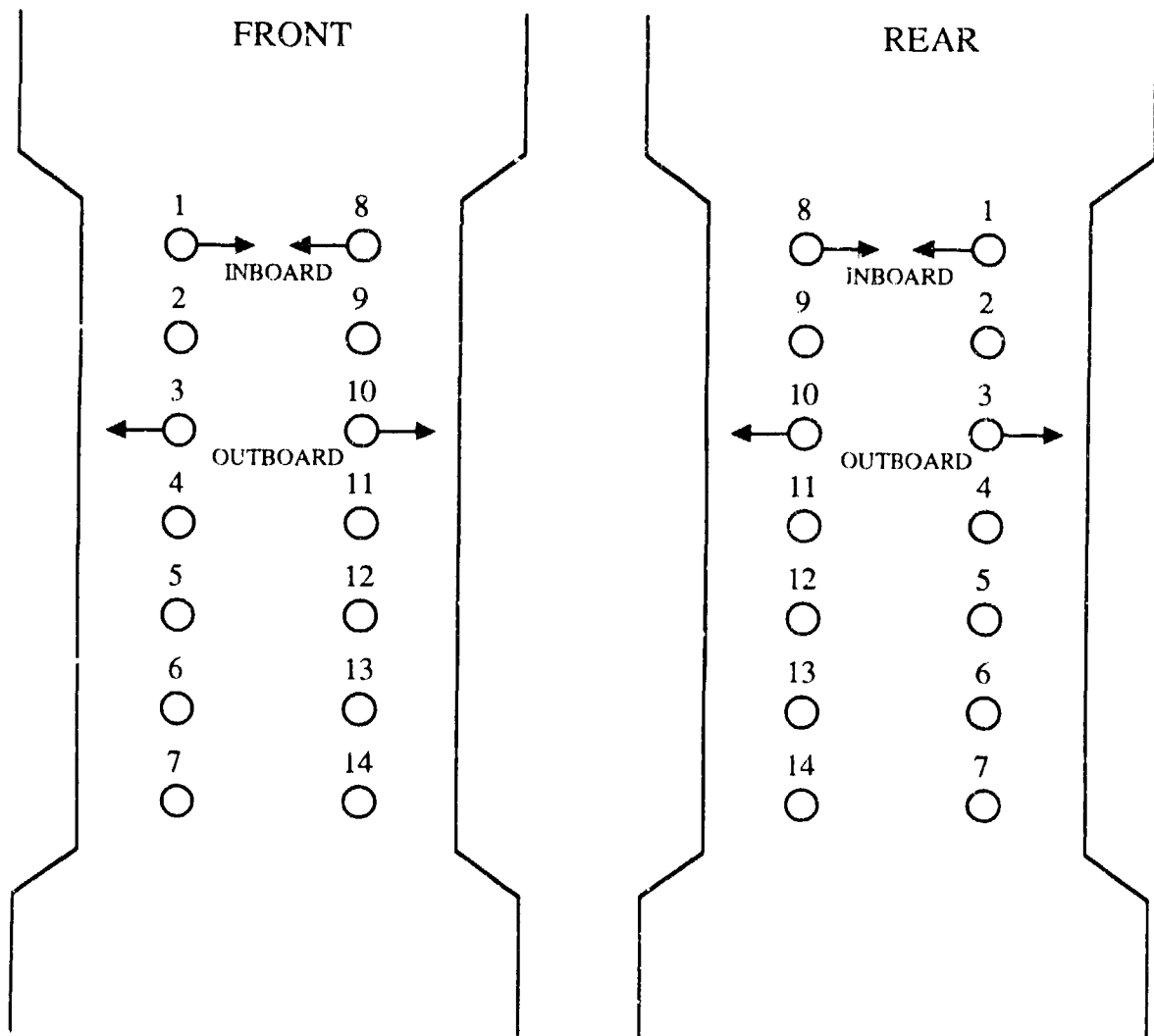


Figure 98. Hole Number Assignment for Multihole Durability Specimens

particle acting as an initiation site is given in the micrograph in Figure 99 (for crack 2-R-0 in specimen Q7A3). A crack initiating at a cluster of silicon particles in specimen Q5C1 is shown in Figure 100 (crack 2-F-0). The size of the particle in Figure 99 (determined using the semicircular area method described in Section 7.3.6) is approximately 0.004 inch.

Two of the specimens listed in Table 79, Q6A2 and Q1D1, exhibited significantly shorter crack initiation and fatigue lives than other specimens tested at similar stress levels. Fractographic analysis of Q1D1 (crack 12-F-I) failed to reveal the presence of a defect responsible for crack initiation. Analysis of Q6A2, however, revealed the presence of a large cavity (0.0015 inch) adjacent to the hole surface from which a fatigue crack initiated. An SEM micrograph of this site is shown in Figure 101. The origin of the cavity is not clear; one possibility is that it formed during fatigue from a coalescence of microvoids surrounding eutectic silicon particles. The low fatigue life of Q6A2 is presumably due to early crack initiation at this site.

Other defects revealed by SEM analysis include shrinkage pores and microcracks. However, these defects were observed in only a few specimens. A micrograph of a shrinkage pore found in specimen Q5C1 (crack 6-F-0) is shown in Figure 102. The pore was located away from the hole surface and is not believed to have initiated a fatigue crack. Figure 103 shows a microcrack extending from a hole surface in specimen Q3D3 (crack 2-F-0). The reason for the presence of the crack is unknown. However, given the specimen's relatively long fatigue life, it does not appear to have accelerated failure.

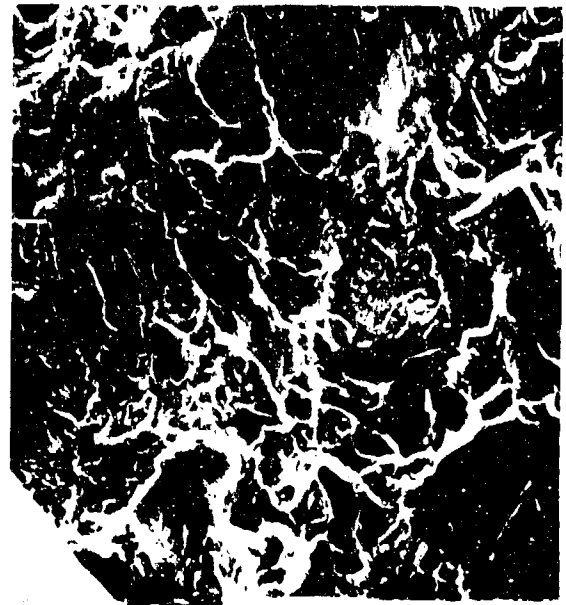
## 10.6 CONCLUSIONS

- The DAS and the silicon particle morphology of the Phase II cast plates and pylons were similar to those of the verification material



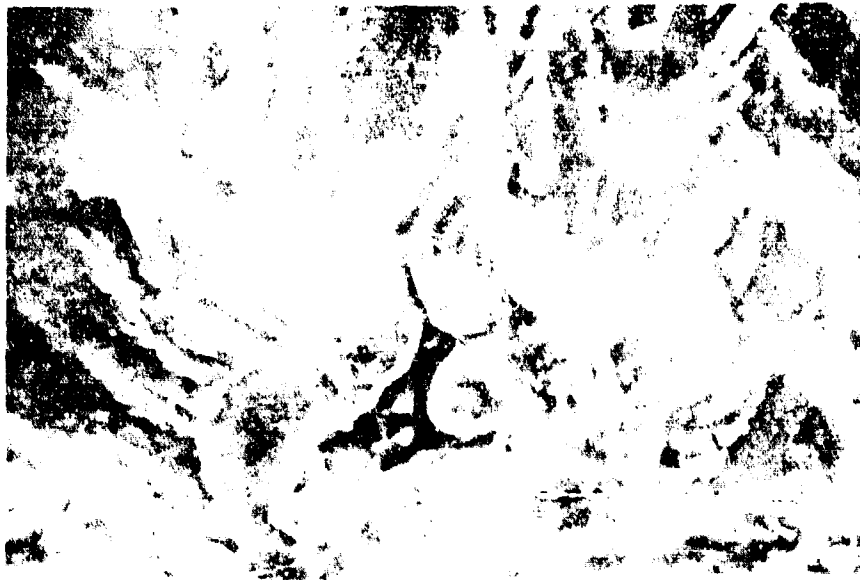
X1.00K 9.95UM 7146

Figure 99. Single Silicon Particle-Initiating a Fatigue Crack



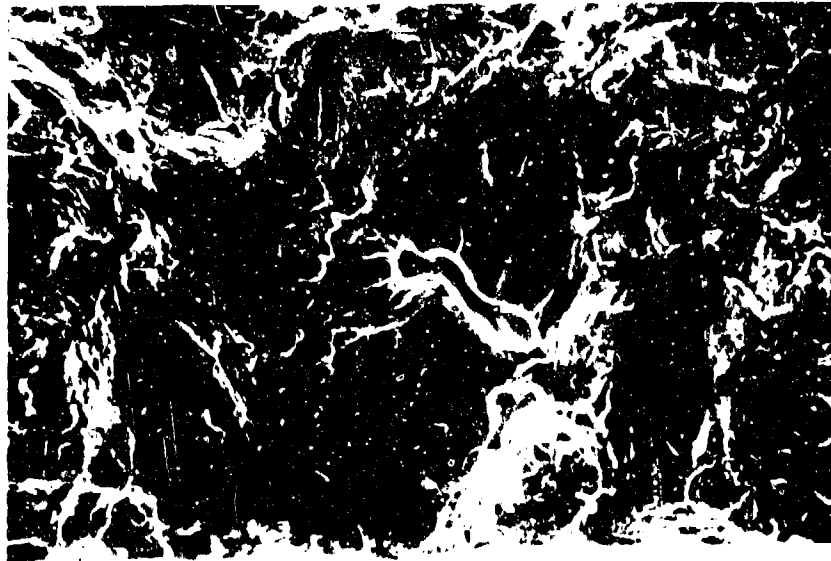
X251 39.7UM 7168

Figure 100. Cluster of Silicon Particles Initiating a Fatigue Crack



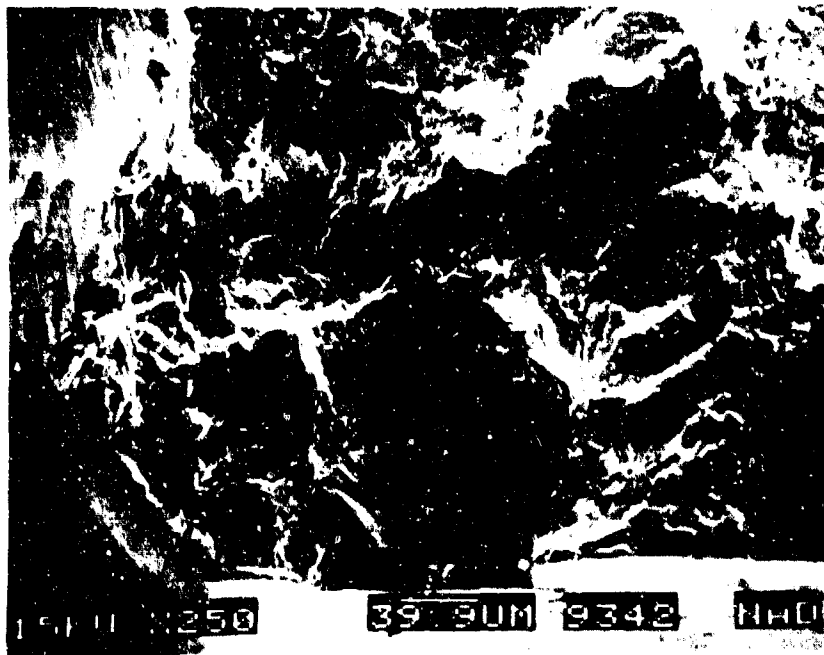
15KV X1.00K 9.90UM 9457 NAD

Figure 101. Cavity Observed in Specimen Q6A?



15KV X250 40.0UM 3179 NAO

Figure 102. Shrinkage Pore Observed in Specimen Q5C1



15KV X250 39.9UM 9342 NAO

Figure 103. Microcrack in Specimen Q3D3

- The average tensile properties of the Phase II castings were slightly different from the verification castings; the yield strength was lower and the ductility was higher. It was concluded that the differences were due to nonoptimized aging conditions, i.e., the Phase II castings were slightly underaged compared with the verification material
- The ductility of the pylons modified using Sr was higher than the ductility of those modified with Na
- The smooth fatigue lives for pylon material were indistinguishable from those of the Phase I verification cast plates
- The fracture toughness of the pylons modified with Sr was higher than the toughness of those modified using Na (27.7 ksi/in versus 25.5 ksi/in). The overall average fracture toughness was 26.7 ksi/in, which is higher than the average value for the verification material (24 ksi/in). This trend is consistent with the lower yield strength observed for the pylons
- The overall pylon properties were similar to those of the verification plates, indicating that the Phase I material and process requirements can be scaled-up for producing large, complex aircraft castings
- Analysis of the durability and damage tolerance test results indicated that the D357-T6 data are consistent with spectrum severities that the material would normally encounter during use.

SECTION 11  
PHASE III - DATA CONSOLIDATION

In Phase III, the Phase I and II results were analyzed to determine if they support the overall program objective of advancing foundry technology and expediting the use of premium quality aluminum castings for durability and damage tolerance applications in aircraft structure. Specifically, emphasis was on recommending material and/or process specifications based on the program results, and on determining if the existing durability and damage tolerance specifications, MIL-A-87221 and MIL-A-83444, are applicable to premium quality aluminum castings.

The specification issues are discussed in the following subsections.

11.1 MATERIAL SPECIFICATIONS

Based on the program results, changes to AMS 4241 (D357) and AMS 4242 (B201) specifications are recommended. The recommendations are discussed in Subsections 11.1.1 and 11.1.2, respectively. Permission was granted by the Society of Automotive Engineers, which publishes the AMS specifications, to reprint copies of AMS 4241 and 4242 (they are protected by copyright law) in this report. The reprints are included in Appendices J (AMS 4241) and K (AMS 4242).

11.1.1 D357-T6

One of the main thrusts of the program was to evaluate the DADT properties of D357-T6 and recommend requirements that can be included in a new AMS specification for durability and damage tolerance applications. Based on the data base developed during the program, in addition to the AMS 4241 tensile properties, requirements for smooth ( $K_t = 1.0$ ) stress-life fatigue, fracture toughness, and DAS are recommended. The inclusion of four additional requirements that might assist foundries in achieving the above minimum properties were also considered. The four requirements were to (1) include a

silicon modifier, (2) limit the silicon particle aspect ratio, (3) limit the hydrogen content, which correlates with gas porosity and fatigue life, and (4) HIP castings to reduce shrinkage porosity.

The introduction of a new specification, based on AMS 4241, for durability and damage tolerance aluminum castings was recommended. The recommended changes to AMS 4241 are outlined in Subsection 11.1.1.1. Supporting data are discussed in Subsection 11.1.1.2. The data that support requirements (1) through (4) above, though not included in the proposed specification, are discussed in Subsection 11.1.1.3.

#### 11.1.1.1 Recommended Changes to AMS 4241

The following changes to the indicated sections of AMS 4241 are recommended to be included in the new D&ET specification. Only the main changes are shown below; full details are included in Appendix J. The modified specification was submitted to the Society of Automotive Engineers for review.

### 3. TECHNICAL REQUIREMENTS

3.6 Properties: Castings and integrally-attached chilled coupons shall conform to the following requirements:

3.6.2 Fatigue Properties: Shall be as follows, determined in accordance with ASTM E 466.

3.6.2.1 Integrally-Attached Coupons: Three specimens shall be tested under constant amplitude fatigue loading at a frequency between 10 and 20 Hz. The maximum stress shall be 40 ksi (276 MPa) at a stress ratio of 0.1, and a stress concentration factor of 1.0.

The log average life of the three specimens shall be 85,000 cycles, with a minimum individual life of 46,000 cycles.

3.6.2.2 Specimens Cut From Castings: If the casting is sufficiently large to permit the provision of the specimens in 3.4.2.2.1, the average and minimum fatigue life requirements in 3.6.2.1 shall apply. If it is not possible to excise 0.5 inch (12.7 mm) diameter specimens from the casting, smaller specimens are permitted. These shall have a 0.250 inch (6.4 mm) or 0.375 inch (9.5 mm) diameter gauge section. The gauge section shall be between 1.5 inches (38.1 mm) and 2.0 inches (50.8 mm) long. All fatigue specimens shall be excised from designated areas of the casting.

The log average life for the 0.250 inch (6.4 mm) and 0.375 inch (9.5 mm) specimens shall be 68,000 and 78,000 cycles, respectively. The minimum fatigue life for each individual specimen shall be 36,000 and 42,000 cycles for the 0.250 inch (6.4 mm) and 0.375 inch (9.5 mm) diameter gauge sections, respectively.

3.6.3 Fracture Toughness Properties: Shall be not less than 21 ksi/in. determined in accordance with ASTM E 1304.

3.6.5 Microstructure: The microstructure of the casting surface in the designated areas of the casting shall have a dendrite arm spacing that does not exceed 0.0020 inch (0.05 mm), determined in accordance with ARP 1947. Castings which exhibit an unacceptable microstructure, but which meet the requirements of 3.6.1, 3.6.2, and 3.6.3, shall be held for disposition by purchaser's cognizant engineering personnel.

#### 11.1.1.2 Supporting Data for the Recommended DADT Specification Requirements

##### Dendrite Arm Spacing

That DAS influences the mechanical properties of D357 is generally recognized by the castings community. DAS is reduced by increasing the solidification rate (Figure 16); the effect of solidification rate on ductility is shown by the results in Table 24. The elongation of D357-T6 solidified at a faster rate is higher than that for material solidified more slowly (6.2 percent versus 4.0 percent) over a range of different

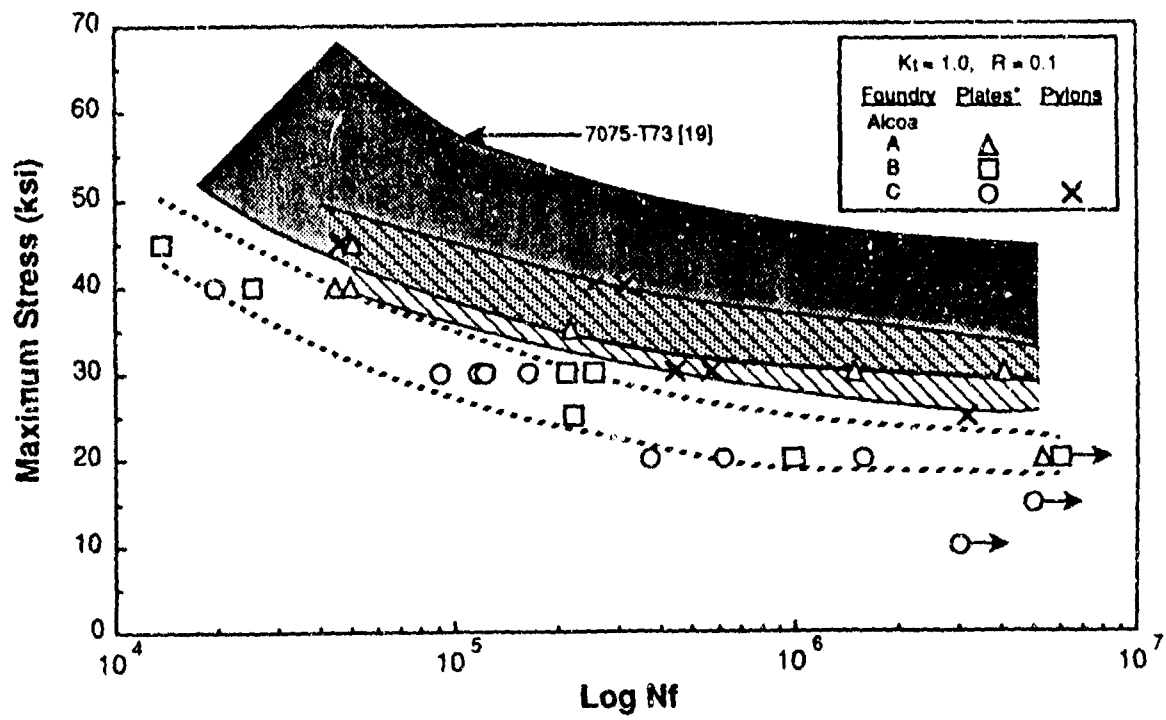
compositions. Similar trends were observed for notched tensile strength and the NTS/YS ratio (Table 2f), which is a toughness indicator. Hence, it is essential that the DAS, which reflects the solidification rate, is maintained below a maximum value. During the verification testing, DAS values were obtained for 21 cast plates (Appendix Table C8), each 1.25-inch-thick, of which eight were glycol-quenched. The DAS range was 0.0008 to 0.0020 inch, with an average value of 0.0013 inch and a standard deviation of 0.00035 inch. Based on these results a maximum DAS value of 0.0020 inch was recommended.

### Stress-Life Fatigue

The stress-life fatigue ( $K_t = 1.0$ ) data for D357-T6 are shown in Figure 28a (verification plates) and Figure 77 (pylons). The two data sets are combined and shown in Figure 104. The data for Foundries B and C plates fall significantly below results for 7075-T73. The fatigue results for Foundry A verification plates, and for the pylons produced by Alcoa during Phase II form a band that is similar to the lower bound for 7075-T73. The conclusion is that it is possible to obtain fatigue lives for D357-T6 that approach those currently achieved for 7075-T73. The data for Foundry A plates and the Alcoa pylons were subsequently selected for use in the development of the proposed AMS specification.

The reason why Foundries B and C were not able to achieve results similar to Foundry A is not clear. There were no obvious differences in microstructure or any other material parameters measured during the program. The fatigue performance may be a function of foundry practice. Details are not clear, but the key factor may be associated with turbulence and/or the molten metal flow distance. The important fact is that a D357-T6 fatigue life similar to the lower bound of 7075-T73 plate was achieved for both plates and large castings.

The following paragraphs include a description of the procedure used to define the fatigue life requirements included in the proposed D357 casting



\* Verification Plates: Water- and Glycol-Quenched

Figure 104. Combined Plate and Pylon Stress-Life Fatigue Data for D357-T6

specification for durability and damage tolerance applications. The data obtained for the Foundry A verification plates and Alcoa's cast pylons were used. The results for the two data sets are very similar and represent the best fatigue lives achieved during the program. In addition, they are similar to those for 7075-T73. Two different specimen sizes were used for the plates (0.5-inch diameter) and pylons (0.375-inch diameter), which was taken into account during the analysis. The pylon cross-section thickness was insufficient for excision of the larger diameter specimens.

The procedure follows a similar approach to that currently used to monitor the acceptable level of mid-plane microporosity occurring in thick ( $\geq 3.0$  inch) 7050-T7451 aluminum plate being delivered to Northrop for use on the F/A-18 program. This requirement is specified in McAir/Northrop Material Specification EO F09070 to MMS-1420.

The F/A-18 specification requires that at least four smooth round bar fatigue specimens are excised from the mid-plane of the plate. These specimens have a 2-inch-long, 0.50-inch-diameter gage section and are tested to failure under constant amplitude fatigue in accordance with ASTM E466 at a maximum stress of 35 ksi, with a stress ratio  $R = 0.1$ . Failures at machining defects are discounted and are replaced with a further specimen. The plate is considered to be acceptable if each specimen exhibits a life of greater than 80,000 cycles and the log average life of the specimens is greater than 100,000 cycles. At the time these criteria were established, they were based on the life trends obtained from plate that was considered to be acceptable, according to prescribed penetrant inspection requirements, as opposed to fatigue lives obtained from plate with unacceptable mid-plane porosity. The selected limits were an engineering judgement based on observed trends rather than a rigorous statistical approach. However, the quality verification of D357-T6 castings was based on a statistical analysis of the data after confirming the approach using 7050-T7451 plate data and comparing the results with the current acceptance limits.

The EIFS distribution obtained from tests run [21] on a series of 2-inch-long, 0.50-inch-diameter 7050-T7451 specimens is shown in Figure 105. This represents the current standard acceptable material quality for this

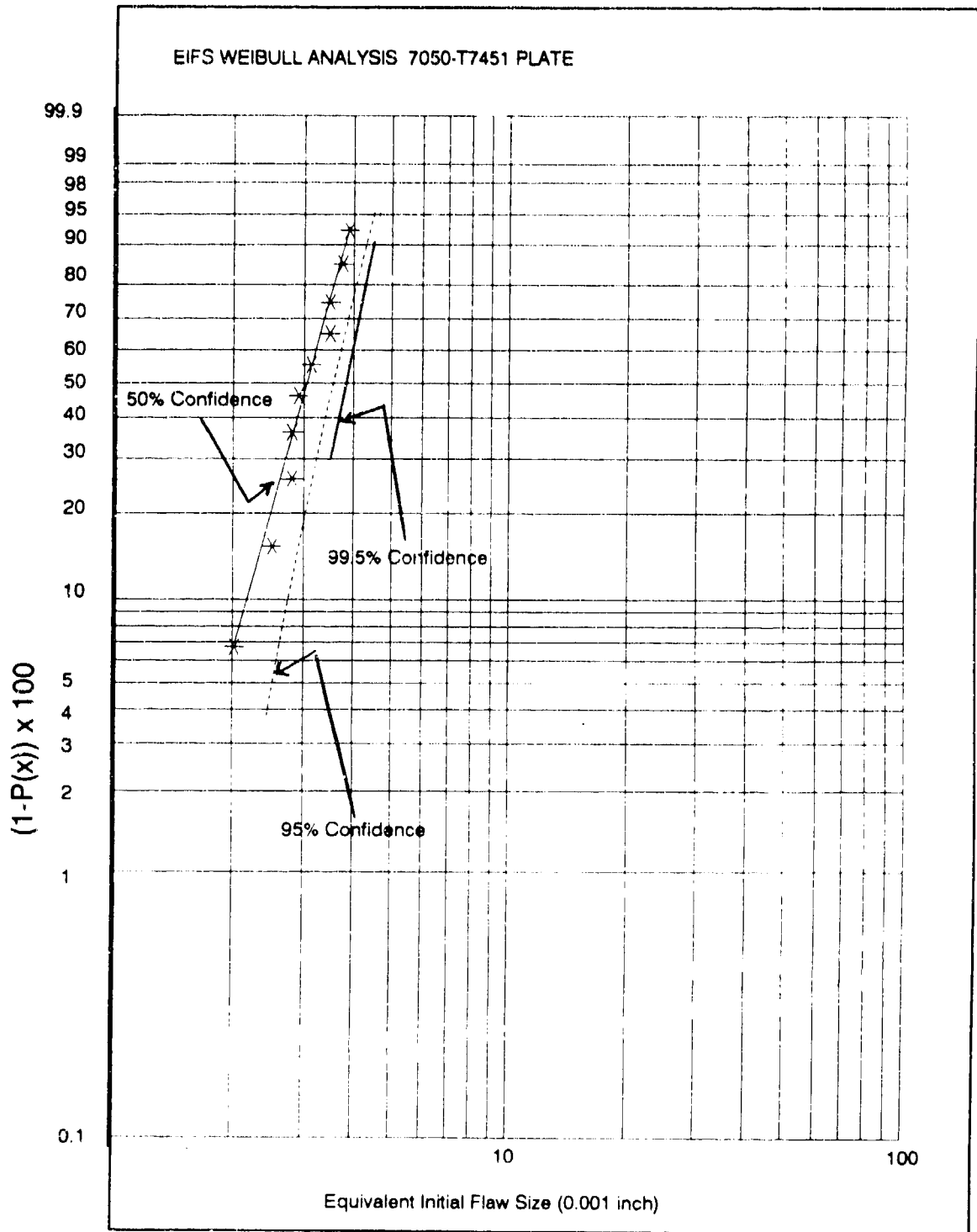


Figure 105. EIFS Weibull Analysis of 7050-T7451 Plate

product. To demonstrate equivalent quality for subsequent material, it will be assumed that it is necessary for the derived EIFS values to fall below the 95 percent confidence line established for the standard. These subsequent results can be plotted using the same theory of ranking approach for establishing the standard distribution. Thus, for a sample of four specimens, the highest EIFS value will be plotted at a median rank probability level of 84 percent [16]. The value of EIFS relating to the 95 percent confidence level at 84 percent probability is 0.0043 inch (from Figure 105). The relationship between EIFS and life for a 0.50-inch-diameter 7050-T7451 specimen is determined via the method given in Section 7.2.3 and is shown in Figure 106. The minimum expected life associated with a pore of this size is obtained from Figure 106 (87,000 cycles). The acceptable average EIFS value is obtained from the 95 percent confidence level at 50 percent probability as 0.0035 inch, and the associated minimum expected average life is obtained from Figure 106 (103,000 cycles).

When the confidence band is expanded to 99.5 percent, the maximum allowable pore size increases to 0.0045 inch and the maximum average pore size increases to 0.0037 inch. Using these pore sizes gives a minimum expected life of 84,000 cycles and a minimum expected average life of 99,000 cycles.

The acceptance criteria established by this method are thus shown to guarantee maximum pore sizes below the upper 99.5 percent confidence level of the standard distribution that agree very closely with the Northrop/McAir specification established in EO F09070 to MMS-1420. Hence, a similar approach for castings is proposed. However, the fatigue lives required to guarantee inherent material quality will be determined for the D357-T6 specification based on the more stringent 95 percent confidence boundary limit of the defect size distribution established for the superior Foundry A plates and Alcoa pylons.

The plate analysis was carried out based on specimens with a fairly large (2-inch-long x 0.50-inch-diameter) critical zone surface area. However, the practical size for the specimens cut from production aircraft castings is likely to be smaller than this. The effect of specimen size is determined as follows:

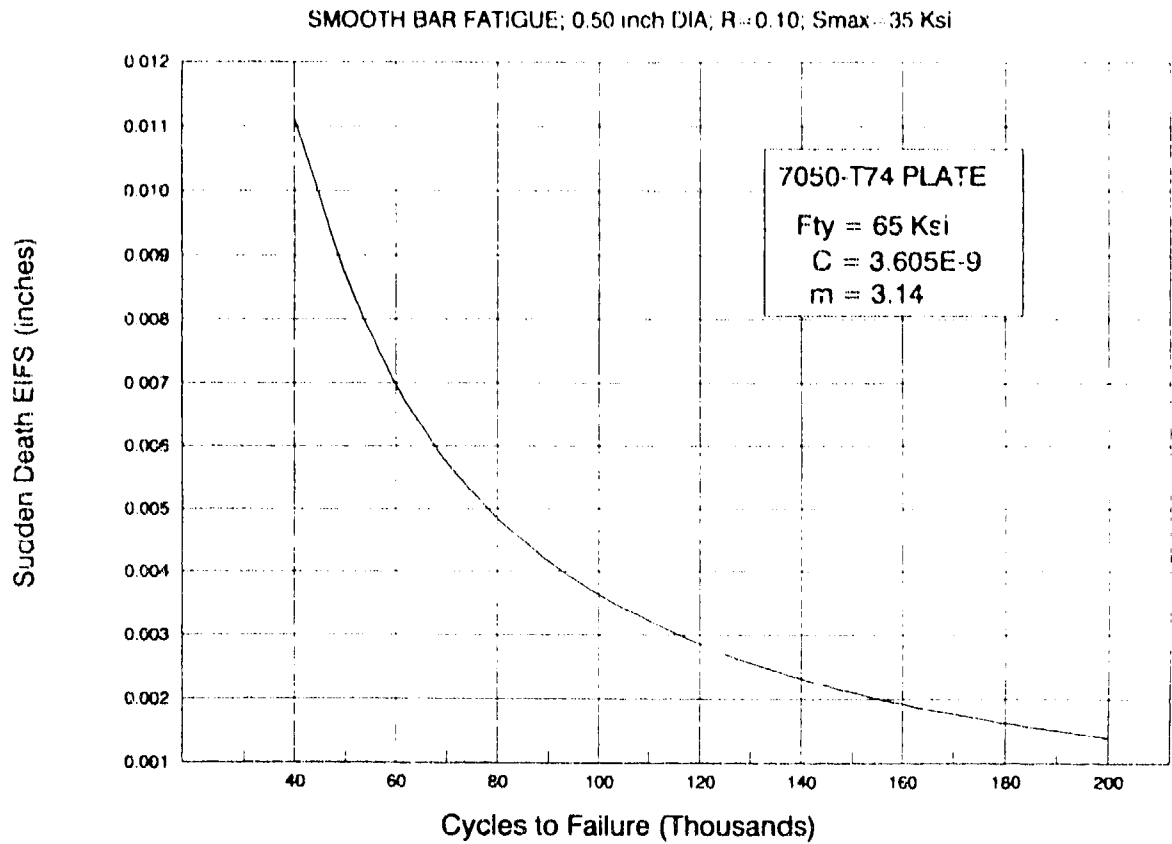


Figure 106. Variation of Inferred Sudden Death EIFS of 7050-T7451 Plate Based on Fatigue Life

Assuming a 0.050-inch-deep critical surface volume for a 2-inch-long, 0.50-inch-diameter specimen gives a critical zone volume (V) of:

$$V = 0.050 \ell \pi D$$

Where D = 0.50-inch diameter

$\ell$  = 2-inch gage length

$$\text{Therefore, } V = 0.1571 \text{ inch}^3$$

Assuming that the critical zone volume ( $V_{\text{hole}}$ ) for a typical 0.25-inch-diameter hole in a thickness of 0.25 inch occurs at  $\pm 20$  degrees from the normal hole axis, then

$$V_{\text{hole}} = 0.050 \pi d t (80/360)$$

Where d = hole diameter of 0.25 inch

t = 0.25 inch thickness

$$\text{Therefore } V_{\text{hole}} = 0.002182 \text{ inch}^3$$

Therefore, the number of 0.25-inch-diameter holes, drilled through a thickness of 0.25 inch, that have the same critical zone volume as a 2-inch-long, 0.50-inch-diameter test specimen is equal to  $0.1571/0.002182 = 72$ .

Hence, the failure of the fatigue specimen can be considered to represent the "sudden death" failure of a set of 72 holes. Based on the theory of ranking, a series of similar test groups would result in lives that would cluster about the 1.15 percent probability level of the life distribution expected from the general hole population. Conversely, the EIFS values (obtained from the application of the method given in Subsection 7.2.3) will cluster about the 98.8 percent probability level of the general EIFS population.

The test specimen (or "sudden death") EIFS values are plotted as a Weibull distribution using ranking tables and the median and 95 percent confidence limits established by regression analysis. These trends can then be used to provide the statistics for the general population by translating them from the 50 percent probability median "sudden death" value to the 98.8 percent probability level.

This exercise was carried out for D357-T6 based on the fatigue results from smooth round specimens excised from the Foundry A verification plates and the Alcoa pylons. Although the specimen geometries for these two lots were slightly different (2 inches long x 0.50 inch diameter for the verification material, and 1.5 inch long x 0.375-inch diameter for the pylons), the resulting surface volumes were still considered to be close enough for the data to be combined. The results of this analysis are shown in Figure 107.

The resulting general population distribution can now be regressed back to a "sudden death" trend for other specimen geometries, as shown below.

The general equation for the number of 0.25-inch-diameter holes drilled in a 0.25-inch-thick layer that are represented by a smooth round bar coupon with gage length  $\ell$  and diameter  $D$  is:

$$N_{equiv} = 0.050 \pi D \ell / 0.002182 = 72 D \ell$$

The number of holes is shown below for a range of gage section length and diameter combinations.

| DIA<br>(in) | GAGE LENGTH (in) |     |     |
|-------------|------------------|-----|-----|
|             | 2.0              | 1.0 | 0.5 |
| 0.50        | 72               | 36  | 18  |
| 0.25        | 36               | 18  | 9   |
| 0.125       | 18               | 9   | 4.5 |

Based on the theory of ranking, the "sudden death" EIFS values obtained from the above specimen geometries will cluster about the probability values for the general population as shown below.

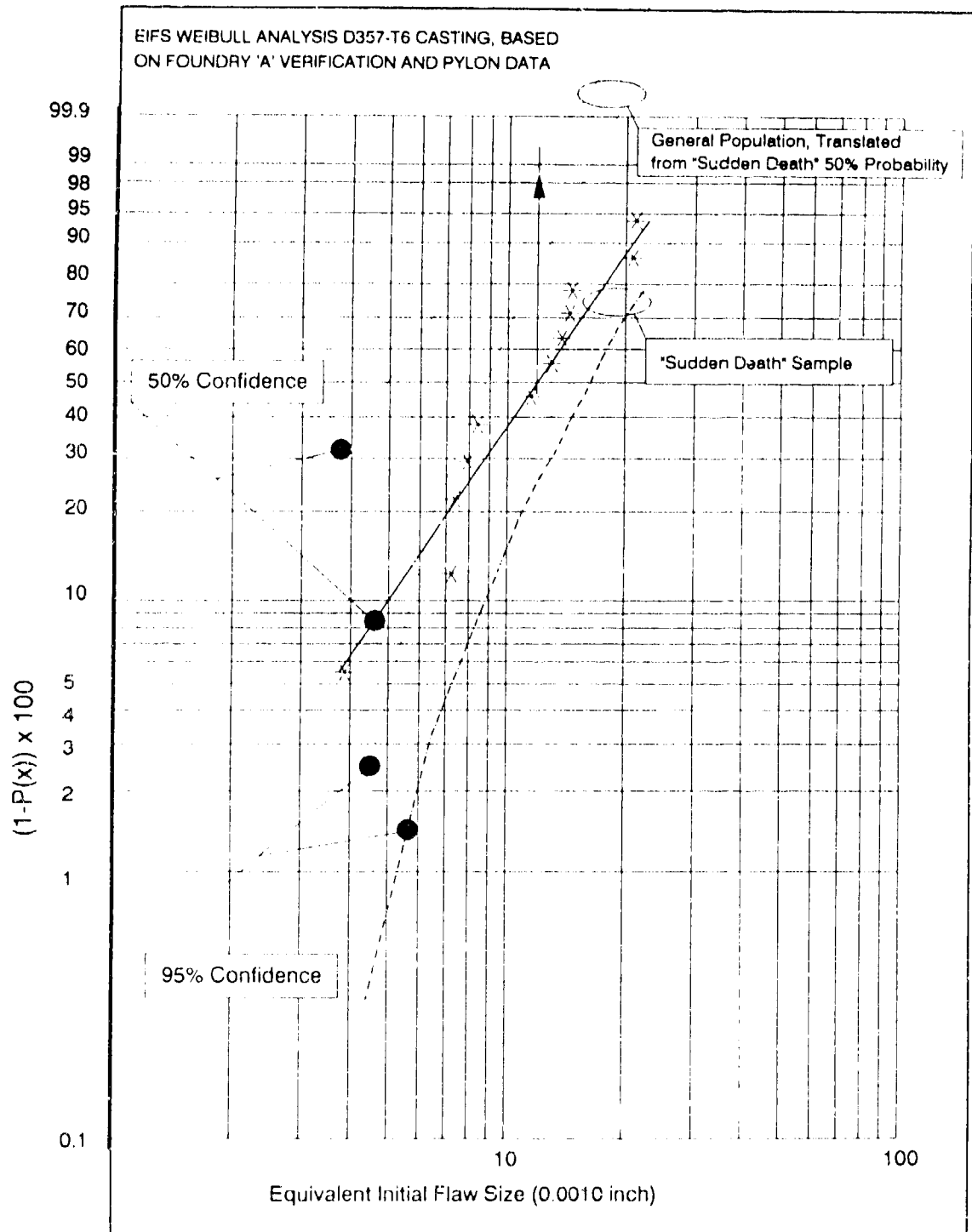


Figure 107. Weibull Distribution of D357-T6 Pylon and Foundry A Verification Plate Data

| DIA<br>(in) | GAGE LENGTH (in) |            |            |
|-------------|------------------|------------|------------|
|             | 2.0<br>(%)       | 1.0<br>(%) | 0.5<br>(%) |
| 0.50        | 98.8             | 98.1       | 96.2       |
| 0.25        | 98.1             | 96.2       | 92.6       |
| 0.125       | 96.2             | 92.6       | 85.5       |

Hence, the "sudden death" statistics for the above specimen geometries can be obtained by translating the median line of the previously generated "general population" distribution from the above cluster points back to the 50 percent probability level.

The maximum expected "sudden death" EIFS is then read at the highest ranking probability for the number of specimens to be run from the 95 percent confidence line for the specimen type under investigation. Based on the theory of ranking, these probabilities are:

| NUMBER OF<br>SPECIMENS TESTED | HIGHEST RANK<br>PROBABILITY (%) |
|-------------------------------|---------------------------------|
| 2                             | 70.7                            |
| 3                             | 79.4                            |
| 4                             | 84.1                            |

The maximum expected average "sudden death" EIFS is read from the 95 percent confidence line at the 50 percent probability level for the specimen type under investigation. This value is independent of the number of specimens tested.

The relationship between EIFS and life for various D357-T6 specimen cross-section diameters is determined via the method given in Subsection 7.2.3 and is shown in Figure 108.

The minimum lives and the minimum average lives that can be accepted, as a function of the number and geometry of the coupons tested are obtained from Figure 108. These results are based on the 95 percent confidence upper rank and 50 percent probability EIFS values determined from the statistical manipulation described above. These are summarized in Tables 80 and 81 and plotted for specimens with a 1-inch gage length in Figure 109.

Based on the above analysis, fatigue life acceptance requirements for D357-T6 were recommended based on test results for three specimens. For integrally-attached coupons, 2-inch-long x 0.5-inch-diameter specimens are specified. For castings, specimens of this size may not be feasible, and reduced length specimens with diameters of 0.25 or 0.375 inch are acceptable, with the minimum and log average allowable fatigue lives adjusted accordingly. Details are included in Subsection 11.1.1.1 and Appendix J.

#### Fracture Toughness

A fracture toughness of 21 ksi/in was included in the specification, based on data obtained during the verification task of Phase I (Table C7, Appendix C). A total of 11 compact tension tests were performed. Seven were for water-quenched material; the remaining four were quenched in glycol. In addition, five chevron-notched specimens, excised from the failed compact tension specimens, were tested. The correlation between the two types of tests was excellent.

The lowest compact tension fracture toughness value obtained was 21 ksi/in. This particular test yielded a valid  $K_{Ic}$  result, unlike most of the compact tension tests. The lowest chevron-notch test result was almost exactly the same (21.5 ksi/in). Thus, 21 ksi/in was selected for inclusion in the specification. The selected test method was the chevron-notch, which is now a valid ASTM test (E1304). The compact tension method was not recommended because of the difficulties obtaining valid results for aluminum castings.

SMOOTH BAR FATIGUE;  $S_{max}=40$  Ksi;  $R=0.10$

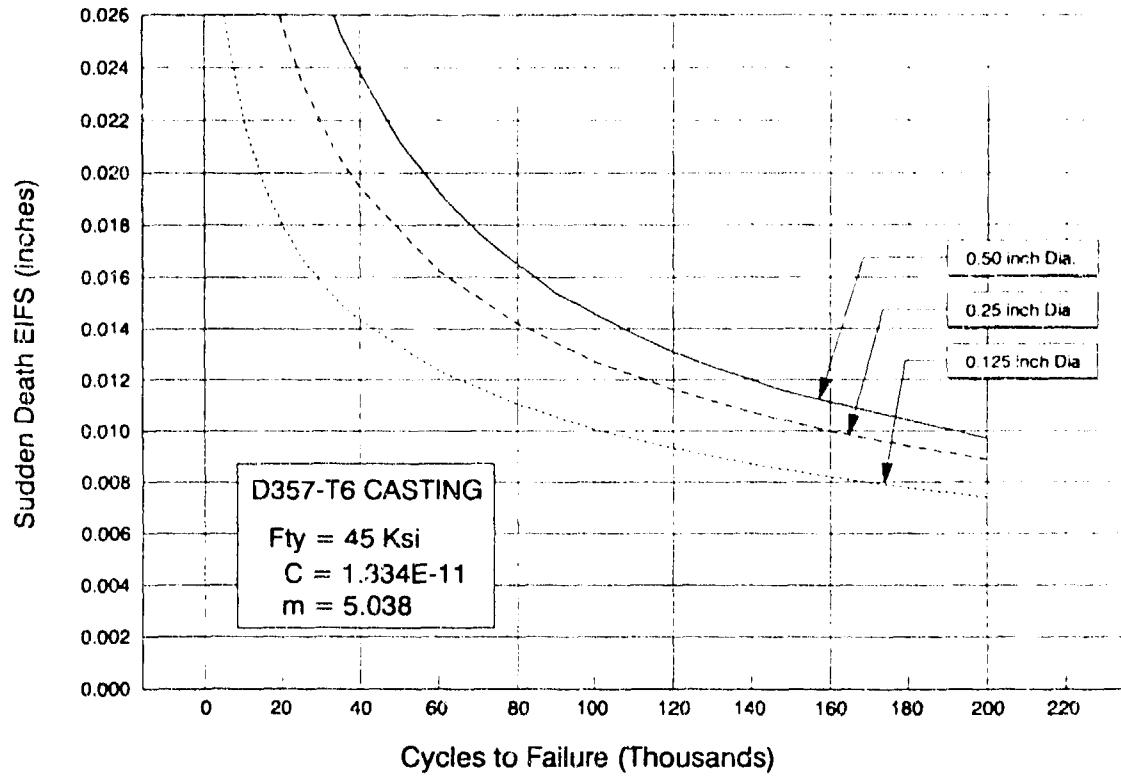


Figure 108. Variation of Inferred Sudden Death EIFS of D357-T6 Based on Fatigue Life

TABLE 80. MAXIMUM EIFS AND MINIMUM FATIGUE LIFE VS.  
SPECIMEN SIZE AND NUMBER OF TESTS  
( $S_{max} = 40$  ksi;  $R = 0.1$ )

| SPECIMEN<br>DIA (in) | MAXIMUM EIFS (in)         |        |        | MINIMUM LIFE (CYCLES)     |       |       |
|----------------------|---------------------------|--------|--------|---------------------------|-------|-------|
|                      | SPECIMEN GAGE LENGTH (in) |        |        | SPECIMEN GAGE LENGTH (in) |       |       |
|                      | 2.0                       | 1.0    | 0.50   | 2.0                       | 1.0   | 0.50  |
| (a) Two Tests        |                           |        |        |                           |       |       |
| 0.500                | 0.0200                    | 0.0190 | 0.0175 | 56000                     | 62000 | 72000 |
| 0.250                | 0.0190                    | 0.0175 | 0.0160 | 43000                     | 50000 | 63000 |
| 0.125                | 0.0175                    | 0.0160 | 0.0145 | 22000                     | 29000 | 40000 |
| (b) Three Tests      |                           |        |        |                           |       |       |
| 0.500                | 0.0220                    | 0.0210 | 0.0195 | 46000                     | 51000 | 59000 |
| 0.250                | 0.0210                    | 0.0195 | 0.0175 | 33000                     | 40000 | 50000 |
| 0.125                | 0.0195                    | 0.0175 | 0.0160 | 15000                     | 22000 | 29000 |
| (c) Four Tests       |                           |        |        |                           |       |       |
| 0.500                | 0.0240                    | 0.0230 | 0.0215 | 39000                     | 43000 | 49000 |
| 0.250                | 0.0230                    | 0.0215 | 0.0190 | 26000                     | 30000 | 43000 |
| 0.125                | 0.0215                    | 0.0190 | 0.0170 | 10000                     | 17000 | 25000 |

TABLE 81. MAXIMUM AVERAGE EIFS AND MINIMUM AVERAGE  
FATIGUE LIFE VS. SPECIMEN SIZE

| SPECIMEN<br>DIA (in) | MAXIMUM AVERAGE EIFS (in) |        |        | MINIMUM AVG LIFE (CYCLES) |       |       |
|----------------------|---------------------------|--------|--------|---------------------------|-------|-------|
|                      | SPECIMEN GAGE LENGTH (in) |        |        | SPECIMEN GAGE LENGTH (in) |       |       |
|                      | 2.0                       | 1.0    | 0.50   | 2.0                       | 1.0   | 0.50  |
| 0.500                | 0.0160                    | 0.0155 | 0.0150 | 85000                     | 90000 | 95000 |
| 0.250                | 0.0155                    | 0.0150 | 0.0140 | 67000                     | 70000 | 83000 |
| 0.125                | 0.0150                    | 0.0140 | 0.0125 | 35000                     | 44000 | 57000 |

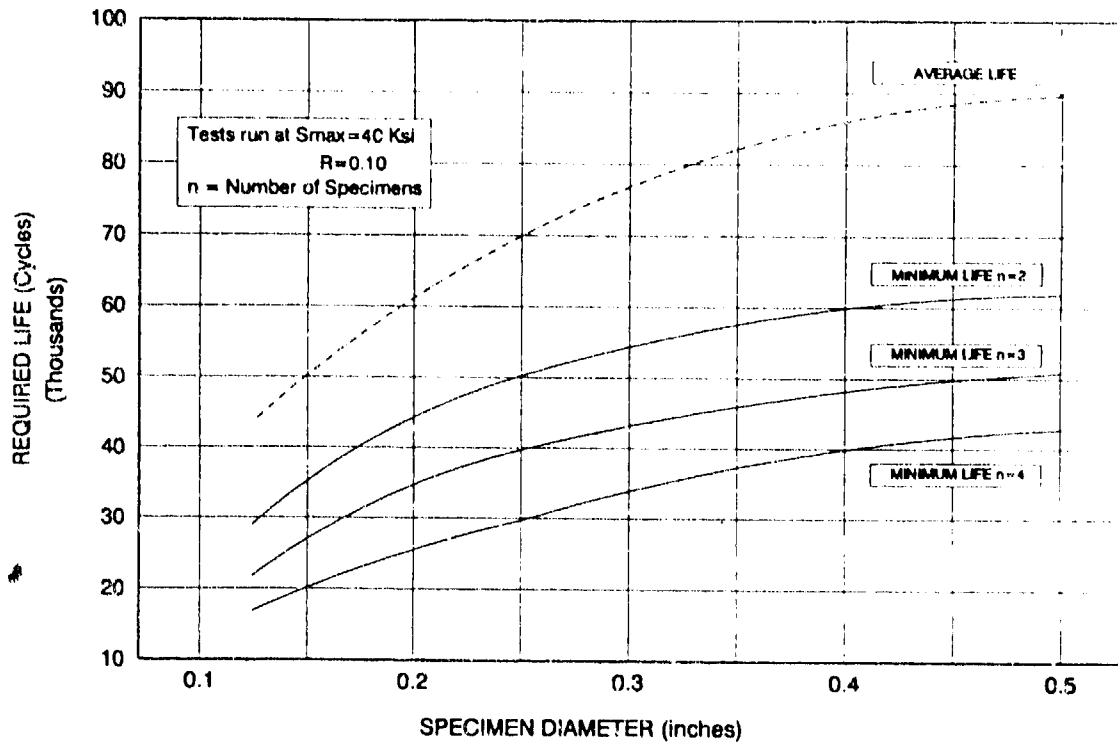


Figure 109. Variation of D357-T6 Specification Fatigue Life Requirements vs. Specimen Diameter (1.0-inch gage length)

#### 11.1.1.3 Supporting Data for Specification Changes Not Selected

During data consolidation (Phase III), the DADTAC data were analyzed to select requirements for inclusion in a proposed new D357-T6 AMS specification for ductility and damage tolerance applications. Three new requirements were selected, as discussed in Subsection 11.1.1.2. In addition to the three selected recommendations, four other issues were investigated but were not selected for inclusion in the proposed new specification. All four were approaches that could help achieve the target tensile, fatigue, and fracture toughness values. However, after discussions with the foundry community and the Air Force, it was decided that their use should be at the discretion of the foundry. The four issues are discussed below. The data presented indicate that, by carefully controlling the silicon particle size morphology and hydrogen content, and perhaps by HIPing the casting, an improvement in fatigue life might be attained. These factors should, therefore, be considered by the foundry when producing castings to meet the requirements listed in Subsection 11.1.1.1.

#### Silicon Modifier

The inclusion of a silicon modifier was considered because there was a clear indication of improvement (Subsection 5.3) in ductility, notched tensile strength, NTS/YS ratio (an indicator of fracture toughness) and the silicon particle morphology (Figure 17) of material at the edge of the cast plate (i.e., not under the chill). With adequate chilling it is possible to achieve similar results as those obtained by adding a silicon modifier. However, the latter promotes the formation of smaller silicon particles in those areas of a casting that are not chilled. Silicon particles were shown to be the primary crack initiation sites in the multihole durability specimens tested under fatigue loading (Subsection 10.5.7). Therefore, for fatigue-critical applications, the likelihood of forming large, irregularly-shaped particles of a brittle phase such as silicon could be reduced by the use of a modifier, with a possible improvement in fatigue life.

Both Sr and Na were evaluated in otherwise identical cast pylons produced by the same foundry (Alcoa). There were differences in the balance

of mechanical properties achieved with the two modifiers (Subsection 10.4). These differences may have been due to nonoptimized aging, though it is possible that Sr may have provided better properties than did Na. Specifically, the ductility and fracture toughness were higher for Sr- than for Na-modified material.

Either Sr or Na could be used, depending on the foundry preference. Some foundries believe that gas porosity is more readily controlled by using Na, though no significant difference in measured porosity was observed between the Na- and Sr-modified cast pylons evaluated in Phase II (Table 74).

#### Silicon Particle Aspect Ratio

The investigation described in Subsection 10.5.7 showed that, in the absence of porosity, fatigue cracks typically initiate at silicon particles. This is to be expected because the silicon is a brittle inclusion in a relatively ductile matrix, which would promote a local increase in stress. Compared with "spherical" silicon particles, the effect will be amplified for elongated particles, which should therefore be avoided. Thus, a low silicon particle aspect ratio is preferred. Of the three basic silicon particle morphology parameters, the aspect ratio was also recommended by Boeing [26] as being the most useful for controlling ductility. The other two parameters are particle area and spacing.

The average aspect ratio for the verification plates from all three foundries (Subsection 7.3.2) was  $1.66 \pm 0.07$ . The total number of data points was 37. Based on this average value and standard deviation, the inclusion of a maximum aspect ratio of 1.80 was considered, i.e., average value plus  $2\sigma$ . No specific data relating aspect ratio and fatigue life were obtained during the program. However, based on the fact that irregularly-shaped brittle phases are intuitively detrimental to mechanical properties, in an effort to maximize fatigue life, a maximum aspect ratio was considered for inclusion in the specification. This is supported by information in the literature [27]; it was reported that the fatigue life of A356 was dependent upon the distance from the chill (solidification rate). Specifically, the fatigue life was related to the dendrite cell size and the morphology of the silicon particles which are stress raisers.

## Hydrogen Content

The stress-life fatigue data shown in Figure 48 indicate that the fatigue life of D357-T6 is shorter than that of 7075-T73 and is dependent on the amount of gas porosity present (Grade). Grade A/B material has a much longer average fatigue life than Grade D, and it is comparable to the lower bound for 7075-T73. The gas pores in the cast material nucleate fatigue failure; hence, the higher the average porosity (Grade D), the shorter is the fatigue life. Conversely, the maximum fatigue life for D357-T6 can only be achieved by minimizing the gas porosity.

D357-T6 cannot be used for fatigue critical applications unless a useful minimum fatigue life (maximum gas porosity) can be guaranteed. The gas porosity in aluminum castings is hydrogen that comes out of solution during alloy solidification, forming spherical pores in the solidified metal. Hydrogen solubility is much greater in the liquid than the solid phase. Minimizing the hydrogen gas in the alloy will assist in obtaining the best possible fatigue life. To more clearly define the relationship between gas porosity and fatigue life, the hydrogen gas content of 33 of the failed fatigue specimens from Task 3 of Phase I was determined. The results were obtained by Wright Laboratory using the DADTAC contract specimens. The individual test results are detailed in Appendix L. Their significance is discussed below, with the objective of determining if a maximum hydrogen content could be included in an AMS specification to guarantee a minimum fatigue life.

If the bulk hydrogen gas content is plotted against fatigue life, a curve for each maximum fatigue stress is obtained. These are typified by those shown in Figure 110 for 20 and 30 ksi. The results show that there is a clear correlation between hydrogen content and fatigue life. However, selection of a maximum hydrogen content (minimum fatigue life) is complicated by the fact that the fatigue data are spread across a range of stress levels (25 to 45 ksi). A common denominator was needed so that the individual results could be normalized into a single data set. This was achieved by calculating the equivalent initial flaw size (EIFS) for each specimen. The

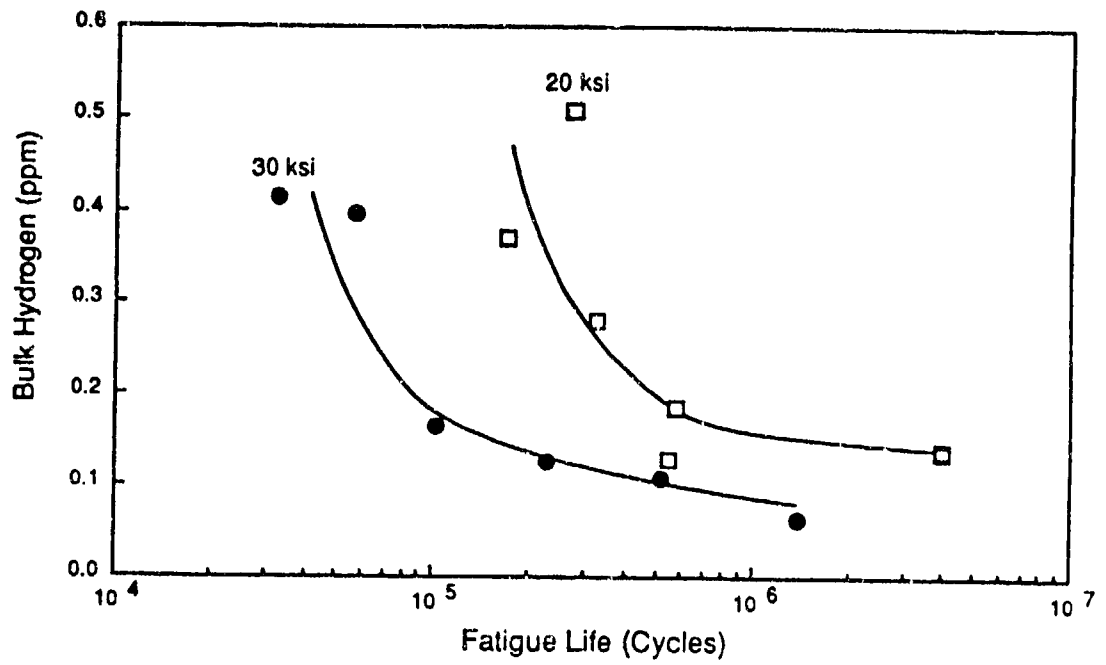


Figure 110. Relationship Between Fatigue Life and Bulk Hydrogen Content of D357-T6

EIFS is calculated from a relationship that includes parameters derived from constant amplitude fatigue test results, fatigue crack growth rate, and yield strength (Subsection 7.2.3.1).

A plot of EIFS versus bulk hydrogen content is shown in Figure 111, indicating a clear correlation. The regression equation for Grades A/B, B, C, and D (Figure 111a) data is:

$$\text{EIFS} = 0.065 + 0.411 \text{ Log } (H_2)$$

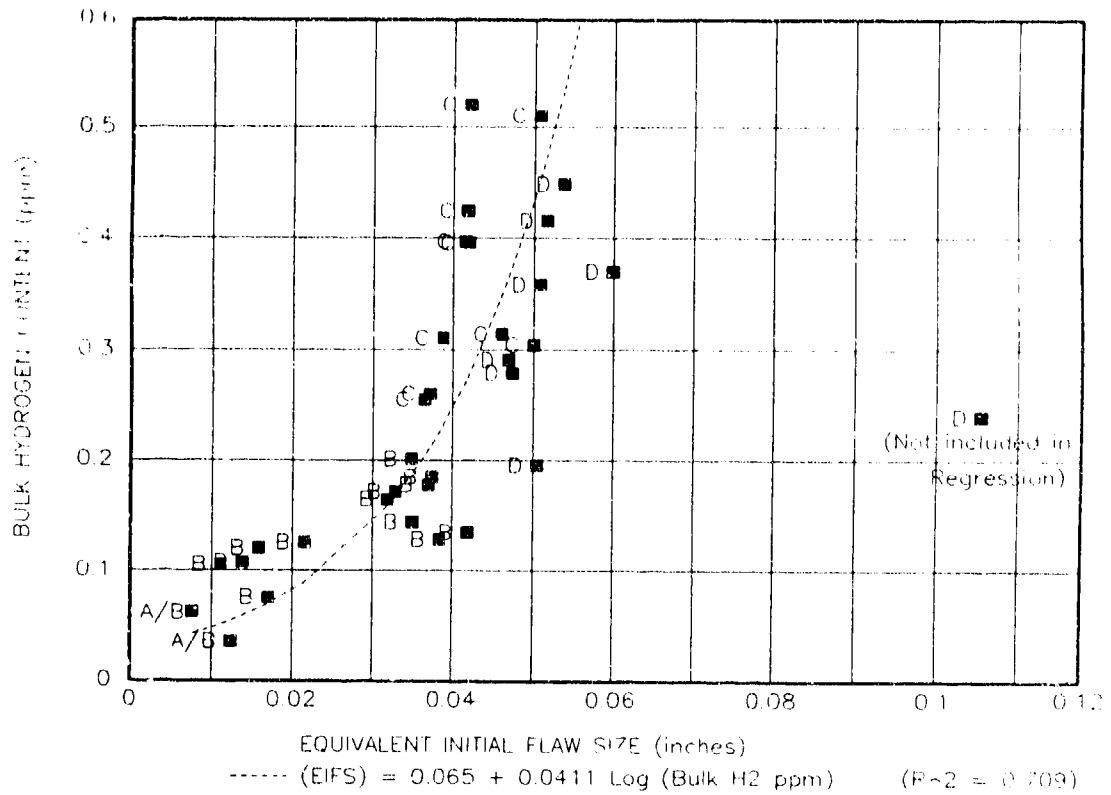
The region of the curve of most interest is at the lower hydrogen content values (Grades A/B and B). The objective was to determine if a maximum hydrogen content that will assure an acceptable, guaranteed fatigue life could be identified. The Grade A/B and B data are plotted separately in Figure 111b using an expanded scale. These data are defined by the linear relationship:

$$\text{EIFS} = 0.2 \times (H_2)$$

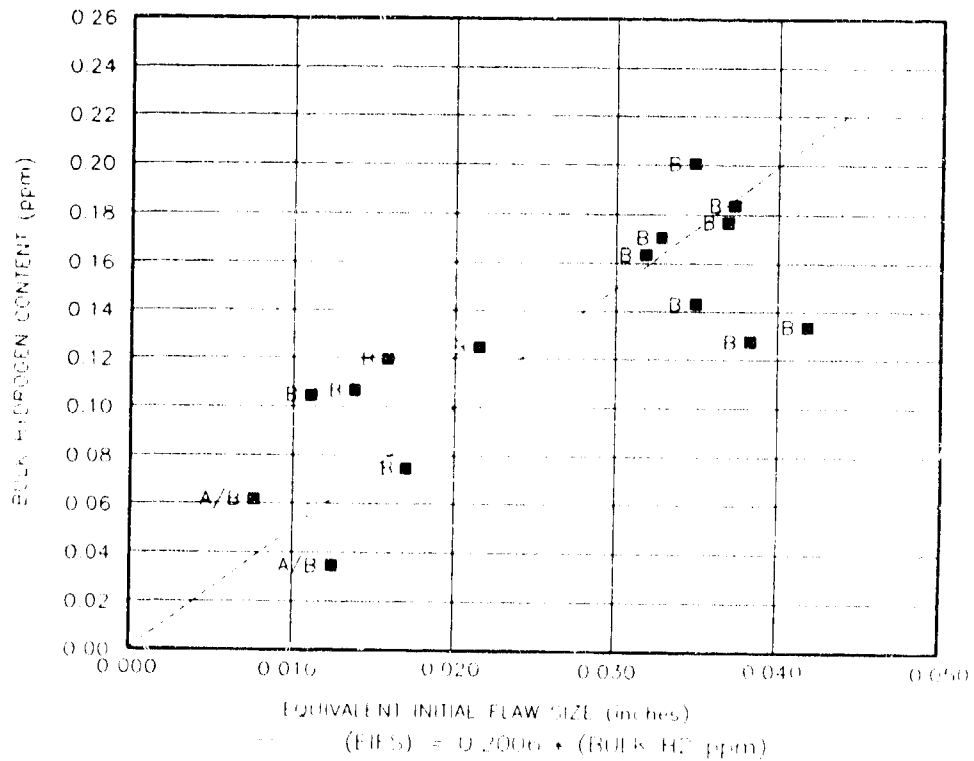
The Grade B data segregate into two groups, spanning an EIFS value of about 0.025 (0.13 ppm hydrogen). The fatigue life of the specimens with less than 0.15 ppm hydrogen are those that are in the upper end of the stress-life data band shown in Figure 48. Based on these results, a value of 0.15 ppm was considered for selection as the minimum allowable hydrogen content.

#### Hot Isostatic Pressing

Because the fatigue life of D357 was shown to be significantly shorter than that of a wrought aluminum alloy (Figure 28), every possible means to attain an improvement was considered. HIPing of B201 was shown in a previous contract to provide a significant increase in fatigue life by reducing shrinkage porosity [12]. Though the effect of HIPing on the fatigue life of D357 was not specifically investigated, shrinkage porosity was observed during the program. Hence, HIPing of D357 to reduce the amount of shrinkage, which can be a nucleation site for failure under fatigue loading, was considered.



a. Grades A/B-D



b. Grades A/B and E Only

Figure 111. Bulk Hydrogen Content of D357-T6 vs. Equivalent Initial Flaw Size

### 11.1.2 B201-T7

Only one change to AMS 4242 is recommended; it should include a provision for HIPing, which reduces microshrinkage and improves fatigue life [12]. The suggested changes to the indicated sections of AMS 4242 are shown below. All sections not indicated remain unchanged. AMS 4242 is reprinted in its entirety in Appendix K.

### 3. TECHNICAL REQUIREMENTS

3.5 Heat Treatment: Castings and integrally-attached test coupons shall be hot isostatically pressed (HIP) as specified in 3.5.3 and shall be solution and precipitation heat treated in accordance with MIL-H-6088 except as specified in 3.5.1 and 3.5.2.

3.5.3 Hot Isostatic Pressing: All castings and integrally-attached coupons shall be HIPed prior to heat treatment. A step treatment of 910-930°F (490-500°C) for not less than two hours, followed by 940-960°F (505-515°C) at a pressure of 15,000 psi for not less than three hours, is recommended.

### 11.2 PROCESS SPECIFICATIONS

No unusual processing methods were employed for producing any of the cast plates or pylons for the DADTAC program. For the D357 and B201 verification plates, Alcoa cast the aluminum into a vertical mold; Hitchcock Industries and Fansteel Wellman Dynamics both used a horizontal arrangement (Subsection 7.2.1). Each foundry used different chill types and configuration. The inboard wing pylons evaluated in Phase II were cast by Alcoa using the same molds previously employed over many years for the production pylons. However, some indications of guidelines for producing D357-T6 and B201-T7 castings can be derived from analysis of the test data, as described in the following sections.

### 11.2.1 D357-T6

Analysis of the microstructural and mechanical property data for D357-T6 reveals information that might facilitate the production of castings with improved properties. For D357-T6, Foundry A verification plates had the longest fatigue lives (Figure 28) and the lowest equivalent initial flaw size (Table 49). The other two foundries were similar to each other in this regard, but not as good as Foundry A. The smooth fatigue ( $K_t = 1.0$ ) stress-life test is very sensitive to the presence of casting defects, which are potential crack initiators. The more defects that are present in a material, the higher is the likelihood that one will be positioned at a critical location that results in early failure under fatigue loading, e.g., on the surface of the gage section of a fatigue specimen. The indications are, therefore, that Foundry A produced "cleaner" material.

In Phase II, it was observed that fatigue crack initiation of the multihole specimens often occurred at silicon particles. It is clear, therefore, that silicon particles should be as small and as spherical as possible. An analysis of the percent porosity of the verification plates that met the property requirements (Table 45) shows that there is little difference from foundry-to-foundry. While there are differences in silicon particle morphology between plates from the three foundries, there are no major trends. However, several plates from Foundries B and C were rejected because they failed to meet the tensile property requirements. Data for these plates were not included in Table 45. If silicon particle morphology and percent porosity data for the rejected verification plates are included in the overall assessment, the results are more revealing (Table 82). The average DAS, silicon particle spacing and area, and percent porosity are now all smaller for the Foundry A plates than for Foundries B and C. In light of the smooth fatigue results, the absence of measurable porosity and the smaller silicon particles in the Foundry A material may be major contributors to its excellent fatigue properties. Also, the rejected plates from Foundries B and C were observed to have inclusions (dross) on the surface of tensile specimens that did not meet the specification minimum ductility value. These inclusions probably contributed to the shorter fatigue lives of Foundry B and C material.

TABLE 82. SILICON PARTICLE MORPHOLOGY AND POROSITY  
FOR ALL D357-T6 VERIFICATION PLATES

| FOUNDRY | Si PARTICLE MORPHOLOGY |                             |                              |                 | POROSITY<br>(%) |
|---------|------------------------|-----------------------------|------------------------------|-----------------|-----------------|
|         | DAS<br>(INCH)          | AREA<br>( $\mu\text{m}^2$ ) | SPACING<br>( $\mu\text{m}$ ) | ASPECT<br>RATIO |                 |
| A       | 0.0011                 | 13                          | 37                           | 1.6             | 0               |
| B       | 0.0017                 | 20                          | 43                           | 1.6             | 0.11            |
| C       | 0.0015                 | 16                          | 46                           | 1.7             | 0.18            |

The effect of a nonoptimum microstructure on the properties of D357-T6 (Subsection 8.4) was significant. The mechanical properties, particularly tensile properties and fracture toughness, were reduced by the development of a much more coarse microstructure.

The main conclusion is that, from the Foundry A data, it is possible to produce castings that result in improved fatigue properties. The fatigue life for Foundry A material (Figure 28a) more closely approaches that of 7075-T73 than Foundries B and C, and exhibits a higher value for both the upper and lower extremities of the data scatter. Unless the fatigue life of aluminum castings can be both consistent and close to that of conventional ingot alloys, they are unlikely to be used in fatigue-critical applications. Foundry A showed that this goal might be achievable by attaining a fine microstructure with little or no detectable porosity. Verification of this quality can be achieved by the use of a fatigue test.

To achieve the improved fatigue properties exhibited by Foundry A, foundry practices must include significant precautions to ensure that the fine microstructure and, in particular, a very low porosity content is achieved.

#### 11.2.2 B201-T7

All the cast B201-T7 verification plates met the AMS 4242 specification requirements and the mechanical properties were essentially unaffected by significantly increasing the grain size (Subsection 8.5); only the limited spectrum fatigue life results showed an indication of deterioration. All plates were HIPed, which reduced the amount of porosity in the castings (Subsection 7.4.8). Similar to D357-T6, B201-T7 supplied by Foundry A had the lowest EIFS and longest fatigue lives (Figure 41) which is an indication of "cleaner" material.

Similar to D357-T6, Foundry A showed that good fatigue lives can be achieved, presumably through careful control of those foundry practices that can affect the amount of porosity present in the castings.

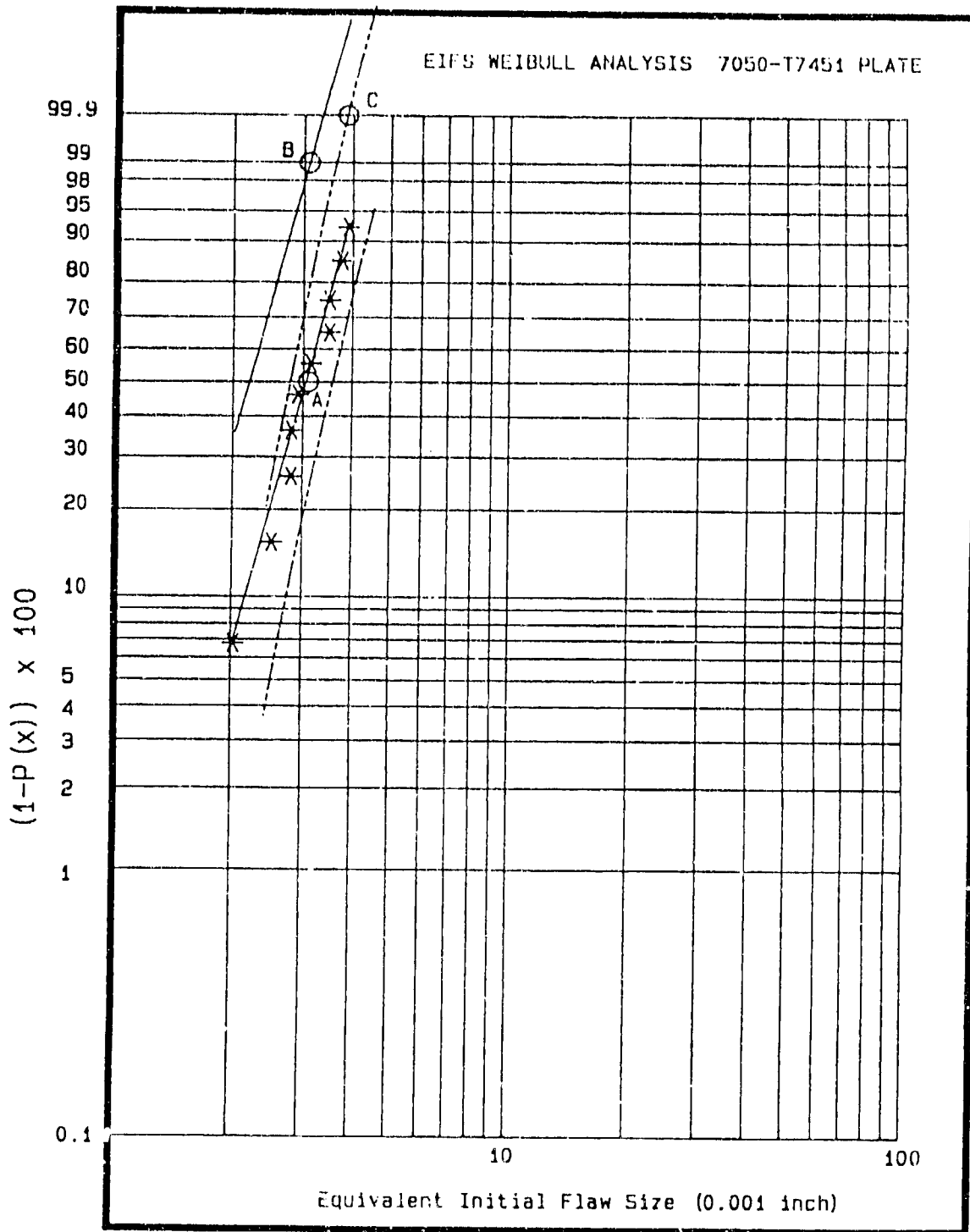
### 11.3 APPLICABILITY OF MIL-A-87221 AND MIL-A-83444 TO PREMIUM QUALITY CASTINGS

Based on a comparison of inherent flaw size Weibull distributions obtained for 7050-T7451 plate (Figure 112) using Northrop IR&D data [15] and the verification casting material (Figures 33 and 46), the inherent flaws present in Grade B D357-T6 and B201-T7 provided by all three foundries are an order of magnitude greater than those found in wrought aluminum alloys. However, Foundry A material demonstrated significantly longer fatigue lives than Foundries B and C (Figures 28 and 41). Foundry A D357-T6 verification and Alcoa pylon fatigue data were selected for developing the requirements to be included in the proposed new AMS specification (Section 11.1.1.2) and are used as a basis for assessing compliance with the durability requirements in MIL-A-87221.

For wrought alloys, initial flaw size assumptions tend to be based on demonstrated manufacturing procedures; any inherent material defects are overshadowed by flaws that occur during manufacturing of the part. However, castings tend to have upper bound defects that are more a function of inherent material quality than part manufacture or aircraft assembly procedures. The guidelines for durability analysis given in MIL-A-87221 require that:

*"the durability analysis should demonstrate that an assumed initial flaw in typical quality structure would not propagate to a size which would cause functional impairment in two lifetimes of the service usage spectrum and that, additionally, it is unlikely that, by means of crack initiation analysis, fatigue cracks will initiate in the same period of time."*

For initial design, MIL-A-87221 defines the assumed initial flaw size at a stress riser as a 0.010-inch-radius corner flaw. This initial flaw size requirement is adequately satisfied by the upper 95 percent confidence limit determined for the average (or "typical quality") EIFS value obtained for the Foundry A plates and the Alcoa pylons selected as a basis to develop the proposed D357-T6 specification.



Note: Weibull Mean (A) of the Sudden Death Data Clusters About the 99% Probability Level of the General Population (B). The Maximum Expected Flaw (99.9% Probability With 95% Confidence) is Indicated by Point (C)

Figure 112. Weibull Distribution of 7050-T7451 Plate EIFS Data

The requirements of MIL A-87221 are thus satisfied for specification-controlled premium quality castings by conducting a standard crack growth analysis from an initial flaw of 0.010 inch to a size that is assumed to cause functional impairment.

MIL-A-87221 indicates that reductions in the initial flaw size assumptions used for both durability and damage tolerance analyses may be negotiated when certain fatigue improvement techniques or assembly procedures are used. However, reductions in initial flaw size assumptions are not proposed for premium quality castings. This is because initial flaw sizes are primarily a function of inherent material quality rather than subsequent part manufacturing methods.

The equivalent initial flaw size for D357-T6 and B201-T7 verification plates (Subsections 7.3.6 and 7.4.7) was less than the MIL-A-83444 damage tolerance value (0.05 inch). Thus, the requirements of MIL-A-83444 can be applied without modification. However, because the flaws are inherently associated with the casting process, the possibility of negotiating a reduction in the 0.05 inch requirement based on demonstrated improvements in subsequent manufacturing quality (e.g., machining) should not be considered.

Any application of durability and damage tolerance requirements also requires that demonstrated lives and crack growth trends can be accurately predicted by analytical techniques and that the material behaves in a consistent manner. It has been demonstrated that the data spread for D357-T6 premium quality castings was within the bounds normally expected for this type of testing and that the results can be estimated via the Northrop unified life prediction method [13].

SECTION 12  
SUMMARY OF DADTAC PROGRAM CONCLUSIONS

Conclusions and/or recommendations are listed at the end of each of the major sections of this report. The main conclusions are summarized below. For further details, refer to the appropriate section.

12.1 PHASE I, TASK 1 - NDI ASSESSMENT

1. The FAI NDI method provides a qualitative correlation with X-ray grades, particularly for castings that contain gas porosity. Part of the scatter in the FAI results can be explained by a wide variation of the number of defects observed in the radiographs of Grade B material. Further development is needed before data for foreign material can be correlated with X-ray results
2. The eddy current technique can be used to detect the presence of cracks under fasteners in castings, and to determine crack length.

12.2 PHASE I, TASK 2 - SCREENING TESTS

1. The inclusion of a silicon modifier in D357-T6 improves mechanical properties, particularly ductility and toughness
2. The requirements for optimizing the DADT and tensile properties of D357-T6 and B201-T7 do not conflict.

12.3 PHASE I, TASK 2 - PROPERTY VERIFICATION

1. D357-T6 and B201-T7 made according to the modified AMS 4241 and 4242 specifications, respectively, had inherent material equivalent initial flaw sizes that are less than the value currently assumed (0.050 inch) for standard damage tolerance analysis. Therefore, D357-T6 and B201-T7 can be considered for damage tolerance

applications based on the existing requirements of MIL-A-83444 and MIL-A-87221.

#### 12.4 PHASE I, TASK 3 - EFFECT OF DEFECTS

1. Increased soundness resulted in an improvement in the overall balance of mechanical properties of D357-T6. The best properties were observed for Grade A/B, essentially defect-free, and weld material (also Grade A/B). The effect of soundness was particularly noticeable for fatigue life ( $K_t = 1.0$ ). The fatigue crack growth rate was insensitive to soundness.
2. A nonoptimum (coarse) microstructure significantly reduced the mechanical properties of D357-T6, but had little effect on HIPed B201-T7.

#### 12.5 PHASE II - CASTINGS QUALIFY VERIFICATION

1. The cast plate technology evaluated in Phase I can be successfully scaled up to make large, complex-shaped, aircraft castings.

#### 12.6 PHASE III - DATA CONSOLIDATION

1. The durability and damage tolerance test data indicated that the D357-T6 results are consistent and predictable for the spectrum severities that would normally be encountered for its usage
2. The durability requirements of MIL-A-87221 were met by D357-T6 (Foundry A plates and Alcoa pylons) and B201-T7 (combined verification data from all three foundries)
3. A new D357 specification should be introduced for durability and damage tolerance aircraft applications. The specification should be based on AMS 4241 and include requirements for fatigue life, fracture toughness, and dendrite arm spacing. A draft specification is included in Appendix J. The specification varies from AMS 4241 as follows:

- a) *Requirements for fatigue life and fracture toughness are included.*
  - b) *A maximum DAS of 0.0020 inch in the designated areas of the casting should be achieved.*
4. AMS 4242 (B201-T7) should include a provision for HIPing to reduce the amount of microshrinkage.

SECTION 13  
SPECIAL CONSIDERATIONS

The technology developed under the DADTAC contract will not require the development of any environmental regulations or other special considerations from the standpoint of potential future scale-up to production quantities. All recommended specification changes are within the scope of current technology. Both Na and Sr can readily be used as silicon modifiers for D357, and HIPing is standard technology and can be applied to D357 or B201 without problem.

#### REFERENCES

1. Aerospace Materials Specification, AMS 4241, 1986, Society of Automotive Engineers, Warrendale, Pennsylvania 15096.
2. Aerospace Material Specification, AMS 4242, 1986, Society of Automotive Engineers, Warrendale, Pennsylvania 15096.
3. L. Adler, J. Rose, and C. Mobley, J. Appl. Phys., Vol. 59, p. 336, 1986.
4. P. Nagy, D. Rypien, and L. Adler, to be published.
5. J. Gubernatis and E. Domany, Review of Progress in Quantitative Nondestructive Evaluation, edited by D. Thompson and D. Chementi, Plenum, New York, 1983, Vol. 2A, p. 833.
6. "Determination of Dendrite Arm Spacing in Aluminum Castings," Northrop Process Specification IT-72.
7. B. Chamberlin and J. Sulzer, "Gas Content and Solidification Rate Effect on Tensile Properties and Soundness of Aluminum Casting Alloys," Modern Castings, Vol. 46, October 1964.
8. M. R. James and W. L. Morris, "The Fracture of Constituent Particles During Fatigue," Material Science and Engineering, Vol. 56, 1982, pp. 63-71.
9. D. S. Saunders, B. A. Parker, and J. F. Griffiths, "The Fracture Toughness of an Aluminum Casting Alloy," Journal of Australian Institute of Metals, 1975.
10. M. D. Hanna, S. Z. Lu, and A. Hallawell, "Modification in the Aluminum Silicon System," Metallurgical Transactions, Vol. 15A, March 1984.

11. G. R. Turk, "Fatigue Performance and Phase Structure of 3XX Cast Aluminum Alloys Due to Cerium Additions and Anodic Coatings," MS Thesis, University of Virginia, May 1985.
12. G. V. Scarich and K. C. Wu, "Hot Isostatic Pressing of Aluminum Castings," Final Report, Contract N00019-80-C-0276, February 1986.
13. P. G. Porter, "A Unified Approach to Crack Initiation and Growth Analysis," Northrop Report No. NOR 87-102, October 1987.
14. "Northrop Fatigue/Damage Tolerance Manual," Vol. I, Section III.
15. "Airplane Damage Tolerance Design Requirements," MIL-A-83444, July 1974.
16. C. Lipson and N. J. Sheth, "Statistical Design and Analysis of Engineering Experiments," Section 5.5, McGraw-Hill, 1973.
17. "Fatigue-Endurance Data," Vol. 2., Aeronautical Series of Engineering Sciences Data, Item No. 68016, The Royal Aeronautical Society, London, England, 1968.
18. I. J. Polmear, "Light Alloys - Metallurgy of the Light Metals," ASM International, Metals Park, Ohio, 1982, p. 119.
19. Alcoa Green Letter, GL-206, 1971.
20. Alcoa Green Letter, GL-216, 1985.
21. Unpublished Data, Northrop Aircraft Division.
22. Northrop IR&D Program 84-R-1098.
23. Unpublished Data from the Premium Casting Task Force, American Foundrymen's Society, Committee 2D.

24. I. J. Polmear, "Development of an Experimental Wrought Aluminum Alloy for Use at Elevated Temperatures." Vol. 1, pp. 664-665, published in Aluminum Alloys, Their Physical and Mechanical Properties, proceedings of an International Conference at University of Virginia, June 1986.
25. P. G. Porter and A. F. Liu, "A Rapid Method to Predict Fatigue Crack Initiation; Vol. I--Technical Summary; Vol II--Computer Program Users Manual," Report No. NADC-81010-60, NADC Contract N62269-82-C-0044, February 1983.
26. D. L. McLellan and M. M. Tuttle, "Manufacturing Methodology Improvement for Aluminum Casting Ductility," Final Report, AFWAL-TR-82-4135, Contract No. F33615-80-C-3209.
27. W. A. Bailey, "Fatigue of 356 Aluminum Alloy," Foundry, October 1965, p. 97.

APPENDIX A  
PHASE I, TASK 2  
D357-T6 SCREENING TEST DATA

TABLE A1. EFFECT OF PROCESS VARIABLES ON THE ULTIMATE TENSILE STRENGTH OF D357-T6 WITHIN COMPOSITION SPECIFICATION

| COMPOSITION <sup>1</sup> | ULTIMATE TENSILE STRENGTH (ksi)                      |          |  |          | AVERAGE |
|--------------------------|--|----------|--|----------|---------|
|                          | AGE  |          | AGE  |          |         |
|                          | <u>SLOW SOLIDIFICATION</u> <sup>2</sup><br>315F/12HR | 335F/6HR | <u>FAST SOLIDIFICATION</u> <sup>3</sup><br>315F/12HR | 335F/6HR |         |
| 0.19Ti-0.10Mn-0.053Be    | 51.8   | 52.5     | 52.6   | 54.0     |         |
|                          | 49.0   | 48.1     | 49.8   | 52.7     |         |
| Average                  | 50.4   | 50.3     | 51.2   | 53.4     | 51.3    |
| 0.07Ti-0.00Mn-0.04Be     | 48.5   | 52.5     | 48.6   | 55.1     |         |
|                          | 49.6   | 51.1     | 49.6   | 53.2     |         |
| Average                  | 49.0   | 51.8     | 49.1   | 54.2     | 51.0    |
| 0.60Mg                   | 50.8   | 53.3     | 52.3   | 54.7     |         |
|                          | 48.6   | 50.4     | 51.8   | 54.5     |         |
| Average                  | 49.7   | 51.8     | 52.0   | 54.6     | 52.0    |
| 0.56Mg                   | 52.3   | 52.8     | 54.0   | 55.4     |         |
|                          | 49.2   | 51.4     | 53.1   | 54.2     |         |
|                          | 48.8   | -        | -  | 52.6     |         |
| Average                  | 50.1   | 52.1     | 53.5   | 54.1     | 52.5    |
| 7.41Si                   | 50.8   | 52.5     | 53.4   | 54.7     |         |
|                          | 48.3   | 50.3     | 48.5   | 48.8     |         |
| Average                  | 49.5   | 51.4     | 51.0   | 51.8     | 50.9    |
| 6.53Si                   | 51.5   | 54.2     | 54.0   | 54.3     |         |
|                          | 50.8   | 52.3     | 49.3   | 50.8     |         |
|                          | 47.2   | -        | -  | 49.1     |         |
| Average                  | 49.8   | 53.2     | 51.6   | 51.4     | 51.5    |
| 0.18Fe                   | 50.6   | 51.7     | 54.1   | 54.6     |         |
|                          | 49.5   | 50.7     | 50.4   | 49.4     |         |
| Average                  | 50.0   | 51.2     | 52.2   | 52.0     | 51.4    |
| 0.00Sr                   | 50.9   | 51.7     | 53.6   | 53.9     |         |
|                          | 48.3   | 50.8     | 51.4   | 51.5     |         |
| Average                  | 49.6   | 51.2     | 52.5   | 52.7     | 51.5    |
| Nominal                  | 51.4   | 48.6     | 51.0   | 49.6     |         |
|                          | 51.5   | 50.4     | 50.4   | 53.2     |         |
| Average                  | 51.5   | 49.5     | 50.7   | 51.4     | 50.8    |
| Average                  | 50.0   | 51.4     | 51.5   | 52.8     | 51.4    |

1) Other elements; mid-range of the specification

2) Fe chill; 1440F pour temperature

3) Cu chill; 1380F pour temperature

TABLE A2. EFFECT OF PROCESS VARIABLES ON THE ULTIMATE TENSILE STRENGTH OF D357-T6 OUTSIDE COMPOSITION SPECIFICATION

| COMPOSITION <sup>1</sup> | ULTIMATE TENSILE STRENGTH (ksi)                      |          |  |          | AVERAGE |
|--------------------------|--|----------|--|----------|---------|
|                          | AGE  |          | AGE  |          |         |
|                          | <u>SLOW SOLIDIFICATION</u> <sup>2</sup><br>315F/12HR | 335F/6HR | <u>FAST SOLIDIFICATION</u> <sup>3</sup><br>315F/12HR | 335F/6HR |         |
| 0.45Mg                   | 51.0   | 51.8     | 51.0   | 47.5     |         |
|                          | 50.2   | 51.8     | 50.0   | 50.6     |         |
| Average                  | 50.6   | 51.8     | 50.5   | 49.0     | 50.5    |
| 0.00Ti                   | 50.5   | 47.9     | 51.6   | 51.0     |         |
|                          | 51.4   | 49.9     | 52.4   | 52.1     |         |
| Average                  | 51.0   | 48.9     | 52.0   | 51.5     | 50.9    |
| 0.027Fe-0.0005Be         | 52.2   | 51.2     | 52.8   | 50.6     |         |
|                          | 52.9   | 52.3     | 45.3   | 54.0     |         |
| Average                  | 52.5   | 51.8     | 49.0   | 52.3     | 51.4    |
| Average                  | 51.4   | 50.8     | 50.0   | 51.5     | 50.9    |

1) Other elements; mid-range of the specification

2) Fe chill; 1440F pour temperature

3) Cu chill; 1380F temperature

TABLE A3. EFFECT OF PROCESS VARIABLES ON THE YIELD STRENGTH OF D357-T6 WITHIN COMPOSITION SPECIFICATION

| COMPOSITION <sup>1</sup>  | YIELD STRENGTH (ksi)                                 |          |  |          | AVERAGE |
|---------------------------|--|----------|--|----------|---------|
|                           | AGE  |          | AGE  |          |         |
|                           | <u>SLOW SOLIDIFICATION</u> <sup>2</sup><br>315F/12HR | 335F/6HR | <u>FAST SOLIDIFICATION</u> <sup>3</sup><br>315F/12HR | 335F/6HR |         |
| 0.1°C Ti-0.10 Mn-0.053 Be | 41.8   | 43.9     | 41.8   | 44.4     |         |
|                           | 42.5   | 43.4     | 41.7   | 44.5     |         |
| Average                   | 42.1   | 43.6     | 41.8   | 44.5     | 43.0    |
| 0.07 Ti-0.00 Mn-0.04 Be   | 42.1   | 44.1     | 41.5   | 45.3     |         |
|                           | 41.6   | 43.5     | 41.8   | 44.0     |         |
| Average                   | 41.9   | 43.8     | 41.6   | 44.6     | 43.0    |
| 0.60 Mg                   | 40.7   | 44.6     | 42.8   | 45.4     |         |
|                           | 41.6   | 44.7     | 43.3   | 46.0     |         |
| Average                   | 41.2   | 44.7     | 43.1   | 45.7     | 43.7    |
| 0.56 Mg                   | 42.6   | 44.3     | 43.2   | 46.5     |         |
|                           | 41.2   | 43.5     | 42.4   | 45.4     |         |
|                           | 42.2   | -        | -  | 45.5     |         |
| Average                   | 42.0   | 43.9     | 42.8   | 45.8     | 43.6    |
| 7.41 Si                   | 42.2   | 44.9     | 41.8   | 44.3     |         |
|                           | 41.6   | 44.1     | 41.7   | 43.8     |         |
| Average                   | 41.9   | 44.5     | 41.8   | 44.0     | 43.0    |
| 6.53 Si                   | 42.1   | 44.6     | 42.5   | 44.8     |         |
|                           | 41.5   | 44.7     | 41.4   | 43.5     |         |
|                           | 41.1   | -        | -  | 43.0     |         |
| Average                   | 41.6   | 44.7     | 42.0   | 43.8     | 43.0    |
| 0.18 Fe                   | 42.9   | 45.3     | 44.0   | 44.6     |         |
|                           | 42.6   | 45.2     | 42.6   | 45.5     |         |
| Average                   | 42.8   | 45.2     | 43.3   | 45.0     | 44.1    |
| 0.00 Sr                   | 42.5   | 45.5     | 42.5   | 44.3     |         |
|                           | 42.5   | 45.5     | 43.5   | 44.4     |         |
| Average                   | 42.5   | 45.5     | 43.0   | 44.3     | 43.8    |
| Nominal                   | 41.9   | 42.1     | 41.4   | 44.4     |         |
|                           | 43.8   | 42.6     | 41.8   | 45.8     |         |
| Average                   | 42.8   | 42.4     | 41.6   | 45.1     | 43.0    |
| Average                   | 42.1   | 44.2     | 42.3   | 44.8     | 43.4    |

1) Other elements; mid-range of the specification

2) Fe chill; 1440F pour temperature

3) Cu chill; 1380F pour temperature

TABLE A4. EFFECT OF PROCESS VARIABLES ON YIELD STRENGTH OF D357-T6 OUTSIDE COMPOSITION SPECIFICATION

| COMPOSITION <sup>1</sup> | YIELD STRENGTH (ksi)                          |          |   |          | AVERAGE |
|--------------------------|---|----------|---|----------|---------|
|                          | AGE   |          | AGE   |          |         |
|                          | SLOW SOLIDIFICATION <sup>2</sup><br>315F/12HR | 335F/6HR | FAST SOLIDIFICATION <sup>3</sup><br>315F/12HR | 335F/6HR |         |
| 0.45Mg                   | 40.8  | 43.2     | 39.0  | 40.7     |         |
|                          | 39.4  | 42.4     | 38.8  | 41.4     |         |
| Average                  | 40.1  | 42.8     | 38.9  | 41.0     | 40.7    |
| 0.00Ti                   | 41.5  | 41.2     | 42.2  | 43.1     |         |
|                          | 42.1  | 42.4     | 41.9  | 43.3     |         |
| Average                  | 41.8  | 41.8     | 42.0  | 43.2     | 42.2    |
| 0.027Fe-0.0005Be         | 42.7  | 45.2     | 43.6  | 43.9     |         |
|                          | 42.9  | 44.6     | 41.9  | 44.9     |         |
| Average                  | 42.8  | 44.9     | 42.8  | 44.4     | 43.7    |
| Average                  | 41.6  | 43.2     | 41.2  | 42.9     | 42.2    |

1) Other elements; mid-range of the specification

2) Fe chill; 1440F pour temperature

3) Cu chill; 1380F temperature

TABLE A5. EFFECT OF PROCESS VARIABLES ON THE ELONGATION OF D357-T6 WITHIN COMPOSITION SPECIFICATION

| COMPOSITION <sup>1</sup> | ELONGATION (%)                                       |          |  |          | AVERAGE |
|--------------------------|--|----------|--|----------|---------|
|                          | AGE  |          | AGE  |          |         |
|                          | <u>SLOW SOLIDIFICATION</u> <sup>2</sup><br>315F/12HR | 335F/6HR | <u>FAST SOLIDIFICATION</u> <sup>3</sup><br>315F/12HR | 335F/6HR |         |
| 0.19Ti-0.10Mn-0.053Be    | 7.5  | -        | 8.5  | 8.5      |         |
|                          | 3.0  | 1.5      | 4.5  | 5.0      |         |
| Average                  | 5.2  | 1.5      | 6.5  | 6.8      | 5.0     |
| 0.07Ti-0.00Mn-0.04Be     | 3.5  | 5.5      | 3.0  | 12.0     |         |
|                          | 4.5  | 4.5      | 4.0  | 6.5      |         |
| Average                  | 4.0  | 5.0      | 3.5  | 9.2      | 5.4     |
| 0.60Mg                   | 6.0  | 6.0      | 7.0  | 7.5      |         |
|                          | 3.0  | 2.5      | 5.0  | 6.5      |         |
| Average                  | 4.5  | 4.2      | 6.0  | 7.0      | 5.4     |
| 0.56Mg                   | 6.5  | 6.0      | 10.5   | 8.0      |         |
|                          | 4.0  | 5.0      | 8.5  | 7.0      |         |
|                          | 3.4  | -        | -  | 5.9      |         |
| Average                  | 4.6  | 5.5      | 9.5  | 7.0      | 6.7     |
| 7.41Si                   | 5.0  | 3.5      | 10.5   | 9.0      |         |
|                          | 3.0  | 3.0      | 3.0  | 1.5      |         |
| Average                  | 4.0  | 3.2      | 6.8  | 5.2      | 4.8     |
| 6.53Si                   | 6.0  | 7.0      | 13.5   | 9.5      |         |
|                          | 6.0  | 5.0      | 4.5  | 4.0      |         |
|                          | 3.2  | -        | -  | 3.7      |         |
| Average                  | 5.1  | 6.0      | 9.0  | 5.7      | 6.5     |
| 0.13Fe                   | 3.5  | 3.5      | 7.0  | 9.5      |         |
|                          | 3.0  | 2.5      | 3.5  | 1.0      |         |
| Average                  | 3.2  | 3.0      | 5.2  | 5.2      | 4.2     |
| 0.00Sr                   | 3.5  | 2.0      | 8.0  | 6.0      |         |
|                          | 1.5  | 1.5      | 3.0  | 2.5      |         |
| Average                  | 2.5  | 1.8      | 5.5  | 4.2      | 3.5     |
| Nominal                  | 6.8  | 3.1      | 5.7  | 2.0      |         |
|                          | 4.9  | 5.1      | 4.9  | 5.3      |         |
| Average                  | 5.8  | 4.1      | 5.3  | 3.6      | 4.7     |
| Average                  | 4.3  | 3.8      | 6.4  | 6.0      | 5.1     |

1) Other elements; mid-range of the specification

2) Fe chill; 1440F pour temperature

3) Cu chill; 1380F pour temperature

TABLE A6. EFFECT OF PROCESS VARIABLES ON ELONGATION OF D357-T6 OUTSIDE COMPOSITION SPECIFICATION

| COMPOSITION <sup>1</sup> | ELONGATION (%)                                |          |   |          | AVERAGE |
|--------------------------|---|----------|---|----------|---------|
|                          | AGE   |          | AGE   |          |         |
|                          | SLOW SOLIDIFICATION <sup>2</sup><br>315F/12HR | 335F/6HR | FAST SOLIDIFICATION <sup>3</sup><br>315F/12HR | 335F/6HR |         |
| 0.45Mg                   | 11.5  | 6.1      | 14.4  | 4.3      |         |
|                          | 10.8  | 9.1      | 12.8  | 8.4      |         |
| Average                  | 11.2  | 7.6      | 13.6  | 6.3      | 9.7     |
| 0.00Ti                   | 5.2   | 2.7      | 6.3   | 5.9      |         |
|                          | 6.7   | 3.8      | 8.0   | 7.4      |         |
| Average                  | 6.0   | 3.2      | 7.2   | 6.7      | 5.8     |
| 0.027Fe-0.0005Be         | 10.9  | 5.2      | 11.4  | 2.8      |         |
|                          | 11.0  | 8.4      | 8.7   | 8.4      |         |
| Average                  | 10.9  | 6.8      | 10.1  | 5.6      | 8.3     |
| Average                  | 9.3   | 5.9      | 10.3  | 6.2      | 7.9     |

- 1) Other elements; mid-range of the specification  
 2) Fe chill; 1440F pour temperature  
 3) Cu chill; 1380F temperature

TABLE A7. EFFECT OF PROCESS VARIABLES ON THE NOTCHED TENSILE STRENGTH OF D357-T6 WITHIN COMPOSITION SPECIFICATION

| COMPOSITION <sup>1</sup> | NOTCHED TENSILE STRENGTH (ksi)                |          |   |          | AVERAGE |
|--------------------------|---|----------|---|----------|---------|
|                          | AGE   |          | AGE   |          |         |
|                          | SLOW SOLIDIFICATION <sup>2</sup><br>315F/12HR | 335F/6HR | EAST SOLIDIFICATION <sup>3</sup><br>315F/12HR | 335F/6HR |         |
| 0.19Ti-0.10Mn-0.053Be    | 52.2  | 48.7     | 56.4  | 56.6     |         |
|                          | 51.6  | 48.0     | 55.7  | 57.2     |         |
| Average                  | 51.9  | 48.4     | 56.0  | 56.9     | 53.3    |
| 0.07Ti-0.00Mn-0.04Be     | 56.7  | 55.0     | 55.5  | 57.9     |         |
|                          | 54.7  | 52.3     | 54.9  | 59.9     |         |
| Average                  | 55.7  | 53.6     | 55.2  | 58.9     | 55.9    |
| 0.60Mg                   | 51.5  | 53.1     | 56.4  | 57.4     |         |
|                          | 51.8  | 54.6     | 55.7  | 56.4     |         |
| Average                  | 51.6  | 53.9     | 56.0  | 56.9     | 54.6    |
| 0.56Mg                   | 48.9  | 51.6     | 58.1  | 59.4     |         |
|                          | 48.7  | 57.2     | 57.2  | 56.8     |         |
| Average                  | 48.8  | 54.4     | 57.7  | 58.1     | 54.7    |
| 7.41Si                   | 50.6  | 52.5     | 52.7  | 49.4     |         |
|                          | 51.6  | 52.0     | 53.3  | 50.6     |         |
| Average                  | 51.1  | 52.2     | 53.0  | 50.0     | 51.6    |
| 6.53Si                   | 49.4  | 48.8     | 55.3  | 56.3     |         |
|                          | 48.1  | 52.9     | 55.1  | 55.6     |         |
| Average                  | 48.8  | 50.8     | 55.2  | 56.0     | 52.7    |
| 0.18Fe                   | 53.3  | 47.8     | 53.8  | 50.5     |         |
|                          | 52.4  | 49.5     | 53.8  | 54.1     |         |
| Average                  | 52.8  | 48.6     | 53.8  | 52.3     | 51.9    |
| 0.00Sr                   | 53.2  | 42.2     | 44.4  | 42.9     |         |
|                          | 43.2  | 43.1     | 47.5  | 45.9     |         |
| Average                  | 43.2  | 42.7     | 46.0  | 44.4     | 44.1    |
| Nominal                  | 56.8  | 52.6     | 55.8  | 51.9     |         |
|                          | 55.0  | 52.1     | 55.9  | 47.7     |         |
| Average                  | 55.9  | 52.4     | 55.8  | 49.8     | 53.5    |
| Average                  | 51.1  | 50.8     | 54.3  | 53.7     | 52.5    |

1) Other elements; mid-range of the specification

2) Fe chill; 1440F pour temperature

3) Cu chill; 1380F pour temperature

TABLE A8. EFFECT OF PROCESS VARIABLES ON THE NOTCHED TENSILE STRENGTH OF D357-T6 OUTSIDE COMPOSITION SPECIFICATION

| COMPOSITION <sup>1</sup> | NOTCHED TENSILE STRENGTH (ksi)                       |          |  |          | AVERAGE |
|--------------------------|--|----------|--|----------|---------|
|                          | AGE  |          | AGE  |          |         |
|                          | <u>SLOW SOLIDIFICATION</u> <sup>2</sup><br>315F/12HR | 335F/6HR | <u>FAST SOLIDIFICATION</u> <sup>3</sup><br>315F/12HR | 335F/6HR |         |
| 0.45Mg                   | 58.7   | 54.7     | 55.4   | 50.7     |         |
|                          | 57.4   | 55.5     | 56.6   | 55.0     |         |
| Average                  | 58.0   | 55.1     | 56.0   | 52.9     | 55.5    |
| 0.00Ti                   | 53.1   | 46.4     | 52.5   | 53.5     |         |
|                          | 52.6   | 43.4     | 49.9   | 54.7     |         |
| Average                  | 52.9   | 44.9     | 51.2   | 54.1     | 50.8    |
| 0.027Fe-0.0005Be         | 61.7   | 56.3     | 57.7   | 53.6     |         |
|                          | 60.6   | 57.8     | 57.4   | 57.5     |         |
| Average                  | 61.2   | 57.0     | 57.5   | 58.0     | 58.5    |
| Average                  | 57.4   | 52.4     | 54.9   | 55.0     | 54.9    |

1) Other elements; mid-range of the specification

2) Fe chill; 1440F pour temperature

3) Cu chill; 1380F temperature

TABLE A9. EFFECT OF PROCESS VARIABLES ON THE NTS/TYS RATIO OF D357-T6 WITHIN COMPOSITION SPECIFICATION

| COMPOSITION <sup>1</sup> | NTS/TYS RATIO  |          |  |          | AVERAGE |
|--------------------------|--|----------|--|----------|---------|
|                          | AGE  |          | AGE  |          |         |
|                          | <u>SLOW SOLIDIFICATION</u> <sup>2</sup><br>315F/12HR | 335F/6HR | <u>FAST SOLIDIFICATION</u> <sup>3</sup><br>315F/12HR | 335F/6HR |         |
| 0.19Ti-0.10Mn-0.053Bc    | 1.25   | 1.11     | 1.35   | 1.27     |         |
|                          | 1.21   | 1.11     | 1.34   | 1.29     |         |
| Average                  | 1.23   | 1.11     | 1.34   | 1.28     | 1.24    |
| 0.07Ti-0.00Mn-0.04Bc     | 1.35   | 1.25     | 1.34   | 1.28     |         |
|                          | 1.31   | 1.20     | 1.31   | 1.36     |         |
| Average                  | 1.33   | 1.22     | 1.33   | 1.32     | 1.30    |
| 0.60Mg                   | 1.27   | 1.19     | 1.31   | 1.26     |         |
|                          | 1.25   | 1.22     | 1.29   | 1.23     |         |
| Average                  | 1.26   | 1.21     | 1.30   | 1.25     | 1.25    |
| 0.56Mg                   | 1.15   | 1.16     | 1.34   | 1.28     |         |
|                          | 1.18   | 1.31     | 1.35   | 1.25     |         |
| Average                  | 1.16   | 1.24     | 1.35   | 1.26     | 1.25    |
| 7.41Si                   | 1.20   | 1.17     | 1.26   | 1.12     |         |
|                          | 1.24   | 1.18     | 1.28   | 1.16     |         |
| Average                  | 1.22   | 1.17     | 1.27   | 1.14     | 1.20    |
| 6.53Si                   | 1.17   | 1.09     | 1.30   | 1.26     |         |
|                          | 1.16   | 1.18     | 1.33   | 1.28     |         |
| Average                  | 1.17   | 1.14     | 1.32   | 1.27     | 1.22    |
| 0.18Fe                   | 1.24   | 1.06     | 1.22   | 1.13     |         |
|                          | 1.23   | 1.10     | 1.26   | 1.19     |         |
| Average                  | 1.24   | 1.08     | 1.24   | 1.16     | 1.18    |
| 0.00Sr                   | 1.02   | 0.93     | 1.04   | 0.97     |         |
|                          | 1.02   | 0.95     | 1.09   | 1.03     |         |
| Average                  | 1.02   | 0.94     | 1.07   | 1.00     | 1.01    |
| Nominal                  | 1.36   | 1.25     | 1.35   | 1.17     |         |
|                          | 1.26   | 1.22     | 1.34   | 1.04     |         |
| Average                  | 1.31   | 1.24     | 1.34   | 1.11     | 1.25    |
| Average                  | 1.21   | 1.15     | 1.28   | 1.20     | 1.21    |

- 1) Other elements; mid-range of the specification  
 2) Fe chill; 1440F pour temperature  
 3) Cu chill; 1380F pour temperature

TABLE A10. EFFECT OF PROCESS VARIABLES ON THE NTS/TYS RATIO OF D357-T6 OUTSIDE COMPOSITION SPECIFICATION

| COMPOSITION <sup>1</sup> | NTS/TYS RATIO  |          |  |          | AVERAGE |
|--------------------------|--|----------|--|----------|---------|
|                          | AGE  |          | AGE  |          |         |
|                          | <u>SLOW SOLIDIFICATION</u> <sup>2</sup><br>315F/12HR | 335F/6HR | <u>FAST SOLIDIFICATION</u> <sup>3</sup><br>315F/12HR | 335F/6HR |         |
| 0.45Mg                   | 1.44   | 1.27     | 1.42   | 1.25     |         |
|                          | 1.46   | 1.31     | 1.46   | 1.33     |         |
| Average                  | 1.45   | 1.29     | 1.44   | 1.29     | 1.37    |
| 0.00Ti                   | 1.28   | 1.13     | 1.24   | 1.24     |         |
|                          | 1.25   | 1.02     | 1.19   | 1.26     |         |
| Average                  | 1.26   | 1.07     | 1.22   | 1.25     | 1.20    |
| 0.027Fe-0.0005Be         | 1.44   | 1.25     | 1.32   | 1.33     |         |
|                          | 1.41   | 1.30     | 1.37   | 1.28     |         |
| Average                  | 1.43   | 1.27     | 1.35   | 1.31     | 1.34    |
| Average                  | 1.38   | 1.21     | 1.33   | 1.28     | 1.30    |

1) Other elements; mid-range of the specification

2) Fe chill; 1440F pour temperature

3) Cu chill; 1380F temperature

TABLE A11. EFFECT OF PROCESS VARIABLES ON THE FATIGUE LIFE OF D357-T6 WITHIN COMPOSITION SPECIFICATION

| COMPOSITION <sup>1</sup> | FATIGUE LIFE (CYCLES TO FAILURE)*             |          |   |          | AVERAGE |
|--------------------------|---|----------|---|----------|---------|
|                          | AGE   |          | AGE   |          |         |
|                          | SLOW SOLIDIFICATION <sup>2</sup><br>315F/12HR | 335F/6HR | FAST SOLIDIFICATION <sup>3</sup><br>315F/12HR | 335F/6HR |         |
| 0.19Ti-0.10Mn-0.053Be    | 135809  | 131993   | 266713  | 248401   | 149223  |
|                          | 70317   | 81367    | 110664  | 199227   |         |
|                          | --  | --       | 244896  | --       |         |
| Log Average              | 97722   | 103633   | 193349  | 222459   |         |
| 0.07Ti-0.00Mn-0.04Be     | 134390  | 95497    | 157622  | 129575   | 165251  |
|                          | 210300  | 195147   | 168357  | 307069   |         |
|                          | 169113  | 136513   | 162901  | 199470   |         |
| Log Average              | 169113  | 136513   | 162901  | 199470   |         |
| 0.60Mg                   | 91589   | 138636   | 612997  | 414731   | 150463  |
|                          | 66727   | 74555    | 227710  | 73997    |         |
|                          | --  | --       | --  | 146970   |         |
| Log Average              | 78175   | 101666   | 373611  | 164884   |         |
| 0.56Mg                   | 147835  | 84636    | 573030  | 634933   | 252449  |
|                          | 142523  | 87737    | 671856  | 431329   |         |
|                          | 145154  | 86172    | 620478  | 523321   |         |
| Log Average              | 145154  | 86172    | 620478  | 523321   |         |
| 7.41Si                   | 55629   | 90454    | 61153   | 43679    | 75519   |
|                          | 77129   | 38451    | 209015  | 76517    |         |
|                          | --  | --       | 125333  | --       |         |
| Log Average              | 65502   | 58974    | 117009  | 57811    |         |
| 6.53Si                   | 106671  | 183851   | 100145  | 69402    | 104042  |
|                          | 83548   | 93809    | 106207  | 121013   |         |
|                          | 94404   | 131327   | 103131  | 91643    |         |
| Log Average              | 94404   | 131327   | 103131  | 91643    |         |
| 0.18Fe                   | 67594   | 80450    | 73759   | 304864   | 118240  |
|                          | 71749   | 88287    | 158423  | 402408   |         |
|                          | --  | --       | 91485   | --       |         |
| Log Average              | 69640   | 84277    | 102249  | 350256   |         |
| 0.00Sr                   | 41127   | 60504    | 56235   | 103076   | 99183   |
|                          | 67121   | 92936    | 164092  | 60872    |         |
|                          | --  | --       | 1019540                                       | --       |         |
| Log Average              | 52540   | 74986    | 175362  | 79224    |         |
| Nominal                  | 66881   | 61351    | 40848   | 48123    | 50663   |
|                          | 47787   | 71954    | 39361   | 39762    |         |
|                          | 56533   | 66441    | 40097   | 43743    |         |
| Log Average              | 56533   | 66441    | 40097   | 43743    |         |
| Log Average              | 85275   | 90396    | 156214  | 143842   | 117354  |

\* Specimen with a hole;  $K_t=2.42$ , 20 ksi net maximum stress

1) Other elements; mid-range of the specification

2) Fe chill; 1440F pour temperature

3) Cu chill; 1380F pour temperature

TABLE A12. EFFECT OF PROCESS VARIABLES ON THE FATIGUE LIFE OF D357-T6 OUTSIDE COMPOSITION SPECIFICATION

| COMPOSITION <sup>1</sup> | FATIGUE LIFE (CYCLES TO FAILURE*)                    |          |  |          | AVERAGE |
|--------------------------|--|----------|--|----------|---------|
|                          | AGE  |          | AGE  |          |         |
|                          | <u>SLOW SOLIDIFICATION</u> <sup>2</sup><br>315F/12HR | 335F/6HR | <u>FAST SOLIDIFICATION</u> <sup>3</sup><br>315F/12HR | 335F/6HR |         |
| 0.45Mg                   | 77984  | 53464    | 83258  | 61960    |         |
|                          | 77769  | 64874    | 92214  | 49888    |         |
| Log Average              | 77876  | 58893    | 87621  | 55597    | 68751   |
| 0.00Ti                   | 81977  | 71298    | 42198  | 74891    |         |
|                          | 74162  | 41332    | 74501  | 67000    |         |
| Log Average              | 77971  | 54285    | 56069  | 70835    | 64032   |
| 0.027Fe-0.0005Be         | 73279  | 62341    | 46169  | 52650    |         |
|                          | 91157  | 85196    | 60064  | 54739    |         |
| Log Average              | 81730  | 72878    | 52660  | 53684    | 64058   |
| Log Average              | 79172  | 61533    | 63719  | 59573    | 65577   |

\* Specimen with a hole;  $K_t=2.42$ , 20 ksi net maximum stress

1) Other elements; mid-range of the specification

2) Fe chill; 1440F pour temperature

3) Cu chill; 1380F temperature

APPENDIX B  
PHASE I, TASK 2  
B201-T7 SCREENING TEST DATA

TABLE B1. EFFECT OF PROCESS VARIABLES ON THE ULTIMATE TENSILE STRENGTH OF B201-T7 WITHIN COMPOSITION SPECIFICATION

| COMPOSITION <sup>1</sup> | ULTIMATE TENSILE STRENGTH (ksi)              |          |  |          | AVERAGE |
|--------------------------|--|----------|--|----------|---------|
|                          | AGE  |          | AGE  |          |         |
|                          | SLOW SOLIDIFICATION <sup>2</sup><br>360F/8HR | 380F/5HR | FAST SOLIDIFICATION <sup>3</sup><br>360F/8HR | 380F/5HR |         |
| 0.35Ti-0.43Mn            | 65.7   | 63.4     | 63.5   | 62.5     |         |
|                          | 62.9   | 59.4     | 66.4   | 62.3     |         |
| Average                  | 64.3   | 61.4     | 65.0   | 62.4     | 63.3    |
| 0.19Ti-0.24Mn            | 65.5   | 65.1     | 66.1   | 64.2     |         |
|                          | 67.4   | 66.1     | 66.1   | 66.3     |         |
| Average                  | 66.5   | 65.6     | 66.1   | 65.2     | 65.8    |
| 4.95Cu-0.98Ag-0.32Mg     | 70.9   | 68.6     | 69.0   | 69.9     |         |
|                          | 69.3   | 70.1     | 70.5   | 68.5     |         |
| Average                  | 70.1   | 69.3     | 69.8   | 69.2     | 69.6    |
| 4.65Cu-0.57Ag-0.26Mg     | 64.4   | 65.4     | 64.4   | 65.4     |         |
|                          | 66.1   | 63.9     | 65.8   | 62.1     |         |
| Average                  | 65.2   | 64.7     | 65.1   | 63.8     | 64.7    |
| 0.041Fe-0.043Si          | 64.1   | 58.0     | 64.8   | 60.8     |         |
|                          | 64.9   | 61.9     | 63.8   | 59.9     |         |
| Average                  | 64.5   | 60.0     | 64.3   | 60.3     | 62.3    |
| Nominal                  | 57.9   | 58.3     | 72.0   | 70.8     |         |
|                          | 62.9   | 61.0     | 70.5   | 68.3     |         |
| Average                  | 60.4   | 59.6     | 71.2   | 69.5     | 65.2    |
| Average                  | 65.2   | 63.4     | 66.9   | 65.1     | 65.1    |

1) Other elements; mid-range of the specification

2) Fe chill; 1450F pour temperature

3) Cu chill; 1350F pour temperature

TABLE B2. EFFECT OF PROCESS VARIABLES ON THE ULTIMATE TENSILE STRENGTH OF B201-T7 OUTSIDE COMPOSITION SPECIFICATION

| COMPOSITION <sup>1</sup> | ULTIMATE TENSILE STRENGTH (ksi)                     |          |   |          | AVERAGE |
|--------------------------|---|----------|---|----------|---------|
|                          | AGE   |          | AGE   |          |         |
|                          | <u>SLOW SOLIDIFICATION</u> <sup>2</sup><br>360F/8HR | 380F/5HR | <u>FAST SOLIDIFICATION</u> <sup>3</sup><br>360F/8HR | 380F/5HR |         |
| 0.052Ti                  | 68.1  | 66.4     | 69.1  | 66.7     |         |
|                          | 69.1  | 67.9     | 69.0  | 68.4     |         |
| Average                  | 68.6  | 67.2     | 69.0  | 67.6     | 68.1    |
| 5.25Cu-1.45Ag-0.43Mg     | 77.8  | 76.1     | 78.0  | 75.5     |         |
|                          | 71.0  | 72.0     | 76.9  | 76.4     |         |
| Average                  | 74.4  | 74.0     | 77.5  | 76.0     | 75.5    |
| Average                  | 71.5  | 70.6     | 73.2  | 71.8     | 71.8    |

1) Other elements; mid-range of the specification

2) Fe chill; 1450F pour temperature

3) Cu chill; 1350F temperature

TABLE B3. EFFECT OF PROCESS VARIABLES ON THE YIELD STRENGTH OF B201-T7 WITHIN COMPOSITION SPECIFICATION

| COMPOSITION <sup>1</sup> | YIELD STRENGTH (ksi)                         |          |  |          | AVERAGE |
|--------------------------|--|----------|--|----------|---------|
|                          | AGE  |          | AGE  |          |         |
|                          | SLOW SOLIDIFICATION <sup>2</sup><br>360F/8HR | 380F/5HR | FAST SOLIDIFICATION <sup>3</sup><br>360F/8HR | 380F/5HR |         |
| 0.35Ti-0.43Mn            | 58.7   | 56.0     | 57.0   | 54.8     |         |
|                          | 59.6   | 56.3     | 60.1   | 57.3     |         |
| Average                  | 59.2   | 56.1     | 58.5   | 56.0     | 57.5    |
| 0.19Ti-0.24Mn            | 60.1   | 59.3     | 60.1   | 57.9     |         |
|                          | 61.9   | 60.4     | 60.5   | 60.2     |         |
| Average                  | 61.0   | 59.8     | 60.3   | 59.0     | 60.0    |
| 4.95Cu-0.98Ag-0.32Mg     | 66.1   | 62.6     | 62.9   | 64.0     |         |
|                          | 63.6   | 64.3     | 64.7   | 62.4     |         |
| Average                  | 64.8   | 63.5     | 63.8   | 63.2     | 63.8    |
| 4.65Cu-0.57Ag-0.26Mg     | 57.4   | 58.2     | 57.0   | 58.0     |         |
|                          | 59.7   | 56.5     | 59.2   | 54.7     |         |
| Average                  | 58.5   | 57.4     | 58.1   | 56.4     | 57.6    |
| 0.041Fe-0.043Si          | 59.1   | 55.7     | 59.7   | 54.2     |         |
|                          | 59.0   | 55.4     | 57.7   | 56.9     |         |
| Average                  | 59.0   | 55.5     | 58.7   | 55.5     | 57.2    |
| Nominal                  | 57.3   | 57.2     | 65.4   | 63.3     |         |
|                          | 62.1   | 59.4     | 59.9   | 60.8     |         |
| Average                  | 59.7   | 58.3     | 62.7   | 62.0     | 60.7    |
| Average                  | 60.4   | 58.4     | 60.4   | 58.7     | 59.5    |

1) Other elements; mid-range of the specification

2) Fe chill; 1450F pour temperature

3) Cu chill; 1350F pour temperature

TABLE B4. EFFECT OF PROCESS VARIABLES ON THE YIELD STRENGTH OF B201-T7 OUTSIDE COMPOSITION SPECIFICATION

| COMPOSITION <sup>1</sup> | YIELD STRENGTH (ksi)                                |          |   |          | AVERAGE |
|--------------------------|---|----------|---|----------|---------|
|                          | AGE   |          | AGE   |          |         |
|                          | <u>SLOW SOLIDIFICATION</u> <sup>2</sup><br>360F/8HR | 380F/5HR | <u>FAST SOLIDIFICATION</u> <sup>3</sup><br>360F/8HR | 380F/5HR |         |
| 0.052Ti                  | 63.5  | 61.7     | 64.0  | 61.8     |         |
|                          | 64.4  | 63.1     | 64.2  | 63.2     |         |
| Average                  | 64.0  | 62.4     | 64.1  | 62.5     | 63.2    |
| 5.25Cu-1.45Ag-0.43Mg     | 74.0  | 70.8     | 73.1  | 69.4     |         |
|                          | 71.0  | 69.4     | 71.7  | 70.3     |         |
| Average                  | 72.5  | 70.1     | 72.4  | 69.8     | 71.2    |
| Average                  | 68.2  | 66.2     | 68.2  | 66.2     | 57.2    |

1) Other elements; mid-range of the specification

2) Fe chill; 1450F pour temperature

3) Cu chill; 1350F temperature

TABLE B5. EFFECT OF PROCESS VARIABLES ON THE ELONGATION OF R201-T7 WITHIN COMPOSITION SPECIFICATION

| COMPOSITION <sup>1</sup> | ELONGATION (%)                                      |                  |   |          | AVERAGE |
|--------------------------|---|------------------|---|----------|---------|
|                          | AGE   |                  | AGE   |          |         |
|                          | <u>SLOW SOLIDIFICATION</u> <sup>2</sup><br>360F/8HR | 380F/5HR         | <u>FAST SOLIDIFICATION</u> <sup>3</sup><br>360F/8HR | 380F/5HR |         |
| 0.35Ti-0.43Mn            | 11.3  | 7.5              | 12.0  | 1.3      |         |
|                          | 3.0   | 3.0              | 9.4   | 3.3      |         |
| Average                  | 7.2   | 5.2              | 10.7  | 2.3      | 6.3     |
| 0.19Ti-0.24Mn            | 6.0   | 5.3              | 10.7  | 10.6     |         |
|                          | 6.4   | 6.9              | 8.6   | 8.4      |         |
| Average                  | 6.2   | 6.1              | 9.6   | 9.5      | 7.9     |
| 4.95Cu-0.98Ag-0.32Mg     | 3.3   | 6.5              | 9.9   | 6.8      |         |
|                          | 5.5   | 5.5              | 7.5   | 7.8      |         |
| Average                  | 4.4   | 6.0              | 8.7   | 7.3      | 6.6     |
| 4.65Cu-0.57Ag-0.26Mg     | 8.3   | 8.5              | 11.5  | 8.4      |         |
|                          | 6.1   | 9.0              | 7.5   | 11.0     |         |
| Average                  | 7.2   | 8.8              | 9.5   | 9.7      | 8.8     |
| 0.041Fe-0.043Si          | 4.1   | 2.0              | 6.3   | 12.0     |         |
|                          | 10.0  | 9.3              | 10.9  | 2.5      |         |
| Average                  | 7.0   | 5.7              | 8.6   | 7.2      | 7.1     |
| Nominal                  | 0.3   | 0.4              | 8.7   | 7.8      |         |
|                          | 0.4   | 0.6              | 10.0  | 8.7      |         |
| Average                  | 0.3   | 0.5              | 9.3   | 8.2      | 4.6     |
| Average                  | 6.4 <sup>4</sup>                                    | 6.3 <sup>4</sup> | 9.4   | 7.4      | 6.9     |

1) Other elements; mid-range of the specification

2) Fe chill; 1450F pour temperature

3) Cu chill; 1350F pour temperature

4) Data for the nominal composition variant were not used to compute the average value because they were below the minimum specification value.

TABLE B6. EFFECT OF PROCESS VARIABLES ON ELONGATION OF B201-T7  
OUTSIDE COMPOSITION SPECIFICATION

| COMPOSITION <sup>1</sup> | ELONGATION (%)                                      |          |   |          | AVERAGE |
|--------------------------|---|----------|---|----------|---------|
|                          | AGE   |          | AGE   |          |         |
|                          | <u>SLOW SOLIDIFICATION</u> <sup>2</sup><br>360F/8HR | 380F/5HR | <u>FAST SOLIDIFICATION</u> <sup>3</sup><br>360F/8HR | 380F/5HR |         |
| 0.052Ti                  | 2.9   | 2.7      | 3.5   | 3.1      |         |
|                          | 3.2   | 3.1      | 3.0   | 3.1      |         |
| Average                  | 3.0   | 2.9      | 3.2   | 3.1      | 3.1     |
| 5.25Cu-1.45Ag-0.43Mg     | 2.8   | 3.8      | 5.0   | 6.3      |         |
|                          | 0.1   | 0.9      | 6.4   | 4.4      |         |
| Average                  | 1.4   | 2.4      | 5.7   | 5.3      | 3.7     |
| Average                  | 2.2   | 2.6      | 4.5   | 4.2      | 3.4     |

1) Other elements; mid-range of the specification

2) Fe chill; 1450F pour temperature

3) Cu chill; 1350F temperature

TABLE B7. EFFECT OF PROCESS VARIABLES ON THE NOTCHED TENSILE STRENGTH OF B201-T7 WITHIN COMPOSITION SPECIFICATION

| COMPOSITION <sup>1</sup> | NOTCHED TENSILE STRENGTH (ksi)                      |          |   |          | AVERAGE |
|--------------------------|---|----------|---|----------|---------|
|                          | AGE   |          | AGE   |          |         |
|                          | <u>SLOW SOLIDIFICATION</u> <sup>2</sup><br>360F/8HR | 380F/5HR | <u>EAST SOLIDIFICATION</u> <sup>3</sup><br>360F/8HR | 380F/5HR |         |
| 0.35Ti-0.43Mn            | 89.0  | 85.2     | 89.8  | 86.1     |         |
|                          | 81.9  | 83.3     | 92.6  | 89.6     |         |
| Average                  | 85.5  | 84.2     | 91.2  | 87.8     | 87.2    |
| 0.19Ti-0.24Mn            | 89.1  | 86.1     | 91.0  | 89.8     |         |
|                          | 85.5  | 88.4     | 92.8  | 91.2     |         |
| Average                  | 87.3  | 87.2     | 91.9  | 90.5     | 89.2    |
| 4.95Cu-0.98Ag-0.32Mg     | 82.0  | 84.2     | 86.6  | 92.9     |         |
|                          | 80.3  | 83.6     | 85.5  | 89.8     |         |
| Average                  | 81.2  | 83.9     | 86.0  | 91.3     | 85.6    |
| 4.65Cu-0.57Ag-0.26Mg     | 82.0  | 80.8     | 89.5  | 90.5     |         |
|                          | 84.4  | 81.0     | 88.5  | 86.9     |         |
| Average                  | 83.2  | 80.9     | 89.0  | 88.7     | 85.5    |
| 0.041Fe-0.043Si          | 87.4  | 80.7     | 88.5  | 84.1     |         |
|                          | 90.5  | 67.2     | 91.5  | 66.3     |         |
| Average                  | 89.0  | 74.0     | 90.0  | 75.2     | 82.0    |
| Nominal                  | 84.9  | 70.0     | 97.1  | 89.7     |         |
|                          | 81.7  | 86.6     | 97.5  | 92.1     |         |
| Average                  | 83.3  | 78.3     | 97.3  | 90.9     | 87.5    |
| Average                  | 84.9  | 81.4     | 90.9  | 87.4     | 86.2    |

1) Other elements; mid-range of the specification

2) Fe chill; 1450F pour temperature

3) Cu chill; 1350F pour temperature

TABLE B8. EFFECT OF PROCESS VARIABLES ON THE NOTCHED TENSILE STRENGTH OF B201-T7 OUTSIDE COMPOSITION SPECIFICATION

| COMPOSITION <sup>1</sup> | NOTCHED TENSILE STRENGTH (ksi)               |          |  |          | AVERAGE |
|--------------------------|--|----------|--|----------|---------|
|                          | AGE  |          | AGE  |          |         |
|                          | SLOW SOLIDIFICATION <sup>2</sup><br>360F/8HR | 380F/5HR | FAST SOLIDIFICATION <sup>3</sup><br>360F/8HR | 380F/5HR |         |
| 0.052Ti                  | 74.9   | 73.0     | 70.5   | 73.4     |         |
|                          | 74.3   | 70.7     | 70.9   | 75.1     |         |
| Average                  | 74.6   | 71.8     | 70.7   | 74.2     | 72.8    |
| 5.25Cu-1.45Ag-0.43Mg     | 76.3   | 80.4     | 88.6   | 88.0     |         |
|                          | 82.4   | 75.3     | 90.8   | 83.1     |         |
| Average                  | 79.3   | 77.8     | 89.7   | 85.5     | 83.1    |
| Average                  | 77.0   | 74.8     | 80.2   | 79.9     | 78.0    |

1) Other elements; mid-range of the specification

2) Fe chill; 1450F pour temperature

3) Cu chill; 1350F temperature

TABLE B9. EFFECT OF PROCESS VARIABLES ON THE NTS/TYS RATIO OF B201-T7 WITHIN COMPOSITION SPECIFICATION

| COMPOSITION <sup>1</sup> | NTS/TYS RATIO                                |          |  |          | AVERAGE |
|--------------------------|--|----------|--|----------|---------|
|                          | AGE  |          | AGE  |          |         |
|                          | SLOW SOLIDIFICATION <sup>2</sup><br>360F/8HR | 380F/5HR | FAST SOLIDIFICATION <sup>3</sup><br>360F/8HR | 380F/5HR |         |
| 0.35Ti-0.43Mn            | 1.52   | 1.52     | 1.58   | 1.57     |         |
|                          | 1.37   | 1.48     | 1.54   | 1.56     |         |
| Average                  | 1.45   | 1.50     | 1.56   | 1.57     | 1.52    |
| 0.19Ti-0.24Mn            | 1.48   | 1.45     | 1.51   | 1.55     |         |
|                          | 1.38   | 1.46     | 1.53   | 1.51     |         |
| Average                  | 1.43   | 1.46     | 1.52   | 1.53     | 1.49    |
| 4.95Cu-0.98Ag-0.32Mg     | 1.24   | 1.35     | 1.38   | 1.45     |         |
|                          | 1.26   | 1.30     | 1.32   | 1.44     |         |
| Average                  | 1.25   | 1.32     | 1.35   | 1.45     | 1.34    |
| 4.65Cu-0.57Ag-0.26Mg     | 1.43   | 1.39     | 1.57   | 1.56     |         |
|                          | 1.41   | 1.43     | 1.49   | 1.59     |         |
| Average                  | 1.42   | 1.41     | 1.53   | 1.57     | 1.48    |
| 0.041Fe-0.043Si          | 1.48   | 1.45     | 1.48   | 1.55     |         |
|                          | 1.53   | 1.21     | 1.59   | 1.17     |         |
| Average                  | 1.51   | 1.33     | 1.53   | 1.36     | 1.43    |
| Nominal                  | 1.48   | 1.22     | 1.48   | 1.42     |         |
|                          | 1.31   | 1.45     | 1.62   | 1.51     |         |
| Average                  | 1.40   | 1.34     | 1.55   | 1.47     | 1.44    |
| Average                  | 1.43   | 1.40     | 1.51   | 1.49     | 1.45    |

1) Other elements; mid-range of the specification

2) Fe chill; 1450F pour temperature

3) Cu chill; 1350F pour temperature

TABLE B10. EFFECT OF PROCESS VARIABLES ON THE NTS/TYS OF B201-T7  
OUTSIDE COMPOSITION SPECIFICATION

| COMPOSITION <sup>1</sup> | NTS/TYS RATIO                                       |          |   |          | AVERAGE |
|--------------------------|---|----------|---|----------|---------|
|                          | AGE   |          | AGE   |          |         |
|                          | <u>SLOW SOLIDIFICATION</u> <sup>2</sup><br>360F/8HR | 380F/5HR | <u>FAST SOLIDIFICATION</u> <sup>3</sup><br>360F/8HR | 380F/5HR |         |
| 0.052Ti                  | 1.18  | 1.18     | 1.10  | 1.19     |         |
|                          | 1.15  | 1.12     | 1.10  | 1.19     |         |
| Average                  | 1.17  | 1.15     | 1.10  | 1.19     | 1.15    |
| 5.25Cu-1.45Ag-0.43Mg     | 1.03  | 1.14     | 1.21  | 1.27     |         |
|                          | 1.16  | 1.09     | 1.27  | 1.18     |         |
| Average                  | 1.09  | 1.12     | 1.24  | 1.23     | 1.17    |
| Average                  | 1.13  | 1.10     | 1.17  | 1.21     | 1.16    |

1) Other elements; mid-range of the specification

2) Fe chill; 1450F pour temperature

3) Cu chill; 1350F temperature

TABLE B11. EFFECT OF PROCESS VARIABLES ON THE FATIGUE LIFE OF B201-T7 WITHIN COMPOSITION SPECIFICATION

| COMPOSITION <sup>1</sup> | FATIGUE LIFE (CYCLES TO FAILURE)*                   |          |   |          | AVERAGE |
|--------------------------|---|----------|---|----------|---------|
|                          | AGE   |          | AGE   |          |         |
|                          | <u>SLOW SOLIDIFICATION</u> <sup>2</sup><br>360F/8HR | 380F/5HR | <u>FAST SOLIDIFICATION</u> <sup>3</sup><br>360F/8HR | 380F/5HR |         |
| 0.35Ti-0.43Mn            | 118032  | 144753   | 159147  | 475005   |         |
|                          | 177770  | 197633   | 113992  | 162192   |         |
| Log Average              | 144853  | 169138   | 134690  | 278179   | 173968  |
| 0.19Ti-0.24Mn            | 172189  | 403233   | 137642  | 133775   |         |
|                          | 183772  | 127497   | 261575  | 168576   |         |
|                          | -   | 1011030  | -   | -        |         |
| Log Average              | 177886  | 373198   | 189746  | 150170   | 222480  |
| 4.95Cu-0.98Ag-0.32Mg     | 147014  | 119081   | 119938  | 134751   |         |
|                          | 167095  | 34902    | 130781  | 127740   |         |
|                          | --  | 81132    | -   | -        |         |
| Log Average              | 156733  | 150009   | 125242  | 131198   | 141255  |
| 4.65Cu-0.57Ag-0.26Mg     | 123856  | 135611   | 159771  | 108156   |         |
|                          | 112963  | 139320   | 135178  | 117470   |         |
| Log Average              | 118284  | 137452   | 146960  | 112716   | 128105  |
| 0.041Fe-0.043Si          | 106883  | 126074   | 169080  | 125960   |         |
|                          | 346870  | 112366   | 148472  | 118180   |         |
|                          | 86411   | -        | -   | -        |         |
| Log Average              | 147417  | 119022   | 158441  | 122008   | 136962  |
| Nominal                  | 83649   | 71734    | 95457   | 1743370  |         |
|                          | 161968  | 69234    | 54057   | 76568    |         |
| Average                  | 116397  | 70472    | 71833   | 365337   | 121131  |
| Average                  | 142405  | 159123   | 132264  | 173712   | 151184  |

\* Specimen with a hole;  $K_t=2.42$ , 25 ksi net maximum stress

1) Other elements; mid-range of the specification

2) Fe chill; 1450F pour temperature

3) Cu chill; 1350F pour temperature

TABLE B12. EFFECT OF PROCESS VARIABLES ON THE FATIGUE LIFE OF B201-T7 OUTSIDE COMPOSITION SPECIFICATION

| COMPOSITION <sup>1</sup> | FATIGUE LIFE (CYCLES TO FAILURE)*            |          |  |          | AVERAGE |
|--------------------------|--|----------|--|----------|---------|
|                          | AGE  |          | AGE  |          |         |
|                          | SLOW SOLIDIFICATION <sup>2</sup><br>360F/8HR | 380F/5HR | FAST SOLIDIFICATION <sup>3</sup><br>360F/8HR | 380F/5HR |         |
| 0.052Ti                  | 76458  | 58444    | 69116  | 161791   |         |
|                          | 235933                                       | 39379    | 58318  | 53447    |         |
| Log Average              | 134309                                       | 47973    | 63487  | 92990    | 78534   |
| 5.25Cu-1.45Ag-0.43Mg     | 91816  | 86690    | 166953                                       | 53267    |         |
|                          | 72883  | 32807    | 66554  | 115787   |         |
| Log Average              | 81803  | 53329    | 105410                                       | 78534    | 77521   |
| Log Average              | 104818                                       | 50580    | 81806  | 85457    | 78018   |

\* Specimen with a hole;  $K_t=2.42$ , 25 ksi net maximum stress

1) Other elements; mid-range of the specification

2) Fe chill; 1450F pour temperature

3) Cu chill; 1350F temperature

APPENDIX C  
PHASE I, TASK 2  
D357-T6 VERIFICATION TEST DATA

TABLE C1. D357-T6 TENSILE PROPERTIES--FOUNDRY A

| QUENCH  | PLATE THICKNESS (INCH) | PLATE NO. | UTS (ksi) | YS (ksi) | EI (%) | NTS (ksi) | <u>NTS</u><br><u>YS</u> |
|---------|------------------------|-----------|-----------|----------|--------|-----------|-------------------------|
| Water   | 0.75                   | V100      | 56.1      | 48.3     | 7.4    | 61.6      | 1.28                    |
|         |                        |           | 56.1      | 47.6     | 8.6    | 64.1      | 1.35                    |
|         |                        | V101      | 54.8      | 43.9     | 8.4    | 63.1      | 1.44                    |
|         |                        |           | 52.4      | 44.1     | 3.1    | 65.0      | 1.47                    |
|         |                        | V102      | 55.0      | 45.2     | 10.0   | 65.3      | 1.44                    |
|         |                        |           | 55.6      | 44.2     | 10.2   | 65.8      | 1.49                    |
|         | 1.25                   | V110      | 53.7      | 46.7     | 4.2    | 58.3      | 1.25                    |
|         |                        |           | 54.4      | 46.9     | 5.4    | 57.8      | 1.23                    |
|         |                        | V111      | 53.4      | 44.9     | 5.7    | 68.0      | 1.51                    |
|         |                        |           | 53.0      | 46.1     | 4.9    | 65.7      | 1.43                    |
|         |                        | V112      | 54.3      | 44.9     | 7.1    | 65.8      | 1.47                    |
|         |                        |           | 53.0      | 44.7     | 5.7    | 66.9      | 1.50                    |
|         |                        | V113      | 54.8      | 44.0     | 8.5    | 63.2      | 1.44                    |
|         |                        |           | 53.2      | 45.2     | 5.7    | 62.0      | 1.37                    |
| V114    | 54.4                   | 44.1      | 8.2       | 61.0     | 1.38   |           |                         |
|         | 51.2                   | 45.1      | 3.5       | 61.9     | 1.37   |           |                         |
| Glycol  |                        | V115      | 51.6      | 42.3     | 5.8    | 57.2      | 1.35                    |
|         |                        |           | 51.1      | 42.5     | 5.5    | 57.8      | 1.36                    |
|         |                        | V116      | 53.3      | 43.6     | 9.0    | 56.7      | 1.30                    |
|         |                        |           | 52.2      | 43.0     | 5.6    | 56.6      | 1.32                    |
|         |                        | V117      | 54.5      | 44.4     | 7.7    | 58.5      | 1.32                    |
|         |                        |           | 52.9      | 43.5     | 6.0    | 58.5      | 1.34                    |
| Average |                        | WQ-0.75"  | 55.0      | 45.6     | 7.9    | 64.2      | 1.31                    |
|         |                        | WQ-1.25"  | 53.5      | 45.3     | 5.9    | 63.1      | 1.39                    |
|         |                        | GQ-1.25"  | 52.6      | 43.2     | 6.6    | 57.6      | 1.33                    |

Note: WQ = Water Quench  
GQ = Glycol Quench

TABLE C2. D357-T6 TENSILE PROPERTIES--FOUNDRY B

| QUENCH  | PLATE THICKNESS (INCH) | PLATE NO.   | UTS (ksi) | YS (ksi) | EI (%) | NTS (ksi) | <u>NTS</u><br><u>YS</u> |
|---------|------------------------|-------------|-----------|----------|--------|-----------|-------------------------|
| Water   | 0.75                   | V200        | 53.1      | 46.1     | 4.5    | 57.6      | 1.25                    |
|         |                        |             | 53.4      | 44.7     | 6.2    | 61.6      | 1.38                    |
|         |                        | V201        | 52.1      | 44.5     | 4.1    | 68.4      | 1.54                    |
|         |                        |             | 51.1      | 45.1     | 2.3    | 64.9      | 1.44                    |
|         |                        | V202        | 52.2      | 44.9     | 3.6    | 65.4      | 1.46                    |
|         |                        |             | 51.5      | 45.2     | 2.4    | 64.3      | 1.42                    |
|         | 1.25                   | V205        | 52.8      | 45.8     | 4.6    | 59.6      | 1.30                    |
|         |                        |             | 52.0      | 44.9     | 4.3    | 59.8      | 1.33                    |
|         |                        | V206 *      | 50.2      | 44.5     | 2.1    | 63.3      | 1.42                    |
|         |                        |             | 52.0      | 44.8     | 4.2    | 63.8      | 1.42                    |
|         |                        | V207 *      | 50.7      | 44.4     | 3.0    | 64.2      | 1.45                    |
|         |                        |             | 49.6      | 44.2     | 1.5    | 62.6      | 1.42                    |
|         |                        | V208 *      | 52.0      | 45.2     | 3.7    | 62.2      | 1.38                    |
|         |                        |             | 50.8      | 44.8     | 2.3    | 63.9      | 1.43                    |
|         |                        | V209        | 51.9      | 45.1     | 4.0    | 60.8      | 1.35                    |
|         |                        |             | 53.1      | 45.3     | 5.4    | 62.3      | 1.38                    |
|         |                        | V210        | 53.2      | 45.7     | 5.6    | 63.1      | 1.38                    |
|         |                        |             | 51.3      | 45.5     | 3.0    | 64.2      | 1.41                    |
| Glycol  |                        | V211        | 49.4      | 41.4     | 4.3    | 58.4      | 1.41                    |
|         |                        |             | 48.8      | 41.8     | 3.3    | 57.6      | 1.38                    |
|         |                        | V212        | 49.7      | 42.2     | 3.6    | 57.9      | 1.37                    |
|         |                        |             | 48.8      | 42.6     | 2.6    | 58.4      | 1.37                    |
|         |                        | V213        | 47.7      | 41.5     | 2.5    | 56.0      | 1.35                    |
|         |                        |             | 48.8      | 41.3     | 3.9    | 57.0      | 1.38                    |
| Average |                        | WQ-0.75"    | 52.3      | 45.1     | 3.9    | 63.7      | 1.41                    |
|         |                        | WQ-1.25"*** | 52.4      | 45.4     | 4.5    | 61.6      | 1.36                    |
|         |                        | WQ-1.25"*   | 50.9      | 44.7     | 2.8    | 63.3      | 1.42                    |
|         |                        | GQ-1.25"    | 48.9      | 41.8     | 3.4    | 57.6      | 1.38                    |

\* Plates With Low Elongation; Not Used for DADT Evaluations.

\*\* Plates Within Specification

Note: WQ = Water Quench  
GQ = Glycol Quench

TABLE C3. D357-T6 TENSILE PROPERTIES-FOUNDRY C

| QUENCH  | PLATE THICKNESS (INCH) | PLATE NO. | UTS (ksi) | YS (ksi) | EI (%) | NTS (ksi) | <u>NTS</u><br><u>YS</u> |
|---------|------------------------|-----------|-----------|----------|--------|-----------|-------------------------|
| Water   | 0.75                   | V301      | 52.7      | 45.4     | 4.6    | -         | -                       |
|         |                        |           | 50.9      | 44.5     | 2.8    | -         | -                       |
|         |                        | V302      | 50.2      | 44.0     | 2.0    | -         | -                       |
|         |                        |           | 51.2      | 45.0     | 3.5    | -         | -                       |
|         | 1.25                   | VX301     | 54.3      | 47.8     | 5.5    | 48.5      | 1.02                    |
|         |                        |           | 54.3      | 47.5     | 6.4    | 50.0      | 1.05                    |
|         |                        | VX302     | 53.8      | 47.2     | 4.4    | 46.3      | 0.97                    |
|         |                        |           | 53.6      | 47.8     | 3.9    | 46.8      | 0.99                    |
|         |                        | VX304     | 53.2      | 46.5     | 4.3    | 60.8      | 1.32                    |
|         |                        | VX305     | 54.5      | 45.9     | 8.2    | 62.9      | 1.36                    |
| Glycol  |                        | VX310     | 51.2      | 43.8     | 4.8    | 42.9      | 0.99                    |
|         |                        |           | 50.5      | 43.3     | 4.6    | 46.6      | 1.07                    |
|         |                        | VX311     | 51.9      | 44.2     | 5.2    | 43.3      | 0.98                    |
| Average |                        | WQ-0.75"  | 51.2      | 44.7     | 3.2    | -         | -                       |
|         |                        | WQ-1.25"  | 54.0      | 47.1     | 5.4    | 52.5      | 1.12                    |
|         |                        | GQ-1.25"  | 51.2      | 43.8     | 4.9    | 44.3      | 1.01                    |

Note: The VX Plates Were Replacements for the First Batch of Plates, Which Had Very Low Ductility and Failed to Meet the AMS 4241 Specification.

TABLE C4. D357-T6 STRESS-LIFE SMOOTH FATIGUE DATA

| FOUNDRY | QUENCH MEDIUM | PLATE NO. | MAXIMUM STRESS (ksi) | CYCLES TO FAILURE       |                       |
|---------|---------------|-----------|----------------------|-------------------------|-----------------------|
| A       | Water         | V111      | 30                   | 4,069,170               |                       |
|         |               | V111      | 35                   | 220,706                 |                       |
|         |               | V110      | 40                   | 50,158                  |                       |
|         |               | V112      | 45                   | 50,058                  |                       |
|         | Glycol        | V117      | 20                   | 5.3 X 10 <sup>6</sup> * |                       |
|         |               | V115      | 30                   | 1,474,660               |                       |
|         |               | V116      | 40                   | 50,226                  |                       |
|         | B             | Water     | V205                 | 20                      | 6 X 10 <sup>6</sup> * |
|         |               |           | V210                 | 25                      | 223,358               |
|         |               |           | V205                 | 30                      | 213,719               |
| V205    |               |           | 40                   | 25,612                  |                       |
| V209    |               |           | 45                   | 13,822                  |                       |
| Glycol  |               | V213      | 20                   | 981,685                 |                       |
|         |               | V211      | 30                   | 254,149                 |                       |
|         |               | V212      | 40                   | 45,287                  |                       |
| C       |               | Water     | VX302                | 15                      | 5 X 10 <sup>6</sup> * |
|         | VX301         |           | 20                   | 1,569,360               |                       |
|         | VX302         |           | 30                   | 164,874                 |                       |
|         | VX301         |           | 30                   | 118,740                 |                       |
|         | VX301         |           | 40                   | 50,417                  |                       |
|         | VX301         |           | 40                   | 50,417                  |                       |
|         | Glycol        | VX311     | 10                   | 3 X 10 <sup>6</sup> *   |                       |
|         |               | VX310     | 20                   | 373,642                 |                       |
|         |               | VX311     | 20                   | 618,238                 |                       |
|         |               | VX310     | 30                   | 123,238                 |                       |
|         |               | VX311     | 30                   | 90,819                  |                       |
|         |               | VX310     | 30                   | 90,819                  |                       |
|         |               | VX310     | 40                   | 19,697                  |                       |

Note:  $K_t = 1.0$ ,  $R = 0.1$

\* No Failure

TABLE C5. D357-T6 NOTCHED STRESS-LIFE FATIGUE DATA

| FOUNDRY | PLATE NO. | MAXIMUM STRESS (ksi) | CYCLES TO FAILURE     |
|---------|-----------|----------------------|-----------------------|
| A       | V110      | 10                   | 5 X 10 <sup>6</sup> * |
|         | V110      | 12.5                 | 1,312,390             |
|         | V110      | 15                   | 201,421               |
|         | V110      | 25                   | 29,302                |
| B       | V208      | 10                   | 5 X 10 <sup>6</sup> * |
|         | V208      | 15                   | 173,113               |
|         | V208      | 20                   | 41,738                |
| C       | 301       | 10                   | 3 X 10 <sup>6</sup> * |
|         | 304       | 20                   | 191,190               |
|         | 305       | 30                   | 12,028                |

Note:  $K_t = 3.0$ ,  $R = 0.1$

\* No Failure

TABLE C6. D357-T6 STRAIN-LIFE FATIGUE DATA

| FOUNDRY | PL. TE NO. | LOG STRAIN AMPLITUDE | CYCLES TO FAILURE      |
|---------|------------|----------------------|------------------------|
| A       | V113       | -2.70                | 1.16 X 10 <sup>6</sup> |
|         | V114       | -2.60                | 198,539                |
|         | V112       | -2.52                | 78,838                 |
|         | V112       | -2.39                | 10,477                 |
|         | V111       | -2.30                | 2,134                  |
|         | V113       | -2.00                | 47                     |
| B       | V209       | -2.39                | 249,199                |
|         | V205       | -2.30                | 1,037                  |
|         | V210       | -2.09                | 59                     |
| C       | VX305      | -2.52                | 24,801                 |
|         | VX304      | -2.39                | 3,463                  |
|         | VX304      | -2.39                | 25,353                 |

Note:  $K_t = 1.0$ ,  $R = -1.0$ ,

TABLE C7. D357-T6 FRACTURE TOUGHNESS DATA

| FOUNDRY | PLATE NO. | KQ (ksi√in) | KIC (ksi√in) | KIV (ksi√in) |
|---------|-----------|-------------|--------------|--------------|
| A       | V110      | 23.2        | 21.0         | 22.7         |
|         | V111      | 26.2        |              | 26.7         |
|         | V115 *    |             |              | 21.5         |
| B       | V205      | 22.2        | 22.0         | 23.7         |
|         | V209      | 23.4        |              |              |
|         | V210      | 26.9        |              |              |
|         | V211 *    |             |              | 22.4         |
| C       | VX301     | 22.4        | 22.2         |              |
|         | VX302     | 23.4        |              |              |
|         | VX310 *   |             |              | 22.2         |
|         | VX311 *   |             |              | 22.1         |

\* Glycol Quenched; All Others Water Quenched

TABLE C8. DAS VALUES FOR D357-T6

| FOUNDRY | PLATE NO. | DAS (Inch x 10 <sup>-4</sup> ) |
|---------|-----------|--------------------------------|
| A       | V110      | 10                             |
|         | V111      | 16                             |
|         | V112      | 16                             |
|         | V113      | 10                             |
|         | V114      | 10                             |
|         | V115*     | 10                             |
|         | V116*     | 11                             |
|         | V117*     | 8                              |
| B       | V205      | 20                             |
|         | V206      | 17                             |
|         | V207      | 18                             |
|         | V208      | 19                             |
|         | V209      | 17                             |
|         | V210      | 16                             |
|         | V211*     | 10                             |
|         | V212*     | 14                             |
|         | V213*     | 14                             |
| C       | VX301     | 10                             |
|         | VX302     | 12                             |
|         | VX310*    | 13                             |
|         | VX311*    | 11                             |
| Average |           | 13                             |

\* Glycol Quenched

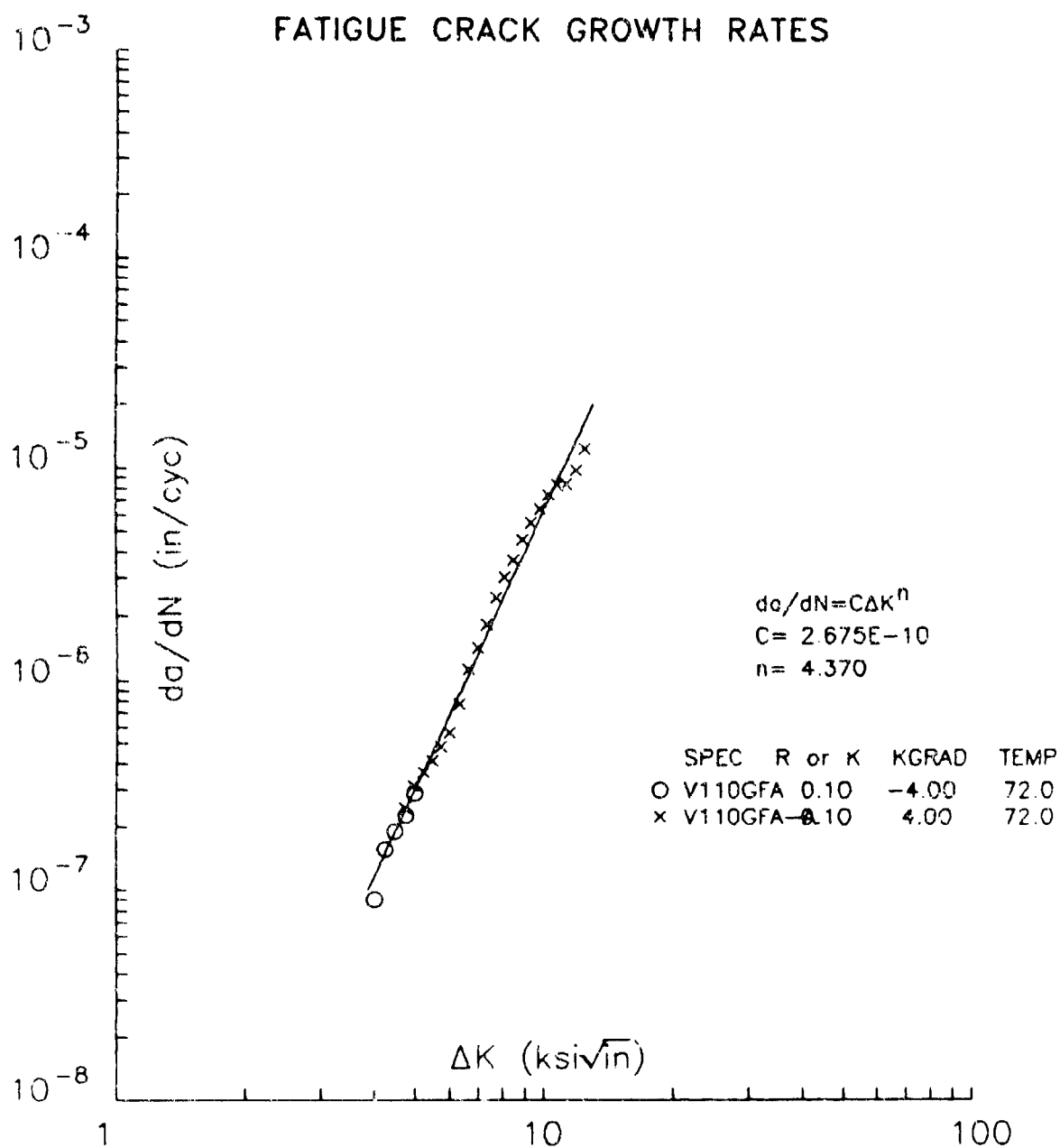


Figure C1. D357-T6 Fatigue Crack Growth Rate Data—Foundry A (Water Quench)

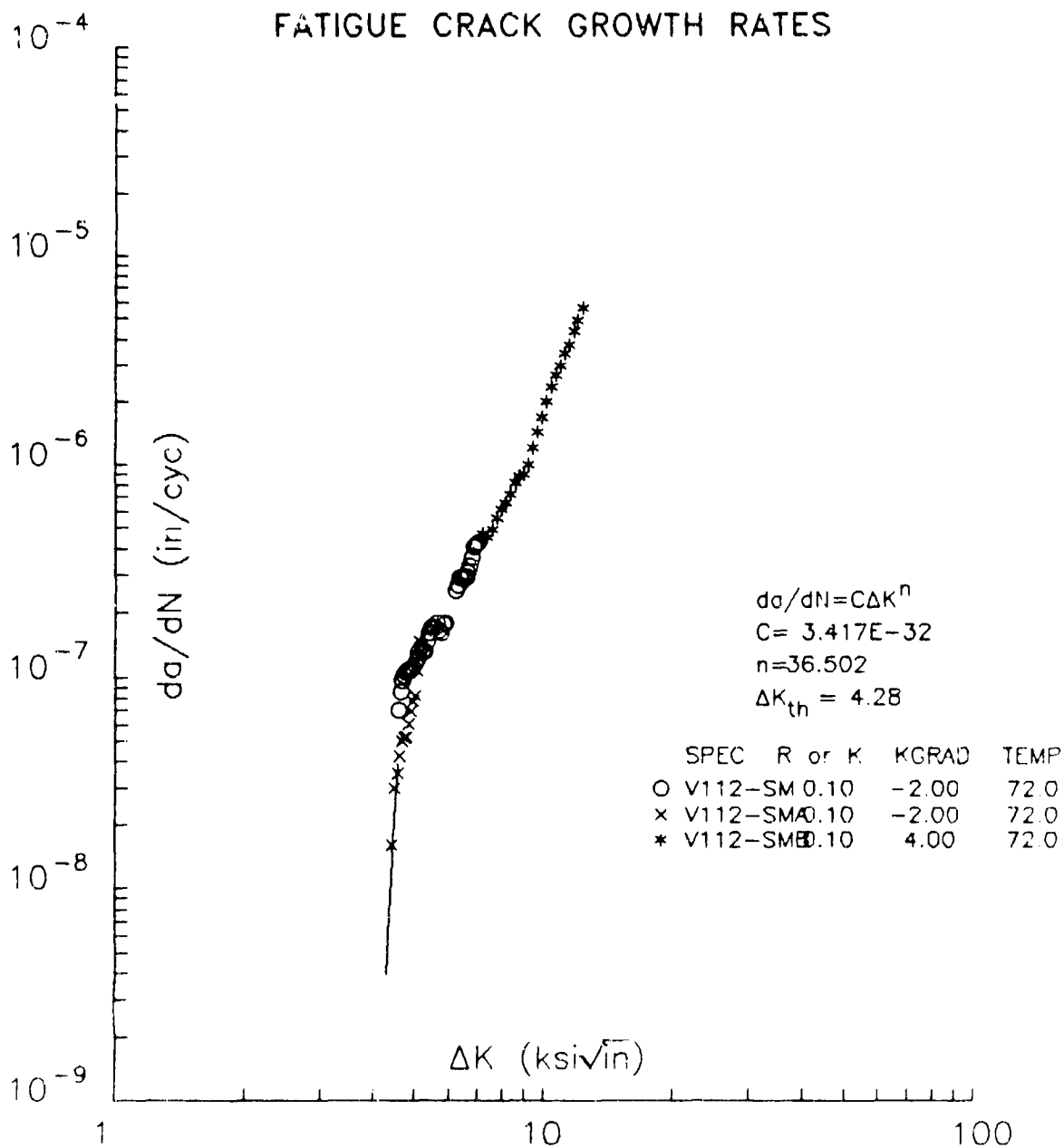


Figure C2. D357-T6 Fatigue Crack Growth Rate Data—Foundry A (Water Quench)

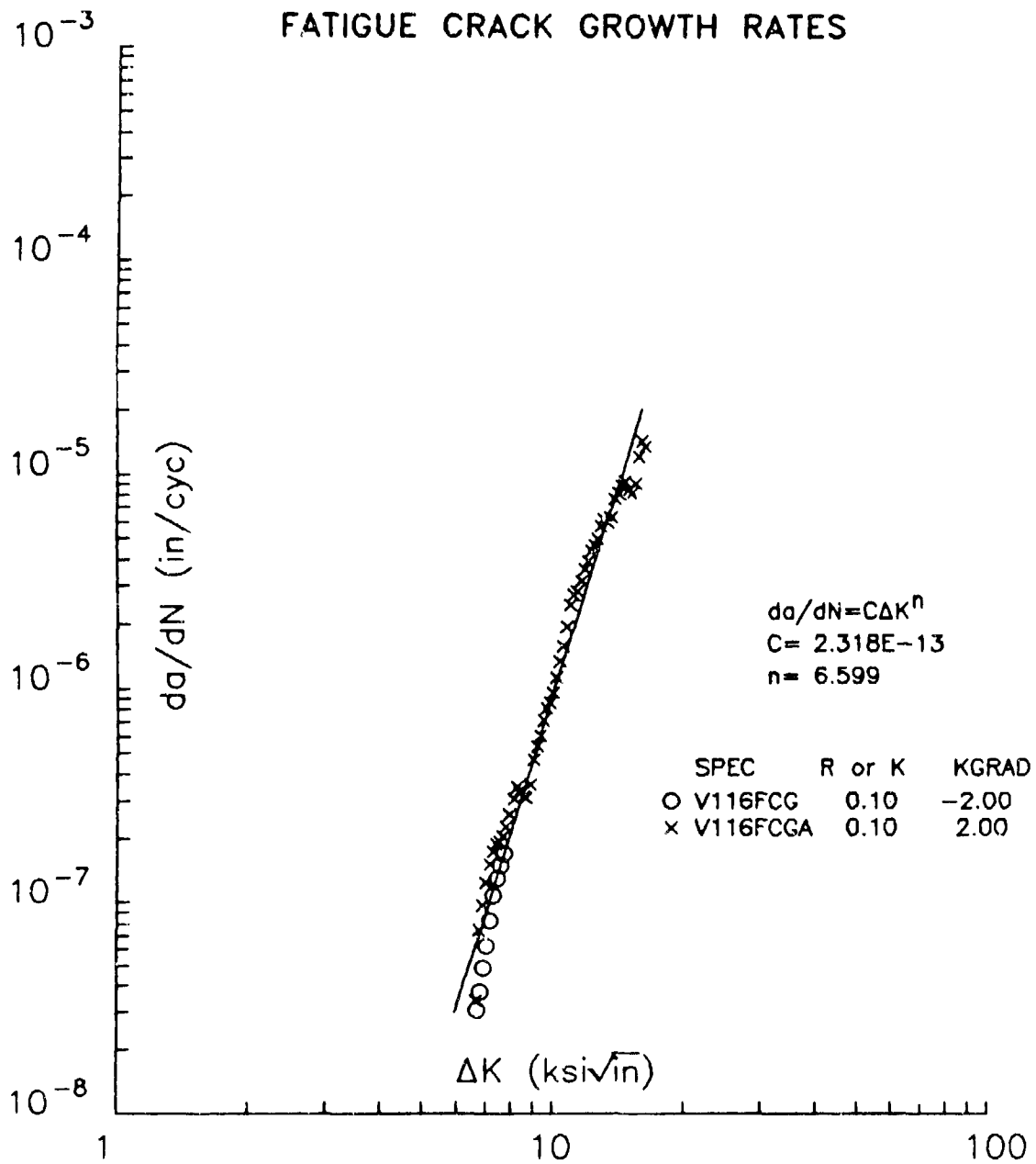


Figure C3. D357-T6 Fatigue Crack Growth Rate Data—Foundry A (Glycol Quench)

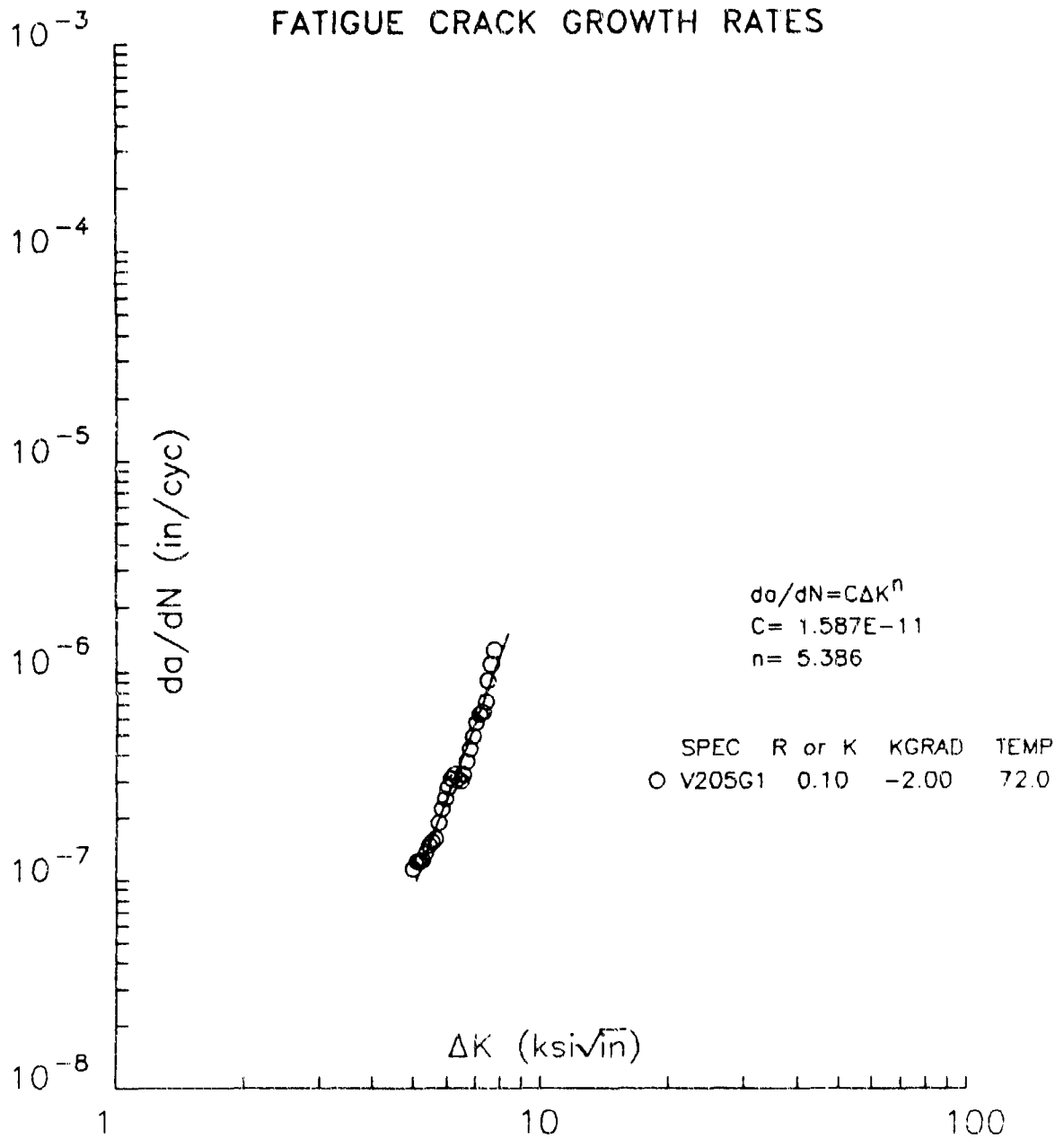


Figure C4. D357-T6 Fatigue Crack Growth Rate Data—Foundry B (Water Quench)

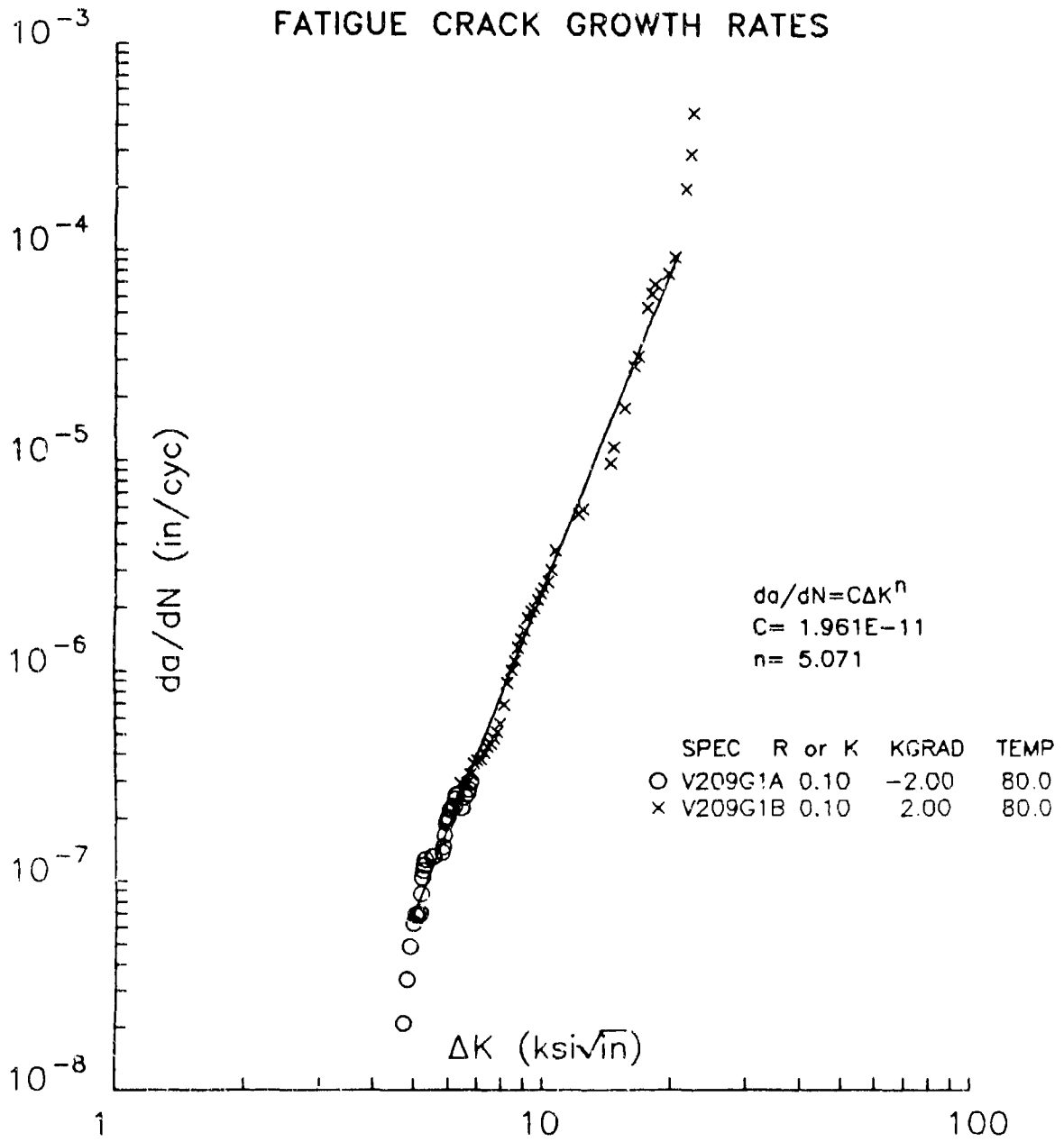


Figure C5. D357-T6 Fatigue Crack Growth Rate—Foundry B (Water Quench)

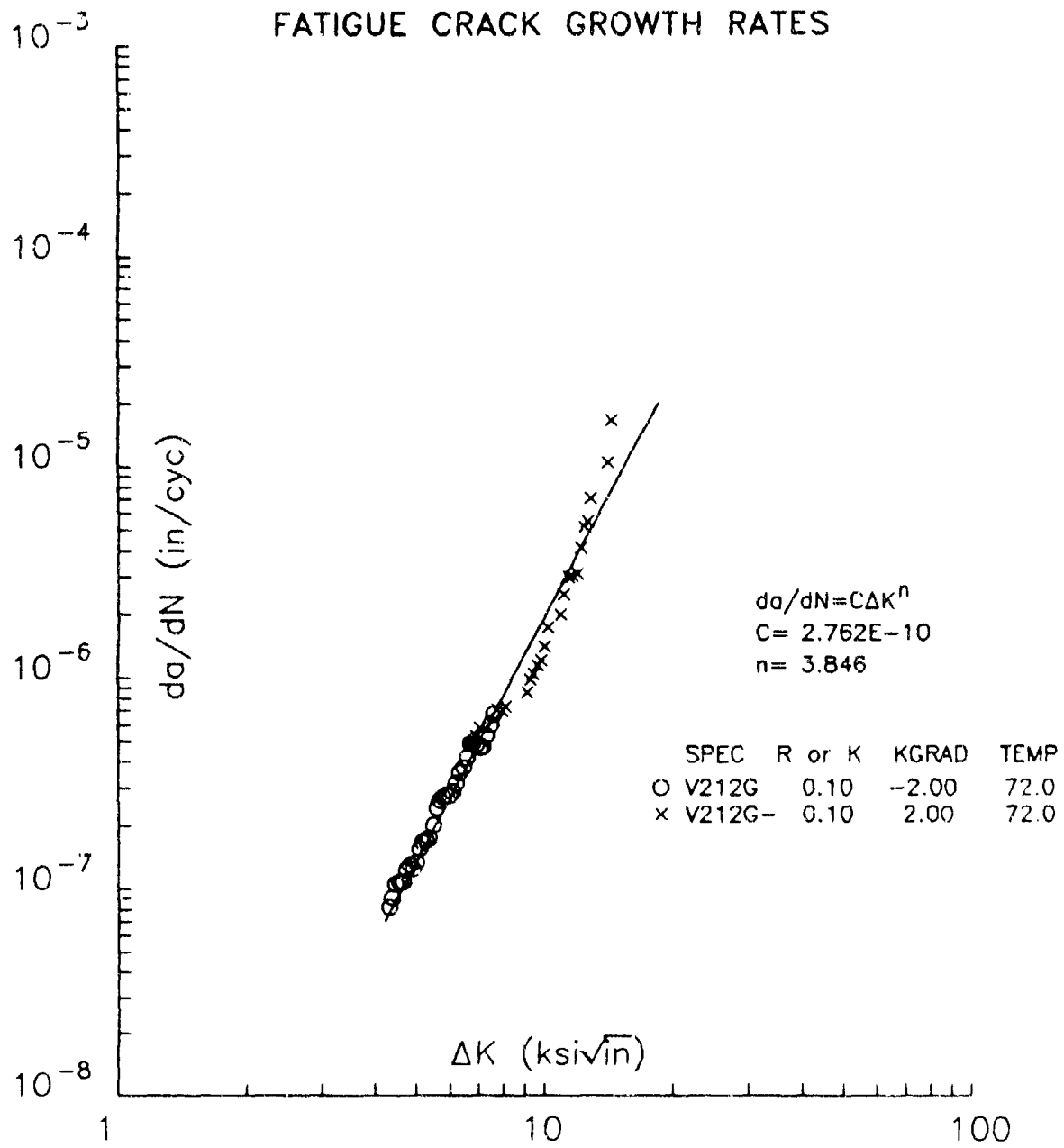


Figure C6. D357-T6 Fatigue Crack Growth Rate Data--Foundry B (Glycol Quench)

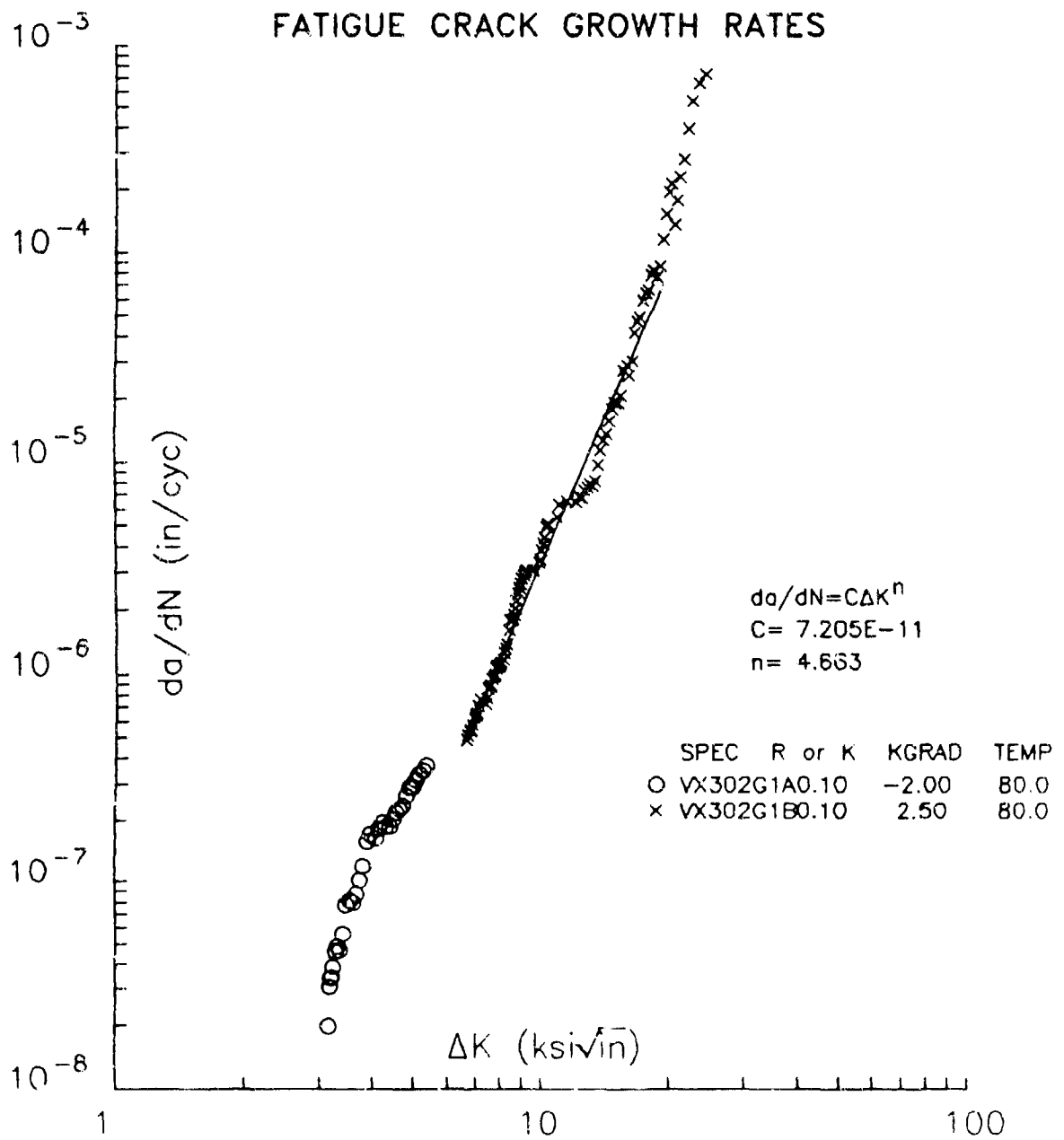


Figure C7. D357-T6 Fatigue Crack Growth Rate Data—Foundry C (Water Quench)

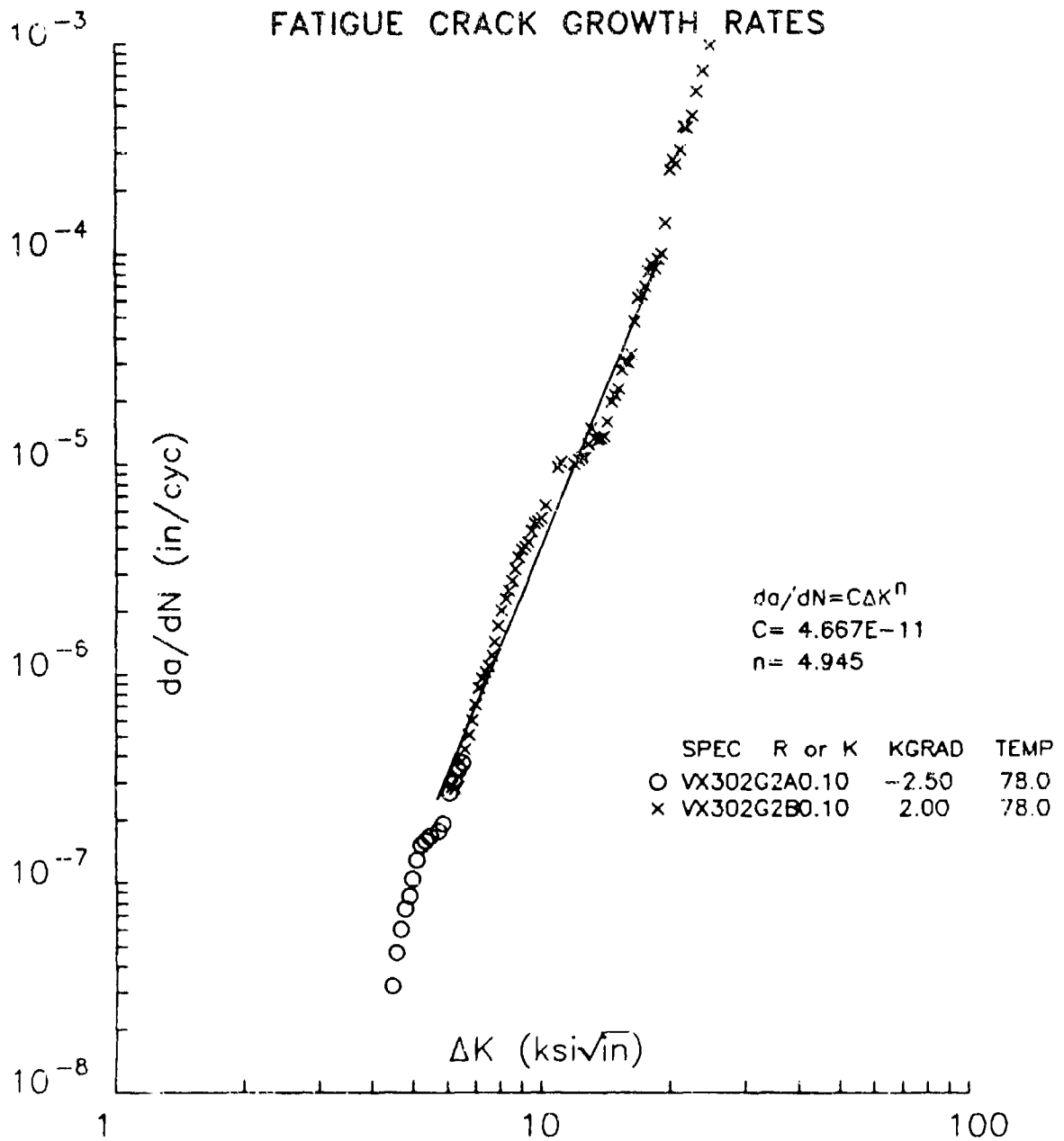


Figure C8. D357-T6 Fatigue Crack Growth Rate Data—Foundry C (Water Quench)

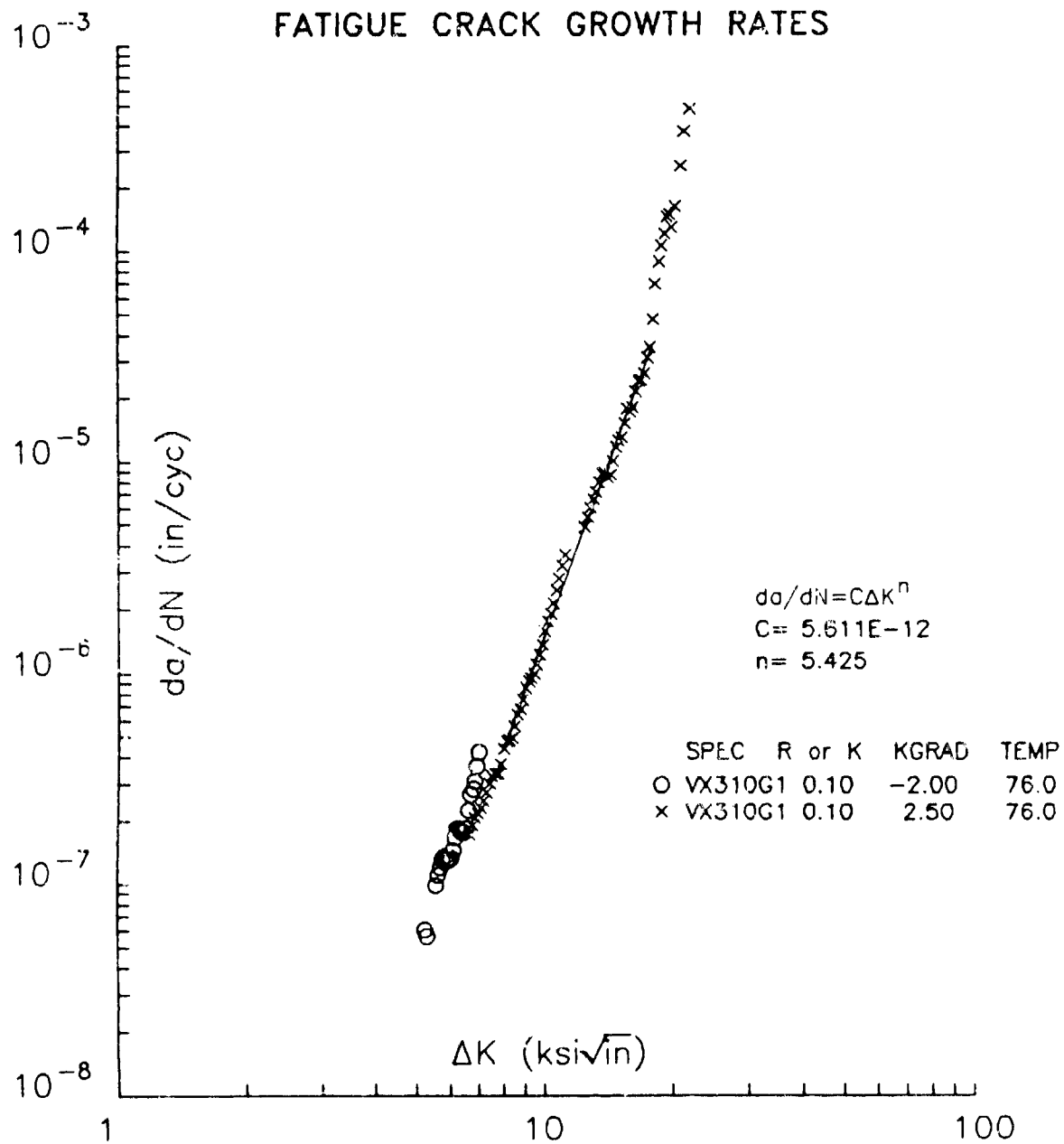


Figure C9. D357-T6 Fatigue Crack Growth Rate Data—Foundry C (Glycol Quench)

APPENDIX D  
PHASE I, TASK 2  
B201-T7 VERIFICATION TEST DATA

TABLE D1. B201-T7 TENSILE PROPERTIES—FOUNDRY A

| PLATE THICKNESS (INCH) | PLATE NO. | UTS (ksi) | YS (ksi) | EI (%) | NTS (ksi) | <u>NTS</u><br><u>YS</u> |
|------------------------|-----------|-----------|----------|--------|-----------|-------------------------|
| 0.75                   | V150      | 64.2      | 55.6     | 8.4    | 89.6      | 1.61                    |
|                        |           | 64.5      | 55.4     | 8.4    | 89.7      | 1.62                    |
| 1.25                   | V155      | 65.3      | 56.9     | 8.4    | 94.0      | 1.65                    |
|                        |           | 65.8      | 57.5     | 8.3    | 91.5      | 1.59                    |
|                        | V156      | 66.6      | 57.1     | 8.4    | 90.6      | 1.59                    |
|                        |           | 66.7      | 57.3     | 8.3    | 86.2      | 1.50                    |
|                        | V157      | 65.7      | 55.3     | 8.4    | 90.9      | 1.64                    |
|                        |           | 64.5      | 53.7     | 11.0   | 88.2      | 1.64                    |
|                        | V158      | 66.0      | 56.8     | 8.4    | 91.3      | 1.61                    |
|                        |           | 66.0      | 57.0     | 8.4    | 89.2      | 1.56                    |
| Average                | 0.75"     | 64.3      | 55.5     | 8.4    | 89.7      | 1.62                    |
|                        | 1.25"     | 65.8      | 56.5     | 8.7    | 90.2      | 1.59                    |

TABLE D2. B201-T7 TENSILE PROPERTIES-FOUNDRY B

| PLATE THICKNESS (INCH) | PLATE NO. | UTS (ksi) | YS (ksi) | $\epsilon$ (%) | NTS (ksi) | $\frac{NTS}{YS}$ |      |
|------------------------|-----------|-----------|----------|----------------|-----------|------------------|------|
| 0.75                   | V250      | 71.1      | 64.4     | 8.2            | 93.7      | 1.45             |      |
|                        |           | 70.0      | 62.9     | 11.0           | 92.8      | 1.48             |      |
|                        | V251      | 67.5      | 60.1     | 10.5           | 92.3      | 1.54             |      |
|                        |           | 68.5      | 61.6     | 8.9            | 91.5      | 1.49             |      |
|                        | V252      | 67.6      | 60.3     | 11.0           | 92.5      | 1.53             |      |
|                        |           | 69.1      | *        | 9.0            | 92.7      | *                |      |
|                        | V253      | 67.9      | 61.0     | 9.2            | 92.8      | 1.52             |      |
|                        |           | 68.5      | 60.9     | 10.7           | 90.8      | 1.49             |      |
|                        | V254      | 68.7      | 61.5     | 10.9           | 91.9      | 1.49             |      |
|                        |           | 70.0      | 63.3     | 8.8            | 96.6      | 1.53             |      |
|                        | 1.25      | V255      | 69.9     | 62.7           | 7.9       | 83.8             | 1.34 |
|                        |           |           | 69.4     | 62.2           | 8.4       | 79.2             | 1.27 |
|                        |           | V256      | 72.8     | 65.6           | 8.5       | 85.7             | 1.31 |
|                        |           |           | 73.1     | 66.0           | 8.0       | 83.9             | 1.27 |
| V257                   |           | 70.4      | 63.3     | 8.8            | 84.8      | 1.34             |      |
|                        |           | 71.3      | 64.5     | 8.8            | 87.4      | 1.36             |      |
| V258                   |           | 67.9      | 60.3     | 8.2            | 78.5      | 1.30             |      |
|                        |           | 68.9      | 61.0     | 8.0            | 84.3      | 1.38             |      |
| V259                   |           | 68.6      | 60.9     | 7.5            | 79.4      | 1.30             |      |
|                        |           | 67.7      | 60.1     | 7.9            | 79.2      | 1.32             |      |
| Average                | 0.75"     | 68.9      | 61.9     | 9.8            | 92.8      | 1.50             |      |
|                        | 1.25"     | 70.0      | 62.7     | 8.2            | 82.6      | 1.32             |      |

\* Extensometer slipped during test - data not available

TABLE D3. B201-T7 TENSILE PROPERTIES-FOUNDRY C

| PLATE THICKNESS (INCH) | PLATE NO. | UTS (ksi) | YS (ksi) | EI (%) | NTS (ksi) | <u>NTS</u><br>YS |
|------------------------|-----------|-----------|----------|--------|-----------|------------------|
| 0.75                   | V350      | 63.8      | 57.8     | 6.5    | 90.9      | 1.57             |
|                        |           | 69.2      | 61.6     | 7.0    | 90.3      | 1.47             |
| 1.25                   | V355      | 66.2      | 58.6     | 9.3    | 89.6      | 1.53             |
|                        |           | 69.3      | 62.0     | 6.9    | 91.0      | 1.47             |
|                        | V356      | 64.1      | 57.8     | 7.0    | 82.7      | 1.43             |
|                        |           | 69.0      | 61.5     | 9.0    | 89.4      | 1.45             |
|                        | V357      | 69.8      | 62.2     | 9.5    | 92.4      | 1.49             |
|                        | 69.7      | 62.0      | 8.9      | 93.7   | 1.51      |                  |
|                        | V358      | 64.3      | 58.2     | 6.5    | 89.6      | 1.54             |
|                        |           | 66.4      | 58.5     | 9.0    | 91.9      | 1.57             |
| Average                | 0.75"     | 66.5      | 59.7     | 6.8    | 90.6      | 1.52             |
|                        | 1.25"     | 67.4      | 60.1     | 8.3    | 90.0      | 1.50             |

TABLE D4. B201-T7 SMOOTH STRESS-LIFE FATIGUE DATA

| FOUNDRY | PLATE NO. | STRESS (ksi) | CYCLES TO FAILURE     |
|---------|-----------|--------------|-----------------------|
| A       | V158      | 20           | 5 X 10 <sup>6</sup> * |
|         | V155      | 30           | 5 X 10 <sup>6</sup> * |
|         | V156      | 40           | 186,703               |
|         | V157      | 45           | 308,543               |
| B       | V255      | 20           | 5 X 10 <sup>6</sup> * |
|         | V256      | 25           | 368,916               |
|         | V256      | 30           | 27,611                |
|         | V258      | 30           | 11,530                |
|         | V259      | 30           | 31,982                |
|         | V257      | 35           | 168,520               |
|         | V255      | 40           | 15,971                |
| C       | V358      | 15           | 5 X 10 <sup>6</sup> * |
|         | V356      | 20           | 1,180,170             |
|         | V357      | 20           | 573,648               |
|         | V355      | 30           | 167,652               |

Note:  $K_t = 1.0$ ,  $R = 0.1$

\* No Failure

TABLE D5. B201-T7 NOTCHED STRESS-LIFE FATIGUE DATA

| FOUNDRY | PLATE NO. | STRESS (ksi) | CYCLES TO FAILURE       |
|---------|-----------|--------------|-------------------------|
| A       | 156       | 25           | 112,825                 |
|         | 158       | 30           | 24,998                  |
| B       | 256       | 20           | 3.2 X 10 <sup>6</sup> * |
|         | 258       | 23           | 237,350                 |
|         | 258       | 27           | 59,632                  |
| C       | 356       | 30           | 16,737                  |
|         | 358       | 25           | 209,254                 |
|         | 358       | 20           | 2.2 X 10 <sup>6</sup> * |

Note:  $K_t = 3.0$ ,  $R = 0.1$

\* No Failure

TABLE D6. B201-T7 STRAIN-LIFE FATIGUE DATA

| FOUNDRY | PLATE NO. | LOG STRAIN AMPLITUDE | CYCLES TO FAILURE |
|---------|-----------|----------------------|-------------------|
| A       | V157      | -2.52                | 90,964            |
|         | V156      | -2.39                | 15,602            |
|         | V158      | -2.30                | 4,659             |
| B       | V257      | -2.60                | 93,835            |
|         | V255      | -2.52                | 54,284            |
|         | V258      | -2.39                | 22,785            |
|         | V259      | -2.30                | 5,130             |
| C       | V358      | -2.70                | 179,112           |
|         | V357      | -2.60                | 92,570            |
|         | V356      | -2.52                | 37,734            |
|         | V355      | -2.30                | 3,388             |
|         | V358      | -2.09                | 432               |

Note:  $K_t = 1.0$ ,  $R = -1.0$

TABLE D7. B201-T7 FRACTURE TOUGHNESS DATA

| FOUNDRY | PLATE NO. | KQ<br>(ksi√in) | KIV<br>(ksi√in) |
|---------|-----------|----------------|-----------------|
| A       | V155      | 46.0           | 55.7            |
|         | V156      | 39.4           | 40.8            |
| B       | V255      | 26.6           | 27.3            |
|         | V256      | 31.5           | 31.1            |
| C       | V355      | 48.8           | 42.9            |
|         | V355      |                | 40.7            |
|         | V356      | 45.6           | 44.4            |

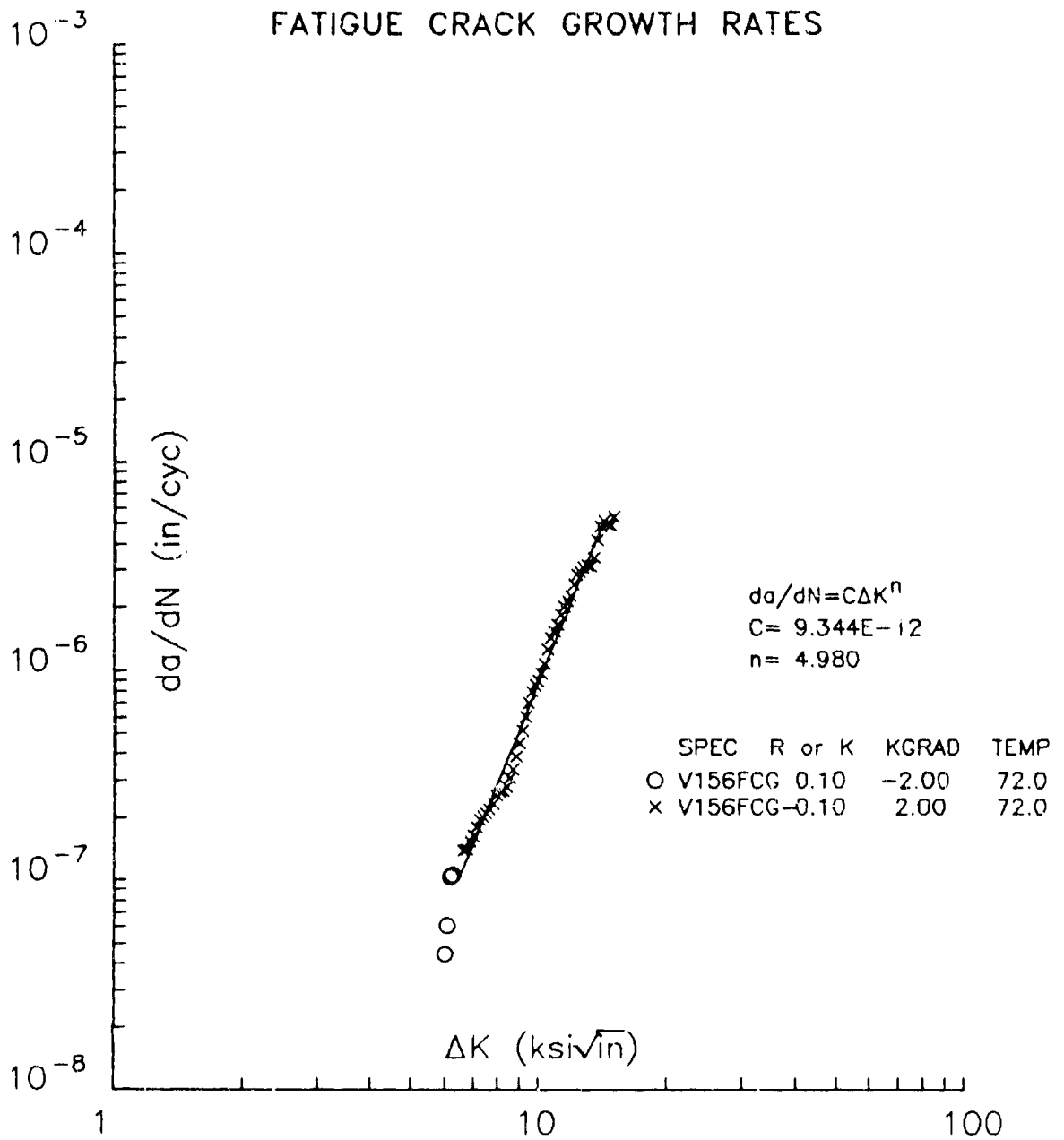


Figure D1. B201-T7 Fatigue Crack Growth Rate Data—Foundry A

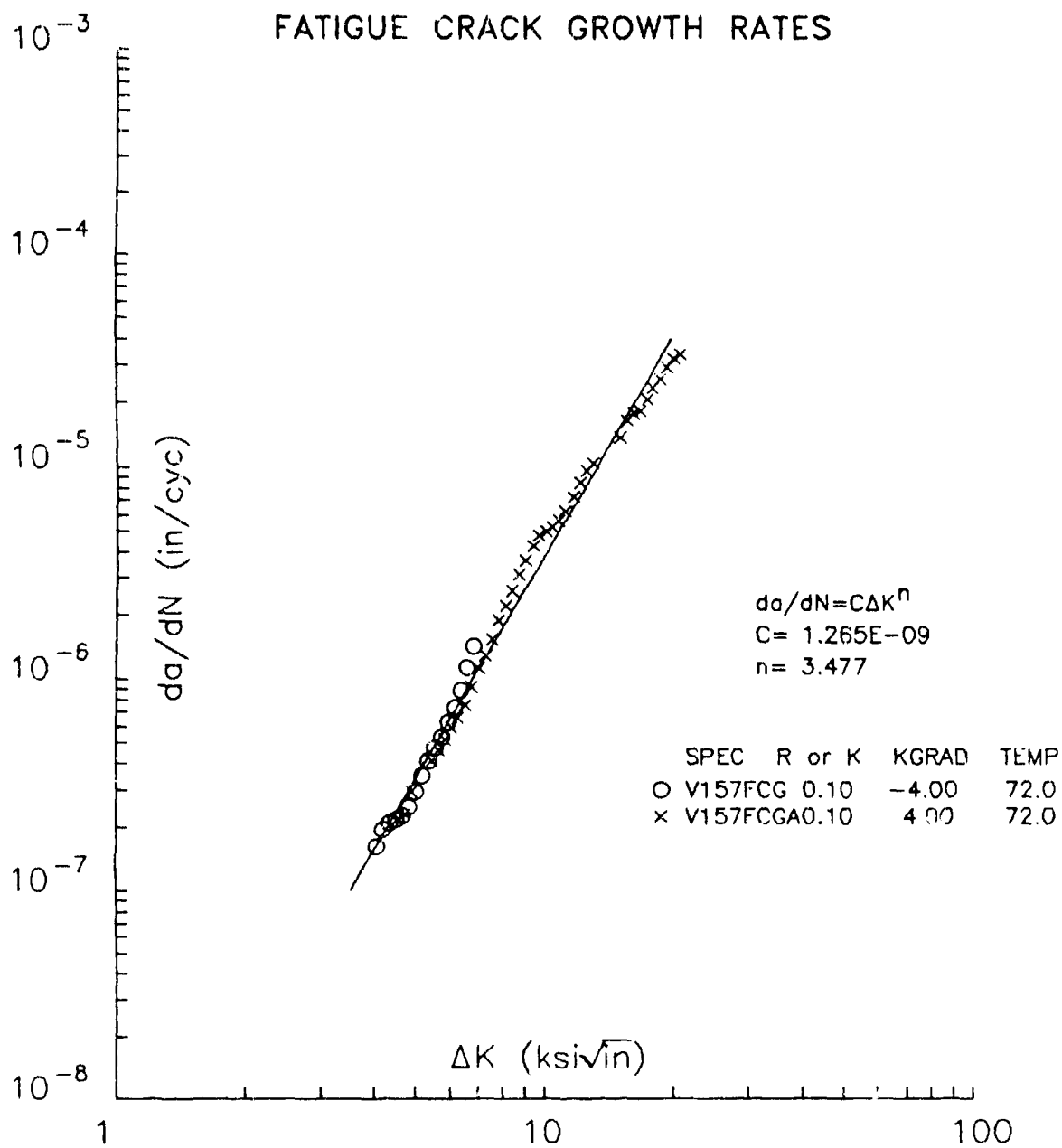


Figure D2. B201-T7 Fatigue Crack Growth Rate Data—Foundry A

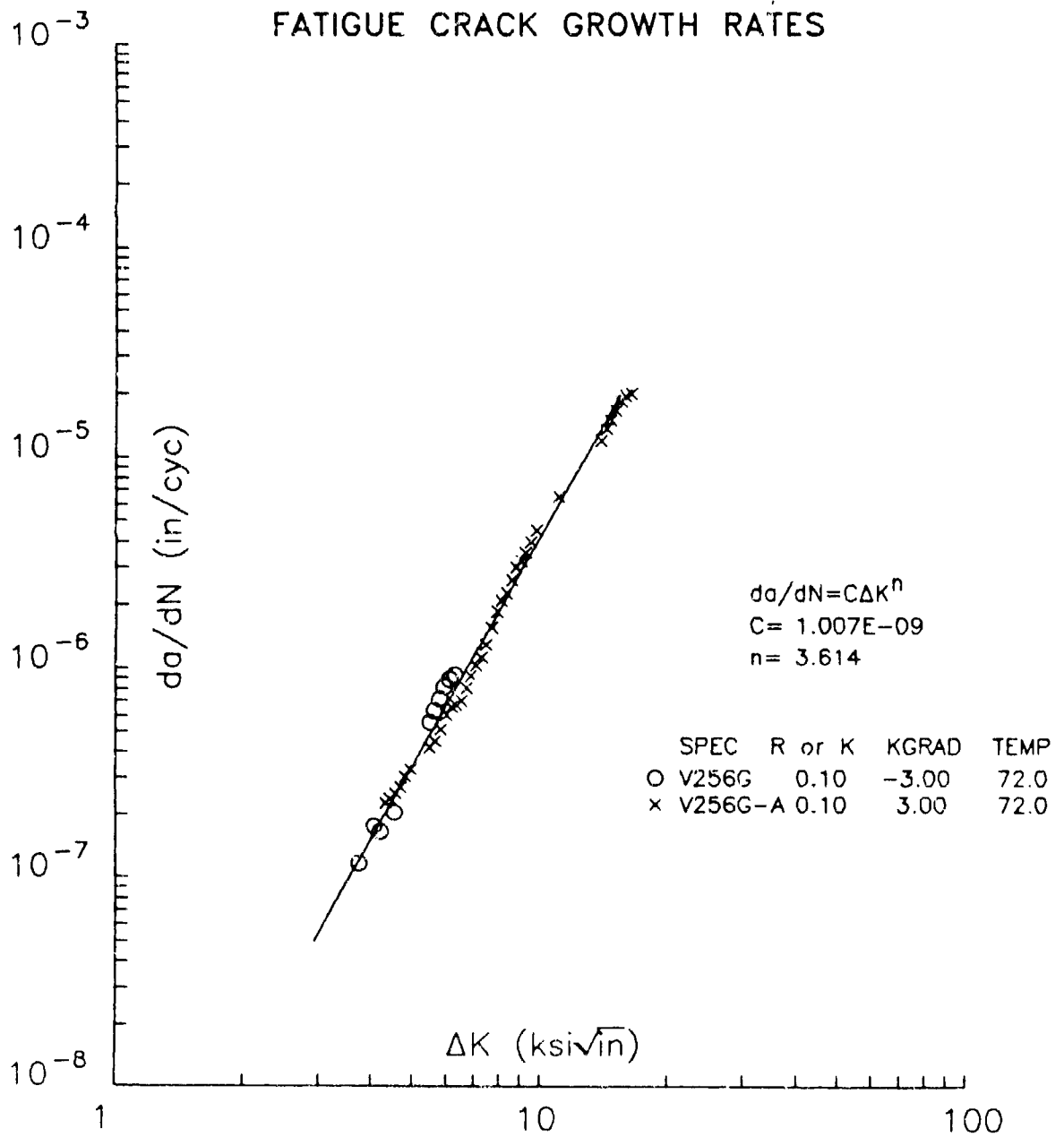


Figure D3. B201-T7 Fatigue Crack Growth Rate Data—Foundry B

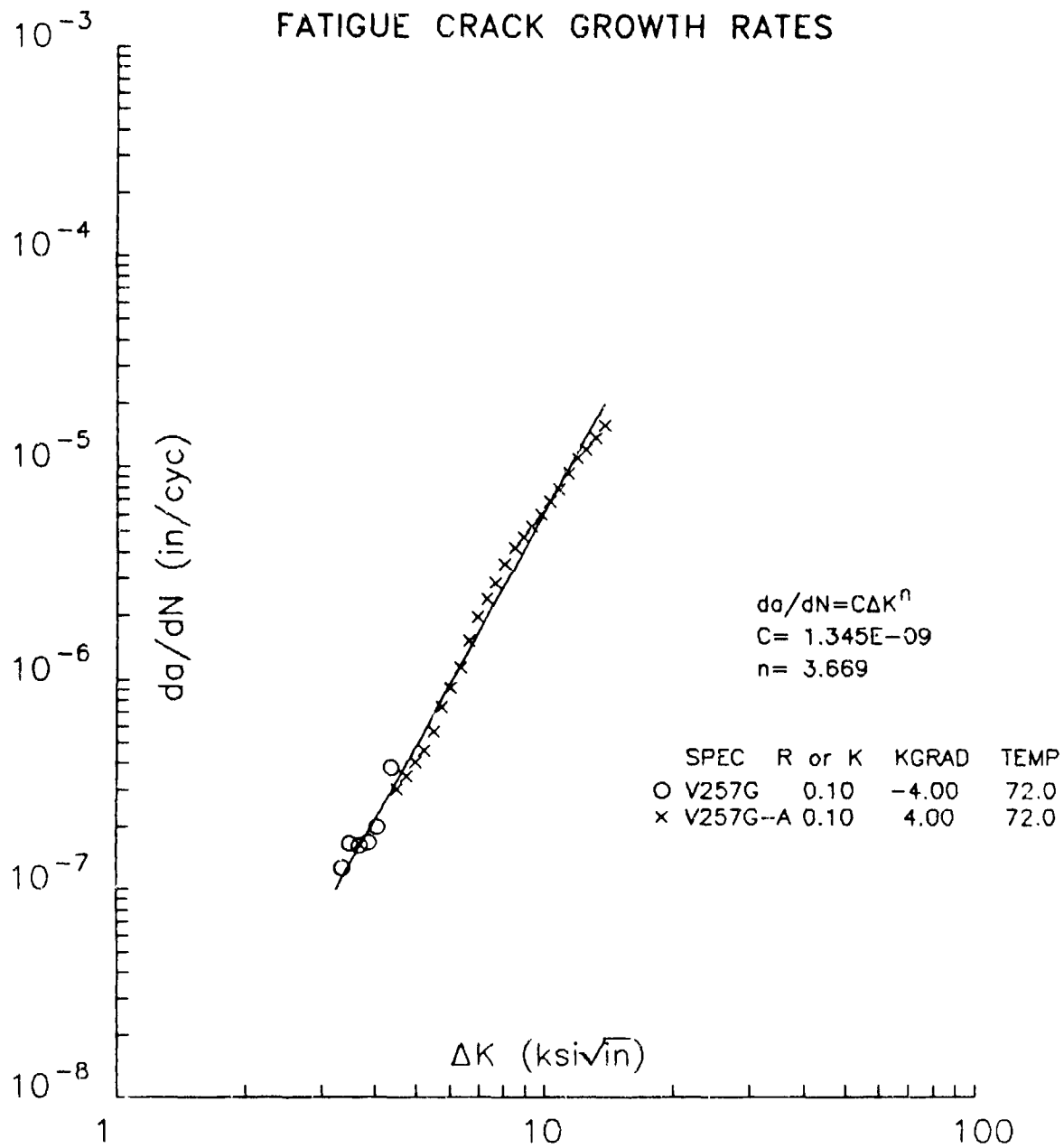


Figure D4. B201-T7 Fatigue Crack Growth Rate Data—Foundry B

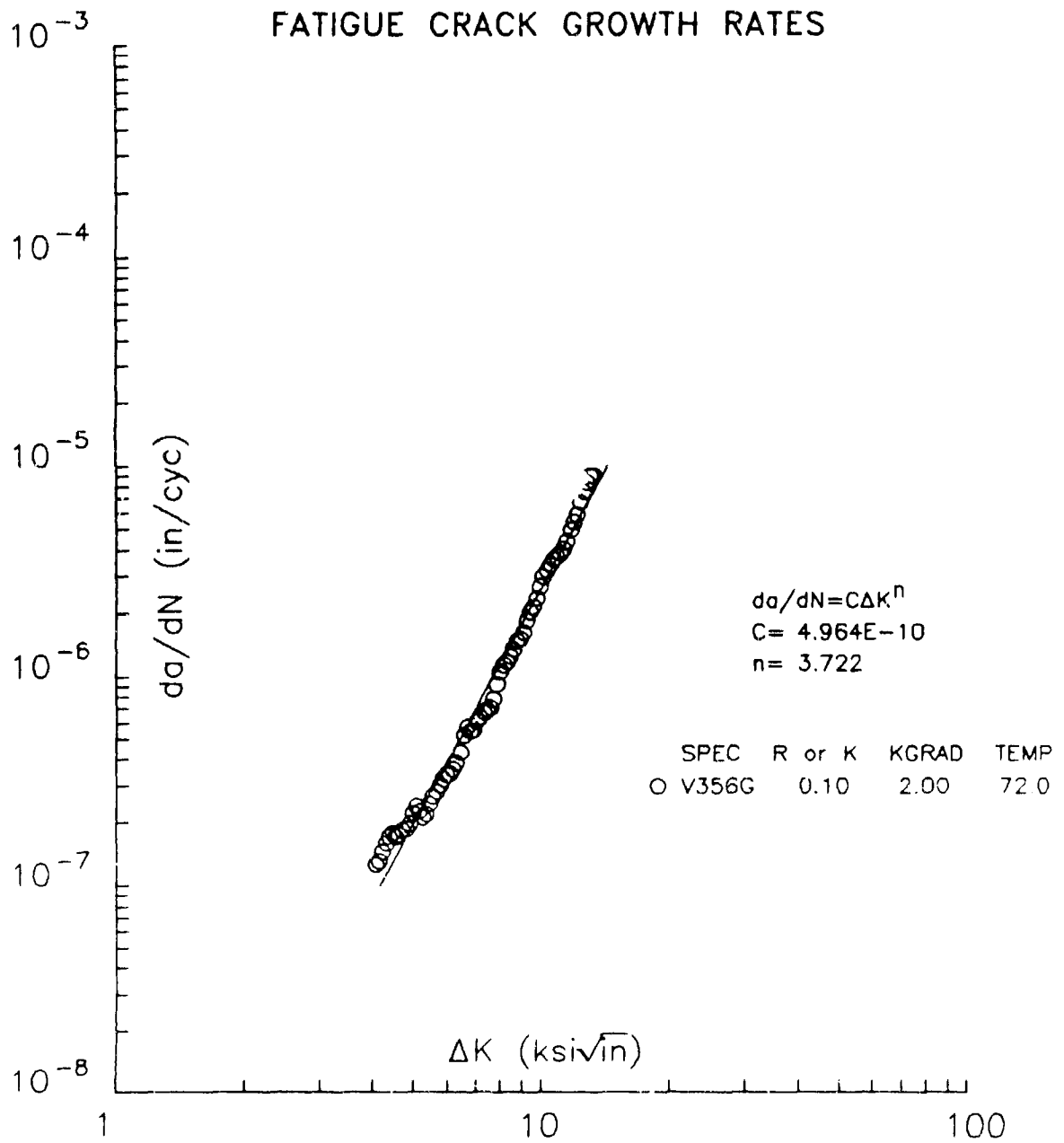


Figure D5. B201-T7 Fatigue Crack Growth Rate Data—Foundry C

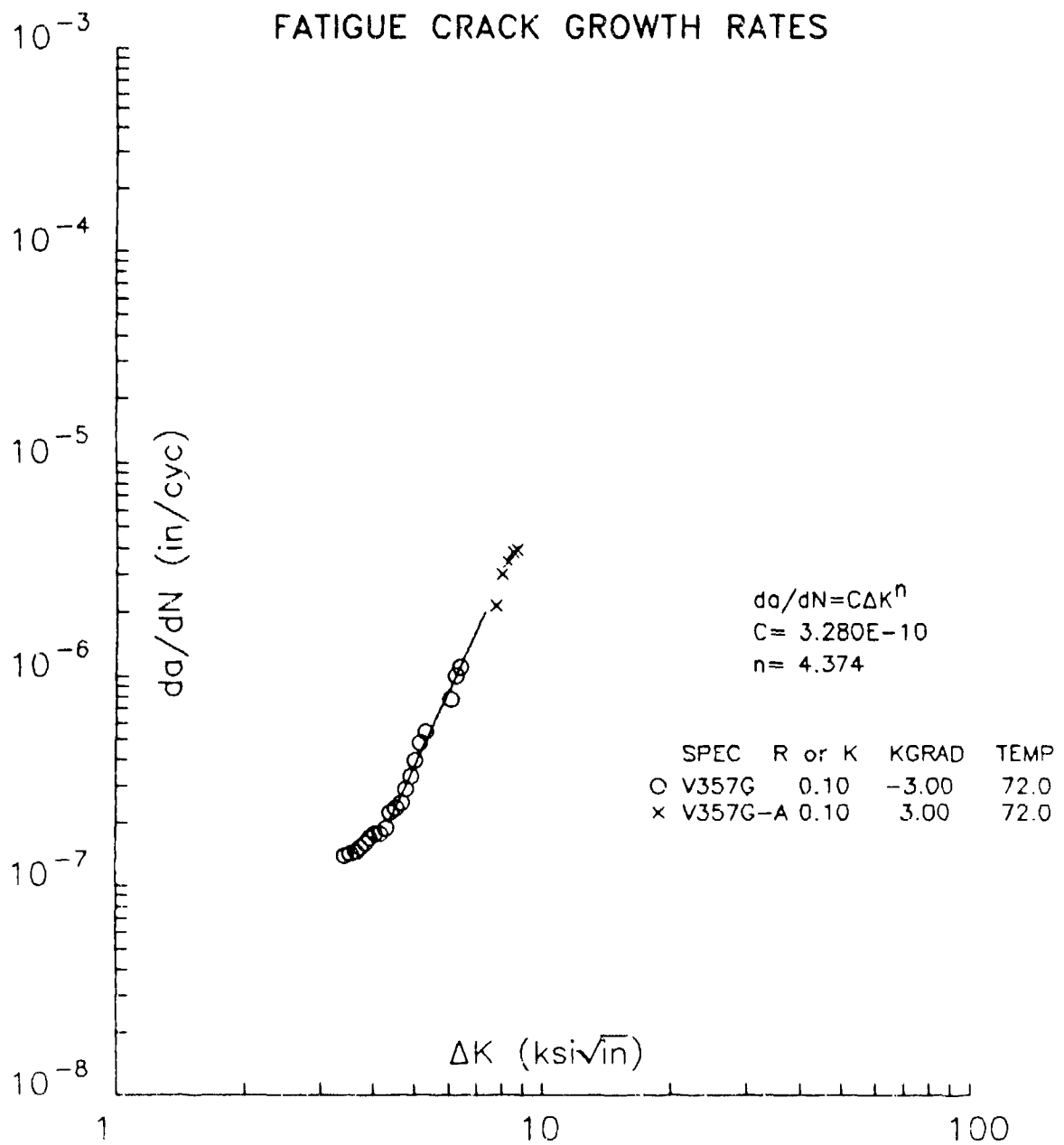


Figure D6. B201-T7 Fatigue Crack Growth Rate Data—Foundry C

APPENDIX E  
PHASE I, TASK 3  
D357-T6 DISCONTINUITY ASSESSMENT

TABLE E1. D357-T6 TENSILE PROPERTIES—GRADE A/B

| GRADE                      | PLATE NO. | UTS (ksi) | YS (ksi) | EI (%) |
|----------------------------|-----------|-----------|----------|--------|
| A/B                        | D1        | 54.7      | 48.5     | 4.3    |
|                            | D1        | 53.7      | 48.6     | 2.6*   |
|                            | D2        | 54.6      | 48.1     | 5.0    |
|                            | D2        | 54.8      | 48.0     | 4.5    |
|                            | D3        | 54.9      | 48.4     | 5.1    |
|                            | D3        | 54.5      | 48.3     | 4.8    |
|                            | D4        | 54.9      | 48.1     | 4.9    |
|                            | D4        | 54.5      | 48.3     | 4.3    |
|                            | D5        | 54.6      | 48.4     | 4.7    |
|                            | D5        | 54.5      | 48.0     | 4.0    |
|                            | D6        | 54.9      | 48.5     | 4.6    |
|                            | D6        | 55.1      | 48.7     | 5.1    |
|                            | D71       | 53.4      | 47.7     | 1.8*   |
|                            | D72       | 53.1      | 47.6     | 1.5*   |
|                            | D72       | 52.5      | 47.5     | 1.1*   |
| Average                    |           | 54.3      | 48.2     | 3.9    |
| Weld Repair<br>(Grade A/B) | D11       | 56.2      | 46.4     | 8.0    |
|                            | D12       | 53.7      | 46.8     | 5.0    |
|                            | D14       | 53.7      | 47.2     | 3.7    |
|                            | D14       | 54.1      | 47.3     | 3.5    |
|                            | D15       | 55.4      | 47.6     | 6.3    |
|                            | D15       | 54.2      | 47.5     | 4.0    |
| Average                    |           | 54.6      | 47.1     | 5.1    |

\* Data Not Meeting AMS 4241 Requirement

TABLE E2. D357-T6 TENSILE PROPERTIES — GAS POROSITY

| GRADE   | PLATE NO. | UTS (ksi) | YS (ksi) | EJ (%) |
|---------|-----------|-----------|----------|--------|
| B       | D20       | 51.2      | 45.6     | 3.6    |
|         | D20       | 49.6*     | 43.4     | 3.5    |
|         | D23       | 51.5      | 45.4     | 2.8*   |
|         | D24       | 51.7      | 46.0     | 2.8*   |
|         | D30       | 50.2      | 44.3     | 3.4    |
|         | D30       | 51.2      | 46.2     | 2.1*   |
|         | D70       | 51.6      | 45.3     | 4.3    |
|         | D70       | 47.4*     | 41.8     | 4.2    |
| Average |           | 50.0      | 44.8     | 3.3    |
| C       | D31       | 50.2      | 44.9     | 2.0*   |
|         | D33       | 51.1      | 45.6     | 2.3*   |
|         | D40       | 50.1      | 43.3     | 4.1    |
|         | D40       | 49.5*     | 43.7     | 3.2    |
|         | D41       | 51.3      | 45.6     | 1.8*   |
|         | D41       | 50.3      | 45.3     | 1.4*   |
|         | D43       | 50.7      | 45.5     | 1.9*   |
|         | D43       | 49.9*     | 45.0     | 1.4*   |
|         | D50       | 50.8      | 45.5     | 2.4*   |
|         | D50       | 50.4      | 45.2     | 2.5*   |
|         | D52       | 48.5*     | 44.8     | 0.9*   |
|         | D52       | 53.0      | 47.3     | 1.6*   |
| Average |           | 50.4      | 45.1     | 2.1    |
| D       | D54       | 49.1*     | 44.9     | 1.3*   |
|         | D60       | 48.4*     | 43.9     | 1.4*   |
|         | D60       | 48.6*     | 44.1     | 1.7*   |
| Average |           | 48.7      | 44.3     | 1.5    |

\* Data Not Meeting AMS 4241 Requirement

TABLE E3. D357-T6 TENSILE PROPERTIES---SHRINKAGE  
POROSITY

| GRADE   | PLATE NO. | UTS (ksi) | YS (ksi) | El (%) |
|---------|-----------|-----------|----------|--------|
| B       | D23       | 51.8      | 46.1     | 2.7*   |
|         | D24       | 51.4      | 45.5     | 2.4*   |
|         | D31       | 49.8*     | 47.6     | 1.6*   |
|         | D32       | 50.6      | 45.1     | 2.5*   |
|         | D32       | 50.7      | 45.4     | 2.7*   |
|         | D32       | 50.3      | 45.5     | 2.3*   |
|         | D32       | 50.9      | 45.6     | 2.3*   |
|         | D32       | 50.6      | 45.7     | 1.5*   |
|         | D32       | 50.1      | 45.0     | 1.5*   |
|         | D42       | 53.0      | 44.3     | 7.9    |
| Average |           | 50.9      | 45.6     | 2.7    |
| C       | D33       | 50.9      | 45.7     | 2.2*   |
|         | D42       | 51.3      | 45.5     | 3.9    |
|         | D44       | 50.4      | 45.2     | 2.5*   |
| Average |           | 50.9      | 45.5     | 2.9    |

\* Data Not Meeting AMS 4241 Requirement

TABLE E4. D357-T6 TENSILE PROPERTIES --- FOREIGN MATERIAL

| GRADE   | PLATE NO. | UTS (ksi) | YS (ksi) | EI (%) |
|---------|-----------|-----------|----------|--------|
| B       | D12       | 55.4      | 45.5     | 7.5    |
|         | D14       | 51.4      | 45.6     | 3.2    |
|         | D42       | 54.1      | 47.6     | 3.1    |
| Average |           | 53.6      | 46.2     | 4.6    |
| C       | D70       | 45.1      | 41.0     | 1.2*   |
|         | D71       | 55.0      | 45.9     | 4.7    |
|         | D72       | 51.9      | 46.3     | 1.2*   |
| Average |           | 50.6      | 44.4     | 2.4    |

\* Data Not Meeting AMS 4241 Requirement

TABLE E5. D357-T6 STRESS-LIFE FATIGUE DATA  
 --DEFECT FREE MATERIAL

| GRADE       | PLATE NO. | MAXIMUM STRESS (ksi) | CYCLES TO FAILURE     |
|-------------|-----------|----------------------|-----------------------|
| Weld Repair | D11       | 20                   | 352,358               |
|             | D11       | 40                   | 51,899                |
|             | D11       | 45                   | 26,224                |
|             | D12       | 30                   | 183,883               |
|             | D12       | 15                   | 4 X 10 <sup>6</sup> * |
|             | D12       | 40                   | 45,007                |
|             | D12       | 20                   | 1,789,060             |
|             | D12       | 30                   | 252,390               |
| A/B **      | D3        | 20                   | 3 X 10 <sup>6</sup> * |
|             | D3        | 30                   | 1,384,680             |
|             | D3        | 30                   | 3 X 10 <sup>6</sup> * |
|             | D3        | 35                   | 1,647,320             |
|             | D3        | 35                   | 636,247               |
|             | D3        | 40                   | 132,188               |
|             | D3        | 40                   | 176,139               |

Note:  $K_t = 1.0$ ,  $R = 0.1$

\* No Failure

\*\* Small Test Specimens - See Text

TABLE E6. D357-T6 STRESS-LIFE FATIGUE DATA  
—GAS POROSITY

| GRADE | PLATE NO. | MAXIMUM STRESS (ksi) | CYCLES TO FAILURE     |
|-------|-----------|----------------------|-----------------------|
| B     | D1        | 20                   | 4 X 10 <sup>6</sup> * |
|       | D1        | 40                   | 86,647                |
|       | D2        | 30                   | 507,830               |
|       | D2        | 30                   | 224,487               |
|       | D3        | 45                   | 84,384                |
|       | D3        | 20                   | 4 X 10 <sup>6</sup> * |
|       | D4        | 40                   | 75,492                |
|       | D20       | 45                   | 9,458                 |
|       | D20       | 20                   | 580,111               |
|       | D70       | 20                   | 547,523               |
|       | D70       | 40                   | 15,835                |
|       | D70       | 30                   | 101,852               |
|       | D70       | 45                   | 11,526                |
|       | D70       | 25                   | 215,005               |
|       | D71       | 25                   | 140,902               |
|       | D71       | 20                   | 773,529               |
|       | D20**     | 10                   | 3 X 10 <sup>6</sup> * |
|       | D20**     | 20                   | 308,660               |
|       | D20**     | 20                   | 254,519               |
|       | D20**     | 30                   | 78,879                |
|       | D20**     | 30                   | 80,806                |
|       | D20**     | 40                   | 22,707                |
|       | D24**     | 15                   | 601,999               |
|       | D24**     | 25                   | 102,921               |

Note:  $K_t = 1.0$ ,  $R = 0.1$

\* No Failure

\*\* Small Specimens (See Text)

TABLE E6. D357-T6 STRESS-LIFE FATIGUE DATA--GAS POROSITY (CONTINUED)

| GRADE | PLATE NO. | MAXIMUM STRESS (ksi) | CYCLES TO FAILURE       |
|-------|-----------|----------------------|-------------------------|
| C     | D23       | 20                   | 272,006                 |
|       | D23       | 10                   | 5 X 10 <sup>6</sup> *   |
|       | D23       | 30                   | 55,829                  |
|       | D23       | 40                   | 16,344                  |
|       | D24       | 45                   | 9,221                   |
|       | D41       | 25                   | 111,408                 |
|       | D43       | 25                   | 138,985                 |
|       | D50       | 20                   | 285,991                 |
|       | D50       | 30                   | 65,456                  |
|       | D50       | 40                   | 15,618                  |
|       | D52       | 10                   | 5.3 X 10 <sup>6</sup> * |
|       | D54       | 15                   | 639,996                 |
|       | D61       | 35                   | 23,419                  |
|       | D62       | 35                   | 23,764                  |
|       | D62       | 45                   | 3,553                   |
| D     | D43       | 15                   | 1,220,750               |
|       | D50       | 20                   | 325,308                 |
|       | D54       | 30                   | 31,957                  |
|       | D60       | 35                   | 15,002                  |
|       | D60       | 35                   | 1,253                   |
|       | D60       | 25                   | 103,377                 |
|       | D61       | 10                   | 5 X 10 <sup>6</sup> *   |
|       | D61       | 20                   | 171,492                 |
|       | D61       | 30                   | 33,188                  |
|       | D62       | 25                   | 73,884                  |
| D62   | 15        | 559,761              |                         |

Note:  $K_t = 1.0$ ,  $R = 0.1$

\* No Failure

TABLE E7. D357-T6 STRESS-LIFE FATIGUE DATA —SHRINKAGE POROSITY

| GRADE | PLATE NO. | MAXIMUM STRESS (ksi) | CYCLES TO FAILURE     |
|-------|-----------|----------------------|-----------------------|
| B     | D4        | 20                   | 5 X 10 <sup>6</sup>   |
|       | D4        | 30                   | 970,197               |
|       | D5        | 40                   | 273,695               |
|       | D5        | 45                   | 52,398                |
|       | D6        | 30                   | 214,275               |
|       | D6        | 30                   | 788,951               |
|       | D6        | 40                   | 19,307                |
|       | D32       | 20                   | 499,010               |
|       | D32       | 20                   | 476,164               |
|       | D32       | 25                   | 69,485                |
|       | D41       | 30                   | 84,264                |
| C     | D31       | 10                   | 5 X 10 <sup>6</sup> * |
|       | D32       | 15                   | 1,802,110             |
|       | D32       | 25                   | 81,757                |
|       | D52       | 20                   | 222,694               |
|       | D52       | 30                   | 42,162                |

Note:  $K_t = 1.0$ ,  $R = 0.1$

\* No Failure

TABLE E8. D357-T6 STRESS-LIFE DATA—FOREIGN MATERIAL

| GRADE | PLATE NO. | MAXIMUM STRESS (ksi) | CYCLES TO FAILURE |
|-------|-----------|----------------------|-------------------|
| B     | D42       | 25                   | 174,571           |
|       | D72       | 30                   | 56,639            |
|       | D72       | 20                   | 628,761           |
|       | D72       | 15                   | 1,022,330         |
|       | D74       | 20                   | 1,557,990         |
| C     | D40       | 25                   | 148,006           |
|       | D74       | 20                   | 490,168           |

Note:  $K_t = 1.0$ ,  $R = 0.1$

TABLE E9. SPECTRUM FATIGUE LIFE DATA\* FOR D357-T6  
CONTAINING INTENTIONALLY ADDED DEFECTS

| GRADE | DEFECT             | PLATE NO. | FLIGHT HOURS TO FAILURE | LOG AVERAGE |
|-------|--------------------|-----------|-------------------------|-------------|
| A/B   | Weld Repair        | D14       | 23,656                  | 30,519      |
|       |                    | D14       | 44,762                  |             |
|       |                    | D14       | 26,843                  |             |
| B     | Gas Porosity       | D5        | 57,462                  | 34,374      |
|       |                    | D70       | 20,562                  |             |
|       | Shrinkage Porosity | D65       | 45,443                  | 45,443      |
| C     | Gas Porosity       | D50       | 8,351                   | 7,061       |
|       |                    | D50       | 8,562                   |             |
|       |                    | D40       | 5,762                   |             |
|       |                    | D23       | 6,031                   |             |
| D     | Gas Porosity       | D60       | 6,762                   | 7,766       |
|       |                    | D60       | 12,743                  |             |
|       |                    | D61       | 5,544                   |             |

\* F-18 Lower Wing Root Spectrum (F18C2) — 32 ksi Gross Maximum Stress

TABLE E10. D357-T6 FRACTURE TOUGHNESS DATA

| DEFECT/<br>GRADE   | PLATE<br>NO. | K <sub>Q</sub><br>(ksi√in) | K <sub>IC</sub><br>(ksi√in) | OVERALL<br>AVERAGE |
|--------------------|--------------|----------------------------|-----------------------------|--------------------|
| Defect-Free        |              |                            |                             |                    |
| A/B                | D3           | 29.3                       |                             | 27.5               |
|                    | D4           | 26.2                       |                             |                    |
|                    | D70          | 26.9                       |                             |                    |
| Weld Repair        | D11          | 36.2                       |                             | 32.2               |
|                    | D12          | 28.3                       |                             |                    |
|                    | D15          | 32.3                       |                             |                    |
| Gas Porosity       |              |                            |                             |                    |
| B                  | D23          |                            | 21.3                        | 21.8               |
|                    | D41          | 22.5                       |                             |                    |
|                    | D50          | 21.4                       |                             |                    |
| C                  | D24          |                            | 22.2                        | 22.6               |
|                    | D62          | 23.1                       |                             |                    |
| Shrinkage Porosity |              |                            |                             |                    |
| B                  | D40          |                            | 20.0                        | 22.4               |
|                    | D44          | 25.0                       |                             |                    |
|                    | D54          | 22.3                       |                             |                    |
| C                  | D61          |                            | 22.6                        | 22.6               |

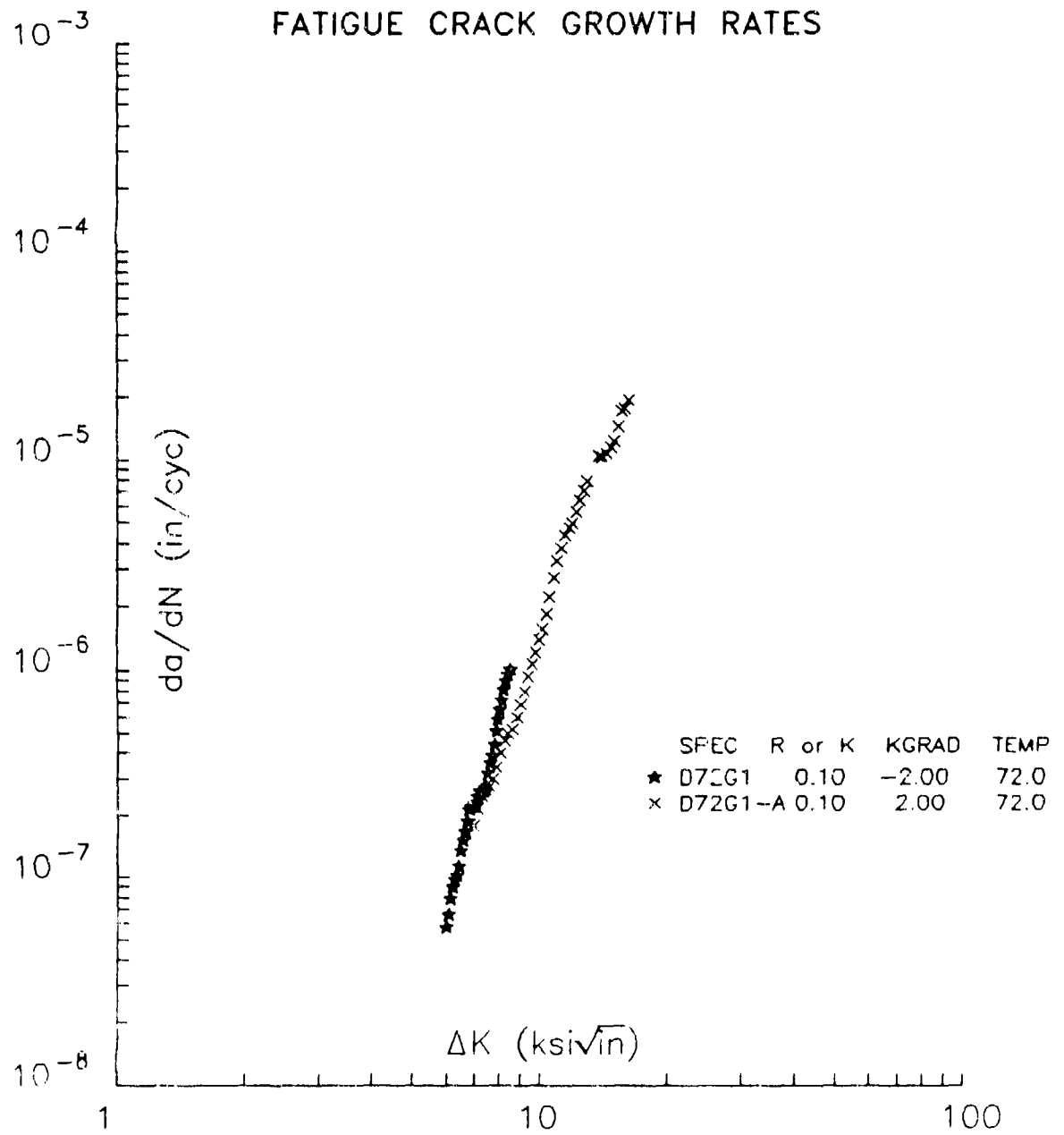


Figure E1. D357-T6 Fatigue Crack Growth Rate Data—Grade A/B

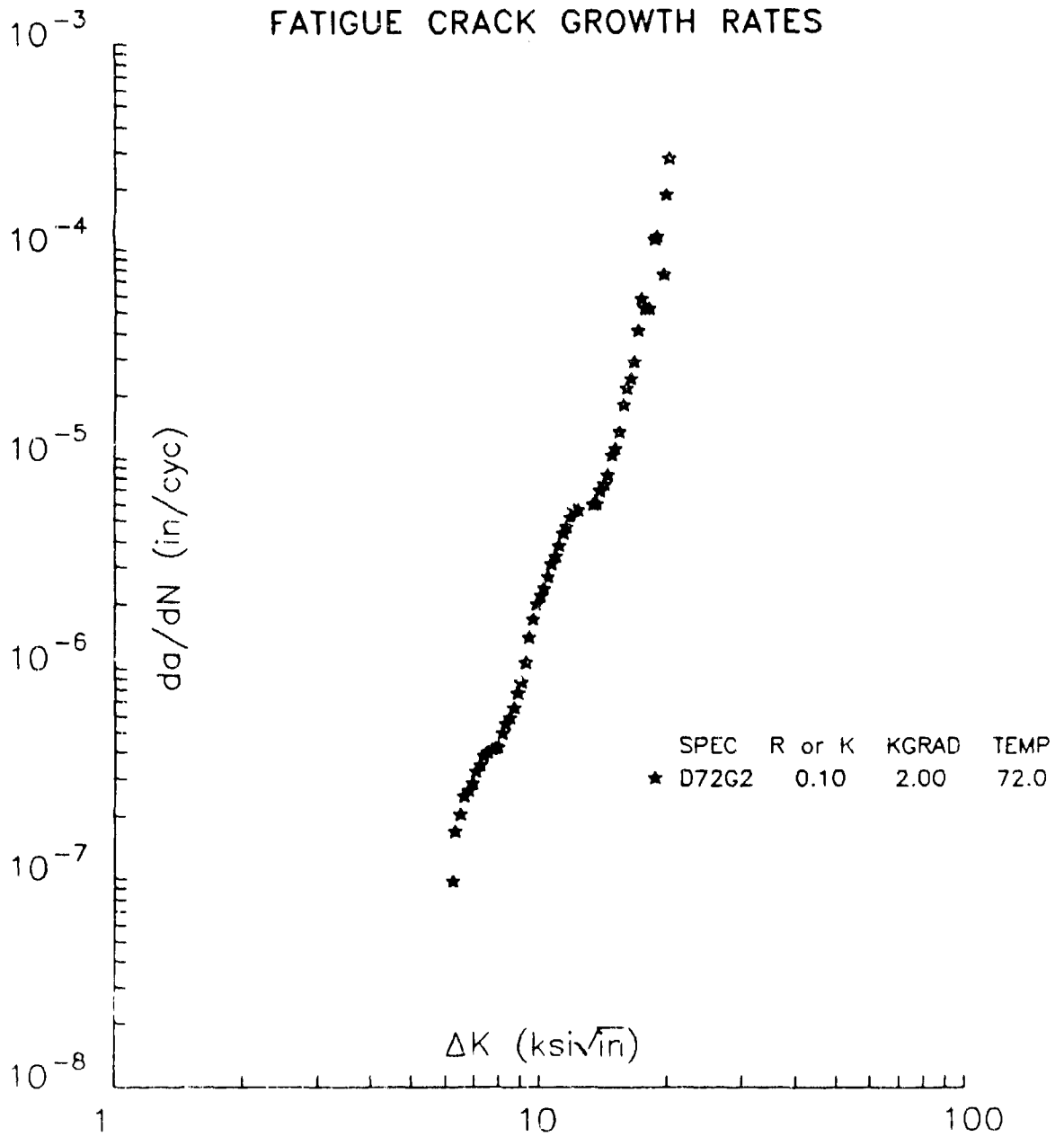


Figure E2. D357-T6 Fatigue Crack Growth Rate Data—Grade A/B

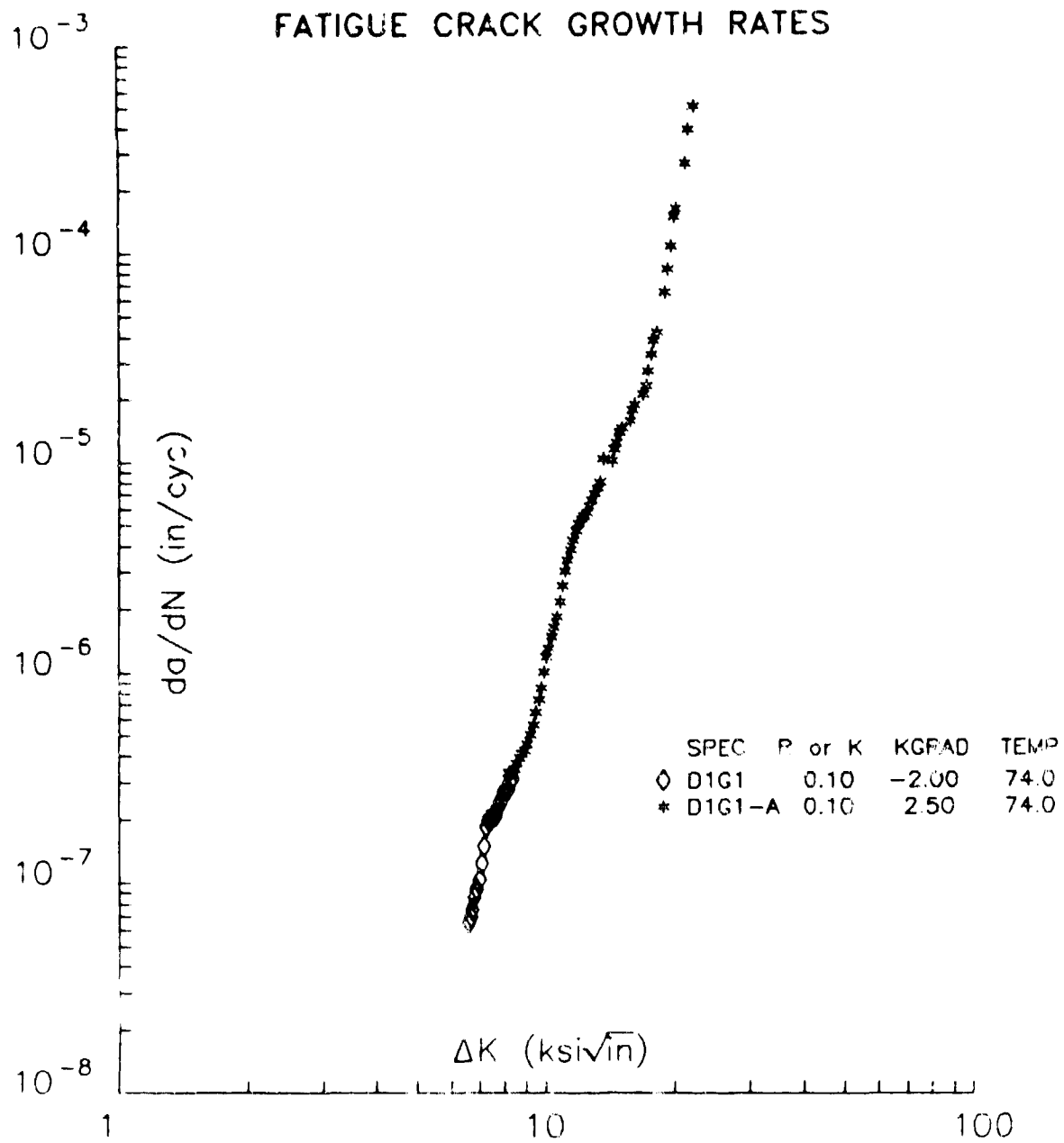


Figure E3. D357-T6 Fatigue Crack Growth Rate Data—Grade B Gas Porosity

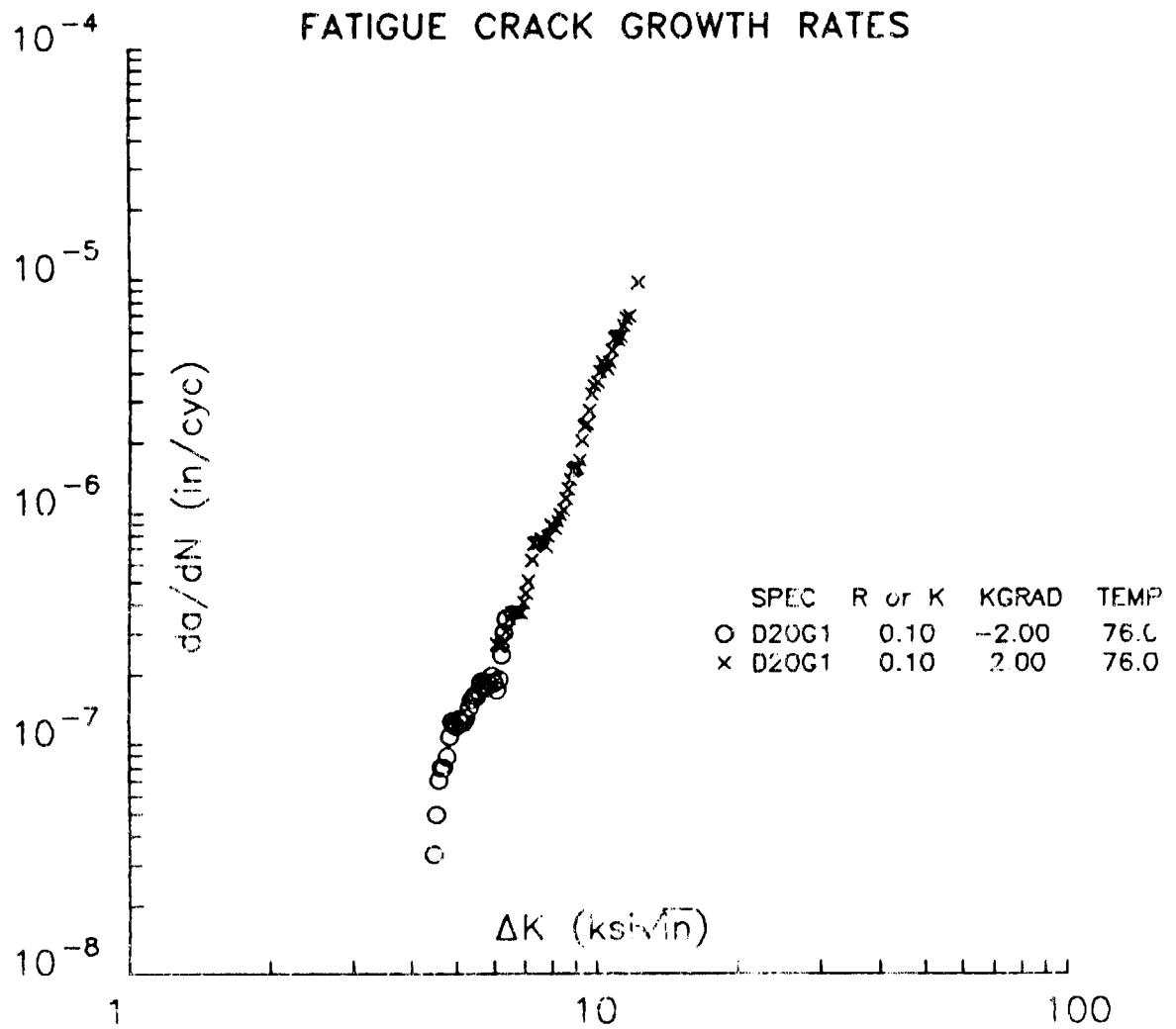


Figure E4. D357-T6 Fatigue Crack Growth Rate Data—Grade B Gas Porosity

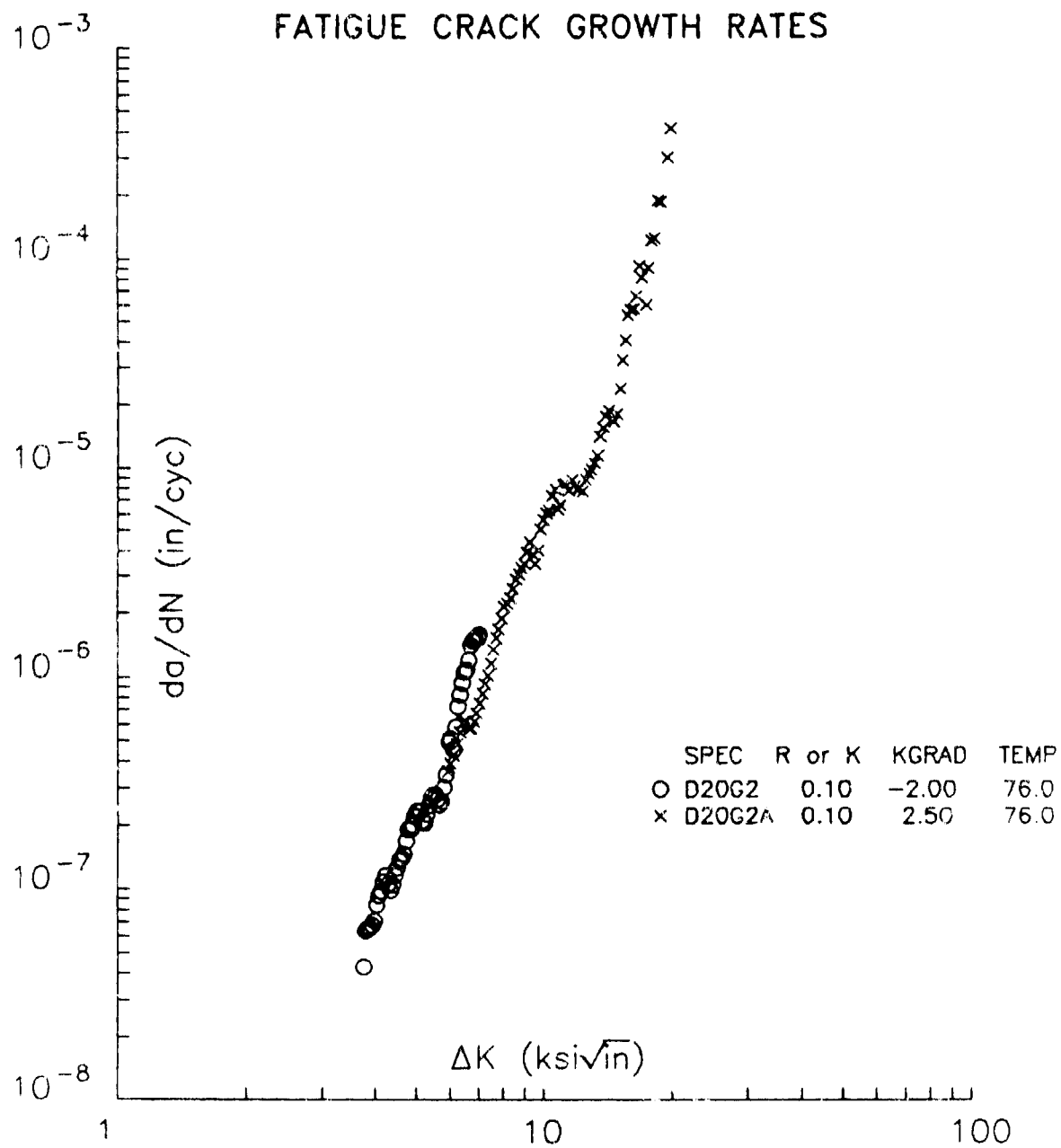


Figure E5. D357-T6 Fatigue Crack Growth Rate Data—Grade B Gas Porosity

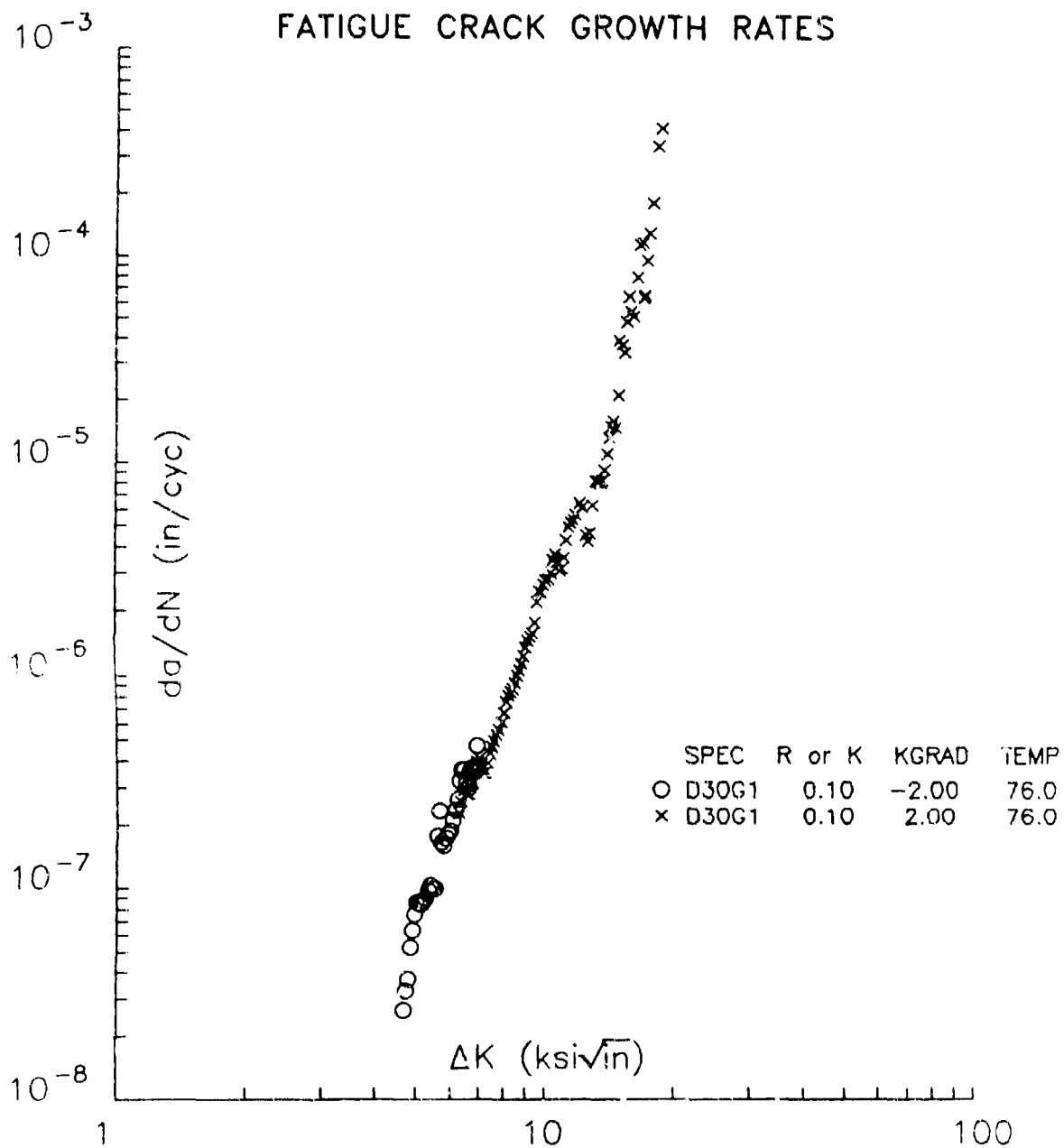


Figure E6. D357-T6 Fatigue Crack Growth Rate Data—Grade B Gas Porosity

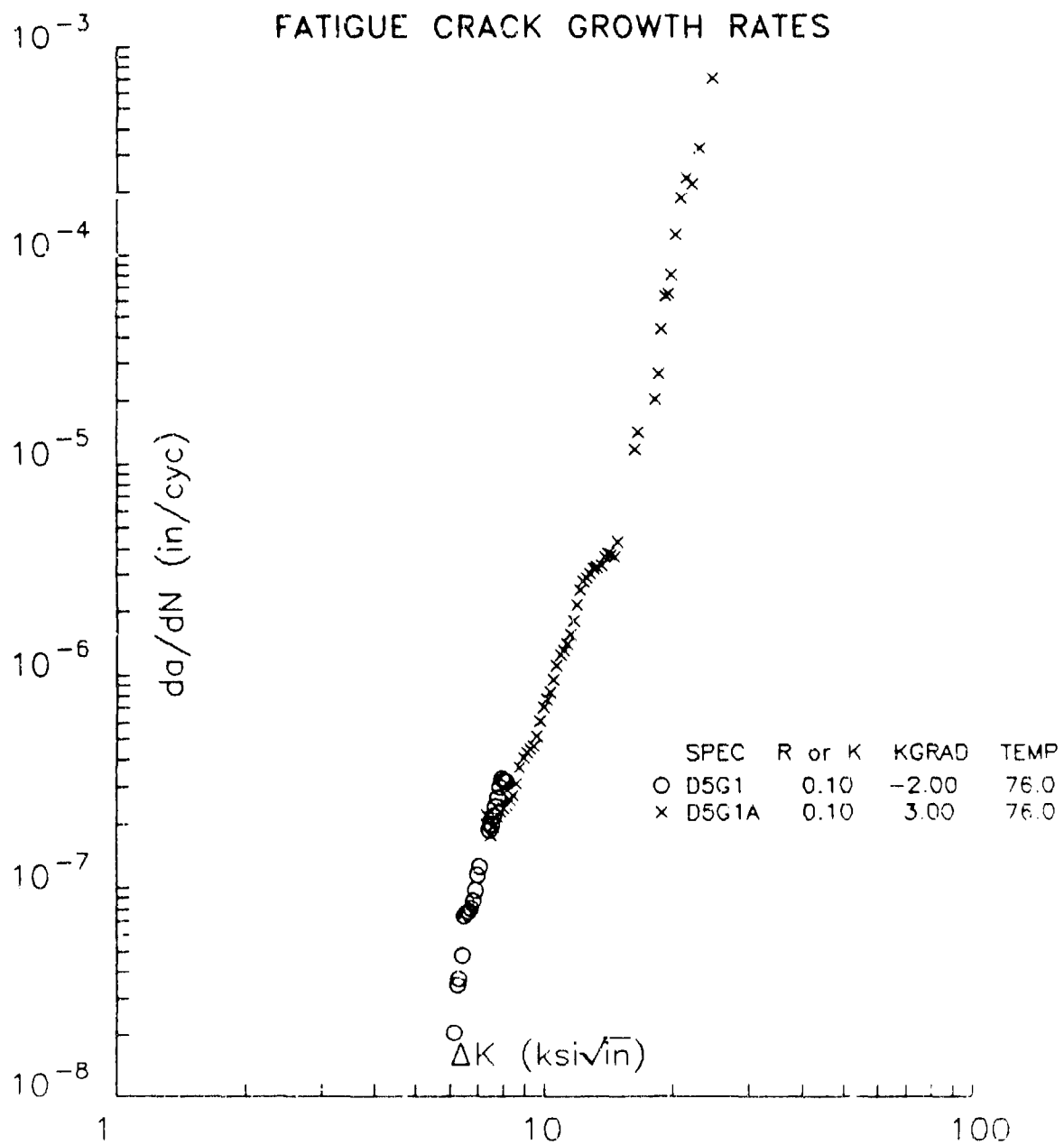


Figure E7. D357-T6 Fatigue Crack Growth Rate Data—Grade C Gas Porosity

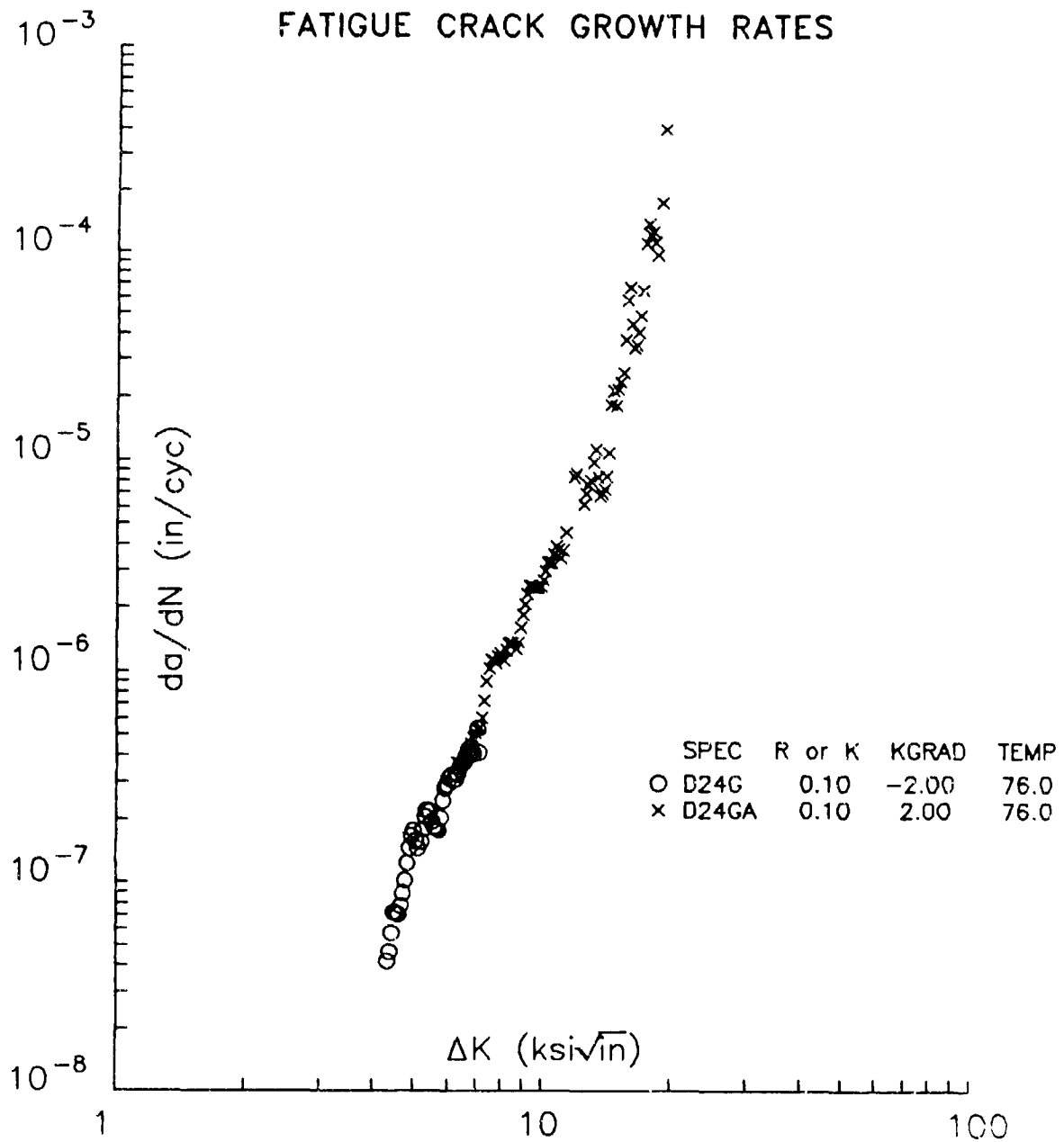


Figure E8. D357-T6 Fatigue Crack Growth Rate Data—Grade C Gas Porosity

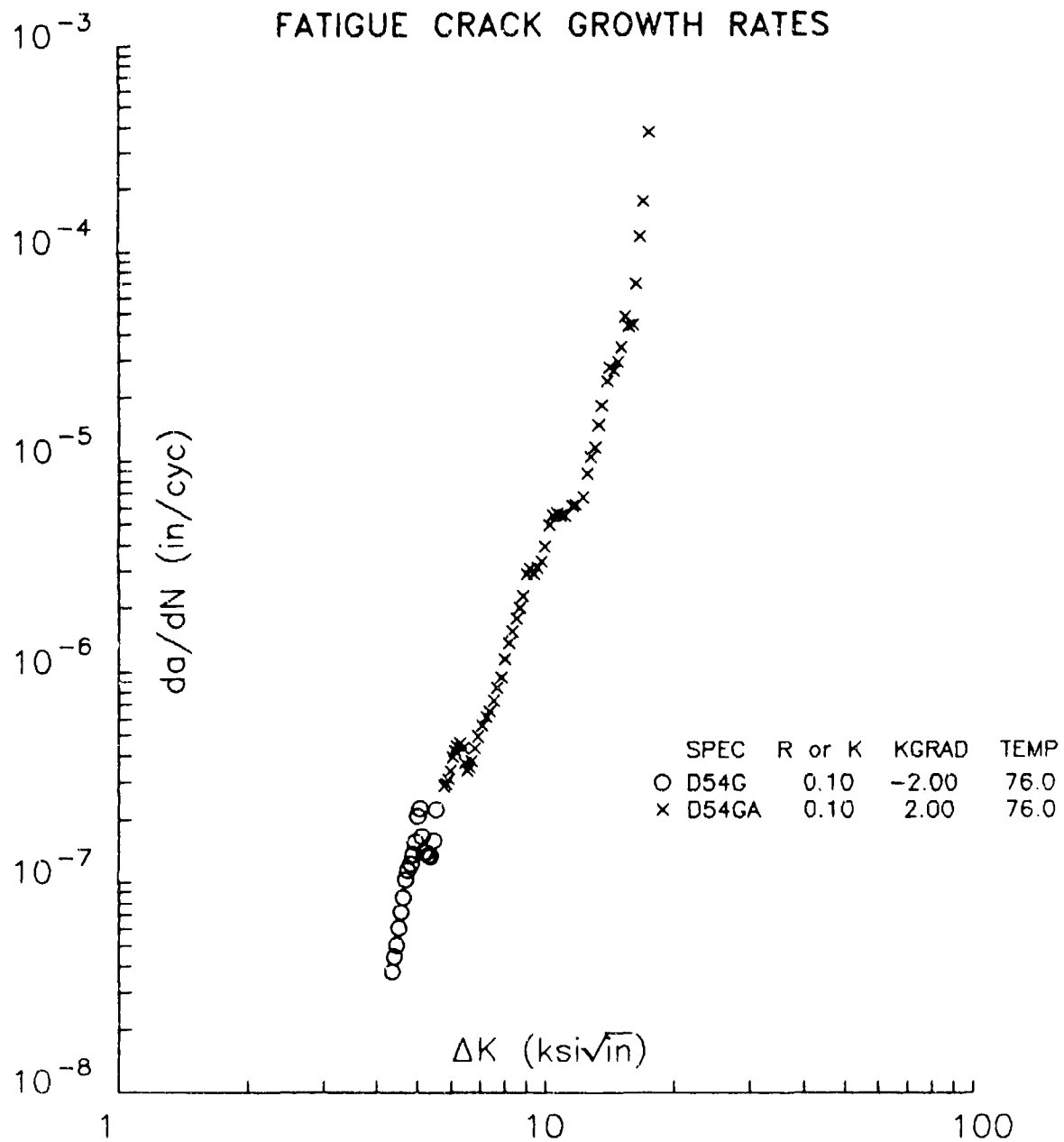


Figure E9. D357-T6 Fatigue Crack Growth Rate Data—Grade D Gas Porosity

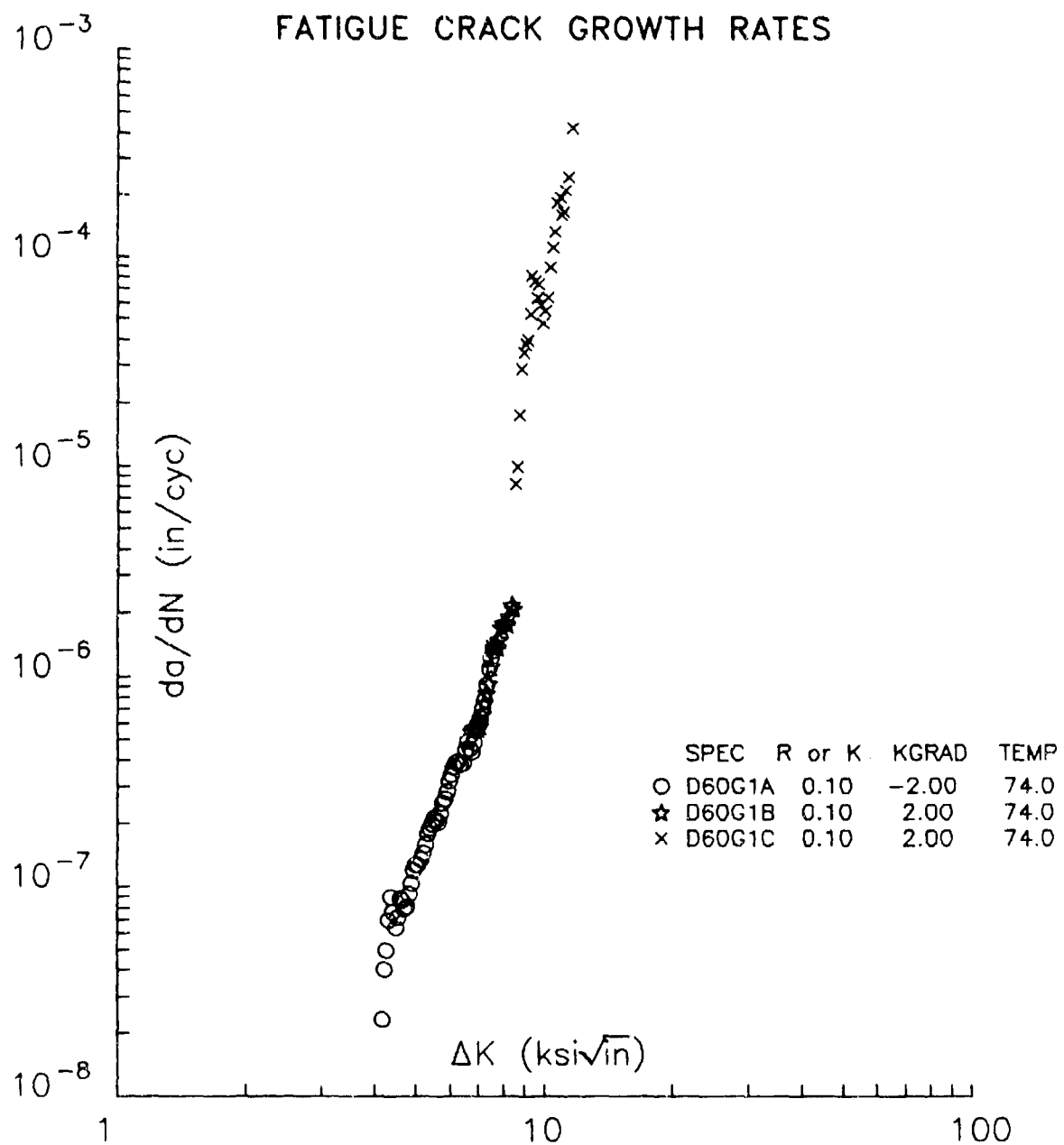


Figure E10. D357-T6 Fatigue Crack Growth Rate Data—Grade D Gas Porosity

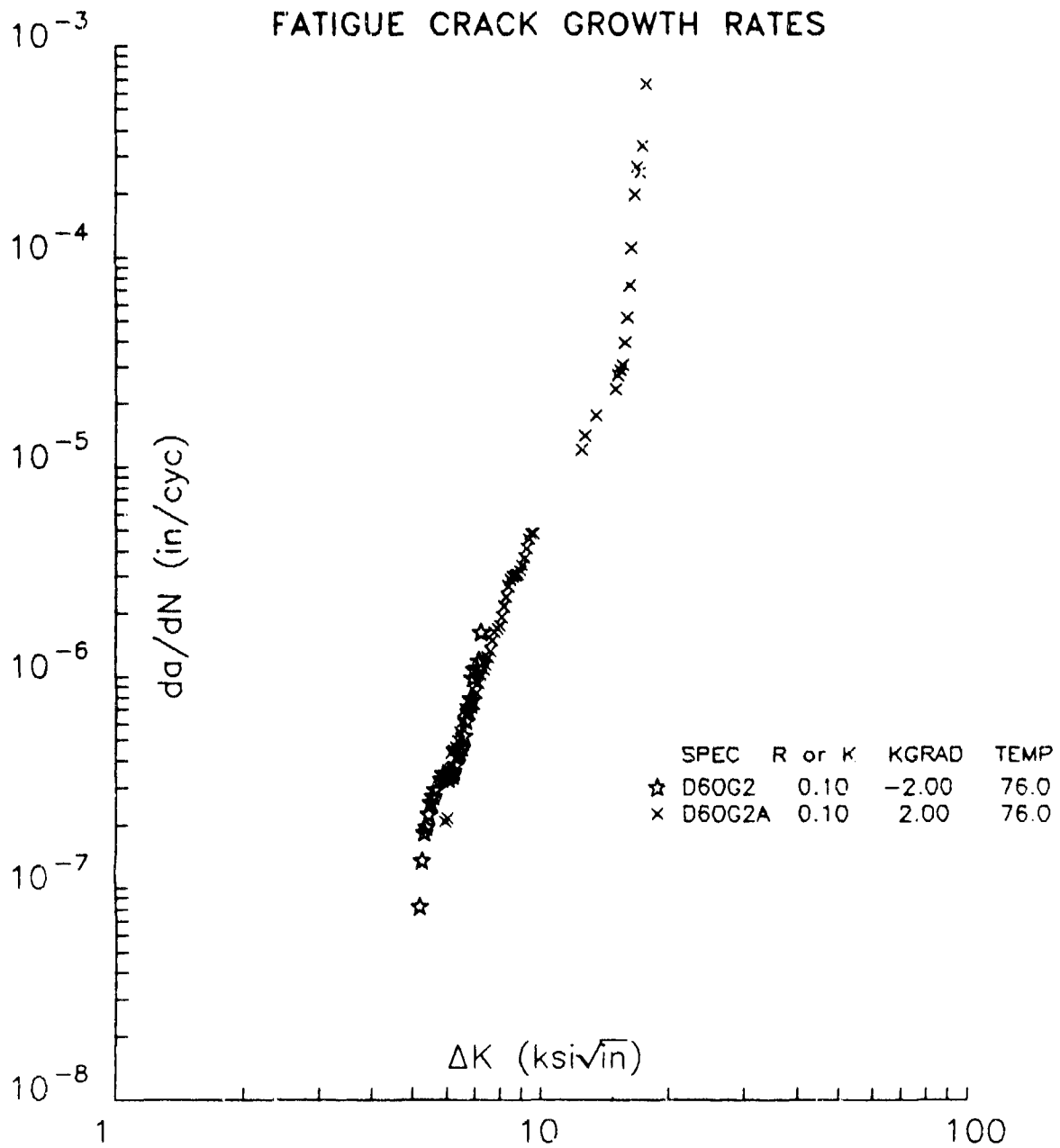


Figure E11. D357-T6 Fatigue Crack Growth Rate Data—Grade D Gas Porosity

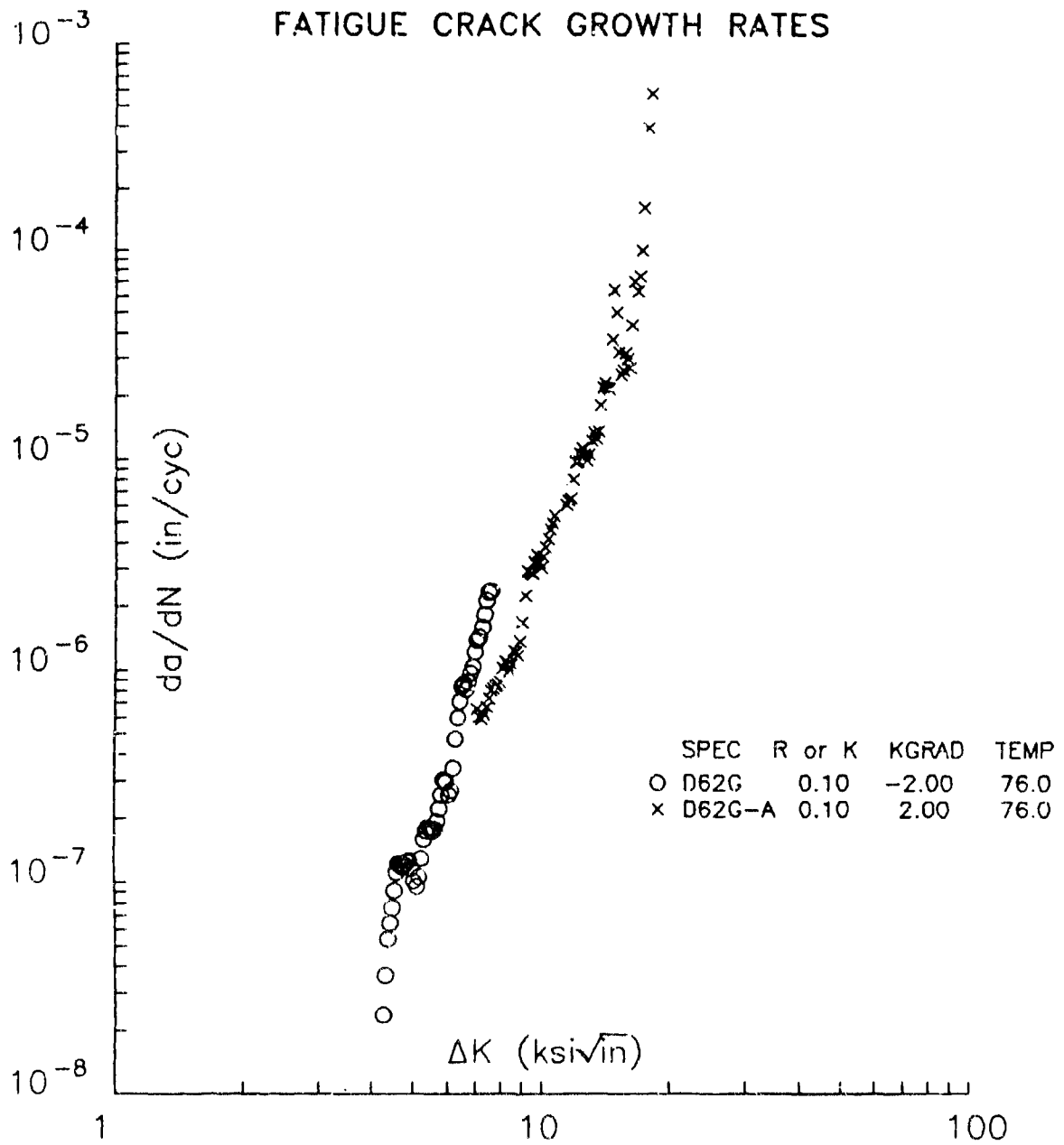


Figure E12. D357-T6 Fatigue Crack Growth Rate Data—Grade D Gas Porosity

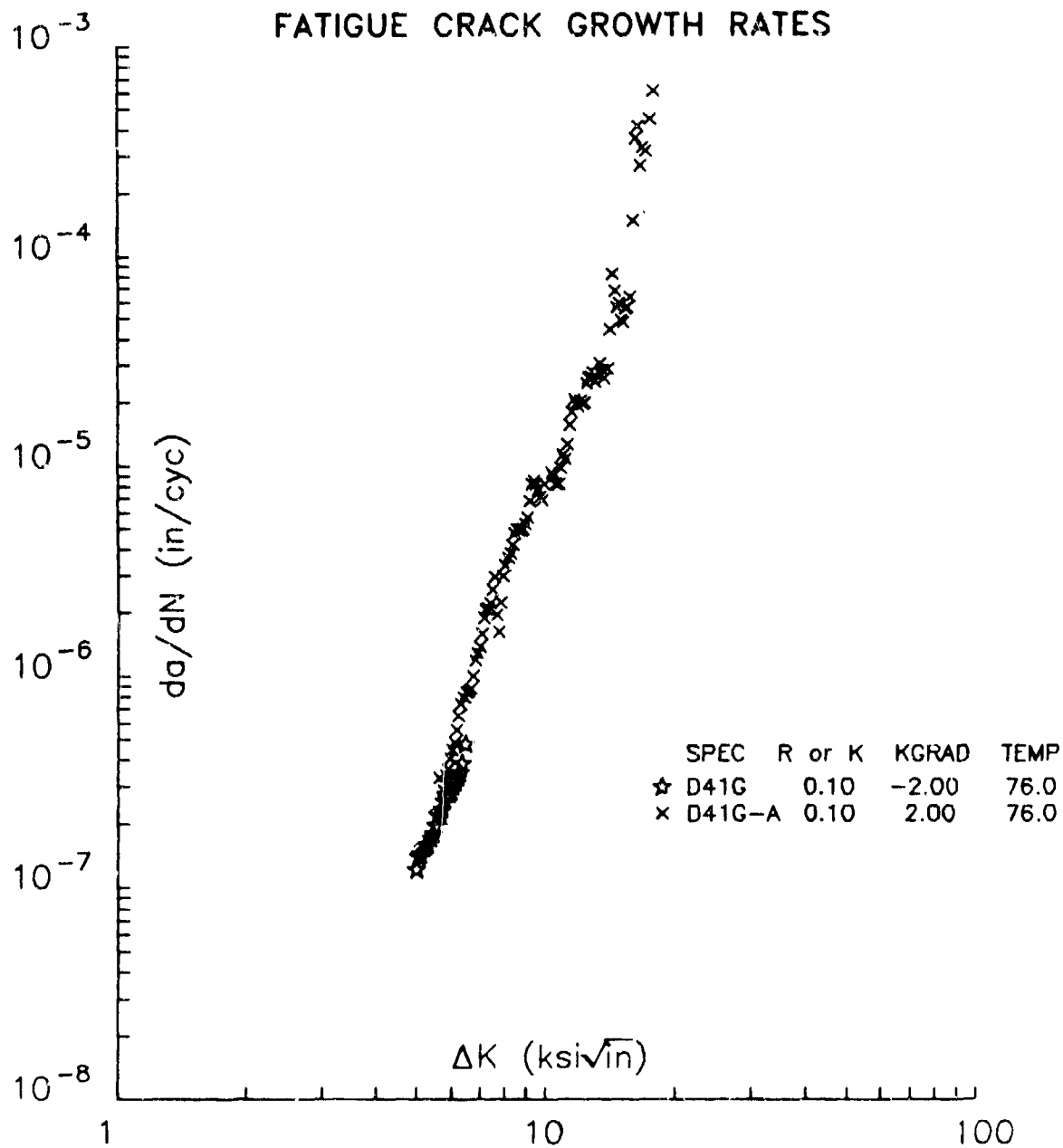


Figure E13. D357-T6 Fatigue Crack Growth Rate Data—Grade B Foreign Material

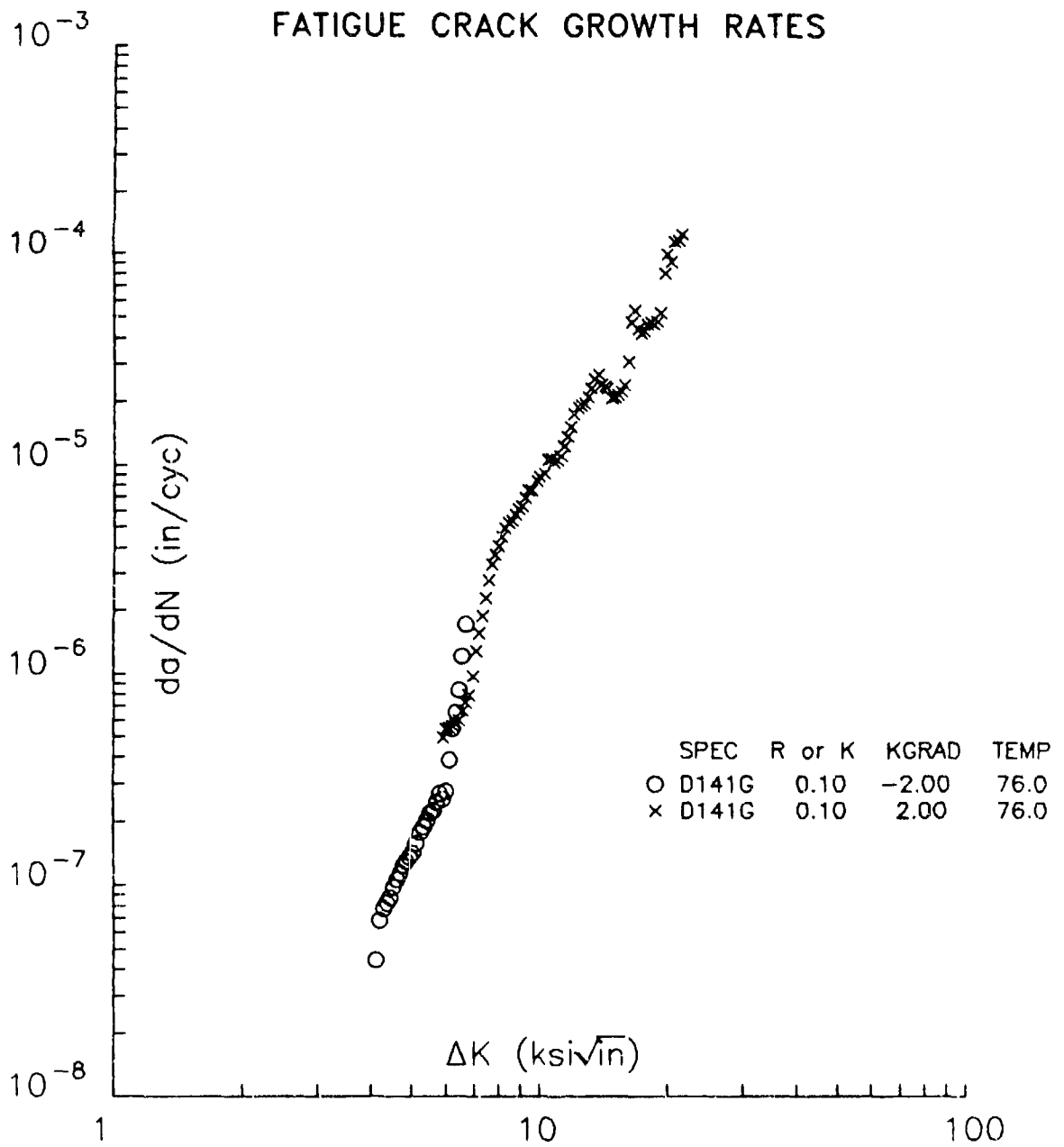


Figure E14. D357-T6 Fatigue Crack Growth Rate Data—Weld Repair

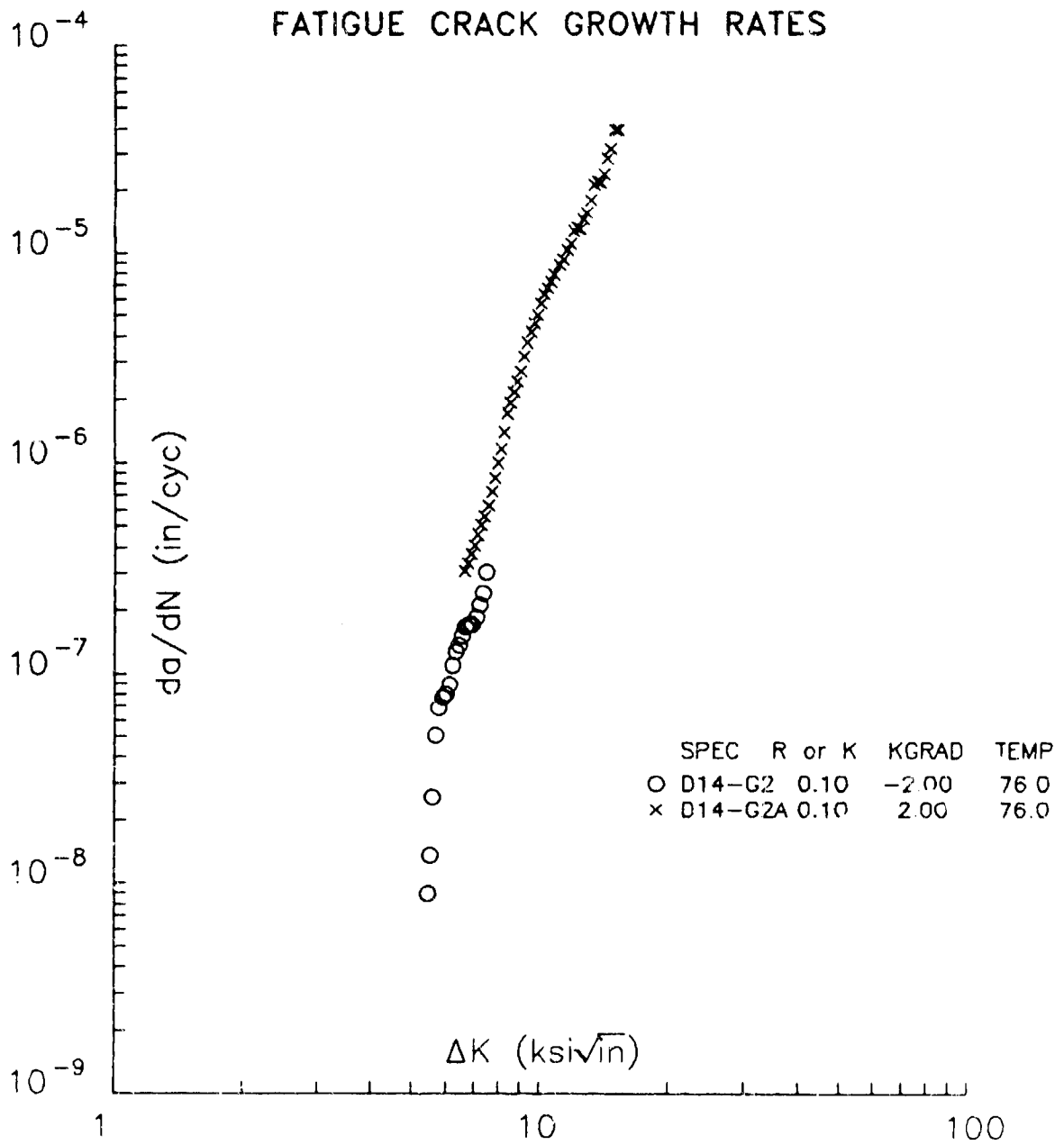


Figure E15. D357 T6 Fatigue Crack Growth Rate Data—Weld Repair

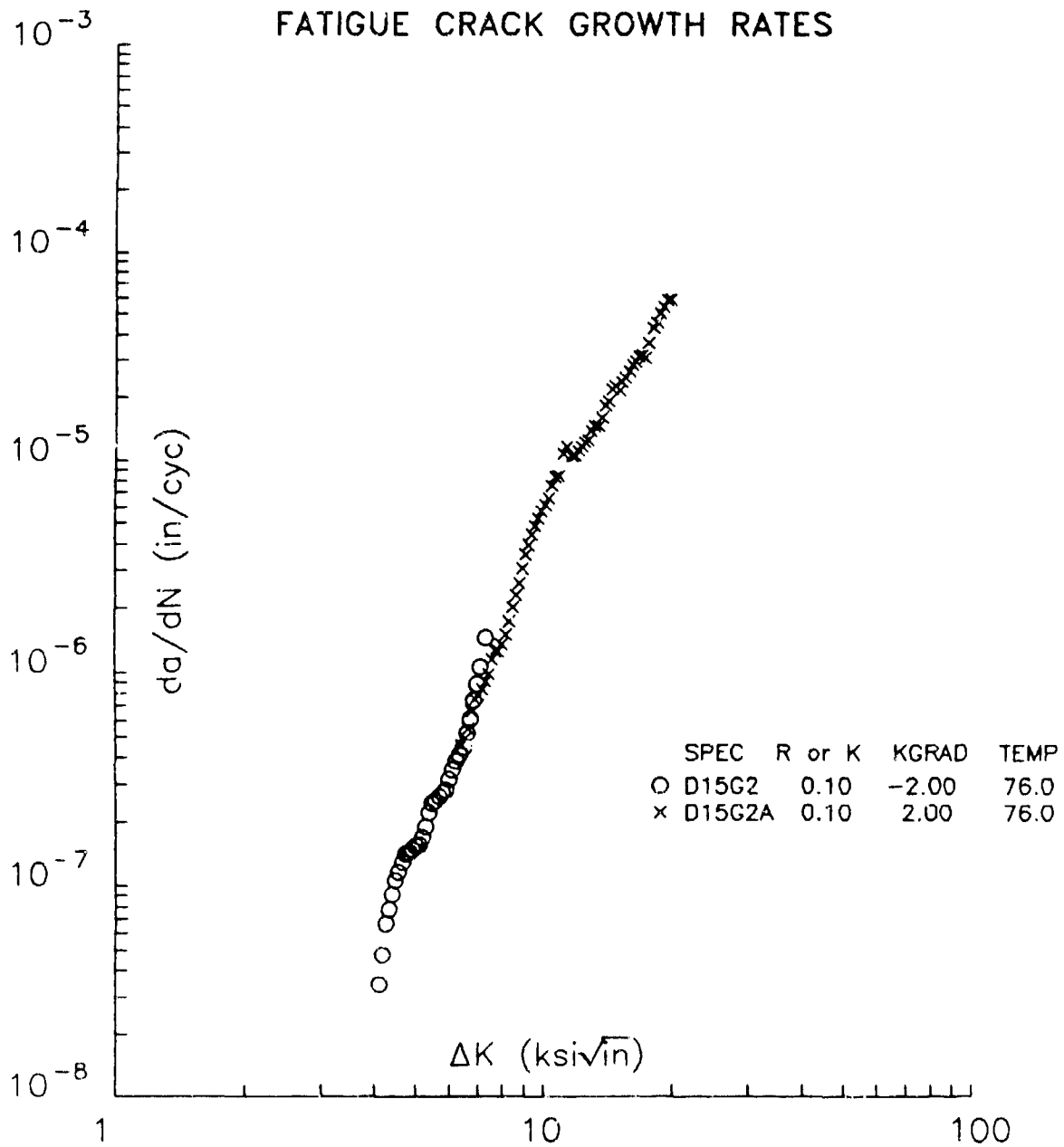


Figure E16. D357-T6 Fatigue Crack Growth Rate Data—Weld Repair

APPENDIX F  
PHASE I, TASK 3  
D357-T6 NONOPTIMUM MICROSTRUCTURE  
ASSESSMENT

TABLE F1. D357-T6 TENSILE PROPERTY DATA ---NONOPTIMUM MICROSTRUCTURE

| PLATE NO. | UTS (ksi) | YS (ksi) | EI (%) |
|-----------|-----------|----------|--------|
| MX31      | 47.5      | 42.6     | 1.1    |
|           | 47.0      | 43.3     | 0.8    |
|           | 46.8      | 42.9     | 0.8    |
|           | 47.0      | 42.4     | 1.1    |
| MX32      | 46.9      | 42.2     | 1.0    |
|           | 46.6      | 43.4     | 0.6    |
|           | 46.7      | 43.3     | 0.7    |
|           | 47.2      | 42.4     | 0.9    |
|           | 47.5      | 43.3     | 0.8    |
| Average   | 47.0      | 42.9     | 0.9    |

TABLE F2. A357-T6 SMOOTH STRESS-LIFE FATIGUE DATA  
 --- NONOPTIMUM MICROSTRUCTURE

| PLATE NO. | MAX. STRESS (ksi) | CYCLES TO FAILURE     |
|-----------|-------------------|-----------------------|
| MX31      | 10                | 5 X 10 <sup>6</sup> * |
|           | 20                | 501,590               |
|           | 25                | 331,393               |
|           | 30                | 54,357                |
| MX32      | 15                | 5 X 10 <sup>6</sup> * |
|           | 17                | 5 X 10 <sup>6</sup> * |
|           | 20                | 235,390               |
|           | 25                | 335,020               |

Note:  $K_t = 1.0$ ,  $R = 0.1$

\* No Failure

TABLE F3. D357-T6 NOTCHED STRESS-LIFE FATIGUE DATA  
 —NONOPTIMUM MICROSTRUCTURE

| PLATE NO. | MAX. STRESS (ksi) | CYCLES TO FAILURE     |
|-----------|-------------------|-----------------------|
| MX31      | 10                | 403,799               |
|           | 20                | 41,401                |
|           | 30                | 3,679                 |
|           | 39.4              | 89                    |
| MX32      | 5                 | 5 X 10 <sup>6</sup> * |
|           | 10                | 407,004               |
|           | 15                | 144,004               |
|           | 20                | 565                   |

Note:  $K_t = 3.0$ ,  $R = 0.1$

\* No Failure

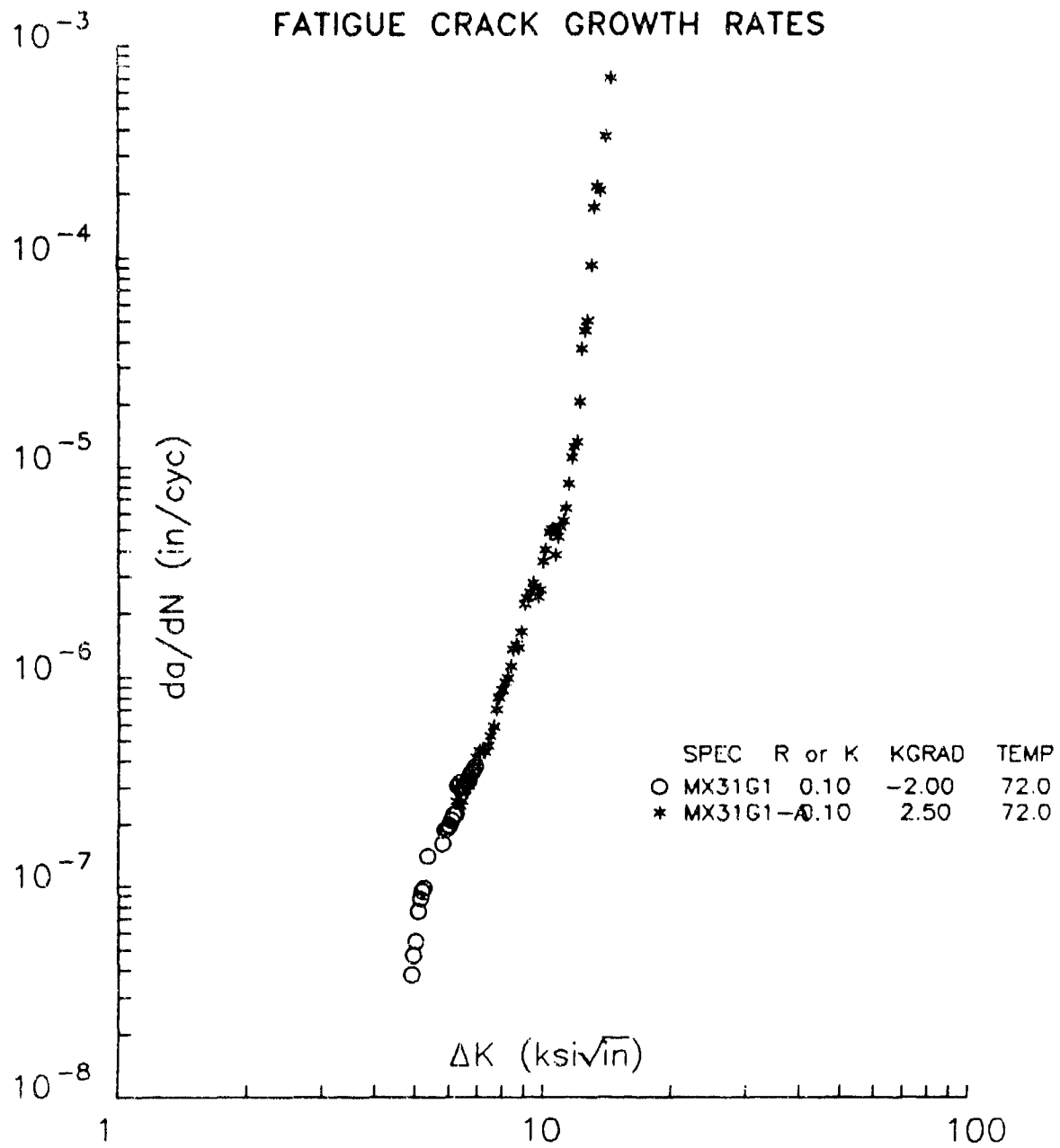


Figure F1. D357-T6 Fatigue Crack Growth Rate Data—Nonoptimum Microstructure

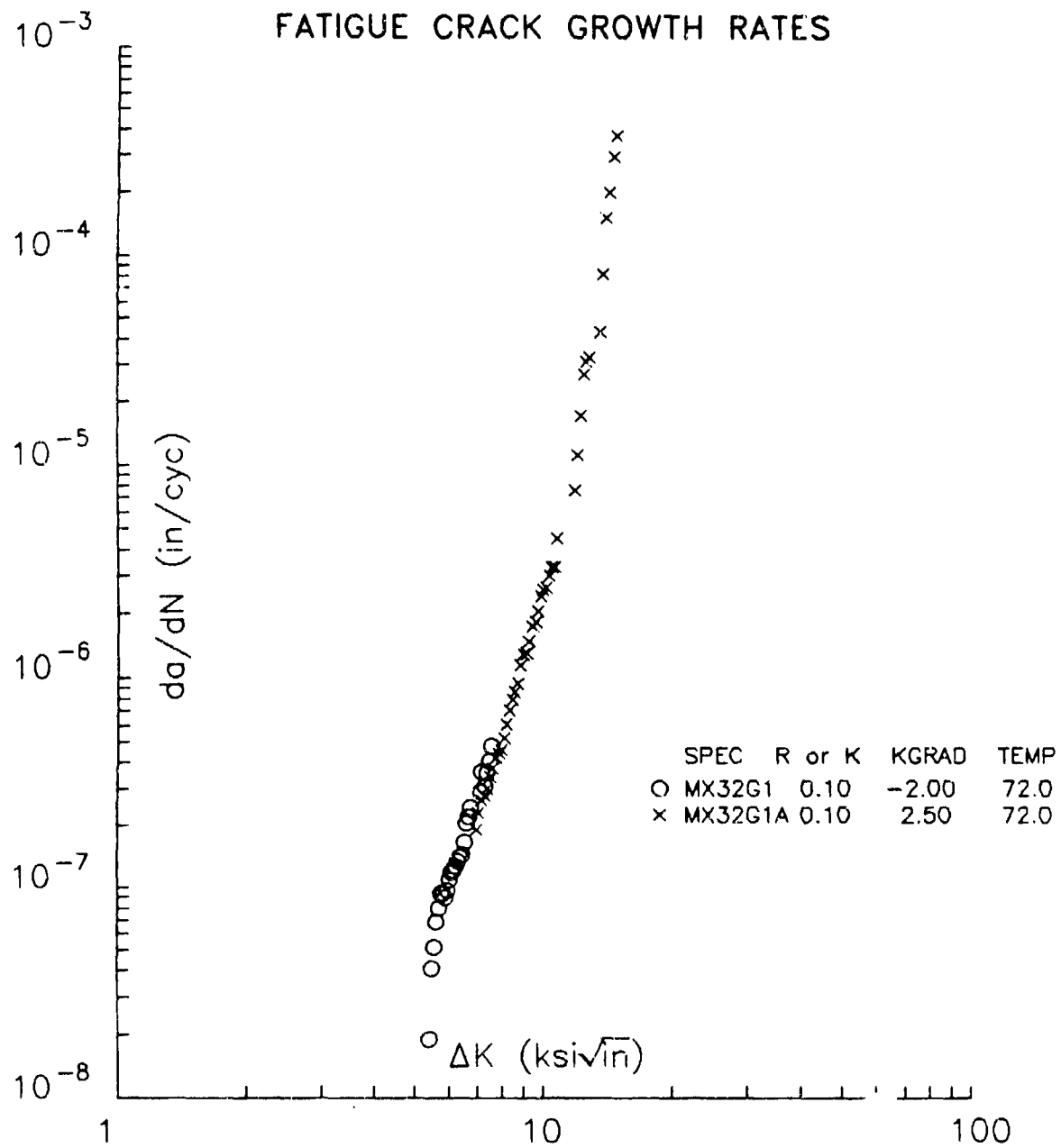


Figure F2. D357-T6 Fatigue Crack Growth Rate Data—Nonoptimum Microstructure

APPENDIX G  
PHASE I, TASK 3  
B201-T7 NONOPTIMUM MICROSTRUCTURE  
ASSESSMENT

TABLE G1. B201-T7 TENSILE PROPERTY DATA — NONOPTIMUM MICROSTRUCTURE

| PLATE NO. | UTS (ksi) | YS (ksi) | EI (%) |
|-----------|-----------|----------|--------|
| MX21      | 65.8      | 58.8     | 11.0   |
|           | 68.0      | 61.2     | 7.9    |
|           | 64.2      | 59.0     | 3.3    |
| MX22      | 64.4      | 58.5     | 5.8    |
|           | 62.0      | 57.6     | 2.7 *  |
|           | 54.3      | 54.3     | 0.1 *  |
| MX23      | 65.6      | 58.8     | 8.9    |
|           | 59.5      | 55.4     | 1.8 *  |
| MX24      | 64.4      | 58.3     | 4.5    |
|           | 59.1      | 56.7     | 1.0 *  |
| Average   | 65.3      | 59.0     | 6.9    |

\* Inclusions Were Observed on the Fracture Surfaces; Data Were Not Used to Compute Average Values.

TABLE G2. B201-T7 SMOOTH STRESS-LIFE FATIGUE DATA  
 -- NONOPTIMUM MICROSTRUCTURE

| PLATE NO. | MAX. STRESS (ksi) | CYCLES TO FAILURE     |
|-----------|-------------------|-----------------------|
| MX21      | 30                | 3 X 10 <sup>6</sup> * |
|           | 40                | 111,434               |
| MX22      | 30                | 97,328                |
| MX23      | 35                | 517,324               |
|           | 45                | 47,377                |
| MX24      | 25                | 748,626               |
|           | 30                | 80,167                |

Note:  $K_t = 1.0$ ,  $R = 0.1$

\* No Failure

TABLE G3. B201-T7 NOTCHED STRESS-LIFE FATIGUE DATA  
 —NONOPTIMUM MICROSTRUCTURE

| PLATE NO. | MAX. STRESS (ksi) | CYCLES TO FAILURE     |
|-----------|-------------------|-----------------------|
| MX21      | 20                | 161,307               |
|           | 30                | 30,286                |
| MX23      | 5                 | 5 X 10 <sup>6</sup> * |
|           | 10                | 5 X 10 <sup>6</sup> * |
|           | 10                | 1,167,690             |
|           | 15                | 5 X 10 <sup>6</sup> * |
|           | 15                | 5 X 10 <sup>6</sup> * |
| MX24      | 17                | 92,164                |
|           | 25                | 52,088                |

Note:  $K_t = 3.0$ ,  $R = 0.1$

\* No Failure

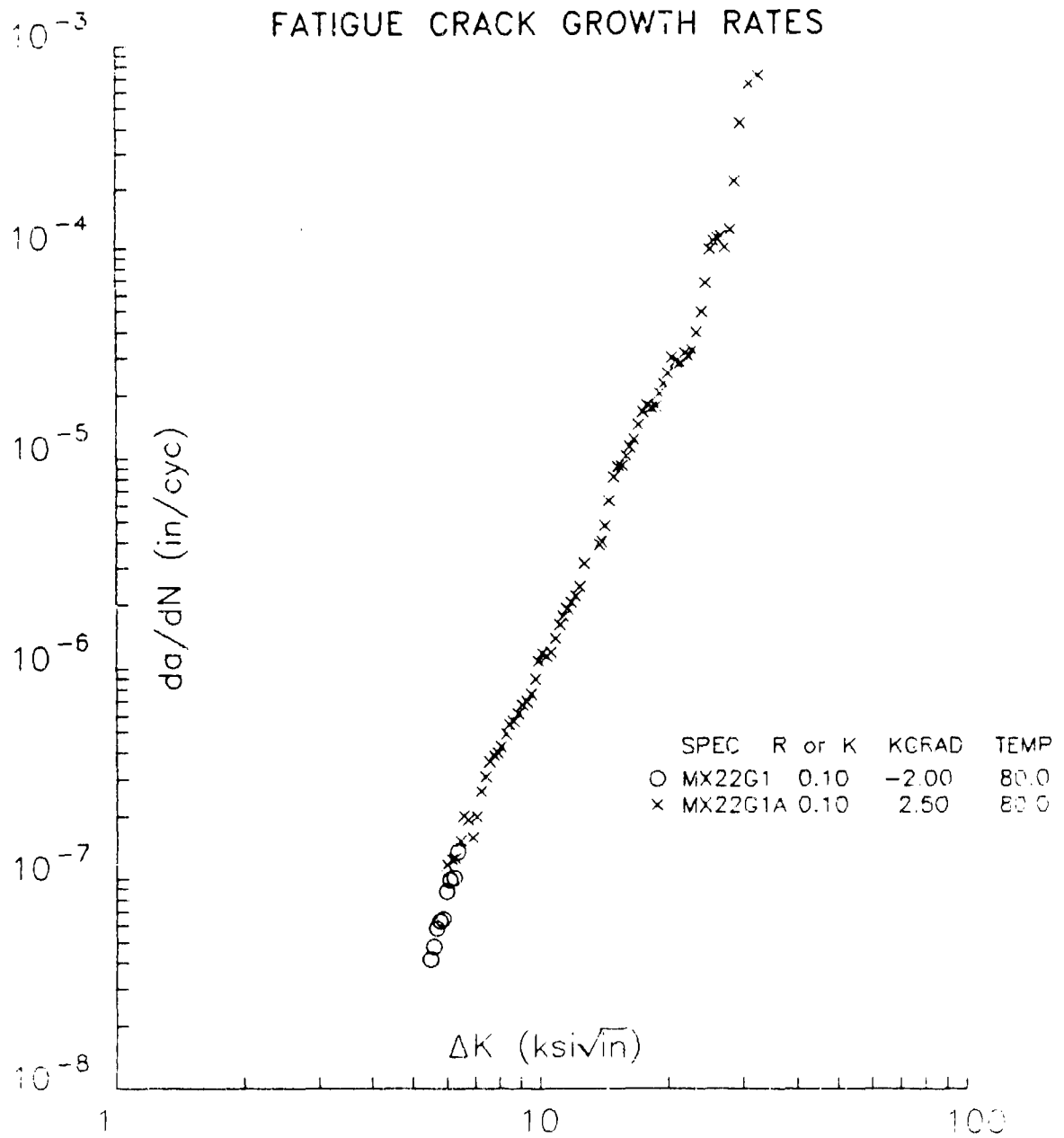


Figure G1. B201-T7 Fatigue Crack Growth Rate Data—Nonoptimum Microstructure

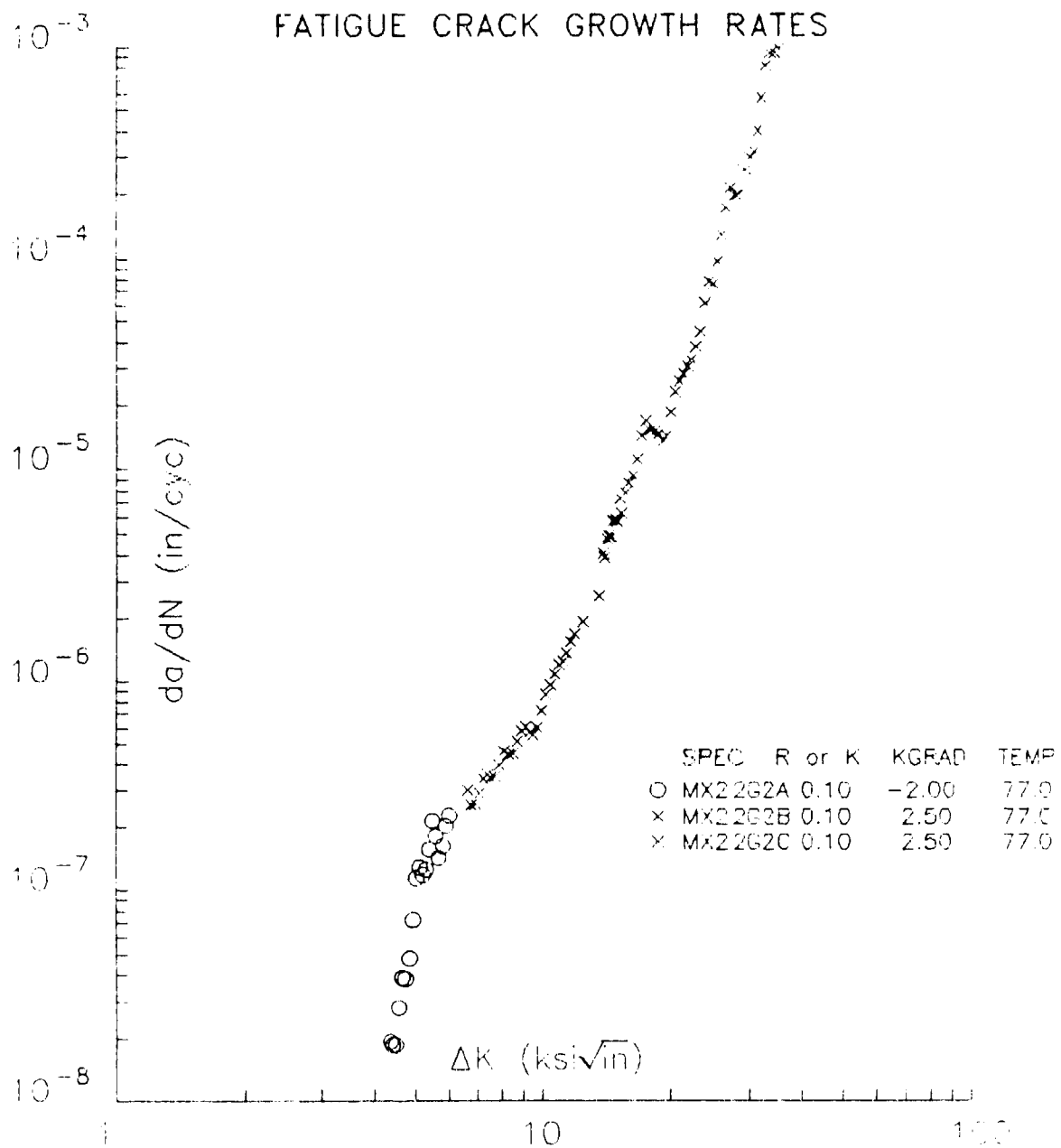


Figure G2. B201-T7 Fatigue Crack Growth Rate Data—Nonoptimum Microstructure

APPENDIX H  
PHASE II, TASK 4  
AIRCRAFT CASTINGS EVALUATION

TABLE H1. D357-T6 PYLON TENSILE PROPERTIES—  
DESIGNATED  
AREAS

| SILICON<br>MODIFIER | PYLON<br>NO. | UTS (ksi) | YS<br>(ksi) | El<br>(%) | NTS<br>(ksi) | <u>NTS</u><br><u>YS</u> |      |
|---------------------|--------------|-----------|-------------|-----------|--------------|-------------------------|------|
| Sodium              | 95           | 51.2      | 42.9        | 5.5       | 63.2         | 1.47                    |      |
|                     |              | 51.8      | 42.1        | 7.0       | 62.1         | 1.48                    |      |
|                     |              | 51.5      | 42.0        | 7.0       | 57.6         | 1.37                    |      |
|                     |              | 52.4      | 42.3        | 8.6       | 61.1         | 1.44                    |      |
|                     | 96           | 51.7      | 43.7        | 6.5       | 59.8         | 1.37                    |      |
|                     |              | 49.3 *    | 41.4        | 3.5       | 63.2         | 1.53                    |      |
|                     |              | 48.9 *    | 39.9 *      | 5.3       | 58.1         | 1.46                    |      |
|                     |              | 51.8      | 42.2        | 7.0       | 59.6         | 1.41                    |      |
|                     |              | Average   | 51.1        | 42.1      | 6.3          | 60.6                    | 1.44 |
|                     | Strontium    | 97        | 52.5        | 41.7      | 10.7         | 60.8                    | 1.45 |
|                     |              |           | 52.8        | 41.7      | 10.7         | 64.3                    | 1.54 |
|                     |              |           | 50.1        | 39.7 *    | 8.6          | 59.9                    | 1.51 |
|                     |              |           | 52.7        | 42.2      | 10.0         | 61.6                    | 1.46 |
| 98                  |              | 53.2      | 42.3        | 11.7      | 64.1         | 1.52                    |      |
|                     |              | 52.9      | 42.1        | 10.5      | 64.7         | 1.54                    |      |
|                     |              | 49.9 *    | 39.9*       | 8.0       | 58.0         | 1.46                    |      |
|                     |              | 53.5      | 43.0        | 9.8       | 61.3         | 1.43                    |      |
|                     |              | Average   | 52.2        | 41.6      | 10.0         | 61.8                    | 1.49 |

\* Below AMS 4241 Specification Requirement (50/40/3)

TABLE H2. D357-T6 PYLON TENSILE PROPERTIES  
 —NONDESIGNATED AREAS

| SILICON<br>MODIFIER | PYLON<br>NO. | UTS<br>(ksi) | YS<br>(ksi) | El<br>(%) |
|---------------------|--------------|--------------|-------------|-----------|
| Sodium              | 95           | 52.5         | 42.4        | 8.0       |
|                     |              | 52.1         | 42.3        | 7.1       |
|                     | 96           | 52.0         | 41.3        | 6.9       |
|                     |              | 51.5         | 41.2        | 7.9       |
|                     | Average      | 52.0         | 41.8        | 7.5       |
| Strontium           | 97           | 53.2         | 40.8        | 11.2      |
|                     |              | 51.9         | 39.9        | 11.1      |
|                     | 98           | 52.9         | 40.3        | 9.8       |
|                     |              | 52.4         | 40.7        | 9.9       |
|                     | Average      | 52.7         | 40.4        | 10.5      |

TABLE H3. D357-T6 TEST PLATE TENSILE DATA

| PLATE NO    | UTS (ksi) | YS (ksi) | EI (%) |
|-------------|-----------|----------|--------|
| Q1          | 50.9      | 40.9     | 6.1    |
|             | 51.1      | 41.9     | 6.1    |
| Q2          | 52.7      | 41.6     | 11.8   |
|             | 52.6      | 41.9     | 9.2    |
| Q3          | 52.0      | 42.0     | 7.4    |
|             | 52.8      | 41.3     | 11.4   |
| Q4          | 53.2      | 42.7     | 9.6    |
|             | 51.9      | 41.4     | 14.5   |
| Q5          | 52.7      | 43.1     | 6.8    |
|             | 52.8      | 43.8     | 6.1    |
| Q6 *        | 52.5      | 37.8*    | 9.3    |
|             | 51.9      | 41.3     | 9.5    |
| Q7*         | 49.1*     | 42.5     | 3.7    |
|             | 50.4      | 42.5     | 5.4    |
| Q8          | 52.1      | 41.6     | 8.7    |
|             | 53.7      | 41.8     | 13.9   |
| Q9          | 51.9      | 41.5     | 8.5    |
|             | 51.4      | 40.7     | 8.7    |
| Q10         | 52.8      | 43.1     | 7.7    |
|             | 52.5      | 41.9     | 9.7    |
| Q11         | 51.3      | 40.2     | 8.8    |
|             | 51.7      | 40.7     | 9.5    |
| Q12         | 52.6      | 41.7     | 11.0   |
|             | 52.5      | 41.3     | 10.1   |
| Q13 **      | 48.5**    | 40.9     | 3.7    |
|             | 47.2**    | 41.1     | 2.6**  |
| Q14 **      | 49.8**    | 41.2     | 6.0    |
|             | 49.4**    | 41.7     | 4.6    |
| Average *** | 52.0      | 41.7     | 8.9    |

\* Data Out of Specification — Plate Used for DADT Analysis

\*\* Data Out of Specification — Plate Not Used for DADT Analysis

\*\*\* Excludes data from plates Q13 and Q14, which were not used for DADT analysis

TABLE H4. D357-T6 SMOOTH STRESS - LIFE FATIGUE DATA  
 — DESIGNATED AREAS

| SILICON<br>MODIFIER | PYLON<br>NO. | MAX. STRESS<br>(ksi) | CYCLES TO<br>FAILURE  |
|---------------------|--------------|----------------------|-----------------------|
| Sodium              | 95           | 20                   | 5 x 10 <sup>6</sup> * |
|                     |              | 30                   | 610,710               |
|                     | 96           | 25                   | 3,336,750             |
|                     |              | 40                   | 334,140               |
| Strontium           | 97           | 30                   | 471,850               |
|                     |              | 40                   | 269,980               |
|                     | 98           | 25                   | 5 x 10 <sup>6</sup> * |
|                     |              | 45                   | 49,430                |

Note:  $K_t = 1.0$ ,  $R = 0.1$

\* No Failure

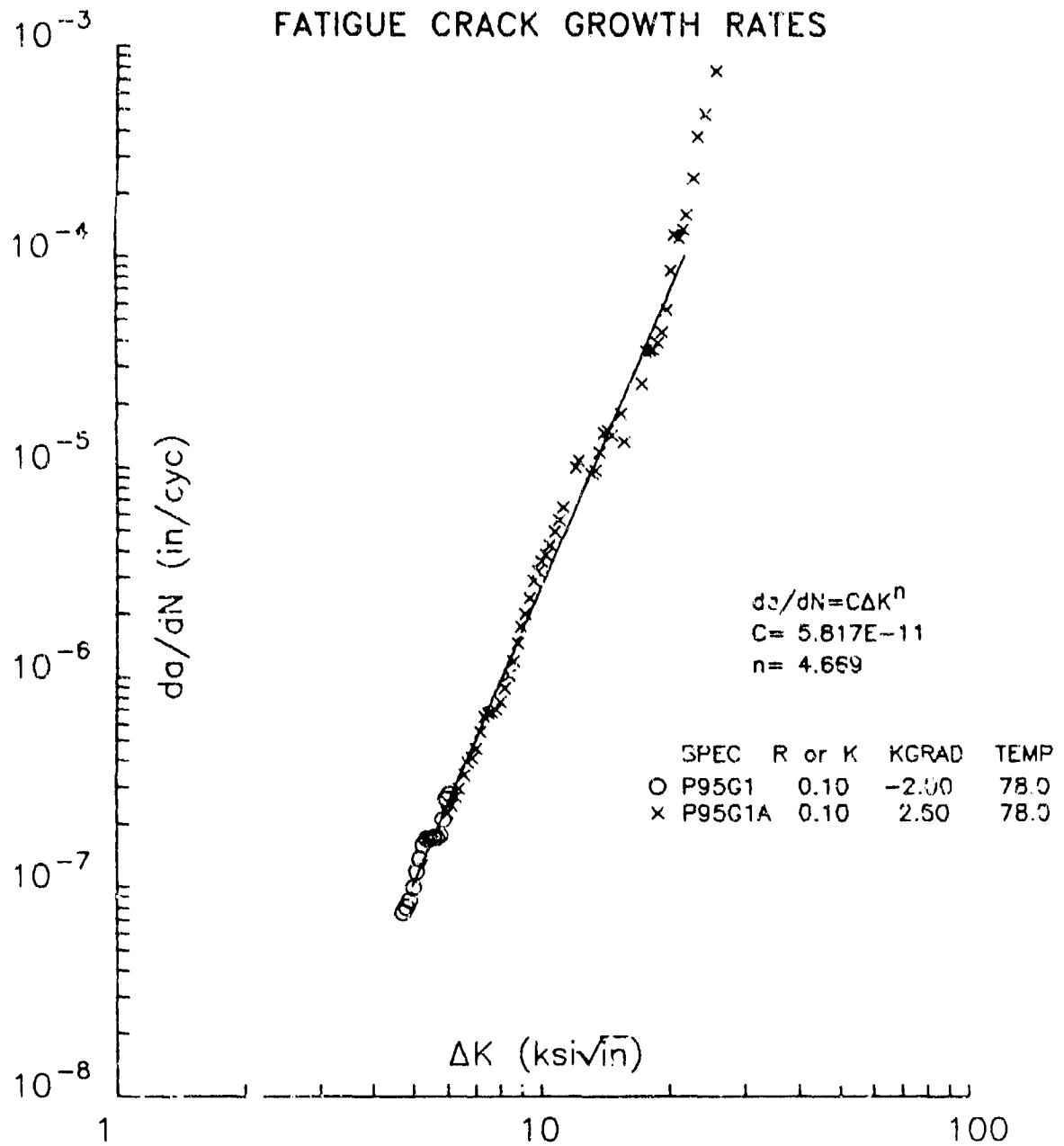


Figure H1. D357-T6 Pylon Fatigue Crack Growth Rate Data

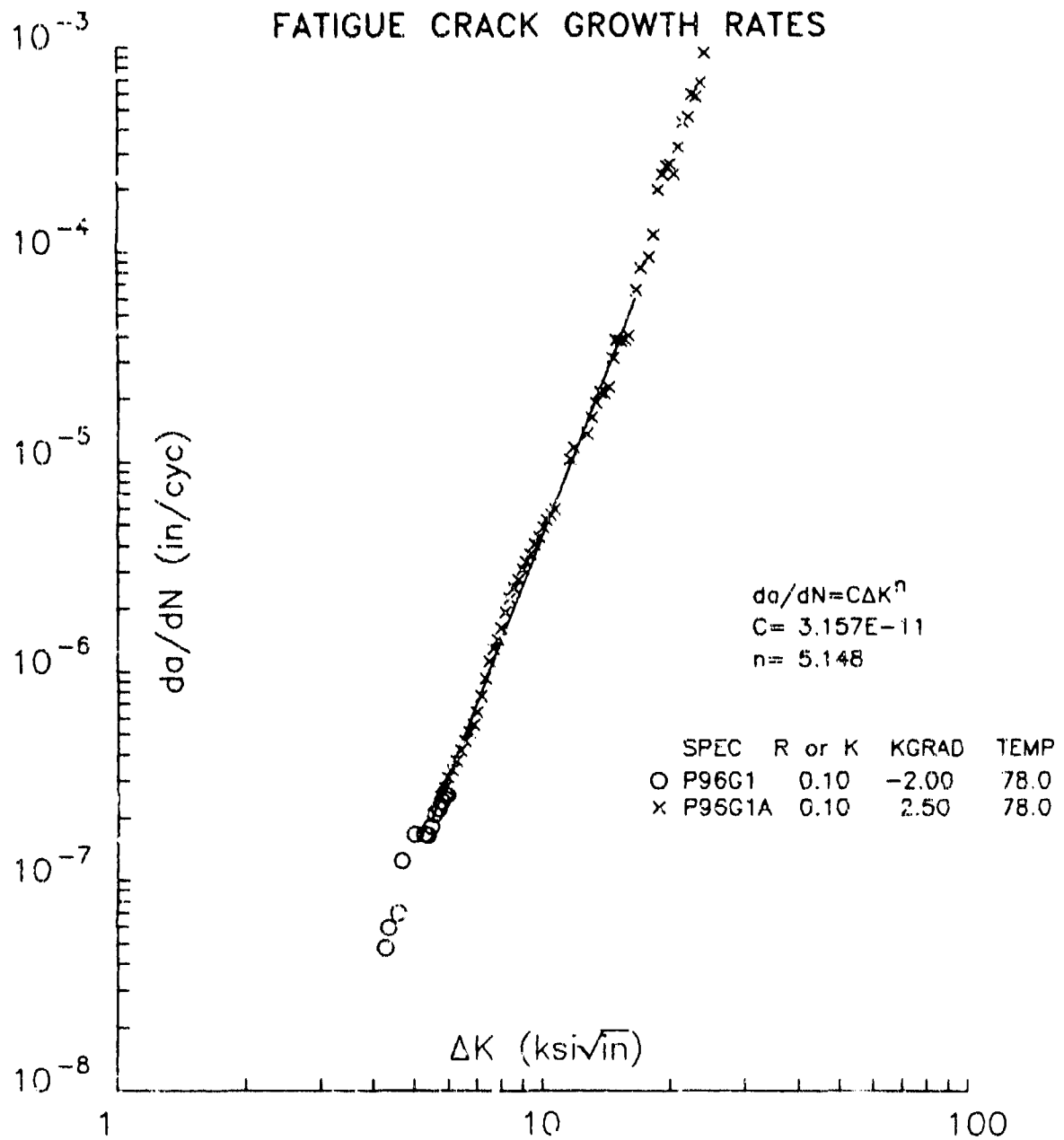


Figure H2. D357-T6 Pylon Fatigue Crack Growth Rate Data

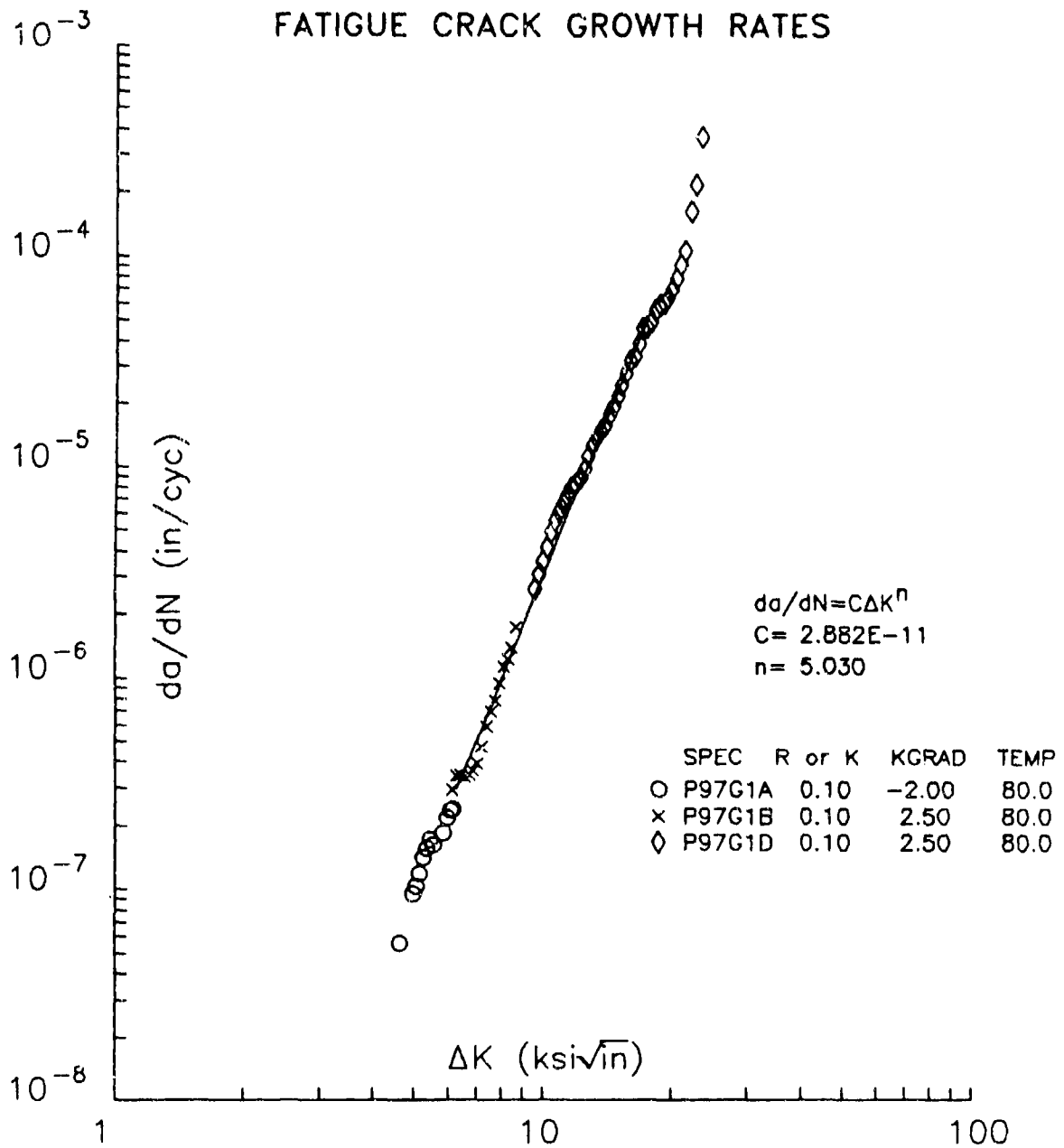


Figure H3. D357-T6 Pylon Fatigue Crack Growth Rate Data

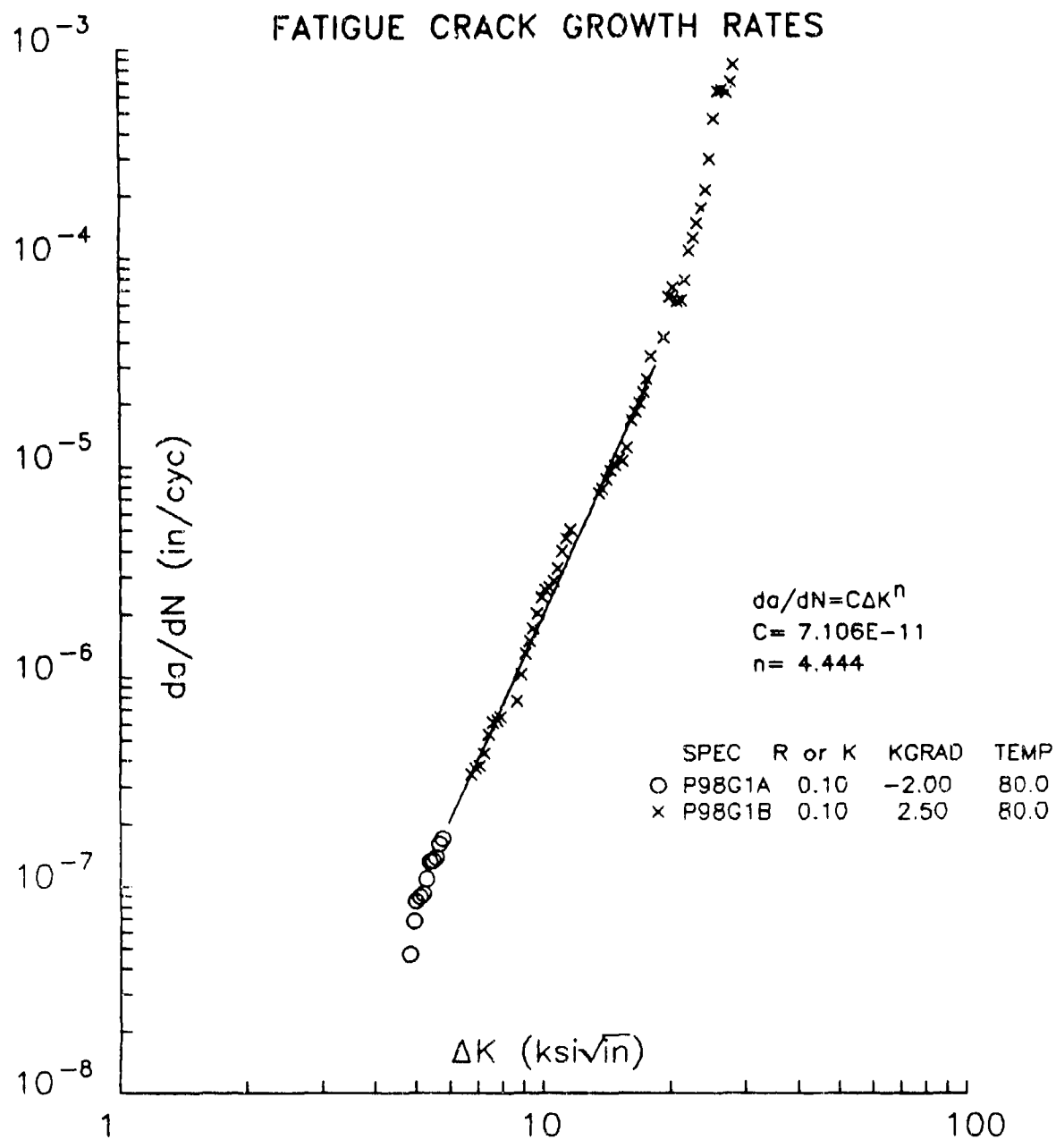


Figure H4. D357-T6 Pylon Fatigue Crack Growth Rate Data

APPENDIX I  
PHASE II, TASK 4  
ELEMENT TEST DATA

## Appendix I

Data summaries for each of the durability and damage tolerance specimens are given below. For the multihole durability specimens, the crack length at failure for each of the four largest cracks observed during testing is recorded along with the initiating defect and approximate defect size.

The location of each crack is identified by the hole number, the face on which the crack appeared (front or rear), and the crack propagation direction (inboard or outboard). Figure I1 illustrates the hole numbering scheme as well as the inboard and outboard directions.

Many of the cracks identified during testing of the multihole specimens occurred at holes at which the sample ultimately failed. For these cracks, the crack length is preceded by a "≥" sign to show that the actual length at failure is presumably greater than the indicated value. The crack length values which are given for these cracks represent the last recorded value prior to specimen failure.

For many of the cracks observed in the multihole specimens, complete identification of the initiating defect was not possible because of smeared fractographic features (a result of the fatigue loading). Where features were observed, in some cases the size could not be defined because of multiple sites. Additional fractographic analysis is required to more clearly identify these sites.

The surface flaw damage tolerance specimen is shown in Figure I2. For each of the four specimens tested, cracks were initiated at the left and right corners of the EDM surface flaw. The data summaries indicate the length of each left hand and right hand crack, as well as the length of any crack which may have broken out of the back surface, as a function of flight hours completed. Similar data summaries are provided for each of the precracked hole specimens.

All specimens were tested under spectrum loading using an F-18 wing root spectrum (F18C2) with the negative loads removed so that the complete test surface was visible. Negative loading would have required the use of lateral buckling constraints, which would have restricted the visibility.

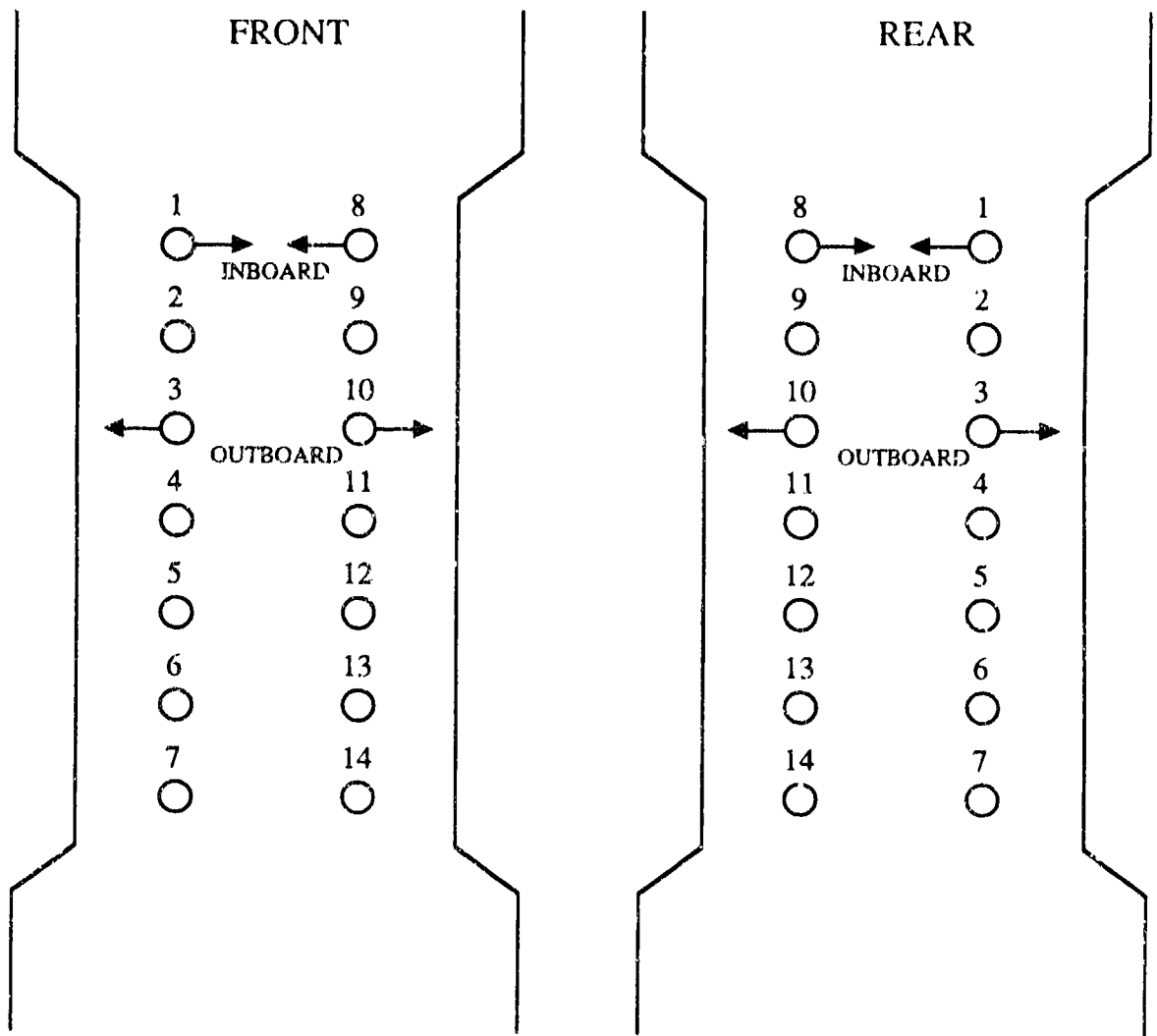


Figure 11. Hole Number Assignment For Multihole Durability Specimens

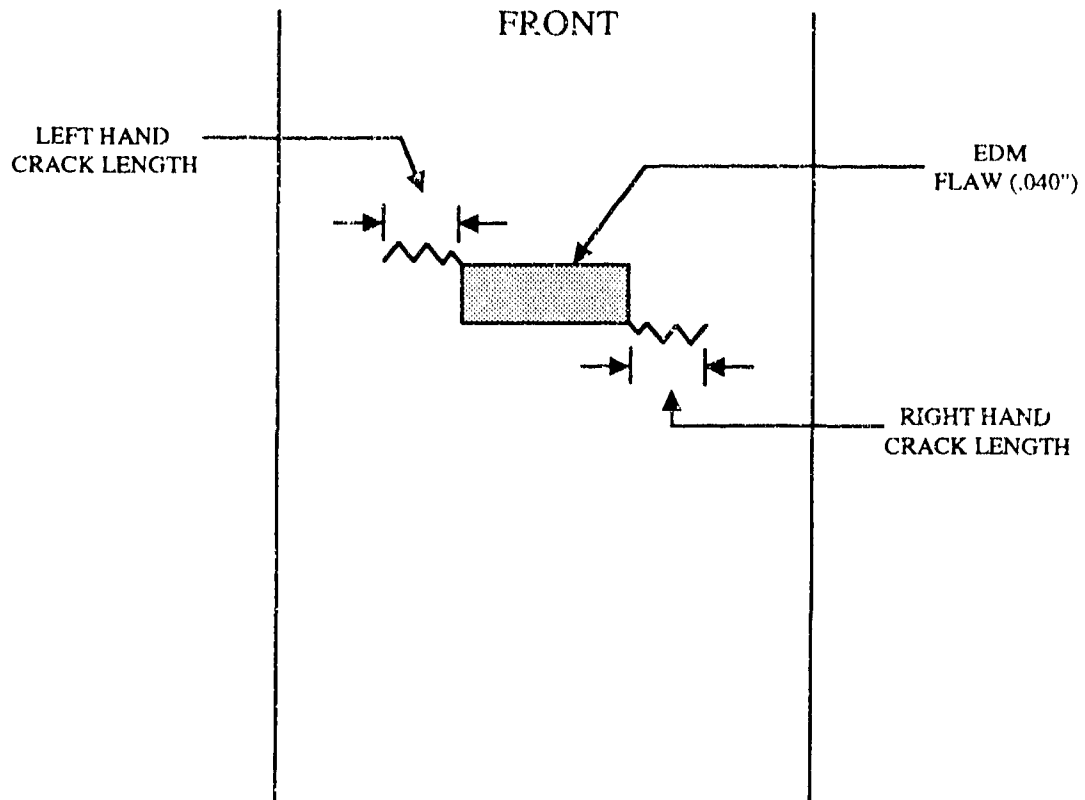


Figure 12. Crack Orientation For Surface Flaw Specimens

## Multihole Durability

|                             |          |
|-----------------------------|----------|
| Specimen:                   | Q1D1     |
| Gross Stress (ksi):         | 37       |
| Total Life (Flight Hours)   | 1528     |
| Specimen Fracture at Holes: | 5 and 12 |

| Crack Number | Hole ID(1) | Crack Length at Failure (inch) | Initiation Site   |             |
|--------------|------------|--------------------------------|-------------------|-------------|
|              |            |                                | Type              | Size (inch) |
| 1            | 13-R-O     | .017                           | NI                | —           |
| 2            | 12-F-I     | >.012                          | NI                | —           |
| 3            | 5-R-O      | .006                           | Silicon Particles | ND          |
| 4            | 13-F-O     | .004                           | NI                | —           |

(1) F = Front; R = Rear; I = Inboard; O = Outboard  
ND = Not defined; identification of complete crack site not possible due to multiple defects  
NI = Not identified; fractographic features obscured

## Multihole Durability

Specimen: Q2D2  
 Gross Stress (ksi): 37  
 Total Life (Flight Hours) 2419  
 Specimen Fracture at Holes: 5 and 12

| Crack Number | Hole ID <sup>(1)</sup> | Crack Length at Failure (inch) | Initiation Site   |             |
|--------------|------------------------|--------------------------------|-------------------|-------------|
|              |                        |                                | Type              | Size (inch) |
| 1            | 6-R-I                  | .016                           | NI                | —           |
| 2            | 6-F-I                  | .010                           | Silicon Particles | .0030       |
| 3            | 5-R-O                  | >.006                          | NI                | —           |
| 4            | 12-F-O                 | N/O                            | Silicon Particles | ND          |

(1) F = Front, R = Rear; I = Inboard; O = Outboard

ND = Not defined; identification of complete crack site not possible due to multiple defects

NI = Not identified

N/O = No surface cracks observed

## Multihole Durability

|                             |         |
|-----------------------------|---------|
| Specimen:                   | Q3D3    |
| Gross Stress (ksi):         | 32      |
| Total Life (Flight Hours)   | 13,528  |
| Specimen Fracture at Holes: | 2 and 9 |

| Crack Number | Hole ID(1) | Crack Length at Failure (inch) | Initiation Site   |             |
|--------------|------------|--------------------------------|-------------------|-------------|
|              |            |                                | Type              | Size (inch) |
| 1            | 2-F-O      | >.090                          | Cavity            | .0006       |
| 2            | 13-F-O     | .049                           | NI                | —           |
| 3            | 9-F-O      | >.046                          | NI                | —           |
| 4            | 2-F-I      | >.024                          | Silicon Particles | ND          |

(1) F = Front; R = Rear; I = Inboard; O = Outboard

ND = Not defined; identification of complete crack site not possible due to multiple defects

NI = Not identified

## Multihole Durability

Specimen: Q4D4  
Gross Stress (ksi): 33  
Total Life (Flight Hours) 6628  
Specimen Fracture at Holes: 5 and 12

| Crack Number | Hole ID <sup>(1)</sup> | Crack Length at Failure (inch) | Initiation Site |             |
|--------------|------------------------|--------------------------------|-----------------|-------------|
|              |                        |                                | Type            | Size (inch) |
| 1            | 6-R-O                  | .086                           | NI              | —           |
| 2            | 6-F-O                  | .042                           | NI              | —           |
| 3            | 12-F-I                 | >.020                          | NI              | —           |
| 4            | 12-R-I                 | >.010                          | NI              | —           |

(1) F = Front; R = Rear; I = Inboard; O = Outboard  
ND = Not defined; identification of complete crack site not possible due to multiple defects  
NI = Not identified

## Multihole Durability

|                             |         |
|-----------------------------|---------|
| Specimen:                   | Q5A1    |
| Gross Stress (ksi):         | 40      |
| Total Life (Flight Hours)   | 28      |
| Specimen Fracture at Holes: | 2 and 9 |

---

No Fatigue Cracks Observed on Front or Rear Faces of the Specimen

## Multihole Durability

Specimen: Q5C1  
 Gross Stress (ksi): 35  
 Total Life (Flight Hours) 6755  
 Specimen Fracture at Holes: 2 and 9

| Crack Number | Hole ID <sup>(1)</sup> | Crack Length at Failure (inch) | Initiation Site                      |             |
|--------------|------------------------|--------------------------------|--------------------------------------|-------------|
|              |                        |                                | Type                                 | Size (inch) |
| 1            | 2-F-O                  | >.054                          | Silicon Particles                    | ND          |
| 2            | 4-F-O                  | .044                           | NI                                   | —           |
| 3            | 6-F-O                  | .018                           | Silicon Particles/<br>Shrinkage Pore | .0015       |
| 4            | 3-F-O                  | .010                           | Silicon Particles                    | ND          |

(1) F = Front; R = Rear; I = Inboard; O = Outboard

ND = Not defined; identification of complete crack site not possible due to multiple defects

NI = Not identified

## Multihole Durability

Specimen: Q6A2  
Gross Stress (ksi): 35  
Total Life (Flight Hours) 3755  
Specimen Fracture at Holes: 6 and 13

| Crack Number | Hole ID(1) | Crack Length at Failure (inch) | Initiation Site   |             |
|--------------|------------|--------------------------------|-------------------|-------------|
|              |            |                                | Type              | Size (inch) |
| 1            | 13-R-I     | .018                           | Silicon Particles | ND          |
| 2            | 11-R-O     | .008                           | NI                | —           |
| 3            | 13-R-O     | N/O                            | Cavity            | .0015       |

(1) F = Front; R = Rear; I = Inboard; O = Outboard

ND = Not defined; identification of complete crack site not possible due to multiple defects

NI = Not identified

N/O = No surface cracks observed

## Multihole Durability

|                             |          |
|-----------------------------|----------|
| Specimen:                   | Q6C2     |
| Gross Stress (ksi):         | 40       |
| Total Life (Flight Hours)   | 253      |
| Specimen Fracture at Holes: | 4 and 11 |

---

No Fatigue Cracks Observed on Front or Rear Faces of the Specimen

## Multihole Durability

Specimen: Q7A3  
 Gross Stress (ksi): 32  
 Total Life (Flight Hours) 11,053  
 Specimen Fracture at Holes: 2 and 9

| Crack Number | Hole ID <sup>(1)</sup> | Crack Length at Failure (inch) | Initiation Site   |             |
|--------------|------------------------|--------------------------------|-------------------|-------------|
|              |                        |                                | Type              | Size (inch) |
| 1            | 2-F-O                  | >.042                          | NI                | —           |
| 2            | 2-R-O                  | >.030                          | Silicon Particle  | .0004       |
| 3            | 2-F-I                  | >.024                          | Silicon Particles | ND          |
| 4            | 4-F-O                  | .020                           | NI                | —           |

(1) F = Front; R = Rear; I = Inboard; O = Outboard  
 ND = Not defined; identification of complete crack site not possible due to multiple defects  
 NI = Not identified

## Multihole Durability

Specimen: Q8A6  
 Gross Stress (ksi): 25  
 Total Life (Flight Hours) 38,428  
 Specimen Fracture at Holes: 2 and 9

| Crack Number | Hole ID(1) | Crack Length at Failure (inch) | Initiation Site   |             |
|--------------|------------|--------------------------------|-------------------|-------------|
|              |            |                                | Type              | Size (inch) |
| 1            | 1-F-O      | .104                           | Silicon Particles | ND          |
| 2            | 2-F-O      | >.098                          | NI                | —           |
| 3            | 2-R-O      | >.074                          | Dross             | ND          |
| 4            | 2-R-I      | >.066                          | Silicon Particles | ND          |

(1) F = Front; R = Rear; I = Inboard; O = Outboard

ND = Not defined; identification of complete crack site not possible due to multiple defects

NI = Not identified

## Multihole Durability

Specimen: Q9B1  
Gross Stress (ksi): 37  
Total Life (Flight Hours) 3628  
Specimen Fracture at Holes: 6 and 13

| Crack Number | Hole ID <sup>(1)</sup> | Crack Length at Failure (inch) | Initiation Site   |             |
|--------------|------------------------|--------------------------------|-------------------|-------------|
|              |                        |                                | Type              | Size (inch) |
| 1            | 13-R-O                 | >.022                          | Silicon Particles | ND          |
| 2            | 12-R-O                 | .012                           | NI                | —           |
| 3            | 11-F-I                 | .010                           | NI                | —           |

(1) F = Front; R = Rear; I = Inboard; O = Outboard

ND = Not defined; identification of complete crack site not possible due to multiple defects

NI = Not identified

## Multihole Durability

Specimen: Q10B2  
 Gross Stress (ksi): 25  
 Total Life (Flight Hours) 48,928  
 Specimen Fracture at Holes: 4 and 11

| Crack Number | Hole ID(1) | Crack Length at Failure (inch) | Initiation Site |             |
|--------------|------------|--------------------------------|-----------------|-------------|
|              |            |                                | Type            | Size (inch) |
| 1            | 11-F-O     | >.136                          | NI              | —           |
| 2            | 10-F-O     | .100                           | NI              | —           |
| 3            | 10-F-I     | .098                           | NI              | —           |
| 4            | 11-R-O     | >.088                          | NI              | —           |

(1) F = Front; R = Rear; I = Inboard; O = Outboard  
 NI = Not identified

## Multihole Durability

Specimen: Q11B3  
Gross Stress (ksi): 35  
Total Life (Flight Hours) 6455  
Specimen Fracture at Holes: 2 and 9

| Crack Number | Hole ID(1) | Crack Length at Failure (inch) | Initiation Site   |             |
|--------------|------------|--------------------------------|-------------------|-------------|
|              |            |                                | Type              | Size (inch) |
| 1            | 10-R-I     | .035                           | Silicon Particles | ND          |
| 2            | 2-R-O      | >.028                          | Silicon Particle  | .0010       |
| 3            | 10-F-I     | .026                           | NI                | ---         |
| 4            | 2-F-O      | >.022                          | NI                | ---         |

(1) F = Front; R = Rear; I = Inboard; O = Outboard

ND = Not defined; identification of complete crack site not possible due to multiple defects

NI = Not identified

## Multihole Durability

Specimen: Q1234  
 Gross Stress (ksi): 32  
 Total Life (Flight Hours) 10,828  
 Specimen Fracture at Holes: 3 and 10

| Crack Number | Hole ID(1) | Crack Length at Failure (inch) | Initiation Site   |             |
|--------------|------------|--------------------------------|-------------------|-------------|
|              |            |                                | Type              | Size (inch) |
| 1            | 10-R-I     | >.050                          | NI                | —           |
| 2            | 10-F-I     | >.045                          | Silicon Particles | ND          |
| 3            | 10-R-O     | >.022                          | Silicon Particle  | ND          |
| 4            | 12-F-O     | .012                           | NI                | —           |

(1) F = Front; R = Rear; I = Inboard; O = Outboard

ND = Not defined; identification of complete crack site not possible due to multiple defects

NI = Not identified

## Surface Flaw

|                           |        |
|---------------------------|--------|
| Specimen:                 | Q1S1   |
| Gross Stress (ksi):       | 40     |
| Total Life (Flight Hours) | 11,428 |

---

| Crack Length (in) |       |      |                              |
|-------------------|-------|------|------------------------------|
| Front             |       | Rear | Total Life<br>(Flight Hours) |
| Left              | Right | Left |                              |
| .016              | .022  | None | 0                            |
| .025              | .027  | None | 3000                         |
| .026              | .028  | .004 | 3600                         |
| .032              | .034  | .005 | 4800                         |
| .037              | .039  | .005 | 6000                         |
| .042              | .042  | .005 | 7200                         |
| .045              | .048  | .005 | 7800                         |
| .054              | .058  | .005 | 8400                         |
| .058              | .059  | .006 | 9000                         |
| .068              | .065  | .006 | 9300                         |
| .072              | .068  | .010 | 9600                         |
| .075              | .076  | .010 | 10,200                       |
| .093              | .087  | .010 | 10,800                       |
| .122              | .112  | .010 | 11,400                       |

---

## Surface Flaw

Specimen: Q3S2  
Gross Stress (ksi): 42  
Total Life (Flight Hours) 7828

---

| Crack Length (inch) |       |                              |
|---------------------|-------|------------------------------|
| Front               |       | Total Life<br>(Flight Hours) |
| Left                | Right |                              |
| .016                | .024  | 0                            |
| .030                | .030  | 2100                         |
| .033                | .035  | 2700                         |
| .040                | .039  | 3300                         |
| .044                | .045  | 3900                         |
| .048                | .051  | 5100                         |
| .056                | .056  | 5700                         |
| .065                | .063  | 6300                         |
| .075                | .074  | 6900                         |
| .084                | .091  | 7500                         |

---

## Surface Flaw

|                           |        |
|---------------------------|--------|
| Specimen:                 | Q10S3  |
| Gross Stress (ksi):       | 35     |
| Total Life (Flight Hours) | 18,328 |

---

| Crack Length (inch) |       |                              |
|---------------------|-------|------------------------------|
| Front               |       | Total Life<br>(Flight Hours) |
| Left                | Right |                              |
| .019                | .021  | 0                            |
| .026                | .028  | 1800                         |
| .026                | .032  | 3900                         |
| .030                | .034  | 5100                         |
| .032                | .041  | 6300                         |
| .037                | .045  | 7500                         |
| .038                | .051  | 8700                         |
| .044                | .052  | 9900                         |
| .052                | .060  | 11,100                       |
| .058                | .067  | 12,300                       |
| .062                | .073  | 13,500                       |
| .069                | .080  | 14,700                       |
| .089                | .093  | 15,900                       |
| .096                | .104  | 16,500                       |
| .111                | .113  | 17,100                       |
| .129                | .136  | 17,700                       |

---

## Surface Flaw

Specimen: Q4S4  
 Gross Stress (ksi): 35  
 Total Life (Flight Hours) 19,933

---

| Crack Length (inch) |       |                              |
|---------------------|-------|------------------------------|
| Front               |       | Total Life<br>(Flight Hours) |
| Left                | Right |                              |
| .022                | .018  | 0                            |
| .038                | .023  | 3300                         |
| .041                | .023  | 4500                         |
| .043                | .024  | 5700                         |
| .046                | .024  | 6900                         |
| .047                | .026  | 8100                         |
| .049                | .032  | 9300                         |
| .053                | .037  | 10,500                       |
| .056                | .038  | 11,700                       |
| .062                | .041  | 12,900                       |
| .068                | .051  | 14,100                       |
| .074                | .055  | 15,300                       |
| .080                | .071  | 16,500                       |
| .098                | .085  | 17,700                       |
| .109                | .099  | 18,300                       |
| .123                | .114  | 18,900                       |
| .141                | .138  | 19,500                       |

---

## Precracked Hole

Specimen: Q1H1  
 Gross Stress (ksi): 30  
 Total Life (Flight Hours) 1655

| Crack Length (in) |       |      |       |      | Total Life<br>(Flight Hours) |
|-------------------|-------|------|-------|------|------------------------------|
| Front             |       | Rear |       |      |                              |
| Left              | Right | Left | Right |      |                              |
| None              | .040  | None | None  | 0    |                              |
| "                 | .044  | .009 | "     | 150  |                              |
| "                 | .047  | .010 | "     | 300  |                              |
| "                 | .054  | .010 | "     | 450  |                              |
| "                 | .055  | .011 | "     | 600  |                              |
| "                 | .058  | .012 | "     | 750  |                              |
| "                 | .062  | .012 | "     | 900  |                              |
| "                 | .063  | .014 | .010  | 1050 |                              |
| "                 | .064  | .014 | .010  | 1200 |                              |
| "                 | .073  | .016 | .012  | 1350 |                              |
| "                 | .073  | .020 | .013  | 1500 |                              |
| .006              | .085  | .034 | .016  | 1650 |                              |

## Precracked Hole

|                           |        |
|---------------------------|--------|
| Specimen:                 | Q3H2   |
| Gross Stress (ksi):       | 23     |
| Total Life (Flight Hours) | 16,055 |

| Crack Length (in) |       |      |                              |
|-------------------|-------|------|------------------------------|
| Front             |       | Rear | Total Life<br>(Flight Hours) |
| Left              | Right | Left |                              |
| None              | .045  | None | 0                            |
| "                 | .056  | "    | 1200                         |
| "                 | .064  | "    | 2400                         |
| "                 | .067  | "    | 3600                         |
| "                 | .071  | "    | 4800                         |
| "                 | .076  | "    | 6000                         |
| "                 | .080  | "    | 7200                         |
| "                 | .090  | "    | 8400                         |
| "                 | .102  | "    | 9600                         |
| "                 | .116  | "    | 10,800                       |
| "                 | .124  | "    | 12,000                       |
| "                 | .140  | "    | 13,200                       |
| .006              | .168  | "    | 14,400                       |
| .008              | .184  | .028 | 15,000                       |
| .008              | .194  | .046 | 15,300                       |
| .010              | .207  | .050 | 15,600                       |
| .024              | .236  | .058 | 15,900                       |

## Precracked Hole

Specimen: Q10H3  
 Gross Stress (ksi): 27  
 Total Life (Flight Hours) 7350

| Crack Length (inch) |      |                              |
|---------------------|------|------------------------------|
| Front               | Rear | Total Life<br>(Flight Hours) |
| Right               | Left |                              |
| .045                | None | 0                            |
| .055                | "    | 600                          |
| .062                | "    | 1200                         |
| .073                | "    | 1800                         |
| .074                | "    | 2400                         |
| .080                | "    | 3000                         |
| .085                | "    | 3600                         |
| .095                | "    | 4200                         |
| .100                | "    | 4800                         |
| .115                | "    | 5400                         |
| .140                | "    | 6000                         |
| .158                | "    | 6600                         |
| .186                | "    | 6900                         |
| .206                | .070 | 7200                         |

## Precracked Hole

|                           |                    |
|---------------------------|--------------------|
| Specimen:                 | Q4H4 (Weld Repair) |
| Gross Stress (ksi):       | 23                 |
| Total Life (Flight Hours) | 10,219             |

| Crack Length (inch) |      | Total Life<br>(Flight Hours) |
|---------------------|------|------------------------------|
| Front               | Rear |                              |
| Right               | Left |                              |
| None                | None | 0                            |
| .009                | "    | 8400                         |
| .026                | "    | 8700                         |
| .048                | "    | 9000                         |
| .062                | "    | 9150                         |
| .071                | "    | 9300                         |
| .085                | .025 | 9450                         |
| .125                | .041 | 9600                         |
| .127                | .068 | 9750                         |
| .140                | .085 | 9900                         |
| .172                | .120 | 10,200                       |

## Precracked Hole

Specimen: Q9H5  
 Gross Stress (ksi): 27  
 Total Life (Flight Hours) 8428

| Crack Length (inch) |      | Total Life<br>(Flight Hours) |
|---------------------|------|------------------------------|
| Front               | Rear |                              |
| Right               | Left |                              |
| .040                | None | 0                            |
| .052                | "    | 1200                         |
| .062                | "    | 2400                         |
| .065                | "    | 3000                         |
| .069                | "    | 3600                         |
| .072                | "    | 4200                         |
| .080                | "    | 4800                         |
| .087                | "    | 5400                         |
| .093                | "    | 6000                         |
| .106                | "    | 6600                         |
| .118                | "    | 7200                         |
| .134                | "    | 7800                         |
| .186                | .060 | 8400                         |

## Precracked Hole

Specimen: Q12H6  
 Gross Stress (ksi): 23  
 Total Life (Flight Hours) 19,333

| Crack Length (in) |       |      |  | Total Life<br>(Flight Hours) |
|-------------------|-------|------|--|------------------------------|
| Front             |       | Rear |  |                              |
| Left              | Right | Left |  |                              |
| None              | .040  | None |  | 0                            |
| "                 | .050  | "    |  | 1200                         |
| "                 | .054  | "    |  | 2400                         |
| "                 | .058  | "    |  | 3600                         |
| "                 | .064  | "    |  | 4800                         |
| "                 | .069  | "    |  | 6000                         |
| "                 | .074  | "    |  | 7200                         |
| "                 | .076  | "    |  | 8400                         |
| "                 | .082  | "    |  | 9600                         |
| "                 | .090  | "    |  | 10,800                       |
| "                 | .098  | "    |  | 12,000                       |
| "                 | .110  | "    |  | 13,200                       |
| "                 | .122  | "    |  | 14,400                       |
| "                 | .134  | "    |  | 15,600                       |
| "                 | .150  | "    |  | 16,800                       |
| "                 | .172  | "    |  | 18,000                       |
| .012              | .191  | .009 |  | 18,600                       |
| .022              | .224  | .088 |  | 19,200                       |

APPENDIX J  
PHASE III, RECOMMENDED CHANGES TO  
AMS 4241 (D357) FOR DURABILITY AND  
DAMAGE TOLERANCE CASTINGS

ALUMINUM ALLOY CASTINGS, SAND COMPOSITE  
7.0Si - 0.58Mg - 0.15Ti - 0.06Be (D357.0-T6)  
SOLUTION AND PRECIPITATION HEAT TREATED  
AIRCRAFT DURABILITY AND DAMAGE TOLERANCE QUALITY

1. SCOPE:

- 1.1 Form: This specification covers an aluminum alloy in the form of sand composite molded castings.
- 1.2 Application: This product is intended to be typically used for durability and damage tolerance structural aircraft components, but usage is not limited to such applications.
- 1.3 Alloy D357.0 has restricted composition within the limits of alloy A357.0.
- 1.4 This specification includes requirements for both fatigue and fracture toughness. If not pertinent to the application, either property requirement can be waived by the purchaser.

2. APPLICATION DOCUMENTS: The following publications form a part of this specification to the extent specified herein. The latest issue of SAE publications shall apply. The applicable issue of other publications shall be the issue in effect on the date of the purchase order.

2.1 SAE Publications: Available from SAE, 400 Commonwealth Drive, Warrendale, PA 15096.

AMS 2350 - Standards and Test Methods  
AMS 2360 - Room Temperature Tensile Properties of Castings  
AMS 2694 - Repair Welding of Aerospace Castings  
AMS 2804 - Identification, Castings  
AMS 4188/5 - Aluminum Alloy Welding Wire, 7.0Si - 0.52Mg

ARP 1947 - Determination and Acceptance of Dendrite Arm Spacing in Aluminum Castings

2.2 ASTM Publications: Available from ASTM, 1916 Race Street, Philadelphia, PA 19103 1187.

ASTM B 557 - Tension Testing of Wrought and Cast Aluminum and Magnesium Alloy Products

ASTM B 660 - Packaging/Packing of Aluminum and Magnesium Products

ASTM E 18 - Rockwell Hardness and Rockwell Superficial Hardness Testing of Metallic Materials

ASTM E 34 - Chemical Analysis of Aluminum and Aluminum Alloys

ASTM E 155 - Reference Radiographs for Inspection of Aluminum and Magnesium Castings

ASTM E 466 - Conducting Constant Amplitude Axial Fatigue Tests of Metallic Materials

ASTM E 1304 - Plane-Strain (Chevron-notch) Fracture Toughness of Metallic Materials

2.3 U.S. Government Publications: Available from Commanding Officer, Naval Publications and Forms Center, 5801 Tabor Avenue, Philadelphia, PA 19120.

2.3.1 Military Specifications:

MIL-H-6088 - Heat Treatment of Aluminum Alloys

MIL-STD-6866 - Inspection, Penetrant Method of

MIL-I 25135 - Inspection Materials, Penetrant

2.3.2 Military Standards:

MIL-STD-410 - Nondestructive Testing Personnel Qualification and Certification (Eddy Current, Liquid Penetrant, Magnetic Particle, Radiographic and Ultrasonic)

MIL-STD-453 - Inspection, Radiographic

2.4 AIA Publications: Available from National Standard Association, Inc., 1321 14th Street, N.W., Washington, DC 20005.

NAS 823 - Cast Surface Comparison Standard

3. TECHNICAL REQUIREMENTS:

3.1 Composition: Shall conform to the percentages by weight shown in Table 1, determined by wet chemical methods in accordance with ASTM E 34, by spectrochemical or by other analytical methods approved by purchaser:

Table 1. Composition

| Element                 | min       | max  |
|-------------------------|-----------|------|
| Silicon                 | 6.5       | 7.5  |
| Magnesium               | 0.55      | 0.60 |
| Titanium                | 0.19      | 0.20 |
| Beryllium               | 0.04      | 0.07 |
| Iron                    | --        | 0.12 |
| Manganese               | --        | 0.10 |
| Other Impurities, each  | --        | 0.05 |
| Other Impurities, total | --        | 0.15 |
| Aluminum                | remainder |      |

- 3.1.1 The use of strontium or sodium as a silicon particle modifier is permitted if approved by the purchaser. When permitted, the maximum percentage by weight shall be 0.014 for strontium or 0.012 for sodium.
- 3.2 Condition: Solution and precipitation heat treated.
- 3.3 Casting: Castings shall be produced in lots from metal conforming to 3.1.
- 3.3.1 A melt shall be a single homogeneous batch of molten metal on which all processing has been completed and the temperature has been adjusted ready for pouring castings.
- 3.3.2 A lot shall be all castings poured from a single melt in not more than eight consecutive hours and solution and precipitation heat treated in the same heat treat batch.
- 3.4 Test Specimens:
- 3.4.1 Chemical Analysis Specimens: Shall be cast from each melt.
- 3.4.2 Integrally-Attached Coupons: Coupons shall be integrally-attached to each casting to permit tensile, fatigue, and fracture toughness testing.
- 3.4.2.1 Each casting shall have at least two integrally-attached tensile coupons. One coupon shall be left attached and used only if repeated heat treatment is necessary. Location and size of the coupons are optional with the following exceptions:
- 3.4.2.1.1 The coupons shall be flat and sufficiently large to permit excision of a sub-size round tensile specimen 0.200 inch (6.35 mm) in diameter with a gage length of 1 inch (25.4 mm), conforming to ASTM B 557.
- 3.4.2.2 Each casting shall have at least three integrally-attached fatigue coupons. Size of the coupons is optional, with the following exceptions:
- 3.4.2.2.1 The coupons shall be sufficiently large to permit excision of a round specimen 0.50 inch (12.7 mm) in diameter, with a minimum gage length of 2.0 inches (50.8 mm), conforming to ASTM E 466. All machining marks shall be removed and the gage section shall be polished parallel to the specimen axis. The final polish shall be with Crocus cloth.
- 3.4.2.3 Each casting shall have at least two integrally-attached fracture toughness coupons. The coupons shall be sufficiently large to permit excision of a specimen that conforms to ASTM E 1304.
- 3.4.2.4 The radiographic quality of the coupons shall meet the requirements for designated areas of Table 2.

3.4.2.5 Testing of integrally-attached coupons for casting acceptance shall be performed by a testing facility which has been approved by purchaser and the foundry, and is independent of the foundry.

TABLE 2. Radiographic Requirements

Maximum acceptance defects in aluminum alloy castings (maximum permissible radiograph in accordance with ASTM E155):

| Defects                       | Radiograph Reference | Designated Area | Other Areas |
|-------------------------------|----------------------|-----------------|-------------|
| Gas holes                     | 1.1                  | 1               | 2           |
| Gas porosity (round)          | 1.21                 | 1               | 3           |
| Gas porosity (elongated)      | 1.22                 | 1               | 3           |
| Shrinkage cavity              | 2.1                  | 1               | 2           |
| Shrinkage porosity or sponge  | 2.2                  | 1               | 2           |
| Foreign material (less dense) | 3.11                 | 1               | 2           |
| Foreign material (more dense) | 3.12                 | 1               | 2           |
| Segregation                   | ---                  | none            | none        |
| Cracks                        | ---                  | none            | none        |
| Cold shuts                    | ---                  | none            | none        |
| Laps                          | ---                  | none            | none        |

NOTES:

- (1) When two or more types of defects are present to an extent equal to or not significantly better than the acceptance standards for respective defects, the parts shall be rejected.
- (2) When two or more types of defects are present and the predominating defect is not significantly better than the acceptance standard, the part shall be considered borderline and shall be reviewed for disposition by the cognizant engineering personnel.
- (3) Gas holes or sand spots and inclusions allowed by this table shall be cause for rejection when closer than twice their maximum dimension to an edge or extremity of a casting.

3.5 Heat Treatment: Castings and integrally-attached coupons shall be solution and precipitation heat treated in accordance with MIL-H-6088 except as specified in 3.5.1 and 3.5.2.

3.5.1 The solution heat treat temperature shall be 1000° - 1020°F (450 - 550°C).

3.5.2 The quenching and precipitation heat treating procedure shall be established to develop the required casting properties.

3.6 Properties: Castings and integrally-attached chilled coupons shall conform to the following requirements:

3.6.1 Tensile Properties: Shall be as follows, determined in accordance with ASTM B 557:

3.6.1.1 Integrally-Attached Chilled Coupons: For heat treat control, the tensile properties shall as shown in Table 3.

TABLE 3. Tensile Properties

|                               |                                  |
|-------------------------------|----------------------------------|
| Tensile Strength, min         | 51.0 ksi (352 MPa)               |
| Yield Strength at 0.2% Offset | 42.0 - 47.0 ksi<br>(290-324 MPa) |

3.6.1.2 Specimens Cut from Castings: Tensile properties of specimens cut from a casting or castings shall be as shown in Table 4 or Table 5.

Table 4. Designated Casting Areas:

|  |                    |
|--|--------------------|
| Tensile Strength, minimum              | 50.0 ksi (345 MPa) |
| Yield Strength at 0.2% Offset, minimum | 40.0 ksi (276 MPa) |
| Elongation in 4D, min (See 3.6.1.2.3)  | 2%                 |

Table 5. Casting Areas Other Than Designated Areas:

|  |                    |
|--|--------------------|
| Tensile Strength, minimum              | 45.0 ksi (310 MPa) |
| Yield Strength at 0.2% Offset, minimum | 36.0 ksi (248 MPa) |
| Elongation in 4D, min (See 3.6.1.2.3)  | 2%                 |

3.6.1.2.1 Excised specimens shall be subsize and proportional to the standard round or sheet type specimens defined in ASTM B557. For sheet type specimens, elongation shall be measured based on a gage length of  $4.5 \times$  (cross-sectional area)<sup>1/2</sup>.

3.6.2 Fatigue Properties: Shall be as follows, determined in accordance with ASTM E 466:

3.6.2.1 Integrally-Attached Coupons: Three specimens shall be tested under constant amplitude fatigue loading at a frequency between 10 and 20 Hz. The maximum stress shall be 40.0 ksi (276 MPa) at a stress ratio of 0.1, and a stress concentration factor of 1.0.

The log average life of the three specimens shall be 85,000 cycles, with a minimum individual life of 46,000 cycles.

- 3.6.2.2 Specimens Cut From Castings: If the casting is sufficiently large to permit the provision of the specimens in 3.4.2.2.1, the average and minimum fatigue life requirements in 3.6.2.1 shall apply. If it is not possible to excise 0.5 inch (12.7 mm) diameter specimens from the casting, smaller specimens are permitted. These shall have a 0.250 inch (6.4 mm) or 0.375 inch (9.5 mm) diameter gauge section. The gauge section shall be between 1.5 inches (38.1 mm) and 2.0 inches (50.8 mm) long. All fatigue specimens shall be excised from designated areas of the casting.

The log average life for the 0.250 inch (6.4 mm) and 0.375 inch (9.5 mm) specimens shall be 68,000 and 78,000 cycles, respectively. The minimum fatigue life for each individual specimen shall be 36,000 and 42,000 cycles for the 0.250 inch (6.4 mm) and 0.375 inch (9.5 mm) diameter gauge sections, respectively.

- 3.6.3 Fracture Toughness Properties: Shall be not less than 21  $\sqrt{\text{inch}}$ , determined in accordance with ASTM E 1304.
- 3.6.4 When properties other than those of 3.6.1, 3.6.2, or 3.6.3 are required specimens taken from locations indicated on the drawing, from a casting or castings chosen at random to represent the lot, shall have the properties indicated on the drawing for such specimens. Tensile property requirements may be designated in accordance with AMS 2360.
- 3.6.5 Microstructure: The microstructure of the casting surface in the designated areas of the casting shall have a dendrite arm spacing that does not exceed 0.0020 inch (0.051 mm), determined in accordance with ARP1947. Castings which exhibit an unacceptable microstructure, but which meet the requirements of 3.6.1, 3.6.2, and 3.6.3, shall be held for disposition by purchaser's cognizant engineering personnel.

### 3.7 Quality:

- 3.7.1 Castings, as received by purchaser, shall be uniform in quality and condition, sound, and free from foreign materials and from imperfections detrimental to usage of the castings.
- 3.7.1.1 Castings shall have a surface finish in accordance with the engineering drawing and NAS 823 or equivalent and shall be well cleaned.
- 3.7.2 Castings shall be produced under foundry control. This control shall consist of preproduction examination of castings until proper foundry technique and controls are established, which will produce castings that will meet the drawing quality and dimensional requirements.
- 3.7.3 Radiographic inspection shall be performed on each casting in accordance with MIL-STD-00453. Type 1 radiographic film shall be used, and a maximum unsharpness value of 0.003 in. (0.08 mm) and flaw sensitivity of 1% shall be maintained. ASTM E 155 shall be used to define radiographic acceptance standards in accordance with Table 1.

- 3.7.4 Each casting shall be subjected to fluorescent penetrant inspection in accordance with MIL-STD-6866.
- 3.7.4.1 The fluorescent penetrant shall have a sensitivity level equivalent to group V of MIL-I-25135
- 3.7.4.2 Personnel conducting the testing shall be qualified and certified in accordance with MIL-STD-410.
- 3.7.4.3 Linear indications, cold shuts, cracks, and seams are not acceptable.
- 3.7.4.4 Surface porosity shall be cause for rejection if the individual pores are closer than twice their maximum dimension to an edge or extremity of the casting or the pores form a linear indication, i.e., three or more are in a line and the distance between each indication is less than twice the maximum dimension of either adjacent indication.
- 3.7.4.5 Any individual indication which is three times longer than it is wide shall be considered a linear indication and is not acceptable.
- 3.7.5 Castings shall not be repaired by peening, plugging, welding, or other methods, except as specified in 3.7.5.1.
- 3.7.5.1 Defects in non-critical areas of the casting may be removed and the castings repaired by welding in accordance with AMS 2694, using AMS 4188/5 alloy filler metal. The vendor's weld procedures shall have prior approval by purchaser.

#### 4. QUALITY ASSURANCE PROVISIONS:

- 4.1 Responsibility for Inspection: The vendor of castings shall be responsible for coordinating all acceptance testing of production castings at purchaser approved facilities. Testing of specimens excised periodically from castings and DAS determinations, when required, shall be performed at a testing facility approved by purchaser and foundry and shall be independent of the foundry. Results of such tests shall be reported to the purchaser as required by 4.5. Purchaser reserves the right to sample and to perform any confirmatory testing deemed necessary to ensure that the castings conform to the requirements of this specification.
- 4.2 Classification of Tests:
- 4.2.1 Acceptance Tests: Tests to determine conformance to requirements for composition (3.1), properties of specimens cut from castings and integrally-attached coupons (3.6), and quality (3.7) are classified as acceptance tests and shall be performed on each casting, melt, or lot as applicable.

- 4.2.2 Preproduction Tests: Tests to determine conformance to all technical requirements of this specification are classified as preproduction tests and shall be performed prior to or on the first-article shipment of casting to a purchaser, when a change in material, processing, or both requires reapproval as in 4.4.2, and when purchaser deems confirmatory testing to be required.
- 4.2.2.1 For direct U.S. Military procurement, substantiating test data and, when requested, preproduction test material shall be submitted to the cognizant agency as directed by the procuring activity, contracting officer, or request for procurement.
- 4.3 Sampling: Shall be in accordance with the following:
- 4.3.1 For Acceptance Tests:
- 4.3.1.1 One chemical analysis specimen in accordance with 3.4.1 from each melt.
- 4.3.1.2 The destructive testing of castings for the evaluation of excised test specimens shall occur at the following frequency:
- 4.3.1.2.1 First 30 Castings Received: One casting from each 10 production castings shall be selected for destructive testing.
- 4.3.1.2.2 Castings Received Thereafter: If no failure occurs in 4.3.1.2.1, one casting from each 25 production castings consecutively received thereafter shall be tested. If a failure occurs, the test frequency reverts to one from each 10 production castings from the next 30 castings received.
- 4.3.1.3 The tensile properties of an integrally-attached coupon required by 3.6.1.1 from each casting shall be determined. Testing shall be performed by a test facility approved by purchaser and independent of the foundry.
- 4.3.1.4 The fatigue properties of three integrally-attached coupons required by 3.6.2.1 from each casting shall be determined. Testing shall be performed by a test facility approved by purchaser and independent of the foundry.
- 4.3.1.5 The fracture toughness properties of an integrally-attached coupon required by 3.6.3.1 from each casting shall be determined. Testing shall be performed by a test facility approved by purchaser and independent of the foundry.
- 4.3.2 For Periodic Tests and Preproduction Tests: As agreed upon by purchaser and vendor and the following:
- 4.3.2.1 When required, specific test sites on the casting and frequency of evaluating castings for surface microstructure shall be defined by purchaser at the time of preproduction approval.

4.4 Approval:

4.4.1 Sample castings from new or reworked patterns shall be approved by purchaser before castings for production use are supplied, unless such approval be waived by purchaser.

4.4.1.1 Two preproduction castings of each part number shall be furnished to purchaser. One casting shall have been dimensionally inspected by the vendor and the results shall be forwarded with the casting for approval. The second casting shall be supplied to purchaser for metallurgical evaluation. All vendor test results obtained to substantiate the metallurgical quality of the casting shall be included.

4.4.2 Vendor shall document the parameters for the process control factors which will produce acceptable castings. These shall constitute the approved casting procedure and shall be used for producing production castings. If necessary to make any change in parameters for the process control factors, vendor shall submit for reapproval a statement of the proposed changes in material, processing, or both and, when requested, integrally attached coupons, sample castings, or both. Production castings incorporating the revised operations shall not be shipped prior to receipt of written reapproval.

4.4.2.1 Control factors for producing castings include, but are not limited to, the following:

Melting practice regarding control of:

- Chemistry
- Gas content
- Melt temperature
- Grain Size

Molding procedure regarding:

- Materials and assembly
- Gating and risering systems
- Solidification rate in designated areas

Heat treatment practice regarding:

- Temperature and time parameters
- Load density
- Quenching procedure

Shop traveler describing the sequence of processing, inspection, and testing.

4.4.2.1.1 Any of the above process control factors for which parameters are considered proprietary by the vendor may be assigned a code designation. Each variation in such parameters shall be assigned a modified code designation.

#### 4.5 Reports:

The vendor of castings shall furnish with each shipment a report showing the results of tests for chemical composition of each melt, tensile, fatigue and fracture toughness properties of attached specimens representing each casting and specimens cut from castings if applicable, penetrant and radiographic inspections of each casting by serial number, and, when performed, microstructure results from each lot. This report shall include the purchase order number, AMS XXXX, part number, and quantity.

#### 4.6 Resampling and Retesting:

##### 4.6.1 Attached Coupons:

4.6.1.1 Replacement of an integrally-attached coupon is permitted when an isolated flaw is evident on the fracture face of a broken specimen.

4.6.1.2 Testing is required of an integrally-attached tensile coupon after reheat treatment. The replacement specimen shall be taken from an additional coupon which has remained integrally attached to the casting through the reheat treat process.

##### 4.6.2 Test Specimens Excised from Castings:

4.6.2.1 Replacement of test specimens shall be allowed for poor machining, incorrect test procedure, malfunction of test equipment, or fracture location.

4.6.2.2 Retesting shall be permitted by testing two adjacent specimens. Should it not be possible to obtain adjacent specimens, or if a replacement specimen also fails, two additional castings shall be tested. Failure of a specimen in a second casting shall be cause to consider the lot of castings suspect and the purchaser contacted for material review action. All castings shipped and in process since the last acceptable tensile test of a casting shall be reviewed for disposition.

4.6.2.3 All retest specimens shall be located to represent as nearly as possible the quality of the metal of the original test.

#### 5. PREPARATION FOR DELIVERY:

5.1 Identification: Shall be in accordance with AMS 2804. Each casting shall be identified by an individual serial number to relate processing of the part with the inspection results for traceability.

5.1.1 Each casting shall be identified by legible raised figures with part number, foundry identification, and serial number in the area indicated on the engineering drawing. The serial number shall be used only on to provide traceability to the processing of a particular part.

5.1.2 Each casting accepted by radiographic inspection shall be ink stamped in accordance with MIL-STD-453.

- 5.1.3 Each casting accepted by penetrant inspection shall be ink stamped in accordance with MIL-I-6866.
- 5.1.4 Integrally-attached coupons shall be identified by a vibroetched serial number corresponding with the casting serial number.
- 5.1.5 Castings and the accompanying reports shall identify the heat treatment and melt analysis of each casting through the serial number.
- 5.1.6 When impregnation is specified or permitted by purchaser, castings so treated shall be marked "IMP".

5.2 Packaging:

- 5.2.1 Castings shall be prepared for shipment in accordance with commercial practice and in compliance with applicable rules and regulations pertaining to the handling, packaging, and transportation of the castings to ensure carrier acceptance and safe delivery.
- 5.2.2 For direct U.S. Military procurement, packaging shall be in accordance with ASTM B 660, Commercial Level unless Level A is specified in the request for procurement.

6. ACKNOWLEDGMENT: A vendor shall mention this specification number in all quotations and when acknowledging purchase orders.

7. REJECTIONS: Castings not conforming to this specification, or to modifications authorized by purchaser, will be subject to rejection.

8. NOTES:

- 8.1 Dimensions and properties in inch/pound units and the Fahrenheit temperatures are primary; dimensions and properties in SI units and Celsius temperatures are shown as the approximate equivalents of the primary units and are presented only for information.
- 8.2 This specification was developed specifically for sand composite molded castings; however, castings produced by other processes may also be capable of satisfying these requirements.
- 8.3 Aircraft durability and damage tolerance structural quality is intended to imply that these castings will exhibit the integrity and reliability required for primary aircraft structural applications, particularly those for which minimum fatigue life and fracture toughness are needed.

8.4 For direct U.S. Military procurement, purchase documents should specify not less than the following:

Title, number, and date of this specification  
Part number or pattern number of castings desired  
Quantity of castings desired  
Level A packaging, if required (See 5.2.2)

8.5 Castings meeting the requirements of this specification have been classified under Federal Standardization Area Symbol "MECA".

PREPARED UNDER JURISDICTION OF AMS COMMITTEE 'D'

ALUMINUM ALLOY CASTINGS, SAND COMPOSITE  
7.0Si - 0.58Mg - 0.15Ti - 0.06Be (D357.0-T6)  
Solution and Precipitation Heat Treated  
Aircraft Structural Quality

UNS A03570

1. SCOPE:

1.1 Form: This specification covers an aluminum alloy in the form of sand composite molded castings.

1.2 Application: Primarily for structural aircraft components.

1.3 Alloy D357.0 has restricted composition within the limits of alloy A357.0.

2. APPLICABLE DOCUMENTS: The following publications form a part of this specification to the extent specified herein. The latest issue of Aerospace Material Specifications and Aerospace Recommended Practices shall apply. The applicable issue of other documents shall be as specified in AMS 2350.

2.1 SAE Publications: Available from SAE, 400 Commonwealth Drive, Warrendale, PA 15096.

2.1.1 Aerospace Material Specifications:

- AMS 2350 - Standards and Test Methods
- AMS 2360 - Room Temperature Tensile Properties of Castings
- AMS 2694 - Repair Welding of Aerospace Castings
- AMS 2804 - Identification, Castings
- AMS 4188/5 - Aluminum Alloy Welding Wire, 7.0Si - 0.52Mg

2.1.2 Aerospace Recommended Practices:

- ARP 1947 - Determination and Acceptance of Dendrite Arm Spacing in Aluminum Castings

SAE Technical Board Rules provide that: "This report is published by SAE to advance the state of technical and engineering sciences. The use of this report is entirely voluntary, and its applicability and suitability for any particular use, including any patent infringement arising therefrom, is the sole responsibility of the user."

AMS documents are protected under United States and international copyright laws. Reproduction of these documents by any means is strictly prohibited without the written consent of the publisher.

- 2.2 ASTM Publications: Available from American Society for Testing and Materials, 1916 Race Street, Philadelphia, PA 19103.

ASTM B557 - Tension Testing Wrought and Cast Aluminum- and Magnesium-Alloy Products  
 ASTM E18 - Rockwell Hardness and Rockwell Superficial Hardness of Metallic Materials  
 ASTM E34 - Chemical Analysis of Aluminum and Aluminum Alloys  
 ASTM E155 - Reference Radiographs for Inspection of Aluminum and Magnesium Castings

- 2.3 U.S. Government Publications: Available from Commanding Officer, Naval Publications and Forms Center, 5801 Tabor Avenue, Philadelphia, PA 19120.

2.3.1 Military Specifications:

MIL-H-6088 - Heat Treatment of Aluminum Alloys  
 MIL-I-6866 - Inspection, Penetrant Method of  
 MIL-I-25135 - Inspection Materials, Penetrant

2.3.2 Military Standards:

MIL-STD-410 - Nondestructive Testing Personnel Qualification and Certification (Eddy Current, Liquid Penetrant, Magnetic Particle, Radiographic and Ultrasonic)  
 MIL-STD-649 - Aluminum and Magnesium Products, Preparation for Shipment and Storage  
 MIL-STD-00453 - Inspection, Radiographic

- 2.4 AIA Publications: Available from National Standard Association, Inc., 1321 14th Street, N.W., Washington, DC 20005.

NAS 823 - Cast Surface Comparison Standard

3. TECHNICAL REQUIREMENTS:

- 3.1 Composition: Shall conform to the following percentages by weight, determined by wet chemical methods in accordance with ASTM E34 or by spectrographic or other analytical methods approved by purchaser:

|                         | min  | max       |
|-------------------------|------|-----------|
| Silicon                 | 6.5  | 7.5       |
| Magnesium               | 0.55 | 0.6       |
| Titanium                | 0.10 | 0.20      |
| Beryllium               | 0.04 | 0.07      |
| Iron                    | --   | 0.12      |
| Manganese               | --   | 0.10      |
| Other Impurities, each  | --   | 0.05      |
| Other Impurities, total | --   | 0.15      |
| Aluminum                |      | remainder |

- 3.2 Condition: Solution and precipitation heat treated.

3.3 Casting: Castings shall be produced from metal conforming to 3.1.

3.3.1 A melt shall be a single homogenous batch of molten metal on which all processing has been completed and the temperature has been adjusted ready for pouring castings.

3.3.2 A lot shall be all castings poured from a single melt in not more than eight consecutive hours and solution and precipitation heat treated in the same heat treat batch.

3.4 Test Specimens:

3.4.1 Chemical Analysis Specimens: Shall be cast from each melt.

3.4.2 Integrally-Attached Coupons: At least two coupons shall be integrally-attached to each casting. The two coupons shall represent a variation of size of Dendrite Arm Spacing (DAS). The chilled coupon exhibiting a small DAS shall be identified as coupon "A"; the coupon of large DAS shall be identified as coupon "B". These coupons shall be used for tensile property determination specified in 3.6.1.1 and microstructure evaluation specified in 3.6.3. Additional coupons may be added for retest and foundry purposes at the option of the foundry.

3.4.2.1 Location and size of the integrally-attached coupons are optional with the following exceptions:

3.4.2.1.1 The coupons shall be flat and at least large enough to permit excision of a sub-size round tensile specimen of 0.250 in. (6.25 mm) diameter conforming to ASTM B557 with a gage length of 1 in. (25 mm).

3.4.2.1.2 The coupons shall be located in such a manner as to avoid any interference with inspection tooling.

3.4.2.2 The two coupons shall be produced with varying solidification rates to develop a minimum DAS size difference of 0.0010 in. (0.025 mm) within a tensile strength range of 47,000 - 57,000 psi (325 - 395 MPa).

3.4.2.3 The radiographic quality of the coupons shall meet the requirements for designated areas of Table I.

3.4.2.4 Removal and testing of integrally-attached coupons for casting acceptance shall be performed by a testing facility which has been approved by purchaser and the foundry and is independent of the foundry.

3.5 Heat Treatment: Castings and integrally-attached coupons shall be solution and precipitation heat treated in accordance with MIL-H-6088 except as specified in 3.5.1 and 3.5.2.

3.5.1 The solution heat treat temperature shall be 1000° - 1020°F (540 - 550°C).

3.5.2 The quenching and precipitation heat treating procedure shall be established to develop the required casting properties.

- 3.6 Properties: Castings and integrally-attached chilled coupon "A" shall conform to the following requirements:
- 3.6.1 Tensile Properties: Shall be as follows, determined in accordance with ASTM B557 and shall be used as basis for acceptance of castings:
- 3.6.1.1 Integrally-Attached Chilled Coupon "A": For heat treat control, the following tensile properties shall be exhibited:
- |                               |  |
|-------------------------------|--|
| Tensile Strength, min         | 51,000 psi (350 MPa)                   |
| Yield Strength at 0.2% Offset | 42,000 - 47,000 psi<br>(290 - 325 MPa) |
- 3.6.1.2 Specimens Cut from Castings: Tensile properties of specimens cut from a casting or castings shall be as follows:
- 3.6.1.2.1 Designated Casting Areas:
- |                                       |                      |
|---------------------------------------|----------------------|
| Tensile Strength, min                 | 50,000 psi (345 MPa) |
| Yield Strength at 0.2% Offset, min    | 40,000 psi (275 MPa) |
| Elongation in 4D, min (See 3.6.1.2.4) | 3%                   |
- 3.6.1.2.2 Casting Areas Other Than Designated Areas:
- |                                       |                      |
|---------------------------------------|----------------------|
| Tensile Strength, min                 | 45,000 psi (310 MPa) |
| Yield Strength at 0.2% Offset, min    | 36,000 psi (260 MPa) |
| Elongation in 4D, min (See 3.6.1.2.4) | 2%                   |
- 3.6.1.2.3 When properties other than those of 3.6.1.2.1 or 3.6.1.2.2 are required, tensile specimens taken from locations indicated on the drawing, from a casting or castings chosen at random to represent the lot, shall have the properties indicated on the drawing for such specimens. Property requirements may be designated in accordance with AMS 2360.
- 3.6.1.2.4 Excised specimens shall be subsize and proportional to the standard round or sheet type specimens defined in ASTM B557. For sheet type specimens, elongation shall be measured based on  $4.5\sqrt{\text{cross-sectional area}}$  *a gage length of*.
- 3.6.2 Hardness of Castings: Should be not lower than 90 HR<sub>A</sub>, determined in accordance with ASTM E18, but castings shall not be rejected on the basis of hardness if the tensile property requirements of 3.6.1.2 are met.
- 3.6.3 Microstructure: The microstructure of the casting surface in the designated areas of the casting shall not exceed the maximum size coarseness, determined in accordance with ARP 1947. Castings which exhibit an unacceptable microstructure, shall be held for disposition by purchaser's cognizant engineering personnel. Castings shall not be rejected, however, if the requirements of 3.6.1.2 are met.

### 3.7 Quality:

- 3.7.1 Castings, as received by purchaser, shall be uniform in quality and condition, sound, and free from foreign materials and from imperfections detrimental to usage of the castings.
- 3.7.1.1 Castings shall have a surface finish in accordance with the engineering drawing and NAS 823 and shall be well cleaned.
- 3.7.2 Castings shall be produced under foundry control. This control shall consist of preproduction examination of castings until proper foundry technique and controls are established which will produce castings that will meet the drawing quality and dimensional requirements.
- 3.7.3 Radiographic inspection shall be performed on each casting in accordance with MIL-STD-00453. In addition, Type 1 radiographic film shall be used, and a maximum unsharpness value of 0.003 in. (0.08 mm) and flaw sensitivity of 1% shall be maintained. ASTM E155 shall be used to define radiographic acceptance standards in accordance with Table I.
- 3.7.4 Each casting shall be subjected to fluorescent penetrant inspection in accordance with MIL-I-6866.
- 3.7.4.1 The fluorescent penetrant shall have a sensitivity level equivalent to group V of MIL-I-25135.
- 3.7.4.2 Personnel conducting the testing shall be qualified and certified in accordance with MIL-STD-410.
- 3.7.4.3 Linear indications, cold shuts, cracks, and seams are not acceptable.
- 3.7.4.4 Surface porosity shall be cause for rejection if the individual pores are closer than twice their maximum dimension to an edge or extremity of the casting or the pores form a linear indication, i.e., three or more are in a line and the distance between each indication is less than twice the maximum dimension of either adjacent indication.
- 3.7.4.5 Any individual indication which is three times longer than it is wide shall be considered a linear indication and is not acceptable.
- 3.7.5 Castings shall not be repaired by peening, plugging, welding, or other methods, except as specified in 3.7.5.1.
- 3.7.5.1 Defects in non-critical areas of the casting may be removed and the castings repaired by welding in accordance with AMS 2694, using AMS 4188/5 alloy filler metal. The vendor's weld procedures shall have prior approval by purchaser.

### 4. QUALITY ASSURANCE PROVISIONS:

- 4.1 Responsibility for Inspection: The vendor of castings shall be responsible for coordinating all acceptance testing of production castings at the purchaser's approved facilities. Tensile testing of specimens excised

## 4.1 (Continued):

periodically from castings and DAS determinations, when required, shall be performed at a testing facility approved by purchaser and foundry and independent of the foundry. Results of such tests shall be reported to the purchaser as required by 4.5. Purchaser reserves the right to sample and to perform any confirmatory testing deemed necessary to ensure that the castings conform to the requirements of this specification.

4.2 Classification of Tests:

- 4.2.1 Acceptance Tests: Tests to determine conformance to requirements for composition (3.1), tensile properties of integrally-attached coupons (3.6.1.1), tensile properties of specimens cut from castings (3.6.1.2), and quality (3.7) are classified as acceptance tests and shall be performed on each casting, melt, or lot as applicable.
- 4.2.2 Periodic Tests: Tests to determine conformance to requirements for hardness (3.6.2) and microstructure (3.6.3), are classified as periodic tests and shall be performed at a frequency selected by the vendor unless frequency of testing is specified by purchaser.
- 4.2.3 Preproduction Tests: Tests to determine conformance to all technical requirements of this specification are classified as preproduction tests and shall be performed prior to or on the first-article shipment of a casting to a purchaser, when a change in material, processing, or both requires reapproval as in 4.4.2, and when purchaser deems confirmatory testing to be required.
- 4.2.3.1 For direct U.S. Military procurement, substantiating test data and, when requested, preproduction test material shall be submitted to the cognizant agency as directed by the procuring activity, the contracting officer, or the request for procurement.
- 4.3 Sampling: Shall be in accordance with the following:
- 4.3.1 For Acceptance Tests:
- 4.3.1.1 One chemical analysis specimen in accordance with 3.4.1 from each melt.
- 4.3.1.2 The destructive testing of castings for the evaluation of excised test specimens shall occur at the following frequency:
- 4.3.1.2.1 First 30 Castings Received: One casting from each 10 production castings shall be selected for destructive testing.
- 4.3.1.2.2 Castings Received Thereafter: If no failure occurs in 4.3.1.2.1, one casting from each 25 production castings consecutively received thereafter shall be tested. If a failure occurs, the test frequency reverts to one from each 10 production castings from the next 30 castings received.

4.3.1.3 The tensile properties of an integrally-attached coupon required by 3.6.1.1 from each casting shall be determined. Removal of the coupon shall only be performed by a test facility approved by purchaser and independent of the foundry.

4.3.2 For Periodic Tests and Preproduction Tests: As agreed upon by purchaser and vendor and the following:

4.3.2.1 When required, specific test sites on the casting and frequency of evaluating castings for surface microstructure shall be defined by purchaser at the time of preproduction approval.

#### 4.4 Approval:

4.4.1 Sample castings from new or reworked patterns shall be approved by purchaser before castings for production use are supplied, unless such approval be waived by purchaser.

4.4.1.1 Two preproduction castings of each part number shall be furnished to purchaser. One casting shall have been dimensionally inspected by the vendor and the results shall be forwarded with the casting for approval. The second casting shall be supplied to purchaser for metallurgical evaluation. All vendor test results obtained to substantiate the metallurgical quality of the casting shall be included.

4.4.2 Vendor shall document the parameters for the process control factors which will produce acceptable castings. These shall constitute the approved casting procedure and shall be used for producing production castings. If necessary to make any change in parameters for the process control factors, vendor shall submit for reapproval a statement of the proposed changes in material, processing, or both and, when requested, integrally-attached coupons, sample castings, or both. Production castings incorporating the revised operations shall not be shipped prior to receipt of written reapproval.

4.4.2.1 Control factors for producing castings include, but are not limited to, the following:

Melting practice regarding control of:

- Chemistry
- Gas content
- Melt temperature
- Grain Size

Molding procedure regarding:

- Materials and assembly
- Gating and risering systems
- Solidification rate in designated areas

## 4.4.2.1 (Continued):

Heat treatment practice regarding:

Temperature and time parameters  
Load density  
Quenching procedure

Shop traveler describing the sequence of processing, inspection, and testing.

- 4.4.2.1.1 Any of the above process control factors for which parameters are considered proprietary by the vendor may be assigned a code designation. Each variation in such parameters shall be assigned a modified code designation.

4.5 Reports:

- 4.5.1 The vendor of castings shall furnish with each shipment a report showing the results of tests for chemical composition of each melt, tensile properties of attached specimens representing each casting and specimens cut from castings if applicable, penetrant and radiographic inspections of each casting by serial number, and, when performed, microstructure and hardness test results from each lot. This report shall include the purchase order number, AMS 4241, part number, and quantity.
- 4.5.2 The vendor of finished or semi-finished parts shall furnish with each shipment a report showing the purchase order number, AMS 4241, contractor or other direct supplier of castings, part number, and quantity. When castings for making parts are produced or purchased by the parts vendor, that vendor shall inspect each lot of castings to determine conformance to the requirements of this specification and shall include in the report either a statement that the castings conform or copies of laboratory reports showing the results of tests to determine conformance.

4.6 Resampling and Retesting:4.6.1 Attached Coupons:

- 4.6.1.1 Replacement of the integrally-attached coupon is permitted when an isolated flaw is evident on the fracture face of the broken tensile specimen.
- 4.6.1.2 Testing is required of an integrally-attached chilled coupon after reheat treatment. The replacement specimen shall be taken from an additional coupon which has remained integrally attached to the casting through the reheat treat process.

4.6.2 Tensile Specimens Excised from Castings:

- 4.6.2.1 Replacement of tensile specimens shall be allowed in accordance with ASTM B557 for poor machining, incorrect test procedure, malfunction of test equipment, or fracture location.

- 4.6.2.2 Retesting of a tensile specimen excised from the castings is permitted only when the fracture face indicates an isolated gas hole or piece of foreign material. Retesting shall be permitted by testing two adjacent specimens. Should it not be possible to obtain adjacent specimens, or if a replacement specimen also fails, two additional castings shall be tested. Failure of a tensile specimen in a second casting shall be cause to consider the lot of castings suspect and the purchaser contacted for material review action. All castings shipped and in process since the last acceptable tensile test of a casting shall be reviewed for disposition.
- 4.6.2.3 All retest tensile specimens shall be located to represent as nearly as possible the quality of the metal of the original test. Isolated gas holes or foreign material that are discernable by production radiography may be avoided.

PREPARATION FOR DELIVERY:

- 5.1 Identification: Shall be in accordance with AMS 2804. Each casting shall be identified by an individual serial number to relate processing of the part with the inspection results for traceability.
- 5.1.1 Each casting shall be identified by legible raised figures with part number, foundry identification, and serial number in the area indicated on the engineering drawing. The serial number shall be used only once to provide traceability to the processing of a particular part.
- 5.1.2 Each casting accepted by radiographic inspection shall be ink stamped in accordance with MIL-STD-00453.
- 5.1.3 Each casting accepted by penetrant inspection shall be ink stamped in accordance with MIL-I-6866.
- 5.1.4 Integrally-attached coupons shall be identified by a vibroetched serial number corresponding with the castings serial number and letter "A" or "B" to indicate the relative size of DAS.
- 5.1.5 Castings and the accompanying reports shall identify the heat treatment and melt analysis of each casting through the serial number.
- 5.1.6 When impregnation is specified or permitted by purchaser, castings shall be marked "IMP".
- 5.2 Packaging:
- 5.2 Castings shall be prepared for shipment in accordance with commercial practice and in compliance with applicable rules and regulations pertaining to the handling, packaging, and transportation of the castings to ensure carrier acceptance and safe delivery. Packaging shall conform to carrier rules and regulations applicable to the mode of transportation.

5.2.2 For direct U.S. Military procurement, packaging shall be in accordance with MIL-STD-649, Level A or Level C, as specified in the request for procurement. Commercial packaging as in 5.2.1 will be acceptable if it meets the requirements of Level C.

6. ACKNOWLEDGMENT: A vendor shall mention this specification number in all quotations and when acknowledging purchase orders.

7. REJECTIONS: Castings not conforming to this specification or to modifications authorized by purchaser will be subject to rejection.

8. NOTES:

- 8.1 Dimensions and properties in inch/pound units and the Fahrenheit temperatures are primary; dimensions and properties in SI units and the Celsius temperatures are shown as the approximate equivalents of the primary units and are presented only for information.
- 8.2 This specification was developed specifically for sand composite molded castings; however, castings produced by other processes may also be capable of satisfying these requirements.
- 8.3 Aircraft structural quality is intended to imply that these castings will exhibit the integrity and reliability required for primary aircraft structural applications.
- 8.4 For direct U.S. Military procurement, purchase documents should specify not less than the following:
- Title, number, and date of this specification
  - Part number or pattern number of castings desired
  - Quantity of castings desired
  - Applicable level of packaging (See 5.2.2)
- 8.5 Castings meeting the requirements of this specification have been classified under Federal Standardization Area Symbol "MECA".

This specification is under the jurisdiction of AMS Committee "D".

TABLE I

Maximum acceptance defects in aluminum alloy castings (maximum permissible radiograph in accordance with ASTM E155):

| Defects                       | Radiograph Reference | Designated Areas | Other Areas |
|-------------------------------|----------------------|------------------|-------------|
| Gas holes                     | 1.1                  | 1                | 2           |
| Gas porosity (round)          | 1.21                 | 1                | 3           |
| Gas porosity (elongated)      | 1.22                 | 1                | 3           |
| Shrinkage cavity              | 2.1                  | 1                | 2           |
| Shrinkage porosity or sponge  | 2.2                  | 1                | 2           |
| Foreign material (less dense) | 3.11                 | 1                | 2           |
| Foreign material (more dense) | 3.12                 | 1                | 2           |
| Segregation                   | ---                  | none             | none        |
| Cracks                        | ---                  | none             | none        |
| Cold shuts                    | ---                  | none             | none        |
| Laps                          | ---                  | none             | none        |

## NOTES:

- (1) When two or more types of defects are present to an extent equal to or not significantly better than the acceptance standards for respective defects, the parts shall be rejected.
- (2) When two or more types of defects are present and the predominating defect is not significantly better than the acceptance standard, the part shall be considered borderline and shall be reviewed for disposition by the cognizant engineering personnel.
- (3) Gas holes or sand spots and inclusions allowed by this table shall be cause for rejection when closer than twice their maximum dimension to an edge or extremity of a casting.

APPENDIX K  
PHASE III, RECOMMENDED CHANGES TO  
AMS 4242 (B201)

## RECOMMENDED CHANGES TO AMS 4242 SPECIFICATION

The following changes to the indicated sections of AMS 4241 specification for aluminum casting alloy B201.0 are recommended. All sections not shown below shall remain per AMS 4242.

### 3. TECHNICAL REQUIREMENTS:

3.5 Heat Treatment: *Castings and integrally-attached test coupons shall be hot isostatically pressed (HIP) as specified in 3.5.3 and shall be solution and precipitation heat treated in accordance with MIL-H-6088 except as specified in 3.5.1 and 3.5.2.*

3.5.3 Hot Isostatic Pressing: *All castings and integrally-attached coupons shall be HIPed prior to heat treatment. A step treatment of 910 to 930°F (490 to 500°C) for not less than two hours then raised to 940 to 960°F (505 to 515°C) at a pressure of 15,000 psi for not less than three hours is recommended.*

Submitted for recognition as an American National Standard

ALUMINUM ALLOY CASTINGS, SAND COMPOSITE  
4.7Cu - 0.60Ag - 0.35Mn - 0.25Mg - 0.25Ti (B201.C-T7)  
Solution Heat Treated and Overaged  
Aircraft Structural Quality

UNS A02010

1. SCOPE:

1.1 Form: This specification covers an aluminum alloy in the form of sand composite molded castings.

1.2 Application: Primarily for structural aircraft components.

1.3 Alloy B201.0 has restricted composition within the limits of alloy A201.0.

2. APPLICABLE DOCUMENTS: The following publications form a part of this specification to the extent specified herein. The latest issue of Aerospace Material Specifications shall apply. The applicable issue of other documents shall be as specified in AMS 2350.

2.1 SAE Publications: Available from SAE, 400 Commonwealth Drive, Warrendale, PA 15096.

2.1.1 Aerospace Material Specifications:

AMS 2350 - Standards and Test Methods

AMS 2360 - Room Temperature Tensile Properties of Castings

AMS 2804 - Identification, Castings

2.2 ASTM Publications: Available from American Society for Testing and Materials, 1916 Race Street, Philadelphia, PA 19103.

ASTM B557 - Tension Testing Wrought and Cast Aluminum- and Magnesium-Alloy Products

ASTM E18 - Rockwell Hardness and Rockwell Superficial Hardness of Metallic Materials

ASTM E34 - Chemical Analysis of Aluminum and Aluminum Alloys

SAE Technical Board Rules provide that: "This report is published by SAE to advance the state of technical and engineering sciences. The use of this report is entirely voluntary, and its applicability and suitability for any particular use, including any patent infringement arising therefrom, is the sole responsibility of the user."

AMS documents are protected under United States and international copyright laws. Reproduction of these documents by any means is strictly prohibited without the written consent of the publisher.

## 2.2 (Continued):

ASTM E155 - Reference Radiographs for Inspection of Aluminum and Magnesium Castings

ASTM G44 - Alternate Immersion Stress Corrosion Testing in 3.5% Sodium Chloride Solution

2.3 U.S. Government Publications: Available from Commanding Officer, Naval Publications and Forms Center, 5801 Tabor Avenue, Philadelphia, PA 19120.

2.3.1 Military Specifications:

MIL-H-6088 - Heat Treatment of Aluminum Alloys

MIL-I-6866 - Inspection, Penetrant Method of

MIL-I-25135 - Inspection Materials, Penetrant

2.3.2 Military Standards:

MIL-STD-410 - Nondestructive Testing Personnel Qualification and Certification (Eddy Current, Liquid Penetrant, Magnetic Particle, Radiographic and Ultrasonic)

MIL-STD-00453 - Inspection, Radiographic

MIL-STD-649 - Aluminum and Magnesium Products, Preparation for Shipment and Storage

MIL-STD-1537 - Electrical Conductivity Test for Measurement of Heat Treatment of Aluminum Alloys, Eddy Current Method

2.4 AIA Publications: Available from National Standards Association, Inc., 1321 14th Street, N.W., Washington, DC 20005.

NAS 823 - Cast Surface Comparison Standard

3. TECHNICAL REQUIREMENTS:

3.1 Composition: Shall conform to the following percentages by weight, determined by wet chemical methods in accordance with ASTM E34 or by spectrographic or other analytical methods approved by purchaser:

|                         | min  | max       |
|-------------------------|------|-----------|
| Copper                  | 4.5  | 5.0       |
| Silver                  | 0.40 | 0.8       |
| Manganese               | 0.20 | 0.50      |
| Magnesium               | 0.20 | 0.30      |
| Titanium                | 0.15 | 0.35      |
| Iron                    | --   | 0.05      |
| Silicon                 | --   | 0.05      |
| Other Impurities, each  | --   | 0.05      |
| Other Impurities, total | --   | 0.15      |
| Aluminum                |      | remainder |

3.2 Condition: Solution and precipitation heat treated (overaged).

3.3 Casting: Castings shall be produced from metal conforming to 3.1.

- 3.3.1 A melt shall be a single homogenous batch of molten metal on which all processing has been completed and the temperature has been adjusted ready for pouring castings.
- 3.3.2 A lot shall be all castings poured from a single melt in not more than eight consecutive hours and solution and precipitation heat treated in the same heat treat batch.

3.4 Test Specimens:

3.4.1 Chemical Analysis Specimens: Shall be cast from each melt.

3.4.2 Integrally-Attached Coupons: Each casting shall have at least two integrally-attached coupons. One coupon shall be left attached and used only in the event that reheat treatment is necessary.

3.5 Heat Treatment: Castings and integrally-attached test coupons shall be solution and precipitation heat treated in accordance with MIL-H-6088 except as specified in 3.5.1 and 3.5.2.

3.5.1 All castings and integrally-attached coupons shall be solution heat treated and overaged in such a manner as to ensure conformance to the requirements of 3.6. A step solution treatment of 945° - 965°F (505° - 520°C) for not less than 2 hr then raised to 970° - 990°F (520° - 530°C) for not less than 14 hr is recommended. Precipitation heat treatment at 365° - 375°F (185° - 190°C) for not less than 5 hr is required.

3.5.2 The integrally-attached coupons shall remain attached to the casting until removed by a test facility approved by purchaser.

3.6 Properties: Castings and integrally-attached test coupons shall conform to the following requirements:

3.6.1 Tensile Properties: Shall be as follows, determined in accordance with ASTM B557 and shall be used as basis for acceptance of castings:

3.6.1.1 Integrally-Attached Coupons:

|                                    |                      |
|------------------------------------|----------------------|
| Tensile Strength, min              | 62,000 psi (425 MPa) |
| Yield Strength at 0.2% Offset, min | 55,000 psi (380 MPa) |
| Elongation in 4D, min              | 5%                   |

3.6.1.2 Specimens Cut from Castings: Tensile properties of specimens cut from a casting or castings shall be as follows:

3.6.1.2.1 Designated Casting Areas:

|                                       |                      |
|---------------------------------------|----------------------|
| Tensile Strength, min                 | 60,000 psi (415 MPa) |
| Yield Strength at 0.2% Offset, min    | 50,000 psi (345 MPa) |
| Elongation in 4D, min (See 3.6.1.2.4) | 3%                   |

3.6.1.2.2 Casting Areas Other Than Designated Areas:

|                                       |                      |
|---------------------------------------|----------------------|
| Tensile Strength, min                 | 56,000 psi (385 MPa) |
| Yield Strength at 0.2% Offset, min    | 48,000 psi (330 MPa) |
| Elongation in 4D, min (See 3.6.1.2.4) | 2%                   |

3.6.1.2.3 When properties other than those of 3.6.1.2.1 or 3.6.1.2.2 are required, tensile specimens taken from locations indicated on the drawing, from a casting or castings chosen at random to represent the lot, shall have the properties indicated on the drawing for such specimens. Property requirements may be designated in accordance with AMS 2360.

3.6.1.2.4 Excised specimens shall be proportional to the standard round or sheet type specimens defined in ASTM B557. For sheet type specimens, elongation shall be measured based on  $4.5 \sqrt{\text{cross-sectional area}}$ .

3.6.2 Hardness of Castings: Should be not lower than 70 HRB, determined in accordance with ASTM E18, but castings shall not be rejected on the basis of hardness if the tensile property requirements of 3.6.1.2 are met.

3.6.3 Electrical Conductivity: Casting shall exhibit a minimum electrical conductivity of 31% IACS, determined by the procedure of MIL-STD-1537.

3.6.4 Stress-Corrosion Resistance: A specimen as in 4.3.5, cut from the designated area of the casting or from an attached coupon shall show no evidence of stress-corrosion cracking when tested for 30 days in accordance with ASTM G44 at a stress of 37,500 psi (260 MPa).

3.7 Quality:

3.7.1 Castings, as received by purchaser, shall be uniform in quality and condition, sound, and free from foreign materials and from imperfections detrimental to usage of the castings.

3.7.1.1 Castings shall have a surface finish in accordance with engineering drawing and NAS 823 and shall be well cleaned.

3.7.2 Castings shall be produced under foundry control. This control shall consist of preproduction examination of castings until proper foundry technique and controls are established which will produce castings that will meet the drawing quality and dimensional requirements.

3.7.3 Radiographic inspection of each casting shall be performed in accordance with MIL-STD-00453. In addition, Type I radiographic film shall be used, and a maximum unsharpness value of 0.003 in. (0.08 mm) and flaw sensitivity of 1% shall be maintained. ASTM E155 shall be used to define radiographic acceptance standards in accordance with Table I.

3.7.4 Each casting shall be subjected to fluorescent penetrant inspection in accordance with MIL-I-6866.

- 3.7.4.1 The fluorescent penetrant shall have a sensitivity level equivalent to group V of MIL-I-25135.
- 3.7.4.2 Personnel conducting the testing shall be qualified and certified in accordance with MIL-STD-410.
- 3.7.4.3 Linear indications, cold shuts, cracks, and seams are not acceptable.
- 3.7.4.4 Surface porosity shall be cause for rejection if the individual pores are closer than twice their maximum dimension to an edge or extremity of the casting or the pores form a linear indication; i.e., three or more are in a line and the distance between each indication is less than twice the maximum dimension of either adjacent indication.
- 3.7.4.5 Any individual indication which is five times longer than it is wide shall be considered a linear indication and is not acceptable.
- 3.7.5 Castings shall not be repaired by peening, plugging, welding, or other methods, except as defined in 3.7.5.1.
- 3.7.5.1 Defects in non-critical areas of the casting may be removed and the castings repaired by welding in accordance with AMS 2694. The vendor's weld procedures shall have prior approval by purchaser.
- 3.7.6 Castings shall not be impregnated, chemically treated, or coated to prevent leakage, unless specified or allowed by written permission of purchaser, designating the method to be used.

#### 4. QUALITY ASSURANCE PROVISIONS:

- 4.1 Responsibility for Inspection: The vendor of castings shall be responsible for obtaining all required tests at purchaser's approved facilities. Removal and testing of tensile specimens from castings in accordance with 3.6.1.2 shall be performed at a facility that is approved by purchaser and foundry and independent of the foundry. Results of such tests shall be reported to the purchaser as required by 4.5. Purchaser reserves the right to sample and to perform any confirmatory testing deemed necessary to ensure that the castings conform to the requirements of this specification.
- 4.2 Classification of Tests:
  - 4.2.1 Acceptance Tests: Tests to determine conformance to requirements for composition (3.1), tensile properties of integrally-attached coupons (3.6.1.1), tensile properties of specimens cut from castings (3.6.1.2), electrical conductivity (3.6.3) and quality (3.7) are classified as acceptance tests and shall be performed on each casting, melt, or lot as applicable.
  - 4.2.2 Periodic Tests: Tests to determine conformance to requirements for hardness (3.6.2) and stress-corrosion resistance (3.6.4) are classified as periodic tests and shall be performed at a frequency selected by the vendor unless frequency of testing is specified by purchaser.

- 4.2.3 Preproduction Tests: Tests to determine conformance to all technical requirements of this specification are classified as preproduction tests and shall be performed prior to or on the first-article shipment of a casting to a purchaser, when a change in material, processing, or both requires reapproval as in 4.4.2, and when purchaser deems confirmatory testing to be required.
- 4.2.3.1 For direct U.S. Military procurement, substantiating test data and, when requested, preproduction test material shall be submitted to the cognizant agency as directed by the procuring activity, the contracting officer, or the request for procurement.
- 4.3 Sampling: Shall be in accordance with the following: -
- 4.3.1 For Acceptance Tests:
- 4.3.1.1 One chemical analysis specimen in accordance with 3.4.1 from each melt.
- 4.3.1.2 The destructive testing of castings for the evaluation of excised tensile specimen shall occur at the following frequency:
- 4.3.1.2.1 First 30 Castings Received: One casting from each 10 production castings shall be selected for destructive testing in accordance with the requirements of 3.6.1.2.
- 4.3.1.2.2 Castings Received Thereafter: If no failure occurs in 4.3.1.2.1, one casting from each 25 production castings consecutively received thereafter shall be tested. If a failure occurs, the test frequency reverts to one from each 10 production castings from the next 30 castings received.
- 4.3.1.2.3 Excised tensile specimens shall be either subsize specimens proportional to the standard round or standard sheet type specimens defined in ASTM B557.
- 4.3.1.3 The tensile properties of an integrally-attached coupon from each casting shall be determined.
- 4.3.1.4 Each casting shall be radiographically and fluorescent penetrant inspected.
- 4.3.1.5 The electrical conductivity of an integrally-attached coupon of each casting shall be determined.
- 4.3.2 For Periodic Tests and Preproduction Tests: As agreed upon by purchaser and vendor and the following:
- 4.3.2.1 Specimens for stress-corrosion tests shall be round specimens, not less than 0.250 in. (6.25 mm) in diameter in the reduced section. Whenever practicable, specimens shall be taken from the designated areas of the casting as shown on the engineering drawing. Specimens from integrally-attached coupons are acceptable if size of the casting does not permit excision of 0.250 in. (6.25 mm) diameter specimen.

#### 4.4 Approval:

4.4.1 Sample castings from new or reworked patterns shall be approved by purchaser before castings for production use are supplied unless such approval be waived by purchaser.

4.4.1.1 Two preproduction castings of each part number shall be furnished to the purchaser. One casting shall have been dimensionally inspected by the vendor and the results shall be forwarded with the casting for approval. The second casting shall be for metallurgical evaluation. All vendor test results obtained to substantiate the metallurgical quality of the casting shall be included.

4.4.2 Vendor shall document the parameters for the process control factors which will produce acceptable castings; these shall constitute the approved casting procedure and shall be used for producing production castings. If necessary to make any change in parameters for the process control factors, vendor shall submit for reapproval a statement of the proposed changes in material, processing, or both and, when requested, test specimens, sample castings, or both. Production castings incorporating the revised operations shall not be shipped prior to receipt of written reapproval.

4.4.2.1 Control factors for producing castings include, but are not limited to, the following:

Melting practice regarding control of:

- Chemistry
- Gas content
- Grain size
- Melt temperature

Molding procedure regarding:

- Materials and assembly
- Gating and risering systems

Heat treatment practice regarding:

- Temperature and time parameters
- Load density
- Quenching procedure

Shop traveler describing the sequence of processing, inspection, and testing.

4.4.2.1.1 Any of the above process control factors for which parameters are considered proprietary by the vendor may be assigned a code designation. Each variation in such parameters shall be assigned a modified code designation.

#### 4.5 Reports:

- 4.5.1 The vendor of castings shall furnish with each shipment a report showing the results of tests or chemical composition of each melt, tensile properties of attached specimens representing each casting and specimens cut from casting, if applicable, and penetrant and radiographic inspection of each casting by serial number. This report shall include the purchase order number, AMS 4242, lot number, part number, and quantity.
- 4.5.2 The vendor of finished or semi-finished parts shall furnish with each shipment a report showing the purchase order number, AMS 4242, contractor or other direct supplier of castings, part number, and quantity. When castings for making parts are produced or purchased by the parts vendor, that vendor shall inspect each lot of castings to determine conformance to the requirements of this specification and shall include in the report either a statement that the castings conform or copies of laboratory reports showing the results of tests to determine conformance.

#### 4.6 Resampling and Retesting:

##### 4.6.1 Attached Coupons.

- 4.6.1.1 Retesting of the integrally-attached coupon is permitted when an isolated flaw is evident on the fracture face of the broken tensile specimen.
- 4.6.1.2 Testing is required of an integrally-attached coupon after reheat treatment. The replacement specimen shall be taken from the second coupon which has remained integrally attached to the casting through the reheat treat process.

##### 4.6.2 Tensile Specimens Excised From Castings:

- 4.6.2.1 Replacement of tensile specimens shall be allowed in accordance with ASTM B557 for poor machining, incorrect test procedure, malfunction of test equipment, or fracture location.
- 4.6.2.2 Retesting of a tensile specimen excised from the castings is permitted only when the fracture face indicates an isolated gas hole or piece of foreign material. Retesting shall be permitted by testing two adjacent specimens. Should it not be possible to obtain adjacent specimens, or if a replacement specimen also fails, two additional castings shall be tested. Failure of a tensile specimen in a second casting shall be cause to consider the lot of castings suspect and the purchaser contacted for material review action. All castings shipped and in process since the last acceptable tensile test of a casting shall be reviewed for disposition.
- 4.6.2.3 All retest tensile specimens shall be located to represent as nearly as possible the quality of the metal of the original test. Isolated flaws that are discernable by production radiography may be avoided.

5. PREPARATION FOR DELIVERY:

- 5.1 Identification: Shall be in accordance with AMS 2804.
- 5.1.1 Each casting shall be identified by legible raised figures with part number, foundry identification, and serial number in the area indicated on the engineering drawing. The serial number shall be used only once to provide traceability to the processing of a particular part.
- 5.1.2 Each casting accepted by radiographic inspection shall be ink stamped in accordance with MIL-STD-00453.
- 5.1.3 Each casting accepted by penetrant inspection shall be ink stamped in accordance with MIL-I-6866.
- 5.1.4 Integrally-attached coupons or prolongations shall be identified by a vibroetched serial number corresponding with the casting serial number.
- 5.1.5 Castings and the accompanying reports shall identify the heat treat batch and melt number to the individual casting through the serial number.
- 5.1.6 When impregnation is specified or permitted by purchaser, castings shall be marked "IMP" by ink stamp.

5.2 Packaging:

- 5.2.1 Castings shall be prepared for shipment in accordance with commercial practice and in compliance with applicable rules and regulations pertaining to the handling, packaging, and transportation of the castings to ensure carrier acceptance and safe delivery. Packaging shall conform to carrier rules and regulations applicable to the mode of transportation.
- 5.2.2 For direct U.S. Military procurement, packaging shall be in accordance with MIL-STD-649, Level A or Level C, as specified in the request for procurement. Commercial packaging as in 5.2.1 will be acceptable if it meets the requirements of Level C.

6. ACKNOWLEDGMENT: A vendor shall mention this specification number in all quotations and when acknowledging purchase orders.

7. REJECTIONS: Castings not conforming to this specification or to modifications authorized by purchaser will be subject to rejection.

8. NOTES:

- 8.1 Dimensions and properties in inch/pound units and the Fahrenheit temperatures are primary; dimensions and properties in SI units and the Celsius temperatures are shown as the approximate equivalents of the primary units and are presented only for information.
- 8.2 Porosity on the surface of the stress-corrosion specimen may accelerate corrosion due to entrapment of the saline solution and result in premature failure.

- 8.3 Aircraft structural quality is intended to imply that these castings will exhibit the integrity and reliability required of primary aircraft structural applications.
- 8.4 This specification was developed specifically for sand composite molded castings however castings produced by other processes may also be capable of satisfying these requirements.
- 8.5 For direct U.S. Military procurement, purchase documents should specify not less than the following:
- Title, number, and date of this specification
  - Part number or pattern number of castings desired
  - Quantity of castings desired
  - Applicable level of packaging (See 5.2.2)
- 8.6 Castings meeting the requirements of this specification have been classified under Federal Standardization Area Symbol "MECA".

This specification is under the jurisdiction of AMS Committee "D".

TABLE I

Maximum acceptance defects in aluminum alloy castings (maximum permissible radiograph in accordance with ASTM E155)

| Defects                       | Radiograph Reference | Designated Areas | Other Areas |
|-------------------------------|----------------------|------------------|-------------|
| Gas holes                     | 1.1                  | 1                | 2           |
| Gas porosity (round)          | 1.21                 | 1                | 3           |
| Gas porosity (elongated)      | 1.22                 | 1                | 3           |
| Shrinkage cavity              | 2.1                  | 1                | 2           |
| Shrinkage porosity or sponge  | 2.2                  | 1                | 2           |
| Foreign material (less dense) | 3.11                 | 1                | 2           |
| Foreign material (more dense) | 3.12                 | 1                | 2           |
| Segregation                   | ...                  | none             | none        |
| Cracks                        | ...                  | none             | none        |
| Cold shuts                    | ...                  | none             | none        |
| Laps                          | ...                  | none             | none        |

## NOTES:

- (1) When two or more types of defects are present to an extent equal to or not significantly better than the acceptance standards for respective defects, the parts shall be rejected.
- (2) When two or more types of defects are present and the predominating defect is not significantly better than the acceptance standard, the part shall be considered borderline and shall be reviewed for disposition by the cognizant engineering personnel.
- (3) Gas holes or sand spots and inclusions allowed by this table shall be cause for rejection when closer than twice their maximum dimension to an edge or extremity of a casting.

APPENDIX L  
PHASE I, TASK 3  
HYDROGEN CONTENT AND EQUIVALENT  
INITIAL FLAW SIZE OF GAS POROSITY  
FATIGUE SPECIMENS

TABLE L-1. HYDROGEN CONTENT AND EQUIVALENT INITIAL FLAW SIZE OF THE PHASE I, TASK 3 STRESS-LIFE FATIGUE SPECIMENS ( $K_t = 1.0$ )

| GRADE | STRESS (KSI) | CYCLES TO FAILURE | BULK (1) HYDROGEN (PPM) | EIFS (INCH) |
|-------|--------------|-------------------|-------------------------|-------------|
| A/B   | 30           | 1,384,680         | 0.062                   | 0.0076      |
|       | 40           | 132,188           | 0.035                   | 0.0124      |
| B     | 20           | 773,529           | 0.171                   | 0.0328      |
|       | 20           | 580,111           | 0.184                   | 0.0373      |
|       | 20           | 547,523           | 0.128                   | 0.0383      |
|       | 25           | 215,005           | 0.201                   | 0.0348      |
|       | 25           | 140,902           | 0.134                   | 0.0418      |
|       | 30           | 507,830           | 0.107                   | 0.0138      |
|       | 30           | 224,487           | 0.125                   | 0.0215      |
|       | 30           | 101,852           | 0.164                   | 0.0318      |
|       | 40           | 75,492            | 0.075                   | 0.0170      |
|       | 40           | 86,647            | 0.120                   | 0.0158      |
|       | 40           | 15,835            | 0.177                   | 0.0369      |
|       | 45           | 84,384            | 0.105                   | 0.0111      |
|       | 45           | 9,458             | 0.144                   | 0.0349      |
| C     | 20           | 285,991           | 0.304                   | 0.0500      |
|       | 20           | 272,006           | 0.510                   | 0.0507      |
|       | 25           | 111,408           | 0.314                   | 0.0460      |
|       | 25           | 138,985           | 0.520                   | 0.420       |
|       | 30           | 65,456            | 0.310                   | 0.0387      |
|       | 30           | 55,829            | 0.397                   | 0.0414      |
|       | 35           | 23,419            | 0.396                   | 0.0419      |
|       | 35           | 23,754            | 0.425                   | 0.0417      |
|       | 40           | 16,344            | 0.255                   | 0.0364      |
|       | 40           | 15,618            | 0.260                   | 0.0371      |
| D     | 20           | 171,492           | 0.370                   | 0.0599      |
|       | 20           | 325,308           | 0.279                   | 0.0474      |
|       | 25           | 103,377           | 0.291                   | 0.0469      |
|       | 25           | 73,884            | 0.449                   | 0.0537      |
|       | 30           | 31,957            | 0.416                   | 0.0516      |
|       | 30           | 33,188            | 0.358                   | 0.0508      |
|       | 35           | 15,002            | 0.195                   | 0.0505      |
|       | 35           | 1,253             | 0.240                   | 0.1055      |

(1) Average of 2 Results — Data Obtained by Wright Laboratory Using DADTAC Contract Fatigue Specimens